PL-TR-92-2232

SPACECRAFT SURFACE CHARGING HANDBOOK

V. A. Davis
L. W. Duncan

Maxwell Laboratories, Inc.
S-Cubed Division
P.O. Box 1620
La Jolla, California 92038-1620

November 1992

Final Report
October 1989 - November 1992

PHILLIPS LABORATORY
Directorate of Geophysics
AIR FORCE MATERIEL COMMAND
HANSCOM AIR FORCE BASE, MA 01731-5000

"This technical report has been reviewed and is approved for publication"

ALLEN G. RUBIN
Contract Manager

DAVID A. HARDY
Branch Chief

WILLIAM SWIDER
Deputy Division Director

This report has been reviewed by the ESC Public Affairs Office (PA) and is releasable to the National Technical Information Service (NTIS).

Qualified requestors may obtain additional copies from the Defense Technical Information Center. All others should apply to the National Technical Information Service.

If your address has changed, or if you wish to be removed from the mailing list, or if the addressee is no longer employed by your organization, please notify PL/TSI, Hanscom AFB, MA 01731-5000. This will assist us in maintaining a current mailing list.

Do not return copies of this report unless contractual obligations or notices on a specific document requires that it be returned.

REPORT DOCUMENTATION PAGE

Form Approved
OMB No. 0704-0188

1. AGENCY USE ONLY *(Leave blank)*	2. REPORT DATE	3. REPORT TYPE AND DATES COVERED
	November 1992	Final Report - 10/89 - 11/92

4. TITLE AND SUBTITLE

Spacecraft Surface Charging Handbook

5. FUNDING NUMBERS

PE 63410F
PR 2821 TA 01 WU AE

Contract F19628-89-C-0209

6. AUTHOR(S)

V. A. Davis and L. W. Gordon

7. PERFORMING ORGANIZATION NAME(S) AND ADDRESS(ES)

Maxwell Laboratories, Inc.
S-Cubed Division
P. O. Box 1620
La Jolla, CA 92038-1620

8. PERFORMING ORGANIZATION REPORT NUMBER

SSS-DPR-91-12305

9. SPONSORING/MONITORING AGENCY NAME(S) AND ADDRESS(ES)

Phillips Laboratory
Hanscom Air Force Base, MA 01731-5000

Contract Manager: Allen G. Rubin/GPSP

10. SPONSORING/MONITORING AGENCY REPORT NUMBER

PL-TR-92-2232

11. SUPPLEMENTARY NOTES

12a. DISTRIBUTION/AVAILABILITY STATEMENT

Approved for public release;
distribution unlimited

12b. DISTRIBUTION CODE

13. ABSTRACT *(Maximum 200 words)*

Spacecraft surface charging is the buildup of net electric charge—and therefore an electrostatic potential—on the external surfaces of a spacecraft due to incident particles with energies in the kilo-electron volt to tens of kilo-electron volts range. Geosynchronous and low-altitude, polar-orbiting spacecraft encounter charging environments.

Surface charging causes problems for operational spacecraft. A primary effect is the occurrence of electronic switching anomalies, which can be triggered by differential charging related discharges. The discharge induced transients can cause system failures and, potentially, material damage. A more common anomaly is a phantom command, requiring intervention from the ground, and possibly resulting in loss of data and/or expendables, thus shortening the operational lifetime of the spacecraft.

The work of the early 1980's provided designers with tools to reduce the number and severity of anomalies. Over the past 10 years, concern has arisen regarding charging on low-altitude, polar orbiting spacecraft due to auroral precipitation. Additionally, with the miniaturization of components, modern spacecraft are more vulnerable to EMI. This handbook was developed to address some of these concerns.

This handbook reviews the scientific issues of concern in spacecraft surface charging, describes the components of a spacecraft surface charging control plan, and summarizes the techniques used to avoid spacecraft surface charging problems. Examples are provided of (1) calculational techniques to evaluate the expected effects of a spacecraft design and (2) experimental techniques to test immunity to spacecraft surface charging effects. Information on the environments found in the geosynchronous and auroral region and the surface material properties that can affect surfaces are also given.

14. SUBJECT TERMS	15. NUMBER OF PAGES
Space Vehicles, Spacecraft, Surface Charging, Spacecraft Charging, Differential Charging, Aurora, Geomagnetic Substorm, Geosynchronous, Polar	352
	16. PRICE CODE

17. SECURITY CLASSIFICATION OF REPORT	18. SECURITY CLASSIFICATION OF THIS PAGE	19. SECURITY CLASSIFICATION OF ABSTRACT	20. LIMITATION OF ABSTRACT
Unclassified	Unclassified	Unclassified	SAR

Table of Contents

Acknowledgments

We wish to express our appreciation to all those who assisted in the development of this handbook by consenting to be interviewed, either formally or informally. This includes H. Koons, R. Briet, and A. L. Vampola of Aerospace Corporation, H. R. Anderson, A. Holman, and J. Manderesse of SAIC, L. Levy of CERT, R. Viswanathan, G. Barbay, P. J. Jupiter, and T. Sartherland of Hughes Aircraft Co., H. B. Garrett and A. C. Whittlesey of the Jet Propulsion Laboratory, K. Pfitzer, and R. Oberman of McDonnell Douglas, D. E. Hastings of the Massachusetts Institute of Technology, R. C. Olsen of the Naval Postgraduate School, C. S. Underwood and N. J. Stevens of TRW, Inc., A. Bogarad and C. Bowman of General Electric, R. Fredrickson of Phillips Laboratory, C. K. Purvis of NASA/LeRC, and A. Reubens of NASA/Johnson. Our thanks to the authors of the object definitions used in the examples. And thanks are due to D. L. Cooke of Phillips Laboratory who supplied the suggested auroral charging environment.

Our thanks to all those who came before. Without twenty years of research in the field of spacecraft charging, this handbook would not be possible.

Our thanks to J. N. Barfield, W. Lockhart, and J. K. Koga of Southwest Research Institute for their participation in the early part of this project. We wish to thank our colleagues at S-Cubed, M. J. Mandell, I. Katz, G. A. Jongeward, J. M. Wilkenfeld, and J. R. Lilley, Jr. for providing text and calculations that have been incorporated in this document. And special thanks to S. M. Tyler for taking care of the details—formatting and editing—that make this a more useful handbook.

Chapter 1
Spacecraft Charging Effects

Spacecraft surface charging is the buildup of net electric charge—and therefore an electrostatic potential—on the external surfaces of a spacecraft due to incident particles with energies in the kilo-electron volt to tens of kilo-electron volts range. A geosynchronous spacecraft charges when the vehicle encounters a region of enhanced plasma associated with a magnetospheric substorm. These enhanced plasma "clouds" have typical particle energies of 1 to 50 keV. Large, low-altitude, polar-orbiting spacecraft charge when they pass through regions of auroral activity. Smaller spacecraft in low-altitude, polar orbits, can charge due to multibody interactions, if they are near a larger spacecraft while passing through an aurora.

Two types of spacecraft charging are of concern. Absolute charging is the development of a potential of the spacecraft frame relative to the surrounding space plasma. Differential charging is the change in the potential of one part of the spacecraft with respect to another. Differential charging may produce strong local electrical fields that can give rise to discharges.

Spacecraft in geosynchronous orbit charge up to tens of kilovolts. The SCATHA satellite demonstrated that differential surface charging on spacecraft during substorms is associated with discharges and operational anomalies. In one event, potential differences of more than 9.5 kV were measured on the satellite [Koons et al., 1988]. At the same time, 29 pulses were detected by the Transient Pulse Monitor. Seventeen of the pulses exceeded the maximum instrument level of 7.4 V. Coincident with the discharges were three anomalies including a two minute loss of data. A survey of nine years of SCATHA data shows a correlation between the current of particles with energies in the tens of kilovolts, the development of surface differential potentials in excess of 100 V, and electrostatic discharges [Koons and Gorney, 1991].

A few severe charging events have been observed in the auroral region. During 1983, instruments on board the Defense Meteorological Satellite 7 (DMSP 7) observed an absolute potential of -800 V [Gussenhoven et al., 1985]. Since then a few events with higher potentials—up to -1.2 kV—have been observed. No anomalies have been associated with any of the observed charging events. However, theory predicts that the larger spacecraft of the future will develop even higher potentials.

Multibody interactions can cause or enhance surface charging if two electrically isolated spacecraft, such as the shuttle and an astronaut during extra-vehicular activity (EVA), are near each other while in a high energy (keV) plasma. Since multiple spacecraft have only been flown in low equatorial orbits (LEO) where high energy

particles do not occur naturally, charging due to multibody interactions has not been observed.

As shown in Figure 1, surface charging causes problems for operational spacecraft. Differential charging can lead to significant potential differences between adjacent surfaces, which can lead to discharges. The discharges are rapid pulses typically of many amperes for nanoseconds to microseconds. A primary effect is the occurrence of electronic switching anomalies, which can be triggered by differential charging related discharges. The discharge induced transients can cause system failures and, potentially, material damage. A more common anomaly is a phantom command, requiring intervention from the ground, and possibly resulting in loss of data and/or expendables, thus shortening the operational lifetime of the spacecraft.

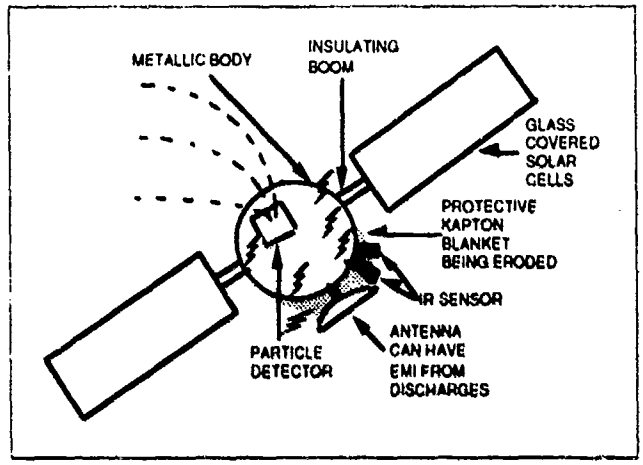

Figure 1. The effects of spacecraft surface charging include EMI, surface degradation, and contamination from discharges, disruption of particle measurements, and enhanced attraction of contaminating ions.

Surface charging can cause increased levels of contamination, resulting in changes in surface characteristics. Spacecraft surface charging can enhance contamination in two ways. First, charged contaminants are attracted to oppositely charged surfaces. Some of the contaminants that would otherwise drift away from the spacecraft are attracted to the charged surfaces and impact at higher energies where chemical bonding is enhanced. Second, the material expelled during a discharge can be deposited on other surfaces.

Contamination on surfaces with special properties, such as lenses, can destroy the special properties. Higher temperatures may result from altered surface optical properties. Charging characteristics may change due to changes in secondary and photoelectron yields. Deposition of dielectric contaminants can also change surface conductivity.

And finally, surface charging on spacecraft can bias plasma measurements of the space environment.

The extent to which these effects interfere with the spacecraft mission varies from spacecraft to spacecraft and charging episode to charging episode. It was in the early 1970s that spacecraft began to experience anomalies, and in one case failure, that

appeared to be spacecraft charging related [Stevens et al., 1987]. The early 1970s is when computer-level logic in electronics subsystems was first introduced. The more sensitive electronics could be upset by transients that did not affect the electronics on earlier spacecraft. As electronics become more sensitive, precautions become more important.

The process of charge accumulation on spacecraft surfaces is understood, and techniques have been developed to minimize the associated problems. NASA developed the *Design Guidelines for Assessing and Controlling Spacecraft Charging Effects*, which describes the understanding of the problem at that time and suggests techniques to avoid problems associated with spacecraft surface charging [Purvis et al., 1984]. Computer codes have been developed to assist designers in the design of spacecraft with minimal surface charging effects.

The first line of defense against differential charging is minimization of the area of surfaces that are insulators or floating conductors. This localizes the problem and reduces the amount of charge that can be rapidly discharged. (Sometimes the potential differences are larger when the areas are smaller, but the total charge and energy stored is smaller.) Careful attention to the design of the parts of the spacecraft where discharges are expected reduces the risk further. Shielding and filtering protect the circuitry from the EMI resulting from any remaining rapid discharging.

For some applications, the reduction of surface charging (both differential and absolute) either by using surface materials with high secondary electron emission, passive charge control, or by using a plasma emitter, active charge control, is necessary.

Over the past 10 years, concern has arisen regarding charging on low-altitude, polar orbiting spacecraft due to auroral precipitation. The 2 m DMSP spacecraft has been observed to charge to −1.2 kV and a 10 m spacecraft could charge to −10 kV. Auroral charging differs from geosynchronous charging in that charging currents tend to be much higher, the vehicle is in a charging environment for only seconds, and the charging rate and the potential reached depend on the vehicle size. In addition, 2-body and wake effects can become important, and differential charging between vehicles such as a shuttle and an astronaut during extra-vehicular activity (EVA) is of concern. The assessment of a low-altitude, polar orbiting spacecraft design for possible charging-related problems requires the consideration of more complicated interactions and the use of different computational tools and environments than for geosynchronous spacecraft. In addition, low-altitude, polar orbiting spacecraft need to work well while in the equatorial regions.

The work of the early 1980s, which provides spacecraft designers with tools to reduce the number and severity of surface charging associated anomalies, leaves some questions unanswered. With the miniaturization of components, modern spacecraft are more vulnerable to EMI, so stricter requirements are needed.

This handbook was developed to address some of these concerns. It addresses auroral charging and provides updated information on geosynchronous charging when available. This handbook focuses on verification. Examples are provided of (1) calculational techniques to evaluate the expected effects of a spacecraft design and (2) experimental techniques to test immunity to spacecraft surface charging effects.

Chapter 2 is a review of the scientific issues of concern in spacecraft surface charging. Chapter 3 describes the components of a spacecraft surface charging control plan.

Chapter 4 summarizes the techniques used to avoid spacecraft surface charging problems. Chapters 5 and 6 provide the heart of this handbook. Chapter 5 provides step-by-step analyses of four different spacecraft. The computer files needed to perform part of the analyses are in Appendix C. Chapter 6 describes the types of experimental tests that may be needed and some of the pitfalls that may be encountered. Appendix A is a general discussion of the environments found in the geosynchronous and auroral region. Appendix B is a discussion of the surface material properties that can affect surfaces. Appendix D is an example of analysis done in connection with discharge testing.

Chapter 2
Review of Spacecraft Charging

2.1 The Spacecraft as a Floating Probe

One way to understand the physics of spacecraft charging is to think of a spacecraft as a Langmuir probe in its local, ionospheric plasma. The Langmuir probe is the most basic instrument used in laboratory plasma experiments. It is used to measure the density and temperature of a plasma. Typically, it is a small metal sphere or long wire whose potential is swept through a limited range of voltages while the current to the probe is measured. The current is due to charged particles from the plasma impinging upon the sphere. When the sphere potential is very positive compared to the kinetic energy of the plasma, only electrons are collected. When the sphere potential is very negative, only ions are collected. Between these two extremes, there is a potential at which the ion current exactly balances the electron current, so that the current to the sphere is exactly zero. This potential, at which the net current is zero, is called the floating potential. Because, at a given energy, electrons move rapidly compared with ions, the floating potential is normally negative a few times the plasma kinetic energy. If the wire to a probe is cut, the probe rapidly achieves the floating potential.

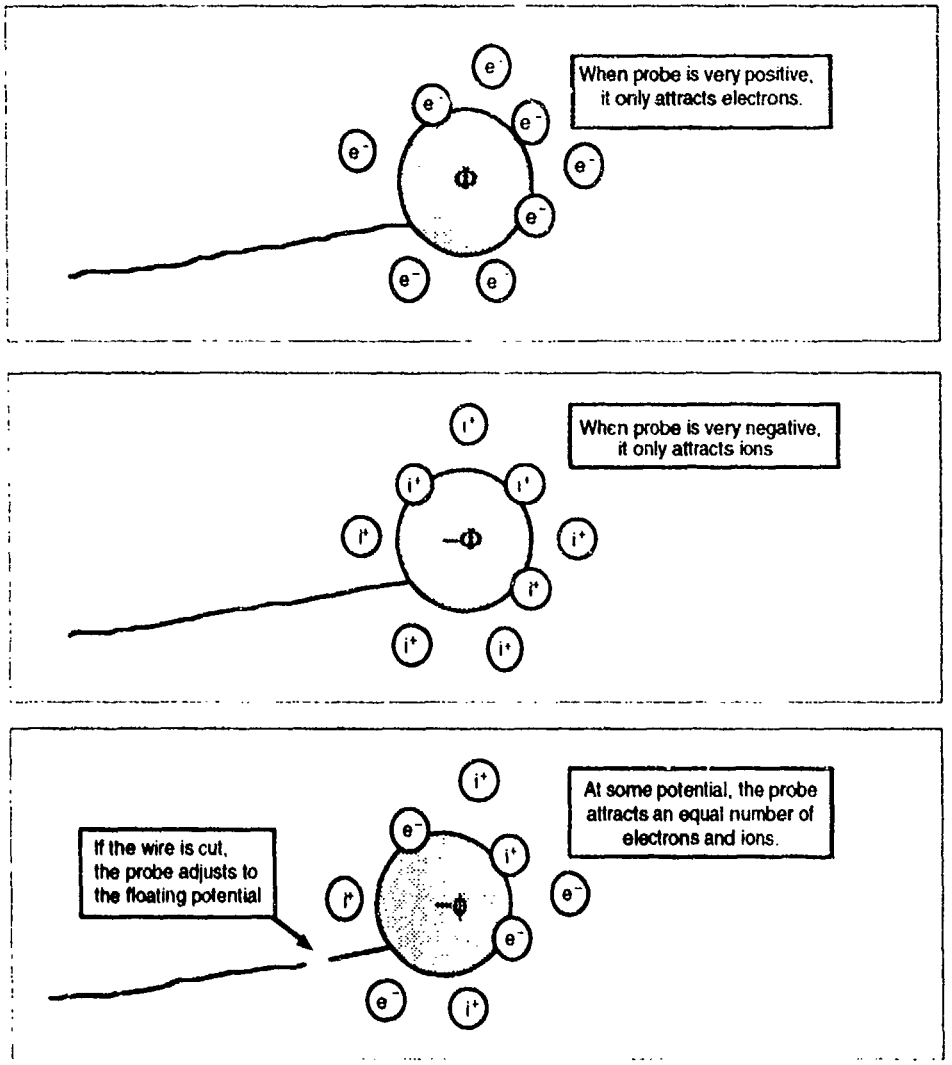

Figure 2. A Langmuir probe attracts electrons and/or ions from the surrounding plasma depending on its potential. The floating potential is the potential at which no net current flows.

In space, since there is no way for a continuous current to flow, the plasma particles rapidly charge the spacecraft to a few times the electron energy. The difference between the laboratory Langmuir probe and a spacecraft immersed in a magnetospheric substorm or an aurora is that the electron energies are a few volts in the laboratory and can be tens of thousands of volts in space. Laboratory floating potentials are typically negative a few volts; in space, potentials as high as –19 kV have been observed [Whipple, 1981].

There are two models of current collection from a plasma. They are referred to as orbit-limited and space-charged-limited. Orbit-limited current collection is appropriate when the potential has a range larger than the largest impact parameter and is sufficiently well behaved so that no angular momentum barriers exist. Potentials that vary more slowly than with the inverse of the radius squared satisfy these conditions. At geosynchronous orbit, the plasma is so dilute that little shielding occurs and the spacecraft potential drops roughly as the inverse of the radius. At lower altitudes, where

the plasma is denser, current collection is space-charge-limited. The space charge of the attracted particles shields the attracting potential and thus limits the range of the potential.

Figure 3 illustrates orbit-limited current collection. In a high energy, low density plasma, the electron current exceeds the ion current and the vehicle charges negatively. As the potential becomes negative, the electron current diminishes because not all the electrons have the energy to overcome the potential. If the plasma has roughly a Maxwellian distribution of energies, the electron current decreases exponentially with the negative potential.

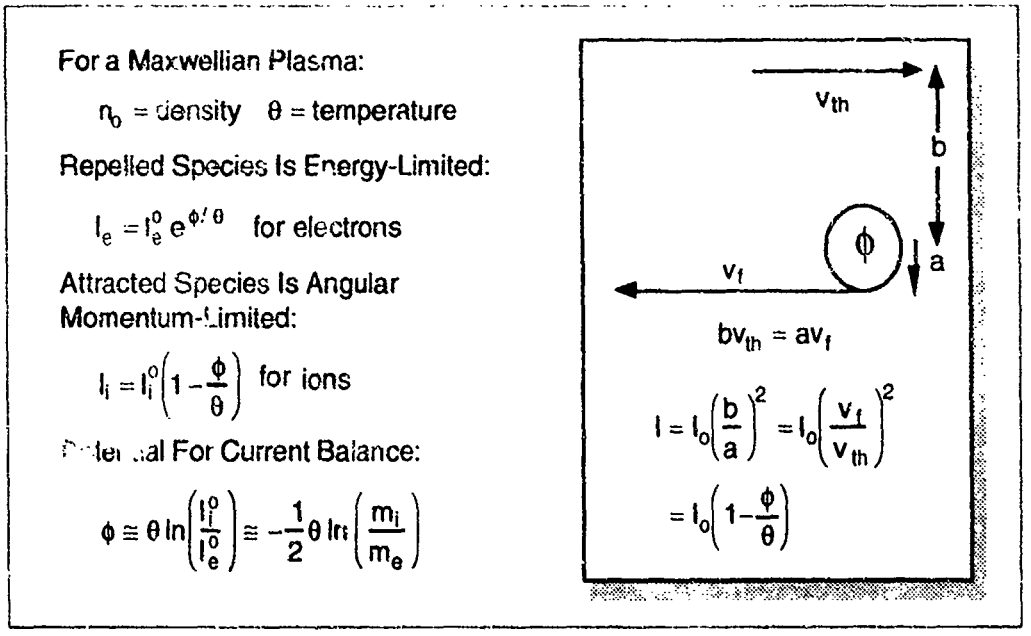

Figure 3. Orbit-limited collection of ions based on conservation of angular momentum.

Additional ions are attracted to the spacecraft as the potential becomes more negative. For the very low density plasma in the magnetosphere, angular momentum limits the collection of ions. The maximum impact parameter from which ions are collected is that for which the ion's collected velocity must be tangent to the spacecraft to conserve energy.

The balancing of ion and electron currents predicts a floating potential on the order of a few times the plasma temperature. Since the electron current diminishes exponentially and the ion current increases linearly, the principal effect of the potential is to decrease the electron current.

Figure 4 illustrates space-charge-limited current collection. Current collection by a spacecraft in a plasma with a Debye length of the order of the spacecraft size is space-charge-limited. As the spacecraft charges negative, the additional ions collected shield and thus limit the range of the potential. To model spacecraft charging in an ionospheric plasma with densities greater than about 10^9 m^{-3}, space-charge-limited collection models should be used.

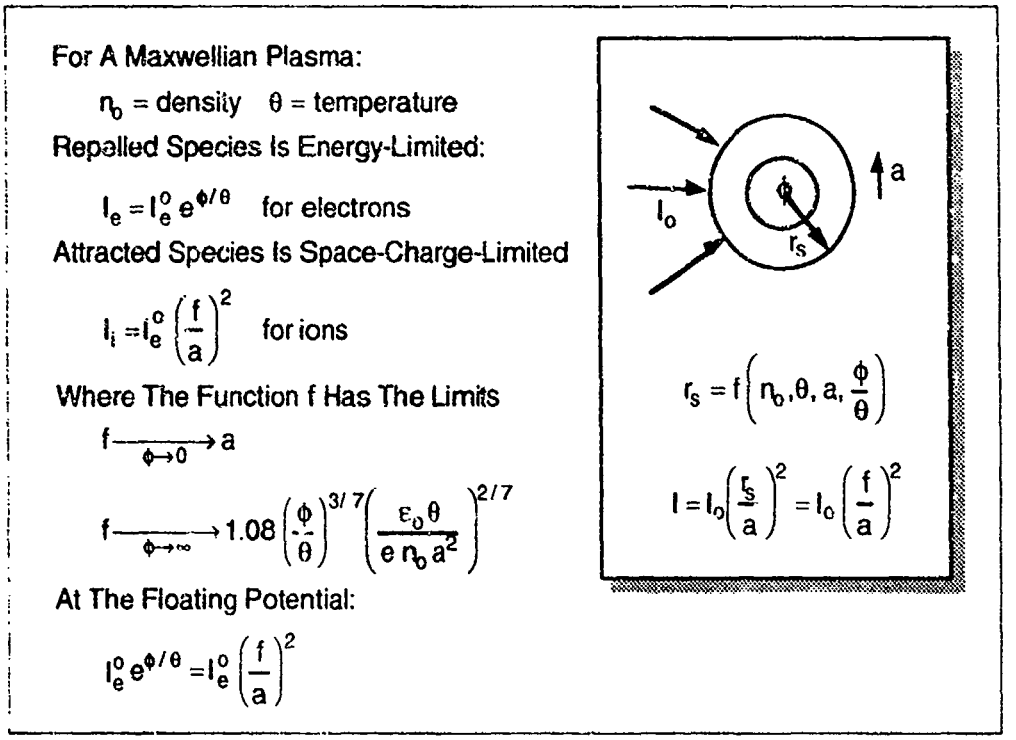

Figure 4. Space-charge-limited collection of ions.

2.2 Charging Environments

Two regions, geosynchronous altitudes and the auroral regions, have plasma conditions where the plasma energy is high enough to charge spacecraft to kilovolts or higher. Figure 14 shows where these regions are located with respect to Earth's size and the radiation belts. At geosynchronous altitudes, spacecraft charge when enveloped in a "plasma cloud" injected during a magnetic substorm. These plasma clouds have particle densities of the order 10^6 to 10^7 m^{-3} and energies of 1 to 50 keV. For calculational purposes, measured fluxes can usually be fit by a Maxwellian or 2-Maxwellian distribution function. Under quiet plasma conditions, particle densities are of the order 10^8 m^{-3} with energies of the order 1 eV. Substorms typically occur every few hours, so the conditions for tens of kilovolt charging at geosynchronous orbit occur frequently.

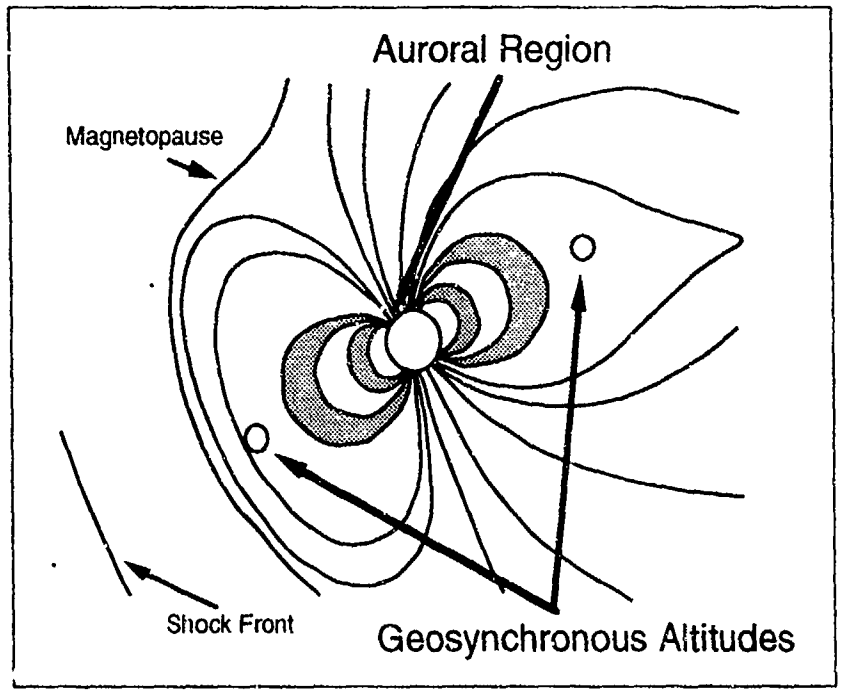

Figure 5. There are two regions where the electron energies can be kilovolts to tens of kilovolts.

The energetic electrons that charge low-altitude, polar-orbiting spacecraft in the auroral region are those that generate the aurora borealis. While of similar origin to substorm electrons in the magnetosphere, the auroral electron fluxes can be as much as a hundred times as intense. Some of the enhanced intensity comes from the convergence of the magnetic field lines as they approach Earth's poles. Measured fluxes can be fit well using the analytical form suggested by Fontheim et al. [1982].

Severe environments that can be used for design calculations are in Table 1 [Cooke, private communication; Cooke et al., 1985; Purvis et al., 1984]. A more detailed discussion of the plasma environment experienced by spacecraft is in Appendix A.

Table 1.
Severe Charging Environments

Geosynchronous Substorm (Maxwellian for each species)		
Electron number density	1.12×10^{6}	m^{-3}
Electron temperature	12	keV
Ion number density	2.36×10^{5}	m^{-3}
Ion temperature	29.5	keV
Ion species	Hydrogen	
Auroral (Cold Single Maxwellian for both species and Fontheim Electrons)		
Ion and cold electron number density	3.55×10^{9}	m^{-3}
Ion and cold electron temperature	0.2	eV
Ion species	Oxygen	
Energetic Maxwellian coefficient	6×10^{5}	m^{-3}
Energetic Maxwellian temperature	8	keV
Power law coefficient	3×10^{11}	m^{-3}
Power law exponent	1.1	
Power law cut off, low	50	eV
Power law cut off, high	1.6×10^{6}	eV
Gaussian coefficient	4×10^{4}	m^{-3}
Gaussian centered about	24	keV
Gaussian width	16	keV

The environment to which spacecraft are exposed consists of more than the plasma environment. Neutral particles, electromagnetic radiation from the sun, high energy charged particles, debris, and meteoroids all affect spacecraft. The atomic oxygen found at low altitudes can erode surface materials and affect the charging characteristics. Incident sunlight generates a photocurrent. Ultraviolet light can change surface characteristics. High energy charged particles can deposit charge in insulators. This deep charging can interact with surface charging to generate discharges that would not occur if charge had not been deposited by both mechanisms. [Garrett et al., 1990] Debris and meteoroids erode surface coating. Atomic oxygen, debris, and meteoroids have densities of concern only at the lower altitudes.

2.3 Charging Currents

Spacecraft are designed for purposes other than acting as plasma probes. Consequently, the interpretation and prediction of the spacecraft potential are complicated due to the complex geometry, multiple surface materials, and the absence of an easily accessible reference ground. Each insulating spacecraft surface interacts separately with the plasma and is capacitively and resistively coupled to the frame and other surfaces. Rather than a single floating potential, there can be a different one

associated with each surface. Computing surface potentials for a spacecraft is a considerably more complex problem than computing the potential on a conducting, spherical probe.

As shown in Figure 6, currents other than incident electrons and ions should be included. Kilovolt electrons generate secondary electrons and can be backscattered (reflected) from surfaces. Kilovolt ions also generate secondary electrons. The current density of low-energy electrons generated by solar UV emission is much greater than the natural charging currents. Because of this, most absolute spacecraft charging has been observed during eclipse, when the spacecraft is in the shadow of the Earth.

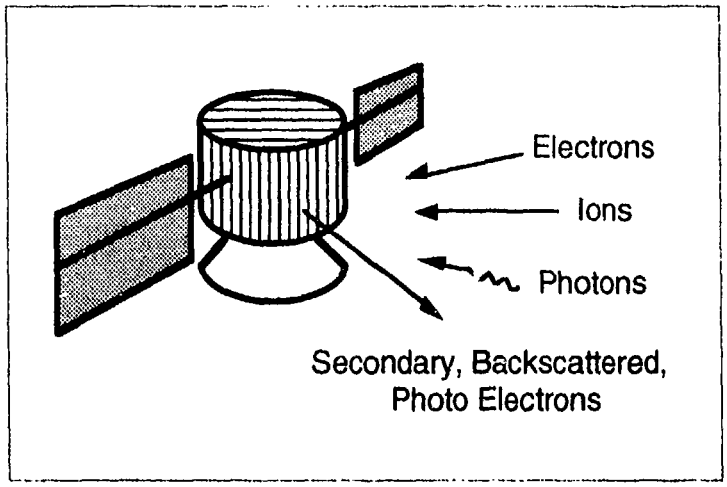

Figure 6. Several currents contribute to the net current to a spacecraft surface.

At equilibrium, each spacecraft surface is at a potential such that the net current to the surface is zero. The net current to each surface is

$$I_{NET} = I_E - I_{SE} - I_B - I_I - I_{SI} - I_P - I_l \qquad (1)$$

where the symbols have the following meanings.

- I_E Electron current to surface
- I_I Ion current to surface
- I_{SE} Secondary electron current due to I_E
- I_{SI} Secondary electron current due to I_I
- I_B Backscattered electron current due to I_E
- I_P Photoelectron current
- I_l Current to adjacent or underlying surfaces.

Each of these currents is a function of the spacecraft geometry and velocity and the plasma conditions.

To get a feel for each of the terms in this equation consider the current to a negatively charged isolated sphere in a Maxwellian plasma in the orbit-limited current collection regime. The electron current is given by

$$I_e = en\sqrt{\frac{e\theta}{2\pi m_e}}e^{\phi/\theta} \tag{2}$$

where e is the electron charge, n is the plasma density, θ is the plasma temperature, m_e is the electron mass, and ϕ is the surface potential. The ion current is given by

$$I_e = en\sqrt{\frac{e\theta}{2\pi m_i}}\left(1-\frac{\phi}{\theta}\right) \tag{3}$$

where m_i is the ion mass.

The interactions of the incident electrons and ions with the spacecraft surfaces have a profound effect on floating potentials. The most important process is secondary electron emission [Katz et al., 1986]. Because secondary electron yields are so high for many surface materials, the spacecraft floating potential is often positive! As seen in Figure 7, for electrons with energies between 50 eV and 2 kV, more than one secondary electron is emitted for every incident electron from a material such as kapton. This results in a positive charging current. Only when the electron energies exceed several thousand volts does the spacecraft charge negatively. Backscatter yields are less than unity and vary little with energy. Ion-generated-secondary electrons enhance the ion current and act to reduce absolute charging levels.

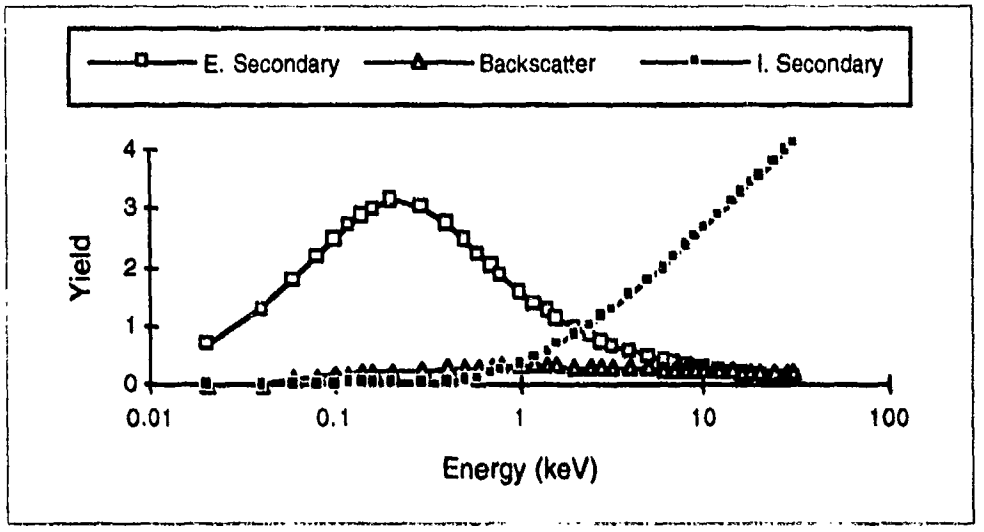

Figure 7. Electron-generated-secondary electron yield, backscatter yield, and proton-generated-secondary electron yield for kapton.

The photoelectron current for sunlit surfaces is of the order of $2\text{-}4 \times 10^{-5}$ A m^{-2} for most spacecraft surfaces. The current to the underlying and adjacent surfaces depends on the surface and bulk conductivities and the geometry.

The computer code **Matchg** was used to compute the various contributions to the current to both a kapton sphere and a silver sphere immersed in the severe substorm environment. The currents are shown in Figures 8 and 9. (See Appendix C, Section C.1

for additional information on these calculations.) As the net current to the kapton sphere is zero at –22 kV, the floating potential is –22 kV. As is shown in Figure 8, at low applied potential, the electron current, which drives the charging, is 3×10^{-6} A m^{-2}, half of which is immediately canceled by secondaries and backscattered electrons. As silver generates more secondary and backscattered electrons, the silver sphere's equilibrium potential is lower. Ion-generated-secondary electrons effectively triple the incident ion current. Because of the secondaries and backscattered electrons, current balance is effected equally by diminishing the electron and increasing the ion currents. Because the incident electron spectrum remains Maxwellian, electron-generated secondaries and backscattered electrons remain a constant fraction of the incident current as the spacecraft charges. The ion-generated secondaries increase compared with the incident ion current because the energy of the ions increases as the spacecraft potential becomes more negative. Ion-generated-secondary electron yields peak for ion energies of several tens of kilovolts.

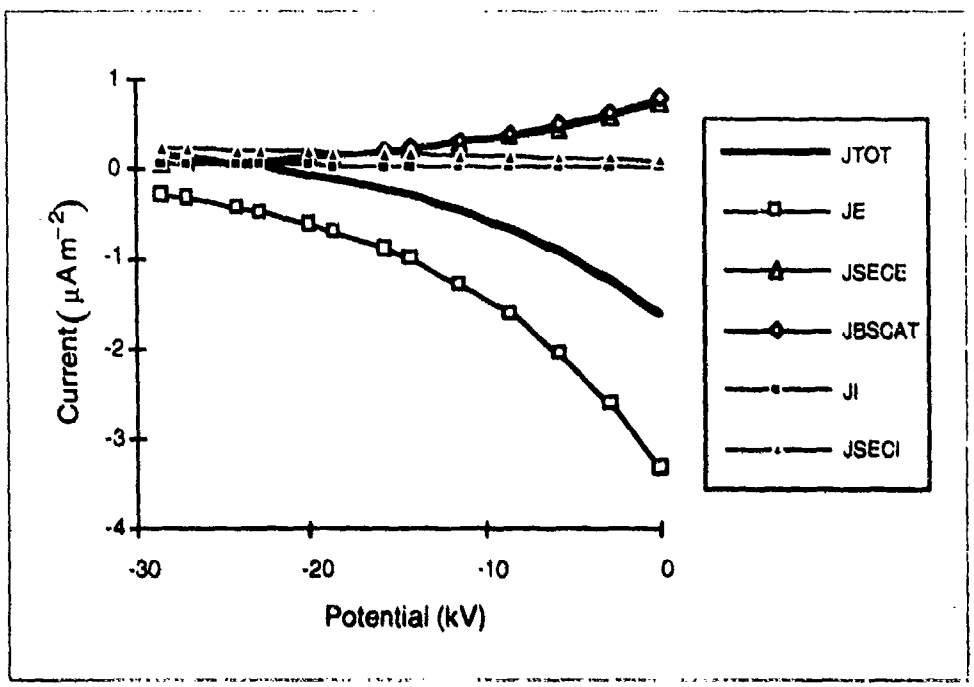

Figure 8. Current versus voltage for a kapton sphere in a severe substorm environment. The floating potential is –22 kV.

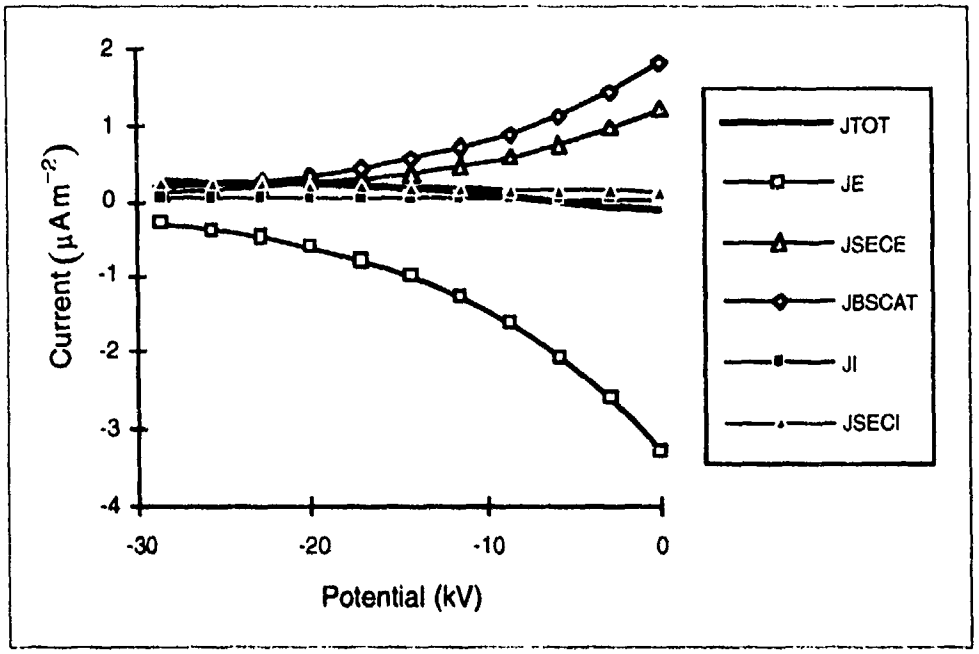

Figure 9. Current versus voltage for a silver sphere in a severe substorm environment. The floating potential is –5.8 kV.

The different conditions of substorms and aurora means that the important contributions to the net current in these two regions are different. Figures 8 and 9 show that charging of geosynchronous spacecraft is dominated by the balance of the incident electron current with the secondary electrons (from incident electrons and ions). Figure 10 shows the current versus voltage for the various currents that contribute to the charging of a 1-meter kapton sphere moving at mach 8 (orbital velocity in low-Earth orbit) in the severe auroral environment. The dominant currents are the space-charge-limited ram ions and the incident electrons. Figure 11 illustrates the difference between these two regimes. Charging of large objects in low-altitude, polar orbit is determined by the balance of the net auroral flux and the space-charge-limited ion flux. These spacecraft leave a substantial ion depleted wake. The lower ion density in the wake region means less ions are available to neutralize the built-up negative charge. The comparison (shown in Table 2) between the potentials calculated ignoring space charge with those calculated including it show more than an order of magnitude difference. The space-charge-limited result agrees with observation. (See Appendix C, Section C.2 for additional information on these calculations.)

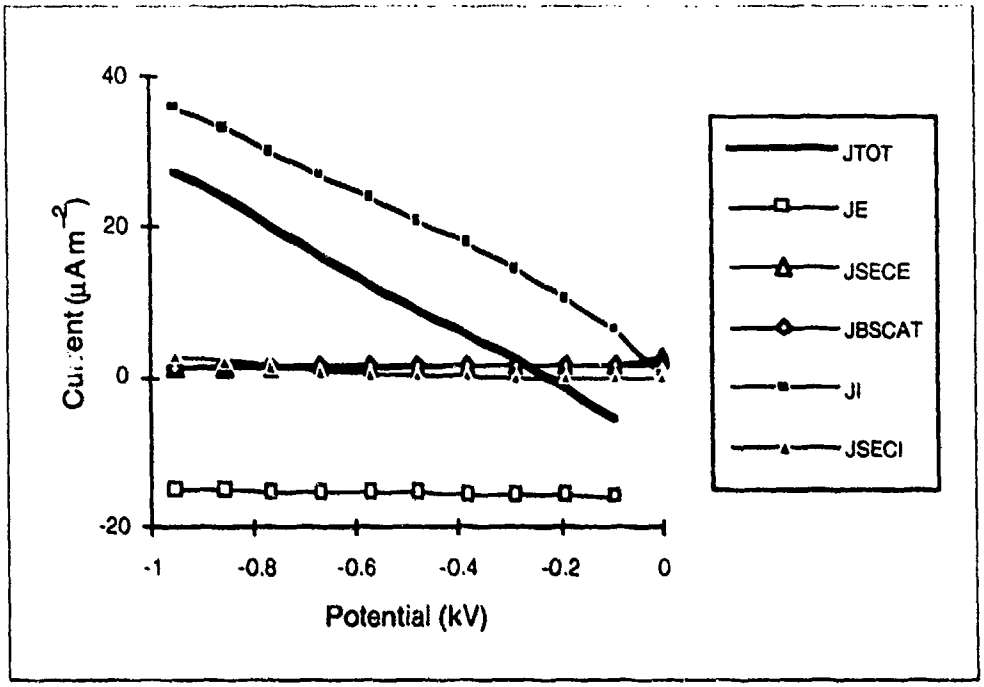

Figure 10. Current versus voltage for a 1-meter kapton sphere moving at mach 8 in a severe auroral environment. The floating potential is -230 V.

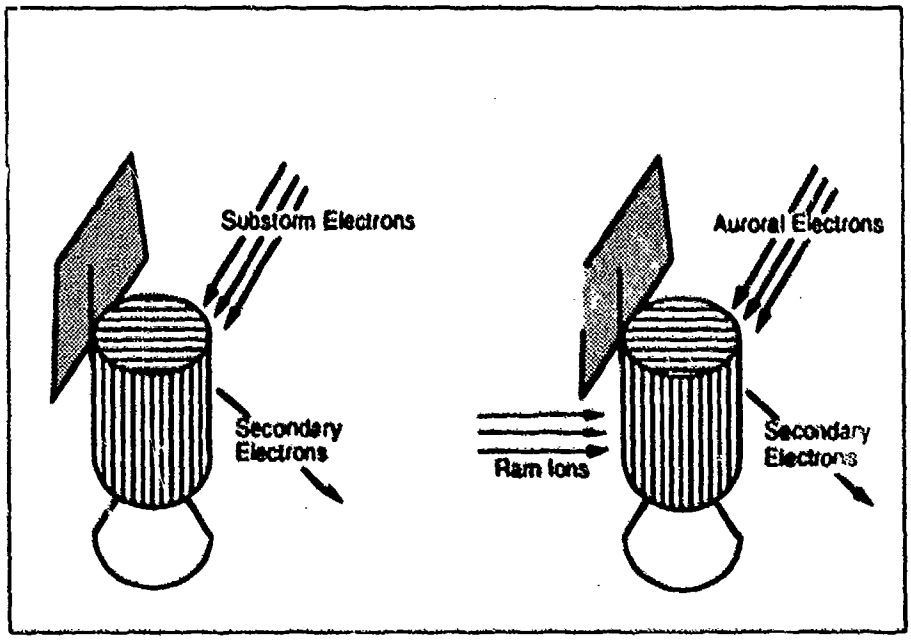

Figure 11. The charging of geosynchronous spacecraft is determined by the balance of the substorm electrons and the secondary electrons. The charging of large spacecraft in the auroral region is determined by the balance of the net auroral flux and the space-charge-limited ion flux.

Table 2.
Equilibrium Potentials Calculated by **suchgr**

Orbit-limited		Space-charge-limited			
Sphere radius		1 m		10 m	
Mach velocity		0.001	8	0.001	8
Kapton	-9 V	-550 V	-230 V	-5400 V	-2900 V
Silver	-5 V	-250 V	-99 V	-3100 V	-1600 V

2.4 Differential Charging

The electrons associated with surface charging penetrate less than a micron into the spacecraft skin. Because of this, surface coatings play a large role in determining spacecraft potentials. While the time to achieve net current balance is very short, the order of a millisecond, the time for each surface to achieve its own equilibrium potential is thousands of times longer. The development of differences between the potentials of different surfaces is referred to as differential charging.

Figure 12 shows mechanisms for the development of differential potentials. Different materials have different equilibrium surface potentials because the secondary and backscatter yield coefficients are different. This effect can lead to potential differences between neighboring surfaces. The ground potential of the spacecraft depends on the average properties of the spacecraft surfaces. Each surface charges differently from spacecraft ground. The difference between the surface potential of a dielectric and the potential of the underlying conductor is another source of differential potentials.

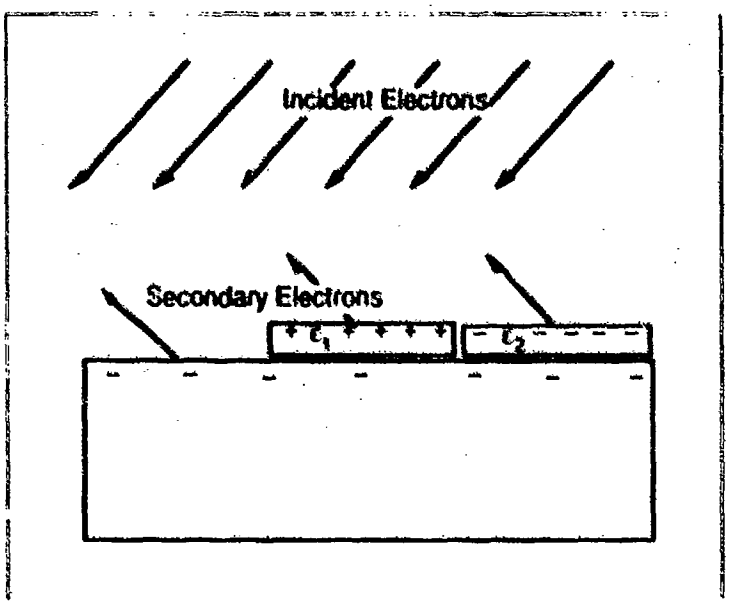

Figure 12. Differential potentials due to differences in secondary emission properties.

The rate of absolute charging is determined by the capacitance of the spacecraft to infinity, while the rate of differential charging is determined by the capacitance of the dielectric layer. The rate of change of the potential on a sphere is given by

$$\frac{d\phi}{dt} = \frac{I}{4\pi\varepsilon_o}\frac{I}{R} = \frac{JR}{\varepsilon_o} \tag{4}$$

where I is the current to the sphere, J is the current density to the sphere surface, and R is the sphere radius. For a 1-meter sphere and a net current of 1 $\mu A\ m^{-2}$, the sphere begins to charge at a rate of 100 $kV\ s^{-1}$. As the potential on the sphere increases, the net current decreases, as can be seen in Figure 8. Therefore, the charging rate decreases with time.

The rate of change of the difference in potential across a dielectric layer is given by

$$\frac{d\phi}{dt} = \frac{Jd}{\varepsilon_o} \tag{5}$$

where d is the thickness of the layer. A 100 μm layer (4 mil) with the same incident current density charges at a rate of 10 $V\ s^{-1}$. Therefore, differential charging takes place 10^4 times more slowly than absolute charging.

Figure 13 shows the equilibrium potential contours calculated by the computer code **Nascap** of the *NASCAP/GEO* codes for a silver quasi-sphere of radius 3.5 m with a 5 mil thick kapton coating over half of the surfaces exposed to the severe substorm environment of Table 1. (See Appendix C, Section C.3 for additional information on this calculation.) The surfaces with the kapton coating are those facing the bottom, the left, and the rear. Figure 13 shows the time history of charging of this sphere. In 1 second the entire sphere charges to −18 kV. After 1500 seconds (25 minutes), a differential potential of 1 kV has developed. By 100,000 seconds (28 hours), the equilibrium potentials of −22.5 kV on the kapton and −10.9 kV on the silver are reached. A thinner kapton coating would charge slower.

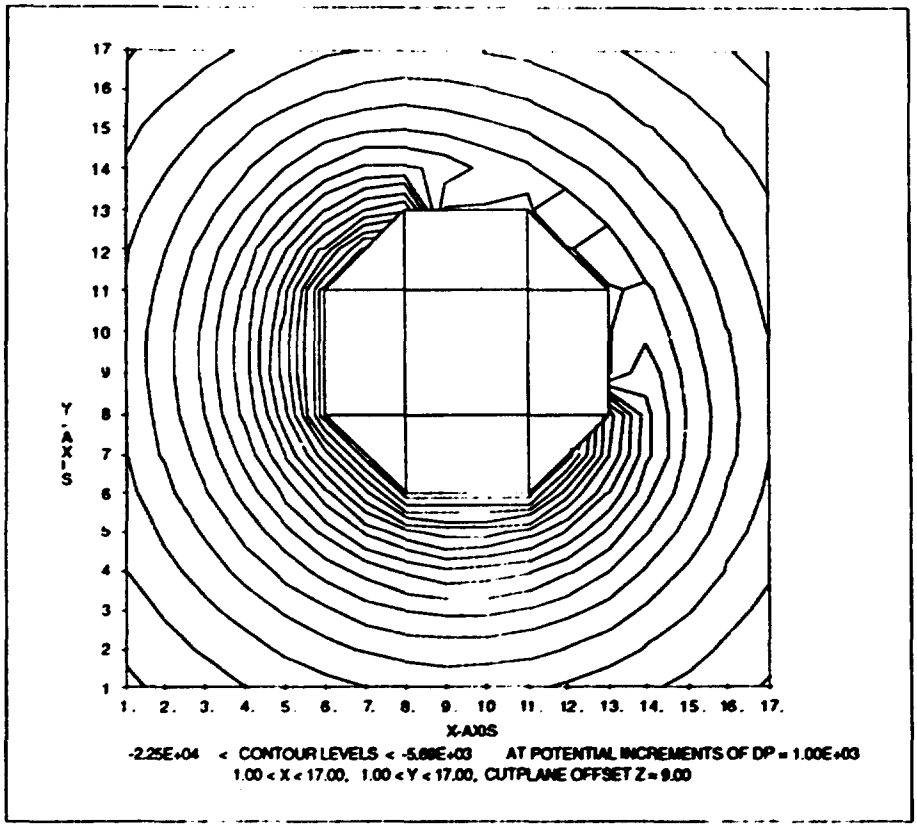

Figure 13. A 3.5 m radius quasi-sphere, half kapton and half silver, exposed to a severe geosynchronous environment develops different potentials on the surfaces coated with different materials. The contour levels are at 1 kV increments. The kapton surfaces charge to –22.5 kV, and the silver surfaces charge to –10.9 kV.

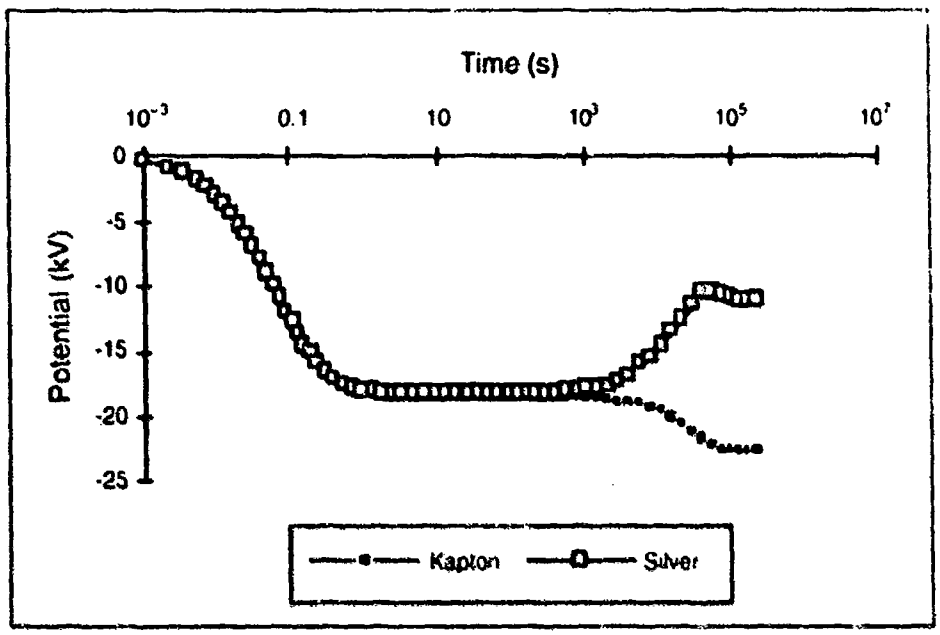

Figure 14. Time history of the potential of the quasi-sphere shown in Figure 13.

The same sphere in the severe auroral environment charges similarly. Figure 15 shows the equilibrium potential contours calculated by the computer code **nterak** of the *POLAR* codes for a 3.5 m radius silver quasi-sphere with a kapton coating over half of the surfaces exposed to the severe auroral environment of Table 1. (See Appendix C, Section C.4 for further information on this calculation.) The surfaces with the kapton coating are those facing the bottom, the left, and the rear. Figure 16 shows the time history of charging of this sphere. In under a hundredth of a second the entire sphere charges to -1.4 kV. In 13 seconds a differential potential of 1 kV has developed. In 60 seconds (1 minute), the surfaces have reached their equilibrium potential of -2.8 kV for the kapton surfaces and -1.0 kV for the silver surfaces (and spacecraft ground).

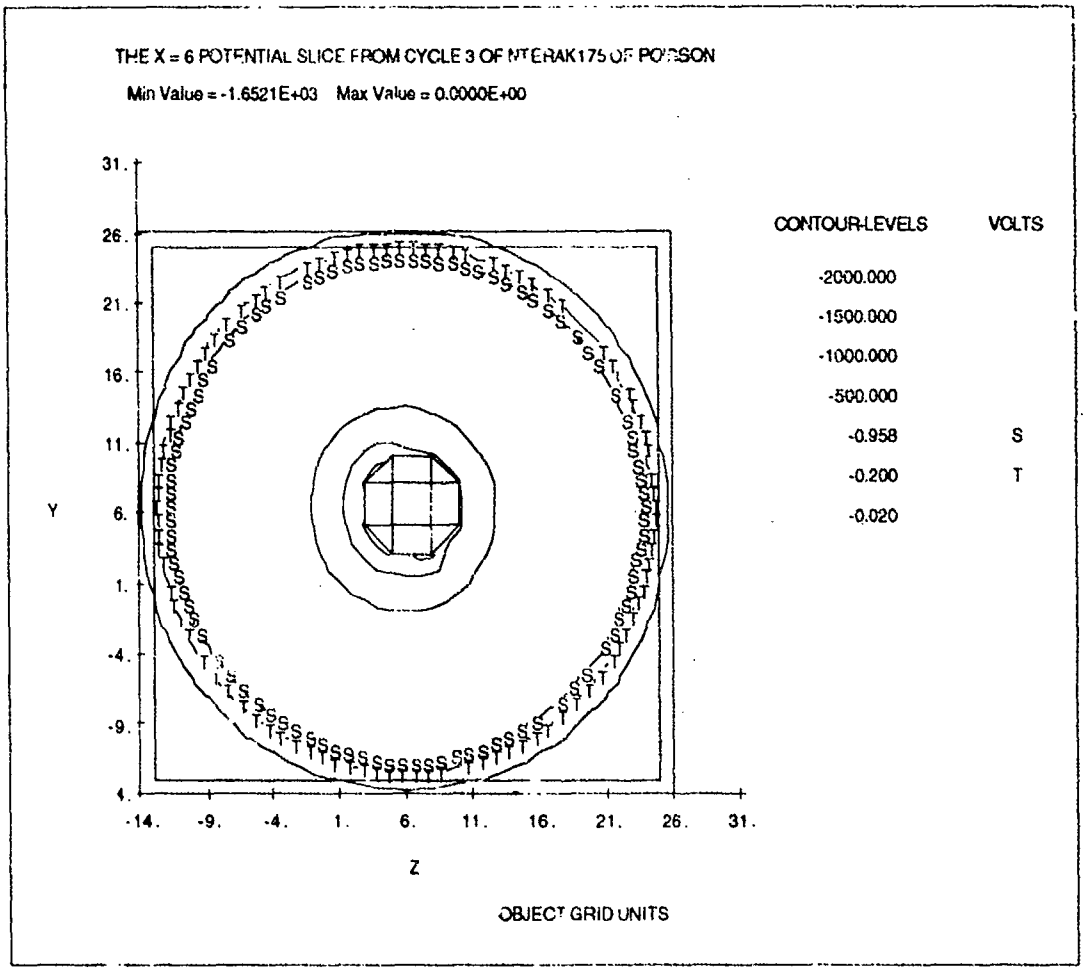

Figure 15. A 3.5 m radius quasi-sphere, half kapton and half silver, exposed to a severe auroral environment develops different potentials on the surfaces coated with different materials. The kapton surfaces charge to –2.8 kV, and the silver surfaces charge to –1.0 kV. The sheath surface is marked with an "s."

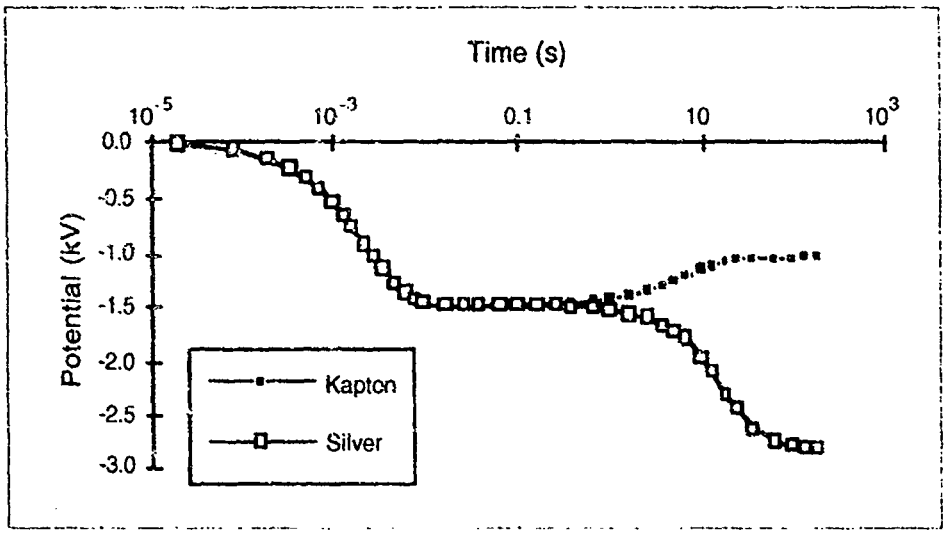

Figure 16. Time history of the potential of the quasi-sphere shown in Figure 15.

Photoelectron current densities are about 2–4 × 10^{-5} A m^{-2}, typically an order of magnitude greater than incident electron currents, even before secondaries are taken into account. As a result, in sunlight, high absolute potentials are rarely observed on spacecraft. However, in an intense substorm, spacecraft surfaces shadowed from the sun slowly charge to thousands of volts negative, while the sunlit surfaces remain a few volts positive. This process can lead to differential charging as illustrated in Figure 17. High differential potentials can develop between shaded and unshaded dielectrics. And high differential potentials can develop between shaded dielectrics and spacecraft ground. The sun-shade interface, and the differential potentials, shifts location through the year. A sun angle that does not cause a problem in one season can in another.

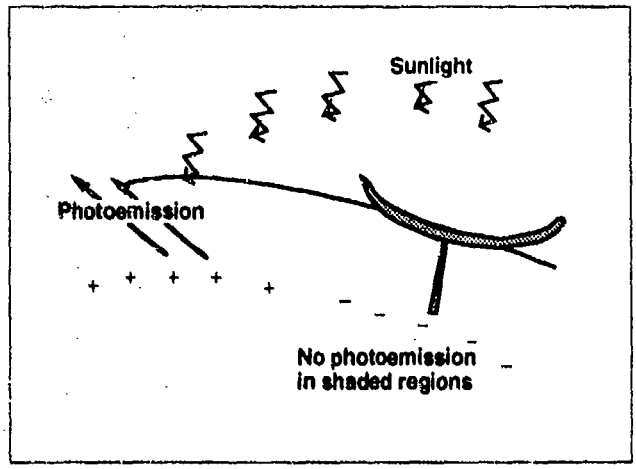

Figure 17. Differential charging between shaded and unshaded surfaces in sunlight

Sunlight differential charging can lead to high spacecraft ground potentials when the low energy photoelectrons can not escape from the spacecraft because of potential

barriers [Fahleson, 1973; Mandell et al., 1978]. Typically, the saddle point is driven by the balance of photo and secondary electrons and has a height of a few volts. All the surfaces then charge negative at a rate corresponding with differential charging, typically a few hundred volts per minute. Figure 18 shows the development of a barrier and the subsequent charging. Figure 19 shows the time history of the ground potential and the surface potential on the sunlit and dark sides. The sunlit side starts out a few volts positive. The dark side charges negatively. After a half second, the dark side is at –8 V and the sunlit side at 3 V. A potential barrier of 1 V has developed. The potential barrier grows until the photoelectrons cannot escape. Once the photoelectrons cannot escape, the entire space charges. Sunlight charging is a multidimensional effect calculable only by models that include the 3-dimensional geometry of real spacecraft.

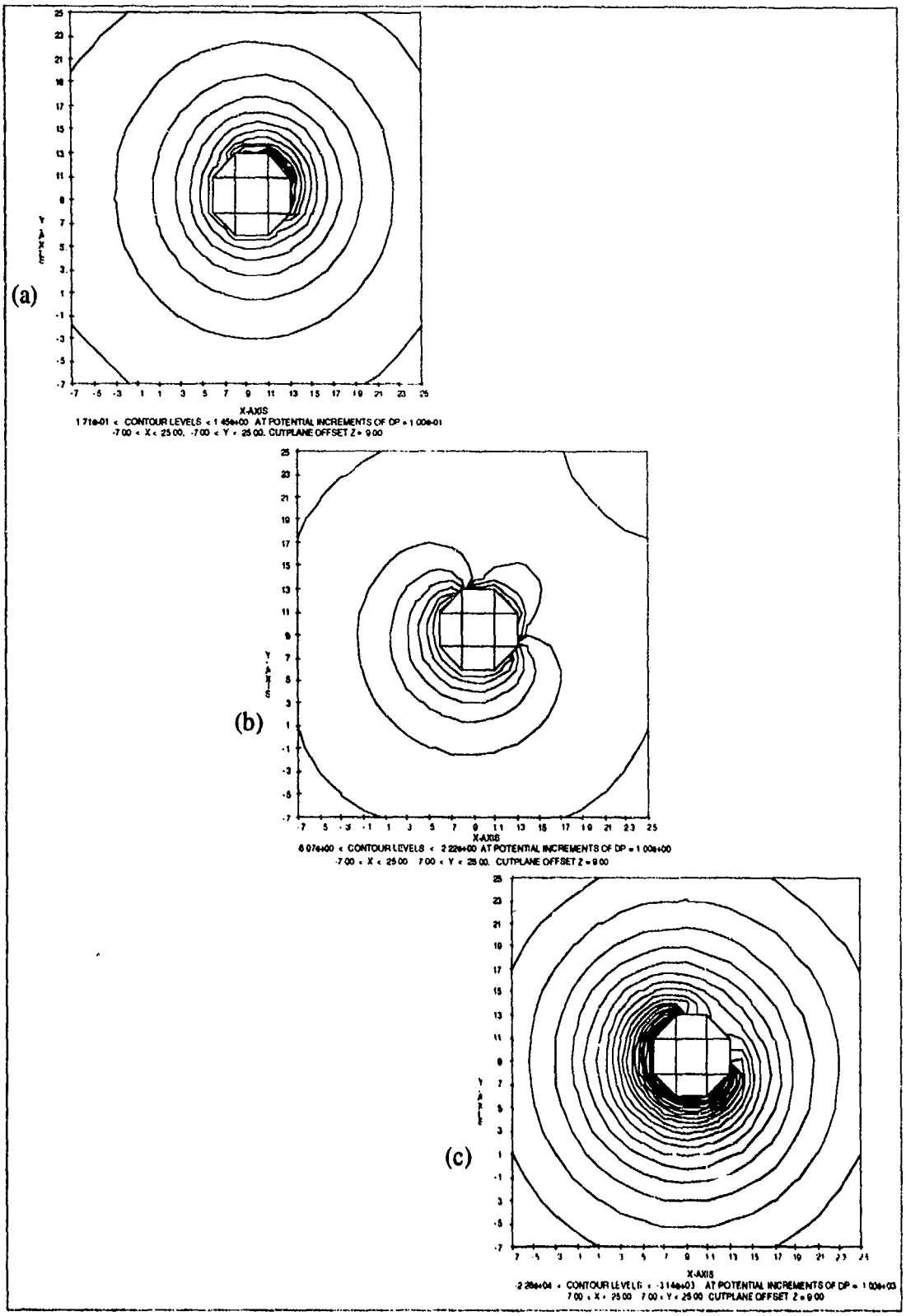

Figure 18. Formation of a barrier. Potentials about a sunlit kapton quasi-sphere at 0.024 s, 0.5 s, and at equilibrium. The sun is in the upper right-hand corner.

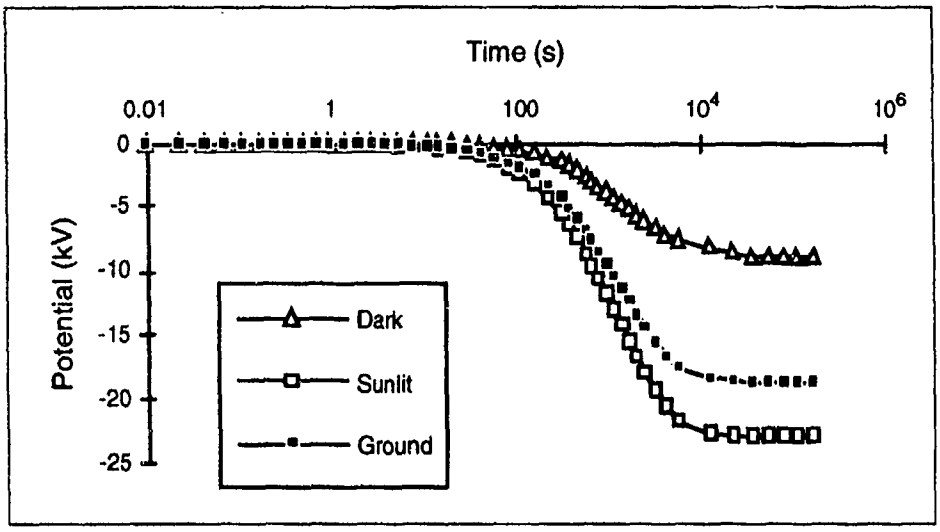

Figure 19. Time history of surface potentials and spacecraft ground on the sunlit kapton quasi-sphere. Charging of spacecraft ground occurs on the differential charging time scale due to the formation of a barrier. The final ground potential of –18 kV is reached after 1000 s (17 minutes).

As illustrated in Figure 20, during aurora, low-altitude, polar-orbiting spacecraft can develop differential potentials between the ram and wake sides of a spacecraft. The ram side of the spacecraft has a much higher ion current than the wake side, which must pull in the ions around the spacecraft. Figure 21 shows potential contours for a kapton quasi-sphere of radius 3.5 m moving at mach 6.7. The ions reaching the wake side of the spacecraft are attracted from the sheath edge. In this calculation a low potential region develops on the wake side of the sphere due to the focusing of ions due to the high symmetry. The ground potential is –650 V, the surfaces in the ram are at –1 V, the surfaces in the center of the wake side are at –100 V, and the peak potential on the wake side is –840 V. The same quasi-sphere with a mach velocity of 0 has an equilibrium potential of –1.9 kV.

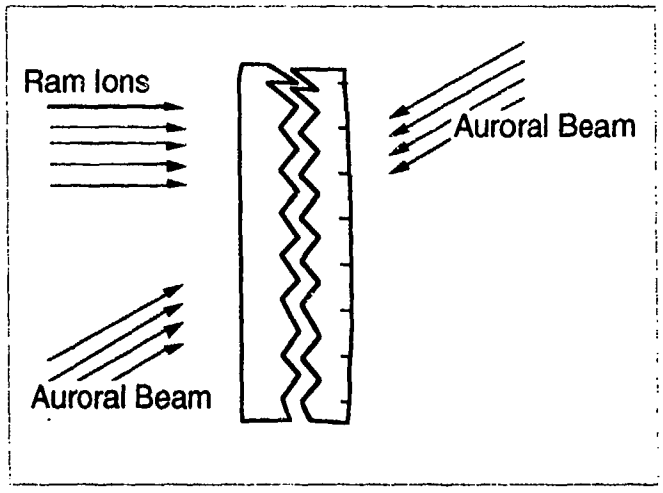

Figure 20. During aurora on low-altitude, polar-orbiting spacecraft, differential potentials can develop between the ram and wake sides of a spacecraft.

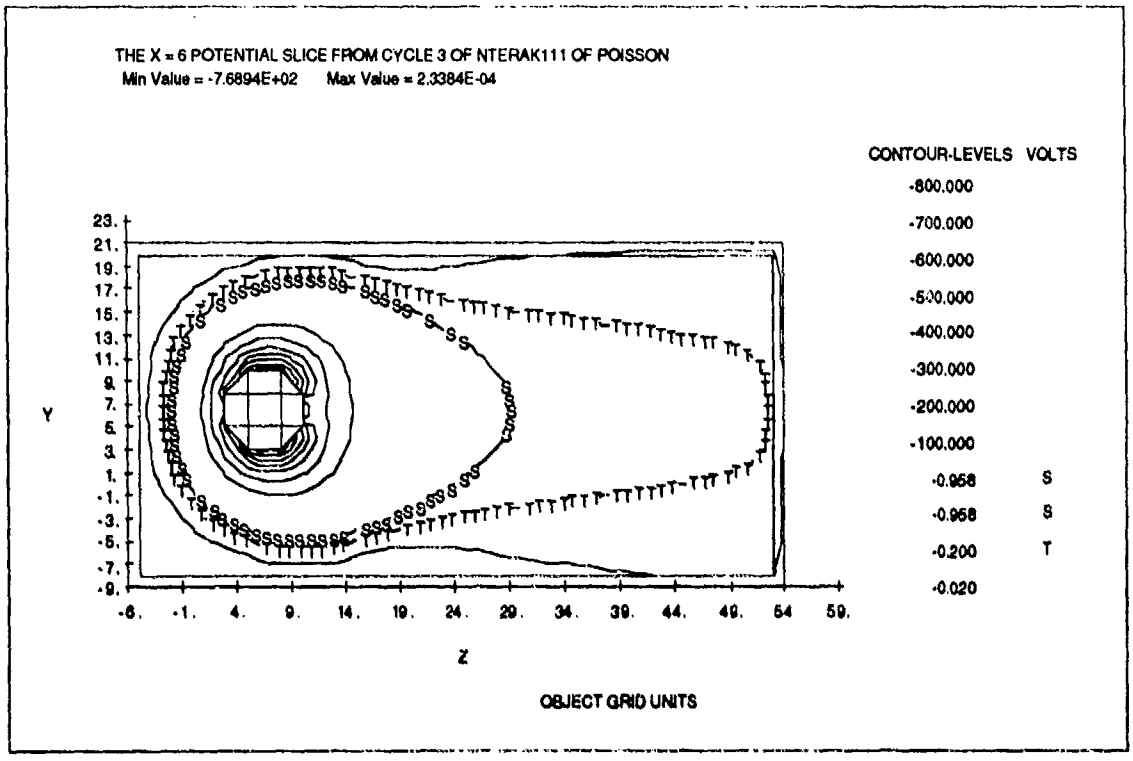

Figure 21. Kapton quasi-sphere in an auroral environment with a ram flux from the positive Z direction. The ground potential is –644 V, the surfaces in the ram are at –1 V, and the highest potential surfaces are at –850 V. The low potential region on the wake side of the sphere is due to the focusing of the ions due to the high symmetry.

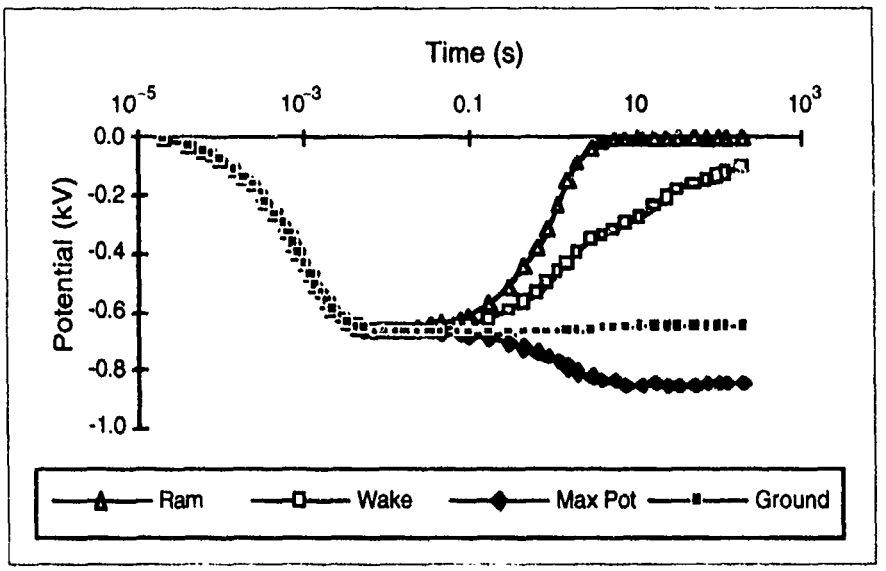

Figure 22. Time history of the surface potentials of the kapton sphere shown in Figure 21.

Table 3 summarizes typical parameters of the geosynchronous and auroral plasmas relevant to surface charging.

Table 3.
Parameters Typical of Spacecraft Charging

Quantity	Magnetosphere	Auroral
Charging plasma density	10^6 m^{-3}	10^5 m^{-3}
Charging electron energy	1-30 keV	1-30 keV
Charging electron current	10^{-5} A m^{-2}	10^{-4} A m^{-2}
Photo current	5×10^{-5} A m^{-2}	5×10^{-5} A m^{-2}
Electron stopping distance	$1\text{-}10 \times 10^{-7}$ m	$1\text{-}10 \times 10^{-7}$ m
$\tau_{\text{uniform charging}}$	10^{-2} s	10^{-1} s
$\tau_{\text{differential charging}}$	10-1000 s	0.1-10 s

2.5 Multibody Charging

If two (or more) vehicles are involved, additional interactions may become important. A small vehicle near a large vehicle may charge even more than would be expected because the large vehicle accelerates the ions to higher energies. This interaction is known as the multibody interaction in plasmas (MIP). This problem, illustrated in Figure 23, is sometimes known as the man-in-the-wake problem because it has been examined carefully for the case of an extravehicular maneuvering unit (EMU) near the shuttle in low-altitude, polar orbit. [Hall et al., 1987; Jongeward et al., 1986] Auroral electrons charge both the shuttle and the EMU. The shuttle collects ions from the ram current. The ambient density is high enough that collection is space-charge-limited. The EMU sees an

ion current of ions accelerated by the shuttle. When exposed to the environment measured by DMSP/F7 during an intense aurora on November 26, 1983, the shuttle will charge to more than –3 kV. The EMU charges even more to pull in ions. Because of material property differences, parts of the EMU charge to higher and lower potentials.

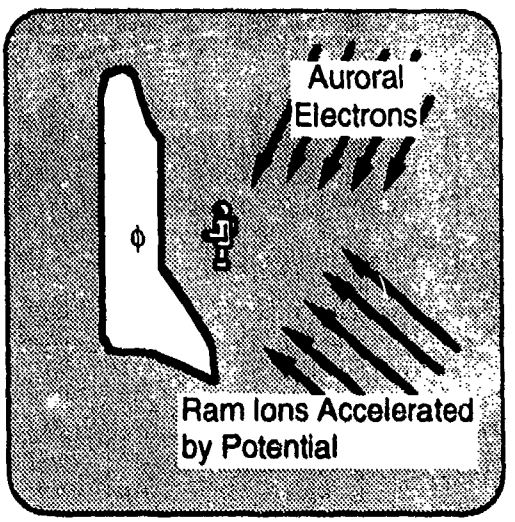

Figure 23. The charging of a small body near a large body is controlled by the balance of auroral electrons and ions accelerated by the potential of the large body.

2.6 Arcing

The primary mechanism by which charging disturbs spacecraft is through discharges. The rapid discharging of surfaces, or arcing, can disrupt operations, disturb measurements, damage instruments, or damage spacecraft surfaces. The mechanism for triggering discharges is an active field of investigation. Measurements made in the laboratory produce results that cannot be extrapolated to on-orbit spacecraft. Part of the problem is the impossibility of adequately simulating the space environment, the spacecraft, and their resultant interaction. Some examples of this inadequacy are the breakdown thresholds, area scaling, and satellite response. It is observed that in space, discharges occur on spacecraft when the calculated and measured potentials and electric fields are lower than those needed to generate discharges in typical electron beam laboratory experiments. Measurements made on uniform, small dielectric samples find that the discharge current scales directly with the square root of the sample area and the fraction of charge blown-off by the discharge is essentially constant for each dielectric type [Balmain, 1979]. Large sample measurements that include lapped and butted seams of materials present in real spacecraft thermal control surfaces differ from the uniform, small sample results [Wilkenfeld et al., 1981]. Analysis of ground based discharge experiments on high voltage solar arrays determined that the measured discharge current pulse was an artifact of the simulation process and did not represent the real discharge pulse [Stevens et al., 1990].

Even though the present understanding about discharges is not complete, there are some well established data, plausible analytical treatments, and useful criteria that can be employed in predicting the location and frequency of discharge. Flashover discharges occur when a layer of neutral gas atoms that has been generated by electron stimulated desorption, breaks down under the local electric field stresses caused by differential potentials of spacecraft dielectrics [Grey, 1985; Hastings et al., 1989]. This type of discharge frequently occurs at the edge of a dielectric next to another surface, at cracks in dielectrics exposing conductors underneath or at exposed conductor-cover cell interfaces in solar arrays. The typical field strengths required for flashover is 2×10^6 V m^{-1} [Grey, 1985], which is an order of magnitude below that for dielectric breakdown

Breakdown of dielectrics also provides discharge paths for spacecraft dielectrics. Dielectric breakdown results from the bulk failure of the dielectric material. Two of the theories of dielectric breakdown are (1) that the energy stress produced by the charged surface potentials exceed the binding energy of the molecules that make up the material, causing rupture of the bonds and loss of the material, and (2) that field enhanced electron emission provides electrons that generate cascades and heating until material vaporizes. Dielectric failure most often occurs at imperfections or dielectric weak points. Dielectric failure at an imperfection usually appears as a pinhole through the dielectric and is referred to as punchthrough. Localized material breakdowns are also observed in trapped charge layers of dielectrics about 1 μm below the dielectric surface. These bulk material failures appear as channels or tunnels just below the dielectric surface and are accompanied by surface damage where the channels penetrate the surface. The typical field strength of dielectrics is 2×10^7 V m^{-1}.

Blowoff is a large scale discharge phenomenon occurring at the surface of the dielectric and sometimes extending over the entire vacuum-dielectric interface. Several models have been proposed for the primary mechanism that initiates blowoff discharges. One of the most promising is a recent surface discharge model by Stettner and DeWald [1985]. The essential idea of the Stettner-DeWald surface discharge model is that the intense electric field on the boundary of the charged and discharged region of dielectric surfaces accelerates ions into the surface. Ions with the necessary velocity and angle to the surface cause kinetic emission of electrons resulting in discharge of the surface. The incident ions also cause sputtering of surface atoms and ions. Newly created ions are also accelerated into the surface producing further discharge and movement of the charge/discharge boundary further into the dielectric's charged region. The initial ions for the Stettner-DeWald model may come from the ions in the ambient plasma or ions desorbed by the incident electrons. A variation of the Stettner-DeWald discharge model termed the localized plasma sheath model has been proposed by Krauss [1988] to overcome some of the shortcomings of the ion surface discharge model. The ion surface discharge model and variants are promising in that they explain most of the observed features of large scale dielectric discharges and are supported by recent surface discharge measurements [Levy et al., 1991]. Unfortunately, a determination of their validity and usefulness for determining where and how often discharges blowoff discharge occur require further theoretical and experimental work.

2.7 Coupling

The discharge process gives rise to replacement currents flowing on nearby conductors such as the conductive layer on the underside of the dielectric. The replacement current restores potential equilibrium in the dielectric as the surface is discharged. All discharge processes can induce significant replacement current on nearby conductors as the charge propagates across or away from the surface. For discharges from punchthrough and flashover, the replacement currents are confined to the local area. Blowoff discharges however produce replacement currents that can be global. The local effect of punchthrough is illustrated by a small dipole model for the punchthrough arc whose current as a function of the distance r from the discharge point is [Woods and Wenaas, 1985]

$$I = I_p \frac{d}{r} \tag{6}$$

where d is the dielectric thickness and I_p is the peak discharge current. Usually d is much less than r for typical satellite system component dimensions. The current amplitude from discharges with local charge motion then falls rapidly with distance from the point of discharge. Thus for satellite systems, the primary replacement current source of interest for dielectric discharges is that due to blowoff discharges because of its large area of coverage.

Chapter 3
Spacecraft Surface Charging Effects Protection Program

Each spacecraft program should have a Spacecraft Surface Charging Effects Protection Program. This program will take a different form for each project. The central point of each Spacecraft Surface Charging Effects Protection Program is that the phenomenon of spacecraft surface charging must be considered along with all other physical phenomena relevant to the design and operation of the spacecraft.

A good Spacecraft Surface Charging Effects Program is a necessary component of spacecraft design, construction, and operation to achieve the objectives of the spacecraft mission. Appropriate measures are taken to reduce or eliminate surface charging related effects that could interfere with the mission. Charging considerations are included in every step of the design and construction process. The earlier in the design process that protection measures are included, the cheaper it is to incorporate them. Spacecraft surface charging protection measures sometimes conflict with other design considerations. The good Spacecraft Surface Charging Effects Program insures that these potential conflicts are identified and resolved early in the design process, when it is still relatively cheap to make changes.

A good Spacecraft Surface Charging Effects Program continues throughout the design, construction, and deployment of a spacecraft. As changes are made in the design, and as construction progresses, spacecraft-charging-related hazards can be inadvertently introduced. The use of a good program, throughout the process, insures that such hazards are identified and mitigating actions are taken. Discussion of spacecraft surface charging concerns during design reviews and a final expert examination are part of the continuing process.

The basics of a good Spacecraft Surface Charging Effects Program are (1) design and build following general guidelines that insure no detrimental charging related effects, (2) use analysis to examine all exceptions, (3) use testing to confirm the analysis and insure that mitigating measures are adequate, and (4) continue the program through design changes, construction, and deployment.

3.1 Develop a Plan

The first step in any project, from a paper airplane to a space station, is to develop a plan. A component of the plan for a spacecraft program is the Spacecraft Surface

Charging Effects Protection Program Plan. The protection plan takes its lead from the overall spacecraft program plan. The basic spacecraft mission, the various subobjectives, the level of importance attached to each, the resources available, and the project complexity determine the nature of the protection plan. The protection plan for a high profile, large budget, complex spacecraft program will be a deliverable document that calls for several reports, formal reviews, and extensive analysis and testing to confirm all decisions. The protection plan for a low budget, piggyback mission will be an internal document that calls for several informal reviews, few formal reviews, and analysis and testing to the same levels of confidence that other phenomena are examined (unless the mission is to study spacecraft charging or related effects.)

For all spacecraft programs, the Spacecraft Surface Charging Effects Protection Program Plan should be a written document. To be effective, the protection plan must be followed. If the original protection plan becomes unworkable during the program, the protection plan must be amended so that it can be used. The protection plan specifies the role of each of the protection program components and specifics about how each of the components will be completed.

3.2 Design and Build Following General Guidelines

The first line of defense against spacecraft surface charging related problems is to design and build the spacecraft using the known techniques of using conductive materials, grounding, shielding, and filtering. These techniques, and a few others, are summarized in Chapter 4 of this document. A detailed discussion of the basic design techniques to minimize surface charging effects is in Chapter 3 of *Design Guidelines for Assessing and Controlling Spacecraft Charging Effects* [Purvis et al., 1984].

3.3 Analysis

All protection programs include some analysis. The type and extent of analysis depend on the specific spacecraft and its mission. The protection program plan should include an analysis plan. An analysis should be done at each stage of the design process. The bulk of the analysis effort should focus on those aspects of the spacecraft design where a tradeoff between the ideal design from a surface charging point of view and the ideal design for another consideration needs to be made. A quantification of the specific risk simplifies the process of finding alternative solutions or deciding that the risk is acceptable.

Chapter 5 discusses the various aspects of an analysis program and how to do the necessary calculations.

3.4 Material Testing

Various properties of the surface materials used on spacecraft affect the surface charging. These properties are the secondary emission yield, the backscatter yield, the photoelectron yield, the conductivity (for insulating surfaces), the dielectric constant, and the thickness. A discussion of these properties is in Appendix B.

The conductivity and thickness of insulating coatings may need to be measured to confirm that the coating conforms to the general guidelines for surface materials.

Values for all of the properties for each material are needed to calculate the charging characteristics of a spacecraft. Literature values are often available and data bases of properties exist. (Many are proprietary.) Whenever adequately accurate values are not available from previous measurements, new measurements are needed. Section 6.1 of this document discusses how some of these measurements would be performed. The testing plan is part of the protection program plan.

3.5 Grounding—Construction Details and Testing

The continuity of the spacecraft ground depends in large part on construction techniques and care in handling. The methods to be used to electrically connect spacecraft components should be specified as part of the protection program. Thermal blankets are often coated with a conducting paint. This paint layer can be brittle. Ground continuity often depends on a small contact area. The protection program should specify the handling techniques to be used to insure ground continuity.

Testing is often necessary to insure that ground continuity is established and maintained. The testing plan is part of the protection program plan. A discussion of the nature of a grounding test plan is in Section 6.3 of this document.

3.6 Discharge Testing

Usually, there are one or more locations on the spacecraft where analysis determines that discharges might occur. Discharge testing should be done for these sites. The testing plan is part of the protection program plan. Section 6.4 of this document discusses the types of discharge tests available and discusses one specific test in detail.

3.7 Design Reviews

At each spacecraft design review, the status of the protection program and any charging concerns should be included. Documentation of spacecraft surface charging related analysis and testing should be included in required reports and presentations.

3.8 As Built Documentation

To evaluate an on-orbit anomaly to determine if it was caused by surface charging, records of how the spacecraft was actually built are necessary. Generally, the actual spacecraft construction differs from the original design in at least minor ways. Records of all aspects of the space vehicle construction relevant to spacecraft surface charging should be maintained by the manufacturer. These records include summaries of all the protection program analyses, descriptions of all the tests, and all the test results. A summary of the expert examination described below and photographs of the space vehicle including close ups of all instruments and booms is part of these records. These records should be kept for at least five years after launch or a year after the end of the mission, whichever is longer. Copies of these records should be available to anyone examining an on-orbit anomaly.

3.9 Expert Examination

The space vehicle should be examined for spacecraft surface charging characteristics as part of the preparation for launch. Multiple examinations may be necessary if there are several instruments that are to be deployed on orbit. A written summary of this examination should be prepared.

3.10 Operational Guidelines

Occasionally operational guidelines are appropriate to the minimization of surface charging related effects. A sensitive instrument might be turned off when a substorm is detected. If such guidelines are contemplated, their effect on the spacecraft design should be considered early in the design process.

3.11 Monitor Charging

All spacecraft should include a device to monitor the spectrum and density of the space plasma and the occurrence of spacecraft surface charging. The information gained from such monitoring not only assists in the analysis of any anomalies that occur, but also is needed for the determination of the risk to future spacecraft. The Compact Environmental Anomalies Sensor Experiment smart detector system under development is such a device.

3.12 Anomaly Analysis

To improve the design and construction of future spacecraft, anomalies that occur should be analyzed to determine if surface charging is implicated. The results from such

analyses should be made available to all those involved in the protection of spacecraft from surface charging related effects.

Chapter 4
Summary of Desirable Design Features

The first defense against spacecraft surface charging related problems is the spacecraft design. The basic design techniques to minimize surface charging effects are described in Chapter 3 of *Design Guidelines for Assessing and Controlling Spacecraft Charging Effects* [Purvis et al., 1984]. They are summarized below in Section 4.1. Some other commonly used and not so commonly used design techniques are discussed in Section 4.2.

4.1 Standard Design Techniques to Minimize Surface Charging Effects on Spacecraft

The primary method to reduce surface charging related problems is to make all exterior surfaces conducting and ground them. In those instances where insulating surfaces or ungrounded surfaces are needed, the area should be minimized. Grounded conducting surfaces do not charge differentially with respect to each other and therefore discharges (due to this mechanism) do not occur. On a well-grounded spacecraft, the remaining areas of insulating or ungrounded surfaces may develop large differential potentials. Small areas can only store a small amount of charge. A rapid discharge or arc releases only a small amount of energy, causing less damage than a larger discharge.

All spacecraft conducting elements with surfaces exposed directly to the plasma environment should be tied by an electrical grounding system so that the DC resistance between any two points is less than or equal to 0.1 Ω.

All thin conducting surfaces exposed to the space plasma environment should be electrically grounded to the common spacecraft structural ground so that the DC resistance between the surface and the structure is less than or equal to 10 Ω. A thin conducting surface is a conductive coating on a dielectric with a thickness of less than 10 μm. Thin conducting surfaces include, but are not limited to, all metallized surfaces of multilayer insulation thermal blankets, metallized dielectric materials in form of sheets, strips, tapes, or tiles, conductive coatings, conductive paints, conductive adhesives, and metallic grids or meshes.

The number of ground points on each thin conducting surface should follow the following prescription:

Surface Area	Number of Ground Points
Under 1.0 m^2	2 or more
1.0 to 4.0 m^2	3 or more
Greater than 4.0 m^2	1 per m^2

Additionally, any point on a thin conducting surface should be within 1 m of a grounding point.

All exterior surfaces of the spacecraft should be partially conductive. For a grounded partially conductive coating over an insulating material, the surface resistivity should not exceed 10^9 ohms per square. For partially conductive coating over a grounded conductor, the thickness times the volume resistivity should not exceed 2×10^9 Ω cm^2.

Where it is impractical or undesirable to implement the above conductivity, thickness, or grounding requirements, analysis, supporting by testing, should be used to insure that spacecraft performance will not degrade below the specified capabilities.

The way to reduce the extraneous signals and potential damage to electronic components from discharges is to provide shielding and filtering for all sensitive components. The use of shielding and filtering increases the spacecraft weight. If the desirability of shielding and filtering is considered in the original design process, it is less likely that maintaining the continuous shield and including filters will conflict with other requirements.

The basic spacecraft structure should be designed as a Faraday cage with a minimum of openings. A Faraday cage is an electromagnetically shielded enclosure, here the conductive metallic structure of the spacecraft. All electronic cables, circuits, and components should be provided with EMI shielding to attenuate radiated fields of frequencies from 1 MHz to 100 MHz from discharges by at least 40 db. The shielding can be provided by the basic spacecraft structure, by enclosures of electronics boxes, and by separate cable shielding. Analysis should be used to carefully examine any breaks in the shielding to insure that the spacecraft performance will not be degraded below the specified capabilities.

All circuits routed through the EMI shielding should be protected by electrical filtering. The filter should be rated to withstand a peak transient voltage of 100 V and a peak transient current of 200 A. The filtering criteria should be chosen to eliminate discharge-induced upsets and not interfere with normal operations.

4.2 Other Design Techniques to Minimize Surface Charging Effects on Spacecraft

Often it is desirable to have an insulating coating over some spacecraft surfaces. These coatings differentially charge when exposed to a severe substorm or severe auroral environment. If the coating is thin enough, the rate of differential charging is so slow that the substorm is over before the potentials are high enough to trigger a discharge. For a

geosynchronous spacecraft, 10 microns is usually thin enough. For low-altitude, polar-orbiting spacecraft, less than 100 microns may be adequate.

The choice of surface material can reduce the severity of surface charging. Teflon has a high secondary emission coefficient (maximum yield of 3) and therefore charges less than kapton with a peak secondary emission coefficient of about 2.1. A spacecraft coated with conducting paint with a high secondary emission coefficient charges less than one coated with a paint with less secondary emission.

Sometimes it may be possible to make design decisions that minimize problems. The choice of instruments or the choice of instrument locations can influence the likelihood of differential charging and the impact of rapid discharges. An instrument sensitive to contamination, such as an optical lens, should be placed away from any probable discharge sites. Differential charging risks can be lessened by avoiding placing instruments that have surfaces with dramatically different secondary emission properties near each other.

On spacecraft where charge control is of particular concern, a plasma emitter such as the Charge Control System can nearly eliminate charging.

Chapter 5
Analysis

A central aspect of any good spacecraft protection program is analysis of any design features that are likely to cause problems. Early in the design process, an assessment of these problems needs to be made. As the design process proceeds, more detailed modeling of the features that are likely to have an impact on the success of the mission is needed. Numerous computer codes have been developed to help in this process. A good analysis program integrates analytic models, computer models, and knowledge of the spacecraft mission to determine if spacecraft surface charging effects will interfere with the spacecraft mission.

Figure 24 graphically illustrates the analysis process. The questions in Figure 24 must be asked of each surface of the spacecraft. Different parts of the process are more important at different stages in the design process. Different people are usually involved in the various determinations. The process can be used to examine the entire spacecraft, a specific instrument, or a small region of concern.

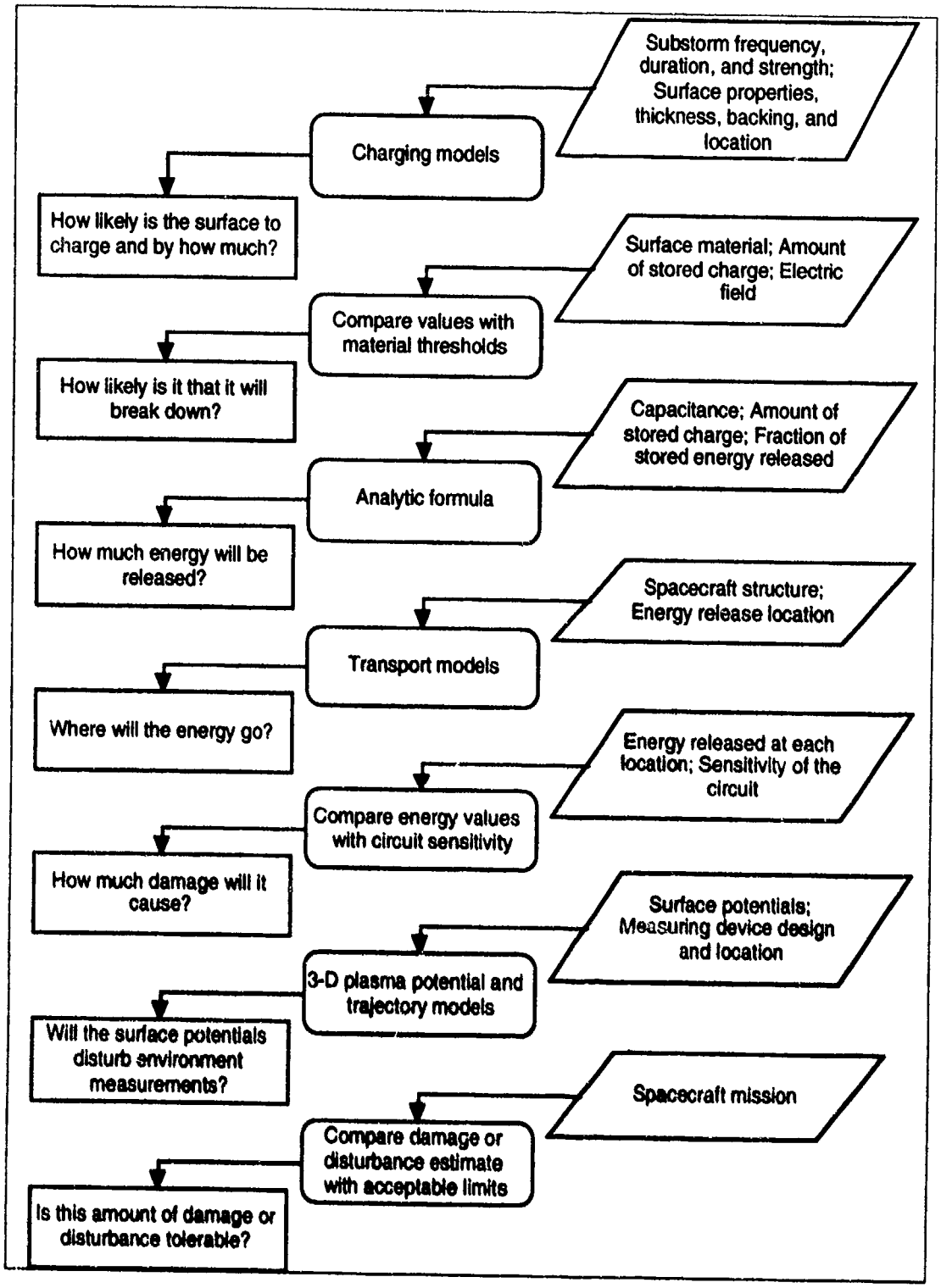

Figure 24. Approach to analysis of a spacecraft for spacecraft surface charging problems. The rectangles give questions that an analysis addresses. The parallelograms give the input needed. The ovals give the technique for analysis.

This chapter uses examples to illustrate how each of these questions might be answered. The focus of the discussion is on those aspects of the analysis that are more complex and less widely known. The examples are simplified, but the process is that used in actual spacecraft charging analyses.

Often the most time-consuming part of an analysis is locating information on the design to be evaluated. The other major difficulty in analysis is the determination of the appropriate way to model the various features of the spacecraft. Included in the examples are some discussions of techniques used. In practice, each person doing analysis develops techniques for the type of analysis she or he does. The discussion in this chapter is not a substitute for experience, but can be a help to those wishing to expand their capabilities.

5.1. Determining the Amount of Charging Expected

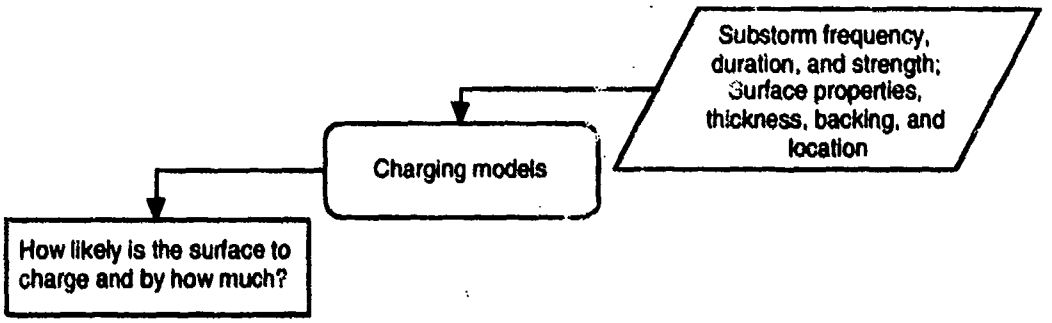

Figure 25. The first step in any analysis of the impact of spacecraft surface charging is to determine how much charging is likely to occur.

The frequency and extent to which a surface charges depends on the space environment, the surface itself, and the rest of the spacecraft. Four spacecraft are used here to illustrate how this determination is made. The input and sometimes the input and output to the computer programs used in this analysis are in Appendix C.

A full analysis of the frequency of charging requires a series of calculations for different environmental conditions. Figure 14 of Purvis et al. [1984] provides the frequency at which different environments occur. If the specifications require a specific potential or electric field to be less than a specific value 95% of the time and the environment at the 95% occurrence level does not change the potential or electric field more than the specified value, the specification is satisfied.

The usual practice for geosynchronous spacecraft is to examine charging for the 90th percentile environment. (The severe substorm environment specified in Chapter 2.) This environment allows the determination of regions of concern where mitigation may be needed. If higher confidence levels are needed, calculations can be done for more severe environments.

5.1.1 Spinning Geosynchronous Spacecraft in Eclipse-SCATHA

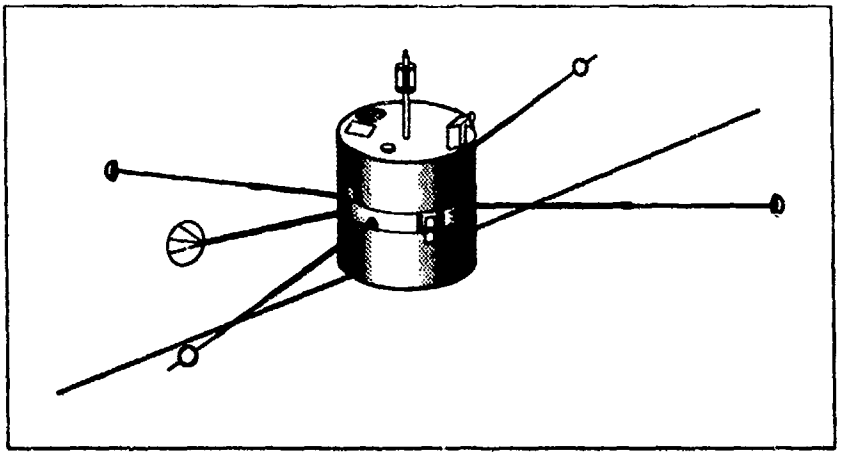

Figure 26. The SCATHA spacecraft.

For a sample calculation, we use the SCATHA (Spacecraft Charging At High Altitudes) spacecraft. The SCATHA program and spacecraft are described in the glossary.

Stannard et al. [1982] and Katz et al. [1983] describe the charging analysis of the SCATHA spacecraft. A sketch of the SCATHA spacecraft is shown in Figure 26.

The first step in an analysis of the charging properties of this spacecraft is to examine the charging of the individual surface materials. The SCATHA surfaces are modeled by 15 distinct exposed surface materials, each of which is specified by the values of 14 parameters. The surface materials are described in Table 4. When available, experimentally measured values for parameters were used; where this was not possible, suitable estimates based on the properties of similar materials were used.

Table 4.
Charging of SCATHA Spacecraft Materials

Material Name	Equilibrium Potential (V)*	Material	Modeled by
GOLD	0.338	Gold plate	Gold
SOLAR	-18200	Solar cells, coated fused silica	Solar cell coverslip
WHITEN	-1230	Nonconducting white paint (STM K792)	Kapton with enhanced conductivity and a thickness appropriate to a paint.
SCREEN	-27600	SC5 screen material	Conducting surface that absorbs but does not emit charged particles.
YELOWC	-21200	Conducting yellow paint	Kapton properties except conductor.
PDGOLD	0.453	88% gold plate with 12% conductive black paint (STM K748 in a polka dot pattern)	Gold except used averaged properties of components for atomic number and secondary yield peak.
BLACKC	-21200	Conductive black paint (STM K748)	Kapton properties except conductor.
KAPTON	-20800	Kapton	Kapton
SIO2	-75.3	SiO_2 fabric	Silicon dioxide with appropriate thickness, enhanced conductivity, and adjusted dielectric constant.
TEFLON	-16900	Teflon	Teflon
INDOX	-18200	Indium oxide	Indium oxide
YGOLDC	-19900	Conducting yellow paint (50%) gold (50%)	Gold except used averaged properties of components for atomic number and secondary yield peak and electron range parameters from Feldman's formula with average density and atomic weight.
ALUMIN	-22200	Aluminum plate	Aluminum
BOMAT	0.124	Platinum banded kapton	Gold except an insulator with enhanced conductivity, average atomic number (platinum and kapton), average photoconductivity. The dielectric constant and thickness for the boom surfaces were chosen to reflect the *effective* capacitance to the underlying cable shield.
ML12	-20600	ML12-3 and ML12-4 surface	Average of the properties of the several materials on the ML12 surfaces.

*The back side of insulating materials is assumed to be grounded.

Table 4 shows the potential each of the surface materials reaches in the severe substorm environment. (See Appendix C for the **Matchg** execution used to determine the charging.) The different materials charge from 0 to -28 kV. Most of the materials are conducting; as long as they are properly grounded little differential charging will occur.

To examine the 3-dimensional charging effects, *NASCAP/GEO* is needed. Perspective views of the model used in the calculations are shown in Figures 27. The *NASCAP/GEO* computer codes are described in the glossary. The main body of the satellite is represented as a right octagonal cylinder, with the aft cavity visible in the figure. Typically, the first calculations are done with a model that reproduces the basic shape and surface materials of the spacecraft. Models that focus on specific instruments or portions of the spacecraft are used to evaluate specific concerns as they arise. The 11.5 cm grid resolution allows the model to reproduce actual SCATHA geometrical features extremely well, as shown in Table 5. Note in particular that the treatment of booms in *NASCAP/GEO* allows the actual boom radii to be reproduced exactly. Monopole boundary conditions are imposed on the edges of the outermost grid, which is a rectangular prism of dimensions $12.8 \times 12.8 \times 25.6$ m. The zone size increases by a factor of 2 in each of the four successive grids. This doubling of zone size, plus the requirements that booms parallel coordinate axes and intercept mesh points in all grids effectively force any long booms to pass through the center of the innermost mesh. Therefore, the model includes only the SC6, SC11, and two SC2 booms with the orientations fixed at right angles to one another. Experiments at the ends of the SCATHA booms were modeled as single boom segments whose radii are chosen to reproduce the exposed surface area of the actual experiment.

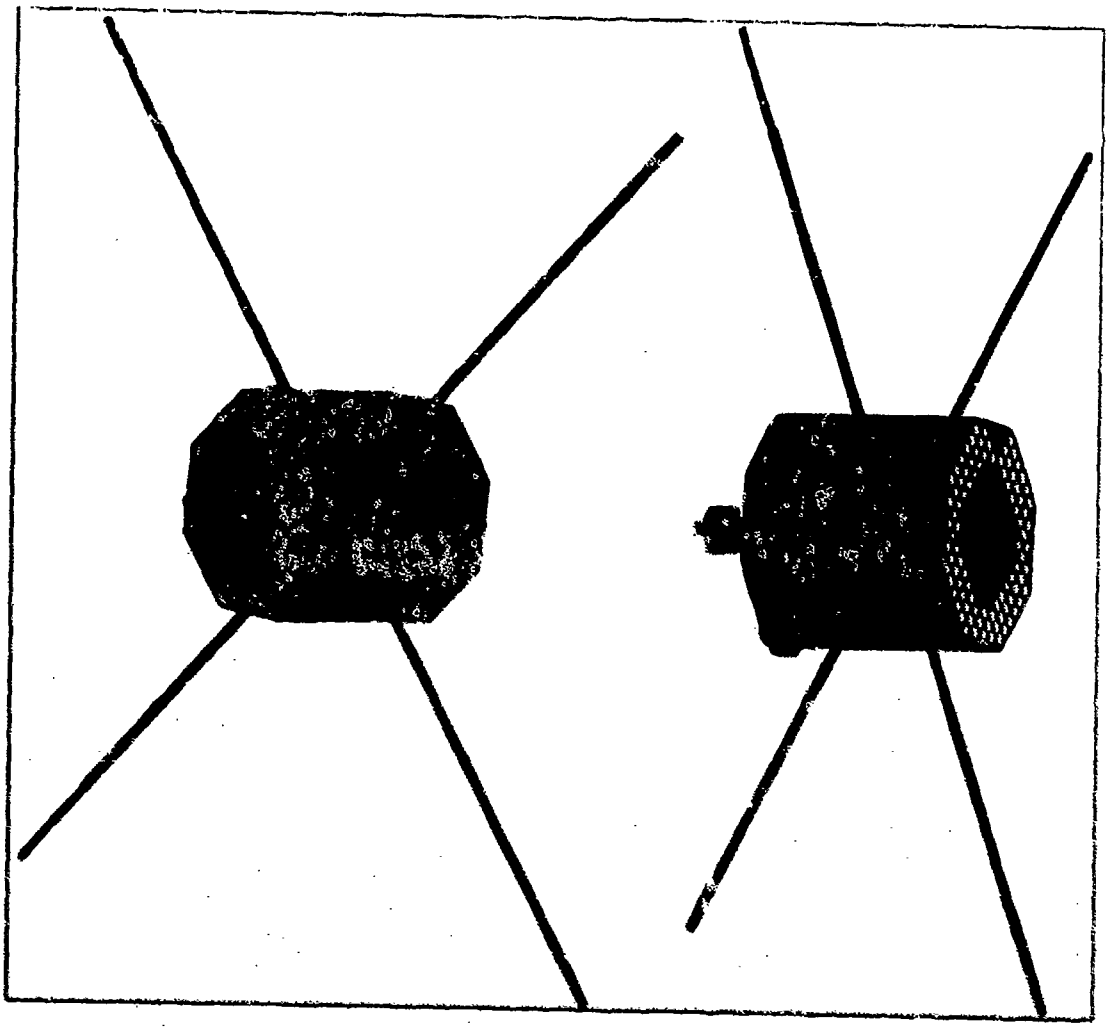

Figure 27. *NASCAP/GEO* model of SCATHA, views from two angles.

Table 5.
Comparison of Actual SCATHA Geometrical Features to 4-Grid *NASCAP/GEO* Model
Zone Size = 4.54 inch (11.5 cm)

	SCATHA	Model
Radius	33.6 inches	32.0 inches
Height	68.7	68.0
Solar array height	29	27.2
Bellyband height	12.0	13.6
SC9-1 experiment	9.2 × 6 × 8	9.1 × 4.5 × 9.1
SC6-1 boom	1.7 (radius) 118 (length)	1.7 113.2
Surface area	2.16×10^6 sq. in.	2.11×10^6 sq. in.
Solar array area	1.23×10^5	1.15×10^5
Forward surface area	0.36×10^6	0.34×10^6

The model also includes six distinct underlying conductors: spacecraft ground, the reference band, and the four experimental mountings SC2-1, SC2-2, SC6-1, and SC6-2. Each of these conductors can be separately biased or floated with respect to spacecraft ground, and each conductor is directly capacitively coupled to spacecraft ground. The values employed for these capacitive couplings are given in Table 6; these values were chosen to represent the capacitance of dielectric spacers separating the conductors from ground.

Table 6.
Capacitive Couplings Employed with the SCATHA Model

Conductor	Representing	Capacitance to Ground (pf)
2	SC2-1 experiment	30
3	SC2-2	30
4	SC6-1	240
5	SC6-2	30
6	Reference band	250

As SOLAR is the primary surface material for this model, the charging properties of SOLAR dominate the charging of the entire spacecraft. The SC2 sensors are at the end of long booms and coupled to the spacecraft ground through capacitances. Their charging properties are dominated by the conducting paint, BLACKC, that they are coated with. The thermal plasma analyzer sensor is also at the end of a long boom and capacitively coupled to spacecraft ground. The sensor charging is dominated by the charging properties of gold.

The potentials of interest are the equilibrium potentials. Therefore the initial potentials are chosen to be the expected equilibrium potentials. The SC2 sensors start at –21 kV and the rest of the spacecraft starts at –18 kV. The results can be analyzed using **Ternitalk** and **Contours** of the *NASCAP/GEO* computer codes. Table 7 shows the surface potentials reached after 20 minutes.

Table 7.
Surface Potentials on SCATHA after 20 Minutes of Charging

Material	Conductor	Potential Reached (V)
GOLD	1	-15200
GOLD	4	-14300
GOLD	5	-4664
GOLD	6	-13900
SOLAR	1	-15600
WHITEN	1	-15400
SCREEN	1	-15200
YELOWC	1	-15200
PDGOLD	1	-15200
BLACKC	1	-15200
BLACKC	2	-22860
BLACKC	3	-22860
KAPTON	1	-16400
SIO2	1	-15180
TEFLON	1	-15700 to 15800
INDOX	1	-15200
YGOLDC	1	-15200
ALUMIN	1	-15200
BOMAT	1	-4370 to -15100
ML12	1	-15200

Figure 28 shows the variation in the potentials of the conductors. The spacecraft reaches its equilibrium in 14 minutes. The SC2 sensors reach nearly 23 kV. The plasma analyzer goes to below 5 kV and the other conductors are all about 14 to 15 kV negative.

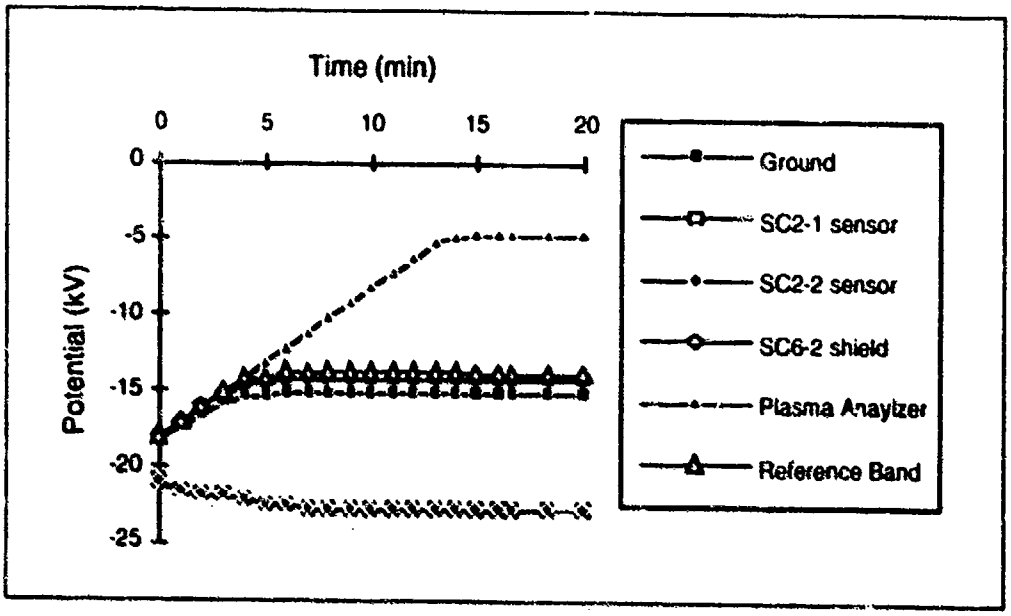

Figure 28. Charging of the SCATHA satellite.

There are two types of differential charging. There are differential potentials between the surface of an insulating surface and the underlying conductor. There are also potential gradients along and between surfaces. The highest electric fields internal to an insulator (due to the first type of differential charging) are within the kapton surfaces below the bellyband. Their surfaces charge to -16.4 kV and the underlying conductor only reaches -15.2 kV. The internal field is $\sim 10^3$ V m^{-1}. The second type of differential charging occurs along the booms. For most of the length of the booms, the high secondary emission coefficient of BOMAT keeps the boom surfaces at the space potential. The SC2 sensors charge to -22.9 and generate high fields at the ends of the booms. The thermal plasma analyzer might seem to be of more concern because it only charges to -4.7 kV for a difference of 10.5 kV. However the analyzer is far enough from the main body that the potential in the space surrounding the analyzer is about -4 kV. Figure 29 shows the contour levels at the Z = 17 plane (through the center of the grid). From this figure it is clear that the high field region is near the ends of the booms. These two regions need to be carefully examined to determine if they present any risk to the spacecraft mission.

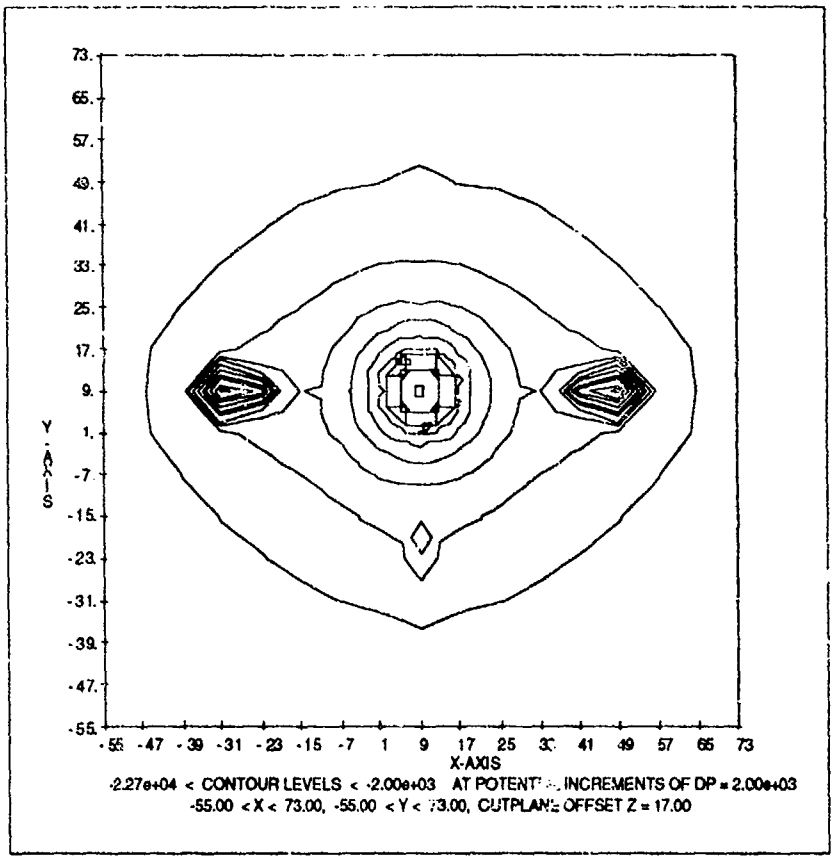

Figure 29. Contours levels of the potential at the Z = 17 plane for the SCATHA model. The booms are not shown in the figure. The high field regions are at the end of the SC2 sensor boom. The thermal plasma analyzer boom extends to Y = -31. The SC11 sensor boom extends to Y = +49.

5.1.2 Three-axis Stabilized Geosynchronous Spacecraft in Sunlight

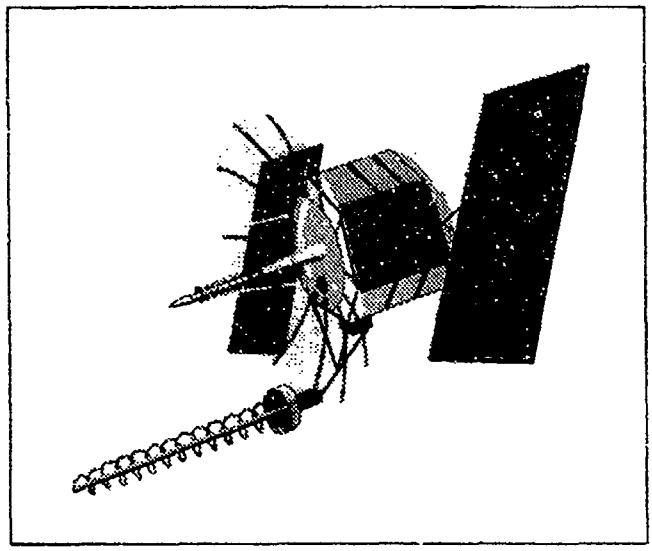

Figure 30. A typical 3-axis-stabilized spacecraft to be analyzed.

This spacecraft is cylindrical in shape and covered with kapton blankets. Second surface mirrors on the sides are exposed. It has a large transparent antenna. It has two large solar arrays, each about the same size as the spacecraft itself.

The spacecraft ground potential can reach high values in eclipse, but as discussed in Chapter 2, sunlight charging can also create problems.

The first step in the analysis is to examine the charging of each surface material on its own. The spacecraft is primarily covered with kapton blankets and paints with properties similar to kapton. The solar array faces can be modeled as silicon dioxide, and the paint on the solar array backs can be modeled as a lossy kapton. The large antenna is modeled as silver. Table 8 shows the materials and the potential they reach in the dark as calculated by **Matchg**. (Input and output files are in Appendix C.)

Table 8.
Charging of Spacecraft Materials

Material Name	Equilibrium Potential (kV)*	Location on Spacecraft	Modeled by
KAP3TN	-20.8	Bottom surface	Kapton with higher surface resistivity
LFALUM	0	Arms to solar arrays and antenna	Kapton with higher conductivity
S13GLO	0	UHF transmission antenna	Nonconducting paint
FSLICA	-5.84	Solar panel faces, second surface mirrors on sides	Silicon dioxide
BLKVEL	0	Solar panel backs	Kapton with higher conductivity
SSMESH	-5.77	Antenna	Silver
KAP1TN	-20.2	Base sides, solar array patches	Kapton with higher surface resistivity
KAP2TN	-17.9	Top surface	Kapton with higher surface resistivity
EHFPRT	-18.2	EHF patch	Indium tin oxide
ALUM	-22.2	UHF antenna, plume shield	Aluminum
CPHENL	-0.045	AKM nozzle	Teflon with higher conductivity and higher dielectric constant

*The back side of insulating materials is assumed to be grounded.

Photoemission generates enough current that if any large conducting grounded area is exposed to sunlight, spacecraft ground remains near plasma ground. Here, the transparent antenna is always oriented away from the earth and therefore partially exposed to the sun whenever the spacecraft is not in eclipse. In all orientations, the transparent antenna generates enough photoelectrons to keep the antenna and therefore the entire spacecraft near plasma ground.

The solar panels always face the sun and remain near plasma ground. The solar panel backs are painted with a material that does not differentially charge even in the dark.

The surfaces that develop the largest surface charging are the shaded kapton surfaces on the top, bottom, and sides of the base. The second surface mirrors on the sides not facing the sun also charge. The areas of concern are shaded–unshaded kapton interfaces, shaded kapton–conductor interfaces, and shaded kapton–second surface mirror interfaces. To examine the charging behavior of this spacecraft in sunlight and look specifically at these areas of concern a *NASCAP/GEO* simulation is needed.

The first step of a *NASCAP/GEO* simulation is to develop a representation of the spacecraft suitable for the desired calculation. (See Appendix C for the input files used.) The mesh size of 1.5 feet is chosen so that the entire spacecraft can fit within the 17 by 17 by 33 grid. The spacecraft body is represented by an octagon of radius 6 and height 4. The second surface mirrors are represented by 1 by 1 patches on the sides of the octagon. The actual mirrors are smaller in area than those of the model. The antenna is composed

of ASLANTs and ATETs. The sides are steeper than the actual spacecraft, but the total collecting area is similar. The arms and transmission antennas are composed of booms of appropriate sizes. The solar arrays are modeled by thin plates. The cavity on the bottom is included in the model because this is an area where severe charging could occur. Other features are represented by small surfaces in appropriate locations. Figure 31 shows the final object from the sunward and anti-sunward directions. Figure 32 shows the surface materials.

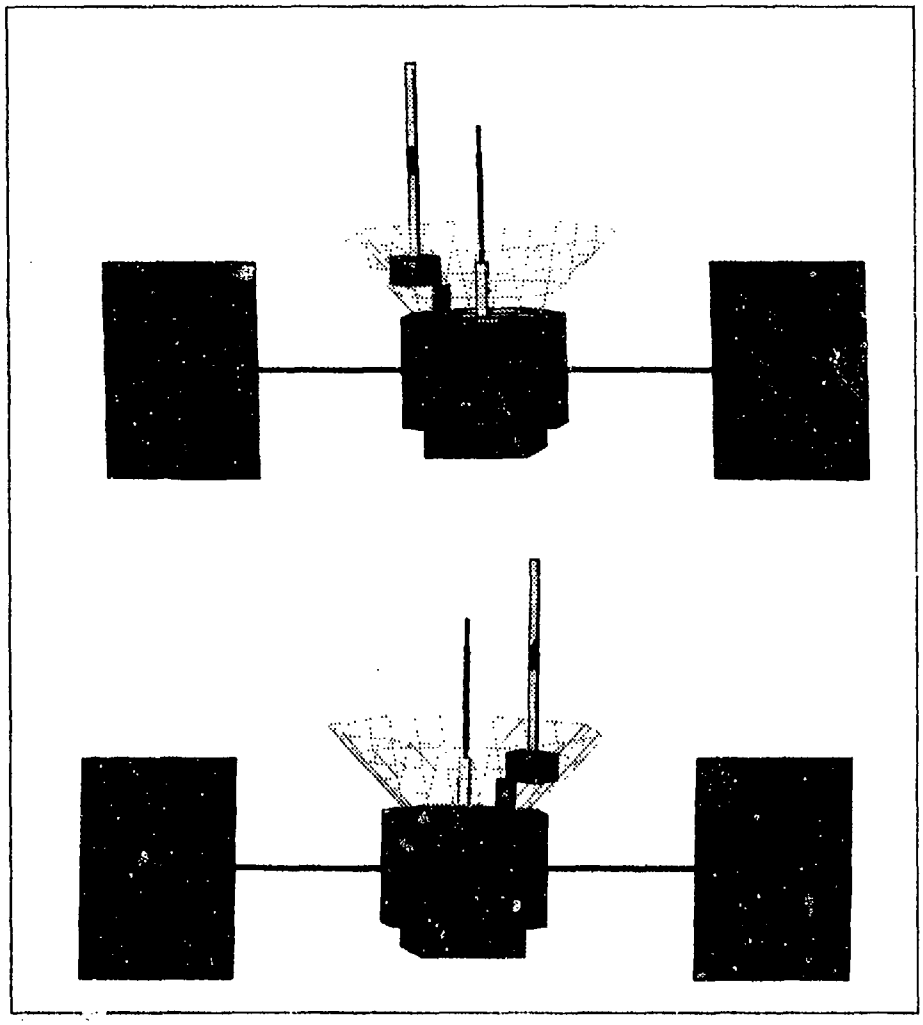

Figure 31. *NASCAP/GEO* model of spacecraft from the sunward and anti-sunward directions.

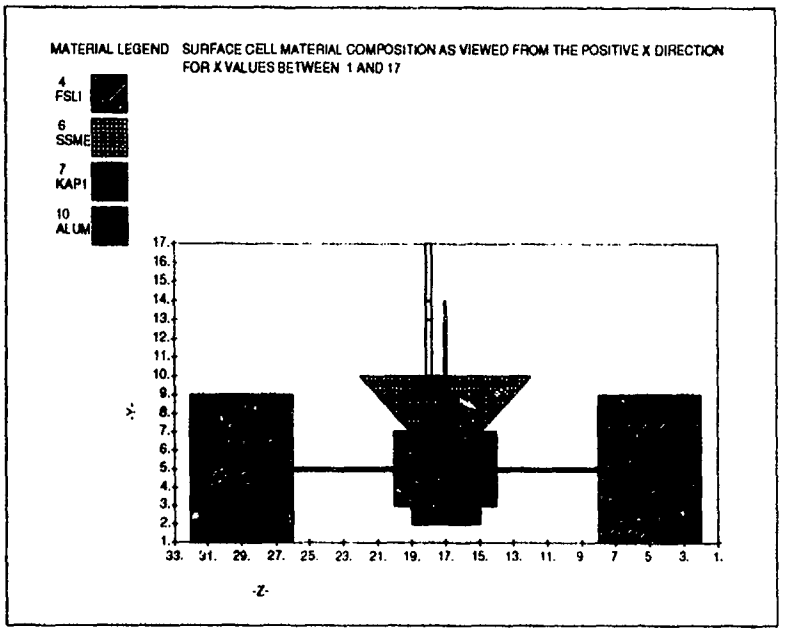

Figure 32. Materials on the surface of the spacecraft as viewed from the +X direction.

Spacecraft ground does not charge significantly because the antenna keeps it near zero. Therefore in the simulation, the charging sequence begins with no initial potential. Table 9 shows the potentials reached by the various materials after 20 minutes.

Table 9.
Surface Potentials After 20 Minutes of Sunlit Charging

Material	Potential Reached (V)
KAP3TN	-6000
LFALUM	-208
S13GLO	-189 to -208
FSLICA	-192 to -2930
BLKVEL	-208
SSMESH	-208
KAP1TN	-202 to -3270
KAP2TN	-53 to -967
EHFPRT	-208
ALUM	-208
CPHENL	-324

Figure 33 shows the charging rate of the shaded bottom of the spacecraft. After 20 minutes the kapton surfaces are continuing to charge. As the most severe portion of a substorm does not last this long, this simulation period is long enough.

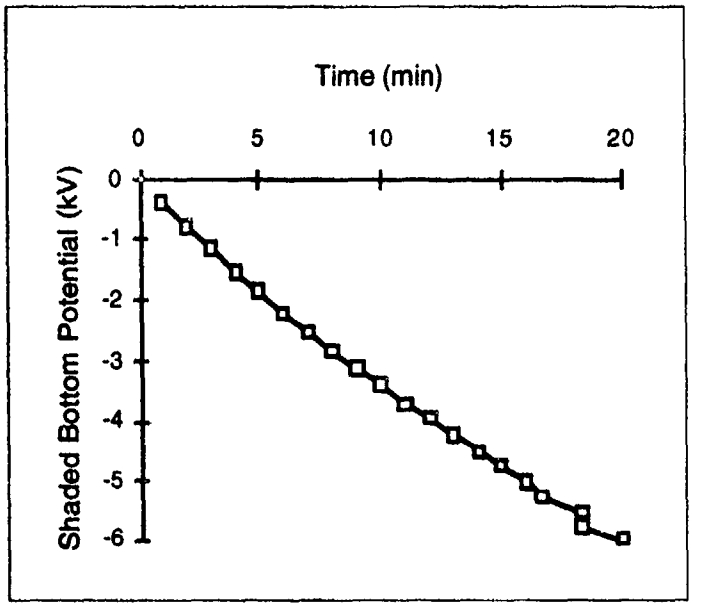

Figure 33. Surface charging rate of the bottom of the spacecraft.

The potentials computed by *NASCAP/GEO's* **Nascap** can now be examined for regions requiring further analysis. *NASCAP/GEO's* **Termtalk** and **Contours** codes give the user the following information. The solar arrays and the antenna have potentials of about –200 V. The potentials on the body vary from about –200 V on the top to about –1 kV at the bottom edge on the sunlit side. On the shaded side, the insulator potentials are over –2.5 kV. Figure 34 is a contour plot of potentials at the Z = 14 points on the grid. The 3 kV m^{-1} electric field is at the sun-shade interface. The regions with the highest electric fields are in the cavity area. Exposed metal at –200 V is adjacent to kapton at –3 kV. Figure 35 shows the contour levels at the Z = 17 plane through the center of the object. The high field within the cavity can be clearly seen.

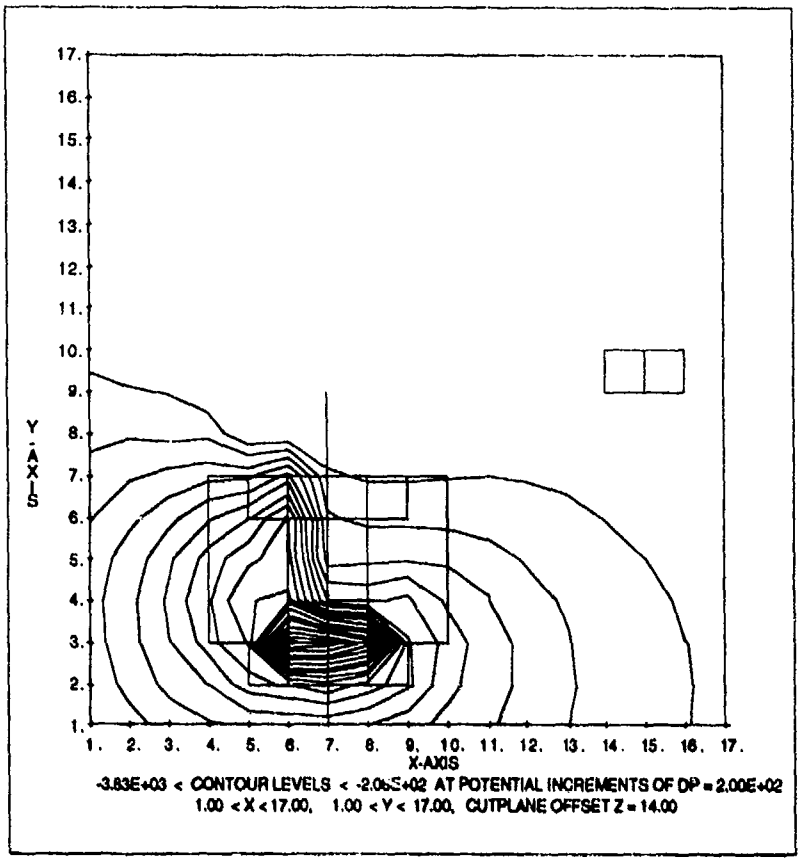

Figure 34. Potential contours at the Z = 14 plane.

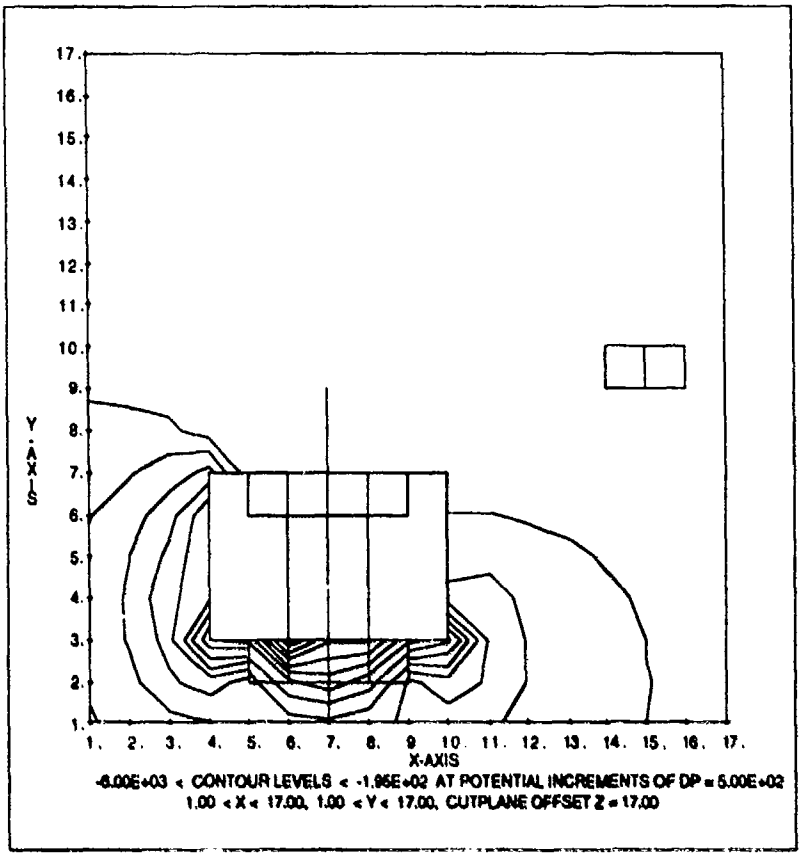

Figure 35. Potential contours at the Z = 17 plane.

If this amount of charging is a risk to the spacecraft mission, further calculations can be done to quantify the problem more precisely.

Cavity charging can also occur on spinning spacecraft when the orientation with respect to the sun is such that the cavity is always shaded.

5.1.3 Polar-orbiting Spacecraft DMSP

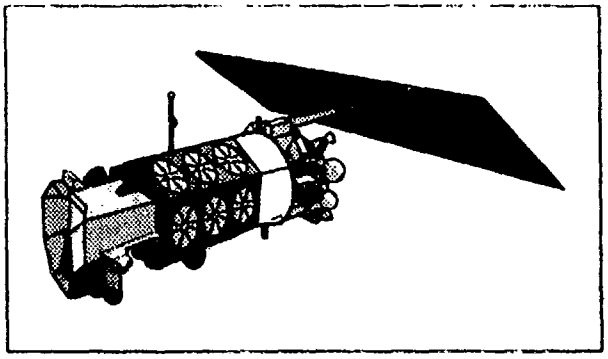

Figure 36. DMSP spacecraft.

For a sample low-altitude, polar-orbiting spacecraft calculation, we use the DMSP spacecraft.

An analysis of the charging of the DMSP spacecraft was done by Cooke et al. [1989]. A sketch of the DMSP spacecraft is shown in Figure 36.

The DMSP spacecraft is roughly a cylinder that is about 4.5 m long and 0.9 m in radius. The solar array is about 4 m by 2 m. The total surface area is about 45 square meters. A sphere with the same surface area has a radius of 1.9 m. The body of the spacecraft is covered with kapton and teflon thermal blankets.

The first step is to examine the charging of the materials in isolation. *POLAR* default material properties are used for all the surface materials. Charging is examined for a spacecraft moving at 7.3 km s^{-1} (mach velocity of 6.7). The severe auroral environment is used. The potentials computed by **suchgr** are shown in Table 10. (See Appendix C for output file.)

Table 10.
Charging of DMSP Surface Materials

Material	Equilibrium Potential (V)*	Sheath Radius (m)
SOLA	-491.25	9.069
NPAI	-541.25	9.39
GOLD	-187.5	6.429
CPAI	-641.25	10
TEFL	-528.75	9.312
AQUA	-603.75	9.775
KAPT	-641.25	10
ALUM	-566.25	9.545
SILV	-294.38	7.519

*The back side of insulating materials is NOT grounded.

Most of the surface materials charge between –500 V and –650 V with a resulting sheath radius of about 9 to 10 m. The gold and the silver charge much less than the other materials. As long as the metals are properly grounded to spacecraft ground, those surfaces will not differentially charge. The largest differentials are between the SOLA and the KAPT. Since the SOLA is on the solar arrays and the KAPT on the body, this does not present a risk.

The next step is to do 3-dimensional calculations to examine ram-wake effects and any other 3-dimensional effects on charging. The *POLAR* computer codes are needed to model such effects. The *POLAR* codes are described in the glossary. The *POLAR* model is shown in Figure 37. The solar arrays are thin plates of solar cell material on one side and nonconducting paint on the other. The spacecraft body is wrapped in teflon and kapton thermal blankets. The SSIE RPA is the round disk located on the boom just above the spacecraft. It is too small to be modeled with *POLAR*.

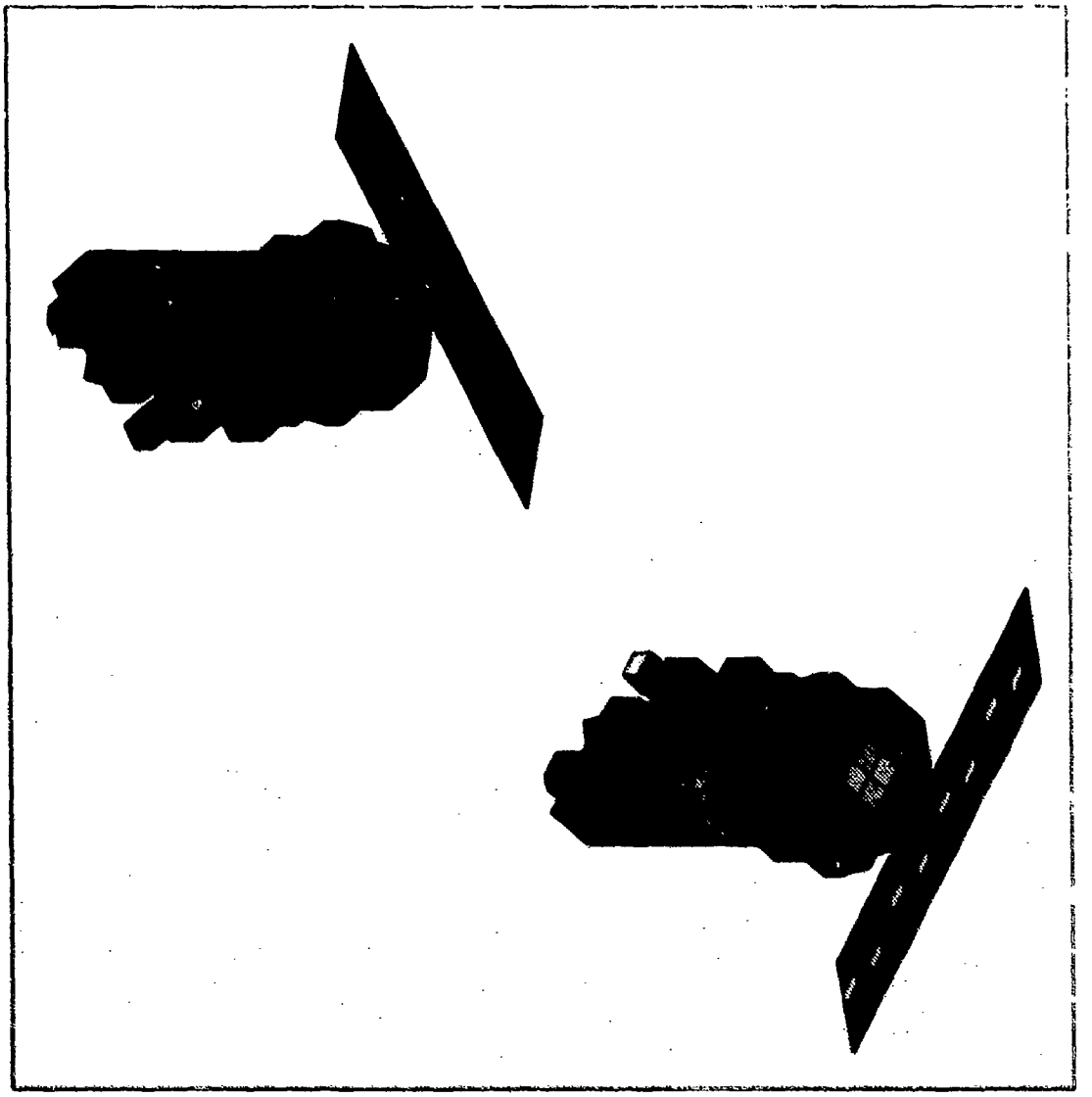

Figure 37. *POLAR* model of the DMSP spacecraft.

The computer code **nterak** of the *POLAR* codes was used to example the charging of DMSP. Figure 38 shows the charging rate of a selection of surfaces. After 10 seconds, the surfaces are continuing to charge.

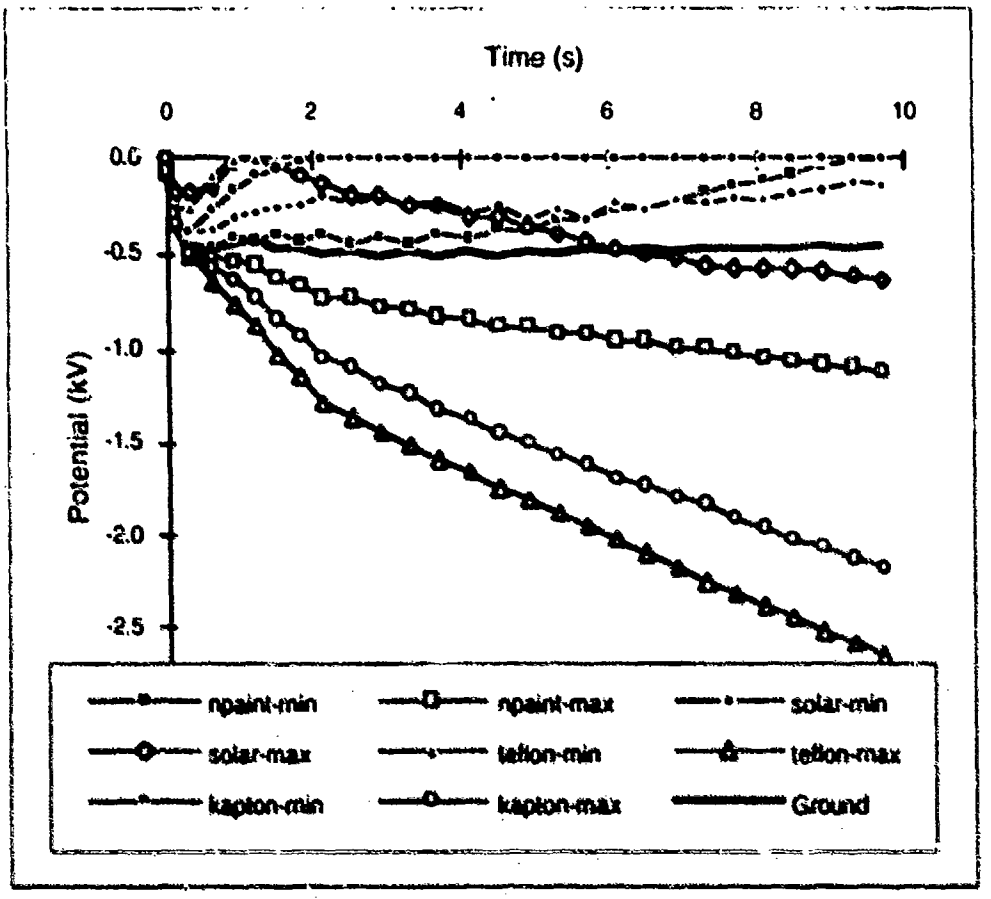

Figure 38. Surface charging rate of selected DMSP surfaces.

The potentials computed by *POLAR*'s **nterak** can now be examined for regions requiring further analysis. The *POLAR* **tmtlk** and **shontl** codes give the user the following information. All the surfaces charge negatively. The maximum potential is -2.25 kV on the sunshade, which is teflon. The highest fields are also in this region. Figures 39 are contour plots of potentials at the center of the grid in the X and Z directions, respectively. The region with the highest electric fields is inside the area between the sunshade and the body. In the model, this region is shielded from the environment so it gets no ion current and continues to charge negatively.

(a)

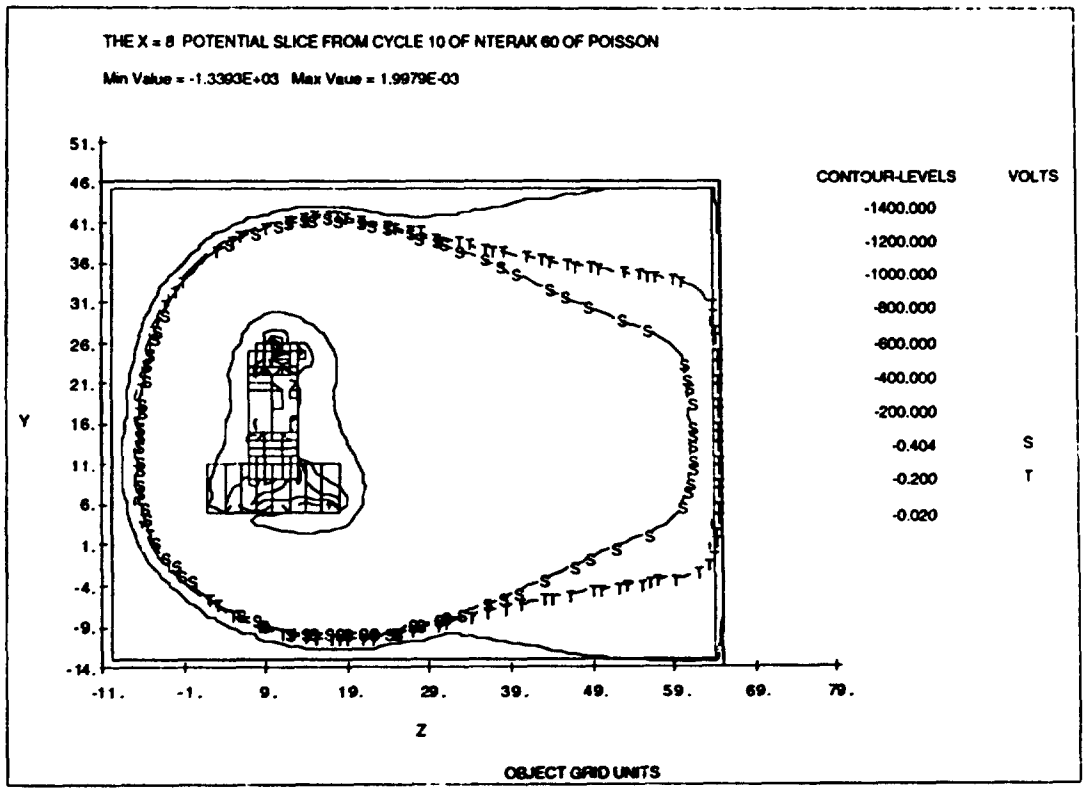

(b)

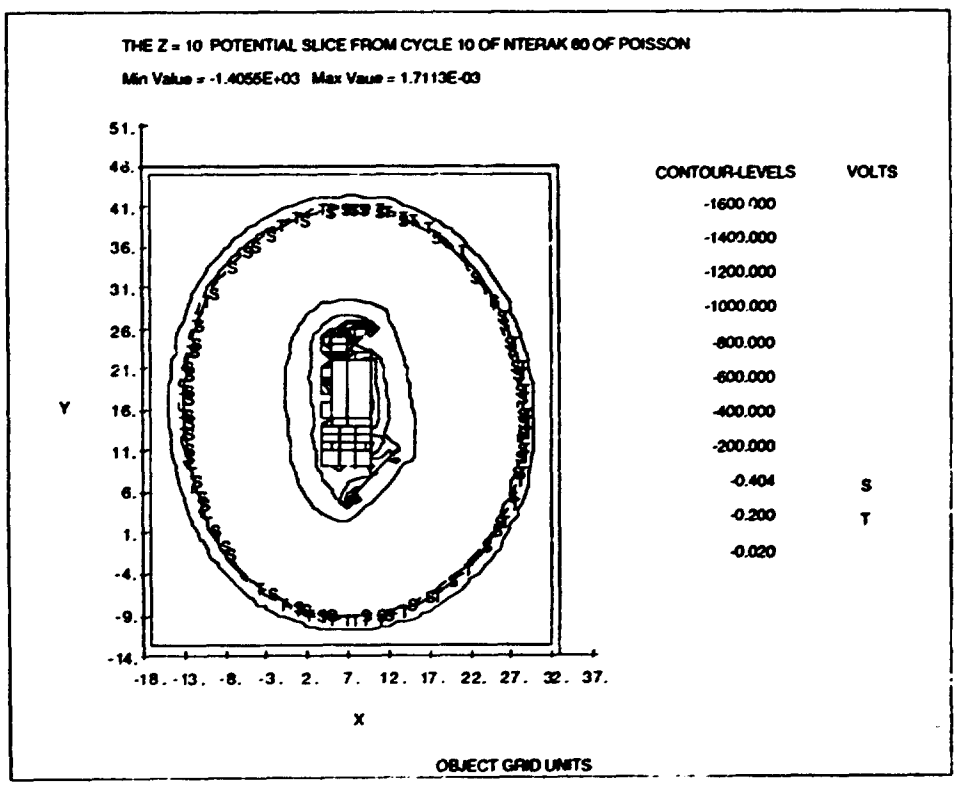

Figure 39. Potential contours for DMSP (a) in the constant X plane of the center of the grid and (b) in the constant Z plane of the center of the grid.

5.1.4 A Multibody Problem–EMU Near the Shuttle

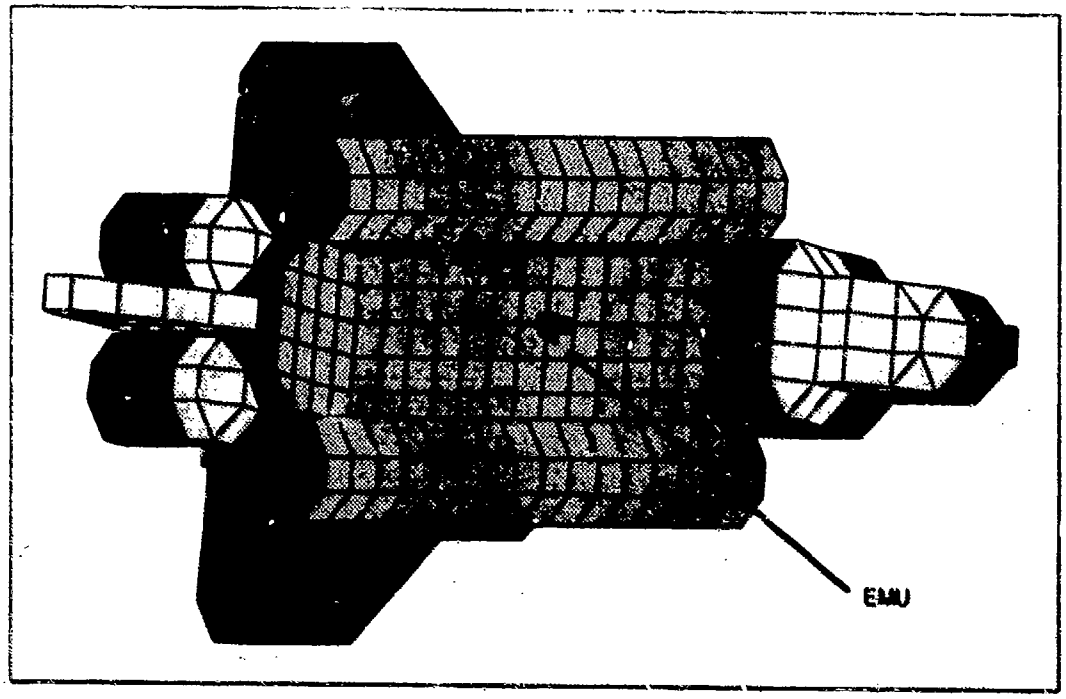

Figure 40. A small spacecraft, such as an Extravehicular Maneuvering Unit (EMU), near a large object, such as the shuttle orbiter, may charge to a large potential in the auroral zone.

An example of how the presence of one spacecraft can affect the charging of another is the charging of a small object near a large one during an aurora. One example of this is the operation of an EMU (Extravehicular Maneuvering Unit) near the much larger shuttle orbiter. The EMU develops surface potentials comparable to those of the shuttle.

To analyze the charging, a 2-part calculation is needed. First, the charging of the large object is examined to determine the appropriate environment of the small object. Second, the charging of the small object is examined in the environment determined by the large object.

The *POLAR* codes are used to determine the charging of the orbiter-EMU pair in the severe auroral environment. Since the orbiter operates at lower altitudes than DMSP, this is not a realistic environment for the shuttle. (At present no missions into the auroral zone are planned for the shuttle orbiter anyway.) The model for the calculations is shown in Figure 41. Although this is a crude model of the orbiter, the size and shape are similar. The material covering the model has secondary properties equivalent to the shuttle white tile material and a small patch on the wake side is TEFLON to simulate the EMU. The computer files used in the calculations are in Appendix C.

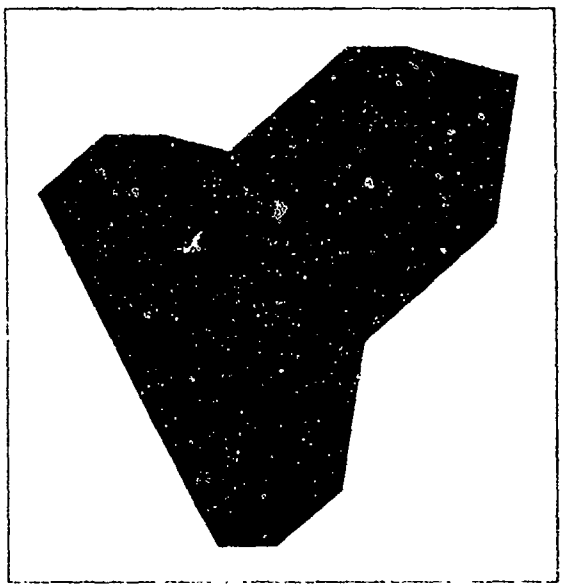

Figure 41. *POLAR* model of shuttle used for calculations of the ion current as a function of voltage.

A series of **nterak** calculations is done using this model to determine the ion current density as a function of the voltage. Figure 42 shows the current collected as a function of voltage. The figure shows the ion current collected and the net electron current including electron generated secondaries and backscattered electrons. The ion generated secondaries are ignored as their contribution is small. The electron current collection values were determined using **suchgr** because they depend only on the potential, the spectrum, and the surface material properties. The voltage at which the lines intersect for zero net current, −1.5 kV, is the equilibrium potential. If the ion generated secondaries had been included in the calculation, the equilibrium potential would be slightly greater. The equilibrium potential could also be found by letting the shuttle charge in this environment until an equilibrium potential is reached. This process takes longer. A charging calculation gives a variation in potential from location to location. Since the current to the EMU is not dependent on the small scale potential variations, these can be ignored for this calculation.

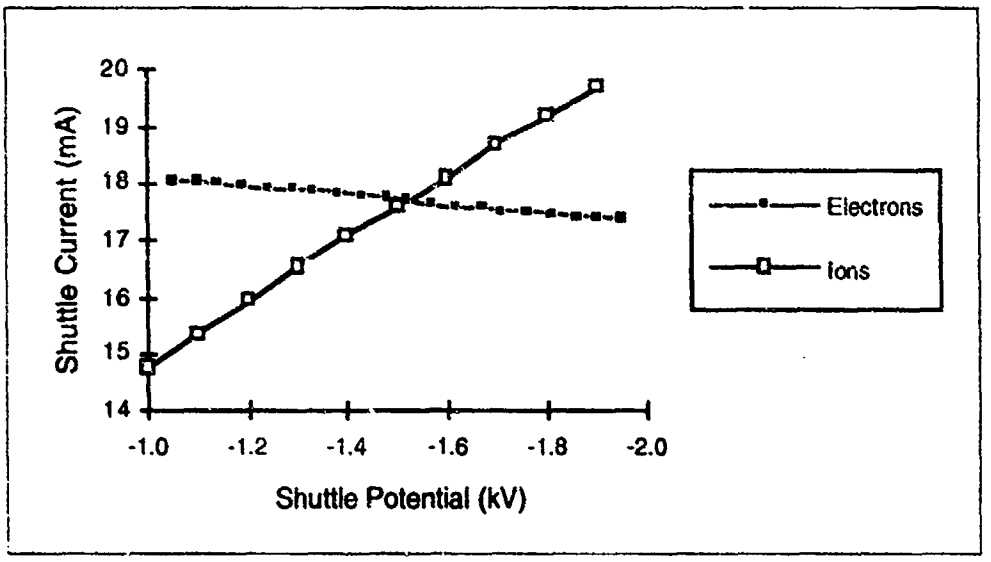

Figure 42. Shuttle current collection as a function of shuttle voltage. The potential at which the electron and ion currents are equal is the equilibrium potential.

The ion current as a function of voltage curve is used to determine the appropriate environment in which to evaluate the charging of the EMU. The EMU environment is a monoenergetic beam of ions with energy equal to the orbiter potential. The ions are accelerated to the orbiter potential before they are substantially affected by the EMU electric fields. Ion collection by the small EMU is orbit-limited, with a current density for surfaces at the orbiter potential the same as the average orbiter ion current density. This is because a small object in an ion beam collects according to orbit-limited theory. EMU collection is described by,

$$J(\Delta\phi) = J_o\left(1 + \frac{\Delta\phi}{\phi_s}\right) \tag{7}$$

where J_o is the current density on the shuttle, ϕ_s is the potential of the shuttle, and $\Delta\phi$ is the difference between the shuttle and the EMU's surface potential.

The next step is to evaluate the charging of the EMU in the effective environment. The ion current collected by a negatively biased sphere in a thermal plasma is given by

$$J(\phi) = J_{th}\left(1 + \frac{\phi}{\theta}\right) \tag{8}$$

where θ is the plasma temperature. *POLAR* uses this formula to obtain the ion current to a surface when orbit-limited current collection is requested. One approach to solving for the surface potentials on the EMU is to do an orbit-limited current collection calculation with an ion temperature of ϕ_s and an ion density such that J_{th} equals J_o. The resulting potentials should then be shifted by ϕ_s to give the true potentials. However, this approach gives the wrong secondary emission currents. An alternative is to use the following approximation. Equation 7 can be rewritten as

$$J(\phi) = J_0\left(1 + \frac{\phi - \phi_s}{\phi_s}\right) = J_0\left(\frac{\phi}{\phi_s}\right) = J_0 \frac{\theta}{\phi_s}\left(\frac{\phi}{\theta}\right) \approx J_0 \frac{\theta}{\phi_s}\left(1 + \frac{\phi}{\theta}\right) \tag{9}$$

where θ is a number small with respect to ϕ. The temperature is chosen to be an appropriate temperature for the problem and the density is chosen such that

$$J_{th} = J_0 \frac{\theta}{\phi_s} . \tag{10}$$

To evaluate the charging of the EMU, we use **nterak**. The model of the EMU is shown in Figure 43. The cold plasma environment is chosen to give the correct ion collection properties of the EMU. The temperature is 4.5 eV, which is the ram energy of the oxygen ions. The approximation in Equation 9 is valid as long as θ is small with respect to the shuttle potential of –1.5 kV. A density of 2.2×10^7 m^{-3} gives the correct ion thermal current. The calculation is done assuming orbit-limited ion current collection. The hot electron environment is the same as we used for the shuttle charging. A mach velocity of 0 is used because wake effects are meaningless here. We use as large a grid as possible because the grid boundary is at 0 V.

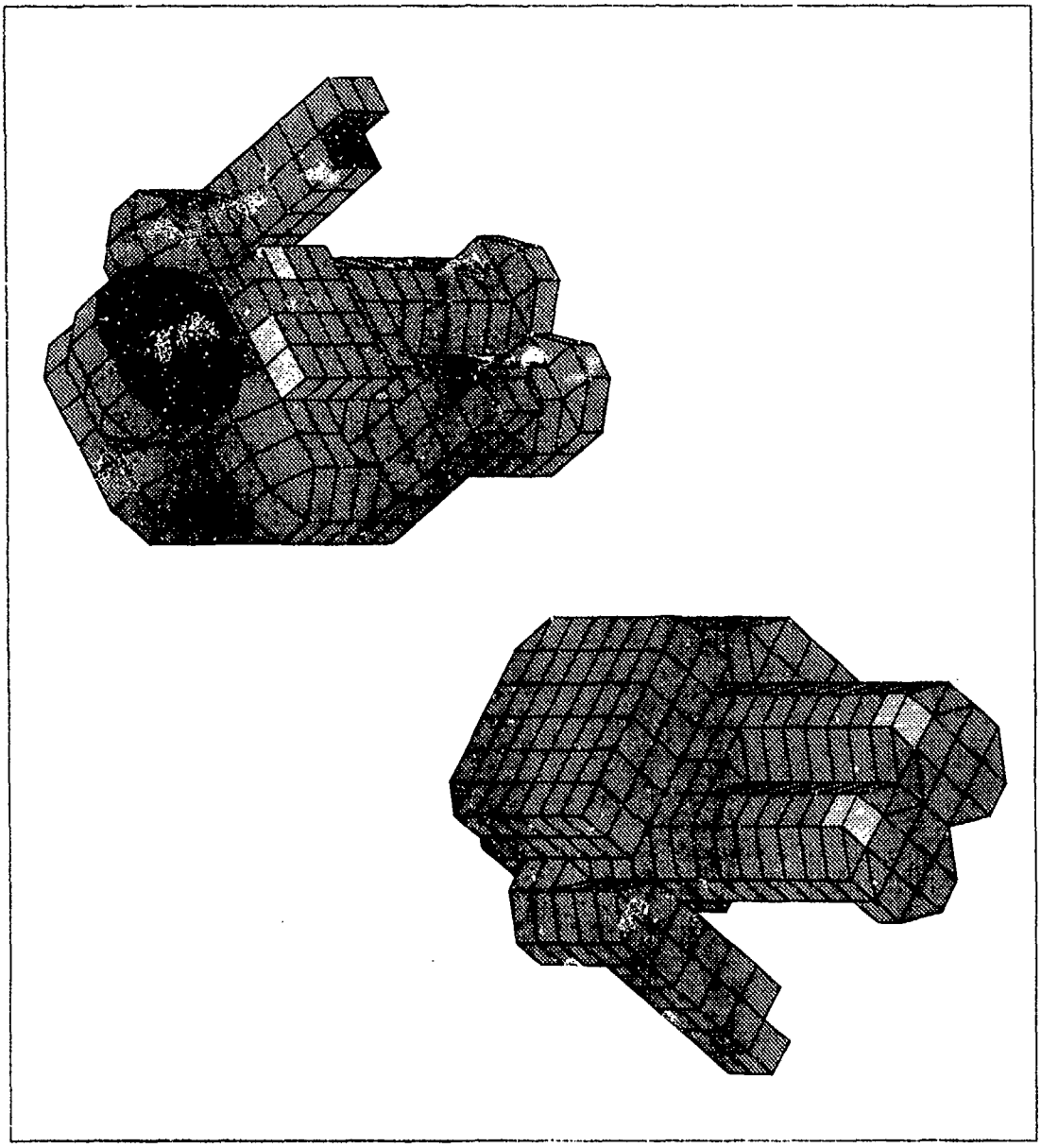

Figure 43. *POLAR* model of the EMU, two views.

We use **suchgr** to estimate the charging. Table 11 shows the final potentials for the various materials. The materials LEXAN, KAPTON, and WHITEN all charge the same (as the secondary properties are the same.) The material ALUM charges slightly more and TEFLON, the predominant material, charges less.

Table 11.
Charging of EMU Materials As Given by **suchgr**

Material Name	Equilibrium Potential (kV)
TEFLON	-2.8
LEXAN	-3.2
ALUM	-3.35
KAPTON	-3.2
WHITEN	-3.2

Figure 44 shows the time history of the potential of the different materials of the EMU as computed by **nterak**. Differential potentials of 450 V develop. The insulating surfaces reach their equilibrium potentials in about 0.2 s. Spacecraft ground is capacitively coupled with the exterior of the insulating surfaces and therefore follows the potential of the most numerous (by far) surfaces for the first second. After about a second, the ground potential begins to increase. This is because the few aluminum surfaces have a net negative current to them from the environment. Eventually, spacecraft ground will reach the floating potential of aluminum in this environment.

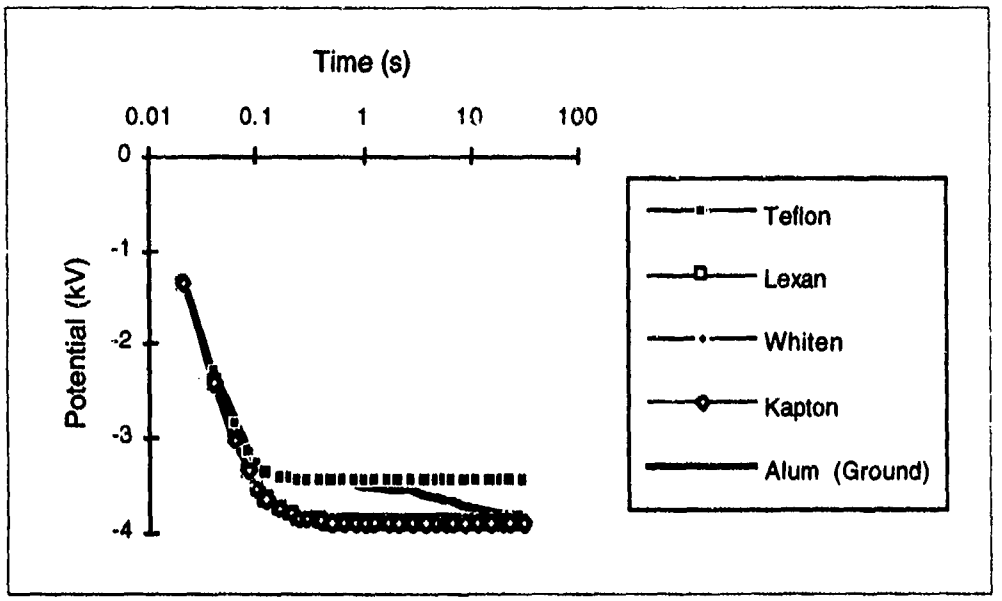

Figure 44. Time history of the EMU surface potentials.

The field over the exterior of the EMU varies from 10^4 to 2×10^5. The high fields are at the hands, heels, and face plate, the surfaces that are not modeled by TEFLON. Figure 45 shows the contour levels in a plane through the center of the EMU.

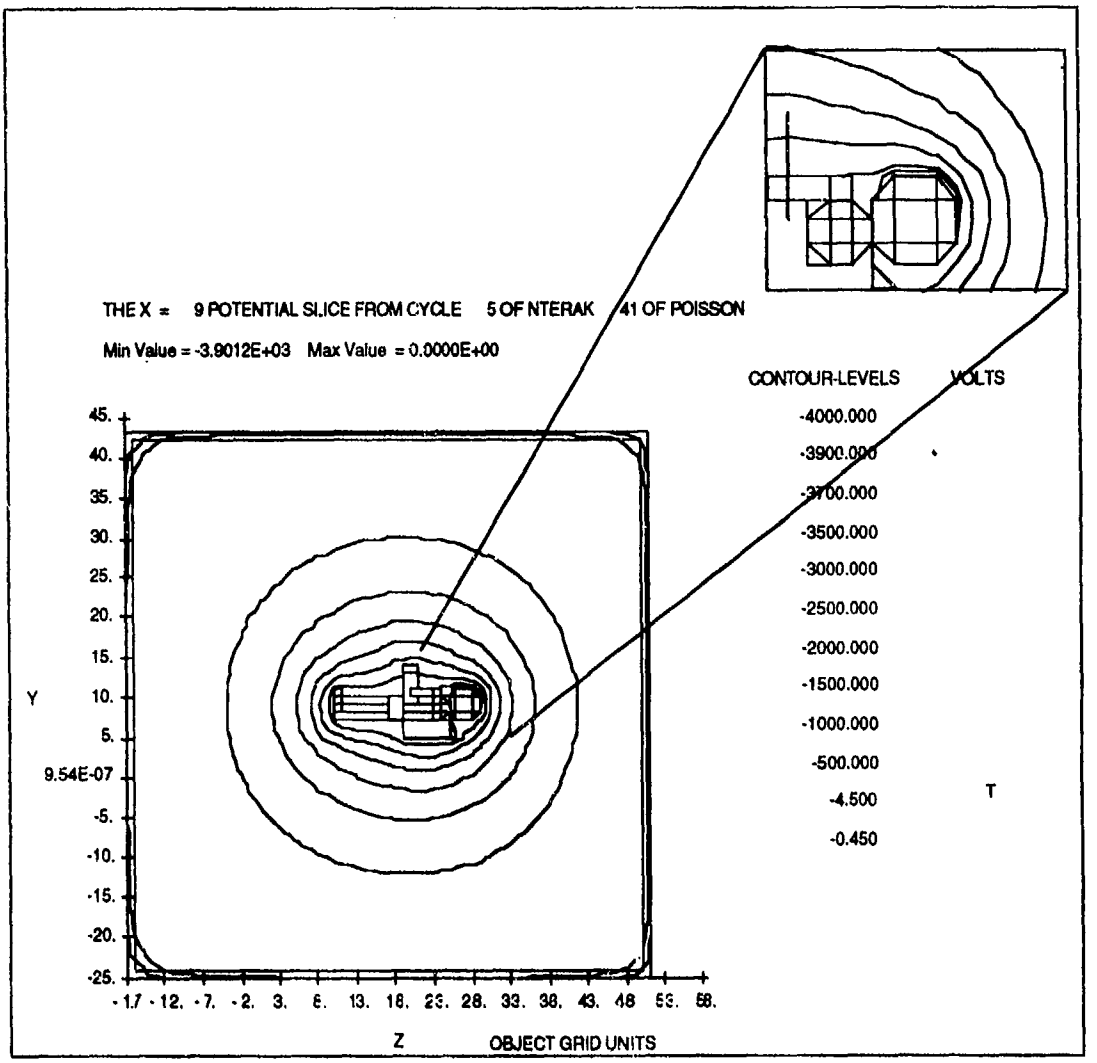

Figure 45. Contour levels in a plane through the center of the grid. The high fields near the face plate can be seen in the inset.

5.1.5 Documentation

Enough documentation of the charging analysis should be kept to allow the calculations to be repeated. Any figures, analytic calculations, and other information that is used to make recommendations should be kept. Frequently, decisions need to be reassessed and it is easier to review the decision if all the information that went into the decision is available. The material contained in this chapter and in Appendix C is the type of material that should be kept.

5.2 Determining the Location and Frequency of Discharges

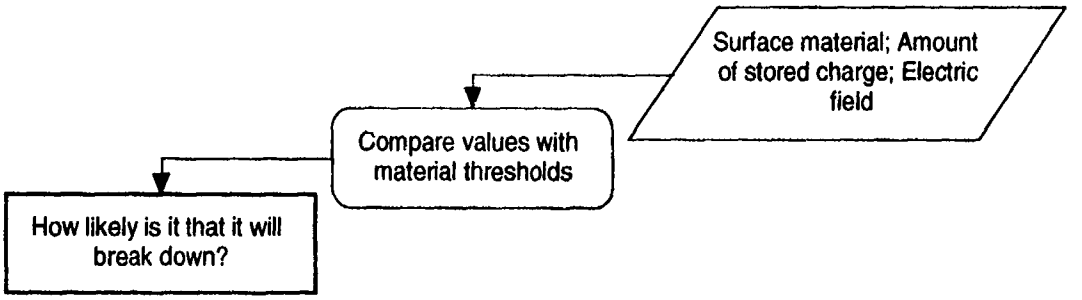

Figure 46. Once we know the surface potentials to expect, we want to locate the likely breakdown locations.

As discussed in Chapter 2, even though our understanding about discharges is not complete, there are some well-established data, plausible analytical treatments, and useful criteria that can be employed in predicting the location and frequency of discharges as discussed below.

The criteria given in Purvis et al. [1984] for determination of expected discharge locations are (a) dielectric surface voltages greater than 500 V positive relative to an adjacent exposed conductor, or (b) an electric field greater than 5×10^7 Vm^{-1} between a dielectric and an exposed conductor. The potentials calculated using the methods discussed in Section 5.1 can be used to determine some discharge sites. Small features, such as edges, points, and corners can enhance the electric field. They are rarely explicitly included in the modeling of charging. To locate high field regions due to these types of features, the spacecraft specifications must be examined.

At present, no proven analytical method exists to determine the sites of discharges or their frequency. To overcome the lack of definitive analytical methods, a rule structured protocol based on the level of differential voltage has been developed by the spacecraft charging community to determine possible discharge sites. The rules for determining the location and charge loss of potential discharges for spacecraft dielectrics from the *NASCAP/GEO* or *POLAR* predictions are as follows [Frezet et al., 1988; Purvis et al., 1984; Stevens et al., 1987]:

1. Discharges are possible from *NASCAP/GEO* or *POLAR* dielectric cells whose surface potential is 1000 V or more negative with respect to the spacecraft structure or adjacent exposed conductors.
2. Discharges are possible from *NASCAP/GEO* or *POLAR* dielectric cells whose surface potential is 500 V or more positive with respect to the spacecraft structure or adjacent exposed conductors.
3. Discharges are possible from *NASCAP/GEO* or *POLAR* dielectric cells where an electric field of 5×10^7 V m^{-1} exists between the dielectric and an exposed conductor.

4. The charge loss in a discharge is normally assumed to be 10%. If there is a differential surface potential between the dielectric cell and an adjacent cell of 1000 V or larger then the charge loss is assumed to be 30%.

5.3. Determining the Severity of Discharges

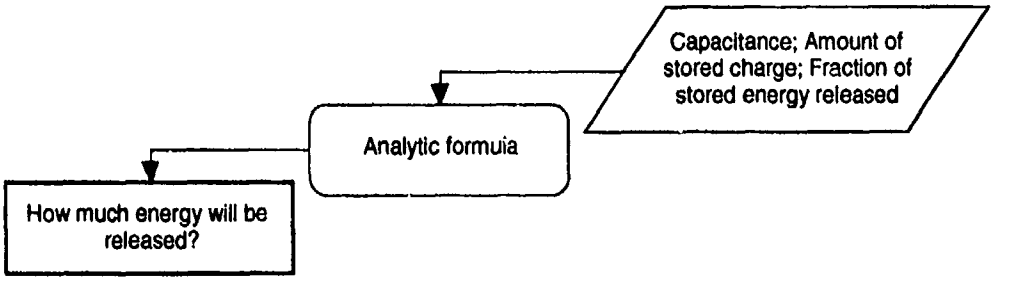

Figure 47. Once we have determined that a discharge is likely at a given location, we would like to determine how severe the discharge is likely to be.

The severity of a discharge can be measured in several different ways: the amount of energy released, the peak current, the voltage change, or the amount of material released.

The replacement current arising from blowoff discharges has a time profile that can be represented by a triangle or double exponential wave shape [Purvis et al., 1984]. The peak amplitude of the wave shape, I_0, depends on C, the capacitance of the dielectric cells where discharges are possible, on V_0, the voltage of the cells before discharge, on κ, the fraction of charge blown off, and on t, the half width of the discharge pulse. It is expressed as

$$I_0 = \kappa C V_0 / t \ . \tag{11}$$

The discharge half width can be estimated by the space-charge limitation time [Woods and Wenaas, 1985] given by

$$t = \frac{2}{v_p}\sqrt{\frac{8 R d}{\kappa \varepsilon_r}} \tag{12}$$

and the pulse rise time is

$$t_r = 2 R / v_p \tag{13}$$

where v_p is the dielectric dependent discharge propagation velocity (typically, 3×10^5 m s^{-1}), R is the average surface dimension of the dielectric undergoing discharge or is the radius of a 3-dimensional structure, d is the dielectric thickness, and ε_r is the relative dielectric constant of the dielectric.

Another means of estimating the peak amplitude and half width of a discharge is to use ground-based measured data. Data based on the measurement of small planar samples is

given by Balmain and Dubois [1979] and O'Donnell and Beers [1982] which find the following scaling laws for dielectric discharges [Wilkenfeld, 1983]

$$I_o = C1\, A^{C2} \tag{14}$$

$$t = C1'\, A^{C2'} \tag{15}$$

where A is the dielectric surface area undergoing discharge and the Cs are the dielectric dependent constants shown in Table 12.

Table 12.
Current and Time Discharge Scaling Parameters [Wilkenfeld, 1983]

	I_o (A)		t (ns)	
Material	C1	C2	C1′	C2′
Kapton	3.8	0.482	01.4	0.669
Teflon	5.146	0.516	8.0	0.511
Mylar	8.359	0.509	7.7	0.461
Fused quartz	0.81	0.6		

5.4 Determining Where the Discharge Energy Will Go

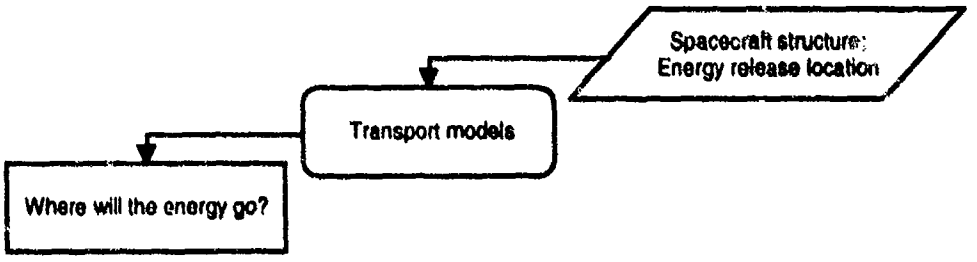

Figure 48. A vital key to a determination of the impact of surface charging is the determination of where the discharge energy, the current, will go.

The transient pulse produced by the discharge couples directly or capacitively to the spacecraft structure and to spacecraft cables. Various methods are available to analyze the coupling of the discharge transient to the spacecraft elements. Some of these different coupling analysis methods are briefly discussed below.

5.4.1 Lumped Element Method

Lumped element modeling (LEM) is the most common analysis method used for discharge coupling. LEM models replace spacecraft structural elements with their equivalent inductance, capacitance, and resistance. LEMs have varied from simple

1-dimensional models where a few circuit elements are used to model the entire spacecraft structure [Bowman et al., 1989; Woods and Wenaas, 1985] to very complex 3-dimensional models where each structural element is modeled by its equivalent RLC circuit [Granger and Ferrante, 1987; Robinson, 1977]. The discharge source is then used to drive the lumped element electrical model at the point in the model associated with the cells identified as locations where discharges are likely to occur. A circuit analysis code such as SPICE is used analyze the lumped element circuit model and to calculate the currents flowing on each structural element due to the discharge source. A LEM model is also generated for cables that are attached to or run near the spacecraft structures. The structure currents calculated by SPICE for the spacecraft LEM are then used to drive the cable LEMs. SPICE runs are made for the cable electrical models using the structure drive sources to determine the coupling of the structure currents to the cable conductors. The conductor currents and the resulting voltage appearing at interface circuits attached to the cable conductors are compared to the interface circuit thresholds to determine if the interfaces will be upset or damaged by the discharge sources.

5.4.2 Numerical Electromagnetic Method

The numerical electromagnetic method uses codes such as the Numerical Electromagnetic Code (NEC) [Burke and Poggio, 1981] to analyze discharge coupling. For NEC the spacecraft structures and cables are modeled as a combination of "sticks" and flat polygonal "plates." The NEC spacecraft model is then driven by direct sources representing the discharge at the model locations identified with the cells that are likely to discharge. NEC is a frequency domain code and thus the time domain discharge sources must be converted to the frequency domain when input to NEC. The NEC program solves both an electric field integral equation (EFIE) and a magnetic field integral equation (MFIE) and accounts for mutual coupling between spacecraft model elements. Individual NEC calculations are performed at a single frequency point and thus must be repeated at a number of specific frequencies that cover the range of interest for the frequency spectrum of the discharge sources. The NEC code output is transformed to the time domain to yield the current flowing on the cables of interest. The cable currents are then used to determine the cable conductor currents via the transfer characteristics of the cables being analyzed or with a lumped element electrical model. Once the conductors' currents are found, the voltages and currents appearing at sensitive interface components are determined using usual network analysis techniques.

5.4.3 Particle Pushing Method

The particle pushing methods use system generated electromagnetic pulse (SGEMP) codes such as the 2-dimensional Arbitrary Body of Revolution Code (ABORC) [Woods and Delmer, 1976] or its 3-dimensional equivalent MEEC [Tumolillo and Wondra, 1977] to calculate spacecraft discharge response. These codes solve Maxwell's equations by direct finite differencing for axisymmetric geometries. Spatial current densities are obtained from finite particles of charge that are followed through the spatial mesh of

zones. In addition to the Maxwell equation routine, ABORC has a Poisson equation solver from which electrostatic fields may be obtained for each time step. Woods and Wenaas [1985] describes the details of using ABORC to perform discharge analysis of spacecraft. Discharge response calculations begin with the static fields arising from the initial charge on the dielectrics. The ABORC discharge model assumes uniform spatial emission, a triangular time history, and zero initial electron kinetic energy. Flashover currents are included to the extent that the potential across the dielectrics varies with time due to both blowoff and flashover effects. Reasonable agreement has been found between discharge results calculated with ABORC and actual measurements made on spacecraft models in the laboratory.

5.4.4 EMC Radiative Coupling Method

The EMC radiative coupling method employs EMC analysis codes such as Intrasystem Electromagnetic Compatibility Analysis Program (IEMCAP) and Specification and Electromagnetic Compatibility Program (SEMCAP) [Heiderbrecht, 1975] to analyze discharge coupling for spacecraft. IEMCAP and SEMCAP contain communications and EMC analysis math models to efficiently evaluate the spectra and transfer modes of electromagnetic energy between generators and receptors within a system. In analyzing a system with these codes, all system emitters are characterized by emission spectra and all receptors are characterized by susceptibility spectra. All ports and coupling mechanisms are assumed to have linear characteristics. Emissions from the various emitter ports are assumed to be statistically independent so that signals from several emitters impinging at a receptor port combine on an RMS or power basis. The function of these codes is to determine, by analysis, whether the signals from one or more emitters entering a receptor port cause interference with the required operation of that receptor. Electromagnetic Interference (EMI) is accessed by computation of an EMI Margin for each receptor port. The EMI Margin is just the ratio of power received at each receptor port to that receptor's susceptibility. Coupling models built into these codes include antenna coupling, wire-to-wire coupling, case-to-case coupling, coupling through filters, field-to-wire coupling. Voyager [Rosen, 1978] and SCATHA [Inouye, 1981] are two spacecraft whose discharge couplings have been analyzed by using the EMC radiative coupling method. Leung et al. [1986] describes discharge induced anomalies that have been observed for Voyager and discusses them in relation to the SEMCAP discharge prediction made for Voyager.

5.4.5 Recommended Coupling Analysis Approach

The present standard practice used for spacecraft discharge response is the LEM method and follows the procedure shown in Figure 49. The analysis procedure is as follows [Elkman et al., 1983; Granger and Ferrante, 1987; Stevens et al., 1987]:

1. Obtain the structural details on the spacecraft to be analyzed.

2. Obtain the physical details on spacecraft cabling that are routed on or near structural elements and connect to sensitive interface circuits that are susceptible to interface or damage.
3. Construct a physical model of the spacecraft using the following library of structural components: rectangular plates, disk plates, hollow cylinders, bars and cones.
4. Construct an electrical model of the spacecraft replacing the structural components with their equivalent electrical RLC models. The equivalent circuits for plates, hollow cylinders, and discs are shown in Figure 50. The structural elements fall into one of two major categories, the exterior structural elements that are capacitively coupled to space and the interior elements that capacitively couple to each other. These free space capacitances and mutual capacitances are included in the electrical model for each model structure. Capacitances and inductances of structure elements may be found in Granger and Ferrante [1987], Elkman et al. [1983], and Rostek [1974]. The electrical model nodes should correspond to structural features with dimensions of 0.3 m or less.
5. Construct LEM electrical coupling models of the spacecraft cabling and insert these cable coupling models at the appropriate location in the spacecraft electrical model. Simple LEM models can only be used for cables that are less than $\lambda/8$ long, where λ is the smallest wavelength used in the analysis. For longer cables, distributed LEMs must be used where the simple LEM is divided into several sections to account for distributed effects.
6. Insert the discharge sources at the appropriate points in the spacecraft electrical model. The sources drive the spacecraft electrical model through their source impedance that is capacitive or resistive depending on their spacecraft injection mechanism. Use a circuit analysis code such as SPICE to solve the spacecraft electrical model for the voltages and currents that appear at the cable conductor loads representing input impedances of the sensitive interface circuits.

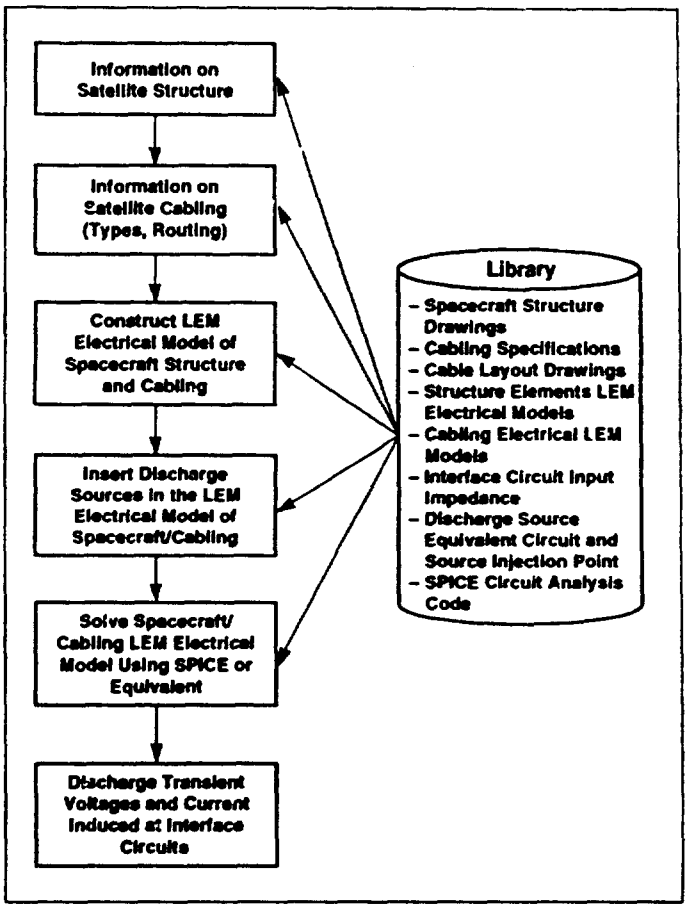

Figure 49. Discharge response modeling using the Lumped Element Method (developed with input from Elkman et al. [1983], Granger and Ferrante [1987], and Stevens et al. [1977]).

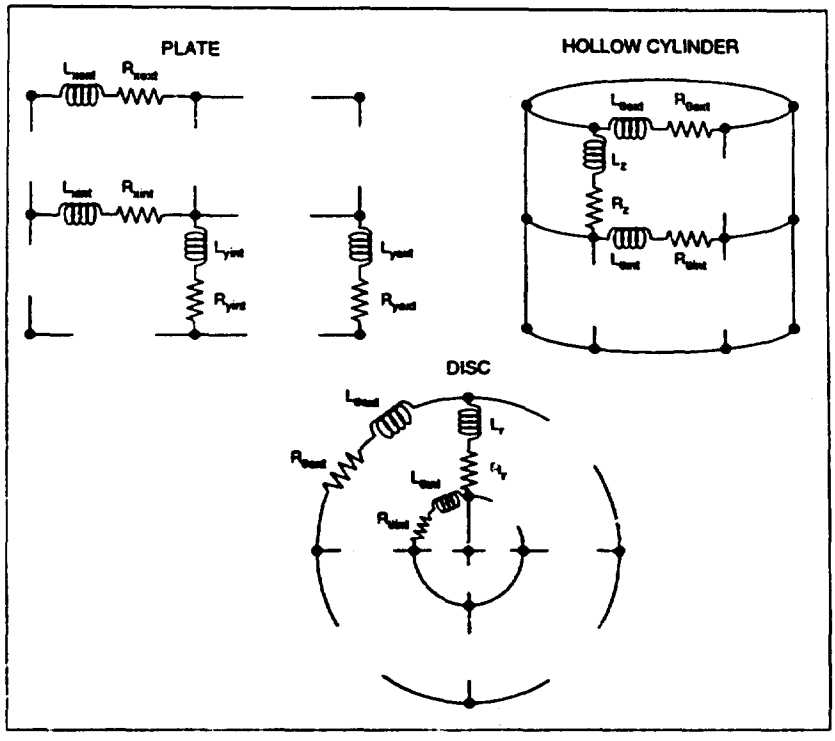

Figure 50. Equivalent circuits for plates, cylinder, and discs [Granger and Ferrante, 1987].

5.5 Determining the Damage Produced by Discharges

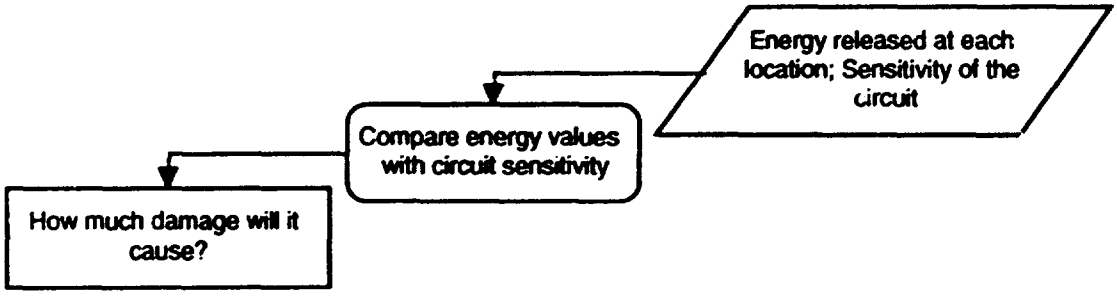

Figure 51. The point of the discharge magnitude and coupling calculations is to determine the stress and ultimately the damage to circuits and components.

We first became aware of spacecraft dielectric discharges because they produce anomalous behavior in spacecraft operation. An anomaly is defined as any spacecraft behavior that is out of the ordinary. Thus our goal in examining discharges is to analyze where the voltage and currents induced by discharges could produce an undesirable spacecraft circuit response and thus possibly produce anomalies. The transient voltages and currents in interface circuit loads transfer through any intervening circuit elements and arrive at and stress sensitive interface components. The transient component stress

can produce one of two undesired responses in spacecraft circuits. One response is upset and the other is component damage. These two types of responses and the analysis procedure for determining if they can occur are discussed below.

5.5.1 Circuit Upset

Circuit upset is a nonpermanent alteration of a circuit or component operational state that is self-correcting or reversible by automatic or manual means. Some examples of upset are provided in Figure 52. The conditions for upset to occur when a circuit is stressed by a discharge transient are as follows:

1. The discharge transient's amplitude must be a significant fraction of or greater than the circuit's operating signal levels.
2. The discharge transient's time scale must be within the circuit's response time.
3. When the discharge transient's time scale is shorter than the circuit's response time, the discharge transient's amplitude required to cause upset exceeds the circuit's operating signal levels by increasing amounts as the time scale differences become larger.
4. For digital logic circuits, when stressing discharge transients have time widths that are within the logic circuits response time, logic upsets occur when the discharge transient's amplitude is greater than the logic circuit's noise margins.

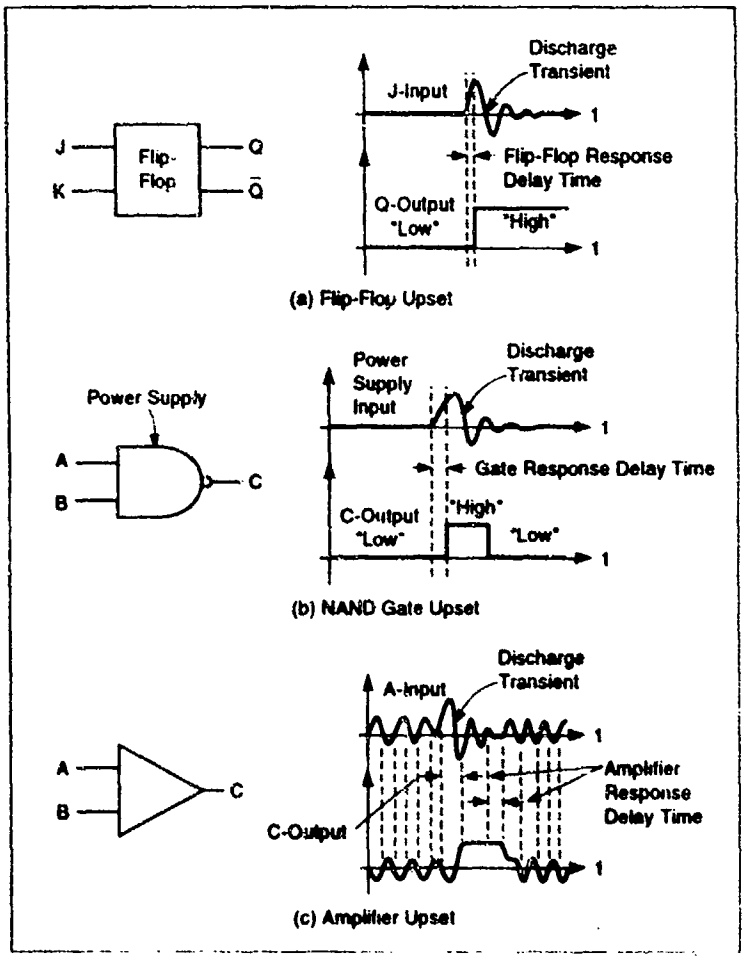

Figure 52. Examples of upset from discharge transient pulses [EMP Susceptibility Threshold Handbook, 1972].

The upset thresholds for representative logic families are given in Table 13. The upset level (e.g., noise margin) for commonly used logic families vary from a few hundred milli-electron-volts to a few volts. Typical upset energy level thresholds range from 1 to 50 nanojoules.

Table 13.
Typical Upset Threshold and Characteristics of Some Logic Families
[Noise Immunity Comparison of CMOS versus Popular Bipolar Logic Families]

Logic Family	Power Supply (V)	Typical Gate Quiescent Power Dissipation (mW)	Typical Propagation Delay (ns)	Typical Signal Line DC Noise Immunity (V)				Typical Signal Line Impedance (Ω)		Logic Voltage Swing (V)	Typical Energy Noise Immunity on Signal Line (Joules × 10^{-9})	
				Low		High						
				Min	Typ #	Min	Typ #	Low	High		Low	High
DTL	5	5	30	0.7	1.2	0.7	3.8	80	1.7k	4.5	3	15
TTL	5	15	10	0.4	1.2	0.4	2.2	30	140	3.5	4	25
HTL	15	30	85	5.0	7.5	4.0	7.0	130	1.6k	13	48	-
SCL	-5.2	25	2	NA	0.35	NA	0.17	7	7	0.8	NA	NA
CMOS	5	0.000025	45	1.5	2.2	1.5	3.4	*600	**1.2k	5	3	15
CMOS	10	0.00010	16	3.0	4.2	3.0	6.0	*400	**800	10	10	5
CMOS	15	0.00023	12	4.5	6.5	4.5	9.0	*250	**450	15	22	13

Typical values are from experimental results of testing a small sample quantity of parts and may not reflect manufacturer's specifications

*Defined at 30% of V_{DD}
**Defined at 70% of V_{DD}
} dc resistance

An example of a discharge induced upset anomaly is the Power-On Reset within the Voyager 1 Flight Data System (FDS) which occurred 42 times during its Jupiter flyby [Leung, 1986]. This anomaly was traced to the upset of a CD4050 CMOS input buffer in the FDS processor delay logic circuit. Investigation determined that a discharge pulse with a current rise of 4 A μs^{-1} to 10 A μs^{-1} on a nearby wire would induce the 3 V to 17 V at the CMOS buffer required to trigger its upset for induced transient pulse widths of 5 ms and 20 ns, respectively.

5.5.2 Component Damage

Component damage is a permanent change in one or more electrical characteristics of a circuit component. Circuit components are vulnerable to thermal damage and electrical breakdown when stressed by dielectric discharge transients. The damage energy threshold for various circuit components for a 100 ns rectangular transient pulse is shown in Figure 53. The damage threshold level ranges from 10 nJ for microwave diodes to several hundred nanojoules for various logic families.

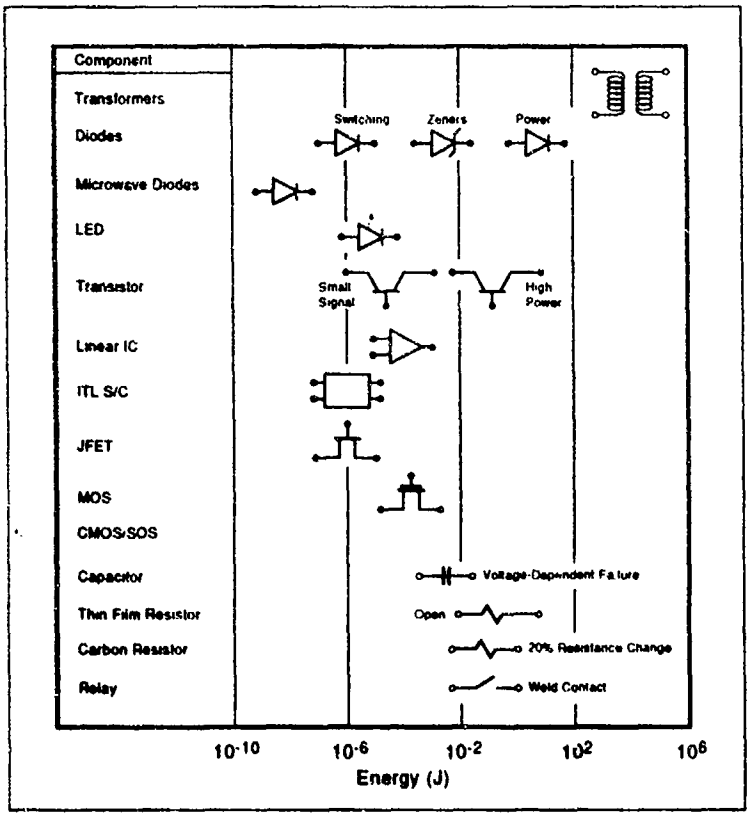

Figure 53. Permanent damage energy threshold of components for 100 ns pulse [Rudie, 1981].

For semiconductors, the most common discharge transient damage mechanism is localized thermal runaway triggered by electrothermal overstress. This condition produces a resolidified melt channel across the junction once the transient is removed where the melt channel appears electrically as a low resistance shunt across the junction. Junction damage is most likely to occur when the discharge transient reverse biases the junction and drives it into second breakdown. Forward stressed junctions also fail but typically have damage thresholds that are three to ten times higher than reverse stressed junctions. For integrated circuits, metallization burnout and gate oxide breakdown (for MOS devices) are also prominent failure mechanisms.

Semiconductor failure thresholds for discharge transients can be predicted from known or measured data using models developed for discrete semiconductors and integrated circuits. These models, which are based on thermal considerations and experimental results, yield the following expression for the failure threshold level

$$P_f = k_1 t^{-k_2} \qquad (16)$$

where P_f is the power in watts required in t seconds to produce device failure, and k_1 and k_2 are device dependent damage constants. As illustrated by Figure 54, for discrete devices, k_2 is unity for discharge pulse widths less than 100 ns, 0.5 for pulse widths between 100 ns and 300 ms, and zero for longer pulse widths. The value of k_1 is determined by test when possible Measured values of k_1 for some common discrete

semiconductors are shown in Table 14. When test data is unavailable, the value of k_1 can be obtained from data sheet information and the analytical expressions given in Durgin, et al. [1983]. The failure models for diodes and transistors are shown in Figure 55. The diode and transistor junctions are modeled by a resistor that represents the junction's bulk resistance and a voltage source that represents the reverse breakdown voltage for the junction. Typical values of junction bulk resistance and reverse breakdown voltage for diodes and transistors are listed in Table 15.

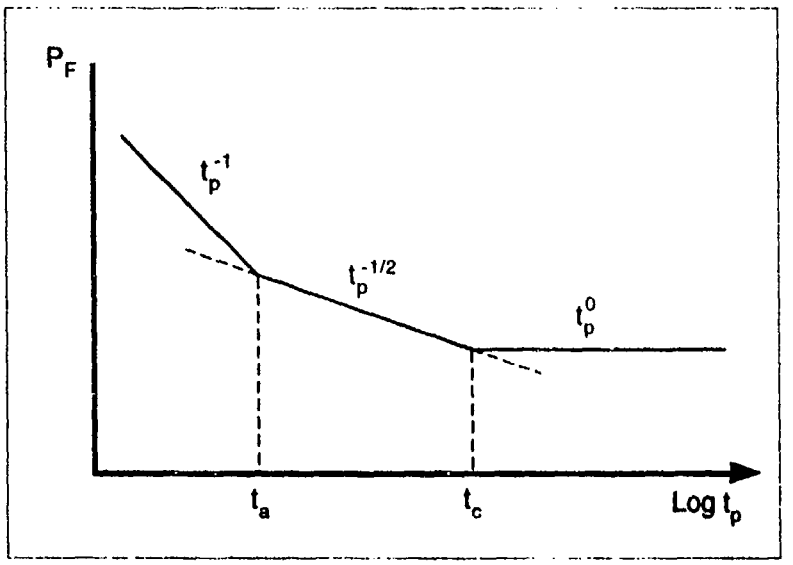

Figure 54. Pulse power failure dependence on pulse width for discrete semiconductors [EMP Susceptibility Threshold Handbook, 1972].

Table 14.
Damage Constants and Junction Breakdown Voltages for Some Typical Discrete Semiconductors

Device	Type	k* ($W s^{1/2}$)	BV_{EBO} (V)	BV_{CBO} (V)	V_{BD} (V)
IN750A	Zener	2.84			4.7
IN756	Zener	20.4			8.2
IN914	Diode	0.096			75
IN3600	Diode	0.18			75
IN4148	Diode	0.011			75
IN4003	Diode	2.2			200
2N918	Transistor	0.0086	3	30	
2N2222	Transistor	0.11	5	60	
2N2857	Transistor	0.0085	2.5	30	
2N2907A	Transistor	0.1	5	60	
2N3019	Transistor	0.44	7	140	
2N3440	Transistor	1.1	7	300	

* $k_1 = k$, $k_2 = 1/2$

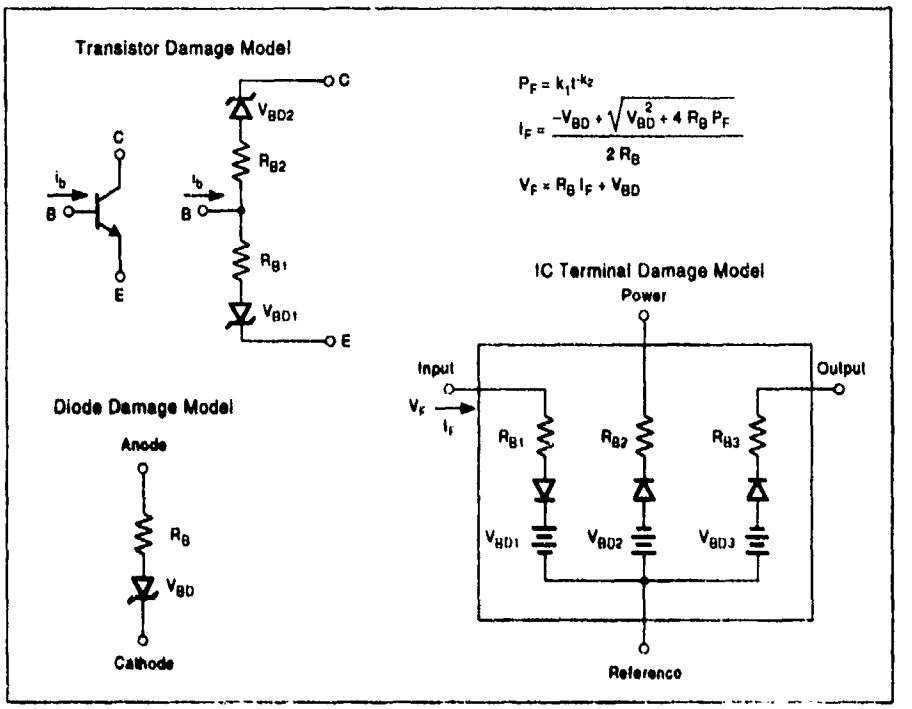

Figure 55. Transient pulse failure models for transistors, diodes, and integrated circuits

Table 15.
Typical Junction Bulk Resistance for Discrete Semiconductors
[Sweton, 1979]

Device Category	Reverse Bias (Ω)	Forward Bias (Ω)
Zener diodes	1.0	0.1
Signal diode	25.0	0.25
Rectifier diode	150.0	0.05
Low power transistor (e-b)	10.0	1.0
High power transistor (e-b)	2.0	0.2

For integrated circuits, k_1 and k_2 are determined experimentally when possible. The constants for some common integrated circuits are presented in Table 16. For the case where test data is not available, typical values of these coefficients for different types of integrated circuits have been determined by tests and are given in Table 17. Tight integrated circuit manufacturing tolerances and standard circuit designs have allowed integrated circuits to be grouped by their technology into generic failure classes and their terminals categorized into one of the following types: input terminal, output terminal, and power terminal. The terminal failure model for integrated circuits is shown in Figure 55. The IC terminal failure model consists of a resistor representing the terminal's bulk resistance and voltage source representing the terminal's reverse breakdown voltage. Typical reverse breakdown voltages and bulk resistance for integrated circuits are listed in Table 17.

Table 16.
Measured Damage Constants for Some Typical Integrated Circuits

Device	Family	Input		Output		Power	
		k_1	k_2	k_1	k_2	k_1	k_2
CD4000AD	CMOS	0.762	0.355	0.0228	0.595	0.24	0.515
CD4024	CMOS	1.6	0.5	0.19	0.5	—	—
MC14000	MOS	1.99	0.184	1.5×10^{-4}	0.991	0.021	0.636
MC1678	ECL	0.2	0.5	—	—	—	—
7400DC	TTL	3.72×10^{-5}	0.955	0.837	0.354	—	—
74163N	TTL	3.5×10^{-1}	0.648	3.4×10^{-4}	0.791	3.9×10^{-4}	0.783
8228	STTL	8×10^{-3}	0.5	—	—	—	—
1402	PMOS	0.041	0.5	—	—	—	—
AM111	Linear	0.01	0.398	0.199	0.669	—	—
LM105H	Linear	3.3×10^{-3}	0.721	0.115	0.429	7.2×10^{-4}	0.877
MC1533	Linear	4.9×10^{-3}	0.566	0.72	0.89	6.4	0.23

Table 17.
Damage Constants and Failure Model Parameters for Various Logic Families
[EMP Assessment Handbook, 1980]

	Category				V_{BD}	R_S	Lower 95%	Upper 95%
	Family	Terminal	k_1	k_2	(V)	(Ω)	k_1	k_2
1	TTL	Input	0.00216	0.689	7	16	0.00052	0.00896
2		Output	0.00359	0.722	13	2.4	0.00098	0.013
3	RTL	Input	0.554	0.384	6	40	0.12	2.6
4		Output	0.0594	0.508	5	18.9	0.0096	0.39
5		Power	0.0875	0.555	5	20.8	0.026	0.70
6	DTL	Input	0.0137	0.580	7	25.2	0.0046	0.041
7		Output	0.0040	0.706	1	15.8	0.012	0.0136
8		Power	0.0393	0.576	1	30.6	0.009	0.17
9	ECL	Input	0.152	0.441	20	15.7	0.045	0.51
10		Output	0.0348	0.558	0.7	7.8	0.0031	0.397
11		Power	0.456	0.493	0.7	8.9	0.22	0.935
12	MOS	Input	0.0546	0.483	30	9.2	0.0063	0.47
13		Output	0.0014	0.819	0.6	11.6	0.00042	0.0046
14		Power	0.105	0.543	3	10.4	0.038	0.29
15	Linear	Input	0.0743	0.509	7	13.2	0.0054	1.01
16		Output	0.0139	0.714	7	5.5	0.0045	0.043

From the failure models for discrete semiconductors and integrated circuits, we find the failure voltage, V_F, and failure current, I_F, at the device terminals are expressed as follows:

$$V_F = V_B + I_F R_B \tag{17}$$

$$I_F = \left(V_B - \sqrt{V_B^2 - 4\,R_B P_F}\right) \Big/ 2\,R_B \tag{18}$$

where V_B is the terminal's breakdown voltage, R_B is the terminal's bulk resistance and P_F is the terminal's failure power given by Equation 16.

The conditions for failure to occur when a circuit is stressed by a discharge transient is as follows:

1. The discharge transient current produced at the terminals of a transistor, diode, or integrated circuit must be equal to or exceed I_F/D where I_F is obtained from Equation 18. D is a derating factor to account for the statistical variation in device failure thresholds. D is 3 for P_F values obtained using measured damage constants and D is 10 for P_F values obtained using damage constants from generic data tables (Table 16) or those obtained from analytical expressions [Durgin, 1983].
2. Or the discharge transient voltage produced at the terminals of a transistor, diode, or integrated circuit must be equal to or exceed $V_F D$ where $V_F D = V_B + I_F R_B/D$ and D is the derating factor given above.

5.5.3 Recommended Analysis Approach for Anomalies

The recommended analysis approach for assessing where discharge induced anomalies are likely to occur and whether the anomaly would be transient or permanent is as follows:

1. Use the discharge coupling analysis results to identify all spacecraft interface circuits that are stressed by discharge transients.
2. Obtain the electrical specifications for each stressed interface circuit and its semiconductors.
3. Compare the discharge induced voltage, current, and transient pulse width with the circuit and semiconductor specifications following the procedure to determine if circuit upset can occur. If circuit upset is possible, then evaluate the circuit's function and the function of circuits that it feeds into to identify all the anomalies that can be produced by this circuit upset. Next, determine if the anomalous condition would be self-correcting, could be corrected from the ground (if not self-correcting) or would be permanent.
4. For interface circuits that can upset, compare the discharge voltage or current induced at the terminals of circuit semiconductor with the semiconductor failure voltage or current obtained for the induced transient pulse width to identify interface semiconductors that can also be damaged. If semiconductor damage is

possible, then evaluate the possible permanent anomalies that the damage could produce.

5.6. Evaluating the Direct Impact of Surface Charging on the Spacecraft Mission

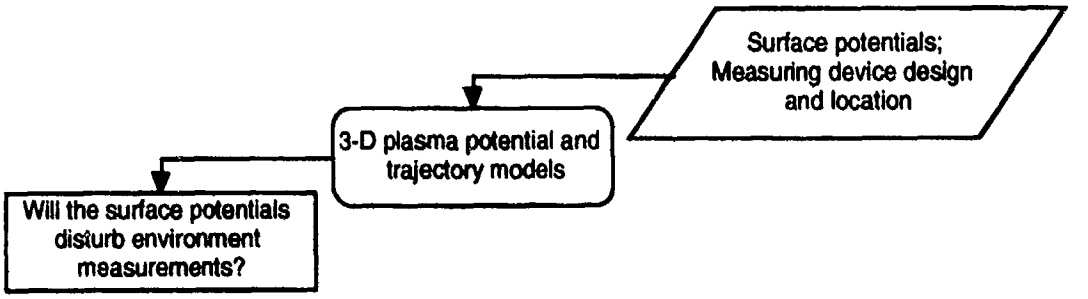

Figure 56. Surface charging can directly affect the spacecraft mission. An assessment of this impact must be made.

Only on a few spacecraft does surface charging itself interfere with the spacecraft mission. The primary cause for concern is spacecraft carrying instruments intended to measure the plasma environment.

The trajectories of charged particles are determined by the local electric and magnetic fields. Charged spacecraft surfaces can create high enough electric fields, which affect the trajectories.

Suppose a particle detector were placed on the side of the spacecraft discussed in Section 5.1.2. In particular, suppose this detector is in the center of the side facing the sun at the time modeled. This would be the east or the west side, depending on if the model is for mid-morning or mid-afternoon. Figure 57 shows the potential contours in a plane along the surface of this side and in two mutually perpendicular planes that are perpendicular to the surface and pass through the center of the spacecraft side. The potential at the detector is -651 V. The fields parallel to the surface will affect trajectories. The files used to do the calculations shown here are in Appendix C.

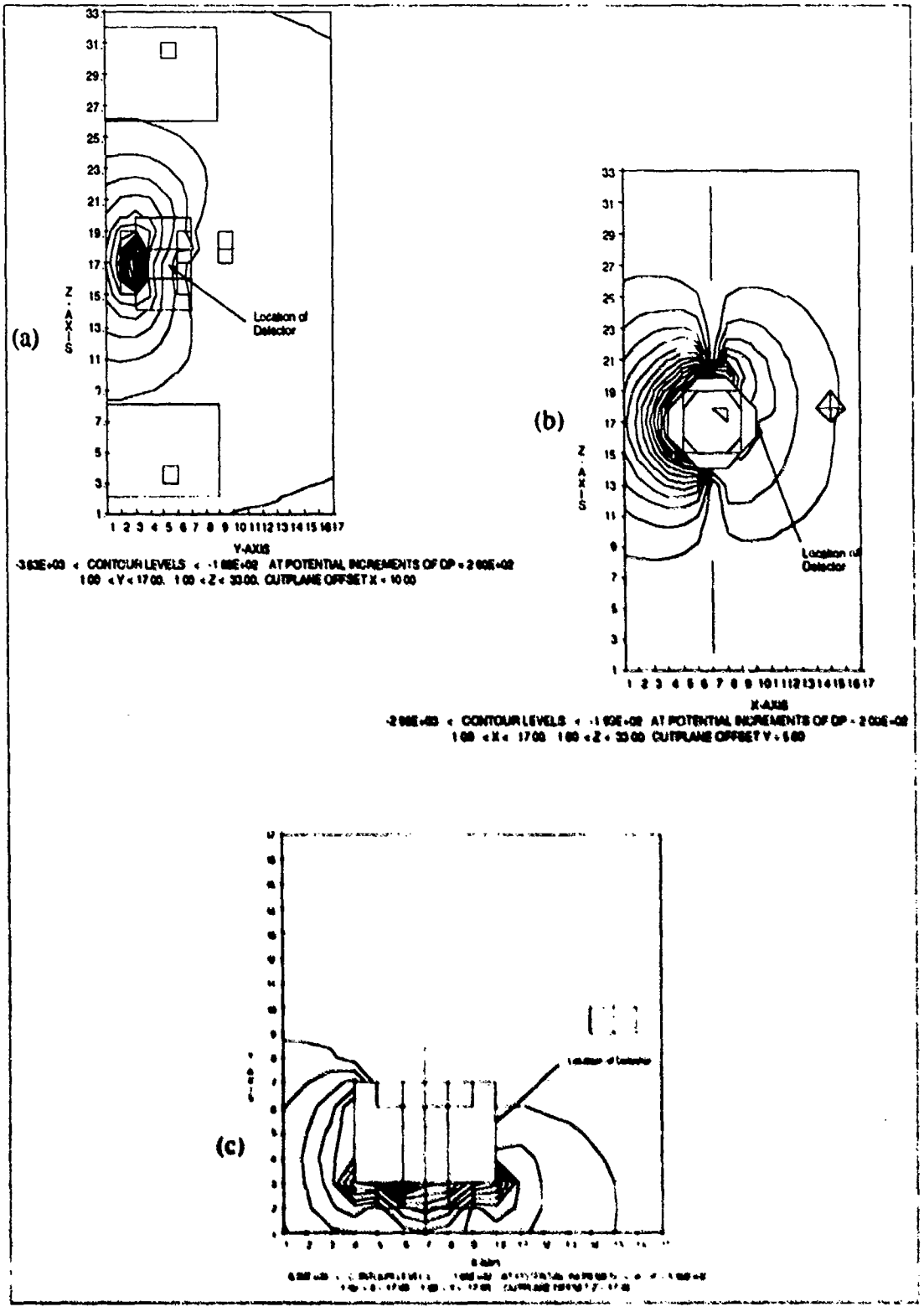

Figure 57. Potential contours in a plane along the surface of the side with the detector (a) and in two mutually perpendicular planes that are perpendicular to the spacecraft surface and pass through the center of the detector (b and c)

Figure 58a shows trajectories of electrons that strike the detector with normal incidence with energies from 100 eV to 1 keV (spaced logarithmically). For electrons below 1 keV, the detector is in the electrostatic shadow of the antenna mesh and boom structure. From these trajectories alone, the spacecraft potential would appear to be +1 kV, because no electrons of lower energy are detected. In actuality, spacecraft ground is at –200 V and the detector is at –651 V. Figure 58b shows higher energy electrons whose trajectories are less disturbed.

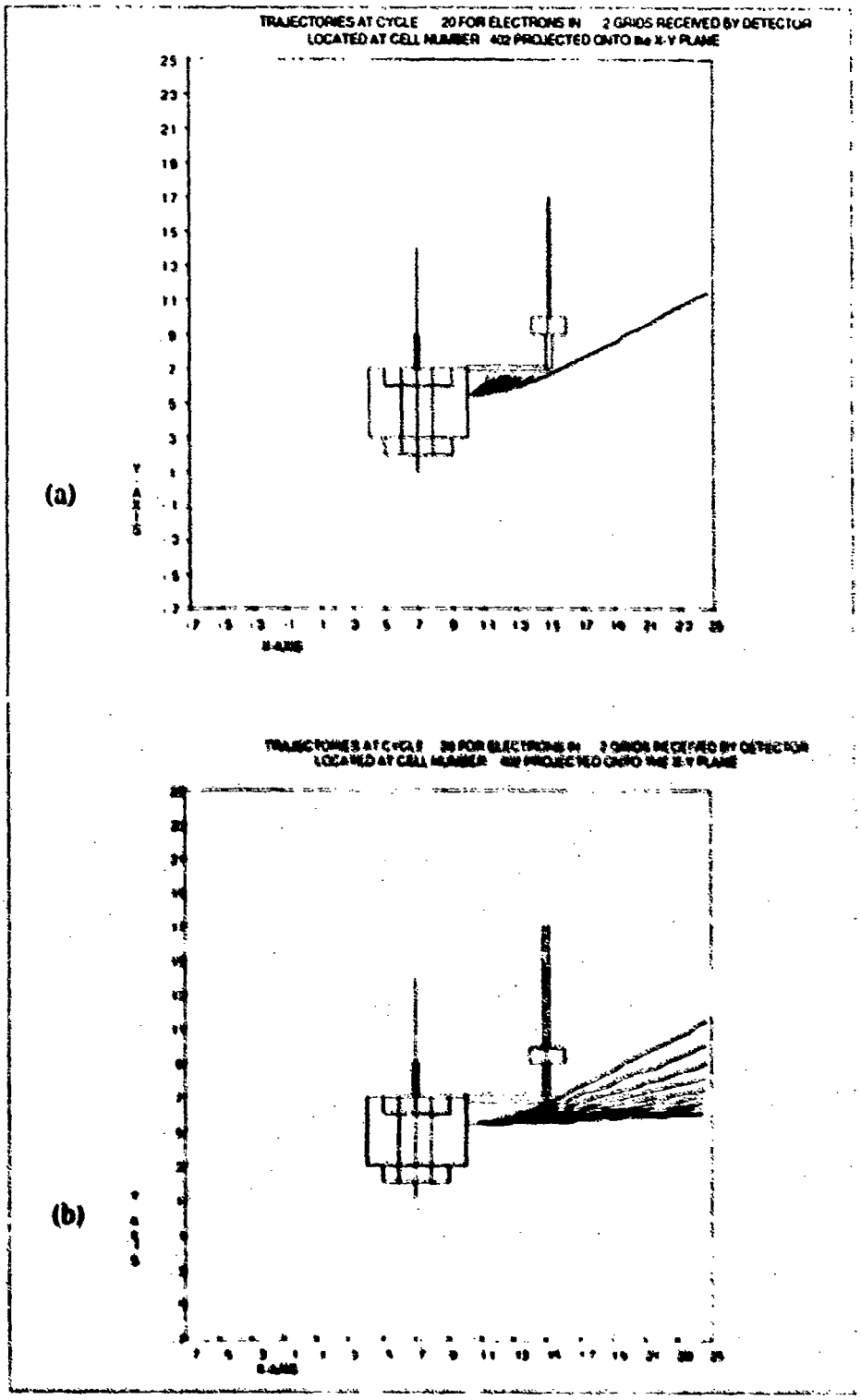

Figure 58. Electron trajectories for electrons that strike the detector with normal incidence with energies from 100 eV to 1 keV (a) and with energies from 1 keV to 10 keV (b)

To further illustrate the problems that can be encountered with particle detectors, Figure 59 shows trajectories for the same particles as Figure 58 for the same spacecraft

with all the surfaces at -651 V. Even with no differential charging, the particle trajectories are disturbed. Here the electrons are bent the other way by the fields.

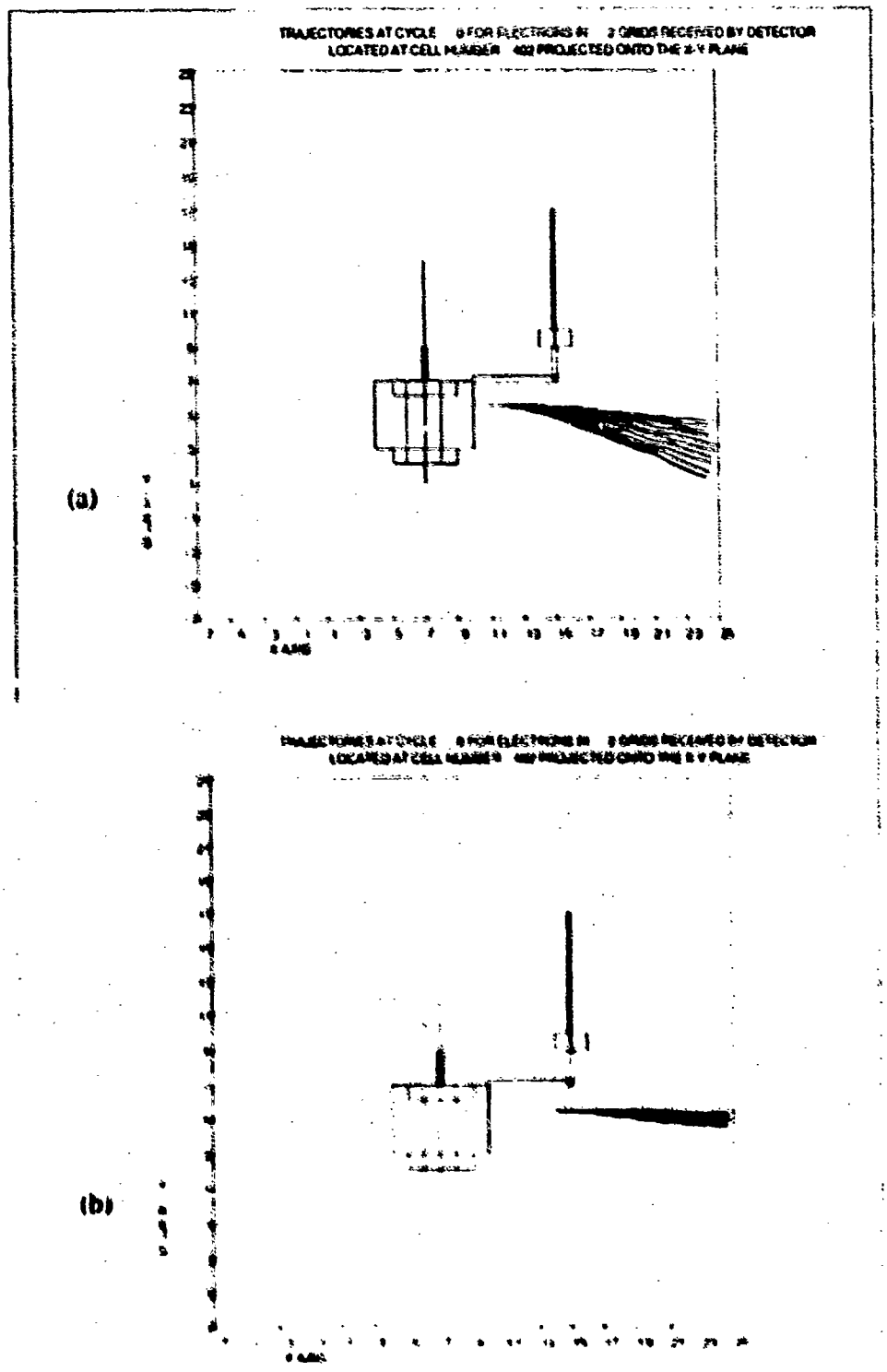

Figure 59 Electron trajectories for electrons that strike the detector with normal incidence with energies from 100 eV to 1 keV (a) and with energies from 1 keV to 10 keV (b)

If care is taken in the design of the spacecraft and the placement of the particle detectors, particle detectors can yield much useful information about the spacecraft environment. However, care must be taken in both the design stage and during interpretation of the measurements.

5.7. Impact Assessment

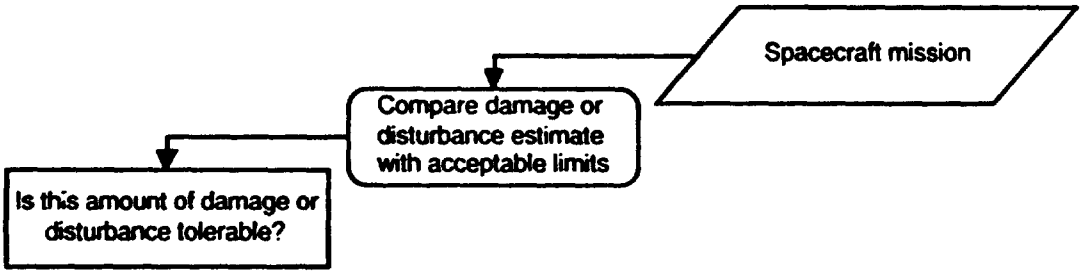

Figure 60. An assessment of the impact of damage or disturbance on the mission and a decision regarding the acceptability of the impact must be made.

The final step of any analysis is to determine the implications of the analysis to the spacecraft program. A minimization of the potential impact on the spacecraft mission due to disturbance or damage to the spacecraft from spacecraft surface charging effects is the desired end result of any analysis.

The likely impact on the spacecraft mission must be compared with acceptable design limits. The comparison may reassure the designers, builders, and ultimate users of the spacecraft that spacecraft surface charging is unlikely to interfere with the mission in an unacceptable way. The comparison may also point out some areas where changes may be needed or special care taken. An examination of the result of an analysis done before the spacecraft design becomes fixed can suggest possible mitigation approaches that do not interfere with other aspects of the design.

For all analyses, if the likely impact on the spacecraft mission exceeds acceptable design limits, mitigation techniques must be employed to eliminate the possible discharge sources and to reduce the coupling between possible discharge sources and stressed interface circuits.

An analysis done late in the design process should identify susceptible design areas and locations for testing and quantify representative test levels. In this manner, test levels and test locations can be an accurate representation of spacecraft surface charging effects on the spacecraft. The testing can then reassure the designers, builders, and ultimate users of the spacecraft that spacecraft surface charging is unlikely to interfere with the mission in an unacceptable way. The tests may also point out some areas where changes may be needed or special care taken.

Chapter 6
Testing

Testing is the final component of a spacecraft surface charging protection program. The necessary tests are divided into the following four types of testing: material property determination, material discharge response testing, ground continuity testing, and discharge immunity testing. Each of these types of testing is described below.

6.1 Material Property Determination

The charging rate and the maximum potential reached are functions of the properties of spacecraft surface materials. The material properties that determine the charging response of the surface materials are the secondary emission yield, the backscatter yield, the photoelectron yield, the conductivity, the dielectric constant, and the thickness. For common spacecraft materials, the measured values of some of these properties are given in the literature [Wall et al., 1977] or are available from the manufacturers of the materials.

For new spacecraft materials one or more of the listed material properties will likely not be available and must be measured. When measurements of these material properties must be made, the standard test techniques available in technical references and test books should be used for the measurement. The bibliography of this document lists references that describe some of the standard test methods used for material property determination. Since spacecraft surface materials are mainly insulators, the measurement technique used to measure the conductivity (or resistivity) must be appropriate for low conductivity (or high resistivity). Any necessary material property determination tests for spacecraft materials should be specified in the spacecraft surface charging test plan. The plan should contain the material property test technique, test setup, and instrumentation for the material property tests.

When evaluating the reliability of published data or that determined from new measurements, it is important to consider that the material properties can vary from sample to sample, one location to another (due to non uniformity), over time, and with environmental exposure. For instance, the conductivity of kapton has been shown to increase after long term exposure to the space environment [Leung et al., 1985]. The atomic oxygen of low-altitude polar orbit can oxide surface materials, reducing their conductivity. Debris and meteoroid particles can erode protective layers.

6.2 Material Discharge Response Testing

Material discharge response testing is performed when measurements of the discharge susceptibility of spacecraft surface materials and coatings [Balmain et al., 1985; Goldstein et al., 1982] the transient currents produced by discharge of the materials [Bogorad et al., 1990; Levy and Sarrail, 1987; Snyder, 1986] or the radiated fields produced by the discharge transients [Leung, 1984; Leung and Plamp, 1982] are needed.

A typical test setup for discharge response testing is shown in Figure 61. The discharge response test setup generally consists of a vacuum chamber to provide the vacuum environment of space, an electron gun to provide the electron charging environment, current probes to measure the discharge current, a faraday cup to set the electron beam density at the test sample, a high-voltage probe to measure the charge voltage of the sample, antennas to measure the discharge radiated fields, and a collection electrode to measure the blowoff charge produced by the discharge. The test sample is normally a small section of the spacecraft material to be studied. It is attached to a conductive holder that represents the spacecraft structure. The holder is placed on a dielectric stand and often grounded with a ground strap [Balmain and Dubois, 1979]. In some cases the holder has been resistively terminated to ground [Wilkenfeld et al., 1981] or resistively connected to a bias supply along with a capacitor-to-ground termination [Levy and Sarrail, 1987]. The test instrumentation used to connect to the current probe and to measure the discharge current is the same as the transient measurement equipment used for discharge immunity testing given in Section 6.4. Test instrumentation that connects to the antennas and measures the discharge radiated fields consists of a spectrum analyzer or a wide-band heterodyne detector as described in Leung and Plamp [1982].

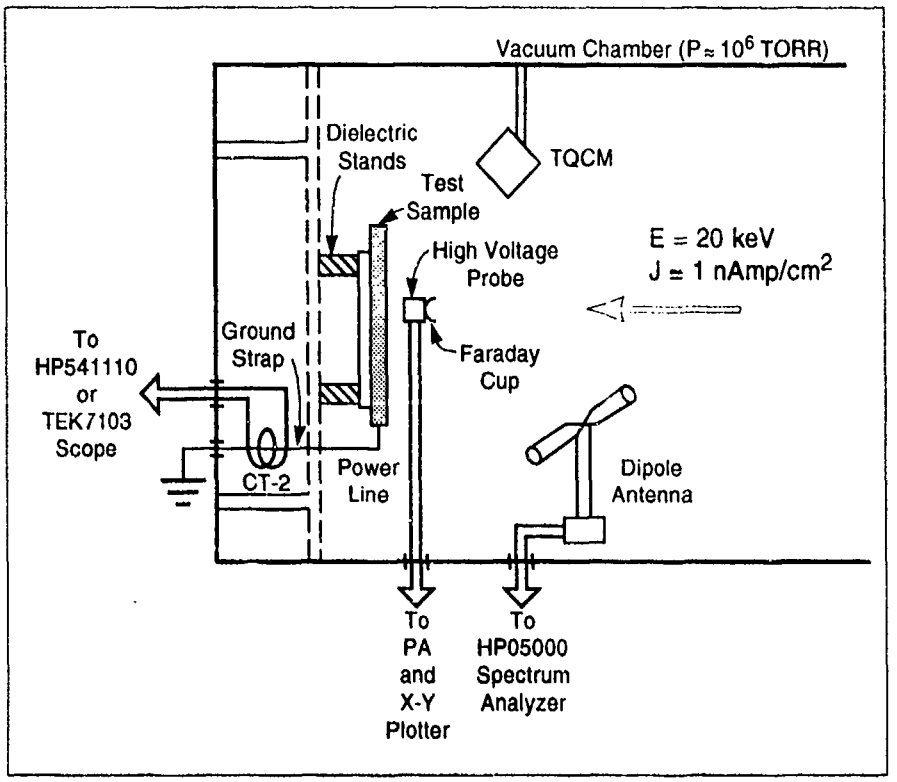

Figure 61. Test setup for surface material discharge response tests (based on [Bogorad et al., 1990]).

6.3 Ground Continuity Testing

Grounding is one of the key design techniques used to prevent charge buildup [Gore, 1977; Ling, 1977; Purvis et al., 1984]. The continuity of the spacecraft grounding system depends on the construction techniques used and the care in handling. Testing is usually necessary to insure that ground continuity exists and that the grounding resistance does not exceed the required level. The ground continuity tests including the test methods to be used, the test setup, and the test instrumentation should be described in the spacecraft surface charging test plan.

Thermal blankets often have thin coatings of conductors such as conducting paint and indium tin oxide (ITO). The coating can be very fragile and easily damaged by handling. When blankets are installed and when they are extensively handled, disturbed, or adjusted, they should be tested to verify their continuity.

Each ground strap should be tested for continuity at installation and each time it is adjusted. All bonds should be tested to verify continuity at the time the bond is made.

Besides testing during assembly, ground straps, bonding, and conducting surfaces should be tested for continuity before discharge testing is begun.

6.4 Spacecraft Discharge Immunity Testing

The most authentic ground-based method of qualifying spacecraft for spacecraft surface charging related discharges would be to expose an operating spacecraft to a true simulated space plasma environment during ground tests. This qualification technique has been used for a few spacecraft. However, it has been found to be not realistic because of our inability to reproduce the space environment causing spacecraft charging and discharging on the ground. Additionally this qualification approach is extremely costly, difficult to implement on a routine basis due to simulation and handling requirements, and requires extensive test facilities [Wilkenfeld et al., 1981].

An evaluation of various discharge qualification test methods has determined that the most practical and technically sound approach for spacecraft surface charging related qualification tests is global discharge immunity (GDI) involving direct current injection onto the spacecraft that simulate the currents caused by surface material discharges [Wilkenfeld et al., 1981]. The advantage of GDI testing is that it is a true system test, can be performed at threat levels, simulates many of the electromagnetic effects produced by discharges, and is consistent with present EMP test practices. GDI testing is the recommended test technique for qualifying spacecraft against spacecraft charging related discharges and is the test technique described below.

6.4.1 Spacecraft GDI Test Plan

GDI spacecraft charging tests are performed by applying a series of current injections to selected locations about the spacecraft, and monitoring the effects of these injected transients on critical system functions. Test instrumentation is installed to monitor system functions and verify safety margins. Injection locations, the coupling methods, and the injection pulse parameters are selected either from an analysis of the spacecraft or are taken from a control document.

The test plan includes at least the following:

1. Critical measurement test points that must be monitored to demonstrate safety margins. (Determination of these points is part of the Spacecraft Analysis Plan.)
2. Failure criteria and limits. (Determination of these is also part of the analysis plan.)
3. Expected wire and structural responses at monitoring points. These are compared to failure thresholds to determine anticipated safety margins.
4. Specification of the critical points to be stressed. (Determination of these is part of the analysis plan.)
5. Test configurations and procedures for all electronic and electrical equipment installed in, or associated with, the system and the response for operations during tests, including switching.
6. A description of all nonstandard equipment such as pulsers, data links, or sensors that cannot be found in referenced manufacturer's equipment manuals or data

sheets. Where available, appropriate manuals or data sheets, can be cited for standard test equipment.

7. Implementation and application of test procedures that include vehicle configuration, modes of operation and monitoring points for each subsystem and operation of test equipment.
8. Data recording requirements.
9. Methods and procedures for data measurement and analysis.
10. A safety plan whose objective is to prevent inadvertent damage to the spacecraft and to ensure personnel safety during the operation of the high voltage/high current power supplies specified in the test.

A post-test analysis in which the measured electrostatic discharge safety margins for critical monitoring points are compared to predictions is part of the test plan. When these margins are negative, impact on vehicle performance is part of the analysis. Where the measured electrostatic discharge safety margins are less than the 6 db required, identification of necessary changes to ensure compliance should be identified.

Test levels should be 6 db (energy) overstress by the injected current above that produced by a worst case discharge occurring at that site for the specified charging environment. Identification of discharge sites, discharge characteristics, and predicted system structural current responses can be determined by the analysis methods discussed in Chapter 5.

6.4.2 Test Setup and Spacecraft Test Configuration

The general test setup for GDI testing is shown schematically in Figure 62. The test setup consists of a high voltage pulser, the spacecraft coupler for injecting current on the spacecraft, test instrumentation data link, command and control data link, the test instrumentation, and the aerospace ground equipment (EAGE). The test should be performed in a large open area such as a high bay. The spacecraft should be in its on-orbit configuration (e.g., with antennas and solar panels extended) in an open area on a dielectrically isolated stand as far away from conducting boundaries as possible. It is recommended that the minimum height of the stand platform be comparable to a center body dimension and that the clear space above the vehicle be similar. The minimum clear space around the satellite should be comparable to the tip-to-tip wing dimension for 3-axis stabilized spacecraft and several body diameters for a spin stabilized vehicle. As a rule of thumb, the capacitance of the vehicle to ground should be no more than twice its capacitance to infinity. The spacecraft coupler can consist of a hardwire connection via a grid of wires [Wilkenfeld et al., 1981] or a coupling capacitor formed by a test ground plane and the metal structure (or portion thereof) of the spacecraft.

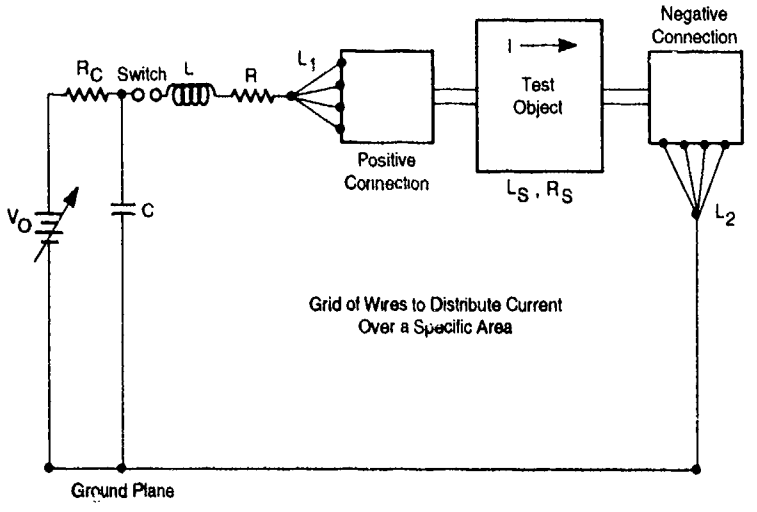

Circuit Elements

V_o	Adjustable power supply with output up to approximately 20 kV
R_c	Charging resistor, typically 100 kΩ
C	Drive capacitor, typically 0.0001 to 0.2 μf, depending on circuit requirements
L	Lumped inductance added if necessary for wave shaping
R	Lumped resistance added if necessary for wave shaping
L'_1, L'_2	Inductance of the connection grids
L_s, R_s	Inductance and resistance of the test object between pulser connection points
I	Current flowing on the test object that simulates the replacement currents flowing as the result of blowoff

The ground plane is to simulate plasma current return paths to the circuit.

The switch is an adjustable, self-breakdown, high-voltage spark gap.

Figure 62. Direct-drive setup for electrostatic discharge simulation testing.

During electrical injection, the vehicle should be electrically isolated from its environment except for controlled impedance paths between the pulser and test object, and test object to common ground as shown in Figure 62.

During testing, the spacecraft should be powered from its internal batteries, and system command and telemetry data that indicates system status should be transmitted via the Radio Frequency (RF) Command and Control links between the spacecraft and the EAGE. The spacecraft surface electric and magnetic field sensor outputs and critical test point current sensor outputs should be transmitted via fiber optics or equivalent isolated data links.

6.4.3 Pulse Injection Method

Pulse injections onto the satellite are made via the hardwire coupler or the capacitive coupler. The selection of which injection scheme to use for exciting a candidate discharge area is made on the basis of an electromagnetic (EM) coupling analysis. The coupling analysis is to determine which aspects of the EM energy produced by the discharge site are important in coupling to nearby spacecraft conductors or points-of-entry (POEs) associated with sensitive electronics. The hardwire coupler is the preferred pulse injection method, if it is necessary to simulate the surface current excitation resulting from the circulation of several-hundred-ampere, microsecond-wide pulses caused by electron blowoff from a large area. Capacitive excitation is better, where excitation of system resonances or normal electric fields is the important coupling mode. The critical test points are the spacecraft dielectric surfaces that are found to be susceptible to discharge by the spacecraft charging analysis.

Unfortunately, neither current injection method provides a uniform global simulation of the electrostatic discharge excited fields on the surface of the spacecraft. The simulation fidelity will vary with spacecraft location and injection method. Thus one may find that a particular selected injection technique and injection point may not provide a correct simulation of fields in another area of interest. Therefore, the coupling analysis may suggest additional points of excitation beyond those determined from the charging analysis to complete the test simulation process.

6.4.3.1 Pulser Injection Points

The following steps define the details on injection points to which the pulser (including the wave shaping network) is attached to the spacecraft.

1. The results of the charging and coupling analyses are used to select the appropriate injection locations to attach the positive and negative leads of the pulse generator (hardwire coupling) or the position and spacing of the coupling plate (capacitive coupling).
2. For each injection location, the coupling analysis results are used to define the surface area over which current is to be injected. This surface area then is used to determine the appropriate number of wires required in each grid (direct injection) or the size and shape of the drive plate (capacitive coupling). The wire grid can be a continuous resistively loaded structure with a total resistance, R', and inductance, L', set to provide both pulse shaping and impedance matching.
3. The coupling connection should be adequate to inject current over the same areas as that which participates in the discharge. This may require driving an entire solar array panel or a thermal blanket.
4. For hardwire injection, L'_1 and L'_2, the total inductance respectively of the wire grid connection to the pulse generator and the return at each injection location, should be measured or calculated. Where current is returned to ground by

capacitive coupling, the coupling of the test object to the ground should be determined and adjusted as required.

5. Calculate or measure the spacecraft inductance, L_s, and resistance, R_s, between each injection location and return location.
6. The wire grid used for hardwire injection should be attached to the conducting substrate surrounding the dielectric surface and not to the dielectric surface itself.
7. Conventional circuit analysis should be performed on Figure 63 (which is the equivalent circuit of Figure 62) to compute the values of V_o, R_c, R, L, C (and C_c for capacitive injection), required to drive the spacecraft with the desired current magnitude and wave shape. The analytical results obtained from analysis of Figure 62 are given in Appendix D.
8. The test setup shown in Figure 62 should then be implemented based on the information and circuit values determined in Steps 1 through 7 above.

6.4.4 Test Instrumentation

The high voltage pulser is to be a capacitive discharge pulser followed by a wave form shaping network, as shown in Figure 63. The pulser can be a self-contained unit such as the ELGAL 103 or one constructed from a high voltage power supply, a charging network, and a remotely triggered spark gap. The pulser must be capable of peak output voltages of 20 to 100 kV, peak currents of several hundred amps, and a pulse width (full width to half maximum (FWHM)) of greater than 1 μs. The component values for the wave shaping network are determined from the results of the circuit analysis performed in Section 6.4.3.1, Step 7.

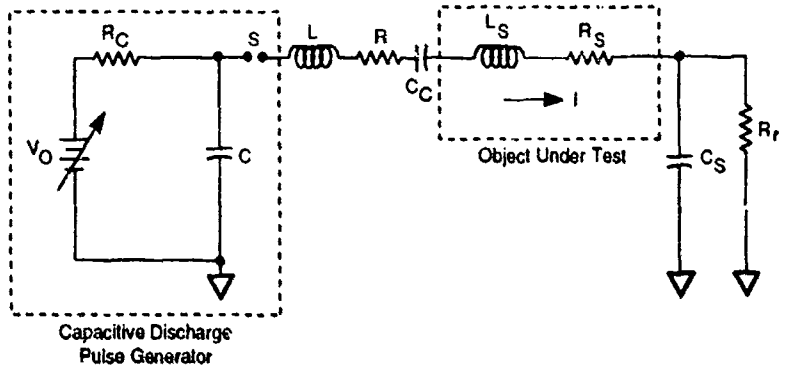

Adjustable Circuit Parameters

V_o	Adjustable charging voltage
R_c	Charging resistor
C	Drive capacitor
L	Added inductance for wave shaping
R	Added resistance for wave shaping
C_c	Capacitive coupling between pulse generator and test object
L_s	Nominal inductance of test object
R_s	Nominal resistance of test object
C_s	Capacitance between test object and pulse generator ground
I	body current of test object that is charging current for C_s
R_r	Resistance of return line to ground
S	Spark gap

For direct drive, C_c and C_s are removed from circuit.

Figure 63. General capacitive discharge injection model.

Spacecraft operation during testing is determined through the on-board status monitors of the telemetry system with the data being transmitted via the telemetry radio link to provide electrical isolation. Comprehensive post-test functional performance checks are made using a direct cable link from the spacecraft to the vehicle EAGE.

Other measurements to be made during the tests are pulser source measurements, local EM environment measurements and EM coupling measurements. The source measurements consist of the discharge voltage of the pulser and the drive current. If multipoint drive is employed, then measurement of the current through each of the individual drive wires may be desired. A summary of representative source measurements is given in Table 18 and typical instrumentation is given in Table 19.

Table 18.
Source Measurements

Measurement	Charging voltage	Drive current	Wire currents
Type	DC voltage	Pulse current	Pulse current
Representative Characteristics	50 kV DC	I_p<1000 A, $\tau_p \leq 5$ μs	I_p/n, $\tau_p \leq 5$ μs
Location	High potential side of C	Pulser output	Wires on drive plate
Sensor	High-voltage probe	Current probe	Current probe
Connection	Hardwired	Hardwired fiber optic link	Hardwired fiber optic link
Recording	Voltmeter	Digitizing oscilloscope or oscilloscope and transient digitizer	Digitizing oscilloscope or oscilloscope and transient digitizer
Comments	Removable during test	Removable during test	Removable during test

n = number of drive wires

Table 19.
Typical Test Equipment for System Spacecraft Charging Related Discharge Tests

Equipment Mfr.	Model	Frequency Range		Other Characteristics	Comments
RF Amplifiers					
Avantek	AWL 500	0.001-500 MHz		26 db gain, input voltage ±30μV-22 mV	
Hewlett Packard	8447D, E	0.05-1300 MHz		26 db gain, input voltage ≤ ±20 mV	
Oscilloscopes					
Tektronix	TDS 520	0-500 MHz		Input voltage sensitivity 1 mV/diV	Digitizing oscilloscope
	2420	0-100 MHz		Input voltage sensitivity 200 μV/diV	"
Hewlett Packard	54510A	0-250 MHz		Input voltage sensitivity 1 mV/diV	Digitizing oscilloscope
	54511D	0-500 MHz		Input voltage sensitivity 1 mV/diV	"
	54502A	0-100 MHz		Input voltage sensitivity 2 mV/diV	"
Analog Fiber Optic Links					
Tesco	OAM04	200 Hz-250 MHz		Includes programmable attenuators in 3 db steps	
EG&G	ODS-F	1 KHz-150 MHz		Includes programmable 40 db amplifier, programmable attenuator	
Coaxial Switches					
Nowack		0-300 MHz		8 in, 1 out	Mechanical
Matrix		0-300 MHz		8 in, 1 out	Programmable
Daico	100C1159	0-250 MHz		8 in, 1 out	Mechanical
Pulse Generators					
Elgal	EM 103			V_{max} = 100 kV, I_{pk} = 10 kA (50 Ω), $t_r \geq 8$ ns, t_f = 12.5 μs	
	EM101/ 1012 exp			V_{max} = 20 kV, I_{pk} = 2 kA (50 Ω), $t_r \leq 10$ ns, $t_f \leq 5$ μs	
Active Integrator					
EG&G	IA-300	0.4 kHz-200 MHz		6 db insertion loss	
Balun					
EG&G	DMB-3	20 kHz-1 GHz			
D Sensor					
EG&G	CFD-1	> 300 MHz (3 db)		200 A/m²	
	HSD-3	> 150 MHz (3 db)		10^3 A/m² max time rate of change	
B Sensors					
				Maximum Field Change (Teslas/Second)	
EG&G	CML-3	≤ 632 MHz (3 db)		2×10^7	For surface current measurements
Prodyne	CML-X3	≤ 700 MHz (3 db)		6×10^6	
	CML-X5	≤ 500 MHz (3 db)		3×10^6	
	CML-6	≤ 175 MHz (3 db)		6×10^5	
Surface Current (H) Sensors					
			Peak Current (A)	*Nominal Z (Ohms) into 50 Ohms*	
TEGAM	95210-1	0.1-100 MHz	300	3	
	95210-2	0.1-100 MHz	300	3	
Fischer	F-91	1-100 MHz	500	0.1	

Table 19.
(Continued)

Equipment Mfr.	Model	Frequency Range		Other Characteristics		Comments
Clamp On Current Probes						
			Peak Current (A)	*Nominal Z_t (Ohms) into 50 Ohms*	*Gap (Inches))*	
TEGAM	91550-3	0.01-100 MHz	500	0.033	1 1/4	For measuring currents on struts and cable bundles
	91550-4	0.02-100 MHz	500	0.1	1 1/4	
	91550-5	0.1-100 MHz	100	1.0	1 1/4	
	91550-7	0.01-150 MHz	4000	0.003	1 1/4	
	93686-2	0.01-50 MHz	100	5	2 5/8	
	93686-3	0.01-140 MHz	100	2	2 5/8	
	93686-4	0.01-100 MHz	500	0.06	2 5/8	
	93686-4M	0.01-100 MHz	5000	0.005	2 5/8	
	94430-1	0.01-250 MHz	70	8	3/4	
	94430-2	0.01-250 MHz	10	1	3/4	
	94430-3	0.01-250 MHz	500	0.1	3/4	
	94430-4	0.01-250 MHz	500	0.05	3/4	
	94456-1	0.01-100 MHz	100	5	4	
	94456-2	0.01-100 MHz	200	1	4	
	94456-3	0.01-100 MHz	500	0.1	4	
	94456-4	0.01-100 MHz	500	0.06	4	
Tektronix	CT-1	0.3-1000 MHz	100	5		For individual wire measurements
	CT-2	1.2 kHz-100 MHz	100	1		"
Voltage Probes						
			V_{max} (V)	*Attenuation*	*Impedance (MΩ, pf)*	
Tektronix	6015	DC-75 MHz	± 20,000			For high voltage source measurements
	P6046	< 100 MHz	± 50	1X,10X	(1,10),(10,3)	Diff/Amp
	P6201	< 1 GHz	± 60	2X,10X,100X	(0.1,3),(1,1.5),(1,1.5)	FET
	P6202A	< 500 MHz	± 60	10X,100X	(10,2)	FET
	P6230	> 1 GHz	± 30	10X	450 Ω, 1.3 pf	50 Ω
	P6057	> 3 GHz	± 50			50 Ω
	P6106A	< 300 MHz	± 500	100X	5 kΩ, 1.1 pf	Passive, Bandwidth decreased to 153 MHz for 3M code.
				10	(10, 10.5)	

The pulser source is calibrated by measuring the pulse output current into a short circuit and a known load. The current probe output should be transmitted back to the transient data recording system via fiber optics or a semi-rigid coaxial cable.

To validate the test results, one must ensure that the desired electromagnetic environment is reproduced on the outer surface of the spacecraft. The critical parameters to be measured are the tangential magnetic field $\mathbf{H}_t$, which is proportional to the surface current density $\mathbf{K}$, and the normal electric displacement $\mathbf{D}_n$, related to the surface charge density. In addition, it is useful to measure boom currents. The joints between the spacecraft and booms on which antennae or the solar array panels are mounted often serve as a major penetration for the coupling of energy into the interior of the spacecraft.

Surface current measurements for surface currents of significantly large magnitude and in absence of ionizing radiation, can be made with surface current sensors like the

TEGAM 95210–1 or 95210-2. These small, surface mounted sensors have an active area of about 1/4 to 1/2 square inch. If sensitivity is a problem, then $\dot{B}$ or $\dot{J}$ sensors, which measure the rate of change of B or magnetic induction field can be used. Specifications for the 95210 surface current sensors and the CML $\dot{B}$ sensors are provided in Table 19.

One problem to be faced with using sensors that measure time rate of change is that the relative amplitude of the higher frequency components is magnified, even though these components contain relatively little energy. Therefore it is advisable to integrate the output of these sensors, where possible, using active integrators (such as the IA-300) with time constants long compared to pulse width (about a factor of 10 is recommended).

The rate of change of the normal displacement field or surface charge density $\dot{D}_n$ can be measured with a surface mounted sensor like the CFD-1 or the HSD-3 $\dot{D}$sensors.

Currents flowing along booms or cable bundles can be measured by clamp-on current sensors such as those given in Table 19.

Some of the sensors such as the CML $\dot{B}$ sensors have differential outputs. A balun such as the DMB-3 or impedance matching transformer is required to convert the output from double-ended to single-ended. The sensors should be mounted directly on the satellite surface or boom. This may pose practical problems for means of adhesion and avoidance of surface contamination. Signal cables should be run from these sensors to the fiber optic data links in a manner least likely to perturb the electromagnetic environment, i.e., along ground planes. The use of radio frequency tight, semi-rigid Cujack or Aljack cable and locking connectors for the sensor signal cable runs to the fiber optics is recommended.

Monitoring of specific response points should be done in addition to performance data that may be received via the spacecraft telemetry. Given the mode of electrostatic discharge coupling, the monitoring points are most likely to be the currents and voltages on critical signal lines, or at inputs to the interface circuits of critical functional units. The measurements are of two types, currents on individual wires and input voltages at critical box pins. A variety of standard current and voltage probes are available to perform these measurements. A representative set of these is given in Table 19.

These measurements must be implemented without disturbing the operation of the spacecraft. Practically, this may mean modifying cable bundles by including interior wires on which can be mounted current probes, putting monitoring points in critical circuits that can be accessed through box pins, or by providing breakout boxes that interface between the normal cable harness and the input connectors of the box under test. These boxes contain necessary current and voltage sensors, coupling circuitry to isolate the measured cable or test point from the measuring device, and output connectors. The output of the sensors is then run via separate cables back to a J-box located at the satellite where the coaxial switches and fiber optic or other data transmission links are gathered. The breakout box approach has been used to perform SGEMP electrical testing [FLTSATCOM Phase II Experiment Plan, 1981; Lowell et al., 1980]

In addition, it may be desirable to measure the internal electromagnetic environment of the spacecraft to ensure that it is correctly driven and to locate any points of entry. This may be done with the environment sensors previously described. In particular, it is useful to measure the currents flowing on interior cable bundles using one of the clamp-on

current sensors described in Table 19. This is because one of the major coupling modes is through the electrical and magnetic field penetration of cable shields to individual wires.

The signals to be monitored during testing are of two kinds: electromagnetic response data such as surface currents and electromagnetic fields and satellite telemetry data that indicates the status of system components. The former is relatively high frequency (1-200 MHz) analog data, while the latter consists of much slower digital data. The preferred test configuration described is one in which the spacecraft is electrically isolated except for current injection and return over paths with controlled characteristics. These requirements in turn determine the characteristic of the required data systems.

Transmissions of high frequency analog data should be via wide band analog fiber optic data links such as the OAM04 or the ODS-F fiber optics links. The type of system required consists of:

1. Wide band (DC-300 MHz), many in - one out coaxial switches
2. Wide band (0.01-150 MHz minimum) analog fiber optic data links
3. Digital controlled wide band RF attenuator, 0-60 db
4. Radio frequency amplifier; 2-26 db gain, 0.01 to 500 MHz (3 db bandwidth)
5. Digital fiber optic control link
6. Digital control circuitry.

The function of these systems is to provide a means of monitoring several critical points with one data link. Because the range of possible signal amplitudes is large, it is necessary to provide both amplification for small signals and attenuation for large ones as the normal operating range of the LED in the FO transmitter is typically $\pm$ 5 to $\pm$ 500 mV and often less. The systems can monitor signals from a few hundred microvolts to 1 kV over a bandwidth of 0.01-150 MHz.

Spacecraft status information during testing should be provided by the spacecraft telemetry system. To provide for electrical isolation, this information should be transmitted via the spacecraft's radio frequency links. In some cases it may be desired to use the EAGE to supplement or in place of the spacecraft telemetry to monitor system status during the discharge testing. If the EAGE is used during testing, the hardwire link between the spacecraft and the EAGE must be isolated via ferrite isolators such as that described by Siedler et al. [1981a; 1981b] or other suitable isolation techniques to prevent coupling of discharge transients to the EAGE during testing.

Generally, fast transient data should be recorded on oscilloscopes and cameras, transient digitizers, or digitizing oscilloscopes. Transient digitizers or digitizing oscilloscopes are preferred as both an analog and digital signal are obtained and the digitized data can be displayed on a digital plotter. The digital signal can also be stored and processed off-line with the data obtained from the spacecraft telemetry. To avoid degradation, the bandwidth (upper 3 db point) of the oscilloscopes and digitizers should be as high as possible. While the major discharge response currents have characteristic frequencies of 1 to 20 MHz, vehicle structural resonances can exceed 150 MHz. It is recommended that transient recording devices have a minimum bandwidth of 100 MHz and should preferably be 200 MHz or above.

6.4.5 Test Conduct

The following steps form the major elements of the test:

1. A complete pretest functional checkout should be performed using the EAGE. The nature of the checkout is specified in the test plan.
2. The spacecraft should be disconnected from the EAGE and placed on battery power and the radio frequency telemetry system for command and status monitoring should be activated.
3. A series of electrical injections should be performed according to the steps given. During injection, the vehicle should be operated in representative on-orbit flight modes and in the on-orbit configuration. The spacecraft's on board housekeeping capability should be used to monitor its behavior for out-of-spec operation.
4. At the end of a series of injections at a given point and drive level, a quick look functional checkout of the spacecraft should be made before performing tests at the next drive level. The nature of this checkout should be specified in the test plan.
5. Following the complete series of electrical injection tests, the spacecraft should be reconnected to the EAGE and the system functional tests performed in Step 1 should be repeated.

The assumptions on which the proposed electrical injection schemes have been based have been reviewed in Wilkenfeld et al. [1981]. For convenience they are summarized in Table 20. The primary one is that the principal electromagnetic driver in generating surface electromagnetic fields is the blowoff of electrons. From this premise, it is possible to predict the response of spacecraft-like objects if one makes certain assumptions about the emission characteristics of the blowoff charge (magnitude, energy and angular distributions, surface albedo, presence and characteristics of an associated plasma). However, these calculations have not been able to predict the response of real spacecraft. The prediction problem is enhanced for spacecraft with reentrant geometries such as booms and antennae, largely because of a lack of a well-validated discharge model, but also in part because of the inaccuracies inherent in trying to predict the response of complicated systems with simplified models. In addition, the number of cases for which a calculation has been performed is extremely limited. In a sense, response prediction is in its infancy.

Table 20.
Summary of Assumptions Used to Derive Current Source Terms

1.	The predominant mode of excitation is the blowoff of electrons.
2.	Punch through and flash over serve primarily to reduce the potential of the dielectric relative to the structure.
3.	The emitted electrons move in fields whose sources are electrons trapped in the dielectric, replacement charges and currents, and other emitted electrons.
4.	Spacecraft isolation ensures space charge limiting so that most electrons return to the structure, hence, current flow is limited, decreasing in amplitude and pulse width as the distance from the dielectric increases.
5.	A worst-case is taken to be the response of the satellite grounded for which the skin currents are equal to the blowoff currents.
6.	Following standard practice, replacement current characteristics are described by the scaling laws presented in Table 21.
7.	The scaling is based on mono-energetic, circular samples, grounded edges. Real samples show order of magnitude variations about the mean.
8.	Coupling is based on limited validation.
9.	More complicated environmental simulations (UV, high-energy electrons) typically diminish or eliminate discharging.
10.	Scaling laws may reflect the effect of typical test fluxes (1 nA cm^{-2}) that are much higher than the fluxes occurring in space.
11.	Real dielectrics do not show regular discharging patterns (edges, seams).
12.	Neglects plasma effects (Debye screening).
13.	Does not handle reentrant geometries.
14.	Probably worst-case.

Thus, one must fall back on the limited body of data that connects inferred discharge characteristics to the observed response of simple systems such as planar dielectric surfaces. On the basis of simple scaling laws, the simple coupling models, and the limited data base, one can derive predictions as to the anticipated skin currents generated because of electrostatic discharge, in particular dielectrics.

Therefore, in the spirit of doing what one can at this time with the available data base, these scaling laws have been adopted as the provisional injection current amplitude and pulse width characteristics. The specification as it stands is incomplete because no information is given on the normal electric fields associated with charge density. The coupling experiments described in Wilkenfeld et al. [1981] and Treadaway et al. [1980] did not measure this quantity. Planar sample measurements reported in Milligan et al. [1979] indicate that they can be tens of kilovolts per meter. The normal electric fields on the surface of the test objects can be calculated with the modeling approach described in Treadaway et al. [1980] and Keyser et al. [1978]. It would be useful to publish such data if it exists and to perform additional calculations and measurements for realistic spacecraft configurations.

The question of emission pulse characteristics has a crucial bearing on possible current injection and experiment configuration issues. If the blowoff discharges were smaller (say less than 50 A) and narrower (less than 200 ns) it would be more feasible to employ capacitive coupling in a threat level simulation. It might also be possible to use ferrite isolation of power supplies, data links and the satellite EAGE that would make experimental implementation much less complex.

6.4.5.1 Direct Injection Excitation

1. The critical stress points are to be driven by a direct current injection with direct return of the type specified above. The pulser circuit parameters are adjusted to yield an exciting pulse that has a maximum peak amplitude I_p and approximately equal rise and fall times $t_r = t_f = \tau_p$ chosen as follows in order of preference:
   a. Scaled values of I_p, τ_p based on laboratory electron spraying measurements on materials of the same type as used on the spacecraft. The laboratory data are scaled according to the area scaling laws given in Table 21 for FEP teflon, mylar, fused quartz and kapton. For other types of materials it can be assumed that:

$$\frac{\tau_p(\text{Drive})}{\tau_p(\text{Measured})} = \frac{I_p(\text{Drive})}{I_p(\text{Measured})} = \frac{A^{1/2}(\text{Spacecraft})}{A^{1/2}(\text{Test})}, \tag{19}$$

   where τ_p (Measured) and I_p (Measured) are the discharge pulse widths, and total return currents (edge + back plane) for the test sample of area A (test). I_p (Drive) and τ_p (Drive), are the corresponding current injection peak current amplitude and pulse widths for an actual spacecraft material configuration with a dielectric area A (Spacecraft).

   b. On the basis of a coupling analysis whose source terms and method of calculation yield the surface replacement currents for an excitation over the critically stressed area produced by a blowoff discharge.

In all cases, the value of I_p so determined should be increased by 3 db to provide for the 6 db overstress (energy) above those levels calculated by Method a or b.

2. Current is returned to the pulser at locations remote from the current injection area. The response produced by the return at several different locations should be determined. These locations should be chosen to provide maximum excitation of points of entry for the coupling of electromagnetic energy into the interior of the spacecraft adjacent to the excitation location.
3. The testing should be conducted by injecting current pulses with the correct τ_p, but at an initial peak current I_p, which is 21 db below the amplitude as defined in 1. The pulse amplitude should be increased in approximately 6 db steps until the level defined in 1 (I_p + 3 db) is reached. That at least three pulses be injected at each level for each pair of excitation and return points is recommended.

Table 21.
Summary of Discharge Scaling Laws

	$I_p(A) = K_I A(cm^2)^{n_I}$		$\tau_p(ns) = K_p A(cm^2)^{n_p}$		$Q_p(\mu C) = K_Q A(cm^2)^{n_Q}$	
Material	K_I	n_I	K_p	n_p	k_Q	n_Q
Teflon[a]	10	0.58	16.5	0.48	0.18	1.06
Kapton[a]	5.6	0.51	21.9	0.59	0.15	1.00
Mylar[a]	10	0.59	18.2	0.46	0.21	1.05
Fused silica[b]	0.81	0.6				

a. [Balmain and Dubois, 1979]

b. [Wilkenfeld et al., 1981]

6.4.5.2 Capacitive Injection

1. The critical stress points should be driven by capacitive injection that may either be through capacitive coupling with capacitive return or direct coupling with capacitive return. The pulser circuit parameters should be adjusted to yield an exciting pulse that has a first lobe peak amplitude I_p and time to first zero crossing t_1 chosen according to Method a or b given for direct injection.
2. The capacitive coupler or direct connections to the critically stressed area should be designed to excite the same area as participates in the discharge. This may be assumed to be the entire conductivity bounded dielectric surface.
3. The current return to the pulser should be through the capacitive coupling of the test object to the common pulser test object ground plane, for direct injection or through either direct or capacitive coupling for capacitive coupling of the pulser to the test object.
4. The testing should be conducted by injecting current pulses with the correct t_1 but at an initial peak current I_p that is 21 db below the amplitude defined in 1. The pulse amplitude should be increased in approximately 6 db steps until the smaller of the maximum attainable level or 3 db overstress level is reached. It is recommended that at least three pulses be injected at each level for each point of excitation.
5. If it is not feasible to capacitively drive the spacecraft at I_p + 3 db, then additional internal sensors of the type described in the above should be added to the spacecraft at internal monitoring points in sufficient number to provide data to determine whether the spacecraft would show improper responses if driven at full criteria levels based on the susceptibility thresholds for systems and subsystems. Subsystem electrical testing of those system components for which the above analysis indicates negative safety margins at critical internal test points is recommended to verify the analytical results.

Appendix A
Environments

The region of space dominated by the plasma surrounding the earth is called the magnetosphere. A popular visualization of the magnetosphere is shown in Figure 64.

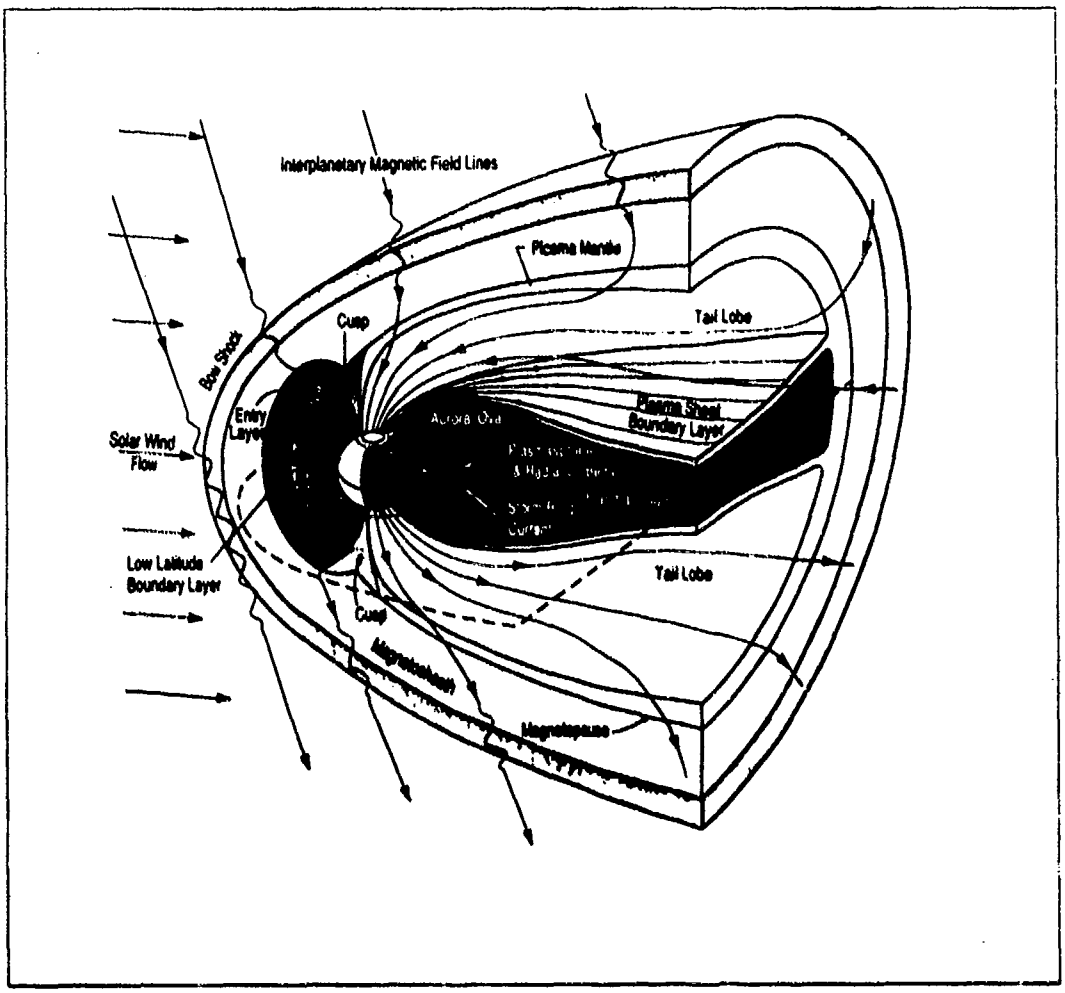

Figure 64. Magnetosphere geometry.

The plasma in the magnetosphere can be divided into three regions: (1) the plasmasphere containing cool (less than 1 eV) plasma consisting of electrons, ions, and oxygen ions, (2) the plasma sheet containing warm (5 keV) plasma, and (3) the radiation

belts, with plasma energies up to several MeV. The auroral oval is that region where the plasma from the plasma sheet and radiation belts extends to low-altitudes.

The space environments for which spacecraft charging is a concern are encountered in geosynchronous and low-altitude, polar orbits. In either of these orbital regimes, spacecraft charging results when a spacecraft encounters a plasma population associated with a geomagnetic substorm—a warm plasma with particle energies in the 1–50 keV range. The spatial and temporal variations of the plasma environment in either the geosynchronous or polar regime are quite complex and a large body of work has been devoted to characterization of those variations. (See the Bibliography.)

A.1 Geosynchronous Environment

Table 22 shows the environmental parameters at geosynchronous altitudes during a quiet period.

Table 22.
Typical Environmental Parameters At Geosynchronous Altitudes

Plasma density	$10^{6} m^{-3}$
Plasma thermal energy	0.1 eV
Debye length	20 cm
Ion species	H^{+}
Ram ion current	5×10^{-9} A m^{-2}
Ram ion energy	0.05 eV
Ion mach number	0.7
Magnetic field	10^{-5} Gauss
Debris and meteoroids	Little
Photoemission current	30 μA m^{-2}

Spacecraft charging at geosynchronous orbit generally occurs when the spacecraft is enveloped in the "plasma cloud" injected near local midnight during a magnetospheric substorm. This plasma cloud may be characterized as low density (1–10 particles cm^{-3}) with energies of 1–50 keV, in contrast to the "quiet" plasma conditions of higher density shown in Table 22. Since a substorm typically occurs every few hours, the conditions for spacecraft charging at geosynchronous orbit exist quite often. A geosynchronous spacecraft can be immersed in the substorm cloud for many minutes to hours, causing possible durations of hours for geosynchronous charging events. When the plasma is thin or tenuous, the spacecraft charges more slowly than when the plasma is dense. Table 23 shows environmental parameters during a typical substorm.

Table 23.
Environmental Parameters During A Typical Substorm

Charging current intensity	1 to 10 $\mu A\ m^{-2}$
Charging current directionality	Isotropic
Charging plasma density	10^6 to $10^7\ m^{-3}$
Characteristic plasma energy	1 to 50 keV
Spectrum	Broadly distributed
Background plasma density	No background plasma
Time spacecraft in most disturbed region	30 minutes

While the spectrum of a geosynchronous plasma is quite complex, it is usually described in terms of a Maxwell-Boltzmann distribution—either a Maxwellian or a 2-Maxwellian (two populations each represented by a Maxwellian distribution) for each species. The first four moments of such a distribution then equate to the number density, number flux, energy density, and energy flux, which can be compared to actual observations. This parameterization of the plasma affords a convenient means of describing the average plasma conditions, the standard deviation about that average, and the worst case plasma conditions.

For risk analysis, the geosynchronous plasma can be described by a Maxwellian [Purvis et al., 1984]. Table 24 gives a 90th percentile Maxwellian representation of the geosynchronous plasma environment. The probability of observing given current densities and temperatures of a given magnitude or larger are given in Purvis et al. [1984].

Table 24.
Severe Geosynchronous Substorm Plasma Environment (from Purvis et al. [1984])

Quantity	Value
Electron density	1.12 cm^{-3}
Proton density	0.236 cm^{-3}
Electron temperature	12.0 keV
Proton temperature	29.5 keV
Electron current density	0.33 $nA\ cm^{-2}$
Proton current density	2.5 $pA\ cm^{-2}$

Figure 65 shows a Maxwellian distribution function and a 2-Maxwellian distribution function.

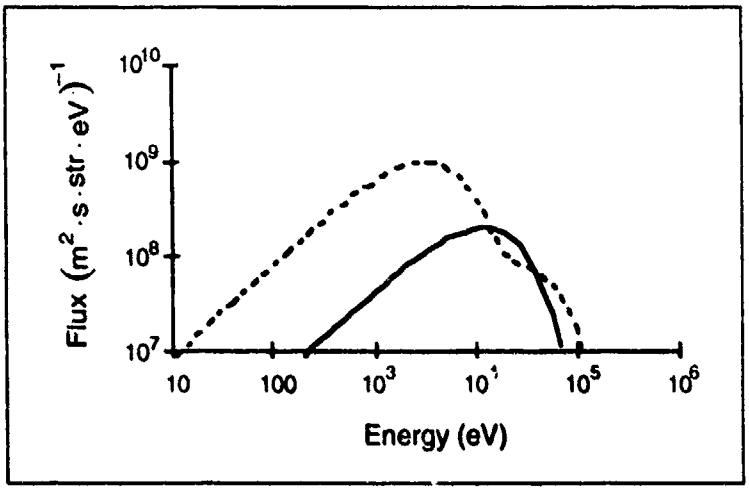

Figure 65. Spectrum for Maxwellian and 2-Maxwellian distributions. The parameters of the Maxwellian distribution are 1.12 cm^{-3} and 12 keV. The parameters of the 2-Maxwellian distribution are 2.67 cm^{-3}, 3.1 keV, 0.625 cm^{-3}, and 25.1 keV. Note that the total flux for the 2-Maxwellian is twice that of the Maxwellian.

The SCATHA satellite determined that significant levels of spacecraft charging (greater than −100 V) can occur under the following conditions [Mullen and Gussenhoven, 1982]:

- Between 1900 and 0900 Local Time
- Any distance between 5.3 R_e and 7.8 R_e
- Any magnetic latitude between +19 and −19 degrees
- Any L-shell value between 5.5 and 8.6
- Any period where $K_p \geq 2+$, where K_p is the magnetic activity index.

Charging outside this region can occur at any time electron fluxes at energies between about 30 and 70 keV exceed 6×10^2 cm^{-2} s^{-1} sr^{-1} eV^{-1} in a plasma-sheet-type low-energy particle environment.

A worst-case event occurred on March 13, 1989 at 0700 UT, the "Great Magnetic Storm," where the magnetosphere was compressed from 10 R_e to 6.6 R_e [Wilkinson, 1990]. Satellites in geosynchronous orbit were exposed directly to the solar wind. There were several other storms during the peak of the solar cycle. There is no information on particle fluxes or distribution functions below 2 MeV presently available.

When doing a post-anomaly analysis it is usually desirable to use an environmental description that fits the actual environment. Two-Maxwellian distributions are better approximations to space plasmas than Maxwellian distributions (since they have more free parameters). This representation, in most cases, fits the data quite adequately over the energy range of importance to spacecraft charging. It incorporates the simplicity of the Maxwellian distribution while maintaining a physically reasonable picture of the plasma [Purvis et al., 1984].

A.2 The Auroral Environment

The plasma environment of a spacecraft in low-altitude, polar orbit is more complex than that of geosynchronous spacecraft. Table 25 shows the environmental parameters in the auroral region. The auroral zones are characterized by visible auroral displays and intense particle and field variations. The necessary conditions for charging appear to be a thermal plasma density less than 10^4 cm^{-3} and a high integral electron number flux for energies greater than 14 keV.

Table 25.
Environmental Parameters in the Auroral Region during Quiet Times

Plasma density	10^{10} to 10^{12} m^{-3}
Plasma thermal energy	0.1 eV
Debye length	1 cm
Ion species	O^+, H^+, and others
Ram ion current	5×10^{-8} A m^{-2}
Ram ion energy	5 eV
Ion mach number	7
Magnetic field	0.3 to 0.7 Gauss
Debris and meteoroids	Significant
Photoemission current	30 μA m^{-2}

The environment at auroral latitudes in the ionosphere is different from that of geosynchronous orbit in two major ways. First, there exists a large reservoir of high-density, cold plasma that tends to suppress charging effects by providing an ample source of neutralizing current. Second, auroral electrons are often observed to undergo field-aligned accelerations of several kilovolts. Severe charging environments at auroral latitudes are more intense. Since a low-altitude, polar-orbiting spacecraft is in the auroral region only part of the time, severe charging events occur less frequently than on geosynchronous spacecraft. Table 26 shows the environmental parameters during an aurora.

Table 26.
Environmental Parameters during Aurora

Charging current intensity	100 mA m^{-2}
Charging current directionality	Anisotropic
Charging plasma density	10^6 to 10^7 m^{-3}
Characteristic plasma energy	1 to 100 keV
Spectrum	Accelerated distribution
Background plasma density	10^8 to 10^9 m^{-3}
Time spacecraft in most disturbed region	Under 1 minute

Using several million high latitude spectra from the DMSP satellites, Hardy et al.[1985] show two distinct regions of plasma. The hot plasma that causes spacecraft charging is in an annular region about the pole. The plasma between the poleward edge of the annular region and the pole is colder.

The most severe charging environments for low-altitude, polar-orbiting satellites are associated with westward traveling surges and inverted-V events. Within the poleward bulge of the westward surge, significant numbers of electrons extending out to high energies appear to be present. This indicates that the bulge region may be a severe charging region. Whereas the westward traveling surge is generally localized to the night side near local midnight, extending toward local dusk, the inverted Vs have been reported at all magnetic local times [Lin and Hoffman, 1979a; Lin and Hoffman, 1979b]. Mullen and Gussenhoven [1982] showed that the most severe charging events are associated with strong fluxes with energies greater than 10 keV. In two inverted-V events in January, 1983, the satellite was shown to charge significantly, and the charging level appeared to be directly correlated with the integral flux of electrons over 10 keV.

The severe charging environments appear on the night side of the aurora and can have electron current density values up to 10^3 nA cm^{-2} and characteristic energies of up to 15 keV. The ambient thermal plasma—particles with energy under 2 eV—also varies. At times, severe auroras can be accompanied by low ambient plasma density. It is during these events that the highest spacecraft potentials develop.

The charging events in the auroral region tend to be more intense than at geosynchronous altitudes but are of shorter duration, tens of seconds rather than minutes.

Charging over 100 V is likely to occur under the following conditions [Gussenhoven et al., 1985]:

- The plasma density is less than 10^4 cm^{-3}.
- The integral number flux for energies greater than 14 keV is greater than 10^6 cm^{-2} s^{-1} sr^{-1})

The highest potentials develop when there is a severe localized dropout of ion plasma density. This condition occurs more often during solar minimum conditions [Frooninckx and Sojka, 1992].

One worst-case event was observed by the DMSP satellite on December 31, 1983 [Gussenhoven et al., 1985]. This event had the longest charging duration seen on any DMSP satellite, 62 seconds [Yeh and Gussenhoven, 1987]. The spacecraft potential reached a peak value of –462 V.

The measured parameters were as follows:

Thermal ion density	$12.2\ cm^{-3}$
Integrated flux of electrons	$2.39 \times 10^{9}\ cm^{-2}\ s^{-1}\ sr^{-1}$
Integrated flux of electrons (greater than 14 keV)	$2.33 \times 10^{9}\ cm^{-2}\ s^{-1}\ sr^{-1}$
Integrated flux (ion peak)	$1.48 \times 10^{8}\ cm^{-2}\ s^{-1}\ sr^{-1}$

Fontheim et al. [1982] suggested that high-latitude precipitating electrons that would be expected to influence spacecraft charging significantly could be represented by the superposition of three distributions: a power law, a Maxwellian, and a Gaussian. Analytic functions are easily manipulated to find the charging potential of a spacecraft and provide physical parameters that give insight to the nature of the precipitating electron environment. The sum of three distributions is used to fit the energy spectra of precipitating electrons.

$$\Phi(E) = \Phi_p + \Phi_m + \Phi_G \tag{20}$$

where

$$\Phi_p = \begin{cases} A_p E^{-\alpha}, & E_{pL} \le E \le E_{pH} \\ 0, & \end{cases} \tag{21}$$

$$\Phi_m = \frac{1}{\sqrt{2\pi^3 m_e}} n \frac{E}{\theta^{3/2}} e^{-E/\theta} \tag{22}$$

$$\Phi_G = A_G E e^{-\left(\frac{E - E_m}{\Delta}\right)^2} . \tag{23}$$

Φ_p represents a power law population linked to the energy of the precipitating primary electron beam, composed of secondaries and backscattered primaries. Φ_m represents a Maxwellian distribution with temperature θ describing the ambient flux for medium and high energies. Φ_G represents auroral enhancements that can best be described by a Gaussian distribution. Figure 66 shows a Fontheim distribution.

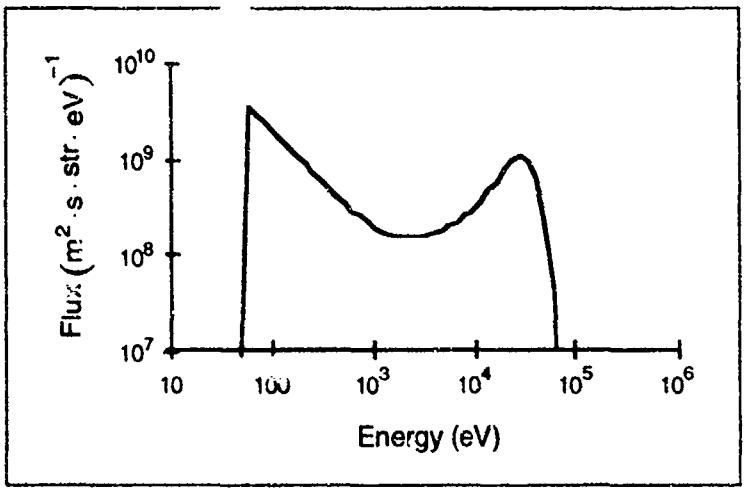

Figure 66. Fontheim distribution for $A_p = 3 \times 10^{11}\ m^{-3}$, $\alpha = 1.1$, $E_{PH} = 50$ eV, $E_{PH} = 1.6 \times 10^6$, $n = 6 \times 10^5\ m^{-3}$, $\Theta = 8$ keV, $A_G = 4 \times 10^4\ m^{-3}$ $E_o = 24$ keV, $\Delta = 16$ keV.

Fontheim distributions for most environments have the parameters given in Table 27.

Table 27.
Typical Fontheim Distribution Parameters
[Barker, 1986]

E_{EP}	10–20 eV
E_{PH}	1 keV
α	2.5–4.5
Δ	1–10 keV
E_o	5–15 keV
n	10^5–$10^7\ m^{-3}$
kT	1–20 keV

The parameters A_p and A_G can be expressed through ρ_p and ρ_G that express the fraction of current contained in the power and Gaussian portion of the distribution:

$$\rho_p = \frac{J_p}{J_p + J_m + J_G} \qquad \rho_G = \frac{J_G}{J_p + J_m + J_G} \tag{24}$$

A.3 Effect of Electron Energy on Charging

In Chapter 2 specific environments are given for use in hazard analysis. Figures 67 and 68 show how charging is affected by how energetic the environment is. Figure 67 shows **Matchg** results of the equilibrium potential for spheres in environments of different energies. For most materials, over most of the temperature range, the equilibrium

potential increases roughly linearly with temperature. Some materials show a threshold effect, where little charging occurs until a threshold temperature is reached. The threshold effect seen here for some materials is an example of the threshold effect seen on all spacecraft [Laframboise and Kamitsuma, 1983; Lai et al., 1983; Olsen, 1983].

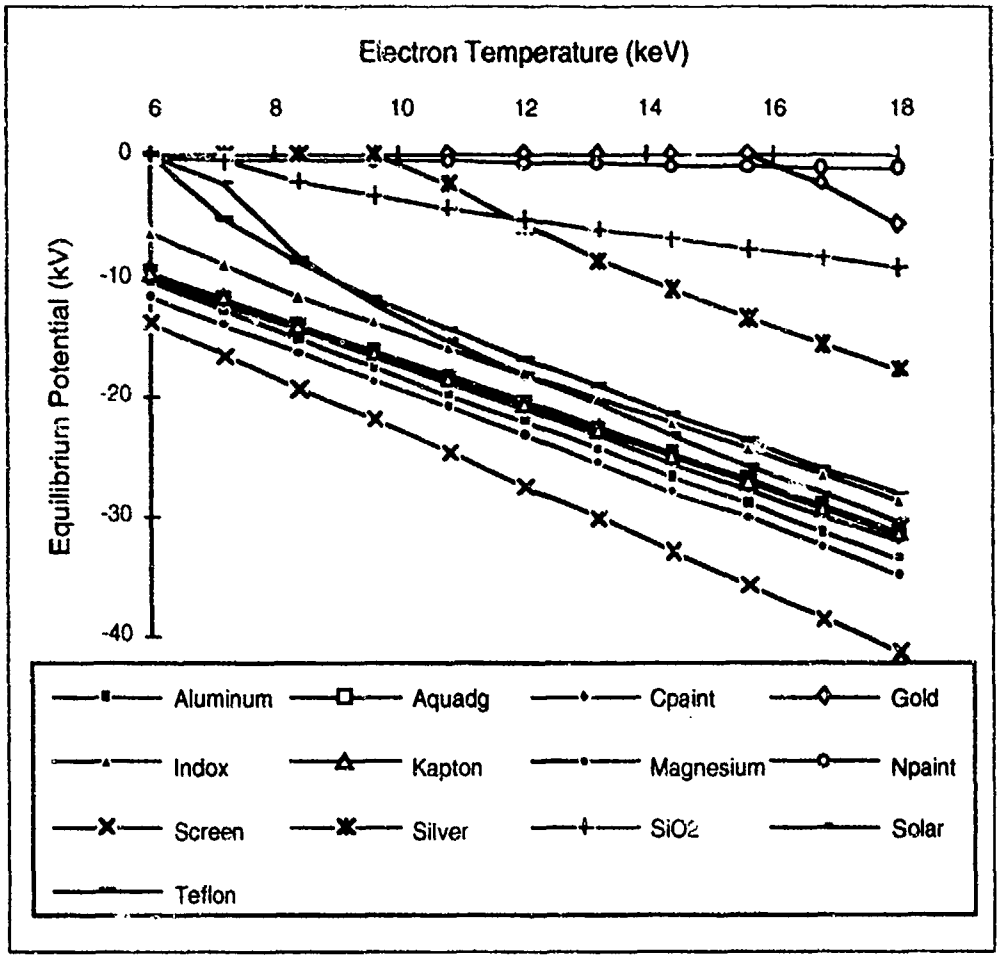

Figure 67. Equilibrium potential of a sphere in a geosynchronous substorm as a function of substorm energy for various materials. The environment is the severe substorm environment except for the electron and ion Maxwellian temperatures. Their ratio is kept constant for all the calculations.

Figure 68 shows **suchgr** results of the equilibrium potential for 1-meter-radius spheres in auroral environments of different energies. The equilibrium potential increases slightly faster than linearly and no threshold effect is seen in this range of energies.

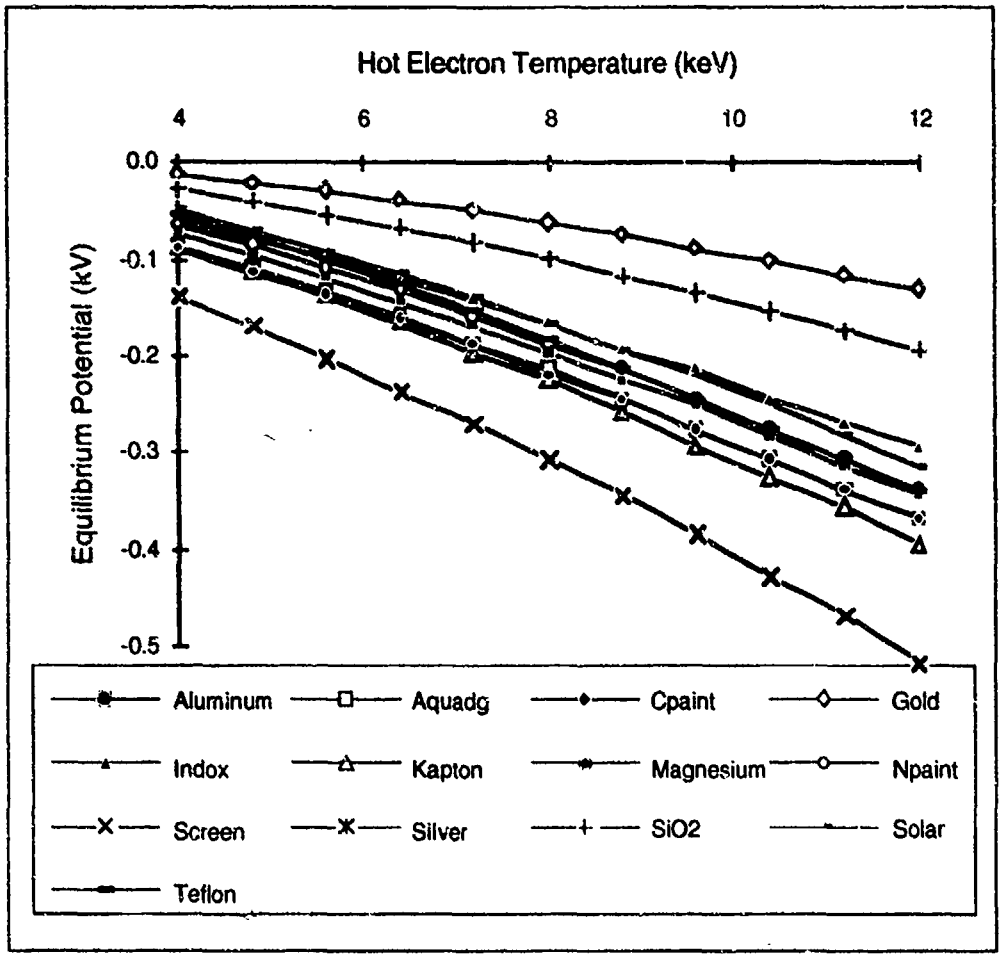

Figure 68. Equilibrium potential of a sphere in an aurora as a function of aurora energy for various materials. The environment is the severe auroral environment except for the electron Maxwellian temperature, the upper and lower cutoffs of the power law, and the energy the Gaussian is centered about. The ratio between these quantities is kept constant for all the calculations.

Appendix B
Material Properties

The properties of the spacecraft surface materials determine the charging rates and total charging of spacecraft. The properties used in the calculations are the secondary emission yield, the backscatter yield, the photoelectron yield, the conductivity, the dielectric constant, and the thickness. The models described here are those used by the *NASCAP/GEO* and *POLAR* codes.

B.1 Secondary Electron Emission Due to Electron Impact

Secondary electrons are those emitted from a surface, with energies below 50 eV, due to the impingement of higher energy particles. Their energy distribution is usually peaked below 10 eV. The secondary yield, δ, is the ratio of primary to secondary electron current.

$$\delta = \frac{\text{emitted secondary current due to electron impact}}{\text{primary electron current}} \tag{25}$$

The secondary electron emission yield, δ, can be calculated using the empirical formula [Katz et al., 1977a]:

$$\delta(\theta) = C\int_0^R \left|\frac{dE}{dx}\right| e^{-\alpha x \cos\theta} dx \tag{26}$$

where x is the path length of penetration of a primary electron beam into the material, R is the "range," or maximum penetration length, and θ is the angle of incidence of the primary electron.

This equation is based upon a simple physical model [Hackenberg and Brauer, 1959]:

1. The number of secondary electrons produced by the primary beam at a distance x is proportional to the energy loss of the beam or "stopping power" of the material, $S(E) = \left|\frac{dE}{dx}\right|$.
2. The fraction of the secondaries that migrate to the surface and escape decreases exponentially with depth ($f = e^{-\alpha x \cos\theta}$). Thus only those produced within a few multiples of the distance $1/\alpha$ (the depth of escape) from the surface contribute significantly to the observed yield.

The stopping power for incident electrons of energy E is related to the range of these electrons through the equation

$$S(E) = \left|\frac{dE}{dx}\right| = \left|\frac{dR}{dE}\right|^{-1} \tag{27}$$

The usual formulation for the range is that it increases with the energy, E, of the incident electrons in a way that approximates a simple power law [Feldman, 1960]:

$$R = bE^n \tag{28}$$

where $1.0 < n < 2.0$.

Because the primary beam loses energy as it passes through the material, E, and $S(E_0, x)$ (where E_0 is the initial electron energy) depend on the path length x. The stopping power can be written as

$$S(E_0, x) = \left|\frac{dE}{dx}\right| = \left|\frac{dR}{dE}\right|^{-1} = \frac{1}{nb}\left(\frac{b}{R-x}\right)^{1-1/n} \tag{29}$$

Figure 69 shows $S(E_0, x)$ plotted against x for several values of E_0. Inspection of Figure 69 and the equation for S(x) illustrates the following points:

1. $S(E_0, x)$ increases with x, slowly at first, before reaching a singularity as x approaches R.
2. The initial value of $S(E_0, x)$ decreases with increasing initial energy E_0.

Both of these observations are due to the decrease in electron-atom collision cross-section with increasing energy.

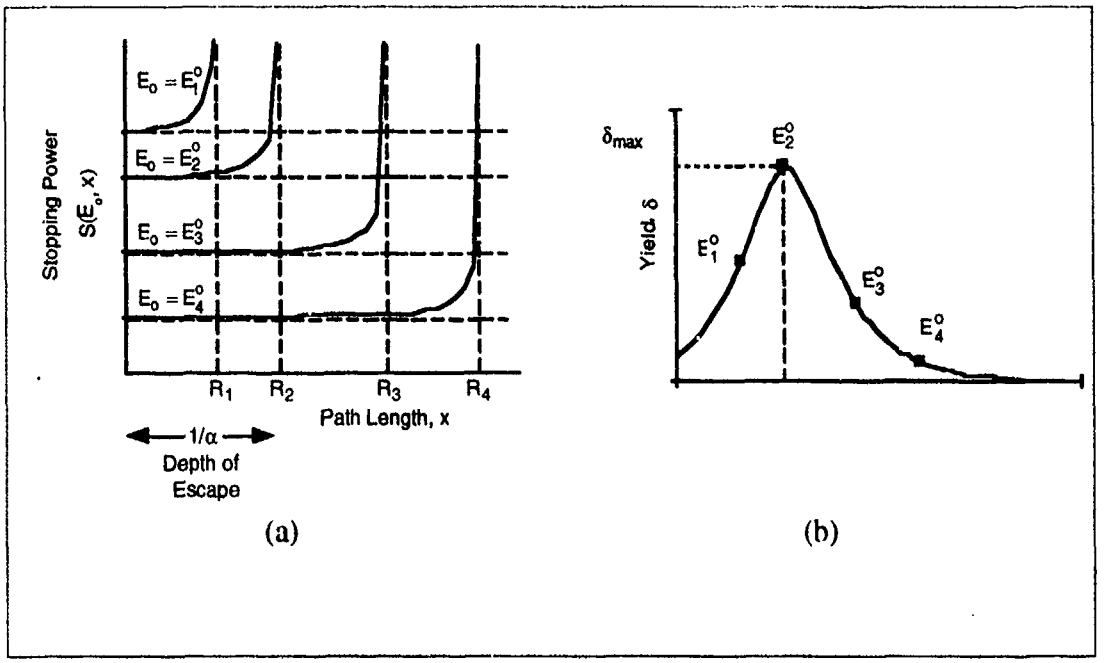

Figure 69. Energy deposition profiles of normally incident primary electrons for four incident energies E_1^o, E_2^o, E_3^o, and E_4^o and corresponding yield curve.

The yield is only sensitive to the details of the stopping-power depth-dependence for initial energies with ranges of the same order as the escape depth, $R \sim 1/\alpha$ (i.e., about the maximum of the yield curve). For lower energies, $R << 1/\alpha$, essentially all the primary energy is available for detectable secondary production, leading to a linear increase in yield with increasing E_o. At higher energies, where $R >> 1/\alpha$, $S(E_o, x)$ remains almost constant over the depth of escape. Therefore along with $S(E_o, x)$ the yield decreases as E_o increases.

Taking this into account, the stopping power can be approximated by a linear expansion in x, about x = 0.

$$\frac{dE}{dx} = \left(\frac{dR}{dE_o}\right)^{-1} + \left(\frac{d^2R}{dE_o^2}\right)\left(\frac{dR}{dE_o}\right)^{-1} x \ . \tag{30}$$

Equation 28 does not adequately describe the available experimental data. The range has different exponents for low energy and high energy. A biexponential range law with four parameters b_1, b_2, n_1, n_2 fits the experimental data better.

$$R = b_1 E_o^{n_1} + b_2 E_o^{n_2} \ . \tag{31}$$

For materials where no suitable data is available, a monoexponential form can be generated using Feldman's empirical relationships [Feldman, 1960], connecting b and n to atomic data.

$$b = 250 A / \rho Z^{n/2} \tag{32}$$

$$n = 1.2 / \left(1 - 0.29 \log_{10} Z\right) \tag{33}$$

where A is the atomic or molecular weight of the material, Z is the atomic number, and ρ is the density in gm cm^{-3}. Then E is in keV and R is in angstroms in Equation 28. The stopping power is then obtained indirectly with the equation above. Theoretical estimates of the stopping power for a number of materials are available from Ashley et al. [1978]. Comparison of these values with those implied by the range data showed significant discrepancies, particularly for those materials fit using Feldman's formula. The best approach is to fit the four parameters in the equation for R directly to the stopping power data.

$$S = \left(n_1 b_1 E^{n_1 - 1} + n_2 b_2 E^{n_2 - 1}\right)^{-1} . \tag{34}$$

Burke et al. [1970] propose a relationship between secondary emission due to electrons below 1 keV and secondary emission due to higher energy particles, including gamma radiation from Co^{60}.

B.2 Secondary Electron Emission Due to Ion Impact

Secondary emission of electrons due to ion impact can be treated in a way similar to that for electron impact. The yield Δ is given by

$$\Delta(\theta) = C \int_0^t \left|\frac{dE}{dx}\right| e^{-\alpha x \sec\theta} dx \ . \tag{35}$$

The stopping power is assumed to be independent of path length x over the thickness, t, of the sample. At low energies the stopping power is proportional to the velocity, and at high energies it is inversely proportional to the velocity [Sternglass, 1957].

$$\left|\frac{dE}{dx}\right| = \frac{\beta E^{1/2}}{1 + E / E_{max}} \ . \tag{36}$$

E_{max} is the energy at the maximum in the yield curve. This is approximately 50 keV for most materials. The yield curve for aluminum is shown in Figure 70.

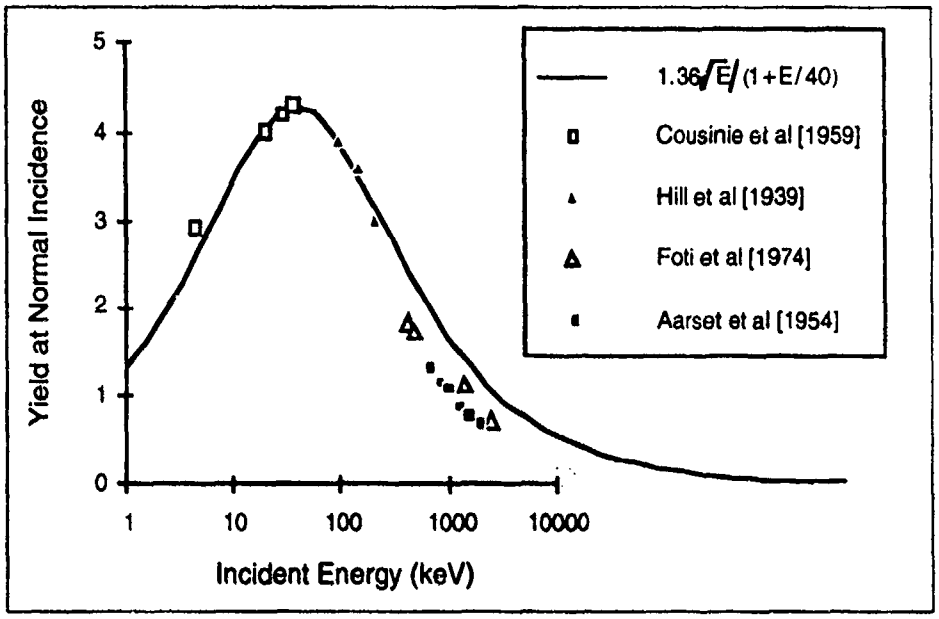

Figure 70. Secondary electron emission by aluminum for proton impact at normal incidence; experimental points as indicated.[Aarset et al., 1954; Cousinie et al., 1959; Foti et al., 1974; Hill et al., 1939].

B.3 Backscatter

Backscattered electrons are those emitted from the surface with energies above 50 eV. Their energy distribution is usually peaked close to the primary incident energy and they may be considered as reflected electrons.

The *NASCAP/GEO* and *POLAR* codes use a backscattering theory [Katz et al., 1977b] based on that of Everhart [1960] as extended by McAfee [1976]. It assumes a single scattering in accordance with the Rutherford cross-section and the Thomson-Widdington slowing down law,

$$\frac{dE}{dx} \propto E^{-1} \tag{37}$$

(valid for most metals for E > 10 keV). For normal incidence the backscattering coefficient is given by

$$\eta = 1 - \left(\frac{2}{e}\right)^{a} \tag{38}$$

where a is taken to be 0.0375 Z and where Z is the atomic number of the material. This expression matches the experimental data.

The large-angle scattering theory, together with Monte Carlo data and experiments by Darlington and Cosslett [1972] indicate that the angular dependence of backscattering is well-described by

$$\eta(\theta) = \eta_0 \exp\left[\eta_1 (1 - \cos\theta)\right] \tag{39}$$

where the value of η_1 is, within the uncertainty in the data, what would be obtained by assuming total backscattering at glancing incidence, $\eta_1 = -\log \eta_0$. The net albedo for an isotropic flux is then

$$A_0 = 2\frac{1 - \eta_0(1 - \log \eta_0)}{(\log \eta_0)^2} \quad . \tag{40}$$

As the energy is decreased below 10 keV, the backscattering increases. Data cited by Shimizu [1974] indicate an increase of about 0.1, almost independent of Z. This component of backscattering can be approximated by

$$\delta\eta_0 = 0.1 \exp\left[-E / 5\,\text{keV}\right]. \tag{41}$$

At very low energies, the backscattering coefficient becomes very small and, below 50 eV, backscattering and secondary emission are indistinguishable. This can be taken into account by a factor of

$$\Theta(E - 50\text{eV})\left[\frac{1}{\log 20}\right]\log\left(\frac{E}{50\text{eV}}\right) \quad . \tag{42}$$

The formula for energy-dependent backscattering, incorporating these assumptions, is then

$$\eta_0 = \left(\Theta(1 - E)\Theta(E - 0.05)\left(\frac{1}{\log 20}\right)\log\left(\frac{E}{0.05}\right) + \Theta(E - 1)\right) \times \left(\frac{e^{-E/5}}{10} + 1 - \left(\frac{2}{e}\right)^{0.37E}\right) \tag{43}$$

where energies are measured in keV.

B.4 Photoemission

Usually the quantity known is the yield, or number of electrons emitted for a surface normally exposed to the solar spectrum, an "earth distance" from the sun. The photocurrent from a surface exposed to the sun at an angle θ is given by the formula

$$i_{\text{photo}} = (\text{Area exposed}) \cdot Y \cdot \cos\theta \quad . \tag{44}$$

This assumes that the yield per photon is, on average, independent of θ.

B.5 Conductivity

The bulk conductivity σ_v is usually constant. The conductivity can be enhanced by fields across the dielectric film and by high energy electron fluxes.

B.5.1 Field-Induced Conductivity

Consider a thin dielectric film of thickness d covering an underlying conductor. If the potential of the dielectric surface V_s differs from the potential of the conductor V_c, current will flow from the surface to its underlying conductor due to bulk conductivity.

$$I_c = G\Delta V = G(V_s - V_c) \quad . \tag{45}$$

G is the bulk conductance of the sample in mhos. If σ is the conductivity in mhos m^{-1} and A is the area of the sample in m^2.

$$G = \frac{\sigma A}{d} \tag{46}$$

$$I_c = -\frac{\sigma A(V_s - V_c)}{d} \quad . \tag{47}$$

I_c depends on $(V_s - V_c)$ in a nonlinear way due to the electric field enhancement of σ. Assuming a thin film, the field E is given by

$$E = \frac{V_s - V_c}{d} \quad . \tag{48}$$

Ademec and Calderwood [1975] have shown that σ depends on E in the following way:

$$\sigma(E) = \frac{\sigma_v}{3}\left[2 + \cosh\left(\frac{\beta_s |E|^{1/2}}{2kT}\right)\right] \tag{49}$$

where

$$\beta_s = \left(\frac{|q|^3}{\pi\epsilon}\right)^{1/2} \tag{50}$$

and q is the charge on the electron and ϵ is the dielectric constant of the material.

B.5.2 Radiation-Induced Conductivity

Dielectric materials have characteristically small bulk conductivities due to their electron band structure. Unlike metals, the delocalized conduction bands are empty at normal temperatures and electrons are strongly localized in the regions close to individual nuclei. However, under the influence of an exciting source, nonconducting electrons can be promoted into the conduction bands, leading to an increase in the bulk conductivity. High energy electrons passing through the dielectric provide such an excitation source.

Studies [Schnuelle et al., 1981] suggest that the penetrating fluxes may influence the degree of differential charging by increasing the bulk conductivity. This enhancement due to high energy electron fluxes is described as the "radiation-induced" conductivity σ_r.

Frederickson [1977] has expressed σ_r in terms of the dose rate $\dot{D}$ and two parameters k and Δ.

$$\sigma_r = k \dot{D}^{\Delta} \tag{51}$$

k and Δ are characteristic of each material and Δ usually lies between 0.5 and 1.0. The dose rate can be estimated from the stopping power S for electrons in the medium of interest.

$$S(E) = \frac{dE}{dx} . \tag{52}$$

The dose rate is measured as energy deposited per unit mass per second (i.e., rad s^{-1} = 100 erg g^{-1} s^{-1}). Stopping power is measured as energy deposited per particle per unit thickness of the sample. Dividing S(E) by the density ρ of the sample gives the energy deposited per particle per unit mass of the material multiplied by unit area. The product of this quantity with the flux (particles per unit area per second) gives the required dose rate:

$$\dot{D} = \text{flux} \frac{S(E)}{\rho} . \tag{53}$$

The flux of incident electrons due to a plasma with distribution function f(E) is given by:

$$(nf) = \frac{2}{m^2} \int E\, f(E)\, dE \tag{54}$$

$$\dot{D} = \frac{2}{\rho m^2} \int E\, f(E)\, S(E)\, dE . \tag{55}$$

A number of models for the energy spectrum of high energy fluxes in space have been measured. All show a Maxwellian like behavior, i.e.,

$$f(E) = N\left(\frac{m}{2\pi T}\right)^{3/2} e^{-E/T} \quad . \tag{56}$$

The AE3 model [Hilbert, 1979] implies a value of 3×10^2 m^{-3} for the density N and 2.5×10^2 keV for the temperature T at geosynchronous orbit. Electrons in this energy range are relativistic; i.e., their velocity is close to that of light and so the weight function E in the integral above should be replaced by mc^2. This is confirmed by a plot of <nf> against E, which shows the same exponential behavior.

$$\dot{D} = \frac{2c^2}{\rho m} N\left(\frac{m}{2\pi T}\right)^{3/2} \int_{\omega}^{\infty} e^{-k/T} S(E)\, dE \tag{57}$$

(where we assumed the contribution from nonpenetrating electrons with energies below 50 keV is negligible.)

The dose rate is calculated for each material by integrating the above equation from 50 keV to 4 T. If all energies are in keV and S(E) is in keV Å^{-1} and I is the value of the integral:

$$\dot{D} = \frac{2c^2}{\rho m} N\left(\frac{m}{2\pi T}\right)^{3/2} I \quad \text{keV}^2 \text{Å}^{-1} \quad . \tag{58}$$

Substituting:

$$\dot{D} = 1.38 \times 10^{-3} \frac{NI}{\rho T^{3/2}} \text{m}^2 \text{s}^{-3} \tag{59}$$

where N is in m^{-3}, ρ is in kg m^{-3}, and T is in keV.

Frederickson [1977] has pointed out that k is often known to within only 2 orders of magnitude and Δ values are usually close to 1. Reasonable values of $k = 1 \times 10^{17}$ mhos cm^{-1} (rad s^{-1})$^{-1}$ = 1×10^{-13} mhos m^{-1} (m^2 s^{-1})$^{-1}$ and Δ = 1. The density of plastics and other insulators depends very much on the particular sample and manufacturer. A reasonable value is 1×10^3 kg m^{-3}.

Appendix C
Calculations Shown in the Text

C.1 Yields and Current Voltage Relations

Matchg is used to compute the yields and current-voltage relations shown in Figures 7, 8, and 9 of Chapter 2. The change environment command is used to set the environment to the severe substorm environment. The surface material is set to be kapton and the default properties displayed. A table and then a plot of the secondary and backscatter emission coefficients are requested. The range of potentials for which currents are to be calculated is set and then a current-voltage table and plot are requested. A table and a plot of potential and current as a function of time are requested. And finally a summary of potentials and currents before and after charging is requested. Similar information is requested for silver. For additional information on the use of **Matchg** see Mandell, et al. [1984].

```
WELCOME TO 'MATCHG', A MATERIAL CHARGING
PROGRAM. TYPE 'HELP' AT ANY TIME FOR ASSISTANCE.
MATERIAL IS GOLD
ENVIRONMENT NOW SINGLE MAXWELLIAN

change envi te1 12

ENVIRONMENT IS A SINGLE MAXWELLIAN

ELECTRONS: NE1 =  1.00E+06 (M**-3)     TE1 =    12.000 KEV
IONS     : NI1 =  1.00E+06 (M**-3)     TI1 =     1.000 KEV

change envi ti1 29.5

ENVIRONMENT IS A SINGLE MAXWELLIAN

ELECTRONS: NE1 =  1.00E+06 (M**-3)     TE1 =    12.000 KEV
IONS     : NI1 =  1.00E+06 (M**-3)     TI1 =    29.500 KEV

change envi ne1 1.12e6

ENVIRONMENT IS A SINGLE MAXWELLIAN

ELECTRONS: NE1 =  1.12E+06 (M**-3)     TE1 =    12.000 KEV
IONS     : NI1 =  1.00E+06 (M**-3)     TI1 =    29.500 KEV

change envi ni1 .236e6

ENVIRONMENT IS A SINGLE MAXWELLIAN

ELECTRONS: NE1 =  1.12E+06 (M**-3)     TE1 =    12.000 KEV
```

IONS : NI1 = 2.36E+05 (M**-3) TI1 = 29.500 KEV

list angle

ANGULAR DISTRIBUTION IS ISOTROPIC

list emission

EMISSION FORMULATION IS ANGL.

change mate kapt

MATERIAL IS kapt

list properties all

MATERIAL = kapt.

	PROPERTY	INPUT VALUE	CODE VALUE
1	DIELECTRIC CONSTANT	3.50E+00 (NONE)	3.50E+00 (NONE)
2	THICKNESS	1.27E-04 METERS	1.27E-04 MESH
3	CONDUCTIVITY	1.00E-16 MHO/M	1.00E-16 MHO/M
4	ATOMIC NUMBER	5.00E+00 (NONE)	5.00E+00 (NONE)
5	DELTA MAX>COEFF	2.10E+00 (NONE)	4.06E+01 (NONE)
6	E-MAX >DEPTH**-1	1.50E-01 KEV	8.74E-02 ANG-01
7	RANGE	7.15E+01 ANG.	4.29E+01 ANG.
8	EXPONENT> RANGE	6.00E-01 (NONE)	5.52E+02 ANG.
9	RANGE> EXPONENT	3.12E+02 ANG.	6.00E-01 (NONE)
10	EXPONENT	1.77E+00 (NONE)	1.77E+00 (NONE)
11	YIELD FOR 1KEV PROTONS	4.55E-01 (NONE)	4.55E-01 (NONE)
12	MAX DE/DX FOR PROTONS	1.40E+02 KEV	1.40E+02 KEV
13	PHOTOCURRENT	2.00E-05 A/M**2	2.00E-05 A/M**2
14	SURFACE RESISTIVITY	1.00E+16 OHMS	8.85E+04 V-S/Q

table all

TABLE GENERATED USING ISOTROPI))	EL. SEC.	EL. BKSCAT.	PR. SEC.
0.100	2.484	0.165	0.036
0.200	3.153	0.230	0.051
0.300	3.033	0.262	0.062
0.400	2.742	0.282	0.072
0.500	2.460	0.296	0.090
0.600	2.219	0.307	0.144
0.700	2.019	0.315	0.201
0.800	1.852	0.322	0.260
1.000	1.592	0.333	0.375
2.000	0.965	0.316	0.855
3.000	0.712	0.302	1.236
4.000	0.573	0.290	1.535
5.000	0.483	0.286	1.787
6.000	0.423	0.272	2.067
7.000	0.374	0.265	2.202
8.000	0.338	0.259	2.378
9.000	0.308	0.254	2.538
10.000	0.285	0.250	2.686
20.000	0.167	0.234	3.561
30.000	0.122	0.232	4.105
40.000	0.098	0.232	4.476
50.000	0.083	0.232	4.741

plot secon

4.00E+00+
I

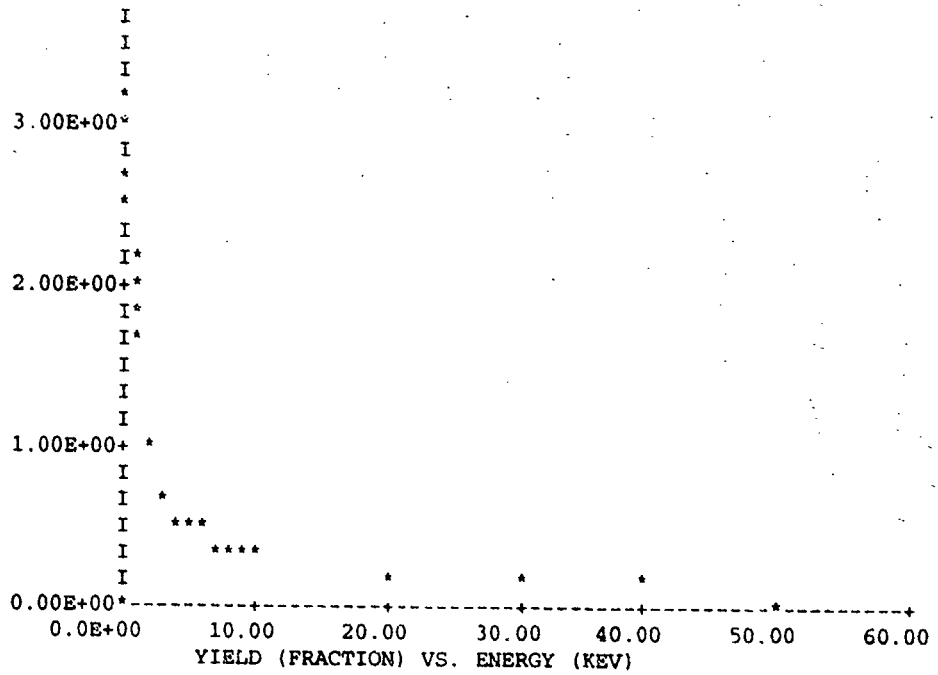

change vend -30

VEND = -3.00E+01 KEV

table iv

V	JTOT	JE	JSECE	JBSCAT	JI	JSECI
0.00E+00	-1.62E-06	-3.30E-06	7.33E-07	8.01E-07	2.54E-08	1.14E-07
-1.43E+00	-1.42E-06	-2.93E-06	6.51E-07	7.11E-07	2.66E-08	1.20E-07
-2.86E+00	-1.23E-06	-2.60E-06	5.78E-07	6.31E-07	2.79E-08	1.25E-07
-4.29E+00	-1.07E-06	-2.31E-06	5.13E-07	5.60E-07	2.91E-08	1.31E-07
-5.71E+00	-9.22E-07	-2.05E-06	4.55E-07	4.97E-07	3.03E-08	1.37E-07
-7.14E+00	-7.91E-07	-1.82E-06	4.04E-07	4.41E-07	3.15E-08	1.44E-07
-8.57E+00	-6.73E-07	-1.61E-06	3.59E-07	3.92E-07	3.28E-08	1.50E-07
-1.00E+01	-5.68E-07	-1.43E-06	3.19E-07	3.48E-07	3.40E-08	1.56E-07
-1.14E+01	-4.73E-07	-1.27E-06	2.83E-07	3.09E-07	3.52E-08	1.63E-07
-1.29E+01	-3.88E-07	-1.13E-06	2.51E-07	2.74E-07	3.64E-08	1.69E-07
-1.43E+01	-3.11E-07	-1.00E-06	2.23E-07	2.43E-07	3.77E-08	1.76E-07
-1.57E+01	-2.42E-07	-8.90E-07	1.98E-07	2.16E-07	3.89E-08	1.83E-07
-1.71E+01	-1.79E-07	-7.90E-07	1.76E-07	1.92E-07	4.01E-08	1.89E-07
-1.86E+01	-1.23E-07	-7.01E-07	1.56E-07	1.70E-07	4.13E-08	1.96E-07
-2.00E+01	-7.15E-08	-6.23E-07	1.38E-07	1.51E-07	4.26E-08	2.03E-07
-2.14E+01	-2.50E-08	-5.53E-07	1.23E-07	1.34E-07	4.38E-08	2.10E-07
-2.29E+01	1.75E-08	-4.91E-07	1.09E-07	1.19E-07	4.50E-08	2.17E-07
-2.43E+01	5.62E-08	-4.36E-07	9.69E-08	1.06E-07	4.62E-08	2.24E-07
-2.57E+01	9.16E-08	-3.87E-07	8.60E-08	9.39E-08	4.75E-08	2.31E-07
-2.71E+01	1.24E-07	-3.43E-07	7.64E-08	8.34E-08	4.87E-08	2.38E-07
-2.86E+01	1.54E-07	-3.05E-07	6.78E-08	7.40E-08	4.99E-08	2.45E-07

plot iv

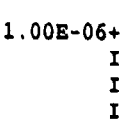

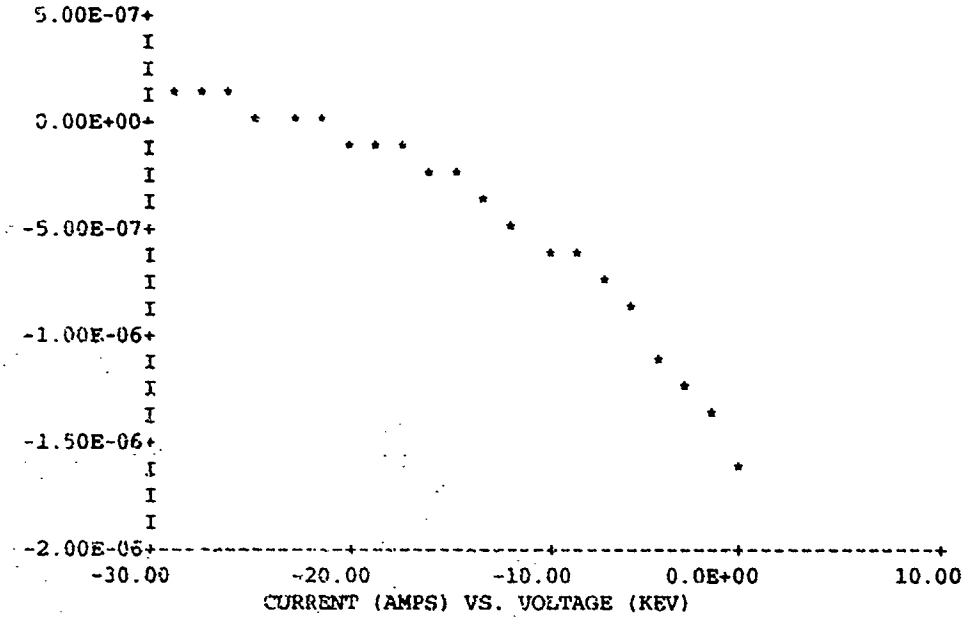

change vend -1

VEND = -1.00E+00 KEV

table charge

T (SEC)	V (VOLTS)	I(AMPS/M**2)
0.00E+00	0.00E+00	-1.62E-06
3.61E+02	-2.07E+03	-1.33E-06
7.21E+02	-3.80E+03	-1.12E-06
1.08E+03	-5.28E+03	-9.65E-07
1.44E+03	-6.57E+03	-8.42E-07
1.80E+03	-7.70E+03	-7.43E-07
2.16E+03	-8.71E+03	-6.62E-07
2.52E+03	-9.62E+03	-5.95E-07
2.89E+03	-1.04E+04	-5.38E-07
3.25E+03	-1.12E+04	-4.89E-07
3.61E+03	-1.18E+04	-4.47E-07
3.97E+03	-1.25E+04	-4.10E-07
4.33E+03	-1.30E+04	-3.78E-07
4.69E+03	-1.36E+04	-3.49E-07
5.05E+03	-1.41E+04	-3.23E-07
5.41E+03	-1.45E+04	-3.00E-07
5.77E+03	-1.49E+04	-2.79E-07
6.13E+03	-1.53E+04	-2.60E-07
6.49E+03	-1.57E+04	-2.43E-07
6.85E+03	-1.60E+04	-2.28E-07
7.21E+03	-1.63E+04	-2.13E-07
7.57E+03	-1.66E+04	-2.00E-07
7.93E+03	-1.69E+04	-1.88E-07
8.30E+03	-1.72E+04	-1.77E-07
8.66E+03	-1.74E+04	-1.67E-07
9.02E+03	-1.77E+04	-1.57E-07
9.38E+03	-1.79E+04	-1.49E-07
9.74E+03	-1.81E+04	-1.40E-07
1.01E+04	-1.83E+04	-1.33E-07
1.05E+04	-1.85E+04	-1.25E-07

1.08E+04	-1.87E+04	-1.19E-07
1.12E+04	-1.88E+04	-1.12E-07
1.15E+04	-1.90E+04	-1.07E-07
1.19E+04	-1.92E+04	-1.01E-07
1.23E+04	-1.93E+04	-9.59E-08
1.26E+04	-1.94E+04	-9.11E-08
1.30E+04	-1.96E+04	-8.65E-08
1.33E+04	-1.97E+04	-8.22E-08
1.37E+04	-1.98E+04	-7.81E-08
1.41E+04	-1.99E+04	-7.43E-08
1.44E+04	-2.00E+04	-7.06E-08
1.48E+04	-2.01E+04	-6.72E-08
1.51E+04	-2.02E+04	-6.40E-08
1.55E+04	-2.03E+04	-6.09E-08
1.59E+04	-2.04E+04	-5.80E-08
1.62E+04	-2.05E+04	-5.53E-08
1.66E+04	-2.06E+04	-5.27E-08
1.70E+04	-2.06E+04	-5.02E-08
1.73E+04	-2.07E+04	-4.79E-08
1.77E+04	-2.08E+04	-4.57E-08

plot charge

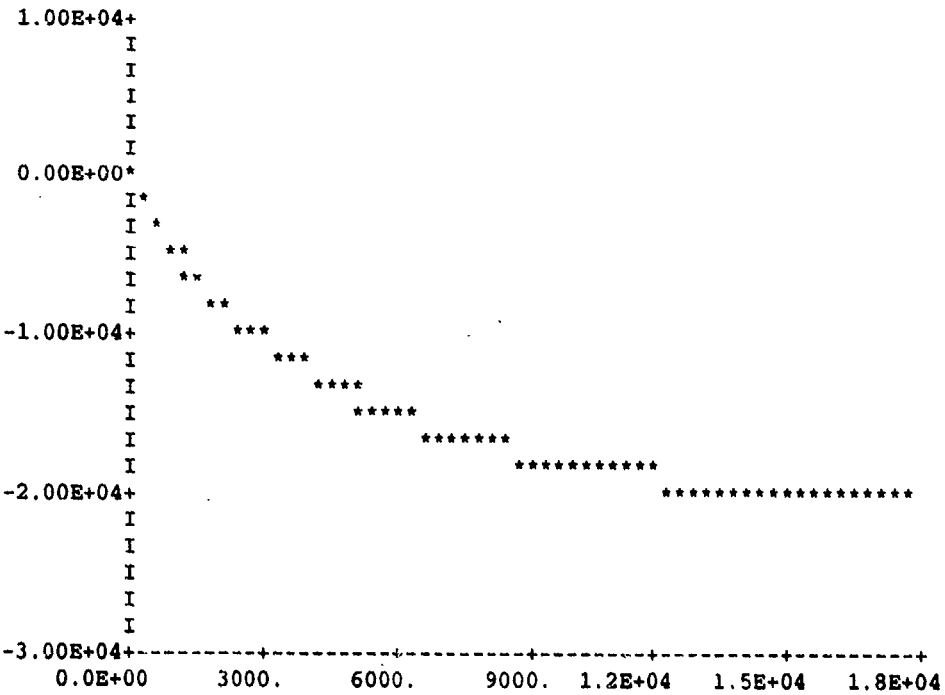

result charge

```
CYCLE     1   TIME  0.00E+00 SECONDS     POTENTIAL  0.00E+00 VOLTS
INCIDENT ELECTRON CURRENT            -3.30E-06
         SECONDARY ELECTRONS          7.33E-07
         BACKSCATTERED ELECTRONS      8.01E-07
INCIDENT PROTON CURRENT               2.54E-08
         SECONDARY ELECTRONS          1.14E-07
BULK CONDUCTIVITY CURRENT             0.00E+00
                                     ----------
```

```
                    NET CURRENT  -1.62E-06  AMPS/M**2
CYCLE   99   TIME  1.77E+04 SECONDS    POTENTIAL -2.08E+04 VOLTS
INCIDENT ELECTRON CURRENT          -5.84E-07
         SECONDARY ELECTRONS        1.30E-07
         BACKSCATTERED ELECTRONS    1.42E-07
INCIDENT PROTON CURRENT             4.32E-08
         SECONDARY ELECTRONS        2.07E-07
BULK CONDUCTIVITY CURRENT           1.64E-08
                                  -------------
                    NET CURRENT  -4.57E-08  AMPS/M**2
```

change mate silver

```
MATERIAL IS silv
```

list properties all

```
   MATERIAL = silv.
    PROPERTY                          INPUT VALUE          CODE VALUE
  1     DIELECTRIC CONSTANT           1.00E+00 (NONE)       1.00E+00 (NONE)
  2     THICKNESS                     1.00E-03 METERS       1.00E-03 MESH
  3     CONDUCTIVITY                 -1.00E+00 MHO/M       -1.00E+00 MHO/M
  4     ATOMIC NUMBER                 4.70E+01 (NONE)       4.70E+01 (NONE)
  5     DELTA MAX>COEFF               1.00E+00 (NONE)       3.09E+00 (NONE)
  6     E-MAX >DEPTH**-1              8.00E-01 KEV          1.58E-02 ANG-01
  7     RANGE                         8.45E+01 ANG.         6.93E+01 ANG.
  8     EXPONENT> RANGE               8.20E-01 (NONE)       1.38E+02 ANG.
  9     RANGE> EXPONENT               7.94E+01 ANG.         8.20E-01 (NONE)
 10     EXPONENT                      1.74E+00 (NONE)       1.74E+00 (NONE)
 11     YIELD FOR 1KEV PROTONS        4.90E-01 (NONE)       4.90E-01 (NONE)
 12     MAX DE/DX FOR PROTONS         1.23E+02 KEV          1.23E+02 KEV
 13     PHOTOCURRENT                  2.90E-05 A/M**2       2.90E-05 A/M**2
 14     SURFACE RESISTIVITY          -1.00E+00 OHMS        -8.85E-12 V-S/Q
```

table all

```
TABLE GENERATED USING ISOTROPIC INCIDENT FLUX
ENERGY(KEV)      EL. SEC.      EL. BKSCAT.      PR. SEC.
    0.020          0.061          0.000          0.017
    0.040          0.120          0.000          0.024
    0.060          0.178          0.139          0.030
    0.080          0.234          0.218          0.035
    0.100          0.289          0.266          0.039
    0.120          0.342          0.302          0.042
    0.140          0.394          0.330          0.046
    0.160          0.444          0.353          0.049
    0.200          0.541          0.390          0.055
    0.400          0.935          0.493          0.077
    0.600          1.194          0.547          0.155
    0.800          1.341          0.582          0.280
    1.000          1.411          0.608          0.404
    1.200          1.446          0.605          0.522
    1.400          1.428          0.603          0.634
    1.600          1.391          0.600          0.739
    1.800          1.345          0.598          0.837
    2.000          1.295          0.596          0.930
    4.000          0.903          0.577          1.647
    6.000          0.696          0.565          2.149
    8.000          0.573          0.556          2.542
   10.000          0.491          0.551          2.866
```

plot secon

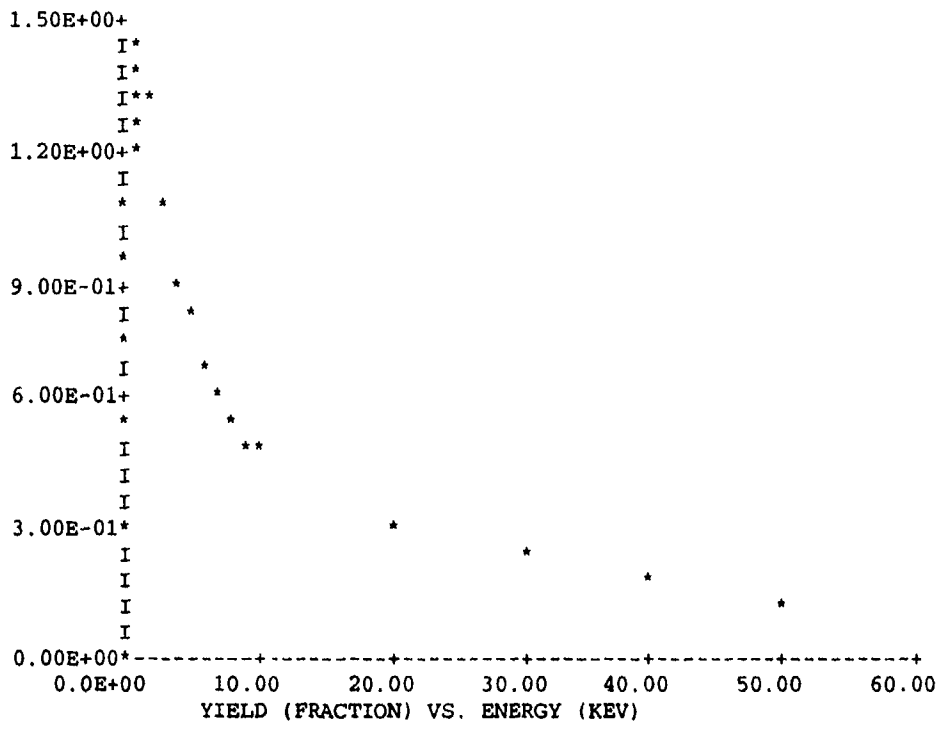

change vend -30

VEND = -3.00E+01 KEV

table iv

V	JTOT	JE	JSECE	JBSCAT	JI	JSECI
0.00E+00	-1.37E-07	-3.30E-06	1.22E-06	1.80E-06	2.54E-08	1.18E-07
-1.43E+00	-9.83E-08	-2.93E-06	1.08E-06	1.60E-06	2.66E-08	1.24E-07
-2.86E+00	-6.32E-08	-2.60E-06	9.58E-07	1.42E-06	2.79E-08	1.30E-07
-4.29E+00	-3.10E-08	-2.31E-06	8.51E-07	1.26E-06	2.91E-08	1.36E-07
-5.71E+00	-1.44E-09	-2.05E-06	7.55E-07	1.12E-06	3.03E-08	1.42E-07
-7.14E+00	2.57E-08	-1.82E-06	6.70E-07	9.93E-07	3.15E-08	1.49E-07
-8.57E+00	5.08E-08	-1.61E-06	5.95E-07	8.81E-07	3.28E-08	1.55E-07
-1.00E+01	7.40E-08	-1.43E-06	5.28E-07	7.82E-07	3.40E-08	1.62E-07
-1.14E+01	9.56E-08	-1.27E-06	4.69E-07	6.95E-07	3.52E-08	1.68E-07
-1.29E+01	1.16E-07	-1.13E-06	4.16E-07	6.17E-07	3.64E-08	1.75E-07
-1.43E+01	1.34E-07	-1.00E-06	3.70E-07	5.47E-07	3.77E-08	1.82E-07
-1.57E+01	1.52E-07	-8.90E-07	3.28E-07	4.86E-07	3.89E-08	1.89E-07
-1.71E+01	1.69E-07	-7.90E-07	2.91E-07	4.31E-07	4.01E-08	1.96E-07
-1.86E+01	1.84E-07	-7.01E-07	2.59E-07	3.83E-07	4.13E-08	2.03E-07
-2.00E+01	1.99E-07	-6.23E-07	2.30E-07	3.40E-07	4.26E-08	2.10E-07
-2.14E+01	2.13E-07	-5.53E-07	2.04E-07	3.02E-07	4.38E-08	2.17E-07
-2.29E+01	2.27E-07	-4.91E-07	1.81E-07	2.68E-07	4.50E-08	2.24E-07
-2.43E+01	2.40E-07	-4.36E-07	1.61E-07	2.38E-07	4.62E-08	2.31E-07
-2.57E+01	2.52E-07	-3.87E-07	1.43E-07	2.11E-07	4.75E-08	2.38E-07
-2.71E+01	2.64E-07	-3.43E-07	1.27E-07	1.87E-07	4.87E-08	2.45E-07
-2.86E+01	2.76E-07	-3.05E-07	1.12E-07	1.66E-07	4.99E-08	2.52E-07

plot iv

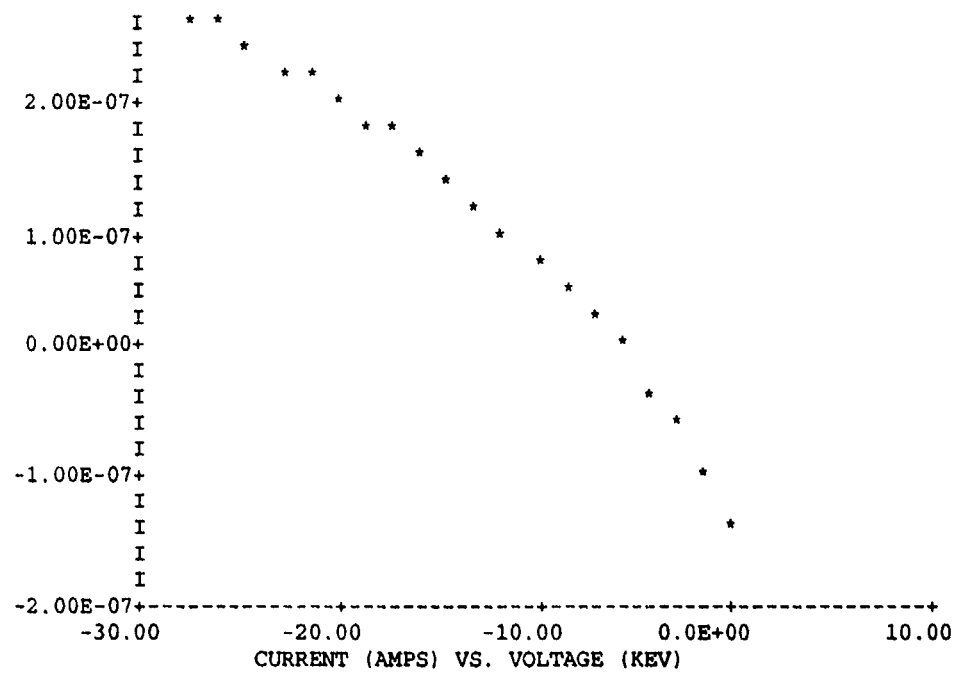

change vend -1

VEND = -1.00E+00 KEV

table charge

T (SEC)	V (VOLTS)	I(AMPS/M**2)
0.00E+00	0.00E+00	-1.37E-07
1.55E+02	-1.76E+03	-8.99E-08
3.10E+02	-2.94E+03	-6.11E-08
4.66E+02	-3.76E+03	-4.25E-08
6.21E+02	-4.34E+03	-2.99E-08
7.76E+02	-4.74E+03	-2.12E-08
9.31E+02	-5.03E+03	-1.52E-08
1.09E+03	-5.24E+03	-1.09E-08
1.24E+03	-5.39E+03	-7.87E-09
1.40E+03	-5.50E+03	-5.68E-09
1.55E+03	-5.58E+03	-4.11E-09
1.71E+03	-5.64E+03	-2.98E-09
1.86E+03	-5.68E+03	-2.16E-09
2.02E+03	-5.71E+03	-1.57E-09
2.17E+03	-5.73E+03	-1.14E-09
2.33E+03	-5.75E+03	-8.26E-10
2.48E+03	-5.76E+03	-6.00E-10
2.64E+03	-5.77E+03	-4.36E-10
2.79E+03	-5.77E+03	-3.17E-10
2.95E+03	-5.78E+03	-2.30E-10

plot charge

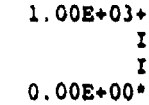

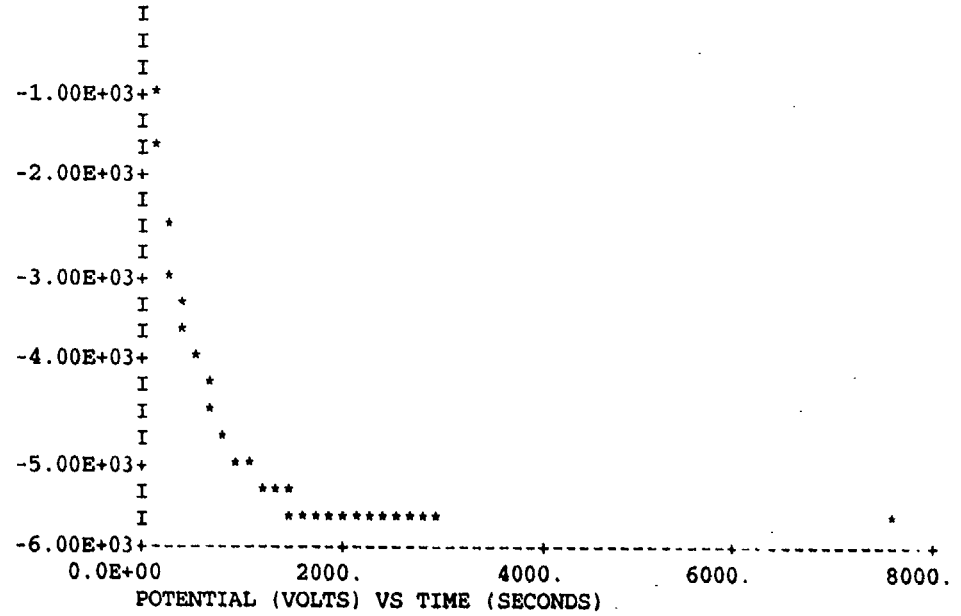


```
result charge

CYCLE    1   TIME  0.00E+00 SECONDS     POTENTIAL  0.00E+00 VOLTS
INCIDENT ELECTRON CURRENT          -3.30E-06
         SECONDARY ELECTRONS        1.22E-06
         BACKSCATTERED ELECTRONS    1.80E-06
INCIDENT PROTON CURRENT             2.54E-08
         SECONDARY ELECTRONS        1.18E-07
                                   ----------
                     NET CURRENT   -1.37E-07  AMPS/M**2
CYCLE   40   TIME  7.61E+03 SECONDS     POTENTIAL -5.78E+03 VOLTS
INCIDENT ELECTRON CURRENT          -2.04E-06
         SECONDARY ELECTRONS        7.51E-07
         BACKSCATTERED ELECTRONS    1.11E-06
INCIDENT PROTON CURRENT             3.04E-08
         SECONDARY ELECTRONS        1.43E-07
                                   ----------
                     NET CURRENT   -1.96E-10  AMPS/M**2

exit
```

C.2 Equilibrium Potential of Spacecraft in Aurora

Suchgr is used to compute the current-voltage relation shown in Figure 10 in Chapter 2 and the potentials shown in Table 2 in Chapter 2. The environment commands are used to set the environment to the severe auroral environment. The spacecraft mach velocity is set to 0.001. Orbit-limited current collection is requested. The surface material is set to be kapton and the default properties displayed. A summary of potentials and currents before and after charging is requested. Similar information is requested for silver. Then space-charge-limited current collection is requested and the spacecraft radius is set to be 1 m. The surface material is set to be kapton and a summary of potentials and currents before

and after charging is requested. Similarly for silver. The spacecraft radius is set to 10 m and the potentials and currents for kapton and silver. The mach velocity is set to 8. The current-voltage relation is requested for a 1 m kapton sphere with a mach velocity of 8. And finally, the space-charge-limited calculations are repeated. For additional information on the use of **suchgr** see Lilley et al. [1989].

```
Welcome to SUCHGR 1.3

***ERROR - READMS - LUN 11 KEY=       1 NOT PREVIOUSLY WRITTEN.
***ERROR - READMS - LUN 19 KEY=CONT NOT PREVIOUSLY WRITTEN.
***ERROR - READMS - LUN 19 KEY=MT19 NOT PREVIOUSLY WRITTEN.
    Default material is
    Default environment is DMSP

 SUCHGR command >>  DEN1 3.55e9

 SUCHGR command >>  TEMP1 0.2

 SUCHGR command >>  DEN2   6.0E5

 SUCHGR command >>  TEMP2  8.0E3

 SUCHGR command >>  GAUCO  4.0e4

 SUCHGR command >>  EMAUT  2.4E4

 SUCHGR command >>  DELTA  1.6E4

 SUCHGR command >>  PONCO  3.0E11

 SUCHGR command >>  PALPHA 1.1

 SUCHGR command >>  PCUTL  50.0

 SUCHGR command >>  PCUTH  1.6E6

 SUCHGR command >>  vend -5000

 SUCHGR command >>  avmach .001

 SUCHGR command >>  orbit

 SUCHGR command >>  mate kapton
Setting default values for material KAPT

 SUCHGR command >>  show mate

              Material Properties Keywords & Current Settings
 Keyword   Description                Values        Units
 -------   -----------                ------        -----
 MATNAM    Material Name              KAPT          (none)
 DIELEC    Dielectric Constant        3.5000e+00    (none)
 THICK     Thickness                  1.2700e-04    meters
 CONDUCT   Conductivity               1.0000e-16    MHO/M
 ATOMNUMB  Atomic Number              5.0000e+00    (none)
 DELTAMAX  Delta Max                  2.1000e+00    (none)
 EMAX      E-Max                      1.5000e-01    keV
 RANGE1    Range_1                    7.1480e+01    angstroms
 EXP1      Exponent_1                 6.0000e-01    (none)
 RANGE2    Range_2                    1.1210e+02    angstroms
 EXP2      Exponent_2                 1.7700e+00    (none)
```

```
PROYIELD Yield for 1keV Protons        4.5500e-01    (none)
PROMAX   Max de/dx for Protons         1.4000e+02    keV
PHOTOCUR Photo Current                 2.0000e-05    amps/meter**2
RESIST   Surface Resistivity           1.0000e+16    ohms
SPDISCHR Space Discharge Potential     1.0000e+04    volts
INDISCHR Interal Discharge Potential   2.0000e+03    volts
RICCOEFF Radn-Induced Cond. Coeff      1.0000e-13    MHOMS3
RICPOWER Radn-Induced Cond. Power      1.0000e+00    (none)
MATDENS  Density                       1.0000e+03    kg/m*3

SUCHGR command >>  charge

Charged under Orbit Limited Regime
                                    Initial       Final        Units
                                    -------       -----        -----
   Surface Potential               0.0000e+00   -9.4500e+00 volts
   Conductor Potential             0.0000e+00    0.0000e+00 volts

Flux Breakdown:
   Incident Electron Flux         -5.8523e-05   -1.5818e-05 A/m**2
   Electron Secondary Flux         2.8429e-06    2.1478e-06 A/m**2
   Backscattered Electron Flux     1.7080e-06    1.7026e-06 A/m**2

   Incident Ion Flux               2.4901e-07    1.1965e-05 A/m**2
   Ion Secondary Flux              0.0000e+00    3.3425e-08 A/m**2

   Photo Flux                      0.0000e+00    0.0000e+00 A/m**2
   Conduction Flux                 0.0000e+00    0.0000e+00 A/m**2
                                  -----------   -----------
   Total Flux                     -5.3723e-05    3.0142e-08 A/m**2

SUCHGR command >>  mate silver
Setting default values for material SILV

SUCHGR command >>  show mate

              Material Properties Keywords & Current Settings
Keyword  Description                   Values        Units
-------  -----------                   ------        -----
MATNAM   Material Name                 SILV          (none)
DIELEC   Dielectric Constant           1.0000e+00    (none)
THICK    Thickness                     1.0000e-03    meters
CONDUCT  Conductivity                 -1.0000e+00    MHO/M
ATOMNUMB Atomic Number                 4.7000e+01    (none)
DELTAMAX Delta Max                     1.0000e+00    (none)
EMAX     E-Max                         8.0000e-01    keV
RANGE1   Range_1                       8.4460e+01    angstroms
EXP1     Exponent_1                    8.2000e-01    (none)
RANGE2   Range_2                       7.9430e+01    angstroms
EXP2     Exponent_2                    1.7400e+00    (none)
PROYIELD Yield for 1keV Protons        4.9000e-01    (none)
PROMAX   Max de/dx for Protons         1.2300e+02    keV
PHOTOCUR Photo Current                 2.9000e-05    amps/meter**2
RESIST   Surface Resistivity          -1.0000e+00    ohms
SPDISCHR Space Discharge Potential     1.0000e+04    volts
INDISCHR Interal Discharge Potential   2.0000e+03    volts
RICCOEFF Radn-Induced Cond. Coeff      1.0000e-13    MHOMS3
RICPOWER Radn-Induced Cond. Power      1.0000e+00    (none)
MATDENS  Density                       1.0000e+03    kg/m*3

SUCHGR command >>  charge

Charged under Orbit Limited Regime
                                    Initial       Final        Units
```

```
                                        -------      -----      -----
   Surface Potential                  0.0000e+00  -5.1500e+00 volts
   Conductor Potential                0.0000e+00   0.0000e+00 volts

 Flux Breakdown:
   Incident Electron Flux            -5.8523e-05  -1.5829e-05 A/m**2
   Electron Secondary Flux            2.8423e-06   2.7837e-06 A/m**2
   Backscattered Electron Flux        6.3595e-06   6.3535e-06 A/m**2

   Incident Ion Flux                  2.4901e-07   6.6337e-06 A/m**2
   Ion Secondary Flux                 0.0000e+00   1.4865e-08 A/m**2

   Photo Flux                         0.0000e+00   0.0000e+00 A/m**2
   Conduction Flux                    0.0000e+00   0.0000e+00 A/m**2
                                     -----------  -----------
   Total Flux                        -4.9072e-05  -4.3569e-08 A/m**2

 SUCHGR command >>  spclim

 SUCHGR command >>  robj 1

 SUCHGR command >>  mate kapton
Material is changed to KAPT

 SUCHGR command >>  charge

 Charged under Space Charge Limited Regime
                                       Initial      Final      Units
                                       -------      -----      -----
   Surface Potential                  0.0000e+00  -5.5375e+02 volts
   Conductor Potential                0.0000e+00   0.0000e+00 volts

 Flux Breakdown:
   Incident Electron Flux            -5.8523e-05  -1.5145e-05 A/m**2
   Electron Secondary Flux            2.8429e-06   1.5278e-06 A/m**2
   Backscattered Electron Flux        1.7080e-06   1.5926e-06 A/m**2

   Incident Ion Flux                  2.4805e-07   1.1645e-05 A/m**2
   Ion Secondary Flux                 0.0000e+00   3.4522e-07 A/m**2

   Photo Flux                         0.0000e+00   0.0000e+00 A/m**2
   Conduction Flux                    0.0000e+00   0.0000e+00 A/m**2
                                     -----------  -----------
   Total Flux                        -5.3724e-05  -3.4618e-08 A/m**2

 Init  Sheath Radius= 1.000e+00 meters  AVMACH= 1.000e-03
 Final Sheath Radius= 6.852e+00 meters  ROBJ  = 1.000e+00 meters

 SUCHGR command >>  mate silver
Material is changed to SILV

 SUCHGR command >>  charge

 Charged under Space Charge Limited Regime
                                       Initial      Final      Units
                                       -------      -----      -----
   Surface Potential                  0.0000e+00  -2.5063e+02 volts
   Conductor Potential                0.0000e+00   0.0000e+00 volts

 Flux Breakdown:
   Incident Electron Flux            -5.8523e-05  -1.5427e-05 A/m**2
   Electron Secondary Flux            2.8423e-06   2.6179e-06 A/m**2
   Backscattered Electron Flux        6.3595e-06   6.1970e-06 A/m**2
```

```
   Incident Ion Flux                 2.4805e-07    6.4516e-06 A/m**2
   Ion Secondary Flux                0.0000e+00    9.8712e-08 A/m**2

   Photo Flux                        0.0000e+00    0.0000e+00 A/m**2
   Conduction Flux                   0.0000e+00    0.0000e+00 A/m**2
                                     ----------    ----------
   Total Flux                       -4.9073e-05   -6.1657e-08 A/m**2

 Init  Sheath Radius= 1.000e+00 meters  AVMACH= 1.000e-03
 Final Sheath Radius= 5.100e+00 meters  ROBJ  = 1.000e+00 meters

 SUCHGR command >>  robj 10

 SUCHGR command >>  mate kapton
Material is changed to KAPT

 SUCHGR command >>  charge

 Charged under Space Charge Limited Regime
                                    Initial       Final       Units
                                    -------       -----       -----
   Surface Potential                0.0000e+00   -5.4475e+03 volts
   Conductor Potential              0.0000e+00    0.0000e+00 volts

 Flux Breakdown:
   Incident Electron Flux          -5.8523e-05   -1.1677e-05 A/m**2
   Electron Secondary Flux          2.8429e-06    1.0731e-06 A/m**2
   Backscattered Electron Flux      1.7080e-06    1.1673e-06 A/m**2

   Incident Ion Flux                2.4805e-07    6.4942e-06 A/m**2
   Ion Secondary Flux               0.0000e+00    3.0669e-06 A/m**2

   Photo Flux                       0.0000e+00    0.0000e+00 A/m**2
   Conduction Flux                  0.0000e+00    0.0000e+00 A/m**2
                                    ----------    ----------
   Total Flux                      -5.3724e-05    1.2409e-07 A/m**2

 Init  Sheath Radius= 1.000e+01 meters  AVMACH= 1.000e-03
 Final Sheath Radius= 5.117e+01 meters  ROBJ  = 1.000e+01 meters

 SUCHGR command >>  mate silver
Material is changed to SILV

 SUCHGR command >>  charge

 Charged under Space Charge Limited Regime
                                    Initial       Final       Units
                                    -------       -----       -----
   Surface Potential                0.0000e+00   -3.1038e+03 volts
   Conductor Potential              0.0000e+00    0.0000e+00 volts

 Flux Breakdown:
   Incident Electron Flux          -5.8523e-05   -1.3243e-05 A/m**2
   Electron Secondary Flux          2.8423e-06    2.1735e-06 A/m**2
   Backscattered Electron Flux      6.3595e-06    5.2689e-06 A/m**2

   Incident Ion Flux                2.4805e-07    4.3153e-06 A/m**2
   Ion Secondary Flux               0.0000e+00    1.4709e-06 A/m**2

   Photo Flux                       0.0000e+00    0.0000e+00 A/m**2
   Conduction Flux                  0.0000e+00    0.0000e+00 A/m**2
                                    ----------    ----------
   Total Flux                      -4.9073e-05   -1.4301e-08 A/m**2
```

```
 Init  Sheath Radius= 1.000e+01 meters  AVMACH= 1.000e-03
 Final Sheath Radius= 4.171e+01 meters  ROBJ  = 1.000e+01 meters

 SUCHGR command >>  avmach 8

 SUCHGR command >>  robj 1

 SUCHGR command >>  mate kapt
Material is changed to KAPT

 SUCHGR command >> table iv


Fluxes(A/m**2) as functions of Surface Voltage(eV)

  SRFVLT     FTOT       FEIN       FESEC      FEBAK      FIIN       FISEC
  0.00E+00 -5.35E-05 -5.85E-05  2.84E-06  1.71E-06  4.96E-07  0.00E+00
 -4.76E+01 -8.01E-06 -1.57E-05  1.96E-06  1.68E-06  4.04E-06  2.51E-08
 -9.52E+01 -5.62E-06 -1.56E-05  1.83E-06  1.67E-06  6.44E-06  5.66E-08
 -1.43E+02 -3.47E-06 -1.56E-05  1.75E-06  1.66E-06  8.58E-06  9.21E-08
 -1.90E+02 -1.47E-06 -1.55E-05  1.70E-06  1.65E-06  1.05E-05  1.31E-07
 -2.38E+02  4.57E-07 -1.54E-05  1.66E-06  1.64E-06  1.24E-05  1.72E-07
 -2.86E+02  2.35E-06 -1.54E-05  1.63E-06  1.63E-06  1.41E-05  2.16E-07
 -3.33E+02  4.15E-06 -1.53E-05  1.61E-06  1.62E-06  1.60E-05  2.62E-07
 -3.81E+02  5.97E-06 -1.53E-05  1.58E-06  1.62E-06  1.78E-05  3.11E-07
 -4.29E+02  7.55E-06 -1.53E-05  1.57E-06  1.61E-06  1.93E-05  3.58E-07
 -4.76E+02  9.13E-06 -1.52E-05  1.55E-06  1.60E-06  2.08E-05  4.06E-07
 -5.24E+02  1.09E-05 -1.52E-05  1.54E-06  1.60E-06  2.23E-05  5.72E-07
 -5.71E+02  1.26E-05 -1.51E-05  1.52E-06  1.59E-06  2.39E-05  7.65E-07
 -6.19E+02  1.44E-05 -1.51E-05  1.51E-06  1.58E-06  2.54E-05  9.85E-07
 -6.67E+02  1.63E-05 -1.50E-05  1.50E-06  1.58E-06  2.70E-05  1.23E-06
 -7.14E+02  1.82E-05 -1.50E-05  1.49E-06  1.57E-06  2.86E-05  1.50E-06
 -7.62E+02  2.01E-05 -1.50E-05  1.48E-06  1.57E-06  3.03E-05  1.80E-06
 -8.10E+02  2.21E-05 -1.49E-05  1.47E-06  1.56E-06  3.19E-05  2.11E-06
 -8.57E+02  2.38E-05 -1.49E-05  1.46E-06  1.56E-06  3.32E-05  2.43E-06
 -9.05E+02  2.55E-05 -1.49E-05  1.45E-06  1.55E-06  3.46E-05  2.77E-06
 -9.52E+02  2.72E-05 -1.49E-05  1.45E-06  1.55E-06  3.59E-05  3.13E-06

 SUCHGR command >> plot iv
```

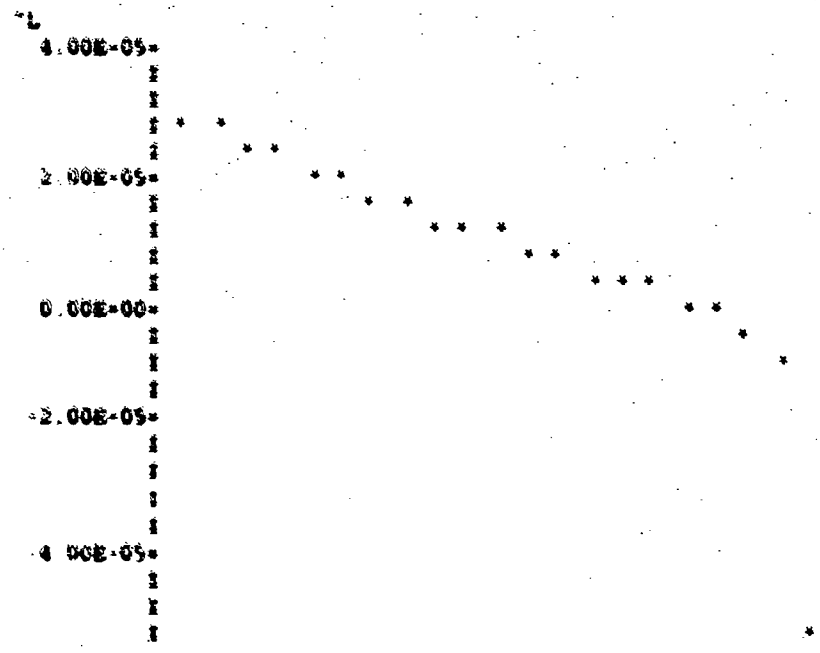

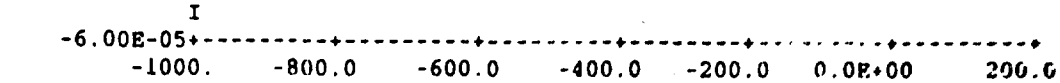

SUCHGR command >> **charge**

Charged under Space Charge Limited Regime

	Initial	Final	Units
Surface Potential	0.0000e+00	-2.2563e+02	volts
Conductor Potential	0.0000e+00	0.0000e+00	volts
Flux Breakdown:			
Incident Electron Flux	-5.8523e-05	-1.5454e-05	A/m**2
Electron Secondary Flux	2.8429e-06	1.6711e-06	A/m**2
Backscattered Electron Flux	1.7080e-06	1.6409e-06	A/m**2
Incident Ion Flux	4.9610e-07	1.1952e-05	A/m**2
Ion Secondary Flux	0.0000e+00	1.6118e-07	A/m**2
Photo Flux	0.0000e+00	0.0000e+00	A/m**2
Conduction Flux	0.0000e+00	0.0000e+00	A/m**2
Total Flux	-5.3476e-05	-2.8665e-08	A/m**2

Init Sheath Radius= 1.000e+00 meters AVMACH= 8.000e+00
Final Sheath Radius= 4.908e+00 meters ROBJ = 1.000e+00 meters

SUCHGR command >> **mate silver**
Material is changed to SILV

SUCHGR command >> **charge**

Charged under Space Charge Limited Regime

	Initial	Final	Units
Surface Potential	0.0000e+00	-9.8750e+01	volts
Conductor Potential	0.0000e+00	0.0000e+00	volts
Flux Breakdown:			
Incident Electron Flux	-5.8523e-05	-1.5616e-05	A/m**2
Electron Secondary Flux	2.8423e-06	2.6936e-06	A/m**2
Backscattered Electron Flux	6.3595e-06	6.2739e-06	A/m**2
Incident Ion Flux	4.9610e-07	6.5983e-06	A/m**2
Ion Secondary Flux	0.0000e+00	6.3513e-08	A/m**2
Photo Flux	0.0000e+00	0.0000e+00	A/m**2
Conduction Flux	0.0000e+00	0.0000e+00	A/m**2
Total Flux	-4.8825e-05	1.3294e-08	A/m**2

Init Sheath Radius= 1.000e+00 meters AVMACH= 8.000e+00
Final Sheath Radius= 3.647e+00 meters ROBJ = 1.000e+00 meters

SUCHGR command >> **robj 10**

SUCHGR command >> **mate kapton**
Material is changed to KAPT

SUCHGR command >> **charge**

Charged under Space Charge Limited Regime

```
                                  Initial      Final       Units
                                  -------      -----       -----
   Surface Potential             0.0000e+00  -2 9163e+03 volts
   Conductor Potential           0.0000e+00   0.0000e+00 volts

 Flux Breakdown:
   Incident Electron Flux       -5.8523e-05  -1.3373e-05 A/m**2
   Electron Secondary Flux       2.8429e-06   1.2596e-06 A/m**2
   Backscattered Electron Flux   1.7080e-06   1.3658e-06 A/m**2

   Incident Ion Flux             4.9610e-07   8.2339e-06 A/m**2
   Ion Secondary Flux            0.0000e+00   2.4872e-06 A/m**2

   Photo Flux                    0.0000e+00   0.0000e+00 A/m**2
   Conduction Flux               0.0000e+00   0.0000e+00 A/m**2
                                -----------  -----------
   Total Flux                   -5.3476e-05  -2.6873e-08 A/m**2

 Init  Sheath Radius= 1.000e+01 meters  AVMACH= 8.000e+00
 Final Sheath Radius= 4.074e+01 meters  ROBJ  = 1.000e+01 meters

 SUCHGR command >>  mate silver
Material is changed to SILV

 SUCHGR command >>  charge

 Charged under Space Charge Limited Regime
                                  Initial      Final       Units
                                  -------      -----       -----
   Surface Potential             0.0000e+00  -1.5569e+03 volts
   Conductor Potential           0.0000e+00   0.0000e+00 volts

 Flux Breakdown:
   Incident Electron Flux       -5.8523e-05  -1.4354e-05 A/m**2
   Electron Secondary Flux       2.8423e-06   2.3563e-06 A/m**2
   Backscattered Electron Flux   6.3595e-06   5.7335e-06 A/m**2

   Incident Ion Flux             4.9610e-07   5.3209e-06 A/m**2
   Ion Secondary Flux            0.0000e+00   9.5343e-07 A/m**2

   Photo Flux                    0.0000e+00   0.0000e+00 A/m**2
   Conduction Flux               0.0000e+00   0.0000e+00 A/m**2
                                -----------  -----------
   Total Flux                   -4.8825e-05   9.9690e-09 A/m**2

 Init  Sheath Radius= 1.000e+01 meters  AVMACH= 8.000e+00
 Final Sheath Radius= 3.279e+01 meters  ROBJ  = 1.000e+01 meters

 SUCHGR command >>  quit
Want to save a copy of the session?  >>  yes

Exit SUCHGR.
```

C.3 Geosynchronous Kapton-Silver Quasi-sphere

The following files are the input and output files for the Geosynchronous Kapton-Silver Quasi-sphere problem shown in Figures 13 and 14 of Chapter 2. For additional information on the use of *NASCAP/GEO* see Mandell et al. [1984].

The problem was completed in four steps with a slightly different standard input file for each step. The first input file shows the options chosen, the object definition, and the environment description.

Geosynchronous Kapton-Silver Quasi-sphere Standard Input

```
RDOPT 5
   SURFACE CELL 1
   SURFACE CELL 5
   LONGTIMESTEP 1000
   DELTA .001
   DELFAC 1.2
   XMESH 1
   NCYC 20
   NG 2
   NZ 17
   END
OBJDEF 5
   QSPHERE
    CENTER 0 0 0
    DIAMETER 7
    SIDE 3
    MATERIAL KAPTON
    ENDOBJ
   PATCHR
    CORNER 3 -1 -1
    DELTAS 1  3  3
    SURFACE +X SILVER
    ENDOBJ
   PATCHR
    CORNER -1 3 -1
    DELTAS 3  1  3
    SURFACE +Y SILVER
    ENDOBJ
   PATCHR
    CORNER -1 -1 3
    DELTAS 3  3  1
    SURFACE +Z SILVER
    ENDOBJ
   PATCHW
    CORNER 2 -1 2
    FACE SILVER 1 0 1
    LENGTH 2 3 2
    ENDOBJ
   PATCHW
    CORNER -1 2 2
    FACE SILVER 0 1 1
    LENGTH 3 2 2
    ENDOBJ
   PATCHW
    CORNER 2 2 -1
    FACE SILVER 1 1 0
    LENGTH 2 2 3
    ENDOBJ
   PATCHW
    CORNER -1 -1 2
    FACE SILVER -1 0 1
    LENGTH 2 3 2
    ENDOBJ
   PATCHW
    CORNER -1 -1 2
```

```
    FACE SILVER 0 -1 1
    LENGTH 3 2 2
    ENDOBJ
   TETRAH
    CORNER 2 2 2
    FACE SILVER 1 1 1
    LENGTH 2 2 2
    ENDOBJ
   TETRAH
    CORNER -1 2 2
    FACE SILVER -1 1 1
    LENGTH 2 2 2
    ENDOBJ
   TETRAH
    CORNER 2 -1 2
    FACE SILVER 1 -1 1
    LENGTH 2 2 2
    ENDOBJ
   TETRAH
    CORNER -1 -1 2
    FACE SILVER -1 -1 1
    LENGTH 2 2 2
    ENDOBJ
   ENDSAT
CAPACI
TRILIN 5
   SINGLE
   1.12 CGS
   13 KEV
   .236 CGS
   29.5 KEV
   END
END
```

Geosynchronous Kapton-Silver Quasi-sphere Standard Input for Continuation

```
RDOPT 5
   SURFACE CELL 1
   SURFACE CELL 5
   LONGTIMESTEP 1000
   RESTART
   DELTA 0.045
   DELFAC 1.4
   XMESH 1
   NCYC 20
   NG 2
   NE 17
   END
TRILIN 5
   SINGLE
   1.12 CGS
   12 KEV
   .236 CGS
   29.5 KEV
   END
END
```

Geosynchronous Kapton-Silver Quasi-sphere Standard Input for Second Continuation

```
RDOPT 5
   SURFACE CELL 1
   SURFACE CELL 5
   LONGTIMESTEP 1000
   RESTART
   DELTA 27
   DELFAC 1.4
   XMESH 1
   NCYC 20
   NG 2
   NZ 17
   END
TRILIN 5
   SINGLE
   1.12 CGS
   12 KEV
   .236 CGS
   29.5 KEV
   END
END
```

Geosynchronous Kapton-Silver Quasi-sphere Standard Input for Third Continuation

```
RDOPT 5
   SURFACE CELL 1
   SURFACE CELL 5
   LONGTIMESTEP 1000
   RESTART
   DELTA 16e3
   DELFAC 1.4
   XMESH 1
   NCYC 5
   NG 2
   NZ 17
   END
TRILIN 5
   SINGLE
   1.12 CGS
   12 KEV
   .236 CGS
   29.5 KEV
   END
END
```

Geosynchronous Kapton-Silver Quasi-sphere Termtalk Execution fort.3 File

A group of all the surface cells of material kapton is defined. The final potential of this group is requested. All the cells are at –22.5 kV. A group of all the surface cells of material silver is defined. The final potential of this group is requested. All the cells are at –10.9 kV. A group of those cells facing in the 1 1 1 or –1 –1 –1 direction is defined. These cells are those in the center of the kapton patch and the silver patch respectively. The history of the potentials on these cells is requested.

```
CHOOSE ANY MODULE
 HELP IS ALWAYS AVAILABLE - TYPE 'HELP'
>HELP
   HELP IS AT HAND - PICK A NUMBER,
(1) BASIC USE                              (7) ERROR MESSAGES
(2) CURRENT MODULE                         (8) COORDINATE SYSTEM
(3) NUMBERING CONVENTIONS                  (9) LINE PRINTER FILE
(4) FLUX,FIELD, POTL, DELTA, STRESS        (10) DEFAULT MODES
(5) SUBSET AND GROUPS                      (11) OLD NASCAP
(6) AIDS                                   (12) COMPLAINTS
                      (13) RETURN TO MAIN
1
-- BASIC USE --
     TERMTALK CONSISTS OF A SET OF MODULES, EACH GIVING
THE USER ACCESS TO A CERTAIN TYPE OF NASCAP INFORMATION.
'HISTORY' FOR EXAMPLE, GIVES THE CHARGING HISTORY OF
INDIVIDUAL SURFACE CELLS. 'LATEST' GIVES INFORMATION
ONLY FROM THE LATEST CHARGING CYCLE.  'SINGLE' GIVES
GEOMETRICAL AND OTHER INFORMATION ABOUT AN INDIVIDUAL
CELL.
     WHICHEVER MODULE YOU ARE IN, YOU HAVE AVAILABLE A
SET OF COMMANDS AND A SET OF MODES.  COMMANDS INITIATE
OUTPUT.  MODES ALTER THE FORM OF SUCCEEDING OUTPUT.
     AT ANY TIME INSTEAD OF TYPING A COMMAND
OR MODE, YOU MAY CHANGE MODULES OR CALL FOR AID.
ALTOGETHER YOU HAVE FOUR CHOICES - TYPE A COMMAND,
A MODE, THE NAME OF A DIFFERENT MODULES, OR THE
NAME OF AN AID.
     AS AN EXAMPLE, YOU ARE IN MODULE SINGLE.  YOU
TYPE THE NUMBER 317.  THIS IS A COMMAND.  THE
TERMINAL PRINTS OUT THE POTENTIAL AND THE SURFACE
NORMAL OF CELL #317.  YOU WANT MORE.
YOU TYPE 'EVERYTHING' (A MODE) AND ON THE NEXT
LINE TYPE '317' AGAIN.  MORE INFORMATION COMES OUT.
TO CHANGE MODULES, YOU TYPE 'HISTORY'.  NOW YOU DON'T
KNOW WHAT TO DO, SO YOU TYPE 'HELP'.  AND YOU GET THIS
MESSAGE.
     FOR ANY COMMAND, MODE, MODULE, OR AID, TERMTALK
RECOGNIZES AN ENTIRE WORD BASED ON THE FIRST THREE
LETTERS.
... PICK ANOTHER NUMBER  -OR- TYPE 'MENU' TO SEE YOUR CHOICES
    -OR-  <CR> TO RETURN TO MAIN

CHOOSE ANY MODULE
 HELP IS ALWAYS AVAILABLE - TYPE 'HELP'
>subset kapton
DEFINITION OF NEW SUBSET NAMED kapt
 159 REMAINING IN GROUP
SUBSET INSTRUCTION PLEASE ?
>matl kapt
  85 REMAINING IN GROUP
SUBSET INSTRUCTION PLEASE ?
>done
GROUP kapt WITH   85 MEMBERS IS NOW DEFINED
RETURNING TO MODULE  'MAIN'
CHOOSE ANY MODULE
 HELP IS ALWAYS AVAILABLE - TYPE 'HELP'
>latest
LATEST COMMAND OR MODE SET ?
>potl
MODE RESET
LATEST COMMAND OR MODE SET ?
>group kapton
```

```
POTL IN VOLTS  FOR NASCAP CYCLE  65 ... TIME = 2.32e+05 SEC
   1-2.25e+04    2-2.25e+04    3-2.25e+04    4-2.25e+04    6-2.25e+04
   7-2.25e+04    8-2.25e+04    9-2.25e+04   11-2.25e+04   12-2.25e+04
  13-2.25e+04   14-2.25e+04   16-2.25e+04   17-2.25e+04   18-2.25e+04
  19-2.25e+04   21-2.25e+04   22-2.25e+04   23-2.25e+04   24-2.25e+04
  26-2.25e+04   27-2.25e+04   28-2.25e+04   29-2.25e+04   31-2.25e+04
  32-2.25e+04   35-2.25e+04   37-2.25e+04   39-2.25e+04   41-2.25e+04
  42-2.25e+04   45-2.25e+04   46-2.25e+04   47-2.25e+04   48-2.25e+04
  50-2.25e+04   51-2.25e+04   52-2.25e+04   53-2.25e+04   55-2.25e+04
  57-2.25e+04   59-2.25e+04   61-2.25e+04   63-2.25e+04   65-2.25e+04
  70-2.25e+04   71-2.25e+04   72-2.25e+04   73-2.25e+04   75-2.25e+04
  77-2.25e+04   79-2.25e+04   81-2.25e+04   83-2.25e+04   85-2.25e+04
  90-2.25e+04   91-2.25e+04   92-2.25e+04   93-2.25e+04   95-2.25e+04
  97-2.25e+04   99-2.25e+04  101-2.25e+04  103-2.25e+04  105-2.25e+04
 110-2.25e+04  111-2.25e+04  112-2.25e+04  113-2.25e+04  115-2.25e+04
 116-2.25e+04  119-2.25e+04  121-2.25e+04  123-2.25e+04  125-2.25e+04
 126-2.25e+04  129-2.25e+04  134-2.25e+04  135-2.25e+04  136-2.25e+04
 137-2.25e+04  139-2.25e+04  144-2.25e+04  149-2.25e+04  154-2.25e+04
LATEST COMMAND OR MODE SET ?
>subset silver
DEFINITION OF NEW SUBSET NAMED silv
 159 REMAINING IN GROUP
SUBSET INSTRUCTION PLEASE ?
>matl silver
  73 REMAINING IN GROUP
SUBSET INSTRUCTION PLEASE ?
>done
GROUP silv WITH   73 MEMBERS IS NOW DEFINED
RETURNING TO MODULE  'LATE'
LATEST COMMAND OR MODE SET ?
>group silver
POTL IN VOLTS  FOR NASCAP CYCLE  65 ... TIME = 2.32e+05 SEC
   5-1.09e+04   10-1.09e+04   15-1.09e+04   20-1.09e+04   25-1.09e+04
  30-1.09e+04   33-1.09e+04   34-1.09e+04   36-1.09e+04   38-1.09e+04
  40-1.09e+04   43-1.09e+04   44-1.09e+04   49-1.09e+04   54-1.09e+04
  56-1.09e+04   58-1.09e+04   60-1.09e+04   62-1.09e+04   64-1.09e+04
  66-1.09e+04   67-1.09e+04   68-1.09e+04   69-1.09e+04   74-1.09e+04
  76-1.09e+04   78-1.09e+04   80-1.09e+04   82-1.09e+04   84-1.09e+04
  86-1.09e+04   87-1.09e+04   88-1.09e+04   89-1.09e+04   94-1.09e+04
  96-1.09e+04   98-1.09e+04  100-1.09e+04  102-1.09e+04  104-1.09e+04
 106-1.09e+04  107-1.09e+04  108-1.09e+04  109-1.09e+04  114-1.09e+04
 117-1.09e+04  118-1.09e+04  120-1.09e+04  122-1.09e+04  124-1.09e+04
 127-1.09e+04  128-1.09e+04  130-1.09e+04  131-1.09e+04  132-1.09e+04
 133-1.09e+04  138-1.09e+04  140-1.09e+04  141-1.09e+04  142-1.09e+04
 143-1.09e+04  145-1.09e+04  146-1.09e+04  147-1.09e+04  148-1.09e+04
 150-1.09e+04  151-1.09e+04  152-1.09e+04  153-1.09e+04  155-1.09e+04
 156-1.09e+04  157-1.09e+04  158-1.09e+04    0 0.00e+00    0 0.00e+00
LATEST COMMAND OR MODE SET ?
>history
HISTORY COMMAND OR MODE SET ?
>subset one
DEFINITION OF NEW SUBSET NAMED one
 159 REMAINING IN GROUP
SUBSET INSTRUCTION PLEASE ?
>normal 1 1 1
   4 REMAINING IN GROUP
SUBSET INSTRUCTION PLEASE ?
>which
MEMBERS OF GROUP one
  127  128  133  158    0    0    0    0    0    0
   4 REMAINING IN GROUP
SUBSET INSTRUCTION PLEASE ?
>done
GROUP one  WITH    4 MEMBERS IS NOW DEFINED
```

```
RETURNING TO MODULE  'HIST'
HISTORY COMMAND OR MODE SET ?
>subset minus
DEFINITION OF NEW SUBSET NAMED minu
 159 REMAINING IN GROUP
SUBSET INSTRUCTION PLEASE ?
>normal -1 -1 -1
   4 REMAINING IN GROUP
SUBSET INSTRUCTION PLEASE ?
>which
MEMBERS OF GROUP minu
    1   26   31   32    0    0    0    0    0    0
   4 REMAINING IN GROUP
SUBSET INSTRUCTION PLEASE ?
>done
GROUP minu WITH    4 MEMBERS IS NOW DEFINED
RETURNING TO MODULE  'HIST'
HISTORY COMMAND OR MODE SET ?
>subset oppose
DEFINITION OF NEW SUBSET NAMED oppo
 159 REMAINING IN GROUP
SUBSET INSTRUCTION PLEASE ?
>numbers 1 to 1
   1 REMAINING IN GROUP
SUBSET INSTRUCTION PLEASE ?
>normal 1 1 1
   0 REMAINING IN GROUP
SUBSET INSTRUCTION PLEASE ?
>or one
   4 REMAINING IN GROUP
SUBSET INSTRUCTION PLEASE ?
>or minus
   8 REMAINING IN GROUP
SUBSET INSTRUCTION PLEASE ?
>done
GROUP oppo WITH    8 MEMBERS IS NOW DEFINED
RETURNING TO MODULE  'HIST'
HISTORY COMMAND OR MODE SET ?
>group oppo
POTL IN VOLTS
  TIME  :     1        26       31       32       127      128      133
--------:-------------------------------------------------------------------
        :    #1       #2       #3       #4       #5       #6       #7
 1.0e-03:-3.63e+02-3.63e+02-3.63e+02-3.63e+02-3.63e+02-3.63e+02-3.63e+02
 2.2e-03:-7.74e+02-7.74e+02-7.74e+02-7.74e+02-7.74e+02-7.74e+02-7.74e+02
 3.6e-03:-1.24e+03-1.24e+03-1.24e+03-1.24e+03-1.24e+03-1.24e+03-1.24e+03
 5.4e-03:-1.76e+03-1.76e+03-1.76e+03-1.76e+03-1.76e+03-1.76e+03-1.76e+03
 7.4e-03:-2.33e+03-2.33e+03-2.33e+03-2.33e+03-2.33e+03-2.33e+03-2.33e+03
 9.9e-03:-2.97e+03-2.97e+03-2.97e+03-2.97e+03-2.97e+03-2.97e+03-2.97e+03
 1.3e-02:-3.66e+03-3.66e+03-3.66e+03-3.66e+03-3.66e+03-3.66e+03-3.66e+03
 1.6e-02:-4.41e+03-4.41e+03-4.41e+03-4.41e+03-4.41e+03-4.41e+03-4.41e+03
 2.1e-02:-5.21e+03-5.21e+03-5.21e+03-5.21e+03-5.21e+03-5.21e+03-5.21e+03
 2.6e-02:-6.06e+03-6.06e+03-6.06e+03-6.06e+03-6.06e+03-6.06e+03-6.06e+03
 3.2e-02:-6.96e+03-6.96e+03-6.96e+03-6.96e+03-6.96e+03-6.96e+03-6.96e+03
 4.0e-02:-7.89e+03-7.89e+03-7.89e+03-7.89e+03-7.89e+03-7.89e+03-7.89e+03
 4.8e-02:-8.85e+03-8.85e+03-8.85e+03-8.85e+03-8.85e+03-8.85e+03-8.85e+03
 5.9e-02:-9.82e+03-9.82e+03-9.82e+03-9.82e+03-9.82e+03-9.82e+03-9.82e+03
 7.2e-02:-1.08e+04-1.08e+04-1.08e+04-1.08e+04-1.08e+04-1.08e+04-1.08e+04
 8.7e-02:-1.18e+04-1.18e+04-1.18e+04-1.18e+04-1.18e+04-1.18e+04-1.18e+04
 1.1e-01:-1.27e+04-1.27e+04-1.27e+04-1.27e+04-1.27e+04-1.27e+04-1.27e+04
 1.3e-01:-1.36e+04-1.36e+04-1.36e+04-1.36e+04-1.36e+04-1.36e+04-1.36e+04
 1.5e-01:-1.44e+04-1.44e+04-1.44e+04-1.44e+04-1.44e+04-1.44e+04-1.44e+04
 1.9e-01:-1.51e+04-1.51e+04-1.51e+04-1.51e+04-1.51e+04-1.51e+04-1.51e+04
 2.3e-01:-1.58e+04-1.58e+04-1.58e+04-1.58e+04-1.58e+04-1.58e+04-1.58e+04
```

```
2.9e-01:-1.65e+04-1.65e+04-1.65e+04-1.65e+04-1.65e+04-1.65e+04-1.65e+04
3.8e-01:-1.70e+04-1.70e+04-1.70e+04-1.70e+04-1.70e+04-1.70e+04-1.70e+04
5.1e-01:-1.74e+04-1.74e+04-1.74e+04-1.74e+04-1.74e+04-1.74e+04-1.74e+04
6.8e-01:-1.77e+04-1.77e+04-1.77e+04-1.77e+04-1.77e+04-1.77e+04-1.77e+04
9.2e-01:-1.79e+04-1.79e+04-1.79e+04-1.79e+04-1.79e+04-1.79e+04-1.79e+04
1.3e+00:-1.80e+04-1.80e+04-1.80e+04-1.80e+04-1.80e+04-1.80e+04-1.80e+04
1.7e+00:-1.81e+04-1.81e+04-1.81e+04-1.81e+04-1.81e+04-1.81e+04-1.81e+04
2.4e+00:-1.82e+04-1.82e+04-1.82e+04-1.82e+04-1.82e+04-1.82e+04-1.82e+04
3.3e+00:-1.82e+04-1.82e+04-1.82e+04-1.82e+04-1.82e+04-1.82e+04-1.82e+04
4.6e+00:-1.82e+04-1.82e+04-1.82e+04-1.82e+04-1.82e+04-1.82e+04-1.82e+04
6.5e+00:-1.82e+04-1.82e+04-1.82e+04-1.82e+04-1.82e+04-1.82e+04-1.82e+04
9.0e+00:-1.82e+04-1.82e+04-1.82e+04-1.82e+04-1.82e+04-1.82e+04-1.82e+04
1.3e+01:-1.82e+04-1.82e+04-1.82e+04-1.82e+04-1.82e+04-1.82e+04-1.82e+04
1.8e+01:-1.82e+04-1.82e+04-1.82e+04-1.82e+04-1.82e+04-1.82e+04-1.82e+04
2.5e+01:-1.82e+04-1.82e+04-1.82e+04-1.82e+04-1.82e+04-1.82e+04-1.82e+04
3.4e+01:-1.82e+04-1.82e+04-1.82e+04-1.82e+04-1.82e+04-1.82e+04-1.82e+04
4.8e+01:-1.82e+04-1.82e+04-1.82e+04-1.82e+04-1.82e+04-1.82e+04-1.82e+04
6.7e+01:-1.82e+04-1.82e+04-1.82e+04-1.82e+04-1.82e+04-1.82e+04-1.82e+04
9.4e+01:-1.83e+04-1.83e+04-1.83e+04-1.83e+04-1.82e+04-1.82e+04-1.82e+04
1.2e+02:-1.83e+04-1.83e+04-1.83e+04-1.83e+04-1.82e+04-1.82e+04-1.82e+04
1.6e+02:-1.83e+04-1.83e+04-1.83e+04-1.83e+04-1.82e+04-1.82e+04-1.82e+04
2.1e+02:-1.83e+04-1.83e+04-1.83e+04-1.83e+04-1.81e+04-1.81e+04-1.81e+04
2.9e+02:-1.83e+04-1.83e+04-1.83e+04-1.83e+04-1.81e+04-1.81e+04-1.81e+04
3.9e+02:-1.83e+04-1.83e+04-1.83e+04-1.83e+04-1.81e+04-1.81e+04-1.81e+04
5.3e+02:-1.83e+04-1.83e+04-1.83e+04-1.83e+04-1.80e+04-1.80e+04-1.80e+04
7.4e+02:-1.84e+04-1.84e+04-1.84e+04-1.84e+04-1.79e+04-1.79e+04-1.79e+04
1.0e+03:-1.84e+04-1.84e+04-1.84e+04-1.84e+04-1.78e+04-1.78e+04-1.78e+04
1.4e+03:-1.85e+04-1.85e+04-1.85e+04-1.85e+04-1.77e+04-1.77e+04-1.77e+04
2.0e+03:-1.86e+04-1.86e+04-1.86e+04-1.86e+04-1.75e+04-1.75e+04-1.75e+04
2.8e+03:-1.88e+04-1.88e+04-1.88e+04-1.88e+04-1.72e+04-1.72e+04-1.72e+04
3.9e+03:-1.89e+04-1.89e+04-1.89e+04-1.89e+04-1.68e+04-1.68e+04-1.68e+04
5.4e+03:-1.88e+04-1.88e+04-1.88e+04-1.88e+04-1.58e+04-1.58e+04-1.58e+04
7.5e+03:-1.93e+04-1.93e+04-1.93e+04-1.93e+04-1.54e+04-1.54e+04-1.54e+04
1.1e+04:-1.95e+04-1.95e+04-1.95e+04-1.95e+04-1.44e+04-1.44e+04-1.44e+04
1.5e+04:-2.00e+04-2.00e+04-2.00e+04-2.00e+04-1.34e+04-1.34e+04-1.34e+04
2.1e+04:-2.05e+04-2.05e+04-2.05e+04-2.05e+04-1.24e+04-1.24e+04-1.24e+04
2.9e+04:-2.10e+04-2.10e+04-2.10e+04-2.10e+04-1.14e+04-1.14e+04-1.14e+04
4.0e+04:-2.16e+04-2.16e+04-2.16e+04-2.16e+04-1.05e+04-1.05e+04-1.05e+04
5.7e+04:-2.22e+04-2.22e+04-2.22e+04-2.22e+04-1.05e+04-1.05e+04-1.05e+04
7.3e+04:-2.25e+04-2.25e+04-2.25e+04-2.25e+04-1.06e+04-1.06e+04-1.06e+04
9.5e+04:-2.26e+04-2.26e+04-2.26e+04-2.26e+04-1.08e+04-1.08e+04-1.08e+04
1.3e+05:-2.26e+04-2.26e+04-2.26e+04-2.26e+04-1.09e+04-1.09e+04-1.09e+04
1.7e+05:-2.26e+04-2.26e+04-2.26e+04-2.26e+04-1.09e+04-1.09e+04-1.09e+04
2.3e+05:-2.25e+04-2.25e+04-2.25e+04-2.25e+04-1.09e+04-1.09e+04-1.09e+04
POTL VERSUS LOG(TIME)
```

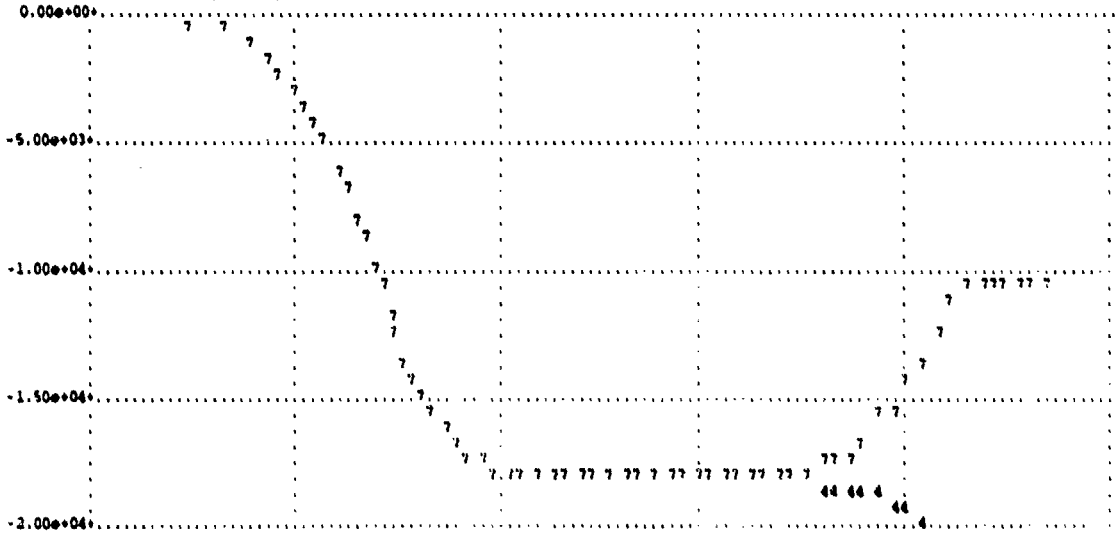

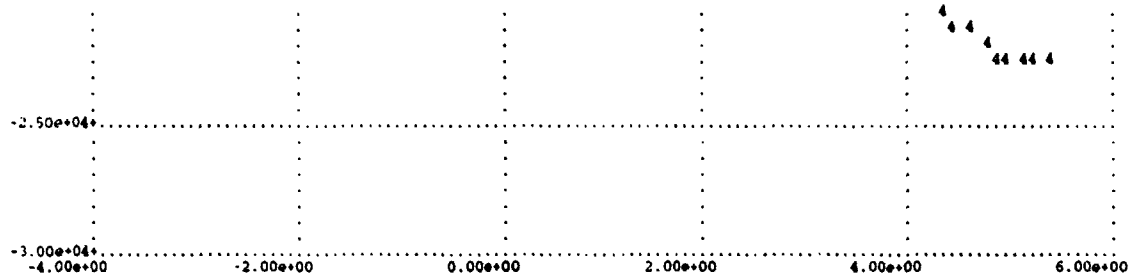

POTL IN VOLTS

TIME : 158

	#1	#2	#3	#4	#5	#6	#7
1.0e-03:	-3.63e+02						
2.2e-03:	-7.74e+02						
3.6e-03:	-1.24e+03						
5.4e-03:	-1.76e+03						
7.4e-03:	-2.33e+03						
9.9e-03:	-2.97e+03						
1.3e-02:	-3.66e+03						
1.6e-02:	-4.41e+03						
2.1e-02:	-5.21e+03						
2.6e-02:	-6.06e+03						
3.2e-02:	-6.96e+03						
4.0e-02:	-7.89e+03						
4.8e-02:	-8.85e+03						
5.9e-02:	-9.82e+03						
7.2e-02:	-1.08e+04						
8.7e-02:	-1.18e+04						
1.1e-01:	-1.27e+04						
1.3e-01:	-1.36e+04						
1.5e-01:	-1.44e+04						
1.9e-01:	-1.51e+04						
2.3e-01:	-1.58e+04						
2.9e-01:	-1.65e+04						
3.8e-01:	-1.70e+04						
5.1e-01:	-1.74e+04						
6.8e-01:	-1.77e+04						
9.2e-01:	-1.79e+04						
1.3e+00:	-1.80e+04						
1.7e+00:	-1.81e+04						
2.4e+00:	-1.82e+04						
3.3e+00:	-1.82e+04						
4.6e+00:	-1.82e+04						
6.5e+00:	-1.82e+04						
9.0e+00:	-1.82e+04						
1.3e+01:	-1.82e+04						
1.8e+01:	-1.82e+04						
2.5e+01:	-1.82e+04						
3.4e+01:	-1.82e+04						
4.8e+01:	-1.82e+04						
6.7e+01:	-1.82e+04						
9.4e+01:	-1.82e+04						
1.2e+02:	-1.82e+04						
1.6e+02:	-1.82e+04						
2.1e+02:	-1.81e+04						
2.9e+02:	-1.81e+04						
3.9e+02:	-1.81e+04						
5.3e+02:	-1.80e+04						
7.4e+02:	-1.79e+04						
1.0e+03:	-1.78e+04						
1.4e+03:	-1.77e+04						
2.0e+03:	-1.75e+04						

```
 2.8e+03:-1.72e+04
 3.9e+03:-1.68e+04
 5.4e+03:-1.58e+04
 7.5e+03:-1.54e+04
 1.1e+04:-1.44e+04
 1.5e+04:-1.34e+04
 2.1e+04:-1.24e+04
 2.9e+04:-1.14e+04
 4.0e+04:-1.05e+04
 5.7e+04:-1.05e+04
 7.3e+04:-1.06e+04
 9.5e+04:-1.08e+04
 1.3e+05:-1.09e+04
 1.7e+05:-1.09e+04
 2.3e+05:-1.09e+04
POTL VERSUS LOG(TIME)
```

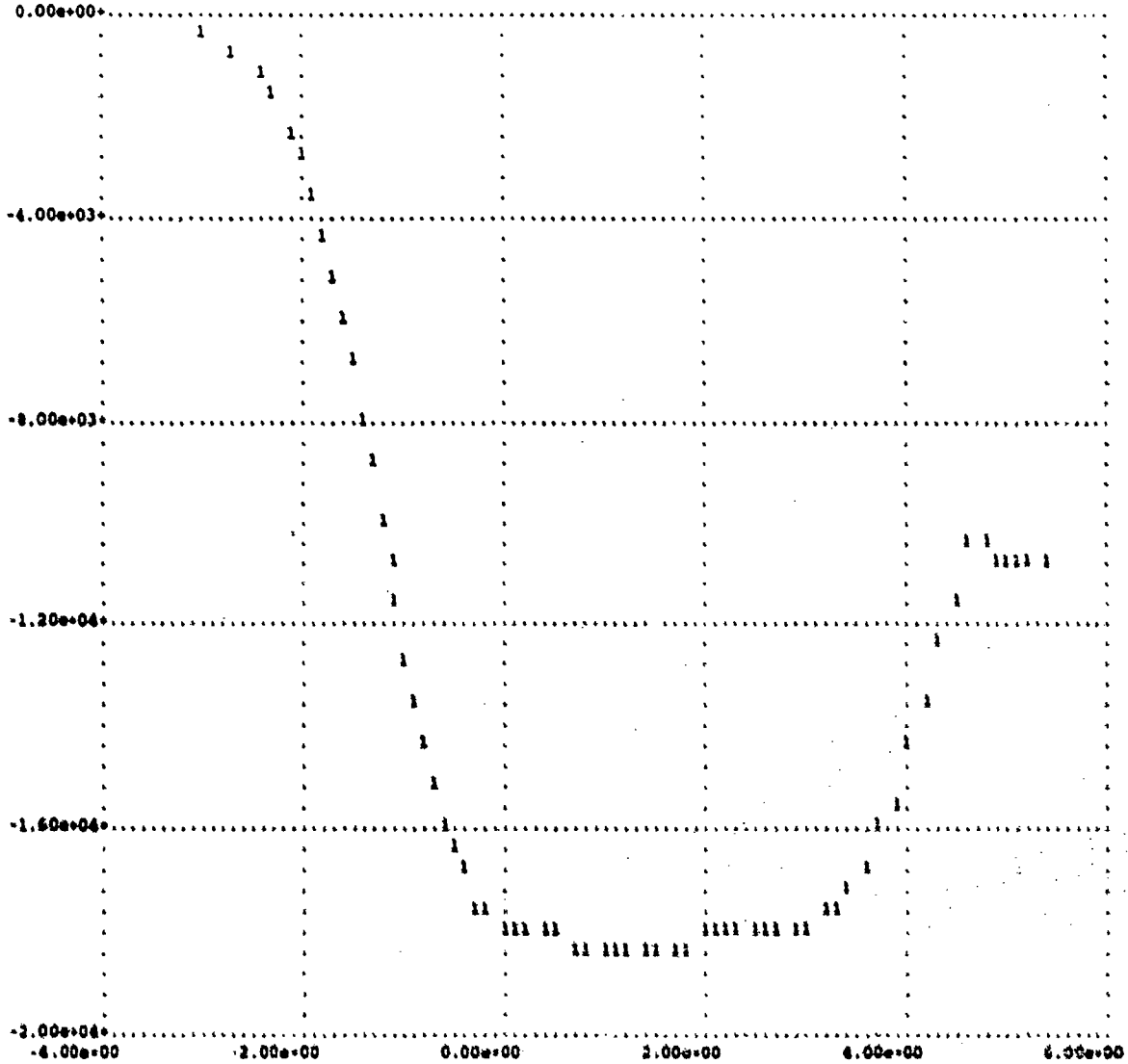


```
HISTORY COMMAND OR MODE SET ?
>exit
```

C.4 Auroral Kapton-Silver Quasi-sphere

The following files are the input and output files for the Auroral Kapton-Silver Quasi-sphere problem shown in Figures 15 and 16 of Chapter 2. For additional information on the use of *POLAR* see Lilley et al. [1989].

The standard input for the execution of vehicle includes general object definition options and the object definition.

Auroral Kapton-Silver Quasi-sphere vehicl Execution Standard Input

```
nxyz 11 11 11
vmach 0 0 0.001
matplots yes
makeplot 4
plotdir 2 3 5
plotdir -2 -3 -5
plotdir 4 -3 -5
plotdir -2 3 5
objdef 5
end
   QSPHERE
    CENTER 0 0 0
    DIAMETER 7
    SIDE 3
    MATERIAL KAPTON
    ENDOBJ
   PATCHR
    CORNER 3 -1 -1
    DELTAS 1  3  3
    SURFACE +X SILVER
    ENDOBJ
   PATCHR
    CORNER -1 3 -1
    DELTAS 3  1  3
    SURFACE +Y SILVER
    ENDOBJ
   PATCHR
    CORNER -1 -1 3
    DELTAS 3  3  1
    SURFACE +Z SILVER
    ENDOBJ
   PATCHW
    CORNER 2 -1 2
    FACE SILVER 1 0 1
    LENGTH 2 3 2
    ENDOBJ
   PATCHW
    CORNER -1 2 2
    FACE SILVER 0 1 1
    LENGTH 3 2 2
    ENDOBJ
   PATCHW
    CORNER 2 2 -1
    FACE SILVER 1 1 0
    LENGTH 2 2 3
    ENDOBJ
   PATCHW
    CORNER -1 -1 2
```

```
    FACE SILVER -1 0 1
    LENGTH 2 3 2
    ENDOBJ
   PATCHW
    CORNER -1 -1 2
    FACE SILVER 0 -1 1
    LENGTH 3 2 2
    ENDOBJ
   TETRAH
    CORNER 2 2 2
    FACE SILVER 1 1 1
    LENGTH 2 2 2
    ENDOBJ
   TETRAH
    CORNER -1 2 2
    FACE SILVER -1 1 1
    LENGTH 2 2 2
    ENDOBJ
   TETRAH
    CORNER 2 -1 2
    FACE SILVER 1 -1 1
    LENGTH 2 2 2
    ENDOBJ
   TETRAH
    CORNER -1 -1 2
    FACE SILVER -1 -1 1
    LENGTH 2 2 2
    ENDOBJ
   ENDSAT
```

The **orient** standard input defines the mach vector. Here the sphere is not moving.

Auroral Kapton-Silver Quasi-sphere orient Execution Standard Input

```
vmach  0.0 0.0 0.001
end
```

The **nterak** execution was completed in three steps with a slightly different standard input file for each step.

Auroral Kapton-Silver Quasi-sphere nterak Execution Standard Input

```
comment  Initialize
  ISTART NEW
comment  Choose Physical Models to be used.
  IGICAL NO
  STEMAKE OFF
  AVEPRTCL ON
  THRMSPRD ON
comment Convergence Parameters
  MAXITT 1
  POTCON 4
  DELTAT 2e-5
  DVLIM 50
comment Define Computat. Grid
  DXMESH 1
  NXADNT 14
```

```
  NXADNB 14
  NYADNT 14
  NYADNB 14
  NZADON 14
  NZTAIL 14
comment Define the plasma environment
  DENS 3.55e9
  TEMP 0.2
  DEN2   6.0E5
  TEMP2  8.0E3
  GAUCO  4.0e4
  ENAUT  2.4E4
  DELTA  1.6E4
  POWCO  3.0E11
  PALPHA 1.1
  PCUTL  50.0
  PCUTH  1.6E6
comment Define the initial potential
  CONDV  1  -1
comment Iterate on the analytical modules
  DELTAT 2e-5
  LOOP 5 PWASON CURREN CHARGE
  DELTAT 5e-5
  LOOP 10 PWASON CURREN CHARGE
  DELTAT 1e-4
  LOOP 10 PWASON CURREN CHARGE
  DELTAT 2e-4
  LOOP 10 PWASON CURREN CHARGE
  DELTAT 5e-4
  LOOP 10 PWASON CURREN CHARGE
  DELTAT 1e-3
  LOOP 10 PWASON CURREN CHARGE
  DELTAT 2e-3
  LOOP 10 PWASON CURREN CHARGE
  endrun
```

Auroral Kapton-Silver Quasi-sphere nterak Execution Standard Input, Continuation Run

```
comment  Initialize
 ISTART CONT
comment Iterate on the analytical modules
  DELTAT 5e-3
  LOOP 10 PWASON CURREN CHARGE
  DELTAT 1e-2
  LOOP 10 PWASON CURREN CHARGE
  DELTAT 2e-2
  LOOP 10 PWASON CURREN CHARGE
  DELTAT 5e-2
  LOOP 10 PWASON CURREN CHARGE
  DELTAT 0.1
  LOOP 10 PWASON CURREN CHARGE
  DELTAT 0.2
  LOOP 10 PWASON CURREN CHARGE
  endrun
```

Auroral Kapton-Silver Quasi-sphere nterak Execution Standard Input, 2nd Continuation Run

```
comment Iterate on the analytical modules
```

```
DELTAT 0.5
LOOP 10 PWASON CURREN CHARGE
DELTAT 1
LOOP 10 PWASON CURREN CHARGE
DELTAT 2
LOOP 4 PWASON CURREN CHARGE
endrun
```

Geosynchronous Kapton-Silver Quasi-sphere trmtlk Execution fort.3 File

The computer code **trmtlk** is used to determine the charging history of the quasi-sphere.

The final potential of all of the surface cells in order by potential magnitude is requested. All the silver cells are at –1.06 kV and the kapton cells are at potentials that range from –1.21 kV to –2.49 kV. The potential history of one silver cell and the highest potential kapton cell is requested.

```
Welcome to POLAR 1.3 TRMTLK ...

Any AID may be called from any MODULE

    MODULES          AIDS
  ***********      ********
    HISTORY          AGAIN
    LATEST           HELP
    SINGLE           LOCATION #
    SPECIAL          OUTLINE
                     SUBSET
                     EXIT
                     SUBSET [GROUP NAME]

Enter any MODULE/AID name or 'HELP' for help >> latest

LATEST command or MODE set >> potl
MODE RESET

LATEST command or MODE set >> magnitude
MODE RESET

LATEST command or MODE set >> list 1 to 159
FROM    1   TO  159   ON LIST OF DECREASING ORDER
POTL IN VOLTS  FOR POLAR CYCLE 150 ... TIME = 2.69E+01 SEC
  -1-1.06E+03  158-1.06E+03  157-1.06E+03  156-1.06E+03  155-1.06E+03
 154-1.06E+03  153-1.06E+03  152-1.06E+03  151-1.06E+03  150-1.06E+03
 149-1.06E+03  148-1.06E+03  147-1.06E+03  146-1.06E+03  145-1.06E+03
 144-1.06E+03  143-1.06E+03  142-1.06E+03  141-1.06E+03  140-1.06E+03
 139-1.06E+03  138-1.06E+03  137-1.06E+03  136-1.06E+03  135-1.06E+03
 134-1.06E+03  133-1.06E+03  132-1.06E+03  131-1.06E+03  130-1.06E+03
 129-1.06E+03  128-1.06E+03  127-1.06E+03  126-1.06E+03  125-1.06E+03
 124-1.06E+03  123-1.06E+03  122-1.06E+03  121-1.06E+03  120-1.06E+03
 119-1.06E+03  118-1.06E+03  117-1.06E+03  116-1.06E+03  115-1.06E+03
 114-1.06E+03  113-1.06E+03  112-1.06E+03  111-1.06E+03  110-1.06E+03
 109-1.06E+03  108-1.06E+03  107-1.06E+03  106-1.06E+03   58-1.06E+03
 104-1.06E+03   84-1.06E+03  102-1.06E+03   64-1.06E+03  100-1.06E+03
  82-1.06E+03   98-1.06E+03   60-1.06E+03   80-1.06E+03   62-1.06E+03
  78-1.06E+03   69-1.06E+03   68-1.06E+03   67-1.06E+03   66-1.06E+03
  89-1.06E+03   88-1.06E+03   87-1.06E+03   86-1.06E+03    5-1.21E+03
  71-1.23E+03   79-1.24E+03   51-1.34E+03   59-1.34E+03   70-1.42E+03
  77-1.42E+03    4-1.46E+03    2-1.46E+03   72-1.47E+03   81-1.47E+03
```

```
 18-1.47E+03   23-1.48E+03    8-1.48E+03   83-1.48E+03    6-1.48E+03
 74-1.48E+03   37-1.52E+03   28-1.52E+03   75-1.53E+03   57-1.54E+03
 73-1.54E+03   50-1.54E+03   17-1.54E+03   12-1.54E+03   52-1.63E+03
 61-1.64E+03   16-1.65E+03   55-1.65E+03   22-1.65E+03   53-1.65E+03
 54-1.67E+03   63-1.67E+03    7-1.68E+03    3-1.68E+03   33-1.68E+03
  1-1.69E+03   42-1.69E+03   24-1.74E+03   35-1.74E+03   20-1.74E+03
 27-1.75E+03   38-1.75E+03   47-1.76E+03   11-1.76E+03   15-1.76E+03
  9-1.77E+03   19-1.78E+03   13-1.78E+03   39-1.78E+03   29-1.79E+03
 32-1.81E+03   41-1.82E+03   30-1.82E+03   34-1.84E+03   85-1.85E+03
 45-1.85E+03   76-1.85E+03   36-1.86E+03   65-1.86E+03   56-1.86E+03
 46-1.86E+03   25-1.88E+03   14-1.90E+03   21-1.90E+03   26-1.92E+03
 31-1.92E+03   43-1.94E+03   99-1.97E+03   91-1.97E+03   10-1.97E+03
 40-2.04E+03   48-2.04E+03   97-2.12E+03   90-2.12E+03  103-2.14E+03
 94-2.14E+03  101-2.14E+03   92-2.15E+03   95-2.27E+03   93-2.27E+03
 49-2.28E+03   44-2.29E+03   96-2.48E+03  105-2.49E+03    0 0.00E+00

LATEST command or MODE set >> history

HISTORY command or MODE set >> potl
MODE RESET

HISTORY command or MODE set >> 58,96

POTL in Volts

  TIME  :    58        96
--------:-------------------------------------------------------------------
        :    #1        #2        #3        #4        #5        #6        #7
 0.0E+00:-1.00E+00-1.00E+00
 2.0E-05:-6.36E+00-6.36E+00
 4.0E-05:-2.33E+01-2.33E+01
 6.0E-05:-4.00E+01-4.00E+01
 8.0E-05:-5.64E+01-5.64E+01
 1.0E-04:-7.27E+01-7.27E+01
 1.5E-04:-1.05E+02-1.05E+02
 2.0E-04:-1.37E+02-1.37E+02
 2.5E-04:-1.68E+02-1.68E+02
 3.0E-04:-1.99E+02-1.99E+02
 3.5E-04:-2.30E+02-2.30E+02
 4.0E-04:-2.60E+02-2.60E+02
 4.5E-04:-2.89E+02-2.89E+02
 5.0E-04:-3.18E+02-3.18E+02
 5.5E-04:-3.46E+02-3.46E+02
 6.0E-04:-3.74E+02-3.74E+02
 7.0E-04:-4.17E+02-4.17E+02
 8.0E-04:-4.59E+02-4.59E+02
 9.0E-04:-5.01E+02-5.01E+02
 1.0E-03:-5.41E+02-5.41E+02
 1.1E-03:-5.81E+02-5.81E+02
 1.2E-03:-6.20E+02-6.20E+02
 1.3E-03:-6.58E+02-6.58E+02
 1.4E-03:-6.94E+02-6.94E+02
 1.5E-03:-7.30E+02-7.30E+02
 1.6E-03:-7.64E+02-7.65E+02
 1.8E-03:-8.15E+02-8.15E+02
 2.0E-03:-8.64E+02-8.64E+02
 2.2E-03:-9.11E+02-9.11E+02
 2.4E-03:-9.56E+02-9.56E+02
 2.6E-03:-9.99E+02-9.99E+02
 2.8E-03:-1.04E+03-1.04E+03
 3.0E-03:-1.08E+03-1.08E+03
 3.2E-03:-1.12E+03-1.12E+03
 3.4E-03:-1.15E+03-1.15E+03
 3.6E-03:-1.18E+03-1.18E+03
```

4.1E-03:-1.23E+03-1.23E+03
4.6E-03:-1.27E+03-1.27E+03
5.1E-03:-1.31E+03-1.31E+03
5.6E-03:-1.34E+03 1.34E+03
6.1E-03:-1.37E+03-1.37E+03
6.6E-03:-1.40E+03-1.40E+03
7.1E-03:-1.42E+03-1.42E+03
7.6E-03:-1.43E+03-1.43E+03
8.1E-03:-1.44E+03-1.44E+03
8.6E-03:-1.45E+03-1.45E+03
9.6E-03:-1.46E+03-1.46E+03
1.1E-02:-1.47E+03-1.47E+03
1.2E-02:-1.47E+03-1.47E+03
1.3E-02:-1.47E+03-1.47E+03
1.4E-02:-1.47E+03-1.47E+03
1.5E-02:-1.47E+03-1.47E+03
1.6E-02:-1.47E+03-1.48E+03
1.7E-02:-1.47E+03-1.48E+03
1.8E-02:-1.47E+03-1.48E+03
1.9E-02:-1.47E+03-1.47E+03
2.1E-02:-1.47E+03-1.47E+03
2.3E-02:-1.47E+03-1.47E+03
2.5E-02:-1.47E+03-1.47E+03
2.7E-02:-1.47E+03-1.47E+03
2.9E-02:-1.47E+03-1.47E+03
3.1E-02:-1.47E+03-1.47E+03
3.3E-02:-1.47E+03-1.47E+03
3.5E-02:-1.47E+03-1.47E+03
3.7E-02:-1.47E+03-1.47E+03
3.9E-02:-1.47E+03-1.47E+03
4.4E-02:-1.47E+03-1.47E+03
4.9E-02:-1.47E+03-1.47E+03
5.4E-02:-1.47E+03-1.47E+03
5.9E-02:-1.46E+03-1.47E+03
6.4E-02:-1.46E+03-1.47E+03
6.9E-02:-1.46E+03-1.47E+03
7.4E-02:-1.46E+03-1.47E+03
7.9E-02:-1.46E+03-1.47E+03
8.4E-02:-1.46E+03-1.47E+03
8.9E-02:-1.46E+03-1.47E+03
9.9E-02:-1.46E+03-1.47E+03
1.1E-01:-1.46E+03-1.47E+03
1.2E-01:-1.46E+03-1.47E+03
1.3E-01:-1.46E+03-1.47E+03
1.4E-01:-1.46E+03-1.47E+03
1.5E-01:-1.46E+03-1.48E+03
1.6E-01:-1.46E+03-1.48E+03
1.7E-01:-1.46E+03-1.48E+03
1.8E-01:-1.46E+03-1.48E+03
1.9E-01:-1.46E+03-1.48E+03
2.1E-01:-1.46E+03 1.48E+03
2.3E-01:-1.45E+03-1.48E+03
2.5E-01:-1.45E+03-1.48E+03
2.7E-01:-1.45E+03-1.48E+03
2.9E-01:-1.45E+03-1.48E+03
3.1E-01:-1.45E+03-1.48E+03
3.3E-01:-1.45E+03-1.48E+03
3.5E-01:-1.45E+03-1.49E+03
3.7E-01:-1.45E+03 1.49E+03
3.9E-01:-1.44E+03-1.49E+03
4.4E-01:-1.44E+03-1.49E+03
4.9E-01: 1.44E+03 1.49E+03
5.4E-01 1.43E+03 1.49E+03
5.9E-01:-1.43E+03-1.50E+03

6.4E-01:-1.43E+03-1.50E+03
6.9E-01:-1.43E+03-1.50E+03
7.4E-01:-1.42E+03-1.50E+03
7.9E-01:-1.42E+03-1.51E+03
8.4E-01:-1.42E+03-1.51E+03
8.9E-01:-1.41E+03-1.51E+03
9.9E-01:-1.41E+03-1.52E+03
1.1E+00:-1.40E+03-1.52E+03
1.2E+00:-1.40E+03-1.53E+03
1.3E+00:-1.39E+03-1.53E+03
1.4E+00:-1.39E+03-1.54E+03
1.5E+00:-1.38E+03-1.54E+03
1.6E+00:-1.38E+03-1.55E+03
1.7E+00:-1.37E+03-1.55E+03
1.8E+00:-1.37E+03-1.56E+03
1.9E+00:-1 36E+03-1.56E+03
2.1E+00:-1.35E+03-1.57E+03
2.3E+00:-1.34E+03-1.58E+03
2.5E+00:-1.33E+03-1.59E+03
2.7E+00:-1.33E+03-1.60E+03
2.9E+00:-1.32E+03-1.61E+03
3.1E+00:-1.31E+03-1.62E+03
3.3E+00:-1.31E+03-1.64E+03
3.5E+00:-1.30E+03-1.65E+03
3.7E+00:-1.29E+03-1.66E+03
3.9E+00:-1.29E+03-1.67E+03
4.4E+00:-1.27E+03-1.69E+03
4.9E+00:-1.25E+03-1.71E+03
5.4E+00:-1.23E+03-1.74E+03
5.9E+00:-1.22E+03-1.76E+03
6.4E+00:-1.21E+03-1.79E+03
6.9E+00:-1.20E+03-1.82E+03
7.4E+00:-1.19E+03-1.84E+03
7.9E+00:-1.18E+03-1.87E+03
8.4E+00:-1.18E+03-1.90E+03
8.9E+00:-1.17E+03-1.93E+03
9.9E+00:-1.15E+03-1.96E+03
1.1E+01:-1.13E+03-2.00E+03
1.2E+01:-1.12E+03-2.04E+03
1.3E+01:-1.11E+03-2.08E+03
1.4E+01:-1.11E+03-2.12E+03
1.5E+01:-1.10E+03-2.16E+03
1 6E+01:-1.10E+03-2.19E+03
1.7E+01:-1.09E+03-2.23E+03
1.8E+01:-1.09E+03-2.27E+03
1.9E+01:-1.08E+03-2.30E+03
2.1E+01:-1.07E+03-2.35E+03
2.3E+01:-1.07E+03-2.40E+03
2.5E+01:-1.06E+03-2.44E+03
2.7E+01:-1.06E+03-2.48E+03

1 POTL versus TIME in Seconds

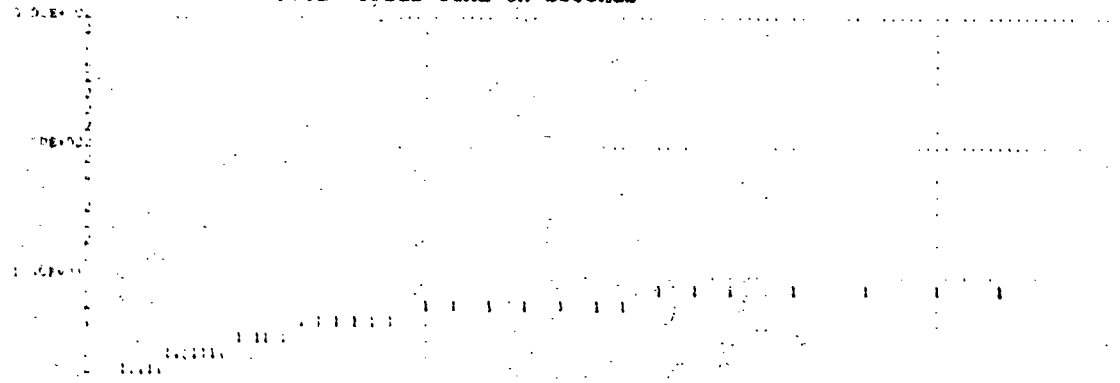

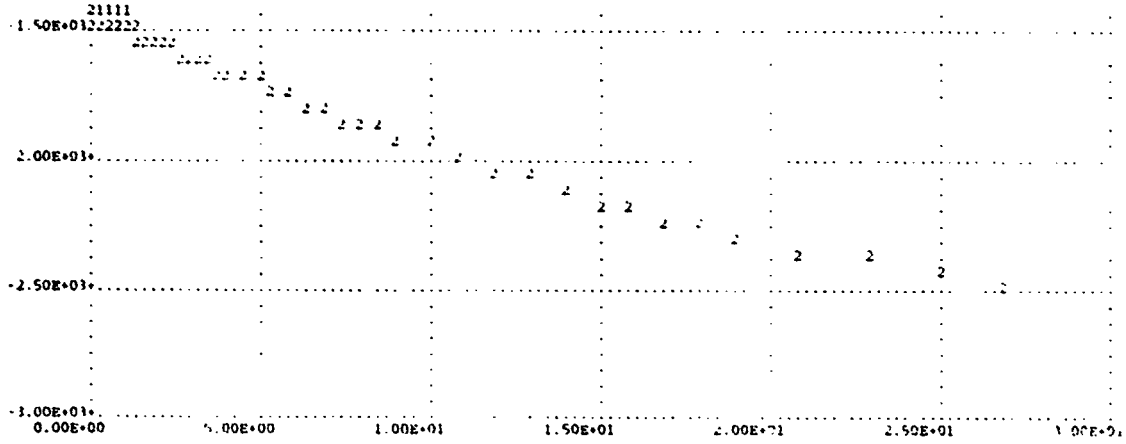


```
HISTORY command or MODE set >> exit
```

C.5 Geosynchronous Sunlit Kapton Quasi-sphere

The following files are the input and output files for the Geosynchronous Sunlit Kapton Quasi-sphere problem shown in Figures 18 and 19 of Chapter 2. The problem was completed in four steps with a slightly different standard input file for each step. The first input file shows the options chosen, the object definition, and the environment description.

Geosynchronous Sunlit Kapton Quasi-sphere Standard Input

```
RDOPT 5
   SURFACE CELL 1
   LONGTIMESTEP 1000
   DELTA .01
   DELFAC 1.4
   NCYC 2
   XMESH 1
   NG 2
   NZ 17
   SUNINT 1.
   END
OBJDEF 5
   QSPHERE
   CENTER 0 0 0
   DIAMETER 7
   SIDE 3
   MATERIAL KAPTON
   ENDOBJ
   ENDSAT
NIDCEL
CAPACI
TRILIN 5
   SINGLE
   1.12 CGS
   12 KEV
   .236 CGS
   29.5 KEV
   END
END
```

Geosynchronous Sunlit Kapton Quasi-sphere Continuation File

```
RDOPT 5
   SURFACE CELL 1
   LONGTIMESTEP 1000
   DELTA .02
   DELFAC 1.4
   RESTART
   NCYC 7
   XMESH 1
   NG 2
   NZ 17
   SUNINT 1.
   END
TRILIN 5
   SINGLE
   1.12 CGS
   12 KEV
   .236 CGS
   29.5 KEV
   END
END
```

Geosynchronous Sunlit Kapton Quasi-sphere 2nd Continuation File

```
RDOPT 5
   SURFACE CELL 1
   LONGTIMESTEP 1000
   DELTA .211
   DELFAC 1.4
   RESTART
   NCYC 20
   XMESH 1
   NG 2
   NZ 17
   SUNINT 1.
   END
TRILIN 5
   SINGLE
   1.12 CGS
   12 KEV
   .236 CGS
   29.5 KEV
   END
END
```

Geosynchronous Sunlit Kapton Quasi-sphere 3rd Continuation File

```
RDOPT 5
   SURFACE CELL 1
   LONGTIMESTEP 1000
   DELTA 84
   DELFAC 1.4
   RESTART
   NCYC 20
   XMESH 1
   NG 2
   NZ 17
   SUNINT 1.
```

```
   END
TRILIN 5
   SINGLE
   1.12 CGS
   12 KEV
   .236 CGS
   29.5 KEV
   END
END
```

Geosynchronous Sunlit Kapton Quasi-sphere Termtalk Execution fort.3 File

The computer code **Termtalk** is used to examine the time history of the surface potentials.

A group of those cells facing in the 1 1 1 or –1 –1 –1 direction is defined. These cells are those facing the sun and directly away from the sun, respectively. The history of the potentials one of the cells of each group and the ground potential is requested.

```
CHOOSE ANY MODULE
 HELP IS ALWAYS AVAILABLE - TYPE 'HELP'
>potl
CHOOSE ANY MODULE
 HELP IS ALWAYS AVAILABLE - TYPE 'HELP'
>history
HISTORY COMMAND OR MODE SET ?
>subset one
DEFINITION OF NEW SUBSET NAMED one
 159 REMAINING IN GROUP
SUBSET INSTRUCTION PLEASE ?
>normal 1 1 1
   4 REMAINING IN GROUP
SUBSET INSTRUCTION PLEASE ?
>which
MEMBERS OF GROUP one
  127  128  133  158    0    0    0    0    0    0
   4 REMAINING IN GROUP
SUBSET INSTRUCTION PLEASE ?
>done
GROUP one  WITH    4 MEMBERS IS NOW DEFINED
RETURNING TO MODULE  'HIST'
HISTORY COMMAND OR MODE SET ?
>subset minus
DEFINITION OF NEW SUBSET NAMED minu
 159 REMAINING IN GROUP
SUBSET INSTRUCTION PLEASE ?
>normal -1 -1 -1
   4 REMAINING IN GROUP
SUBSET INSTRUCTION PLEASE ?
>which
MEMBERS OF GROUP minu
    1   26   31   32    0    0    0    0    0    0
   4 REMAINING IN GROUP
SUBSET INSTRUCTION PLEASE ?
>done
GROUP minu WITH    4 MEMBERS IS NOW DEFINED
RETURNING TO MODULE  'HIST'
HISTORY COMMAND OR MODE SET ?
>127,1,-1
POTL IN VOLTS
```

```
 TIME  :   127        1       -1
--------:-------------------------------------------------------------------
        :    #1       #2       #3       #4       #5       #6       #7
 1.0e-02: 5.52e-01-1.72e-01-1.07e-01
 2.4e-02: 1.54e+00 8.60e-01 1.02e+00
 4.4e-02: 3.49e+00 1.17e+00 1.47e+00
 7.2e-02: 4.18e+00 1.95e+00 2.44e+00
 1.1e-01: 2.04e+00-4.77e-02 7.31e-01
 1.7e-01: 2.48e+00-1.25e+00-1.07e-01
 2.4e-01: 2.80e+00-2.50e+00-8.48e-01
 3.5e-01: 3.01e+00-5.18e+00-2.82e+00
 5.0e-01: 3.07e+00-8.08e+00-4.71e+00
 7.1e-01: 2.93e+00-1.27e+01-7.96e+00
 1.0e+00: 2.39e+00-1.99e+01-1.31e+01
 1.4e+00: 8.60e-01-3.06e+01-2.11e+01
 2.0e+00:-2.55e+00-4.61e+01-3.28e+01
 2.8e+00:-7.02e+00-6.79e+01-4.92e+01
 3.9e+00:-1.40e+01-9.85e+01-7.25e+01
 5.5e+00:-2.31e+01-1.41e+02-1.05e+02
 7.8e+00:-3.63e+01-2.00e+02-1.49e+02
 1.1e+01:-5.38e+01-2.82e+02-2.12e+02
 1.5e+01:-8.08e+01-3.96e+02-2.98e+02
 2.1e+01:-1.13e+02-5.50e+02-4.16e+02
 3.0e+01:-1.64e+02-7.61e+02-5.76e+02
 4.2e+01:-2.26e+02-1.04e+03-7.92e+02
 5.9e+01:-3.18e+02-1.42e+03-1.08e+03
 8.2e+01:-4.33e+02-1.91e+03-1.46e+03
 1.1e+02:-5.97e+02-2.54e+03-1.94e+03
 1.6e+02:-7.89e+02-3.32e+03-2.55e+03
 2.3e+02:-1.06e+03-4.28e+03-3.29e+03
 3.2e+02:-1.37e+03-5.42e+03-4.19e+03
 3.8e+02:-1.77e+03-6.42e+03-5.02e+03
 4.6e+02:-2.16e+03-7.46e+03-5.87e+03
 5.8e+02:-2.59e+03-8.61e+03-6.79e+03
 6.6e+02:-2.98e+03-9.61e+03-7.63e+03
 7.8e+02:-3.44e+03-1.06e+04-8.48e+03
 9.4e+02:-3.82e+03-1.18e+04-9.40e+03
 1.1e+03:-4.27e+03-1.30e+04-1.04e+04
 1.4e+03:-4.68e+03-1.42e+04-1.13e+04
 1.7e+03:-5.18e+03-1.54e+04-1.23e+04
 2.0e+03:-5.61e+03-1.67e+04-1.34e+04
 2.5e+03:-6.15e+03-1.80e+04-1.44e+04
 3.2e+03:-6.60e+03-1.93e+04-1.55e+04
 4.1e+03:-7.15e+03-2.06e+04-1.66e+04
 5.5e+03:-7.61e+03-2.17e+04-1.75e+04
 1.2e+04:-8.16e+03-2.26e+04-1.83e+04
 2.2e+04:-8.53e+03-2.28e+04-1.86e+04
 3.5e+04:-8.86e+03-2.28e+04-1.87e+04
 5.3e+04:-8.92e+03-2.28e+04-1.87e+04
 7.9e+04:-8.98e+03-2.28e+04-1.87e+04
 1.1e+05:-8.97e+03-2.28e+04-1.87e+04
 1.6e+05:-8.97e+03-2.28e+04-1.87e+04
POTL VERSUS LOG(TIME)
 1.00e+04+.....................................................................
         .          .          .          .          .
         .          .          .          .          .
         .          .          .          .          .
         .          .          .          .          .
         .          .          .          .          .
         .          .          .          .          .
         .          .          .          .          .
         .          .          .          .          .
         .          .          .          .          .
         .          .          .          .          .
```

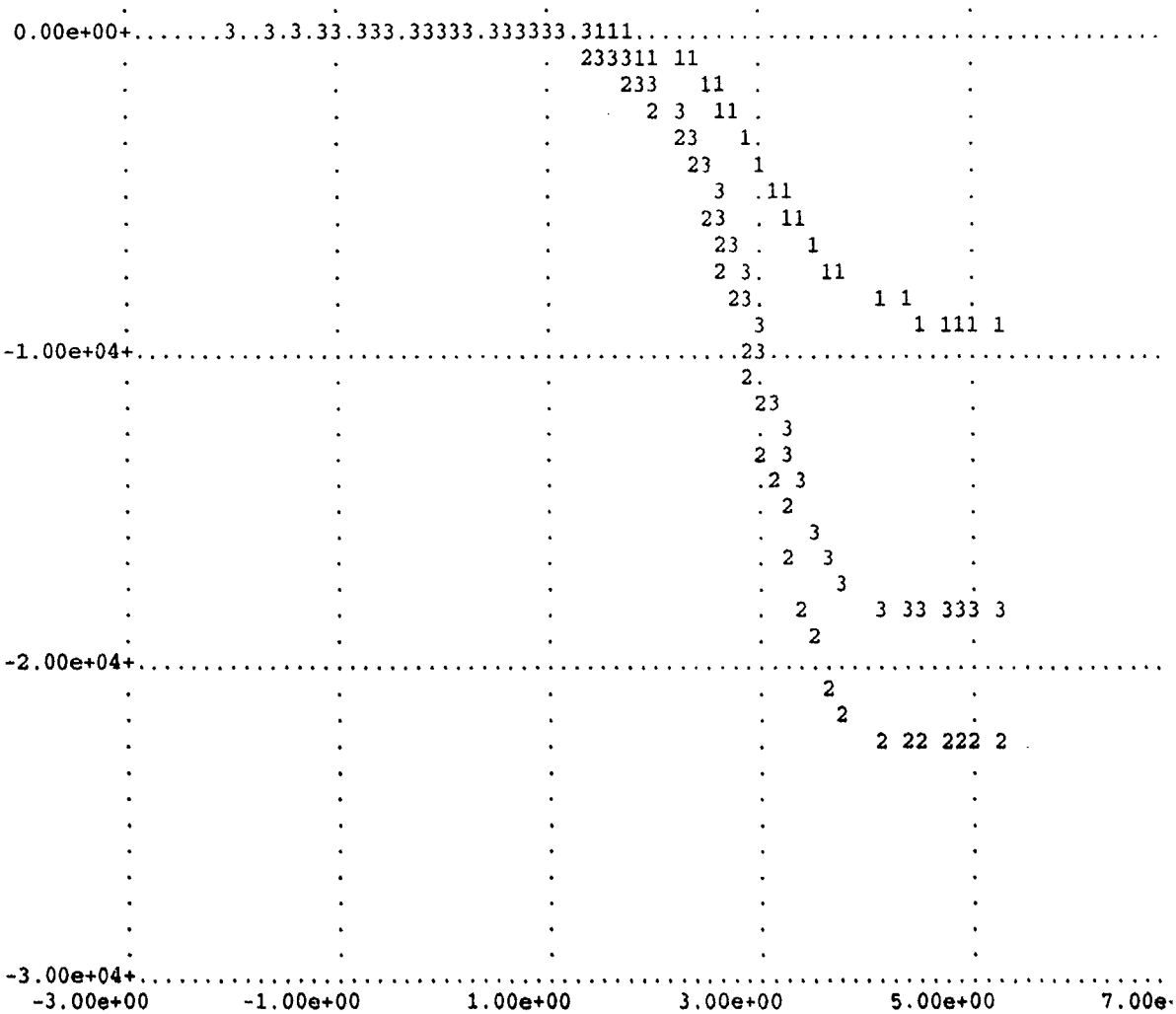


```
HISTORY COMMAND OR MODE SET ?
>exit
```

C.6 Auroral Kapton Quasi-sphere at Orbital Velocity

The following files are the input and output files for the Auroral Kapton Quasi-sphere at Orbital Velocity problem shown in Figures 21 and 22 in Chapter 2. Standard input files are shown for the **vehicl, orient,** and **nterak** executions. **vehicl** defines the object, **orient,** orients the object within the grid, and **nterak** computes the interactions.

Standard Input For vehicl Execution For Kapton Sphere in the Auroral Environment At Orbital Velocity

```
nxyz 11 11 11
vmach 0 0 0.001
matplots yes
makeplot 4
plotdir 2 3 5
plotdir -2 -3 -5
```

```
plotdir 4 -3 -5
plotdir -2 3 5
objdef 5
end
   QSPHERE
    CENTER 0 0 0
    DIAMETER 7
    SIDE 3
    MATERIAL KAPTON
```

Standard Input For orient Execution For Kapton Sphere in the Auroral Environment At Orbital Velocity

```
end
```

Standard Input For nterak Execution For Kapton Sphere in the Auroral Environment At Orbital Velocity

```
comment  Initialize
  ISTART NEW
comment  Choose Physical Models to be used.
  IGICAL YES
  STHWAKE ON
  AVEPRTCL ON
  THRMSPRD ON
comment Convergence Parameters
  MAXITT 1
  POTCON 4
  DELTAT 5e-5
  DVLIM 50
comment Define Computat. Grid
  DXMESH 1
  NXADNT 9
  NXADNB 9
  NYADNT 9
  NYADNB 9
  NZADON 6
  NZTAIL 42
comment Define the plasma environment
  DENS 3.55e9
  TEMP 0.2
  DEN2   6.0E5
  TEMP2  8.0E3
  GAUCO  4.0e4
  ENAUT  2.4E4
  DELTA  1.6E4
  POWCO  3.0E11
  PALPHA 1.1
  PCUTL  50.0
  PCUTH  1.6E6
comment Define the initial potential
  CONDV  1  -1
comment Iterate on the analytical modules
  DELTAT 2e-5
  LOOP 5 PWASON CURREN CHARGE
  DELTAT 5e-5
  LOOP 5 PWASON CURREN CHARGE
  DELTAT 1e-4
  LOOP 5 PWASON CURREN CHARGE
  DELTAT 2e-4
```

```
  LOOP 5 PWASON CURREN CHARGE
  DELTAT 5e-4
  LOOP 5 PWASON CURREN CHARGE
  DELTAT 1e-3
  LOOP 5 PWASON CURREN CHARGE
  DELTAT 2e-3
  LOOP 5 PWASON CURREN CHARGE
  endrun
```

Standard Input For Continuation Run Of nterak For Kapton Sphere in the Auroral Environment At Orbital Velocity

```
comment  Initialize
  ISTART CONT
comment  Choose Physical Models to be used.
  IGICAL NO
  STHWAKE ON
  AVEPRTCL ON
  THRMSPRD ON
comment Convergence Parameters
  MAXITT 1
  POTCON 4
  DELTAT 5e-5
  DVLIM 50
comment Define Computat. Grid
  DXMESH 1
  MXADWT 9
  MXADWB 9
  MYADWT 9
  MYADWB 9
  MZADON 6
  METAIL 42
comment Define the plasma environment
  DENS 3.55e9
  TEMP 0.2
  DEN2   6.0E5
  TEMP2  8.0E3
  GAUCO  4.0e4
  EMAUT  2.4E4
  DELTA  1.6E4
  POWCO  3.0E11
  PALPHA 1.1
  PCUTL  50.0
  PCUTH  1.6E6
comment Define the initial potential
  CONDV  1  -1
comment Iterate on the analytical modules
  DELTAT 5e-3
  LOOP 5 PWASON CURREN CHARGE
  DELTAT 1e-2
  LOOP 5 PWASON CURREN CHARGE
  DELTAT 2e-2
  LOOP 5 PWASON CURREN CHARGE
  DELTAT 5e-2
  LOOP 5 PWASON CURREN CHARGE
  DELTAT 0.1
  LOOP 5 PWASON CURREN CHARGE
  DELTAT 0.2
  LOOP 5 PWASON CURREN CHARGE
  DELTAT 0.5
  LOOP 5 PWASON CURREN CHARGE
  endrun
```

Standard Input For Second Continuation Run of nterak For Kapton Sphere in the Auroral Environment At Orbital Velocity

```
comment  Initialize
  ISTART CONT
comment  Choose Physical Models to be used.
  IGICAL NO
  STHWAKE ON
  AVEPRTCL ON
  THRMSPRD ON
comment Convergence Parameters
  MAXITT 1
  POTCON 4
  DELTAT 5e-5
  DVLIM 50
comment Define Computat. Grid
  DXMESH 1
  NXADMT 9
  NXADMB 9
  NYADMT 9
  NYADMB 9
  NZADON 6
  NZTAIL 42
comment Define the plasma environment
  DENS 3.55e9
  TEMP 0.2
  DEN2   6.0E5
  TEMP2  8.0E3
  GAUCO  4.0e4
  ENAUT  2.4E4
  DELTA  1.6E4
  POWCO  3.0E11
  PALPHA 1.1
  PCUTL  50.0
  PCUTE  1.6E6
comment Define the initial potential
  CONDV  1  -1
comment Iterate on the analytical modules
  DELTAT 1
  LOOP 10 PMASON CURREN CHARGE
  DELTAT 2
  LOOP 10 PMASON CURREN CHARGE
  DELTAT 5
  LOOP 10 PMASON CURREN CHARGE
  DELTAT 10
  LOOP 10 PMASON CURREN CHARGE
  endrun
```

trmtlk Interactive Session For Kapton Quasi-sphere In The Auroral Environment.

The **trmtlk** computer code is used to examine the surface potentials of the quasi-sphere.

The latest module is used to determine the cells with the highest and lowest final potentials. A subset of the ram facing cells is defined and a subset of the wake facing cells is defined. The final surface potentials of each of these two groups is requested. The single module is used to determine the location and potential of each of the wake cells. Full information on the highest potential cell is requested. These high potential cells are

not those that directly face the wake, but have normals that are not parallel with the Z axis. The elevated potentials on the surfaces with normals in the Z direction are due to focusing. Finally, a time history of the surfaces in the center of the +Z and –Z faces, the highest potential surface, and spacecraft ground are requested.

```
Welcome to POLAR 1.3 TRMTLK ...

Any AID may be called from any MODULE

    MODULES          AIDS
  ***********      ********
    HISTORY          AGAIN
    LATEST           HELP
    SINGLE           LOCATION #
    SPECIAL          OUTLINE
                     SUBSET
                     EXIT
                     SUBSET [GROUP NAME]

Enter any MODULE/AID name or 'HELP' for help >> latest

LATEST command or MODE set >> potl
MODE RESET

LATEST command or MODE set >> magnitude
MODE RESET

LATEST command or MODE set >> list 1 to 159
FROM    1   TO  159   ON LIST OF DECREASING ORDER
POTL IN VOLTS  FOR POLAR CYCLE 111 ... TIME = 1.84E+02 SEC
 154-1.15E+00  157-6.01E+00  153-6.50E+00  155-7.61E+00  151-1.40E+01
   5-1.07E+02    4-3.08E+02    2-3.48E+02   18-3.61E+02    8-3.70E+02
   6-3.74E+02   17-3.98E+02   12-4.15E+02   23-4.15E+02  158-4.20E+02
 150-4.22E+02  152-4.22E+02  156-4.23E+02   16-4.79E+02   20-4.80E+02
  19-4.90E+02   15-4.90E+02    1-5.05E+02    7-5.06E+02   24-5.09E+02
  37-5.12E+02   28-5.13E+02    3-5.14E+02   22-5.17E+02    9-5.18E+02
  13-5.18E+02   35-5.19E+02   21-5.21E+02   11-5.22E+02   10-5.25E+02
  39-5.26E+02   25-5.28E+02   14-5.32E+02   40-5.37E+02   36-5.39E+02
  38-5.41E+02   47-5.41E+02   46-5.43E+02   48-5.45E+02   27-5.52E+02
  29-5.61E+02   88-5.88E+02   71-5.92E+02   79-5.92E+02   32-5.94E+02
  33-6.02E+02   42-6.03E+02   80-6.04E+02   43-6.10E+02  136-6.30E+02
 147-6.31E+02  142-6.34E+02  141-6.35E+02   -1-6.44E+02   73-6.56E+02
  34-6.60E+02   74-6.68E+02   44-6.69E+02   31-6.69E+02   70-6.71E+02
  72-6.72E+02   41-6.72E+02   76-6.75E+02   75-6.75E+02   84-6.75E+02
  83-6.78E+02   85-6.79E+02   86-6.81E+02   49-6.82E+02   81-6.83E+02
  89-6.84E+02   87-6.84E+02   45-6.85E+02   82-6.89E+02   78-6.89E+02
  77-6.90E+02   26-7.08E+02   30-7.16E+02   56-7.21E+02  135-7.23E+02
 137-7.26E+02  146-7.27E+02  144-7.27E+02   64-7.28E+02  143-7.28E+02
 140-7.29E+02   53-7.31E+02  148-7.31E+02  139-7.31E+02   55-7.32E+02
 121-7.33E+02  112-7.34E+02  131-7.34E+02  122-7.37E+02   66-7.38E+02
  99-7.40E+02  108-7.40E+02   65-7.41E+02   63-7.41E+02   54-7.42E+02
 105-7.43E+02  106-7.43E+02  104-7.44E+02   95-7.45E+02  103-7.45E+02
  96-7.46E+02   94-7.46E+02   93-7.49E+02  100-7.55E+02   62-7.59E+02
  91-7.60E+02  101-7.60E+02  109-7.61E+02  107-7.62E+02   92-7.67E+02
  98-7.67E+02  102-7.67E+02   97-7.69E+02   58-7.69E+02   67-7.72E+02
  50-7.73E+02   69-7.74E+02   52-7.76E+02   57-7.77E+02   90-7.80E+02
  51-7.80E+02   61-7.88E+02   60-7.88E+02   68-7.92E+02  113-8.02E+02
 119-8.03E+02  130-8.04E+02  120-8.04E+02  124-8.06E+02  111-8.07E+02
 132-8.08E+02   59-8.09E+02  123-8.09E+02  129-8.32E+02  114-8.33E+02
 128-8.33E+02  115-8.33E+02  118-8.33E+02  133-8.34E+02  125-8.36E+02
 110-8.37E+02  126-8.37E+02  127-8.40E+02  117-8.40E+02  116-8.42E+02
 145-8.46E+02  149-8.48E+02  138-8.48E+02  134-8.50E+02    0 0.00E+00
```

```
LATEST command or MODE set >> subset ram
DEFINITION OF NEW SUBSET NAMED RAM
 159 REMAINING IN GROUP

SUBSET command please >> normal 0 0 1
   9 REMAINING IN GROUP

SUBSET command please >> done
GROUP RAM  WITH     9 MEMBERS IS NOW DEFINED
RETURNING TO MODULE  'LATE'

LATEST command or MODE set >> subset wake
DEFINITION OF NEW SUBSET NAMED WAKE
 159 REMAINING IN GROUP

SUBSET command please >> normal 0 0 -1
   9 REMAINING IN GROUP

SUBSET command please >> done
GROUP WAKE WITH     9 MEMBERS IS NOW DEFINED
RETURNING TO MODULE  'LATE'

LATEST command or MODE set >> group ram
POTL IN VOLTS  FOR POLAR CYCLE 111 ... TIME = 1.84E+02 SEC
 154-1.15E+00  157-6.01E+00  153-6.50E+00  155-7.61E+00  151-1.40E+01
 158-4.20E+02  150-4.22E+02  152-4.22E+02  156-4.23E+02     0 0.00E+00

LATEST command or MODE set >> group wake
POTL IN VOLTS  FOR POLAR CYCLE 111 ... TIME = 1.84E+02 SEC
   5-1.07E+02    4-3.08E+02    2-3.48E+02    8-3.70E+02    6-3.74E+02
   1-5.05E+02    7-5.06E+02    3-5.14E+02    9-5.18E+02    0 0.00E+00

LATEST command or MODE set >> single

SINGLE command or MODE set >> 1
-------------------------------------------------------------------------
SURFACE NO.    1                  CENTERED AT   5.50   5.50   3.00
MATERIAL IS KAPT

                    POTENTIAL  = -5.0462E+02 VOLTS

SINGLE command or MODE set >> 2
-------------------------------------------------------------------------
SURFACE NO.    2                  CENTERED AT   6.50   5.50   3.00
MATERIAL IS KAPT

                    POTENTIAL  = -3.4819E+02 VOLTS

SINGLE command or MODE set >> 3
-------------------------------------------------------------------------
SURFACE NO.    3                  CENTERED AT   7.50   5.50   3.00
MATERIAL IS KAPT

                    POTENTIAL  = -5.1379E+02 VOLTS

SINGLE command or MODE set >> 4
-------------------------------------------------------------------------
SURFACE NO.    4                  CENTERED AT   5.50   6.50   3.00
MATERIAL IS KAPT

                    POTENTIAL  = -3.0794E+02 VOLTS

SINGLE command or MODE set >> 5
```

```
------------------------------------------------------------------------
SURFACE NO.    5                    CENTERED AT   6.50   6.50   3.00
MATERIAL IS KAPT

                     POTENTIAL  = -1.0733E+02 VOLTS

SINGLE command or MODE set >> 6
------------------------------------------------------------------------
SURFACE NO.    6                    CENTERED AT   7.50   6.50   3.00
MATERIAL IS KAPT

                     POTENTIAL  = -3.7373E+02 VOLTS

SINGLE command or MODE set >> 7
------------------------------------------------------------------------
SURFACE NO.    7                    CENTERED AT   5.50   7.50   3.00
MATERIAL IS KAPT

                     POTENTIAL  = -5.0558E+02 VOLTS

SINGLE command or MODE set >> 8
------------------------------------------------------------------------
SURFACE NO.    8                    CENTERED AT   6.50   7.50   3.00
MATERIAL IS KAPT

                     POTENTIAL  = -3.6974E+02 VOLTS

SINGLE command or MODE set >> 9
------------------------------------------------------------------------
SURFACE NO.    9                    CENTERED AT   7.50   7.50   3.00
MATERIAL IS KAPT

                     POTENTIAL  = -5.1751E+02 VOLTS

SINGLE command or MODE set >> everything
MODE RESET

SINGLE command or MODE set >> 138
------------------------------------------------------------------------
SURFACE NO.  134                    CENTERED AT   4.33   4.33   9.67
MATERIAL IS KAPT                    NORMAL IS    -1  -1   1
SHAPE IS EQUILATERAL TRIANGLE       SURFACE AREA =  8.6603E-01 M**2

                   POTENTIAL  = -8.4963E+02 VOLTS
                   UNDERLYING CONDUCTOR NUMBER IS  1
                   UNDERLYING CONDUCTOR POTENTIAL = -6.4448E+02 VOLTS
                   DELTA V    = -2.0515E+02 VOLTS
                   INTERNAL FIELD STRESS   = -1.6154E+05 VOLTS/METER
                   EXTERNAL ELECTRIC FIELD = -3.1022E+02 VOLTS/METER
FLUXES IN AMPS/METER**2
       INCIDENT ELECTRONS              -1.4905E-05
            RESULTING SECONDARIES       1.4646E-06
            RESULTING BACKSCATTER       1.5587E-06
       INCIDENT IONS                    1.0949E-05
            RESULTING SECONDARIES       7.8050E-07
       BULK CONDUCTIVITY               -1.6154E-11
       HOPPING CURRENT                  0.0000E+00
       PHOTOCURRENT                     0.0000E+00
                                       ------------
       TOTAL FLUX THROUGH SURFACE      -1.5159E-07
SINGLE command or MODE set >> history

HISTORY command or MODE set >> 154,5,134,-1
```

POTL in Volts

TIME	: 154	5	134	-1			
	: #1	#2	#3	#4		#6	#7
0.0E+00	:-1.00E+00	-1.00E+00	-1.00E+00	-1.00E+00			
2.0E-05	:-7.02E+00	-7.02E+00	-7.02E+00	-7.02E+00			
4.0E-05	:-2.54E+01	-2.54E+01	-2.54E+01	-2.54E+01			
6.0E-05	:-4.25E+01	-4.25E+01	-4.25E+01	-4.25E+01			
8.0E-05	:-5.91E+01	-5.91E+01	-5.91E+01	-5.91E+01			
1.0E-04	:-7.51E+01	-7.50E+01	-7.51E+01	-7.51E+01			
1.5E-04	:-1.06E+02	-1.06E+02	-1.06E+02	-1.06E+02			
2.0E-04	:-1.36E+02	-1.36E+02	-1.36E+02	-1.36E+02			
2.5E-04	:-1.65E+02	-1.65E+02	-1.65E+02	-1.65E+02			
3.0E-04	:-1.92E+02	-1.92E+02	-1.92E+02	-1.92E+02			
3.5E-04	:-2.18E+02	-2.18E+02	-2.18E+02	-2.18E+02			
4.5E-04	:-2.57E+02	-2.57E+02	-2.57E+02	-2.57E+02			
5.5E-04	:-2.94E+02	-2.94E+02	-2.94E+02	-2.94E+02			
6.5E-04	:-3.29E+02	-3.29E+02	-3.29E+02	-3.29E+02			
7.5E-04	:-3.61E+02	-3.61E+02	-3.61E+02	-3.61E+02			
8.5E-04	:-3.90E+02	-3.90E+02	-3.90E+02	-3.90E+02			
1.0E-03	:-4.32E+02	-4.32E+02	-4.32E+02	-4.32E+02			
1.2E-03	:-4.70E+02	-4.69E+02	-4.70E+02	-4.70E+02			
1.4E-03	:-5.02E+02	-5.02E+02	-5.02E+02	-5.02E+02			
1.6E-03	:-5.30E+02	-5.30E+02	-5.31E+02	-5.31E+02			
1.9E-03	:-5.55E+02	-5.55E+02	-5.56E+02	-5.56E+02			
2.1E-03	:-5.86E+02	-5.86E+02	-5.87E+02	-5.87E+02			
2.9E-03	:-6.11E+02	-6.11E+02	-6.12E+02	-6.12E+02			
3.4E-03	:-6.30E+02	-6.30E+02	-6.31E+02	-6.31E+02			
3.9E-03	:-6.39E+02	-6.40E+02	-6.41E+02	-6.41E+02			
4.4E-03	:-6.49E+02	-6.49E+02	-6.51E+02	-6.51E+02			
5.4E-03	:-6.56E+02	-6.56E+02	-6.59E+02	-6.58E+02			
6.4E-03	:-6.60E+02	-6.61E+02	-6.64E+02	-6.63E+02			
7.4E-03	:-6.62E+02	-6.64E+02	-6.67E+02	-6.66E+02			
8.4E-03	:-6.63E+02	-6.65E+02	-6.69E+02	-6.68E+02			
9.4E-03	:-6.63E+02	-6.65E+02	-6.70E+02	-6.68E+02			
1.1E-02	:-6.63E+02	-6.65E+02	-6.70E+02	-6.69E+02			
1.3E-02	:-6.61E+02	-6.65E+02	-6.70E+02	-6.69E+02			
1.5E-02	:-6.61E+02	-6.65E+02	-6.71E+02	-6.69E+02			
1.7E-02	:-6.59E+02	-6.64E+02	-6.71E+02	-6.69E+02			
1.9E-02	:-6.58E+02	-6.63E+02	-6.72E+02	-6.69E+02			
2.4E-02	:-6.54E+02	-6.62E+02	-6.72E+02	-6.69E+02			
2.9E-02	:-6.52E+02	-6.61E+02	-6.73E+02	-6.69E+02			
3.4E-02	:-6.48E+02	-6.59E+02	-6.73E+02	-6.69E+02			
3.9E-02	:-6.46E+02	-6.58E+02	-6.74E+02	-6.69E+02			
4.4E-02	:-6.42E+02	-6.56E+02	-6.74E+02	-6.69E+02			
5.4E-02	:-6.37E+02	-6.54E+02	-6.76E+02	-6.69E+02			
6.4E-02	:-6.30E+02	-6.51E+02	-6.77E+02	-6.69E+02			
7.4E-02	:-6.25E+02	-6.49E+02	-6.79E+02	-6.69E+02			
8.4E-02	:-6.18E+02	-6.46E+02	-6.80E+02	-6.69E+02			
9.4E-02	:-6.13E+02	-6.44E+02	-6.81E+02	-6.69E+02			
1.1E-01	:-6.01E+02	-6.39E+02	-6.84E+02	-6.69E+02			
1.3E-01	:-5.92E+02	-6.34E+02	-6.87E+02	-6.70E+02			
1.5E-01	:-5.79E+02	-6.29E+02	-6.88E+02	-6.69E+02			
1.7E-01	:-5.70E+02	-6.24E+02	-6.91E+02	-6.69E+02			
1.9E-01	:-5.57E+02	-6.19E+02	-6.93E+02	-6.69E+02			
2.4E-01	:-5.37E+02	-6.09E+02	-7.00E+02	-6.70E+02			
2.9E-01	:-5.12E+02	-5.98E+02	-7.05E+02	-6.70E+02			
3.4E-01	:-4.92E+02	-5.88E+02	-7.10E+02	-6.70E+02			
3.9E-01	:-4.68E+02	-5.77E+02	-7.15E+02	-6.69E+02			
4.4E-01	:-4.48E+02	-5.67E+02	-7.19E+02	-6.69E+02			
5.4E-01	:-4.10E+02	-5.50E+02	-7.29E+02	-6.70E+02			
6.4E-01	:-3.78E+02	-5.33E+02	-7.38E+02	-6.70E+02			
7.4E-01	:-3.40E+02	-5.17E+02	-7.45E+02	-6.69E+02			

8.4E-01	[illegible]	-5.01E+02	-7.52E+02	-6.68E+02
9.4E-01	-2.74E+02	-4.84E+02	-7.56E+02	-6.67E+02
1.1E+00	-2.[illegible]E+02	-4.58E+02	-7.69E+02	-6.67E+02
1.3E+00	-1.77E+02	-4.46E+02	-7.78E+02	-6.66E+02
1.5E+00	-1.45E+02	-4.34E+02	-7.87E+02	-6.65E+02
1.7E+00	-1.07E+02	-4.09E+02	-7.93E+02	-6.64E+02
1.9E+00	-8.38E+01	-3.91E+02	-7.99E+02	-6.62E+02
2.4E+00	-5.09E+01	-3.64E+02	-8.12E+02	-6.63E+02
2.9E+00	-3.30E+01	-3.48E+02	-8.22E+02	-6.61E+02
3.4E+00	-1.83E+01	-3.38E+02	-8.26E+02	-6.60E+02
3.9E+00	-9.62E+00	-3.31E+02	-8.33E+02	-6.58E+02
4.4E+00	-3.96E+00	-3.25E+02	-8.36E+02	-6.57E+02
5.4E+00	-2.00E+00	-3.15E+02	-8.37E+02	-6.55E+02
6.4E+00	-1.9[illegible]E+00	-3.09E+02	-8.44E+02	-6.54E+02
7.4E+00	-1.8[illegible]E+00	-2.97E+02	-8.41E+02	-6.53E+02
8.4E+00	-1.75E+00	-2.93E+02	-8.44E+02	-6.52E+02
9.4E+00	-1.69E+00	-2.81E+02	-8.43E+02	-6.50E+02
1.0E+01	-1.64E+00	-2.78E+02	-8.46E+02	-6.50E+02
1.1E+01	-1.59E+00	-2.71E+02	-8.45E+02	-6.49E+02
1.2E+01	-1.56E+00	-2.61E+02	-8.45E+02	-6.48E+02
1.3E+01	-1.52E+00	-2.45E+02	-8.47E+02	-6.47E+02
1.4E+01	-1.49E+00	-2.48E+02	-8.41E+02	-6.46E+02
1.6E+01	-1.47E+00	-2.33E+02	-8.46E+02	-6.46E+02
1.8E+01	-1.44E+00	-2.25E+02	-8.47E+02	-6.46E+02
2.0E+01	-1.42E+00	-2.18E+02	-8.48E+02	-6.46E+02
2.2E+01	-1.40E+00	-2.11E+02	-8.48E+02	-6.46E+02
2.4E+01	-1.38E+00	-2.03E+02	-8.45E+02	-6.46E+02
2.6E+01	-1.36E+00	-1.98E+02	-8.47E+02	-6.46E+02
2.9E+01	-1.35E+00	-1.91E+02	-8.46E+02	-6.46E+02
3.0E+01	-1.33E+00	-1.86E+02	-8.46E+02	-6.46E+02
3.2E+01	-1.32E+00	-1.80E+02	-8.47E+02	-6.46E+02
3.4E+01	-1.30E+00	-1.75E+02	-8.45E+02	-6.46E+02
3.9E+01	-1.29E+00	-1.71E+02	-8.46E+02	-6.45E+02
4.4E+01	-1.29E+00	-1.67E+02	-8.47E+02	-6.45E+02
4.9E+01	-1.27E+00	-1.61E+02	-8.49E+02	-6.45E+02
5.4E+01	-1.26E+00	-1.56E+02	-8.41E+02	-6.45E+02
5.9E+01	-1.25E+00	-1.52E+02	-8.51E+02	-6.45E+02
6.4E+01	-1.24E+00	-1.48E+02	-8.44E+02	-6.45E+02
6.9E+01	-1.23E+00	-1.44E+02	-8.47E+02	-6.45E+02
7.4E+01	-1.22E+00	-1.40E+02	-8.49E+02	-6.45E+02
7.9E+01	-1.22E+00	-1.37E+02	-8.47E+02	-6.45E+02
8.4E+01	-1.21E+00	-1.34E+02	-8.52E+02	-6.45E+02
9.4E+01	-1.20E+00	-1.32E+02	[illegible]	-6.45E+02
1.0E+02	-1.20E+00	-1.28E+02	-8.4[illegible]E+02	-6.44E+02
1.1E+02	-1.19E+00	-1.26E+02	-8.45E+02	-6.45E+02
1.2E+02	-1.18E+00	-1.23E+02	-8.50E+02	-6.45E+02
1.3E+02	-1.18E+00	-1.20E+02	-8.40E+02	-6.44E+02
1.4E+02	-1.17E+00	-1.17E+02	-8.47E+02	-6.44E+02
1.5E+02	-1.16E+00	-1.15E+02	-8.47E+02	-6.45E+02
1.6E+02	-1.16E+00	-1.12E+02	-8.43E+02	-6.44E+02
1.7E+02	-1.16E+00	-1.10E+02	-8.43E+02	-6.44E+02
1.8E+02	-1.15E+00	-1.07E+02	-8.50E+02	-6.44E+021

POTL versus TIME in Seconds

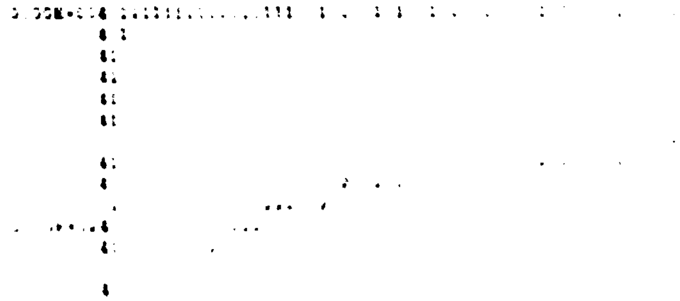

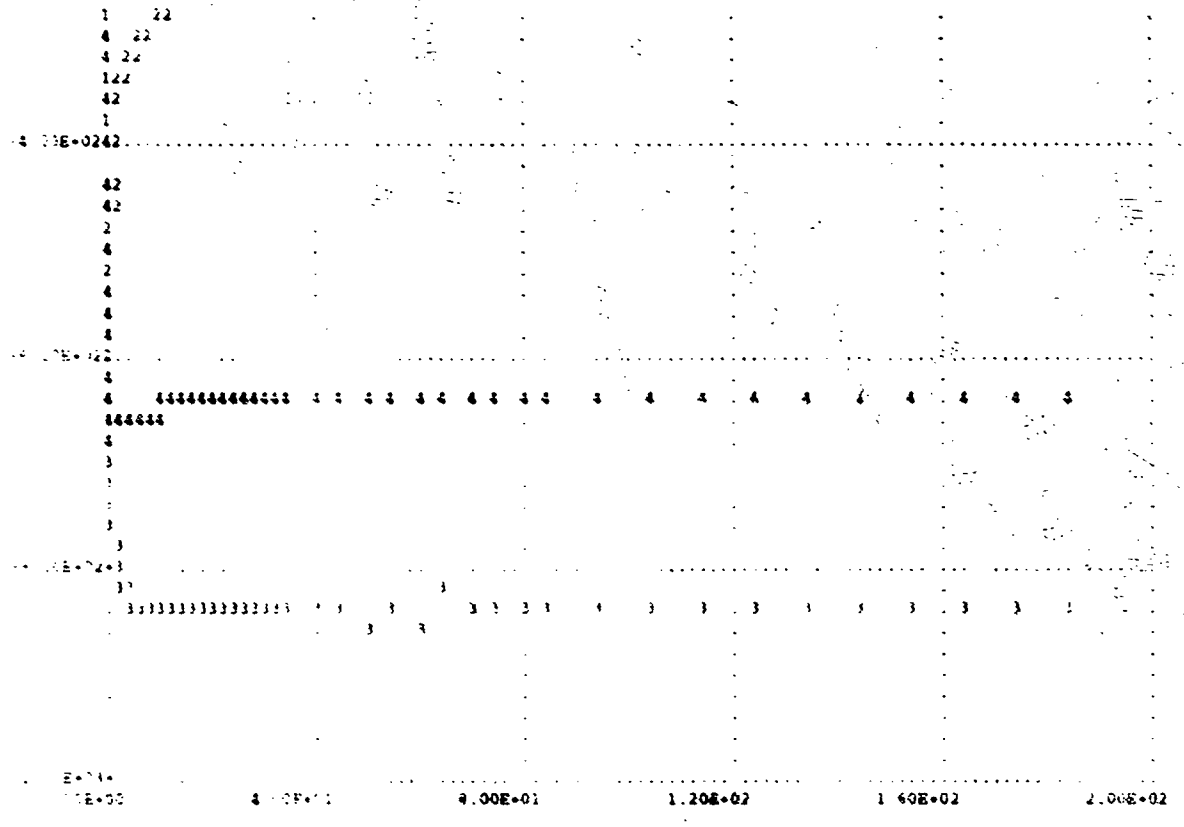


```
HISTORY command or MODE set >> exit
```

C.7 Spinning Spacecraft in Geosynchronous Orbit–SCATHA

The following files are the input and output files from the various computer codes used in Section 5.1.1.

Matchg Execution (fort.3) for Spinning Spacecraft in Geosynchronous Orbit SCATHA

This is the fort.3 file generated from the execution of **Matchg** to create Table 4. The environment is set to the severe substorm environment using the change environment command. The material is set to gold. A summary of potentials and currents before and after charging is requested. The process is repeated for all of the surface materials. During the execution, the object definition file (below) was used as a fort.8 for material definitions

```
WEL  ME TO  MATCHG   A MATERIAL CHARGING
PR  PAM  TYPE  HELP  AT ANY TIME FOR ASSISTANCE
MATERIAL I" GOLD
ENVIR NMENT NOW SINGLE MAXWELLIAN

change envi nel 1.12e6
```

```
ENVIRONMENT IS A SINGLE MAXWELLIAN

ELECTRONS: NE1 =  1.12e+06 (M**-3)     TE1 =     1.000 KEV
IONS     : NI1 =  1.00e+06 (M**-3)     TI1 =     1.000 KEV

change envi te1 12

ENVIRONMENT IS A SINGLE MAXWELLIAN

ELECTRONS: NE1 =  1.12e+06 (M** 3)     TE1 =    12.000 KEV
IONS     : NI1 =  1.00e+06 (M** 3)     TI1 =     1.000 KEV

change envi ni1 2.36e5

ENVIRONMENT IS A SINGLE MAXWELLIAN

ELECTRONS: NE1 =  1.12e+06 (M** 3)     TE1 =    12.000 KEV
IONS     : NI1 =  2.36e+05 (M** 3)     TI1 =     1.000 KEV

change envi ti1 29.5

ENVIRONMENT IS A SINGLE MAXWELLIAN

ELECTRONS: NE1 =  1.12e+06 (M**-3)     TE1 =    12.000 KEV
IONS     : NI1 =  2.36e+05 (M**-3)     TI1 =    29.500 KEV

change material GOLD

MATERIAL IS GOLD

result charge

CYCLE    1   TIME  0.00e+00 SECONDS     POTENTIAL  0.00e+00 VOLTS
INCIDENT ELECTRON CURRENT          -3.30e-06
         SECONDARY ELECTRONS        1.29e-06
         BACKSCATTERED ELECTRONS    2.10e-06
INCIDENT PROTON CURRENT             2.54e-08
         SECONDARY ELECTRONS        1.02e-07
                                   ----------
                    NET CURRENT     2.17e-07  AMPS/M**2
CYCLE   16   TIME  8.00e-01 SECONDS     POTENTIAL  3.38e-01 VOLTS
INCIDENT ELECTRON CURRENT          -3.30e-06
         SECONDARY ELECTRONS        1.09e-06
         BACKSCATTERED ELECTRONS    2.10e-06
INCIDENT PROTON CURRENT             2.54e-08
         SECONDARY ELECTRONS        8.64e-08
                                   ----------
                    NET CURRENT     2.83e-10  AMPS/M**2

change material SOLAR

MATERIAL IS SOLA

result charge

CYCLE    1   TIME  0.00e+00 SECONDS     POTENTIAL  0.00e+00 VOLTS
INCIDENT ELECTRON CURRENT          -3.30e-06
         SECONDARY ELECTRONS        1.45e-06
         BACKSCATTERED ELECTRONS    1.07e-06
INCIDENT PROTON CURRENT             2.54e-08
         SECONDARY ELECTRONS        6.92e-08
BULK CONDUCTIVITY CURRENT           0.00e+00
                                   ----------
                    NET CURRENT     6.84e-07  AMPS/M**2
```

```
CYCLE   99   TIME  3.23e+04 SECONDS    POTENTIAL -1.82e+04 VOLTS
INCIDENT ELECTRON CURRENT          -7.24e-07
         SECONDARY ELECTRONS        3.19e-07
         BACKSCATTERED ELECTRONS    2.34e-07
INCIDENT PROTON CURRENT             4.10e-08
         SECONDARY ELECTRONS        1.19e-07
BULK CONDUCTIVITY CURRENT           1.02e-09
                                  ------------
                      NET CURRENT  -1.02e-08  AMPS/M**2
```

change material WHITEM

```
MATERIAL IS WHIT
```

result charge

```
CYCLE    1   TIME  0.00e+00 SECONDS    POTENTIAL  0.00e+00 VOLTS
INCIDENT ELECTRON CURRENT          -3.30e-06
         SECONDARY ELECTRONS        7.33e-07
         BACKSCATTERED ELECTRONS    8.01e-07
INCIDENT PROTON CURRENT             2.54e-08
         SECONDARY ELECTRONS        1.14e-07
BULK CONDUCTIVITY CURRENT           0.00e+00
                                  ------------
                      NET CURRENT  -1.62e-06  AMPS/M**2
CYCLE   14   TIME  4.49e+04 SECONDS    POTENTIAL -1.23e+03 VOLTS
INCIDENT ELECTRON CURRENT          -2.98e-06
         SECONDARY ELECTRONS        6.62e-07
         BACKSCATTERED ELECTRONS    7.23e-07
INCIDENT PROTON CURRENT             2.65e-08
         SECONDARY ELECTRONS        1.19e-07
BULK CONDUCTIVITY CURRENT           1.45e-06
                                  ------------
                      NET CURRENT  -2.32e-10  AMPS/M**2
```

change material SCREEM

```
MATERIAL IS SCRE
```

result charge

```
CYCLE    1   TIME  0.00e+00 SECONDS    POTENTIAL  0.00e+00 VOLTS
INCIDENT ELECTRON CURRENT          -3.30e-06
         SECONDARY ELECTRONS        0.00e+00
         BACKSCATTERED ELECTRONS    3.24e-07
INCIDENT PROTON CURRENT             2.54e-08
         SECONDARY ELECTRONS        0.00e+00
                                  ------------
                      NET CURRENT  -2.95e-06  AMPS/M**2
CYCLE   99   TIME  3.53e+04 SECONDS    POTENTIAL -2.76e+04 VOLTS
INCIDENT ELECTRON CURRENT          -3.31e-07
         SECONDARY ELECTRONS        0.00e+00
         BACKSCATTERED ELECTRONS    3.26e-08
INCIDENT PROTON CURRENT             4.91e-08
         SECONDARY ELECTRONS        0.00e+00
                                  ------------
                      NET CURRENT  -2.50e-07  AMPS/M**2
```

change material YELOWC

```
MATERIAL IS YELO
```

result charge

```
CYCLE    1   TIME  0.00e+00 SECONDS     POTENTIAL  0.00e+00 VOLTS
INCIDENT ELECTRON CURRENT          -3.30e-06
         SECONDARY ELECTRONS        7.33e-07
         BACKSCATTERED ELECTRONS    8.01e-07
INCIDENT PROTON CURRENT             2.54e-08
         SECONDARY ELECTRONS        1.14e-07
                                   ----------
                     NET CURRENT   -1.62e-06  AMPS/M**2
CYCLE   99   TIME  2.24e+03 SECONDS     POTENTIAL -2.12e+04 VOLTS
INCIDENT ELECTRON CURRENT          -5.65e-07
         SECONDARY ELECTRONS        1.26e-07
         BACKSCATTERED ELECTRONS    1.37e-07
INCIDENT PROTON CURRENT             4.36e-08
         SECONDARY ELECTRONS        2.09e-07
                                   ----------
                     NET CURRENT   -4.99e-08  AMPS/M**2
```

change material PDGOLD

```
MATERIAL IS PDGO
```

result charge

```
CYCLE    1   TIME  0.00e+00 SECONDS     POTENTIAL  0.00e+00 VOLTS
INCIDENT ELECTRON CURRENT          -3.30e-06
         SECONDARY ELECTRONS        1.46e-06
         BACKSCATTERED ELECTRONS    2.03e-06
INCIDENT PROTON CURRENT             2.54e-08
         SECONDARY ELECTRONS        1.02e-07
                                   ----------
                     NET CURRENT    3.17e-07  AMPS/M**2
CYCLE   22   TIME  5.47e-01 SECONDS     POTENTIAL  4.53e-01 VOLTS
INCIDENT ELECTRON CURRENT          -3.30e-06
         SECONDARY ELECTRONS        1.16e-06
         BACKSCATTERED ELECTRONS    2.03e-06
INCIDENT PROTON CURRENT             2.54e-08
         SECONDARY ELECTRONS        8.16e-08
                                   ----------
                     NET CURRENT    2.46e-10  AMPS/M**2
```

change material BLACKC

```
MATERIAL IS BLAC
```

result charge

```
CYCLE    1   TIME  0.00e+00 SECONDS     POTENTIAL  0.00e+00 VOLTS
INCIDENT ELECTRON CURRENT          -3.30e-06
         SECONDARY ELECTRONS        7.33e-07
         BACKSCATTERED ELECTRONS    8.01e-07
INCIDENT PROTON CURRENT             2.54e-08
         SECONDARY ELECTRONS        1.14e-07
                                   ----------
                     NET CURRENT   -1.62e-06  AMPS/M**2
CYCLE   99   TIME  2.24e+03 SECONDS     POTENTIAL -2.12e+04 VOLTS
INCIDENT ELECTRON CURRENT          -5.65e-07
         SECONDARY ELECTRONS        1.26e-07
         BACKSCATTERED ELECTRONS    1.37e-07
INCIDENT PROTON CURRENT             4.36e-08
         SECONDARY ELECTRONS        2.09e-07
                                   ----------
                     NET CURRENT   -4.99e-08  AMPS/M**2
```

change material KAPTON

```
MATERIAL IS KAPT

result charge

CYCLE    1   TIME  0.00e+00 SECONDS    POTENTIAL  0.00e+00 VOLTS
INCIDENT ELECTRON CURRENT          -3.30e-06
         SECONDARY ELECTRONS        7.33e-07
         BACKSCATTERED ELECTRONS    8.01e-07
INCIDENT PROTON CURRENT             2.54e-08
         SECONDARY ELECTRONS        1.14e-07
BULK CONDUCTIVITY CURRENT           0.00e+00
                                  -------------
                      NET CURRENT  -1.62e-06  AMPS/M**2
CYCLE   99   TIME  1.77e+04 SECONDS    POTENTIAL -2.08e+04 VOLTS
INCIDENT ELECTRON CURRENT          -5.84e-07
         SECONDARY ELECTRONS        1.30e-07
         BACKSCATTERED ELECTRONS    1.42e-07
INCIDENT PROTON CURRENT             4.32e-08
         SECONDARY ELECTRONS        2.07e-07
BULK CONDUCTIVITY CURRENT           1.64e-08
                                  -------------
                      NET CURRENT  -4.56e-08  AMPS/M**2

change material SIO2

MATERIAL IS SIO2

result charge

CYCLE    1   TIME  0.00e+00 SECONDS    POTENTIAL  0.00e+00 VOLTS
INCIDENT ELECTRON CURRENT          -3.30e-06
         SECONDARY ELECTRONS        1.33e-06
         BACKSCATTERED ELECTRONS    1.07e-06
INCIDENT PROTON CURRENT             2.54e-08
         SECONDARY ELECTRONS        1.14e-07
BULK CONDUCTIVITY CURRENT           0.00e+00
                                  -------------
                      NET CURRENT  -7.59e-07  AMPS/M**2
CYCLE    4   TIME  1.89e+04 SECONDS    POTENTIAL -7.53e+01 VOLTS
INCIDENT ELECTRON CURRENT          -3.28e-06
         SECONDARY ELECTRONS        1.32e-06
         BACKSCATTERED ELECTRONS    1.06e-06
INCIDENT PROTON CURRENT             2.55e-08
         SECONDARY ELECTRONS        1.14e-07
BULK CONDUCTIVITY CURRENT           7.53e-07
                                  -------------
                      NET CURRENT  -1.56e-10  AMPS/M**2

change material TEFLON

MATERIAL IS TEFL

result charge

CYCLE    1   TIME  0.00e+00 SECONDS    POTENTIAL  0.00e+00 VOLTS
INCIDENT ELECTRON CURRENT          -3.30e-06
         SECONDARY ELECTRONS        1.35e-06
         BACKSCATTERED ELECTRONS    9.25e-07
INCIDENT PROTON CURRENT             2.54e-08
         SECONDARY ELECTRONS        1.14e-07
BULK CONDUCTIVITY CURRENT           0.00e+00
                                  -------------
                      NET CURRENT  -8.80e-07  AMPS/M**2
```

```
CYCLE   99   TIME  1.86e+04 SECONDS    POTENTIAL -1.69e+04 VOLTS
INCIDENT ELECTRON CURRENT          -8.08e-07
         SECONDARY ELECTRONS        3.32e-07
         BACKSCATTERED ELECTRONS    2.27e-07
INCIDENT PROTON CURRENT             3.99e-08
         SECONDARY ELECTRONS        1.88e-07
BULK CONDUCTIVITY CURRENT           1.33e-08
                                  ------------
                      NET CURRENT  -8.63e-09  AMPS/M**2
```

change material INDOX

```
MATERIAL IS INDO
```

result charge

```
CYCLE    1   TIME  0.00e+00 SECONDS    POTENTIAL  0.00e+00 VOLTS
INCIDENT ELECTRON CURRENT          -3.30e-06
         SECONDARY ELECTRONS        6.61e-07
         BACKSCATTERED ELECTRONS    1.46e-06
INCIDENT PROTON CURRENT             2.54e-08
         SECONDARY ELECTRONS        1.18e-07
                                  ------------
                      NET CURRENT  -1.03e-06  AMPS/M**2
CYCLE   99   TIME  1.01e+03 SECONDS    POTENTIAL -1.82e+04 VOLTS
INCIDENT ELECTRON CURRENT          -7.24e-07
         SECONDARY ELECTRONS        1.45e-07
         BACKSCATTERED ELECTRONS    3.21e-07
INCIDENT PROTON CURRENT             4.10e-08
         SECONDARY ELECTRONS        2.01e-07
                                  ------------
                      NET CURRENT  -1.54e-08  AMPS/M**2
```

change material YGOLDC

```
MATERIAL IS YGOL
```

result charge

```
CYCLE    1   TIME  0.00e+00 SECONDS    POTENTIAL  0.00e+00 VOLTS
INCIDENT ELECTRON CURRENT          -3.30e-06
         SECONDARY ELECTRONS        2.29e-07
         BACKSCATTERED ELECTRONS    1.74e-06
INCIDENT PROTON CURRENT             2.54e-08
         SECONDARY ELECTRONS        1.02e-07
                                  ------------
                      NET CURRENT  -1.20e-06  AMPS/M**2
CYCLE   99   TIME  8.68e+02 SECONDS    POTENTIAL -1.99e+04 VOLTS
INCIDENT ELECTRON CURRENT          -6.27e-07
         SECONDARY ELECTRONS        4.36e-08
         BACKSCATTERED ELECTRONS    3.31e-07
INCIDENT PROTON CURRENT             4.25e-08
         SECONDARY ELECTRONS        1.82e-07
                                  ------------
                      NET CURRENT  -2.81e-08  AMPS/M**2
```

change material ALUMIN

```
MATERIAL IS ALUM
```

result charge

```
CYCLE    1   TIME  0.00e+00 SECONDS    POTENTIAL  0.00e+00 VOLTS
INCIDENT ELECTRON CURRENT          -3.30e-06
```

```
         SECONDARY ELECTRONS        6.75e-07
         BACKSCATTERED ELECTRONS    1.18e-06
INCIDENT PROTON CURRENT             2.54e-08
         SECONDARY ELECTRONS        6.92e-08
                                   ----------
                     NET CURRENT  -1.35e-06  AMPS/M**2
CYCLE   99   TIME  7.71e+02 SECONDS    POTENTIAL -2.22e+04 VOLTS
INCIDENT ELECTRON CURRENT          -5.17e-07
         SECONDARY ELECTRONS        1.06e-07
         BACKSCATTERED ELECTRONS    1.85e-07
INCIDENT PROTON CURRENT             4.45e-08
         SECONDARY ELECTRONS        1.31e-07
                                   ----------
                     NET CURRENT  -5.10e-08  AMPS/M**2
```

change material BOMAT

```
MATERIAL IS BOMAT
```

result charge

```
CYCLE    1   TIME  0.00e+00 SECONDS    POTENTIAL  0.00e+00 VOLTS
INCIDENT ELECTRON CURRENT          -3.30e-06
         SECONDARY ELECTRONS        1.28e-06
         BACKSCATTERED ELECTRONS    1.97e-06
INCIDENT PROTON CURRENT             2.54e-08
         SECONDARY ELECTRONS        1.02e-07
BULK CONDUCTIVITY CURRENT           0.00e+00
                                   ----------
                     NET CURRENT   8.39e-08  AMPS/M**2
CYCLE    7   TIME  8.27e-01 SECONDS    POTENTIAL  1.24e-01 VOLTS
INCIDENT ELECTRON CURRENT          -3.30e-06
         SECONDARY ELECTRONS        1.21e-06
         BACKSCATTERED ELECTRONS    1.97e-06
INCIDENT PROTON CURRENT             2.54e-08
         SECONDARY ELECTRONS        9.62e-08
BULK CONDUCTIVITY CURRENT          -2.49e-14
                                   ----------
                     NET CURRENT   2.76e-10  AMPS/M**2
```

change material ML12

```
MATERIAL IS ML12
```

result charge

```
CYCLE    1   TIME  0.00e+00 SECONDS    POTENTIAL  0.00e+00 VOLTS
INCIDENT ELECTRON CURRENT          -3.30e-06
         SECONDARY ELECTRONS        8.22e-07
         BACKSCATTERED ELECTRONS    8.67e-07
INCIDENT PROTON CURRENT             2.54e-08
         SECONDARY ELECTRONS        1.14e-07
                                   ----------
                     NET CURRENT  -1.47e-06  AMPS/M**2
CYCLE   99   TIME  7.09e+02 SECONDS    POTENTIAL  2.06e+04 VOLTS
INCIDENT ELECTRON CURRENT          -5.93e-07
         SECONDARY ELECTRONS        1.48e-07
         BACKSCATTERED ELECTRONS    1.56e-07
INCIDENT PROTON CURRENT             4.31e-08
         SECONDARY ELECTRONS        2.00e-07
                                   ----------
                     NET CURRENT  -4.00e-08  AMPS/M**2
```

exit

```
[EXIT]
```

The following files are used to execute **Nascap** for the SCATHA example. The first is the standard input file, which gives the options and initial potential. The second is the object definition. The third is the environment definition file.

Standard Input to Nascap for Spinning Spacecraft in Geosynchronous Orbit-SCATHA

```
rdopt 5
   delta 60.
   longtimestep
   ncyc 20
   ng 4
   nz 33
   xmesh 0.115
   cij 1  2  30e-12
   cij 1  3  30e-12
   cij 1  4  340e-12
   cij 1  5  30e-12
   cij 1  6  250e-12
   end
objdef 20
capaci
ips
   pcond 1  -18200
   pcond 2  -21200
   pcond 3  -21200
   pcond 4  -18200
   pcond 5  -18200
   pcond 6  -18200
   end
trilin
end
```

Environment File (fort.22) for Spinning Spacecraft in Geosynchronous Orbit-SCATHA

```
single maxwellian
1.12e6 mks
12 kev
2.16e5 mks
29.5 kev
end
```

Object Definition File (fort.20) for Spinning Spacecraft in Geosynchronous Orbit-SCATHA

This file is also used as a fort.8 material definition file for the execution of **Matchg**.

```
GOLD
1.00      .001      -1.       79.       .88       .8        88.8      .92
```

```
53.5      1.73       .413       135.       .000029   -1.        15.        16.
17.       18.        19.        20.
SOLAR
3.8       .000179    1.E-17     10.        2.05          .41     77.5   .45
156       1.73       .244       230.       .00002     1.E+19 15.         16.
17.       18.        19.        20.
WHITEN
3.5       .00005        5.9E-14 5.         2.1        .15        71.5       .6
312       1.77        .455       140.       .00002          1.E+13 15.       16.
17.       18.        19.        20.
SCREEN
1.        .001       -1.        1.         0.         1.         10.        1.5
0.        1.         0.         1.         0.         -1.        15.        16.
17.       18.        19.        20.
YELOWC
3.5       .001       -1.        5.         2.1        .15        71.5       .6
312       1.77       .455       140.       .00002     -1.        15.        16.
17.       18.        19.        20.
PDGOLD
1.        .001       -1.        70.1       1.03       .72        88.8       .92
53.5      1.73        .413       135.       .000029   -1.         15.        16.
17.       18.        19.        20.
BLACKC
3.5       .001       -1.        5.         2.1        .15        71.5       .6
312       1.77      .455       140.       .00002     -1.        15.        16.
17.       18.        19.        20.
KAPTON
3.5       .000127     1.E-16    5.         2.1        .15         71.5       .6
312       1.77        .455       140.       .00002          1.E+16 15.       16.
17.       18.        19.        20.
SIO2
3.8       .000275    2.75E-12     10.       2.4        .4          116       .810
183       1.86        .455       140.       .00002     1.E+11      15.       16.
17.       18.        19.        20.
TEFLON
2.        .000127        1.E-16  7.         3.         .3         45.4       .4
218.      1.77          .455       140.       .00002          1.E+16 15.       16.
17.       18.        19.        20.
INDOX
1.        .001       -1.        24.4       1.4        .8         -1.        0.
7.18      55.5       .490       123.       .000032   -1.         15.        16.
17.       18.        19.        20.
YGOLDC
1.        .001       -1.        42.        1.49       .48        -1.        0.
1.78      1.03       .413       135.       .000024   -1.         15.        16.
17.       18.        19.        20.
ALUMIN
1.        .001       -1.        13.        .97        .3         154.       .8
220.      1.76       .244       230.       .00004    -1.         15.        16.
17.       18.        19.        20.
BOMAT
2.        .005          1.E-15 63.4      .88         .8          88.          .92
53.5      1.73          .413       135.       .0000272       1.E+11 15.       16.
17.       18.        19.        20.
ML12
1.        .001       -1.        6.         1.         .3         -1.        0.
2.        12.        .455       140.       .000021   -1.         15.        16.
17.       18.        19.        20.
OFFSET        0    0   +6
CONDUCTOR     1
COMMENT *** DEFINE SC11-1 BOOM ***
BOOM
AXIS          09   16   11   01   09   14   17   04
RADIUS    0.2
```

```
SURFACE   BOMAT
ENDOBJ
COMMENT *** DEFINE SC6-1 BOOM ***
BOOM
AXIS         09   02   11   01   09   01   17   03
RADIUS    0.196
SURFACE   BOMAT
ENDOBJ
CONDUCTOR     5
COMMENT *** DEFINE SC6-1 THERMAL PLASMA ANAYLZER SENSOR ***
BOOM
AXIS         09   05   17   04   09   04   17   04
RADIUS    0.14
SURFACE   GOLD
ENDOBJ
CONDUCTOR     1
COMMENT *** DEFINE SC2-1 BOOM ***
BOOM
AXIS         16   09   11   01   17   09   17   03
RADIUS    0.178
SURFACE   BOMAT
ENDOBJ
CONDUCTOR     2
COMMENT *** DEFINE SC2-1 SENSOR AND STUB ***
BOOM
AXIS         13   09   17   04   14   09   17   04
RADIUS    0.18
SURFACE   BLACKC
ENDOBJ
CONDUCTOR     1
COMMENT *** DEFINE SC2-2 BOOM ***
BOOM
AXIS         02   09   11   01   01   09   17   03
RADIUS    0.178
SURFACE   BOMAT
ENDOBJ
CONDUCTOR     3
COMMENT *** DEFINE SC2-2 SENSOR AND STUB ***
BOOM
AXIS         05   09   17   04   04   09   17   04
RADIUS    0.18
SURFACE   BLACKC
ENDOBJ
CONDUCTOR     1
COMMENT *** DEFINE 3 INCH DIAMETER OMNI-ANTENNA MAST (BOTTOM) ***
BOOM
AXIS         09   09   19   01   09   09   23   01
RADIUS    0.331
SURFACE   BOMAT
ENDOBJ
COMMENT *** DEFINE 3 INCH DIAMETER OMNI-ANTENNA MAST (TOP) ***
BOOM
AXIS         09   09   25   01   09   09   26   01
RADIUS    0.331
SURFACE   TEFLON
ENDOBJ
COMMENT   OPEN BOTTOM BASIC MATERIAL
COMMENT   EXTERIOR A-FACE WEDGE
WEDGE
CORNER       12   12    4
FACE      SOLAR          1    1    0
LENGTH        4    4    9
SURFACE   -Z        WHITEN
ENDOBJ
```

```
COMMENT   INTERIOR A-FACE WEDGE
WEDGE
CORNER      13    13     4
FACE      GOLD            -1    -1     0
LENGTH       2     2     9
SURFACE   -Z          WHITEN
ENDOBJ
COMMENT   B-FACE RECTANGLE
RECTAN
CORNER      13     6     4
DELTAS       3     6     9
SURFACE   -X          GOLD
SURFACE   +X          SOLAR
SURFACE   -Z          WHITEN
ENDOBJ
COMMENT   EXTERIOR C-FACE WEDGE
WEDGE
CORNER      12     6     4
FACE      SOLAR           1    -1     0
LENGTH       4     4     9
SURFACE   -Z          WHITEN
ENDOBJ
COMMENT   INTERIOR C-FACE WEDGE
WEDGE
CORNER      13     5     4
FACE      GOLD            -1     1     0
LENGTH       2     2     9
SURFACE   -Z          WHITEN
ENDOBJ
COMMENT   D-FACE RECTANGLE
RECTAN
CORNER       6     2     4
DELTAS       6     3     9
SURFACE   -Y          SOLAR
SURFACE   +Y          GOLD
SURFACE   -Z          WHITEN
ENDOBJ
COMMENT   EXTERIOR E-FACE WEDGE
WEDGE
CORNER       6     6     4
FACE      SOLAR           -1    -1     0
LENGTH       4     4     9
SURFACE   -Z          WHITEN
ENDOBJ
COMMENT   INTERIOR E-FACE WEDGE
WEDGE
CORNER       5     5     4
FACE      GOLD            1     1     0
LENGTH       2     2     9
SURFACE   -Z          WHITEN
ENDOBJ
COMMENT   F-FACE RECTANGLE
RECTAN
CORNER       2     6     4
DELTAS       3     6     9
SURFACE   -X          SOLAR
SURFACE   +X          GOLD
SURFACE   -Z          WHITEN
ENDOBJ
COMMENT   EXTERIOR G-FACE WEDGE
WEDGE
CORNER       6    12     4
FACE      SOLAR           -1     1     0
LENGTH       4     4     9
```

```
SURFACE   -Z          WHITEN
ENDOBJ
COMMENT   INTERIOR G-FACE WEDGE
WEDGE
CORNER        5    13     4
FACE      GOLD             1    -1     0
LENGTH        2     2     9
SURFACE   -Z          WHITEN
ENDOBJ
COMMENT   H-FACE RECTANGLE
RECTAN
CORNER        6    13     4
DELTAS        6     3     9
SURFACE   -Y          GOLD
SURFACE   +Y          SOLAR
SURFACE   -Z          WHITEN
ENDOBJ
COMMENT   BELLY BAND BASIC MATERIAL
COMMENT   EXTERIOR A-FACE WEDGE
WEDGE
CORNER       12    12    10
FACE      YELOWC           1     1     0
LENGTH        4     4     3
ENDOBJ
COMMENT   B-FACE RECTANGLE
RECTAN
CORNER       13     6    10
DELTAS        3     6     3
SURFACE   +X          YELOWC
ENDOBJ
COMMENT   EXTERIOR C-FACE WEDGE
WEDGE
CORNER       12     6    10
FACE      YELOWC           1    -1     0
LENGTH        4     4     3
ENDOBJ
COMMENT   D-FACE RECTANGLE
RECTAN
CORNER        6     2    10
DELTAS        6     3     3
SURFACE   -Y          YELOWC
ENDOBJ
COMMENT   EXTERIOR E-FACE WEDGE
WEDGE
CORNER        6     6    10
FACE      YELOWC          -1    -1     0
LENGTH        4     4     3
ENDOBJ
COMMENT   F-FACE RECTANGLE
RECTAN
CORNER        2     6    10
DELTAS        3     6     3
SURFACE   -X          YELOWC
ENDOBJ
COMMENT   EXTERIOR G-FACE WEDGE
WEDGE
CORNER        6    12    10
FACE      YELOWC          -1     1     0
LENGTH        4     4     3
ENDOBJ
COMMENT   H-FACE RECTANGLE
RECTAN
CORNER        6    13    10
DELTAS        6     3     3
```

```
SURFACE   +Y          YELOWC
ENDOBJ
COMMENT   INTERIOR BOTTOM
RECTAN
CORNER        5     5    13
DELTAS        8     8     1
SURFACE   -Z          GOLD
ENDOBJ
COMMENT   TOP BASIC MATERIAL
OCTAGON
AXIS          9     9    13          9     9    19
WIDTH        14
SIDE          6
SURFACE   C           SOLAR
SURFACE   +           PDGOLD
ENDOBJ
COMMENT   OMNI ANTENNA BOX
RECTAN
CORNER        8     8    23
DELTAS        2     2     2
SURFACE   -X          TEFLON
SURFACE   +X          TEFLON
SURFACE   -Y          TEFLON
SURFACE   +Y          TEFLON
SURFACE   -Z          ALUMINUM
SURFACE   +Z          ALUMINUM
ENDOBJ
COMMENT   SC9-1 (TOP)
RECTAN
CORNER        5    14    19
DELTAS        2     1     2
SURFACE   +Z          YGOLDC
SURFACE   +X          BLACKC
SURFACE   -X          BLACKC
SURFACE   +Y          BLACKC
SURFACE   -Y          BLACKC
ENDOBJ
COMMENT   SC9-2 (TOP)
RECTAN
CORNER        5    15    19
DELTAS        1     1     1
SURFACE   +X          GOLD
SURFACE   -X          GOLD
SURFACE   +Y          YELOWC
SURFACE   +Z          GOLD
SURFACE   -Z          GOLD
ENDOBJ
COMMENT   SC9-3 (TOP)
RECTAN
CORNER        4    14    19
DELTAS        1     1     1
SURFACE   -X          YELOWC
SURFACE   +Y          GOLD
SURFACE   -Y          GOLD
SURFACE   +Z          GOLD
SURFACE   -Z          GOLD
ENDOBJ
COMMENT   SC5 SCREEN (TOP)
PATCHR
CORNER        7     2    18
DELTAS        4     3     1
SURFACE   +Z          SCREEN
ENDOBJ
COMMENT   SC1-3A (TOP)
```

```
PATCHR
CORNER        12     5    18
DELTAS         1     1     1
SURFACE    +Z          GOLD
ENDOBJ
COMMENT    SC1-3B (TOP)
PATCHR
CORNER        12     6    18
DELTAS         1     1     1
SURFACE    +Z          KAPTON
ENDOBJ
COMMENT    SC1-3C (TOP)
PATCHR
CORNER        13     6    18
DELTAS         1     1     1
SURFACE    +Z          SIO2
ENDOBJ
COMMENT    SC1-3D (TOP)
PATCHR
CORNER        13     5    18
DELTAS         1     1     1
SURFACE    +Z          TEFLON
ENDOBJ
CONDUCTOR      4
COMMENT    SC6-2 SHIELD (TOP)
PATCHR
CORNER        13    10    18
DELTAS         1     1     1
SURFACE    +Z          GOLD
ENDOBJ
CONDUCTOR      1
COMMENT    SC7-2 SHIELD (TOP)
PATCHR
CORNER         4     4    18
DELTAS         2     2     1
SURFACE    +Z          GOLD
ENDOBJ
COMMENT    ML12-7 SHIELD (TOP,
PATCHR
CORNER         3     8    [illegible]
DELTAS         3     3    [illegible]
SURFACE    +Z          GO[illegible]D
ENDOBJ
COMMENT    ML12-7 (TOP)
PATCHR
CORNER         4     9    [illegible]
DELTAS         1     1    [illegible]
SURFACE    +Z          INDOX
ENDOBJ
COMMENT    BELLY BAND (A-FACE)
PATCHW
CORNER        12    12    10
FACE       YGOLDC           1     1     0
LENGTH         4     4     3
ENDOBJ
COMMENT    ML12-6  (A-FACE)
PATCHW
CORNER        12    15    10
FACE       INDOX            1     1     0
LENGTH         1     1     1
ENDOBJ
COMMENT    ML12-6 DOOR (A-FACE)
PATCHW
CORNER        12    15     9
```

```
FACE      GOLD          1    1    0
LENGTH       1    1    1
ENDOBJ
COMMENT   ML12-3 (A-FACE)
PATCHW
CORNER       13   14   10
FACE      ML12          1    1    0
LENGTH       1    1    2
ENDOBJ
COMMENT   ML-12 MASK (A-FACE)
PATCHW
CORNER       13   14    9
FACE      BLACKC        1    1    0
LENGTH       1    1    1
ENDOBJ
COMMENT   ML-12 MASK (A-FACE)
PATCHW
CORNER       12   14   13
FACE      BLACKC        1    1    0
LENGTH       2    2    1
ENDOBJ
COMMENT   BELLY BAND (B-FACE)
PATCHR
CORNER       15   10   10
DELTAS        1    2    3
SURFACE   +X        YGOLDC
ENDOBJ
COMMENT   SC1 MASK (B-FACE)
PATCHR
CORNER       15    6   10
DELTAS        1    4    3
SURFACE   +X        TEFLON
ENDOBJ
COMMENT   SC1 MASK (B-FACE)
PATCHR
CORNER       15   10   11
DELTAS        1    1    2
SURFACE   +X        TEFLON
ENDOBJ
COMMENT   SC1-1A (B-FACE)
PATCHR
CORNER       15    7   13
DELTAS        1    1    1
SURFACE   +X        GOLD
ENDOBJ
COMMENT   SC1-1B (B-FACE)
PATCHR
CORNER       15    7   14
DELTAS        1    1    1
SURFACE   +X        INDOX
ENDOBJ
COMMENT   SC1-1C (B-FACE)
PATCHR
CORNER       15    8   14
DELTAS        1    1    1
SURFACE   +X        SOLAR
ENDOBJ
COMMENT   SC1-1D (B-FACE)
PATCHR
CORNER       15    8   13
DELTAS        1    1    1
SURFACE   +X        KAPTON
ENDOBJ
COMMENT   SHCI NO. 1 (B-FACE)
```

```
WEDGE
CORNER      16   12   10
FACE      ALUMINUM      1   -1    0
LENGTH       1    1    1
SURFACE   +Z        ALUMINUM
SURFACE   -Z        ALUMINUM
SURFACE   +Y        ALUMINUM
ENDOBJ
COMMENT   SC1-1 MASK (C-FACE)
PATCHW
CORNER      15    6   11
FACE      TEFLON        1   -1    0
LENGTH       1    1    2
ENDOBJ
COMMENT   SC7-1 MASK (D-FACE)
PATCHR
CORNER       6    2    9
DELTAS       2    1    1
SURFACE   -Y        BLACKC
ENDOBJ
COMMENT   SC7-1 MASK (D-FACE)
PATCHR
CORNER       6    2   13
DELTAS       2    1    1
SURFACE   -Y        BLACKC
ENDOBJ
COMMENT   SC5 COVER (D-FACE)
RECTAN
CORNER      10    2   12
DELTAS       1    1    1
SURFACE   -Y        BLACKC
ENDOBJ
COMMENT   SHCI NO. 2 (D-FACE)
WEDGE
CORNER      10    2   10
FACE      ALUMINUM      1   -1    0
LENGTH       1    1    1
SURFACE   +Z        ALUMINUM
SURFACE   -Z        ALUMINUM
SURFACE   -X        ALUMINUM
ENDOBJ
COMMENTCOMMENT   DSAS GLASS PATCH (E-FACE)
COMMENTWEDGE
COMMENTCORNER        4    5   11
COMMENTFACE      SIO2         -1   -1    0
COMMENTLENGTH        1    1    1
COMMENTENDOBJ
COMMENT   SC1-2 MASK (F-FACE)
PATCHR
CORNER       2   10   10
DELTAS       1    2    3
SURFACE   -X        TEFLON
ENDOBJ
COMMENT   SC1-2 MASK (F-FACE)
PATCHR
CORNER       2    8   10
DELTAS       1    2    2
SURFACE   -X        TEFLON
ENDOBJ
COMMENT   SC1-2 (F-FACE)
PATCHR
CORNER       2   10    8
DELTAS       1    2    2
SURFACE   -X        KAPTON
```

```
ENDOBJ
COMMENT   SC9 MASK (G-FACE)
PATCHW
CORNER        6    13    17
FACE      INDOX          -1     1     0
LENGTH        3     3     2
ENDOBJ
COMMENT   SC1-2 MASK (G-FACE)
PATCHW
CORNER        3    12    10
FACE      TEFLON         -1     1     0
LENGTH        1     1     3
ENDOBJ
COMMENT   ML12-4 (H-FACE)
PATCHR
CORNER       10    15    10
DELTAS        1     1     2
SURFACE   +Y          ML12
ENDOBJ
COMMENT   ML12 MASK (H-FACE)
PATCHR
CORNER        6    15     9
DELTAS        6     1     1
SURFACE   +Y          BLACKC
ENDOBJ
COMMENT   ML12 MASK (H-FACE)
PATCHR
CORNER        6    15    13
DELTAS        6     1     1
SURFACE   +Y          BLACKC
ENDOBJ
COMMENT   SC9 MASK (H-FACE)
PATCHR
CORNER        6    15    17
DELTAS        2     1     2
SURFACE   +Y          INDOX
ENDOBJ
COMMENT   SC8 (H-FACE)
PATCHR
CORNER        7    15    11
DELTAS        2     1     1
SURFACE   +Y          BLACKC
ENDOBJ
COMMENT   SC7-3 MASK (BOTTOM)
PATCHR
CORNER       13     4     4
DELTAS        1     2     1
SURFACE   -Z          GOLD
ENDOBJ
COMMENT   SC7-3 MASK (BOTTOM)
PATCHR
CORNER       14     5     4
DELTAS        1     1     1
SURFACE   -Z          GOLD
ENDOBJ
COMMENT   SC7-3 MASK (BOTTOM)
PATCHW
CORNER       14     5     4
FACE      SOLAR          1    -1     0
LENGTH        1     1     1
SURFACE   -Z          GOLD
ENDOBJ
CONDUCTOR     6
COMMENT   REFERENCE BAND (FACE A)
```

```
PATCHW
CORNER      14   13    4
FACE      GOLD          1    1    0
LENGTH       1    1    1
ENDOBJ
COMMENT   REFERENCE BAND (FACE B)
PATCHR
CORNER      15    8    4
DELTAS       1    1    1
SURFACE   +X        GOLD
ENDOBJ
COMMENT   REFERENCE BAND (FACE C)
PATCHW
CORNER      13    4    4
FACE      GOLD          1   -1    0
LENGTH       1    1    1
ENDOBJ
COMMENT   REFERENCE BAND (FACE D)
PATCHR
CORNER       8    2    4
DELTAS       1    1    1
SURFACE   -Y        GOLD
ENDOBJ
COMMENT   REFERENCE BAND (FACE E)
PATCHW
CORNER       4    5    4
FACE      GOLD         -1   -1    0
LENGTH       1    1    1
ENDOBJ
COMMENT   REFERENCE BAND (FACE F)
PATCHR
CORNER       2    9    4
DELTAS       1    1    1
SURFACE   -X        GOLD
ENDOBJ
COMMENT   REFERENCE BAND (FACE G)
PATCHW
CORNER       5   14    4
FACE      GOLD         -1    1    0
LENGTH       1    1    1
ENDOBJ
COMMENT   REFERENCE BAND (FACE H)
PATCHR
CORNER       9   15    4
DELTAS       1    1    1
SURFACE   +Y        GOLD
ENDOBJ
ENDSAT
```

NASCAP/GEO **Contours** is the program used to generate the potential contours plot shown in Figure 29.

Termtalk Execution (fort.3) for Spinning Spacecraft in Geosynchronous Orbit-SCATHA

A group of surface cells is defined for each of the materials. Separate groups are defined for each conductor number. The surface cell number is printed out and a group is not defined for those material conductor number combinations with only one surface cell.

The final potentials for each of the groups is requested. A history of the potential over time for one cell from each of the conductors is requested. The final internal electric field for the cells with the highest field is requested. Detailed information on each of the seven cells with the greatest field is requested. A history of the internal field for two of these high field cells is requested. The results are shown in Figure 28.

```
 CHOOSE ANY MODULE
 HELP IS ALWAYS AVAILABLE - TYPE 'HELP'
>subset GLD1
DEFINITION OF NEW SUBSET NAMED GLD1
267 REMAINING IN GROUP
 SUBSET INSTRUCTION PLEASE ?
>material GOLD
 313 REMAINING IN GROUP
 SUBSET INSTRUCTION PLEASE ?
>cnumb 1
 303 REMAINING IN GROUP
 SUBSET INSTRUCTION PLEASE ?
>done
GROUP GLD1 WITH  303 MEMBERS IS NOW DEFINED
RETURNING TO MODULE  'MAIN'
 CHOOSE ANY MODULE
 HELP IS ALWAYS AVAILABLE - TYPE 'HELP'
>subset GLD4
DEFINITION OF NEW SUBSET NAMED GLD4
267 REMAINING IN GROUP
 SUBSET INSTRUCTION PLEASE ?
>material GOLD
 313 REMAINING IN GROUP
 SUBSET INSTRUCTION PLEASE ?
>cnumb 4
   1 REMAINING IN GROUP
 SUBSET INSTRUCTION PLEASE ?
>done
REMAINING MEMBER IS  #1208
THIS SUBSET HAS 1 MEMBERS
IT WILL NOT BE CATALOGUED
RETURNING TO MODULE 'MAIN'
 CHOOSE ANY MODULE
 HELP IS ALWAYS AVAILABLE - TYPE 'HELP'
>subset GLD5
DEFINITION OF NEW SUBSET NAMED GLD5
267 REMAINING IN GROUP
 SUBSET INSTRUCTION PLEASE ?
>material GOLD
 313 REMAINING IN GROUP
 SUBSET INSTRUCTION PLEASE ?
>cnumb 5
   1 REMAINING IN GROUP
 SUBSET INSTRUCTION PLEASE ?
>done
REMAINING MEMBER IS  #1259
THIS SUBSET HAS 1 MEMBERS
IT WILL NOT BE CATALOGUED
RETURNING TO MODULE 'MAIN'
 CHOOSE ANY MODULE
 HELP IS ALWAYS AVAILABLE - TYPE 'HELP'
>subset GLD6
DEFINITION OF NEW SUBSET NAMED GLD6
267 REMAINING IN GROUP
 SUBSET INSTRUCTION PLEASE ?
```

```
>material GOLD
 313 REMAINING IN GROUP
 SUBSET INSTRUCTION PLEASE ?
>cnumb 6
   8 REMAINING IN GROUP
 SUBSET INSTRUCTION PLEASE ?
>done
GROUP GLD6 WITH    8 MEMBERS IS NOW DEFINED
RETURNING TO MODULE  'MAIN'
 CHOOSE ANY MODULE
 HELP IS ALWAYS AVAILABLE - TYPE 'HELP'
>subset SOLAR
DEFINITION OF NEW SUBSET NAMED SOLA
267 REMAINING IN GROUP
 SUBSET INSTRUCTION PLEASE ?
>material SOLAR
 435 REMAINING IN GROUP
 SUBSET INSTRUCTION PLEASE ?
>done
GROUP SOLA WITH  435 MEMBERS IS NOW DEFINED
RETURNING TO MODULE  'MAIN'
 CHOOSE ANY MODULE
 HELP IS ALWAYS AVAILABLE - TYPE 'HELP'
>subset WHITEN
DEFINITION OF NEW SUBSET NAMED WHIT
267 REMAINING IN GROUP
 SUBSET INSTRUCTION PLEASE ?
>material WHITEN
 116 REMAINING IN GROUP
 SUBSET INSTRUCTION PLEASE ?
>done
GROUP WHIT WITH  116 MEMBERS IS NOW DEFINED
RETURNING TO MODULE  'MAIN'
 CHOOSE ANY MODULE
 HELP IS ALWAYS AVAILABLE - TYPE 'HELP'
>subset SCREEN
DEFINITION OF NEW SUBSET NAMED SCRE
267 REMAINING IN GROUP
 SUBSET INSTRUCTION PLEASE ?
>material SCREEN
  12 REMAINING IN GROUP
 SUBSET INSTRUCTION PLEASE ?
>done
GROUP SCRE WITH   12 MEMBERS IS NOW DEFINED
RETURNING TO MODULE  'MAIN'
 CHOOSE ANY MODULE
 HELP IS ALWAYS AVAILABLE - TYPE 'HELP'
>subset YELOWC
DEFINITION OF NEW SUBSET NAMED YELO
267 REMAINING IN GROUP
 SUBSET INSTRUCTION PLEASE ?
>material YELOWC
  71 REMAINING IN GROUP
 SUBSET INSTRUCTION PLEASE ?
>done
GROUP YELO WITH   71 MEMBERS IS NOW DEFINED
RETURNING TO MODULE  'MAIN'
 CHOOSE ANY MODULE
 HELP IS ALWAYS AVAILABLE - TYPE 'HELP'
>subset PDGOLD
DEFINITION OF NEW SUBSET NAMED PDGO
267 REMAINING IN GROUP
 SUBSET INSTRUCTION PLEASE ?
>material PDGOLD
```

```
 138 REMAINING IN GROUP
 SUBSET INSTRUCTION PLEASE ?
>done
GROUP PDGO WITH  138 MEMBERS IS NOW DEFINED
RETURNING TO MODULE  'MAIN'
 CHOOSE ANY MODULE
 HELP IS ALWAYS AVAILABLE - TYPE 'HELP'
>subset BLK1
DEFINITION OF NEW SUBSET NAMED BLK1
267 REMAINING IN GROUP
 SUBSET INSTRUCTION PLEASE ?
>material BLACKC
  34 REMAINING IN GROUP
 SUBSET INSTRUCTION PLEASE ?
>cnumb 1
  32 REMAINING IN GROUP
 SUBSET INSTRUCTION PLEASE ?
>done
GROUP BLK1 WITH   32 MEMBERS IS NOW DEFINED
RETURNING TO MODULE  'MAIN'
 CHOOSE ANY MODULE
 HELP IS ALWAYS AVAILABLE - TYPE 'HELP'
>subset BLK2
DEFINITION OF NEW SUBSET NAMED BLK2
267 REMAINING IN GROUP
 SUBSET INSTRUCTION PLEASE ?
>material BLACKC
  34 REMAINING IN GROUP
 SUBSET INSTRUCTION PLEASE ?
>cnumb 2
   1 REMAINING IN GROUP
 SUBSET INSTRUCTION PLEASE ?
>done
REMAINING MEMBER IS  #1260
THIS SUBSET HAS 1 MEMBERS
IT WILL NOT BE CATALOGUED
RETURNING TO MODULE 'MAIN'
 CHOOSE ANY MODULE
 HELP IS ALWAYS AVAILABLE - TYPE 'HELP'
>subset BLK3
DEFINITION OF NEW SUBSET NAMED BLK3
267 REMAINING IN GROUP
 SUBSET INSTRUCTION PLEASE ?
>material BLACKC
  34 REMAINING IN GROUP
 SUBSET INSTRUCTION PLEASE ?
>cnumb 3
   1 REMAINING IN GROUP
 SUBSET INSTRUCTION PLEASE ?
>done
REMAINING MEMBER IS  #1261
THIS SUBSET HAS 1 MEMBERS
IT WILL NOT BE CATALOGUED
RETURNING TO MODULE 'MAIN'
 CHOOSE ANY MODULE
 HELP IS ALWAYS AVAILABLE - TYPE 'HELP'
>subset KAPTON
DEFINITION OF NEW SUBSET NAMED KAPT
267 REMAINING IN GROUP
 SUBSET INSTRUCTION PLEASE ?
>material KAPTON
   6 REMAINING IN GROUP
 SUBSET INSTRUCTION PLEASE ?
>done
```

```
GROUP KAPT WITH    6 MEMBERS IS NOW DEFINED
RETURNING TO MODULE  'MAIN'
 CHOOSE ANY MODULE
 HELP IS ALWAYS AVAILABLE - TYPE 'HELP'
>subset SIO2
DEFINITION OF NEW SUBSET NAMED SIO2
267 REMAINING IN GROUP
 SUBSET INSTRUCTION PLEASE ?
>material SIO2
   1 REMAINING IN GROUP
 SUBSET INSTRUCTION PLEASE ?
>done
REMAINING MEMBER IS  # 954
THIS SUBSET HAS 1 MEMBERS
IT WILL NOT BE CATALOGUED
RETURNING TO MODULE 'MAIN'
 CHOOSE ANY MODULE
 HELP IS ALWAYS AVAILABLE - TYPE 'HELP'
>subset TEFLON
DEFINITION OF NEW SUBSET NAMED TEFL
267 REMAINING IN GROUP
 SUBSET INSTRUCTION PLEASE ?
>material TEFLON
  47 REMAINING IN GROUP
 SUBSET INSTRUCTION PLEASE ?
>done
GROUP TEFL WITH   47 MEMBERS IS NOW DEFINED
RETURNING TO MODULE  'MAIN'
 CHOOSE ANY MODULE
 HELP IS ALWAYS AVAILABLE - TYPE 'HELP'
>subset INDOX
DEFINITION OF NEW SUBSET NAMED INDO
267 REMAINING IN GROUP
 SUBSET INSTRUCTION PLEASE ?
>material INDOX
  13 REMAINING IN GROUP
 SUBSET INSTRUCTION PLEASE ?
>done
GROUP INDO WITH   13 MEMBERS IS NOW DEFINED
RETURNING TO MODULE  'MAIN'
 CHOOSE ANY MODULE
 HELP IS ALWAYS AVAILABLE - TYPE 'HELP'
>subset YGOLDC
DEFINITION OF NEW SUBSET NAMED YGOL
267 REMAINING IN GROUP
 SUBSET INSTRUCTION PLEASE ?
>material YGOLDC
  14 REMAINING IN GROUP
 SUBSET INSTRUCTION PLEASE ?
>done
GROUP YGOL WITH   14 MEMBERS IS NOW DEFINED
RETURNING TO MODULE  'MAIN'
 CHOOSE ANY MODULE
 HELP IS ALWAYS AVAILABLE - TYPE 'HELP'
>subset ALUMIN
DEFINITION OF NEW SUBSET NAMED ALUM
267 REMAINING IN GROUP
 SUBSET INSTRUCTION PLEASE ?
>material ALUMIN
  16 REMAINING IN GROUP
 SUBSET INSTRUCTION PLEASE ?
>done
GROUP ALUM WITH   16 MEMBERS IS NOW DEFINED
RETURNING TO MODULE  'MAIN'
```

```
 CHOOSE ANY MODULE
 HELP IS ALWAYS AVAILABLE - TYPE 'HELP'
>subset BOMAT
DEFINITION OF NEW SUBSET NAMED BOMA
267 REMAINING IN GROUP
 SUBSET INSTRUCTION PLEASE ?
>material BOMAT
  41 REMAINING IN GROUP
 SUBSET INSTRUCTION PLEASE ?
>done
GROUP BOMA WITH   41 MEMBERS IS NOW DEFINED
RETURNING TO MODULE  'MAIN'
 CHOOSE ANY MODULE
 HELP IS ALWAYS AVAILABLE - TYPE 'HELP'
>subset ML12
DEFINITION OF NEW SUBSET NAMED ML12
267 REMAINING IN GROUP
 SUBSET INSTRUCTION PLEASE ?
>material ML12
   4 REMAINING IN GROUP
 SUBSET INSTRUCTION PLEASE ?
>done
GROUP ML12 WITH    4 MEMBERS IS NOW DEFINED
RETURNING TO MODULE  'MAIN'
 CHOOSE ANY MODULE
 HELP IS ALWAYS AVAILABLE - TYPE 'HELP'
>latest
 LATEST COMMAND OR MODE SET ?
>potential
MODE RESET
 LATEST COMMAND OR MODE SET ?
>absmag
MODE RESET
 LATEST COMMAND OR MODE SET ?
>group GLD1
POTL IN VOLTS  FOR NASCAP CYCLE  20 ... TIME = 1.20e-03 SEC
1114-1.52e+04 1038-1.52e+04 1021-1.52e+04  997-1.52e+04  996-1.52e+04
 995-1.52e+04  994-1.52e+04  993-1.52e+04  992-1.52e+04  991-1.52e+04
 990-1.52e+04  989-1.52e+04  986-1.52e+04  985-1.52e+04  984-1.52e+04
 983-1.52e+04  982-1.52e+04  981-1.52e+04  980-1.52e+04  979-1.52e+04
 978-1.52e+04  975-1.52e+04  974-1.52e+04  973-1.52e+04  972-1.52e+04
 971-1.52e+04  970-1.52e+04  969-1.52e+04  968-1.52e+04  967-1.52e+04
 964-1.52e+04  963-1.52e+04  962-1.52e+04  961-1.52e+04  960-1.52e+04
 959-1.52e+04  958-1.52e+04  957-1.52e+04  956-1.52e+04  951-1.52e+04
 949-1.52e+04  932-1.52e+04  908-1.52e+04  907-1.52e+04  906-1.52e+04
 905-1.52e+04  904-1.52e+04  903-1.52e+04  902-1.52e+04  901-1.52e+04
 900-1.52e+04  899-1.52e+04  896-1.52e+04  894-1.52e+04  892-1.52e+04
 890-1.52e+04  888-1.52e+04  887-1.52e+04  886-1.52e+04  885-1.52e+04
 884-1.52e+04  883-1.52e+04  882-1.52e+04  881-1.52e+04  880-1.52e+04
 879-1.52e+04  877-1.52e+04  832-1.52e+04  831-1.52e+04  830-1.52e+04
 829-1.52e+04  828-1.52e+04  827-1.52e+04  826-1.52e+04  825-1.52e+04
 824-1.52e+04  823-1.52e+04  820-1.52e+04  818-1.52e+04  816-1.52e+04
 814-1.52e+04  812-1.52e+04  810-1.52e+04  808-1.52e+04  807-1.52e+04
 806-1.52e+04  805-1.52e+04  804-1.52e+04  803-1.52e+04  802-1.52e+04
 801-1.52e+04  800-1.52e+04  799-1.52e+04  756-1.52e+04  755-1.52e+04
 754-1.52e+04  753-1.52e+04  752-1.52e+04  751-1.52e+04  750-1.52e+04
 749-1.52e+04  748-1.52e+04  745-1.52e+04  743-1.52e+04  741-1.52e+04
 739-1.52e+04  737-1.52e+04  735-1.52e+04  733-1.52e+04  731-1.52e+04
 729-1.52e+04  728-1.52e+04  727-1.52e+04  726-1.52e+04  725-1.52e+04
 724-1.52e+04  723-1.52e+04  722-1.52e+04  721-1.52e+04  678-1.52e+04
 677-1.52e+04  676-1.52e+04  675-1.52e+04  674-1.52e+04  673-1.52e+04
 672-1.52e+04  671-1.52e+04  670-1.52e+04  667-1.52e+04  665-1.52e+04
 663-1.52e+04  655-1.52e+04  647-1.52e+04  645-1.52e+04  643-1.52e+04
 641-1.52e+04  639-1.52e+04  638-1.52e+04  637-1.52e+04  636-1.52e+04
```

```
 635-1.52e+04  634-1.52e+04  633-1.52e+04  632-1.52e+04  631-1.52e+04
 590-1.52e+04  589-1.52e+04  588-1.52e+04  587-1.52e+04  586-1.52e+04
 585-1.52e+04  584-1.52e+04  583-1.52e+04  582-1.52e+04  579-1.52e+04
 577-1.52e+04  575-1.52e+04  567-1.52e+04  559-1.52e+04  557-1.52e+04
 555-1.52e+04  553-1.52e+04  551-1.52e+04  550-1.52e+04  549-1.52e+04
 548-1.52e+04  547-1.52e+04  546-1.52e+04  545-1.52e+04  544-1.52e+04
 543-1.52e+04  503-1.52e+04  502-1.52e+04  501-1.52e+04  500-1.52e+04
 499-1.52e+04  498-1.52e+04  497-1.52e+04  496-1.52e+04  495-1.52e+04
 492-1.52e+04  490-1.52e+04  488-1.52e+04  486-1.52e+04  484-1.52e+04
 482-1.52e+04  480-1.52e+04  478-1.52e+04  476-1.52e+04  475-1.52e+04
 474-1.52e+04  473-1.52e+04  472-1.52e+04  471-1.52e+04  470-1.52e+04
 469-1.52e+04  468-1.52e+04  419-1.52e+04  418-1.52e+04  417-1.52e+04
 416-1.52e+04  415-1.52e+04  414-1.52e+04  413-1.52e+04  412-1.52e+04
 411-1.52e+04  410-1.52e+04  407-1.52e+04  405-1.52e+04  403-1.52e+04
 401-1.52e+04  399-1.52e+04  397-1.52e+04  395-1.52e+04  394-1.52e+04
 393-1.52e+04  392-1.52e+04  391-1.52e+04  390-1.52e+04  389-1.52e+04
 388-1.52e+04  387-1.52e+04  386-1.52e+04  363-1.52e+04  362-1.52e+04
 360-1.52e+04  359-1.52e+04  331-1.52e+04  330-1.52e+04  329-1.52e+04
 328-1.52e+04  327-1.52e+04  326-1.52e+04  325-1.52e+04  324-1.52e+04
 323-1.52e+04  322-1.52e+04  320-1.52e+04  319-1.52e+04  318-1.52e+04
 317-1.52e+04  316-1.52e+04  315-1.52e+04  313-1.52e+04  311-1.52e+04
 310-1.52e+04  309-1.52e+04  308-1.52e+04  307-1.52e+04  306-1.52e+04
 305-1.52e+04  304-1.52e+04  303-1.52e+04  302-1.52e+04  300-1.52e+04
 298-1.52e+04  276-1.52e+04  275-1.52e+04  274-1.52e+04  273-1.52e+04
 251-1.52e+04  250-1.52e+04  249-1.52e+04  248-1.52e+04  247-1.52e+04
 246-1.52e+04  245-1.52e+04  244-1.52e+04  243-1.52e+04  242-1.52e+04
 239-1.52e+04  238-1.52e+04  237-1.52e+04  236-1.52e+04  235-1.52e+04
 234-1.52e+04  233-1.52e+04  232-1.52e+04  231-1.52e+04  229-1.52e+04
 228-1.52e+04  227-1.52e+04  226-1.52e+04  225-1.52e+04  224-1.52e+04
 223-1.52e+04  222-1.52e+04  221-1.52e+04  220-1.52e+04  217-1.52e+04
 216-1.52e+04  215-1.52e+04  214-1.52e+04  213-1.52e+04  212-1.52e+04
 211-1.52e+04  210-1.52e+04  209-1.52e+04  205-1.52e+04  203-1.52e+04
 163-1.52e+04  161-1.52e+04  159-1.52e+04    0 0.00e+00    0 0.00e+00
 LATEST COMMAND OR MODE SET ?
>group GLD6
POTL IN VOLTS  FOR NASCAP CYCLE  20 ... TIME = 1.20e+03 SEC
216-1.39e+04 1215-1.39e+04 1214-1.39e+04 1213-1.39e+04 1212-1.39e+04
211-1.39e+04 1210-1.39e+04 1209-1.39e+04    0 0.00e+00    0 0.00e+00
 LATEST COMMAND OR MODE SET ?
>group SOLAR
POTL IN VOLTS  FOR NASCAP CYCLE  20 ... TIME = 1.20e+03 SEC
 365-1.56e+04   19-1.56e+04  103-1.56e+04  778-1.56e+04 1088-1.56e+04
188-1.56e+04  344-1.56e+04 1172-1.56e+04  917-1.56e+04    2-1.56e+04
 839-1.56e+04 1071-1.56e+04  432-1.56e+04  120-1.56e+04  856-1.56e+04
 279-1.56e+04 1103-1.56e+04  793-1.56e+04 1203-1.56e+04  294-1.56e+04
186-1.56e+04 1086-1.56e+04  380-1.56e+04  871-1.56e+04  854-1.56e+04
  17-1.56e+04   34-1.56e+04  932-1.56e+04  118-1.56e+04  135-1.56e+04
  86-1.56e+04   36-1.56e+04  186-1.56e+04  169-1.56e+04  703-1.56e+04
105-1.56e+04  449-1.56e+04 1155-1.56e+04  508-1.56e+04 1022-1.56e+04
005-1.56e+04  761-1.56e+04 1037-1.56e+04 1069-1.56e+04 1020-1.56e+04
 151-1.56e+04   51-1.56e+04 1170-1.56e+04  612-1.56e+04  201-1.56e+04
 464-1.56e+04   53-1.56e+04 1120-1.56e+04  595-1.56e+04  717-1.56e+04
138-1.56e+04  948-1.56e+04 1136-1.56e+04  627-1.56e+04 1153-1.56e+04
 776-1.56e+04  101-1.56e+04  539-1.56e+04   68-1.56e+04   84-1.56e+04
 697-1.56e+04  610-1.56e+04  779-1.56e+04 1089-1.56e+04  104-1.56e+04
  20-1.56e+04  366-1.56e+04   32-1.56e+04 1072-1.56e+04  121-1.56e+04
 345-1.56e+04  280-1.56e+04 1173-1.56e+04  433-1.56e+04 1101-1.56e+04
 840-1.56e+04  918-1.56e+04 1189-1.56e+04 1184-1.56e+04  857-1.56e+04
 791-1.56e+04  378-1.56e+04    3-1.56e+04 1201-1.56e+04  852-1.56e+04
 116-1.56e+04  292-1.56e+04  930-1.56e+04   15-1.56e+04 1084-1.56e+04
 869-1.56e+04  133-1.56e+04  434-1.56e+04 1073-1.56e+04  377-1.56e+04
  14-1.56e+04  281-1.56e+04  841-1.56e+04  790-1.56e+04  346-1.56e+04
183-1.56e+04 1100-1.56e+04  291-1.56e+04  919-1.56e+04  868-1.56e+04
 367-1.56e+04    4-1.56e+04   31-1.56e+04 1090-1.56e+04 1083-1.56e+04
```

21-1.56e+04 780-1.56e+04 122-1.56e+04 858-1.56e+04 105-1.56e+04
200-1.56e+04 929-1.56e+04 1190-1.56e+04 851-1.56e+04 115-1.56e+04
174-1.56e+04 132-1.56e+04 199-1.56e+04 30-1.56e+04 1082-1.56e+04
5-1.56e+04 149-1.56e+04 1018-1.56e+04 123-1.56e+04 1074-1.56e+04
067-1.56e+04 290-1.56e+04 867-1.56e+04 22-1.56e+04 1168-1.56e+04
376-1.56e+04 462-1.56e+04 1118-1.56e+04 49-1.56e+04 946-1.56e+04
859-1.56e+04 13-1.56e+04 1035-1.56e+04 106-1.56e+04 715-1.56e+04
099-1.56e+04 356-1.56e+04 789-1.56e+04 282-1.56e+04 762-1.56e+04
006-1.56e+04 87-1.56e+04 1156-1.56e+04 137-1.56e+04 187-1.56e+04
450-1.56e+04 444-1.56e+04 509-1.56e+04 1023-1.56e+04 170-1.56e+04
259-1.56e+04 934-1.56e+04 1106-1.56e+04 704-1.56e+04 37-1.56e+04
055-1.56e+04 347-1.56e+04 920-1.56e+04 368-1.56e+04 435-1.56e+04
842-1.56e+04 99-1.56e+04 1182-1.56e+04 1091-1.56e+04 1199-1.56e+04
928-1.56e+04 781-1.56e+04 774-1.56e+04 131-1.56e+04 1191-1.56e+04
70-1.56e+04 114-1.56e+04 54-1.56e+04 850-1.56e+04 525-1.56e+04
613-1.56e+04 1122-1.56e+04 1139-1.56e+04 443-1.56e+04 683-1.56e+04
175-1.56e+04 596-1.56e+04 1198-1.56e+04 82-1.56e+04 625-1.56e+04
12-1.56e+04 1181-1.56e+04 6-1.56e+04 436-1.56e+04 1098-1.56e+04
375-1.56e+04 369-1.56e+04 1092-1.56e+04 1081-1.56e+04 355-1.56e+04
354-1.56e+04 1075-1.56e+04 130-1.56e+04 1151-1.56e+04 23-1.56e+04
348-1.56e+04 289-1.56e+04 927-1.56e+04 921-1.56e+04 866-1.56e+04
66-1.56e+04 124-1.56e+04 1134-1.56e+04 860-1.56e+04 849-1.56e+04
843-1.56e+04 788-1.56e+04 283-1.56e+04 113-1.56e+04 537-1.56e+04
29-1.56e+04 442-1.56e+04 112-1.56e+04 28-1.56e+04 1024-1.56e+04
7-1.56e+04 11-1.56e+04 171-1.56e+04 188-1.56e+04 138-1.56e+04
007-1.56e+04 1097-1.56e+04 260-1.56e+04 1080-1.56e+04 1076-1.56e+04
129-1.56e+04 125-1.56e+04 353-1.56e+04 349-1.56e+04 608-1.56e+04
695-1.56e+04 935-1.56e+04 865-1.56e+04 861-1.56e+04 787-1.56e+04
288-1.56e+04 782-1.56e+04 284-1.56e+04 48-1.56e+04 510-1.56e+04
117-1.56e+04 1017-1.56e+04 461-1.56e+04 763-1.56e+04 1167-1.56e+04
714-1.56e+04 1107-1.56e+04 1093-1.56e+04 1066-1.56e+04 705-1.56e+04
24-1.56e+04 451-1.56e+04 1197-1.56e+04 1157-1.56e+04 1192-1.56e+04
148-1.56e+04 98-1.56e+04 88-1.56e+04 945-1.56e+04 198-1.56e+04
773-1.56e+04 38-1.56e+04 1056-1.56e+04 1034-1.56e+04 1180-1.56e+04
057-1.56e+04 1033-1.56e+04 1176-1.56e+04 139-1.56e+04 597-1.56e+04
536-1.56e+04 172-1.56e+04 1025-1.56e+04 1016-1.56e+04 1150-1.56e+04
147-1.56e+04 270-1.56e+04 1008-1.56e+04 944-1.56e+04 684-1.56e+04
624-1.56e+04 1140-1.56e+04 1133-1.56e+04 189-1.56e+04 181-1.56e+04
936-1.56e+04 783-1.56e+04 81-1.56e+04 1123-1.56e+04 526-1.56e+04
520-1.56e+04 71-1.56e+04 614-1.56e+04 1065-1.56e+04 65-1.56e+04
261-1.56e+04 197-1.56e+04 55-1.56e+04 146-1.56e+04 519-1.56e+04
026-1.56e+04 1015-1.56e+04 1009-1.56e+04 943-1.56e+04 39-1.56e+04
158-1.56e+04 190-1.56e+04 937-1.56e+04 772-1.56e+04 511-1.56e+04
180-1.56e+04 764-1.56e+04 607-1.56e+04 179-1.56e+04 89-1.56e+04
452-1.56e+04 269-1.56e+04 706-1.56e+04 268-1.56e+04 140-1.56e+04
108-1.56e+04 1064-1.56e+04 173-1.56e+04 262-1.56e+04 196-1.56e+04
032-1.56e+04 460-1.56e+04 1058-1.56e+04 1166-1.56e+04 97-1.56e+04
116-1.56e+04 713-1.56e+04 694-1.56e+04 47-1.56e+04 938-1.56e+04
191-1.56e+04 141-1.56e+04 1031-1.56e+04 195-1.56e+04 942-1.56e+04
193-1.56e+04 56-1.56e+04 1165-1.56e+04 267-1.56e+04 712-1.56e+04
263-1.56e+04 1149-1.56e+04 178-1.56e+04 535-1.56e+04 693-1.56e+04
174-1.56e+04 145-1.56e+04 1132-1.56e+04 96-1.56e+04 623-1.56e+04
46-1.56e+04 80-1.56e+04 72-1.56e+04 64-1.56e+04 1063-1.56e+04
459-1.56e+04 1027-1.56e+04 518-1.56e+04 512-1.56e+04 453-1.56e+04
615-1.56e+04 1148-1.56e+04 606-1.56e+04 95-1.56e+04 79-1.56e+04
141-1.56e+04 1131-1.56e+04 598-1.56e+04 534-1.56e+04 1124-1.56e+04
63-1.56e+04 1109-1.56e+04 1059-1.56e+04 771-1.56e+04 765-1.56e+04
711-1.56e+04 40-1.56e+04 45-1.56e+04 692-1.56e+04 527-1.56e+04
685-1.56e+04 622-1.56e+04 605-1.56e+04 1164-1.56e+04 707-1.56e+04
159-1.56e+04 57-1.56e+04 73-1.56e+04 1177-1.56e+04 41-1.56e+04
686-1.56e+04 599-1.56e+04 1142-1.56e+04 528-1.56e+04 1125-1.56e+04
110-1.56e+04 78-1.56e+04 1147-1.56e+04 616-1.56e+04 531-1.56e+04
62-1.56e+04 621-1.56e+04 74-1.56e+04 58-1.56e+04 1126-1.56e+04
160-1.56e+04 1143-1.56e+04 708-1.56e+04 529-1.56e+04 617-1.56e+04

```
 LATEST COMMAND OR MODE SET ?
>group WHITEN
POTL IN VOLTS  FOR NASCAP CYCLE  20 ... TIME = 1.20e+03 SEC
187-1.54e+04  343-1.54e+04  916-1.54e+04  119-1.54e+04    1-1.54e+04
 278-1.54e+04  855-1.54e+04 1171-1.54e+04 1154-1.54e+04  431-1.54e+04
 168-1.54e+04  838-1.54e+04  702-1.54e+04  166-1.54e+04   18-1.54e+04
 507-1.54e+04   35-1.54e+04  914-1.54e+04  102-1.54e+04  777-1.54e+04
 185-1.54e+04  364-1.54e+04 1004-1.54e+04  295-1.54e+04  164-1.54e+04
000-1.54e+04  254-1.54e+04  204-1.54e+04  381-1.54e+04  836-1.54e+04
 297-1.54e+04 1050-1.54e+04  335-1.54e+04  423-1.54e+04  912-1.54e+04
 154-1.54e+04  794-1.54e+04 1137-1.54e+04  448-1.54e+04 1104-1.54e+04
  85-1.54e+04   52-1.54e+04  611-1.54e+04  760-1.54e+04  594-1.54e+04
 592-1.54e+04  156-1.54e+04  718-1.54e+04  158-1.54e+04  465-1.54e+04
048-1.54e+04 1046-1.54e+04  162-1.54e+04  505-1.54e+04  628-1.54e+04
 758-1.54e+04  256-1.54e+04  337-1.54e+04  202-1.54e+04  152-1.54e+04
052-1.54e+04  540-1.54e+04 1044-1.54e+04 1002-1.54e+04  680-1.54e+04
042-1.54e+04  160-1.54e+04 1087-1.54e+04  383-1.54e+04  834-1.54e+04
 206-1.54e+04  421-1.54e+04  998-1.54e+04  252-1.54e+04  796-1.54e+04
 333-1.54e+04  910-1.54e+04  299-1.54e+04  872-1.54e+04 1121-1.54e+04
 524-1.54e+04   69-1.54e+04  682-1.54e+04 1040-1.54e+04  720-1.54e+04
 494-1.54e+04  988-1.54e+04  467-1.54e+04  874-1.54e+04  208-1.54e+04
 241-1.54e+04  747-1.54e+04  581-1.54e+04  542-1.54e+04  977-1.54e+04
 966-1.54e+04  219-1.54e+04  230-1.54e+04  669-1.54e+04  630-1.54e+04
 955-1.54e+04  953-1.54e+04  876-1.54e+04  258-1.54e+04 1054-1.54e+04
 136-1.54e+04  409-1.54e+04  385-1.54e+04  898-1.54e+04  321-1.54e+04
 822-1.54e+04  301-1.54e+04  798-1.54e+04 1070-1.54e+04  878-1.54e+04
 933-1.54e+04    0 0.00e+00    0 0.00e+00    0 0.00e+00    0 0.00e+00
 LATEST COMMAND OR MODE SET ?
>group SCREEN
POTL IN VOLTS  FOR NASCAP CYCLE  20 ... TIME = 1.20e+03 SEC
 730-1.52e+04  719-1.52e+04  716-1.52e+04  640-1.52e+04  629-1.52e+04
 626-1.52e+04  552-1.52e+04  541-1.52e+04  538-1.52e+04  477-1.52e+04
 466-1.52e+04  463-1.52e+04    0 0.00e+00    0 0.00e+00    0 0.00e+00
 LATEST COMMAND OR MODE SET ?
>group YELOWC
POTL IN VOLTS  FOR NASCAP CYCLE  20 ... TIME = 1.20e+03 SEC
077-1.52e+04 1030-1.52e+04 1029-1.52e+04 1028-1.52e+04  941-1.52e+04
 940-1.52e+04  939-1.52e+04  864-1.52e+04  863-1.52e+04  862-1.52e+04
 847-1.52e+04  846-1.52e+04  845-1.52e+04  786-1.52e+04  785-1.52e+04
 784-1.52e+04  769-1.52e+04  709-1.52e+04  690-1.52e+04  689-1.52e+04
 688-1.52e+04  620-1.52e+04  619-1.52e+04  618-1.52e+04  603-1.52e+04
 601-1.52e+04  532-1.52e+04  531-1.52e+04  530-1.52e+04  516-1.52e+04
 514-1.52e+04  457-1.52e+04  456-1.52e+04  455-1.52e+04  440-1.52e+04
 439-1.52e+04  438-1.52e+04  373-1.52e+04  372-1.52e+04  371-1.52e+04
 361-1.52e+04  352-1.52e+04  351-1.52e+04  350-1.52e+04  287-1.52e+04
 286-1.52e+04  285-1.52e+04  277-1.52e+04  266-1.52e+04  265-1.52e+04
 264-1.52e+04  194-1.52e+04  193-1.52e+04  192-1.52e+04  177-1.52e+04
 176-1.52e+04  175-1.52e+04  144-1.52e+04  143-1.52e+04  142-1.52e+04
  77-1.52e+04   61-1.52e+04   44-1.52e+04   43-1.52e+04   42-1.52e+04
  27-1.52e+04   26-1.52e+04   25-1.52e+04   10-1.52e+04    9-1.52e+04
   8-1.52e+04    0 0.00e+00    0 0.00e+00    0 0.00e+00    0 0.00e+00
 LATEST COMMAND OR MODE SET ?
>group PDGOLD
POTL IN VOLTS  FOR NASCAP CYCLE  20 ... TIME = 1.20e+03 SEC
202-1.52e+04 1185-1.52e+04 1169-1.52e+04 1152-1.52e+04 1135-1.52e+04
119-1.52e+04 1102-1.52e+04 1085-1.52e+04 1068-1.52e+04 1053-1.52e+04
051-1.52e+04 1049-1.52e+04 1047-1.52e+04 1045-1.52e+04 1043-1.52e+04
041-1.52e+04 1039-1.52e+04 1036-1.52e+04 1019-1.52e+04 1003-1.52e+04
001-1.52e+04  999-1.52e+04  987-1.52e+04  976-1.52e+04  965-1.52e+04
 950-1.52e+04  947-1.52e+04  931-1.52e+04  915-1.52e+04  913-1.52e+04
 911-1.52e+04  909-1.52e+04  897-1.52e+04  895-1.52e+04  893-1.52e+04
 891-1.52e+04  875-1.52e+04  873-1.52e+04  870-1.52e+04  853-1.52e+04
 837-1.52e+04  835-1.52e+04  833-1.52e+04  821-1.52e+04  819-1.52e+04
 817-1.52e+04  815-1.52e+04  813-1.52e+04  811-1.52e+04  809-1.52e+04
```

```
 797-1.52e+04  795-1.52e+04  792-1.52e+04  775-1.52e+04  759-1.52e+04
 757-1.52e+04  746-1.52e+04  744-1.52e+04  742-1.52e+04  740-1.52e+04
 738-1.52e+04  736-1.52e+04  734-1.52e+04  732-1.52e+04  696-1.52e+04
 681-1.52e+04  679-1.52e+04  668-1.52e+04  666-1.52e+04  664-1.52e+04
 656-1.52e+04  648-1.52e+04  646-1.52e+04  644-1.52e+04  642-1.52e+04
 609-1.52e+04  593-1.52e+04  591-1.52e+04  580-1.52e+04  578-1.52e+04
 576-1.52e+04  568-1.52e+04  560-1.52e+04  558-1.52e+04  556-1.52e+04
 554-1.52e+04  522-1.52e+04  506-1.52e+04  504-1.52e+04  493-1.52e+04
 491-1.52e+04  489-1.52e+04  487-1.52e+04  485-1.52e+04  483-1.52e+04
 481-1.52e+04  479-1.52e+04  446-1.52e+04  422-1.52e+04  420-1.52e+04
 408-1.52e+04  406-1.52e+04  404-1.52e+04  402-1.52e+04  400-1.52e+04
 398-1.52e+04  396-1.52e+04  384-1.52e+04  382-1.52e+04  379-1.52e+04
 336-1.52e+04  334-1.52e+04  332-1.52e+04  314-1.52e+04  312-1.52e+04
 296-1.52e+04  293-1.52e+04  257-1.52e+04  255-1.52e+04  253-1.52e+04
 218-1.52e+04  207-1.52e+04  200-1.52e+04  183-1.52e+04  167-1.52e+04
 165-1.52e+04  157-1.52e+04  155-1.52e+04  153-1.52e+04  150-1.52e+04
 134-1.52e+04  117-1.52e+04  100-1.52e+04   83-1.52e+04   67-1.52e+04
  50-1.52e+04   33-1.52e+04   16-1.52e+04    0 0.00e+00    0 0.00e+00
 LATEST COMMAND OR MODE SET ?
>group BLK1
POTL IN VOLTS  FOR NASCAP CYCLE  20 ... TIME = 1.20e+03 SEC
014-1.52e+04 1010-1.52e+04  926-1.52e+04  848-1.52e+04  844-1.52e+04
 770-1.52e+04  766-1.52e+04  710-1.52e+04  691-1.52e+04  687-1.52e+04
 604-1.52e+04  602-1.52e+04  600-1.52e+04  517-1.52e+04  515-1.52e+04
 513-1.52e+04  458-1.52e+04  454-1.52e+04  441-1.52e+04  437-1.52e+04
 430-1.52e+04  429-1.52e+04  428-1.52e+04  426-1.52e+04  425-1.52e+04
 424-1.52e+04  374-1.52e+04  372-1.52e+04  342-1.52e+04  341-1.52e+04
 340-1.52e+04  338-1.52e+04    0 0.00e+00    0 0.00e+00    0 0.00e+00
 LATEST COMMAND OR MODE SET ?
>group KAPTON
POTL IN VOLTS  FOR NASCAP CYCLE  20 ... TIME = 1.20e+03 SEC
 107-1.64e+04   90-1.64e+04  108-1.64e+04   91-1.64e+04 1130-1.64e+04
 889-1.64e+04    0 0.00e+00    0 0.00e+00    0 0.00e+00    0 0.00e+00
 LATEST COMMAND OR MODE SET ?
>group TEFLON
POTL IN VOLTS  FOR NASCAP CYCLE  20 ... TIME = 1.20e+03 SEC
145-1.58e+04 1144-1.58e+04   76-1.58e+04 1128-1.58e+04   60-1.58e+04
127-1.58e+04   75-1.57e+04   59-1.57e+04  653-1.57e+04  654-1.57e+04
 565-1.57e+04  662-1.57e+04  566-1.57e+04  661-1.57e+04  574-1.57e+04
 573-1.57e+04 1225-1.57e+04  650-1.57e+04  651-1.57e+04  563-1.57e+04
 659-1.57e+04  562-1.57e+04  658-1.57e+04  570-1.57e+04  571-1.57e+04
 109-1.57e+04   92-1.57e+04  110-1.57e+04  111-1.57e+04 1096-1.57e+04
129-1.57e+04 1095-1.57e+04   93-1.57e+04 1112-1.57e+04 1079-1.57e+04
111-1.57e+04  128-1.57e+04  127-1.57e+04  126-1.57e+04 1146-1.57e+04
094-1.57e+04 1078-1.57e+04 1113-1.57e+04   94-1.57e+04 1163-1.57e+04
162-1.57e+04  952-1.57e+04    0 0.00e+00    0 0.00e+00    0 0.00e+00
 LATEST COMMAND OR MODE SET ?
>group INDOX
POTL IN VOLTS  FOR NASCAP CYCLE  20 ... TIME = 1.20e+03 SEC
115-1.52e+04  923-1.52e+04  523-1.52e+04  521-1.52e+04  447-1.52e+04
 445-1.52e+04  358-1.52e+04  357-1.52e+04  272-1.52e+04  271-1.52e+04
 240-1.52e+04  184-1.52e+04  182-1.52e+04    0 0.00e+00    0 0.00e+00
 LATEST COMMAND OR MODE SET ?
>group YGOLDC
POTL IN VOLTS  FOR NASCAP CYCLE  20 ... TIME = 1.20e+03 SEC
196-1.52e+04 1195-1.52e+04 1194-1.52e+04 1179-1.52e+04 1178-1.52e+04
161-1.52e+04 1062-1.52e+04 1061-1.52e+04 1060-1.52e+04 1013-1.52e+04
 925-1.52e+04  924-1.52e+04  427-1.52e+04  339-1.52e+04    0 0.00e+00
 LATEST COMMAND OR MODE SET ?
>group ALUMIN
POTL IN VOLTS  FOR NASCAP CYCLE  20 ... TIME = 1.20e+03 SEC
207-1.52e+04 1206-1.52e+04 1205-1.52e+04 1204-1.52e+04  701-1.52e+04
 700-1.52e+04  699-1.52e+04  698-1.52e+04  660-1.52e+04  657 1.52e+04
 652-1.52e+04  649-1.52e+04  572-1.52e+04  569-1.52e+04  564-1.52e+04
```

```
 561-1.52e+04     0 0.00e+00     0 0.00e+00     0 0.00e+00     0 0.00e+00
 LATEST COMMAND OR MODE SET ?
>group BOMAT
POTL IN VOLTS  FOR NASCAP CYCLE  20 ... TIME = 1.20e+03 SEC
221-1.51e+04 1224-1.51e+04 1218-1.50e+04 1217-1.50e+04 1222-1.49e+04
223-1.49e+04 1219-1.36e+04 1220-1.36e+04 1227-1.32e+04 1226-1.31e+04
228-1.27e+04 1229-1.26e+04 1255-1.17e+04 1254-1.17e+04 1236-1.17e+04
241-1.17e+04 1249-1.16e+04 1235-1.15e+04 1230-1.14e+04 1237-1.05e+04
240-1.05e+04 1234-1.03e+04 1231-1.02e+04 1238-9.52e+03 1239-9.52e+03
233-9.23e+03 1232-9.06e+03 1245-8.42e+03 1244-8.42e+03 1256-8.21e+03
253-8.21e+03 1243-7.99e+03 1250-7.82e+03 1257-7.75e+03 1252-7.74e+03
242-7.72e+03 1251-7.04e+03 1246-6.55e+03 1247-5.78e+03 1248-5.14e+03
258-4.37e+03     0 0.00e+00     0 0.00e+00     0 0.00e+00     0 0.00e+00
 LATEST COMMAND OR MODE SET ?
>group ML12
POTL IN VOLTS  FOR NASCAP CYCLE  20 ... TIME = 1.20e+03 SEC
012-1.52e+04 1011-1.52e+04  768-1.52e+04  767-1.52e+04     0 0.00e+00
 LATEST COMMAND OR MODE SET ?
>single
 SINGLE COMMAND OR MODE SET ?
>1208
-------------------------------------------------------------------------
  SURFACE CELL NO. 1208
                                    CENTERED AT      4.5    1.5    8.0
                                    MATERIAL IS  GOLD
                       POTENTIAL =-1.430e+04 VOLTS
 SINGLE COMMAND OR MODE SET ?
>1259
-------------------------------------------------------------------------
  SURFACE CELL NO. 1259
                                    CENTERED AT      0.0  -44.0    0.0
                                    MATERIAL IS  GOLD
                       POTENTIAL =-4.664e+03 VOLTS
 SINGLE COMMAND OR MODE SET ?
>1260
-------------------------------------------------------------------------
  SURFACE CELL NO. 1260
                                    CENTERED AT     36.0    0.0    0.0
                                    MATERIAL IS  BLAC
                       POTENTIAL =-2.286e+04 VOLTS
 SINGLE COMMAND OR MODE SET ?
>1261
-------------------------------------------------------------------------
  SURFACE CELL NO. 1261
                                    CENTERED AT    -44.0    0.0    0.0
                                    MATERIAL IS  BLAC
                       POTENTIAL =-2.286e+04 VOLTS
 SINGLE COMMAND OR MODE SET ?
>954
-------------------------------------------------------------------------
  SURFACE CELL NO.  954
                                    CENTERED AT      4.5   -2.5    8.0
                                    MATERIAL IS  SIO2
                       POTENTIAL =-1.518e+04 VOLTS
 SINGLE COMMAND OR MODE SET ?
>history
 HISTORY COMMAND OR MODE SET ?
>159,1260,1261,1208,1259,1209
POTL IN VOLTS
  TIME  :    159      1260      1261      1208      1259      1209
--------:-------------------------------------------------------------
        :     #1        #2        #3        #4        #5        #6        #7
 6.0e+01:-1.74e+04-2.17e+04-2.17e+04-1.72e+04-1.72e+04-1.72e+04
 1.2e+02:-1.66e+04-2.19e+04-2.19e+04-1.62e+04-1.62e+04-1.62e+04
```

```
 1.8e+02:-1.58e+04-2.20e+04-2.20e+04-1.54e+04-1.52e+04-1.52e+04
 2.4e+02:-1.55e+04-2.23e+04-2.23e+04-1.47e+04-1.42e+04-1.42e+04
 3.0e+02:-1.53e+04-2.25e+04-2.25e+04-1.46e+04-1.32e+04-1.42e+04
 3.6e+02:-1.52e+04-2.26e+04-2.26e+04-1.44e+04-1.22e+04-1.38e+04
 4.2e+02:-1.52e+04-2.28e+04-2.28e+04-1.43e+04-1.12e+04-1.39e+04
 4.8e+02:-1.52e+04-2.28e+04-2.28e+04-1.43e+04-1.02e+04-1.38e+04
 5.4e+02:-1.52e+04-2.28e+04-2.28e+04-1.43e+04-9.20e+03-1.38e+04
 6.0e+02:-1.52e+04-2.29e+04-2.29e+04-1.43e+04-8.20e+03-1.38e+04
 6.6e+02:-1.52e+04-2.29e+04-2.29e+04-1.43e+04-7.20e+03-1.38e+04
 7.2e+02:-1.52e+04-2.29e+04-2.29e+04-1.43e+04-6.20e+03-1.38e+04
 7.8e+02:-1.52e+04-2.29e+04-2.29e+04-1.43e+04-5.20e+03-1.38e+04
 8.4e+02:-1.52e+04-2.29e+04-2.29e+04-1.43e+04-4.80e+03-1.38e+04
 9.0e+02:-1.52e+04-2.29e+04-2.29e+04-1.43e+04-4.70e+03-1.39e+04
 9.6e+02:-1.52e+04-2.29e+04-2.29e+04-1.43e+04-4.67e+03-1.39e+04
 1.0e+03:-1.52e+04-2.29e+04-2.29e+04-1.43e+04-4.67e+03-1.39e+04
 1.1e+03:-1.52e+04-2.29e+04-2.29e+04-1.43e+04-4.67e+03-1.39e+04
 1.1e+03:-1.52e+04-2.29e+04-2.29e+04-1.43e+04-4.67e+03-1.39e+04
 1.2e+03:-1.52e+04-2.29e+04-2.29e+04-1.43e+04-4.66e+03-1.39e+04
POTL VERSUS LOG(TIME)
```

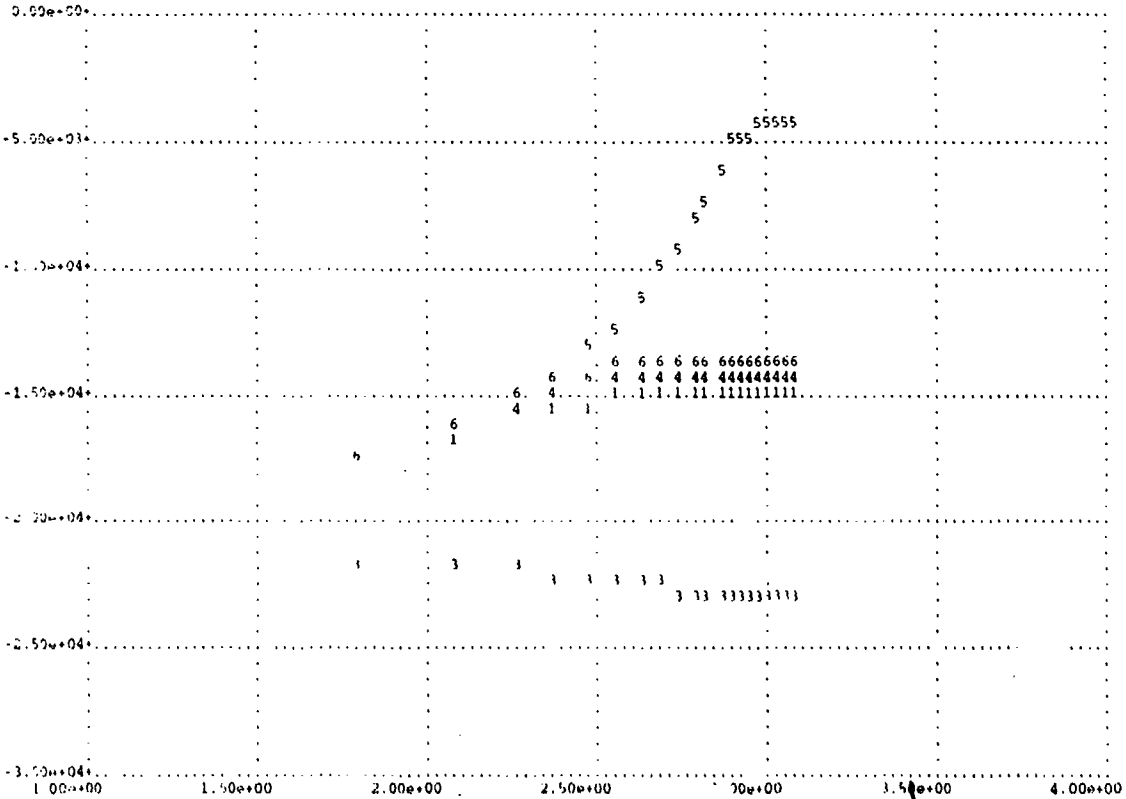


```
 HISTORY COMMAND OR MODE SET ?
>latest
 LATEST COMMAND OR MODE SET ?
>stress
MODE RESET
 LATEST COMMAND OR MODE SET ?
>absmagntitude
MODE RESET
 LATEST COMMAND OR MODE SET ?
>list 1 to 200
FROM    1   TO  200   ON LIST OF DECREASING ABSOLUTE VALUE
STRE IN VOLTS/METER  FOR NASCAP CYCLE  20 ... TIME = 1.20e+03 SEC
 107-9.31e+06   90-9.31e+06  108-9.31e+06   91-9.31e+06 1130-9.31e+06
 889-9.31e+06 1145-4.87e+06 1144-4.83e+06   76-4.59e+06 1128-4.59e+06
  60-4.57e+06 1127-4.52e+06   75-4.48e+06   59-4.47e+06  278-4.01e+06
```

```
 119-4.01e+06  343-4.01e+06 1187-4.01e+06  855-4.01e+06  916-4.01e+06
   1-4.01e+06  702-4.01e+06   35-4.01e+06  364-4.01e+06  838-4.01e+06
004-4.01e+06  777-4.01e+06  168-4.01e+06   18-4.01e+06  507-4.01e+06
 914-4.01e+06 1171-4.01e+06 1154-4.01e+06  166-4.01e+06  102-4.01e+06
 295-4.01e+06  431-4.01e+06  185-4.01e+06  164-4.01e+06 1050-4.01e+06
000-4.01e+06  836-4.01e+06  297-4.01e+06  254-4.01e+06  381-4.01e+06
 423-4.01e+06  154-4.01e+06  794-4.01e+06  335-4.01e+06  912-4.01e+06
 204-4.01e+06  448-4.01e+06  760-4.01e+06   85-4.01e+06   52-4.01e+06
 611-4.01e+06 1137-4.01e+06  594-4.01e+06 1104-4.01e+06  505-4.01e+06
046-4.01e+06  158-4.01e+06  628-4.01e+06  162-4.01e+06  156-4.01e+06
 718-4.01e+06  758-4.01e+06  465-4.01e+06  592-4.01e+06 1048-4.01e+06
052-4.01e+06  202-4.01e+06  256-4.01e+06  152-4.01e+06  337-4.01e+06
002-4.01e+06  540-4.01e+06 1044-4.01e+06 1042-4.01e+06  160-4.01e+06
 680-4.01e+06 1087-4.01e+06  421-4.01e+06  206-4.01e+06  834-4.01e+06
 383-4.01e+06  252-4.01e+06  998-4.01e+06  333-4.01e+06  910-4.01e+06
 796-4.01e+06  299-4.01e+06  872-4.01e+06   69-3.98e+06 1121-3.98e+06
 524-3.98e+06  682-3.98e+06 1040-3.98e+06  988-3.98e+06  208-3.98e+06
 720-3.98e+06  467-3.98e+06  874-3.98e+06  494-3.98e+06  241-3.98e+06
 747-3.98e+06  542-3.98e+06  630-3.98e+06  977-3.98e+06  581-3.98e+06
 669-3.98e+06  219-3.98e+06  966-3.98e+06  230-3.98e+06  955-3.98e+06
 953-3.98e+06  876-3.98e+06 1054-3.94e+06  258-3.94e+06  136-3.94e+06
 898-3.94e+06  409-3.94e+06  321-3.94e+06  822-3.94e+06  301-3.94e+06
 385-3.94e+06  798-3.94e+06 1070-3.94e+06  878-3.94e+06  933-3.87e+06
 653-3.73e+06  654-3.73e+06  565-3.73e+06  662-3.73e+06  566-3.73e+06
 661-3.73e+06  574-3.73e+06  573-3.73e+06 1225-3.73e+06  651-3.73e+06
 650-3.73e+06  659-3.73e+06  562-3.73e+06  563-3.73e+06  658-3.73e+06
 571-3.73e+06  570-3.73e+06  109-3.73e+06   92-3.73e+06 1129-3.73e+06
096-3.73e+06 1095-3.73e+06  110-3.73e+06  111-3.73e+06 1079-3.73e+06
  93-3.73e+06 1112-3.73e+06  126-3.73e+06  128-3.73e+06  127-3.73e+06
111-3.73e+06 1146-3.73e+06 1094-3.73e+06 1078-3.73e+06   94-3.73e+06
113-3.73e+06 1163-3.73e+06 1162-3.73e+06  952-3.73e+06  365-2.21e+06
  19-2.21e+06 1088-2.21e+06  778-2.21e+06  103-2.21e+06 1071-2.21e+06
188-2.21e+06  432-2.21e+06  279-2.21e+06  120-2.21e+06  839-2.21e+06
172-2.21e+06  344-2.21e+06  917-2.21e+06    2-2.21e+06  856-2.21e+06
 793-2.21e+06 1103-2.21e+06  932-2.21e+06  854-2.21e+06  871-2.21e+06
203-2.21e+06 1086-2.21e+06  294-2.21e+06   34-2.21e+06  380-2.21e+06
  17-2.21e+06 1186-2.21e+06  118-2.21e+06  135-2.21e+06 1005-2.21e+06
 LATEST COMMAND OR MODE SET ?
>single
 SINGLE COMMAND OR MODE SET ?
>everything
MODE RESET
 SINGLE COMMAND OR MODE SET ?
>107
-------------------------------------------------------------------------
  SURFACE CELL NO.  107
                                  CODE              420146010
                                  CENTERED AT     -7.0    2.5   -2.5
                                  MATERIAL IS  KAPT
                                  NORMAL          -1  0  0
                                  SHAPE IS SQUARE
                      POTENTIAL =-1.636e+04 VOLTS
                      INTERNAL FIELD STRESS =-9.307e+06  VOLTS/METER
                      EXTERNAL ELECTRIC FIELD =-1.749e+04  VOLTS/METER
                      DELTA V =-1.182e+03 VOLTS
                      UNDERLYING CONDUCTOR IS NUMBER 1
                      UNDERLYING CONDUCTOR POTENTIAL =-1.518e+04 VOLTS
                      LIMITING FACTOR =  1.000e+00
   FLUXES IN A/M**2
        INCIDENT ELECTRONS              8.46e-07
             RESULTING SECONDARIES      1.88e-07
             RESULTING BACKSCATTER      2.05e-07
        INCIDENT PROTONS                3.94e-08
             RESULTING SECONDARIES      1.86e-07
```

```
        BULK CONDUCTIVITY                -9.31e-10
        PHOTOCURRENT                      0.00e+00
                                         ----------
      NET FLUX AFTER LONG-TIME-STEP      -2.23e-07
 SINGLE COMMAND OR MODE SET ?
>90
-------------------------------------------------------------------------
  SURFACE CELL NO.    90
                                  CODE              417536010
                                  CENTERED AT     -7.0    1.5   -2.5
                                  MATERIAL IS  KAPT
                                  NORMAL         -1  0  0
                                  SHAPE IS SQUARE
                     POTENTIAL =-1.636e+04 VOLTS
                     INTERNAL FIELD STRESS =-9.307e+06  VOLTS/METER
                     EXTERNAL ELECTRIC FIELD =-1.617e+04  VOLTS/METER
                     DELTA V =-1.182e+03 VOLTS
                     UNDERLYING CONDUCTOR IS NUMBER 1
                     UNDERLYING CONDUCTOR POTENTIAL =-1.518e+04 VOLTS
                     LIMITING FACTOR =  1.000e+00
   FLUXES IN A/M**2
        INCIDENT ELECTRONS               8.46e-07
             RESULTING SECONDARIES       1.88e-07
             RESULTING BACKSCATTER       2.05e-07
        INCIDENT PROTONS                 3.94e-08
             RESULTING SECONDARIES       1.86e-07
        BULK CONDUCTIVITY               -9.31e-10
        PHOTOCURRENT                     0.00e+00
                                        ----------
      NET FLUX AFTER LONG-TIME-STEP     -2.23e-07
 SINGLE COMMAND OR MODE SET ?
>108
-------------------------------------------------------------------------
  SURFACE CELL NO.  108
                                  CODE              420156010
                                  CENTERED AT     -7.0    2.5   -1.5
                                  MATERIAL IS  KAPT
                                  NORMAL         -1  0  0
                                  SHAPE IS SQUARE
                     POTENTIAL =-1.636e+04 VOLTS
                     INTERNAL FIELD STRESS =-9.307e+06  VOLTS/METER
                     EXTERNAL ELECTRIC FIELD =-1.735e+04  VOLTS/METER
                     DELTA V =-1.182e+03 VOLTS
                     UNDERLYING CONDUCTOR IS NUMBER 1
                     UNDERLYING CONDUCTOR POTENTIAL =-1.518e+04 VOLTS
                     LIMITING FACTOR =  1.000e+00
   FLUXES IN A/M**2
        INCIDENT ELECTRONS               8.46e-07
             RESULTING SECONDARIES       1.88e-07
             RESULTING BACKSCATTER       2.05e-07
        INCIDENT PROTONS                 3.94e-08
             RESULTING SECONDARIES       1.86e-07
        BULK CONDUCTIVITY               -9.31e-10
        PHOTOCURRENT                     0.00e+00
                                        ----------
      NET FLUX AFTER LONG-TIME-STEP     -2.23e-07
 SINGLE COMMAND OR MODE SET ?
>91
-------------------------------------------------------------------------
  SURFACE CELL NO.    91
                                  CODE              417546010
                                  CENTERED AT     -7.0    1.5   -1.5
                                  MATERIAL IS  KAPT
                                  NORMAL         -1  0  0
```

```
                                SHAPE IS SQUARE
                    POTENTIAL =-1.636e+04 VOLTS
                    INTERNAL FIELD STRESS =-9.307e+06  VOLTS/METER
                    EXTERNAL ELECTRIC FIELD =-1.643e+04  VOLTS/METER
                    DELTA V =-1.182e+03 VOLTS
                    UNDERLYING CONDUCTOR IS NUMBER 1
                    UNDERLYING CONDUCTOR POTENTIAL =-1.518e+04 VOLTS
                    LIMITING FACTOR =  1.000e+00
  FLUXES IN A/M**2
        INCIDENT ELECTRONS              8.46e-07
             RESULTING SECONDARIES      1.88e-07
             RESULTING BACKSCATTER      2.05e-07
        INCIDENT PROTONS                3.94e-08
             RESULTING SECONDARIES      1.86e-07
        BULK CONDUCTIVITY              -9.31e-10
        PHOTOCURRENT                    0.00e+00
                                       ----------
      NET FLUX AFTER LONG-TIME-STEP    -2.23e-07
 SINGLE COMMAND OR MODE SET ?
>1130
--------------------------------------------------------------------------
  SURFACE CELL NO. 1130
                                CODE               633372010
                                CENTERED AT      7.0    -.5    2.5
                                MATERIAL IS  KAPT
                                NORMAL          1  0  0
                                SHAPE IS SQUARE
                    POTENTIAL =-1.636e+04 VOLTS
                    INTERNAL FIELD STRESS =-9.306e+06  VOLTS/METER
                    EXTERNAL ELECTRIC FIELD =-1.631e+04  VOLTS/METER
                    DELTA V =-1.182e+03 VOLTS
                    UNDERLYING CONDUCTOR IS NUMBER 1
                    UNDERLYING CONDUCTOR POTENTIAL =-1.518e+04 VOLTS
                    LIMITING FACTOR =  1.000e+00
  FLUXES IN A/M**2
        INCIDENT ELECTRONS              8.46e-07
             RESULTING SECONDARIES      1.88e-07
             RESULTING BACKSCATTER      2.05e-07
        INCIDENT PROTONS                3.94e-08
             RESULTING SECONDARIES      1.86e-07
        BULK CONDUCTIVITY              -9.31e-10
        PHOTOCURRENT                    0.00e+00
                                       ----------
      NET FLUX AFTER LONG-TIME-STEP    -2.23e-07
 SINGLE COMMAND OR MODE SET ?
>889
--------------------------------------------------------------------------
  SURFACE CELL NO.  889
                                CODE               572030110
                                CENTERED AT      3.5   -2.5    8.0
                                MATERIAL IS  KAPT
                                NORMAL          0  0  1
                                SHAPE IS SQUARE
                    POTENTIAL =-1.636e+04 VOLTS
                    INTERNAL FIELD STRESS =-9.305e+06  VOLTS/METER
                    EXTERNAL ELECTRIC FIELD =-1.628e+04  VOLTS/METER
                    DELTA V =-1.182e+03 VOLTS
                    UNDERLYING CONDUCTOR IS NUMBER 1
                    UNDERLYING CONDUCTOR POTENTIAL =-1.518e+04 VOLTS
                    LIMITING FACTOR =  1.000e+00
  FLUXES IN A/M**2
        INCIDENT ELECTRONS              8.46e-07
             RESULTING SECONDARIES      1.88e-07
             RESULTING BACKSCATTER      2.05e-07
```

```
        INCIDENT PROTONS                3.94e-08
             RESULTING SECONDARIES      1.86e-07
        BULK CONDUCTIVITY               -9.31e-10
        PHOTOCURRENT                     0.00e+00
                                        ----------
      NET FLUX AFTER LONG-TIME-STEP     -2.23e-07
 SINGLE COMMAND OR MODE SET ?
>1145
-------------------------------------------------------------------------
  SURFACE CELL NO. 1145
                                  CODE              633762012
                                  CENTERED AT      7.0     .5     .5
                                  MATERIAL IS  TEFL
                                  NORMAL          1  0  0
                                  SHAPE IS SQUARE
                     POTENTIAL =-1.580e+04 VOLTS
                     INTERNAL FIELD STRESS =-4.869e+06  VOLTS/METER
                     EXTERNAL ELECTRIC FIELD =-1.599e+04  VOLTS/METER
                     DELTA V =-6.184e+02 VOLTS
                     UNDERLYING CONDUCTOR IS NUMBER 1
                     UNDERLYING CONDUCTOR POTENTIAL =-1.518e+04 VOLTS
                     LIMITING FACTOR =  1.000e+00
   FLUXES IN A/M**2
        INCIDENT ELECTRONS              8.84e-07
             RESULTING SECONDARIES      3.63e-07
             RESULTING BACKSCATTER      2.48e-07
        INCIDENT PROTONS                3.90e-08
             RESULTING SECONDARIES      1.83e-07
        BULK CONDUCTIVITY               -4.87e-10
        PHOTOCURRENT                     0.00e+00
                                        ----------
      NET FLUX AFTER LONG-TIME-STEP     -5.06e-08
 SINGLE COMMAND OR MODE SET ?
>history
 HISTORY COMMAND OR MODE SET ?
>stress
MODE RESET
 HISTORY COMMAND OR MODE SET ?
>107,1145
STRE IN VOLTS/METER
  TIME  :   107     1145
--------:-------------------------------------------------------------------
        :    #1       #2       #3       #4       #5       #6       #7
 6.0e+01:-3.69e+05-1.48e+06
 1.2e+02:-8.07e+05-1.56e+06
 1.8e+02:-1.31e+06-1.71e+06
 2.4e+02:-1.82e+06-1.89e+06
 3.0e+02:-2.33e+06-2.08e+06
 3.6e+02:-2.84e+06-2.28e+06
 4.2e+02:-3.34e+06-2.49e+06
 4.8e+02:-3.83e+06-2.69e+06
 5.4e+02:-4.32e+06-2.88e+06
 6.0e+02:-4.80e+06-3.08e+06
 6.6e+02:-5.27e+06-3.27e+06
 7.2e+02:-5.74e+06-3.46e+06
 7.8e+02:-6.20e+06-3.64e+06
 8.4e+02:-6.66e+06-3.82e+06
 9.0e+02:-7.11e+06-4.00e+06
 9.6e+02:-7.56e+06-4.18e+06
 1.0e+03:-8.00e+06-4.35e+06
 1.1e+03:-8.44e+06-4.53e+06
 1.1e+03:-8.87e+06-4.70e+06
 1.2e+03:-9.31e+06-4.87e+06
STPE VERSUS LOG(TIME)
```

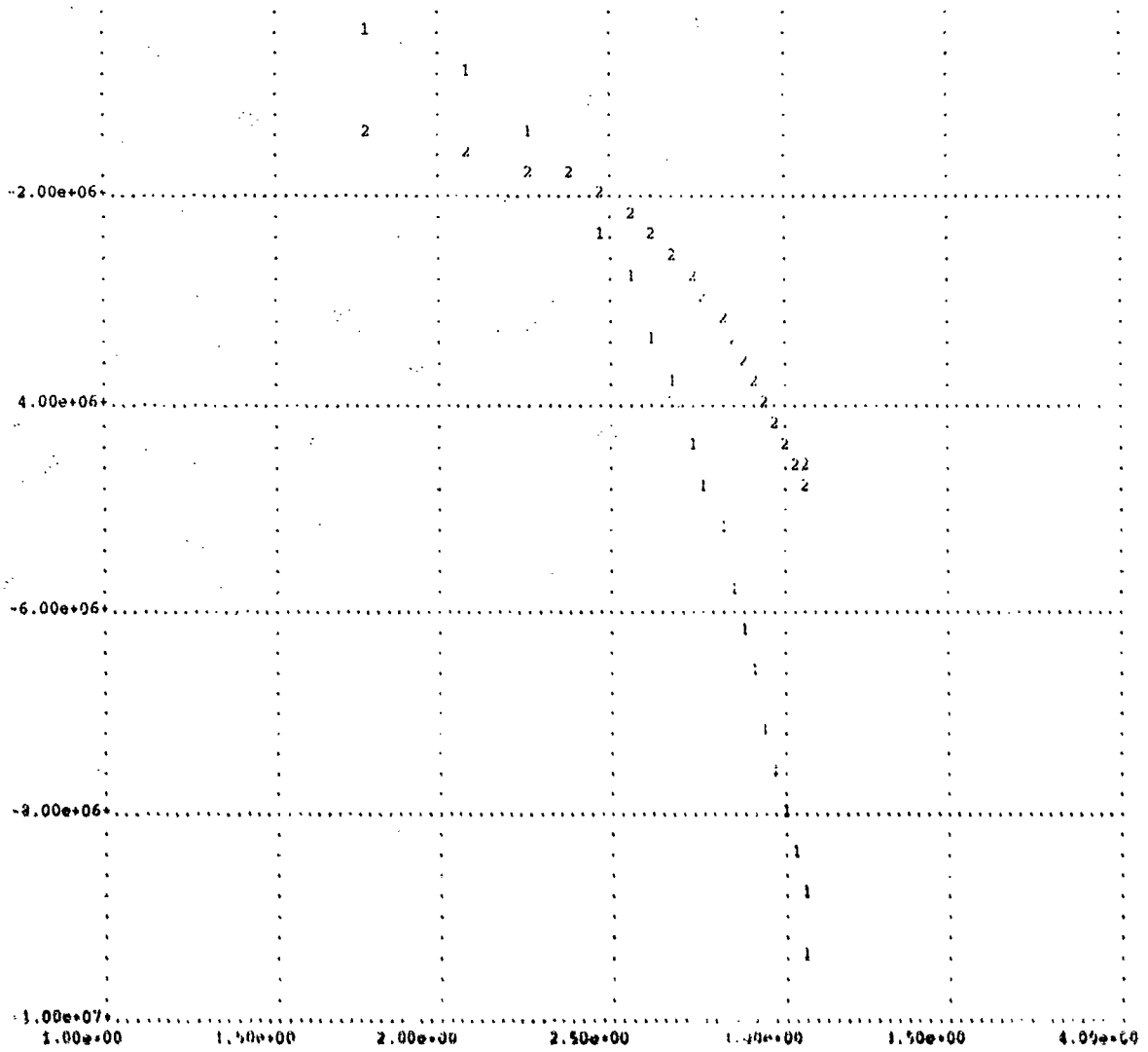


```
 HISTORY COMMAND OR MODE SET ?
>exit
```

Contours Execution for Spinning Spacecraft in Geosynchronous Orbit-SCATHA

```
 ENTER TITLE>:

 asgfil called for lun =   2
 asgfil called for lun =  21

 NZ>33

 NG>4

 ENTER THE CUT-PLANE'S NORMAL DIRECTION  (X,Y,OR    Z), OR QUIT (Q)> Z

 ENTER THE CUT-PLANE'S OFFSET ALONG THE NORMAL>17

ENTER 1 (SINGLE), 2 (DOUBLE), OR 0 (UNIT) TO SPECIFY FORMAT OF ZERO-POTENTIAL>:
 DEFAULT STRING <SINGLE> ASSIGNED.
 ***WARNING*** NUMMOD --- ZERO POINTS FOUND IN LIST.
```

```
ENTER THE CUT-PLANE'S NORMAL DIRECTION  (X,Y,OR    Z), OR QUIT (Q)> q
PREPARING TO DUMP AND QUIT.
[EXIT]
```

C.8 Three-Axis Stabilized Spacecraft in Sunlight

The following files are the input and output files from the various computer codes used in the example shown in Section 5.1.2.

Matchg Execution (fort.3) for 3-Axis Stabilized Spacecraft in Sunlight

This is the fort.3 file generated from the execution of **Matchg** for this problem. The environment is set to the severe substorm environment using the change environment command. The material is KAP3. A summary of potentials and currents before and after charging is requested. The process is repeated for all of the surface materials. During the execution, the object definition files (below) was used as a fort.8 for material definitions. The results are tabulated in Table 8.

```
WELCOME TO 'MATCHG', A MATERIAL CHARGING
PROGRAM. TYPE 'HELP' AT ANY TIME FOR ASSISTANCE.
MATERIAL IS KAP3
ENVIRONMENT NOW SINGLE MAXWELLIAN

change envi nei 1.12e6

ENVIRONMENT IS A SINGLE MAXWELLIAN

ELECTRONS: NEI =  1.12e+06 (M**-3)     TEI =     1.000 KEV
IONS     : NII =  1.00e+06 (M**-3)     TII =     1.000 KEV

change envi tei 12

ENVIRONMENT IS A SINGLE MAXWELLIAN

ELECTRONS: NEI =  1.12e+06 (M**-3)     TEI =    12.000 KEV
IONS     : NII =  1.00e+06 (M**-3)     TII =     1.000 KEV

change envi nii 2.36e5

ENVIRONMENT IS A SINGLE MAXWELLIAN

ELECTRONS: NEI =  1.12e+06 (M**-3)     TEI =    12.000 KEV
IONS     : NII =  2.36e+05 (M**-3)     TII =     1.000 KEV

change envi tii 29.5

ENVIRONMENT IS A SINGLE MAXWELLIAN

ELECTRONS: NEI =  1.12e+06 (M**-3)     TEI =    12.000 KEV
IONS     : NII =  2.36e+05 (M**-3)     TII =    29.500 KEV

result charge

CYCLE    1   TIME  0.00e+00 SECONDS    POTENTIAL  0.00e+00 VOLTS
INCIDENT ELECTRON CURRENT          -3.30e-06
```

```
          SECONDARY ELECTRONS        7.33e-07
          BACKSCATTERED ELECTRONS    8.01e-07
INCIDENT PROTON CURRENT              2.54e-08
          SECONDARY ELECTRONS        1.14e-07
BULK CONDUCTIVITY CURRENT            0.00e+00
                                    -----------
                      NET CURRENT   -1.62e-06  AMPS/M**2
CYCLE   99   TIME  1.77e+04 SECONDS     POTENTIAL -2.08e+04 VOLTS
INCIDENT ELECTRON CURRENT           -5.84e-07
          SECONDARY ELECTRONS        1.30e-07
          BACKSCATTERED ELECTRONS    1.42e-07
INCIDENT PROTON CURRENT              4.32e-08
          SECONDARY ELECTRONS        2.07e-07
BULK CONDUCTIVITY CURRENT            1.64e-08
                                    -----------
                      NET CURRENT   -4.56e-08  AMPS/M**2

change material LFALUM

MATERIAL IS LFAL

result charge

CYCLE    1   TIME  0.00e+00 SECONDS     POTENTIAL  0.00e+00 VOLTS
INCIDENT ELECTRON CURRENT            3.30e-06
          SECONDARY ELECTRONS        7.33e-07
          BACKSCATTERED ELECTRONS    8.01e-07
INCIDENT PROTON CURRENT              2.54e-08
          SECONDARY ELECTRONS        1.14e-07
BULK CONDUCTIVITY CURRENT            0.00e+00
                                    -----------
                      NET CURRENT   -1.62e-06  AMPS/M**2
CYCLE    2   TIME  8.84e+04 SECONDS     POTENTIAL -3.15e-01 VOLTS
INCIDENT ELECTRON CURRENT           -3.30e-06
          SECONDARY ELECTRONS        7.33e-07
          BACKSCATTERED ELECTRONS    8.01e-07
INCIDENT PROTON CURRENT              2.54e-08
          SECONDARY ELECTRONS        1.14e-07
BULK CONDUCTIVITY CURRENT            1.62e-06
                                    -----------
                      NET CURRENT   -4.66e-12  AMPS/M**2

change material S13GLO

MATERIAL IS S13G

result charge

CYCLE    1   TIME  0.00e+00 SECONDS     POTENTIAL  0.00e+00 VOLTS
INCIDENT ELECTRON CURRENT           -3.30e-06
          SECONDARY ELECTRONS        1.42e-06
          BACKSCATTERED ELECTRONS    8.01e-07
INCIDENT PROTON CURRENT              2.54e-08
          SECONDARY ELECTRONS        1.14e-07
BULK CONDUCTIVITY CURRENT            0.00e+00
                                    -----------
                      NET CURRENT   -9.32e-07  AMPS/M**2
CYCLE    2   TIME  3.83e+04 SECONDS     POTENTIAL -1.46e-01 VOLTS
INCIDENT ELECTRON CURRENT           -3.30e-06
          SECONDARY ELECTRONS        1.42e-06
          BACKSCATTERED ELECTRONS    8.01e-07
INCIDENT PROTON CURRENT              2.54e-08
          SECONDARY ELECTRONS        1.14e-07
BULK CONDUCTIVITY CURRENT            9.32e-07
```

```
                                    -------------
                        NET CURRENT  -1.13e-10  AMPS/M**2

change material FSLICA

MATERIAL IS FSLI

result charge

CYCLE    1   TIME  0.00e+00 SECONDS     POTENTIAL  0.00e+00 VOLTS
INCIDENT ELECTRON CURRENT          -3.30e-06
         SECONDARY ELECTRONS        1.33e-06
         BACKSCATTERED ELECTRONS    1.07e-06
INCIDENT PROTON CURRENT             2.54e-08
         SECONDARY ELECTRONS        1.14e-07
BULK CONDUCTIVITY CURRENT           0.00e+00
                                    -------------
                        NET CURRENT  -7.59e-07  AMPS/M**2
CYCLE   49   TIME  3.61e+04 SECONDS     POTENTIAL -5.84e+03 VOLTS
INCIDENT ELECTRON CURRENT          -2.03e-06
         SECONDARY ELECTRONS        8.19e-07
         BACKSCATTERED ELECTRONS    6.56e-07
INCIDENT PROTON CURRENT             3.04e-08
         SECONDARY ELECTRONS        1.38e-07
BULK CONDUCTIVITY CURRENT           3.84e-07
                                    -------------
                        NET CURRENT  -1.82e-10  AMPS/M**2

change material BLKVEL

MATERIAL IS BLKV

result charge

CYCLE    1   TIME  0.00e+00 SECONDS     POTENTIAL  0.00e+00 VOLTS
INCIDENT ELECTRON CURRENT          -3.30e-06
         SECONDARY ELECTRONS        7.33e-07
         BACKSCATTERED ELECTRONS    8.01e-07
INCIDENT PROTON CURRENT             2.54e-08
         SECONDARY ELECTRONS        1.14e-07
BULK CONDUCTIVITY CURRENT           0.00e+00
                                    -------------
                        NET CURRENT  -1.62e-06  AMPS/M**2
CYCLE    2   TIME  4.42e+04 SECONDS     POTENTIAL -5.89e-03 VOLTS
INCIDENT ELECTRON CURRENT          -3.30e-06
         SECONDARY ELECTRONS        7.33e-07
         BACKSCATTERED ELECTRONS    8.01e-07
INCIDENT PROTON CURRENT             2.54e-08
         SECONDARY ELECTRONS        1.14e-07
BULK CONDUCTIVITY CURRENT           1.62e-06
                                    -------------
                        NET CURRENT  -7.73e-12  AMPS/M**2

change material BSME

MATERIAL IS BSME

result charge

CYCLE    1   TIME  0.00e+00 SECONDS     POTENTIAL  0.00e+00 VOLTS
INCIDENT ELECTRON CURRENT          -3.30e-06
         SECONDARY ELECTRONS        1.22e-06
         BACKSCATTERED ELECTRONS    1.80e-06
INCIDENT PROTON CURRENT             2.54e-08
```

```
        SECONDARY ELECTRONS        1.18e-07
                                  ----------
                     NET CURRENT  -1.37e-07  AMPS/M**2
CYCLE   40   TIME  7.62e+03 SECONDS     POTENTIAL -5.77e+03 VOLTS
INCIDENT ELECTRON CURRENT          -2.04e-06
         SECONDARY ELECTRONS        7.52e-07
         BACKSCATTERED ELECTRONS    1.11e-06
INCIDENT PROTON CURRENT             3.04e-08
         SECONDARY ELECTRONS        1.43e-07
                                  ----------
                     NET CURRENT  -1.94e-10  AMPS/M**2

change material KAP1TN

MATERIAL IS KAP1

result charge

CYCLE    1   TIME  0.00e+00 SECONDS     POTENTIAL  0.00e+00 VOLTS
INCIDENT ELECTRON CURRENT          -3.30e-06
         SECONDARY ELECTRONS        7.33e-07
         BACKSCATTERED ELECTRONS    8.01e-07
INCIDENT PROTON CURRENT             2.54e-08
         SECONDARY ELECTRONS        1.14e-07
BULK CONDUCTIVITY CURRENT           0.00e+00
                                  ----------
                     NET CURRENT  -1.62e-06  AMPS/M**2
CYCLE   99   TIME  4.42e+04 SECONDS     POTENTIAL -2.02e+04 VOLTS
INCIDENT ELECTRON CURRENT          -6.11e-07
         SECONDARY ELECTRONS        1.36e-07
         BACKSCATTERED ELECTRONS    1.48e-07
INCIDENT PROTON CURRENT             4.28e-08
         SECONDARY ELECTRONS        2.04e-07
BULK CONDUCTIVITY CURRENT           3.98e-08
                                  ----------
                     NET CURRENT  -3.99e-08  AMPS/M**2

change material KAP2TN

MATERIAL IS KAP2

result charge

CYCLE    1   TIME  0.00e+00 SECONDS     POTENTIAL  0.00e+00 VOLTS
INCIDENT ELECTRON CURRENT          -3.30e-06
         SECONDARY ELECTRONS        7.33e-07
         BACKSCATTERED ELECTRONS    8.01e-07
INCIDENT PROTON CURRENT             2.54e-08
         SECONDARY ELECTRONS        1.14e-07
BULK CONDUCTIVITY CURRENT           0.00e+00
                                  ----------
                     NET CURRENT  -1.62e-06  AMPS/M**2
CYCLE   99   TIME  1.77e+05 SECONDS     POTENTIAL -1.79e+04 VOLTS
INCIDENT ELECTRON CURRENT          -7.40e-07
         SECONDARY ELECTRONS        1.65e-07
         BACKSCATTERED ELECTRONS    1.80e-07
INCIDENT PROTON CURRENT             4.08e-08
         SECONDARY ELECTRONS        1.93e-07
BULK CONDUCTIVITY CURRENT           1.41e-07
                                  ----------
                     NET CURRENT  -2.06e-08  AMPS/M**2

change material EHFPRT
```

```
MATERIAL IS EHFP

result charge

CYCLE     1   TIME  0.00e+00 SECONDS     POTENTIAL  0.00e+00 VOLTS
INCIDENT ELECTRON CURRENT          -3.30e-06
         SECONDARY ELECTRONS        6.61e-07
         BACKSCATTERED ELECTRONS    1.46e-06
INCIDENT PROTON CURRENT             2.54e-08
         SECONDARY ELECTRONS        1.18e-07
                                  -------------
                     NET CURRENT  -1.03e-06  AMPS/M**2
CYCLE    99   TIME  1.01e+03 SECONDS     POTENTIAL -1.82e+04 VOLTS
INCIDENT ELECTRON CURRENT          -7.24e-07
         SECONDARY ELECTRONS        1.45e-07
         BACKSCATTERED ELECTRONS    3.21e-07
INCIDENT PROTON CURRENT             4.10e-08
         SECONDARY ELECTRONS        2.01e-07
                                  -------------
                     NET CURRENT  -1.54e-08  AMPS/M**2

change material ALUM

MATERIAL IS ALUM

result charge

CYCLE     1   TIME  0.00e+00 SECONDS     POTENTIAL  0.00e+00 VOLTS
INCIDENT ELECTRON CURRENT          -3.30e-06
         SECONDARY ELECTRONS        6.75e-07
         BACKSCATTERED ELECTRONS    1.18e-06
INCIDENT PROTON CURRENT             2.54e-08
         SECONDARY ELECTRONS        6.92e-08
                                  -------------
                     NET CURRENT  -1.35e-06  AMPS/M**2
CYCLE    99   TIME  7.71e+02 SECONDS     POTENTIAL -2.22e+04 VOLTS
INCIDENT ELECTRON CURRENT          -5.17e-07
         SECONDARY ELECTRONS        1.06e-07
         BACKSCATTERED ELECTRONS    1.85e-07
INCIDENT PROTON CURRENT             4.45e-08
         SECONDARY ELECTRONS        1.31e-07
                                  -------------
                     NET CURRENT  -5.10e-08  AMPS/M**2

change material CPHENL

MATERIAL IS CPHE

result charge

CYCLE     1   TIME  0.00e+00 SECONDS     POTENTIAL  0.00e+00 VOLTS
INCIDENT ELECTRON CURRENT          -3.30e-06
         SECONDARY ELECTRONS        1.35e-06
         BACKSCATTERED ELECTRONS    9.25e-07
INCIDENT PROTON CURRENT             2.54e-08
         SECONDARY ELECTRONS        1.14e-07
BULK CONDUCTIVITY CURRENT           0.00e+00
                                  -------------
                     NET CURRENT  -8.80e-07  AMPS/M**2
CYCLE     4   TIME  8.15e+02 SECONDS     POTENTIAL -4.45e+01 VOLTS
INCIDENT ELECTRON CURRENT          -3.28e-06
         SECONDARY ELECTRONS        1.35e-06
         BACKSCATTERED ELECTRONS    9.22e-07
INCIDENT PROTON CURRENT             2.55e-08
```

```
        SECONDARY ELECTRONS          1.14e-07
BULK CONDUCTIVITY CURRENT            8.76e-07
                                  -------------
                      NET CURRENT  -4.04e-11  AMPS/M**2

exit

[EXIT]
```

These three files are used in the execution of **Nascap** for the sunlit spacecraft example. The first file is the standard input, which gives the options and the initial potentials. The second file is the object definition, and the third file is the environment definition.

Standard Input to Nascap for 3-Axis Stabilized Spacecraft in Sunlight

```
rdopt 5
   delta 60.
   longtimestep
   ncyc 20
   ng 2
   nz 33
   xmesh 0.457
   sundir 1 .1 -.2
   suniat 1.
   end
objdef 20
capaci
hidcel
trilin
end
```

Object Definition File (fort.20) for 3-Axis Stabilized Spacecraft in Sunlight

This file is also used as a fort.8 material definition file for the execution of **Matchg**.

```
COMMENT PRELIMINARY FLEETSATCOM MODEL (VERSION 1)
COMMENT FLIGHT 7 SPACECRAFT WITH EHF MODULE
COMMENT MESH SIZE IS 1.5FT (0.457 M)
COMMENT S/C ILLUMINATED AT DAWN
COMMENT DEFINE MATERIALS
COMMENT
KAP3TN
3.50E+00  1.27E-04  1.00E-16  5.00E+00  2.10E+00  1.50E-01  7.15E+01  6.00E-01
3.12E+02  1.77E+00  4.55E-01  1.40E+02  2.00E-05  7.90E+19  1.00E+04  2.00E+03
1.00E-13  1.00E+00  1.00E+03  2.00E+01
LFALUM
3.50E+00  2.54E-05  1.23E-08  5.00E+00  2.10E+00  1.50E-01  7.15E+01  6.00E-01
3.12E+02  1.77E+00  4.55E-01  1.40E+02  2.00E-05  3.20E+12  1.00E+04  2.00E+03
1.00E-13  1.00E+00  1.00E+03  2.00E+01
S13GLO
3.50E+00  1.02E-04  6.50E-10  5.00E+00  2.10E+00  1.50E-01  -1.00E+00 0.00E+00
1.05E+00  9.80E+00  4.55E-01  1.40E+02  2.00E-05  1.50E+13  1.00E+04  2.00E+03
1.00E-13  1.00E+00  1.00E+03  2.00E+01
FSLICA
4.00E+00  1.52E-04  1.00E-14  1.00E+01  2.40E+00  4.00E-01  1.16E+02  8.10E-01
1.83E+02  1.86E+00  4.55E-01  1.40E+02  2.00E-05  6.58E+17  1.00E+04  2.00E+03
```

```
1.00E-13  1.00E+00  1.00E+03  2.00E+01
BLKVEL
3.50E+00  5.08E-05  1.40E-08  5.00E+00  2.10E+00  1.50E-01  7.15E+01  6.00E-01
3.12E+02  1.77E+00  4.55E-01  1.40E+02  2.00E-05  1.40E+12  1.00E+04  2.00E+03
1.00E-13  1.00E+00  1.00E+03  2.00E+01
SSMESH
1.00E+00  1.00E-03  -1.00E+00 4.70E+01  1.00E+00  8.00E-01  8.45E+01  8.20E-01
7.94E+01  1.74E+00  4.90E-01  1.23E+02  2.90E-05  -1.00E+00 1.00E+04  2.00E+03
1.00E-13  1.00E+00  1.00E+03  2.00E+01
KAP1TN
3.50E+00  5.08E-05  1.00E-16  5.00E+00  2.10E+00  1.50E-01  7.15E+01  6.00E-01
3.12E+02  1.77E+00  4.55E-01  1.40E+02  2.00E-05  2.00E+20  1.00E+04  2.00E+03
1.00E-13  1.00E+00  1.00E+03  2.00E+01
KAP2TN
3.50E+00  1.27E-05  1.00E-16  5.00E+00  2.10E+00  1.50E-01  7.15E+01  6.00E-01
3.12E+02  1.77E+00  4.55E-01  1.40E+02  2.00E-05  7.90E+20  1.00E+04  2.00E+03
1.00E-13  1.00E+00  1.00E+03  2.00E+01
EHFPRT
1.00E+00  1.00E-03  -1.00E+00 2.44E+01  1.40E+00  8.00E-01  -1.00E+00 0.00E+00
7.18E+00  5.55E+01  4.90E-01  1.23E+02  3.20E-05  -1.00E+00 1.00E+04  2.00E+03
1.00E-13  1.00E+00  1.00E+03  2.00E+01
ALUM
1.00E+00  1.00E-03  -1.00E+00 1.30E+01  9.70E-01  3.00E-01  1.54E+02  8.00E-01
2.20E+02  1.76E+00  2.44E-01  2.30E+02  4.00E-05  -1.00E+00 1.00E+04  2.00E+03
1.00E-13  1.00E+00  1.00E+03  2.00E+01
CPHENL
3.50E+00  5.08E-03  1.00E-10  7.00E+00  3.00E+00  3.00E-01  4.54E+01  4.00E-01
2.18E+02  1.77E+00  4.55E-01  1.40E+02  2.00E-05  1.00E+10  1.00E+04  2.00E+03
1.00E-13  1.00E+00  1.00E+03  2.00E+01
COMMENT
COMMENT DEFINE OBJECT
COMMENT FSC EQUIPMENT MODULE
OCTAGON
AXIS -2 -6 0  -2 -2 0
WIDTH 6
SIDE 2
SURFACE + KAP2TN
SURFACE - KAP3TN
SURFACE C KAP1TN
ENDOBJ
COMMENT
COMMENT EQUIPMENT MODULE SIDES/ SSM PATCHES
PATCHR
CORNER -5 -6 0
DELTAS 1 1 1
SURFACE -X FSLICA
ENDOBJ
PATCHR
CORNER 0 -6 0
DELTAS 1 1 1
SURFACE +X FSLICA
ENDOBJ
PATCHR
CORNER 0 -4 -1
DELTAS 1 1 1
SURFACE +X FSLICA
ENDOBJ
PATCHR
CORNER -2 -3 -3
DELTAS 1 1 1
SURFACE -Z FSLICA
ENDOBJ
PATCHR
CORNER -3 -3 -3
```

```
DELTAS 1 1 1
SURFACE -Z FSLICA
ENDOBJ
PATCHR
CORNER -3 -4 -3
DELTAS 1 1 1
SURFACE -Z FSLICA
ENDOBJ
PATCHR
CORNER -2 -5 -3
DELTAS 1 1 1
SURFACE -Z FSLICA
ENDOBJ
PATCHR
CORNER -3 -6 -3
DELTAS 1 1 1
SURFACE -Z FSLICA
ENDOBJ
PATCHR
CORNER -2 -3 2
DELTAS 1 1 1
SURFACE +Z FSLICA
ENDOBJ
PATCHR
CORNER -3 -3 2
DELTAS 1 1 1
SURFACE +Z FSLICA
ENDOBJ
PATCHR
CORNER -2 -4 2
DELTAS 1 1 1
SURFACE +Z FSLICA
ENDOBJ
PATCHR
CORNER -3 -5 2
DELTAS 1 1 1
SURFACE +Z FSLICA
ENDOBJ
PATCHR
CORNER -2 -6 2
DELTAS 1 1 1
SURFACE +Z FSLICA
ENDOBJ
PATCHW
CORNER 0 -3 1
FACE FSLICA 1 0 1
LENGTH 1 1 1
ENDOBJ
PATCHW
CORNER 0 -5 1
FACE FSLICA 1 0 1
LENGTH 1 1 1
ENDOBJ
PATCHW
CORNER 0 -3 -1
FACE FSLICA 1 0 -1
LENGTH 1 1 1
ENDOBJ
PATCHW
CORNER 0 -5 -1
FACE FSLICA 1 0 -1
LENGTH 1 1 1
ENDOBJ
PATCHW
```

```
CORNER -4 -3 1
FACE FSLICA -1 0 1
LENGTH 1 1 1
ENDOBJ
PATCHW
CORNER -4 -5 1
FACE FSLICA -1 0 1
LENGTH 1 1 1
ENDOBJ
PATCHW
CORNER -3 -4 2
FACE FSLICA -1 0 1
LENGTH 1 1 1
ENDOBJ
PATCHW
CORNER -4 -3 -1
FACE FSLICA -1 0 -1
LENGTH 1 1 1
ENDOBJ
PATCHW
CORNER -4 -5 -1
FACE FSLICA -1 0 -1
LENGTH 1 1 1
ENDOBJ
PATCHW
CORNER -3 -6 -2
FACE FSLICA -1 0 -1
LENGTH 1 1 1
ENDOBJ
COMMENT
COMMENT EQUIPMENT MODULE TOP/UHF TRANSMIT ANTENNA
OCTAGON
AXIS -2 -3 0  -2 -2 0
WIDTH 4
SIDE 2
SURFACE + S13GLO
ENDOBJ
COMMENT EHF ANTENNA PATCH
WEDGE
CORNER -1 -3 1
FACE KAP2TN -1 0 -1
LENGTH 1 1 1
SURFACE +Y EHFPRT
ENDOBJ
COMMENT
COMMENT ANTENNA MESH
ASLANT
CORNER 0 1 -2
FACE SSMESH 1 -1 0
LENGTH 3 3 4
ENDOBJ
ATET
CORNER 0 1 2
FACE SSMESH 1 -1 1
LENGTH 3
ENDOBJ
ASLANT
CORNER -4 1 2
FACE SSMESH 0 -1 1
LENGTH 4 3 3
ENDOBJ
ATET
CORNER -4 1 2
FACE SSMESH -1 -1 1
```

```
LENGTH 3
ENDOBJ
ASLANT
CORNER -4 1 -2
FACE SSMESH -1 -1 0
LENGTH 3 3 4
ENDOBJ
ATET
CORNER -4 1 -2
FACE SSMESH -1 -1 -1
LENGTH 3
ENDOBJ
ASLANT
CORNER -4 1 -2
FACE SSMESH 0 -1 -1
LENGTH 4 3 3
ENDOBJ
ATET
CORNER 0 1 -2
FACE SSMESH 1 -1 -1
LENGTH 3
ENDOBJ
COMMENT
COMMENT UHF TRANSMIT ANTENNA MAST
BOOM
AXIS -2 -2 0  -2 0 0
RADIUS 0.218
SURFACE S13GLO
ENDOBJ
BOOM
AXIS -2 0 0  -2 4 0
RADIUS 0.083
SURFACE ALUM
ENDOBJ
BOOM
AXIS -2 4 0  -2 5 0
RADIUS 0.0416
SURFACE S13GLO
ENDOBJ
COMMENT
COMMENT SOLAR ARRAY PLUME SHIELD
PLATE
CORNER -4 -7 -2
DELTAS 0 1 3
TOP -X KAP1TN
BOTTOM +X ALUM
ENDOBJ
PLATE
CORNER -4 -7 1
DELTAS 0 1 1
TOP -X ALUM
BOTTOM +X ALUM
ENDOBJ
PLATE
CORNER -4 -7 2
DELTAS 3 1 0
TOP +Z KAP1TN
BOTTOM -Z ALUM
ENDOBJ
PLATE
CORNER -1 -7 2
DELTAS 1 1 0
TOP +Z ALUM
BOTTOM -Z ALUM
```

```
ENDOBJ
PLATE
CORNER 0 -7 -1
DELTAS 0 1 3
TOP +X KAP1TN
BOTTOM -X ALUM
ENDOBJ
PLATE
CORNER 0 -7 -2
DELTAS 0 1 1
TOP +X ALUM
BOTTOM -X ALUM
ENDOBJ
PLATE
CORNER -3 -7 -2
DELTAS 3 1 0
TOP -Z KAP1TN
BOTTOM +Z ALUM
ENDOBJ
PLATE
CORNER -4 -7 -2
DELTAS 1 1 0
TOP -Z ALUM
BOTTOM +Z ALUM
ENDOBJ
COMMENT
COMMENT ARM NOZZLE
PATCHR
CORNER -2 -6 0
DELTAS 1 1 1
SURFACE -Y CPHENL
ENDOBJ
COMMENT
COMMENT UHF RECEIVE ANTENNA
COMMENT GROUND PLANE CAVITY
WEDGE
CORNER 6 0 1
FACE ALUM 1 0 1
LENGTH 1 1 1
SURFACE -X ALUM
SURFACE +Y ALUM
SURFACE -Y ALUM
SURFACE -Z ALUM
ENDOBJ
WEDGE
CORNER 6 0 1
FACE ALUM -1 0 1
LENGTH 1 1 1
SURFACE +X ALUM
SURFACE +Y ALUM
SURFACE -Y ALUM
SURFACE -Z ALUM
ENDOBJ
WEDGE
CORNER 6 0 1
FACE ALUM 1 0 -1
LENGTH 1 1 1
SURFACE -X ALUM
SURFACE +Y ALUM
SURFACE -Y ALUM
SURFACE +Z ALUM
ENDOBJ
WEDGE
CORNER 6 0 1
```

```
FACE ALUM -1 0 -1
LENGTH 1 1 1
SURFACE +X ALUM
SURFACE +Y ALUM
SURFACE -Y ALUM
SURFACE +Z ALUM
ENDOBJ
COMMENT ANTENNA MAST
BOOM
AXIS 6 1 1  6 4 1
RADIUS 0.167
SURFACE S13GLO
ENDOBJ
BOOM
AXIS 6 4 1  6 5 1
RADIUS 0.167
SURFACE ALUM
ENDOBJ
BOOM
AXIS 6 5 1  6 8 1
RADIUS 0.167
SURFACE S13GLO
ENDOBJ
COMMENT ANTENNA BOOMS
BOOM
AXIS 1 -2 0  6 -2 0
RADIUS 0.333
SURFACE LFALUM
ENDOBJ
BOOM
AXIS 6 -2 0  6 0 0
RADIUS 0.333
SURFACE LFALUM
ENDOBJ
COMMENT
COMMENT SOLAR ARRAY PANELS
COMMENT PANELS // YZ PLANE
COMMENT CELL SIDE +X
PLATE
CORNER -2 -8 9
DELTAS 0 8 6
TOP +X FSLICA
BOTTOM -X BLKVEL
ENDOBJ
PLATE
CORNER -2 -8 -15
DELTAS 0 8 6
TOP +X FSLICA
BOTTOM -X BLKVEL
ENDOBJ
PLATE
CORNER -2 -4 13
DELTAS 0 1 1
TOP +X KAP1TN
BOTTOM -X BLKVEL
ENDOBJ
PLATE
CORNER -2 -4 -14
DELTAS 0 1 1
TOP +X KAP1TN
BOTTOM -X BLKVEL
ENDOBJ
COMMENT SOLAR ARRAY BOOMS
BOOM
```

```
AXIS -2 -4 3  -2 -4 9
RADIUS 0.06
SURFACE LFALUM
ENDOBJ
BOOM
AXIS -2 -4 -9  -2 -4 -3
RADIUS 0.06
SURFACE LFALUM
ENDOBJ
ENDSAT
```

Flux Defintion File (fort.22) for 3-Axis Stabilized Spacecraft in Sunlight

```
single maxwellian
1.12e6 mks
12 kev
2.36e5 mks
29.5 kev
end
```

Interactive Execution Runstream for Objdisp 3-Axis Stabilized Spacecraft in Sunlight.

The following was used to create Figure 31.

```
 asgfil called for lun =  21

 NZ>33

 NG>1

 XMESH>
0  OBJECT DEFINITION INFORMATION BEING READ FROM FILE
0A SHADOWING TABLE WAS PREVIOUSLY GENERATED
  FOR THIS OBJECT USING THE HIDC OPTION
 asgfil called for lun =   2

MATERIAL PLOTS?>no
0 PERSPECTIVE PLOTS -- <CR> TO EXIT

X> 1

Y> .1

Z> -.2
 HIDCEL - DIR = (  .9759001,  .0975900, -.1951800)
 DISTANCE = 1000.00
 **WARNING**  IN HIDCEL NJT=  12 IPPS=  36001200000 BYPASSED ADDA1
0FINAL NA1 =   298
0 PERSPECTIVE PLOTS -- <CR> TO EXIT

X>
 [EXIT]
```

Termtalk Execution (fort.3) for 3-Axis Stabilized Spacecraft in Sunlight

A group of surface cells is defined for each of the materials. The final potentials for each of the groups is requested. A history of the potential over time for the highest potential cell and for one conducting cell is requested. The results are shown in Figure 33 and Table 9.

```
 CHOOSE ANY MODULE
 HELP IS ALWAYS AVAILABLE - TYPE 'HELP'
>subset KAP3TN
DEFINITION OF NEW SUBSET NAMED KAP3
 487 REMAINING IN GROUP
 SUBSET INSTRUCTION PLEASE ?
>material KAP3TN
  31 REMAINING IN GROUP
 SUBSET INSTRUCTION PLEASE ?
>done
GROUP KAP3 WITH   31 MEMBERS IS NOW DEFINED
RETURNING TO MODULE  'MAIN'
 CHOOSE ANY MODULE
 HELP IS ALWAYS AVAILABLE - TYPE 'HELP'
>subset LFALUN
DEFINITION OF NEW SUBSET NAMED LFAL
 487 REMAINING IN GROUP
 SUBSET INSTRUCTION PLEASE ?
>material LFALUM
  19 REMAINING IN GROUP
 SUBSET INSTRUCTION PLEASE ?
>done
GROUP LFAL WITH   19 MEMBERS IS NOW DEFINED
RETURNING TO MODULE  'MAIN'
 CHOOSE ANY MODULE
 HELP IS ALWAYS AVAILABLE - TYPE 'HELP'
>subset S13GLO
DEFINITION OF NEW SUBSET NAMED S13G
 487 REMAINING IN GROUP
 SUBSET INSTRUCTION PLEASE ?
>material S13GLO
  25 REMAINING IN GROUP
 SUBSET INSTRUCTION PLEASE ?
>done
GROUP S13G WITH   25 MEMBERS IS NOW DEFINED
RETURNING TO MODULE  'MAIN'
 CHOOSE ANY MODULE
 HELP IS ALWAYS AVAILABLE - TYPE 'HELP'
>subset FSLICA
DEFINITION OF NEW SUBSET NAMED FSLI
 487 REMAINING IN GROUP
 SUBSET INSTRUCTION PLEASE ?
>material FSLICA
 117 REMAINING IN GROUP
 SUBSET INSTRUCTION PLEASE ?
>done
GROUP FSLI WITH  117 MEMBERS IS NOW DEFINED
RETURNING TO MODULE  'MAIN'
 CHOOSE ANY MODULE
 HELP IS ALWAYS AVAILABLE - TYPE 'HELP'
>subset BLKVEL
DEFINITION OF NEW SUBSET NAMED BLKV
 487 REMAINING IN GROUP
 SUBSET INSTRUCTION PLEASE ?
```

```
>material BLKVEL
  96 REMAINING IN GROUP
 SUBSET INSTRUCTION PLEASE ?
>done
GROUP BLKV WITH   96 MEMBERS IS NOW DEFINED
RETURNING TO MODULE  'MAIN'
 CHOOSE ANY MODULE
 HELP IS ALWAYS AVAILABLE - TYPE 'HELP'
>subset SSMESH
DEFINITION OF NEW SUBSET NAMED SSME
 487 REMAINING IN GROUP
 SUBSET INSTRUCTION PLEASE ?
>material SSMESH
  84 REMAINING IN GROUP
 SUBSET INSTRUCTION PLEASE ?
>done
GROUP SSME WITH   84 MEMBERS IS NOW DEFINED
RETURNING TO MODULE  'MAIN'
 CHOOSE ANY MODULE
 HELP IS ALWAYS AVAILABLE - TYPE 'HELP'
>subset KAP1TH
DEFINITION OF NEW SUBSET NAMED KAP1
 487 REMAINING IN GROUP
 SUBSET INSTRUCTION PLEASE ?
>material KAP1TH
  55 REMAINING IN GROUP
 SUBSET INSTRUCTION PLEASE ?
>done
GROUP KAP1 WITH   55 MEMBERS IS NOW DEFINED
RETURNING TO MODULE  'MAIN'
 CHOOSE ANY MODULE
 HELP IS ALWAYS AVAILABLE - TYPE 'HELP'
>subset KAP2TH
DEFINITION OF NEW SUBSET NAMED KAP2
 487 REMAINING IN GROUP
 SUBSET INSTRUCTION PLEASE ?
>material KAP2TH
  20 REMAINING IN GROUP
 SUBSET INSTRUCTION PLEASE ?
>done
GROUP KAP2 WITH   20 MEMBERS IS NOW DEFINED
RETURNING TO MODULE  'MAIN'
 CHOOSE ANY MODULE
 HELP IS ALWAYS AVAILABLE - TYPE 'HELP'
>subset EHFPRT
DEFINITION OF NEW SUBSET NAMED EHFP
 487 REMAINING IN GROUP
 SUBSET INSTRUCTION PLEASE ?
>material EHFPRT
   1 REMAINING IN GROUP
 SUBSET INSTRUCTION PLEASE ?
>done
REMAINING MEMBER IS  # 308
THIS SUBSET HAS 1 MEMBERS
IT WILL NOT BE CATALOGUED
RETURNING TO MODULE 'MAIN'
 CHOOSE ANY MODULE
 HELP IS ALWAYS AVAILABLE - TYPE 'HELP'
>subset ALUM
DEFINITION OF NEW SUBSET NAMED ALUM
 487 REMAINING IN GROUP
 SUBSET INSTRUCTION PLEASE ?
>material ALUM
  17 REMAINING IN GROUP
```

```
 SUBSET INSTRUCTION PLEASE ?
>done
GROUP ALUM WITH   37 MEMBERS IS NOW DEFINED
RETURNING TO MODULE  'MAIN'
 CHOOSE ANY MODULE
 HELP IS ALWAYS AVAILABLE - TYPE 'HELP'
>subset CPHEML
DEFINITION OF NEW SUBSET NAMED CPHE
 487 REMAINING IN GROUP
 SUBSET INSTRUCTION PLEASE ?
>material CPHEML
   1 REMAINING IN GROUP
 SUBSET INSTRUCTION PLEASE ?
>done
REMAINING MEMBER IS  # 259
THIS SUBSET HAS 1 MEMBERS
IT WILL NOT BE CATALOGUED
RETURNING TO MODULE 'MAIN'
 CHOOSE ANY MODULE
 HELP IS ALWAYS AVAILABLE - TYPE 'HELP'
>latest
 LATEST COMMAND OR MODE SET ?
>potential
MODE RESET
 LATEST COMMAND OR MODE SET ?
>absmag
MODE RESET
 LATEST COMMAND OR MODE SET ?
>group KAPITN
POTL IN VOLTS  FOR NASCAP CYCLE  20 ... TIME = 1.20e+03 SEC
 358-6.00e+03  361-6.00e+03   72-6.00e+03   69-6.00e+03  134-6.00e+03
 260-6.00e+03   71-6.00e+03  257-6.00e+03   70-6.00e+03  360-6.00e+03
 359-6.00e+03  131-6.00e+03  132-6.00e+03  258-6.00e+03  133-6.00e+03
 262-6.00e+03  256-6.00e+03  136-6.00e+03  130-6.00e+03  362-6.00e+03
 392-6.00e+03  390-6.00e+03  356-6.00e+03  394-6.00e+03   67-6.00e+03
  73-6.00e+03  388-6.00e+03   23-6.00e+03   25-6.00e+03   27-6.00e+03
  21-6.00e+03    0 0.00e+00    0 0.00e+00    0 0.00e+00    0 0.00e+00
 LATEST COMMAND OR MODE SET ?
>group LVALOW
POTL IN VOLTS  FOR NASCAP CYCLE  20 ... TIME = 1.20e+03 SEC
 477-2.08e+02  479-2.08e+02  484-2.08e+02  483-2.08e+02  482-2.08e+02
 478-2.08e+02  472-2.08e+02  485-2.08e+02  481-2.08e+02  480-2.08e+02
 476-2.08e+02  471-2.08e+02  474-2.08e+02  473-2.08e+02  486-2.08e+02
 475-2.08e+02  470-2.08e+02  469-2.08e+02  468-2.08e+02    0 0.00e+00
 LATEST COMMAND OR MODE SET ?
>group S13OLO
POTL IN VOLTS  FOR NASCAP CYCLE  20 ... TIME = 1.20e+03 SEC
 460-2.08e+02  174-2.08e+02  173-2.08e+02  182-2.08e+02   83-2.08e+02
  81-2.08e+02  179-2.08e+02   85-2.08e+02   84-2.08e+02  309-2.08e+02
 462-2.08e+02  463-2.08e+02  370-2.08e+02  372-2.08e+02  180-2.08e+02
 461-2.08e+02  306-2.08e+02  307-2.08e+02  181-2.01e+02  455-2.01e+02
 465-1.99e+02  467-1.99e+02  466-1.99e+02  305-1.98e+02  454-1.89e+02
 LATEST COMMAND OR MODE SET ?
>group PELICA
POTL IN VOLTS  FOR NASCAP CYCLE  20 ... TIME = 1.20e+03 SEC
 310-2.93e+03  183-2.93e+03  290-2.93e+03   44-2.93e+03   38-2.93e+03
  78-2.93e+03  150-2.93e+03   29-2.93e+03   32-2.93e+03  261-2.93e+03
  68-2.93e+03   26-2.93e+03  129-1.45e+03  393-1.27e+03  399-1.17e+03
 396-9.85e+02  279-8.54e+02  161-7.39e+02  177-6.86e+02  401-6.19e+02
 411-5.66e+02  303-5.53e+02  405-4.31e+02  101-3.41e+02  117-3.37e+02
 137-3.27e+02  151-3.14e+02  100-3.12e+02  112-3.06e+02  165-3.00e+02
 128-2.94e+02  102-2.90e+02  118-2.89e+02  185-2.87e+02  138-2.86e+02
 148-2.81e+02  192-2.78e+02  199-2.75e+02  166-2.69e+02   99-2.69e+02
 162-2.68e+02  111-2.66e+02  213-2.61e+02  119-2.61e+02  103-2.61e+02
```

```
127-2.61e+02  186-2.60e+02  139-2.59e+02  176-2.56e+02  153-2.54e+02
147-2.53e+02  200-2.50e+02  167-2.48e+02  196-2.47e+02   98-2.44e+02
161-2.44e+02  110-2.42e+02  214-2.42e+02  187-2.41e+02  210-2.39e+02
126-2.39e+02  104-2.38e+02  120-2.38e+02  140-2.36e+02  175-2.36e+02
201-2.33e+02  146-2.33e+02  154-2.33e+02  168-2.29e+02  195-2.28e+02
215-2.28e+02  160-2.27e+02   97-2.25e+02  188-2.24e+02  209-2.24e+02
109-2.23e+02  105-2.21e+02  174-2.21e+02  121-2.20e+02  125-2.20e+02
141-2.19e+02  202-2.19e+02  155-2.17e+02  145-2.16e+02  194-2.16e+02
216-2.16e+02  208-2.13e+02  159-2.12e+02   96-2.12e+02  189-2.11e+02
106-2.09e+02  108-2.09e+02  122-2.09e+02  173-2.08e+02  203-2.08e+02
142-2.08e+02  124-2.07e+02  217-2.07e+02  156-2.06e+02  193-2.05e+02
144-2.04e+02  207-2.04e+02  170-2.04e+02  190-2.02e+02   95-2.02e+02
204-2.01e+02  107-2.00e+02  218-2.00e+02  172-1.99e+02  123-1.98e+02
192-1.97e+02  206-1.97e+02  143-1.97e+02  157-1.95e+02  171-1.93e+02
191-1.92e+02  205-1.92e+02    0 0.00e+00    0 0.00e+00    0 0.00e+00
 LATEST COMMAND OR MODE SET ?
>group ELEVEL
POTL IN VOLTS  FOR NASCAP CYCLE  20 ... TIME = 1.20e+03 SEC
 232-2.08e+02  227-2.08e+02  226-2.08e+02  229-2.08e+02  228-2.08e+02
 343-2.08e+02  342-2.08e+02  225-2.08e+02  340-2.08e+02  337-2.08e+02
 224-2.08e+02  335-2.08e+02  223-2.08e+02  222-2.08e+02  221-2.08e+02
 231-2.08e+02  230-2.08e+02  264-2.08e+02  344-2.08e+02  341-2.08e+02
 336-2.08e+02  334-2.08e+02  263-2.08e+02  254-2.08e+02  253-2.08e+02
 252-2.08e+02  329-2.08e+02  328-2.08e+02  327-2.08e+02  326-2.08e+02
 323-2.08e+02  322-2.08e+02  321-2.08e+02  320-2.08e+02  251-2.08e+02
 235-2.08e+02  234-2.08e+02  248-2.08e+02  315-2.08e+02  314-2.08e+02
 313-2.08e+02  312-2.08e+02  302-2.08e+02  301-2.08e+02  300-2.08e+02
 299-2.08e+02  247-2.08e+02  246-2.08e+02  245-2.08e+02  295-2.08e+02
 294-2.08e+02  293-2.08e+02  292-2.08e+02  291-2.08e+02  288-2.08e+02
 287-2.08e+02  286-2.08e+02  285-2.08e+02  244-2.08e+02  243-2.08e+02
 283-2.08e+02  281-2.08e+02  280-2.08e+02  279-2.08e+02  278-2.08e+02
 277-2.08e+02  274-2.08e+02  273-2.08e+02  272-2.08e+02  271-2.08e+02
 237-2.08e+02  236-2.08e+02  268-2.08e+02  267-2.08e+02  266-2.08e+02
 265-2.08e+02  270-2.08e+02  284-2.08e+02  316-2.08e+02  250-2.08e+02
 330-2.08e+02  282-2.08e+02  296-2.08e+02  298-2.08e+02  319-2.08e+02
 317-2.08e+02  345-2.08e+02  333-2.08e+02  233-2.08e+02  331-2.08e+02
 249-2.08e+02  269-2.08e+02  283-2.08e+02  297-2.08e+02  318-2.08e+02
 332-2.08e+02    0 0.00e+00    0 0.00e+00    0 0.00e+00    0 0.00e+00
 LATEST COMMAND OR MODE SET ?
>group ERROR
POTL IN VOLTS  FOR NASCAP CYCLE  20 ... TIME = 1.20e+03 SEC
 441-2.08e+02  440-2.08e+02  439-2.08e+02  438-2.08e+02  437-2.08e+02
 436-2.08e+02  435-2.08e+02  434-2.08e+02  433-2.08e+02  432-2.08e+02
 431-2.08e+02  430-2.08e+02  429-2.08e+02  428-2.08e+02  427-2.08e+02
 426-2.08e+02  425-2.08e+02  424-2.08e+02  423-2.08e+02  422-2.08e+02
 421-2.08e+02  420-2.08e+02  419-2.08e+02  418-2.08e+02  417-2.08e+02
 416-2.08e+02  415-2.08e+02  414-2.08e+02  413-2.08e+02  412-2.08e+02
 383-2.08e+02  382-2.08e+02  381-2.08e+02  380-2.08e+02  379-2.08e+02
 378-2.08e+02  347-2.08e+02  346-2.08e+02  339-2.08e+02  338-2.08e+02
 325-2.08e+02  324-2.08e+02  220-2.08e+02  219-2.08e+02  212-2.08e+02
 211-2.08e+02  199-2.08e+02  197-2.08e+02   94-2.08e+02   93-2.08e+02
  92-2.08e+02   91-2.08e+02   90-2.08e+02   89-2.08e+02   58-2.08e+02
  57-2.08e+02   56-2.08e+02   55-2.08e+02   54-2.08e+02   53-2.08e+02
  52-2.08e+02   51-2.08e+02   50-2.08e+02   49-2.08e+02   48-2.08e+02
  47-2.08e+02   46-2.08e+02   45-2.08e+02   16-2.08e+02   15-2.08e+02
  14-2.08e+02   13-2.08e+02   12-2.08e+02   11-2.08e+02   10-2.08e+02
   9-2.08e+02    8-2.08e+02    7-2.08e+02    6-2.08e+02    5-2.08e+02
   4-2.08e+02    3-2.08e+02    2-2.08e+02    1-2.08e+02    0 0.00e+00
 LATEST COMMAND OR MODE SET ?
>group KAPITH
POTL IN VOLTS  FOR NASCAP CYCLE  20 ... TIME = 1.20e+03 SEC
  62-3.27e+03  119-3.26e+03   63-3.26e+03   61-3.14e+03   64-3.14e+03
 241-3.12e+03  164-2.95e+03   88-2.95e+03   80-2.95e+03  276-2.95e+03
  77-2.95e+03   40-2.95e+03   42-2.95e+03   76-2.95e+03   75-2.95e+03
```

```
 33-2.95e+03   36-2.95e+03   34-2.95e+03   35-2.95e+03   30-2.95e+03
 31-2.95e+03  135-2.95e+03   74-2.95e+03   22-2.95e+03   28-2.95e+03
 24-2.95e+03  110-2.75e+03  240-2.57e+03  352-2.54e+03  351-2.51e+03
354-2.36e+03  349-2.33e+03  363-1.62e+03  255-1.51e+03  365-1.44e+03
395-1.41e+03  357-1.32e+03  389-1.26e+03  391-1.25e+03  367-1.10e+03
149-1.05e+03  398-9.86e+02  364-9.77e+02  397-9.55e+02  403-8.42e+02
377-7.90e+02  402-6.51e+02  366-6.48e+02  400-6.46e+02  289-5.37e+02
369-4.44e+02  409-3.98e+02  407-3.74e+02  169-2.14e+02  158-2.02e+02
 LATEST COMMAND OR MODE SET ?
>group KAP2TW
POTL IN VOLTS  FOR NASCAP CYCLE  20 ... TIME = 1.20e+03 SEC
 408-9.67e+02  410-7.48e+02   86-6.38e+02   41-4.73e+02   87-4.36e+02
 375-4.12e+02   82-2.99e+02  178-2.50e+02  184-2.47e+02   39-2.41e+02
 304-2.40e+02  311-2.36e+02  406-2.24e+02  371-2.17e+02  404-1.78e+02
 368-1.49e+02   43-1.40e+02  376-5.76e+01   37-5.27e+01   79-5.27e+01
 LATEST COMMAND OR MODE SET ?
>group ALUM
POTL IN VOLTS  FOR NASCAP CYCLE  20 ... TIME = 1.20e+03 SEC
 464-2.08e+02  459-2.08e+02  458-2.08e+02  457-2.08e+02  456-2.08e+02
 453-2.08e+02  452-2.08e+02  451-2.08e+02  450-2.08e+02  449-2.08e+02
 448-2.08e+02  447-2.08e+02  446-2.08e+02  445-2.08e+02  444-2.08e+02
 443-2.08e+02  442-2.08e+02  387-2.08e+02  386-2.08e+02  385-2.08e+02
 384-2.08e+02  355-2.08e+02  353-2.08e+02  350-2.08e+02  348-2.08e+02
 242-2.08e+02  239-2.08e+02  116-2.08e+02  113-2.08e+02   66-2.08e+02
  65-2.08e+02   60-2.08e+02   59-2.08e+02   20-2.08e+02   19-2.08e+02
  18-2.08e+02   17-2.08e+02    0 0.00e+00    0 0.00e+00    0 0.00e+00
 LATEST COMMAND OR MODE SET ?
>single
 SINGLE COMMAND OR MODE SET ?
>308
------------------------------------------------------------------------
  SURFACE CELL NO.  308
                                  CENTERED AT     -1.3   -2.0     .7
                                  MATERIAL IS  EMPP
                       POTENTIAL =-2.078e+02 VOLTS
 SINGLE COMMAND OR MODE SET ?
>359
------------------------------------------------------------------------
  SURFACE CELL NO.  359
                                  CENTERED AT     -1.5   -6.0     .5
                                  MATERIAL IS  CPHE
                       POTENTIAL =-1.218e+02 VOLTS
 SINGLE COMMAND OR MODE SET ?
>history
 HISTORY COMMAND OR MODE SET ?
>358
POTL IN VOLTS
  TIME  :   358
--------:-------------------------------------------------------------
        :    #1       #2       #3       #4       #5       #6       #7
 6.0e+01:-1.91e+02
 1.2e+02:-8.07e+02
 1.8e+02:-1.16e+03
 2.4e+02:-1.55e+03
 3.0e+02:-1.83e+03
 3.6e+02:-2.21e+03
 4.2e+02:-2.51e+03
 4.8e+02:-2.84e+03
 5.4e+02:-3.13e+03
 6.0e+02:-3.42e+03
 6.6e+02:-3.71e+03
 7.2e+02:-3.98e+03
 7.8e+02:-4.25e+03
 8.4e+02:-4.52e+03
```

```
 9.0e+02:-4.77e+03
 9.6e+02:-5.02e+03
 1.0e+03:-5.26e+03
 1.1e+03:-5.53e+03
 1.1e+03:-5.77e+03
 1.2e+03:-6.00e+03
POTL VERSUS LOG(TIME)
```

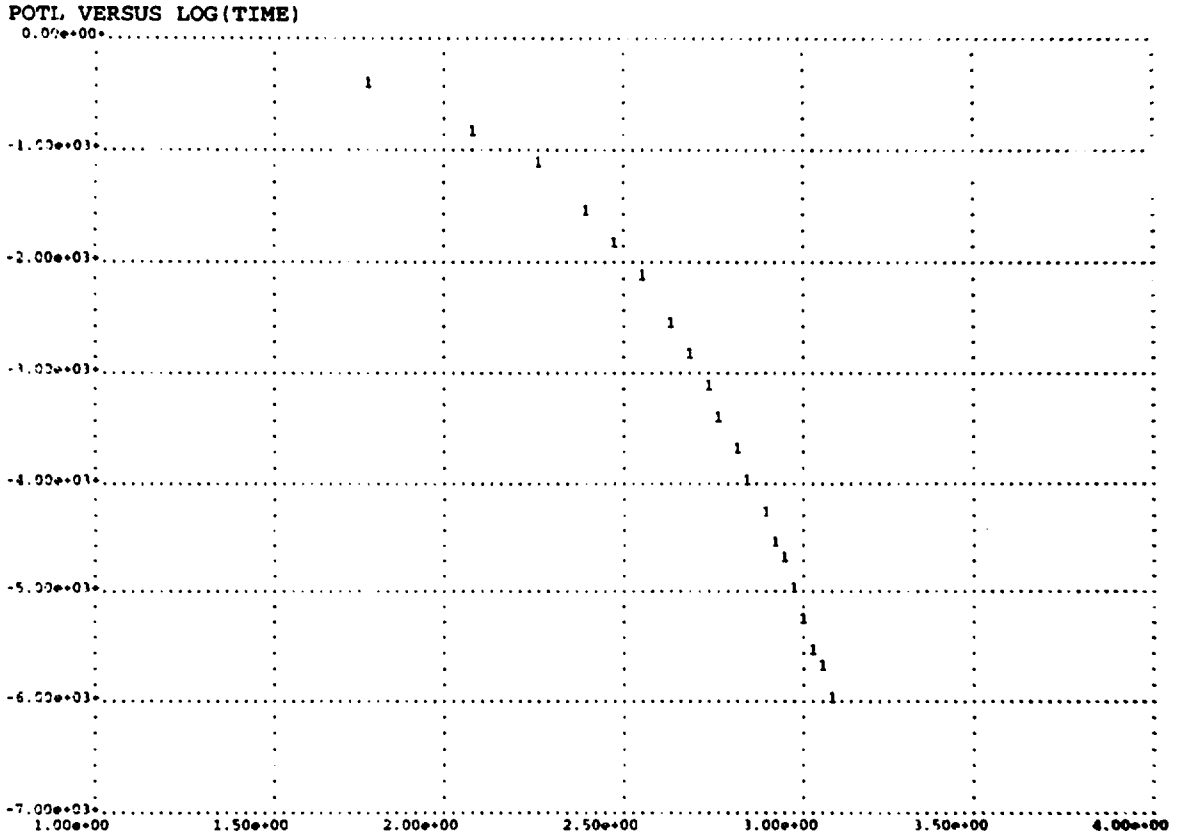


```
 HISTORY COMMAND OR MODE SET ?
>477
POTL IN VOLTS
  TIME  :   477
--------:-------------------------------------------------------------
        :    #1       #2       #3       #4       #5       #6       #7
 6.0e+01:-4.72e+00
 1.2e+02:-5.21e+01
 1.8e+02:-5.14e+01
 2.4e+02:-8.93e+01
 3.0e+02:-8.99e+01
 3.6e+02:-9.52e+01
 4.2e+02:-9.82e+01
 4.8e+02:-1.03e+02
 5.4e+02:-1.07e+02
 6.0e+02:-1.07e+02
 6.6e+02:-1.13e+02
 7.2e+02:-1.20e+02
 7.8e+02:-1.20e+02
 8.4e+02:-1.30e+02
 9.0e+02:-1.36e+02
 9.6e+02:-1.38e+02
 1.0e+03:-1.46e+02
 1.1e+03:-1.80e+02
 1.1e+03:-1.95e+02
 1.2e+03:-2.08e+02
POTL VERSUS LOG(TIME)
```

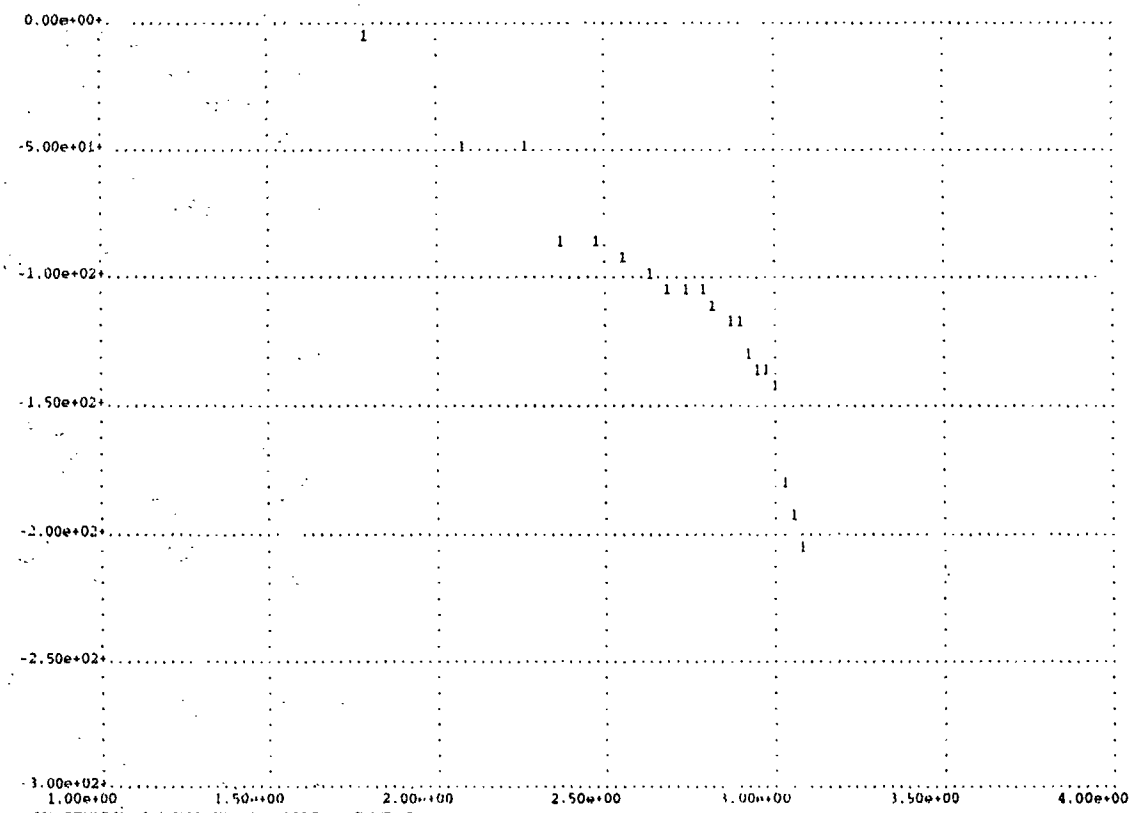


```
 HISTORY COMMAND OR MODE SET ?
>exit
```

Interactive Runstream for the Execution of Contours for 3-Axis Stabilized Spacecraft in Sunlight

The following was used to create Figures 34 and 35.

```
 ENTER TITLE>:

 asgfil called for lun =   2
 asgfil called for lun =  21

 NZ>33

 NG>

 ENTER THE CUT-PLANE"S NORMAL DIRECTION  (X,Y,OR    Z), OR QUIT (Q)> z

 ENTER THE CUT-PLANE"S OFFSET ALONG THE NORMAL>14

ENTER 1 (SINGLE), 2 (DOUBLE), OR 0 (OMIT) TO SPECIFY FORMAT OF ZERO-POTENTIAL>:
 DEFAULT STRING <SINGLE> ASSIGNED.

 ENTER THE CUT-PLANE"S NORMAL DIRECTION  (X,Y,OR    Z), OR QUIT (Q)> z

 ENTER THE CUT-PLANE"S OFFSET ALONG THE NORMAL>17

ENTER 1 (SINGLE), 2 (DOUBLE), OR 0 (OMIT) TO SPECIFY FORMAT OF ZERO-POTENTIAL>:
 DEFAULT STRING <SINGLE> ASSIGNED.
```

```
ENTER THE CUT-PLANE'S NORMAL DIRECTION  (X,Y,OR    Z), OR QUIT (Q)> q
PREPARING TO DUMP AND QUIT.
[EXIT]
```

C.9 Polar Orbiting Spacecraft–DMSP

The following files are the input and output files from the various computer codes used in the example discussed in Section 5.1.3.

suchgr Execution (fort.3) Polar Orbiting Spacecraft—DMSP

This is the fort.3 file generated from the execution of **suchgr** for this problem. The environment is set to the severe auroral environment. Space-charge-limited current collection is requested, the mach velocity is set to 6.7, and the spacecraft radius is set to 1.9 m. The material is set to SOLA. A summary of potentials and currents before and after charging is requested. The process is repeated for all of the surface materials. The results are shown in Table 10.

```
Welcome to SUCHGR 1.3

***ERROR - READMS - LUN 1. KEY=       1 NOT PREVIOUSLY WRITTEN.
***ERROR - READMS - LUN 19 KEY=CONT NOT PREVIOUSLY WRITTEN.
***ERROR - READMS - LUN 19 KEY=MT19 NOT PREVIOUSLY WRITTEN.
    Default material is
    Default environment is DMSP

 SUCHGR command >>  DEN1 3.55e9

 SUCHGR command >>  TEMP1 0.2

 SUCHGR command >>  DEN2   6.0E5

 SUCHGR command >>  TEMP2  8.0E3

 SUCHGR command >>  GAUCO  4.0e4

 SUCHGR command >>  ENAUT  2.4E4

 SUCHGR command >>  DELTA  1.6E4

 SUCHGR command >>  POWCO  3.0E11

 SUCHGR command >>  PALPHA 1.1

 SUCHGR command >>  PCUTL  50.0

 SUCHGR command >>  PCUTH  1.6E6

 SUCHGR command >>  vend -5000

 SUCHGR command >>  spclim

 SUCHGR command >>  avmach 6.7
```

```
 SUCHGR command >>  robj 1.9

 SUCHGR command >>  mate sola
Setting default values for material SOLA

 SUCHGR command >>  charge

 Charged under Space Charge Limited Regime
                                    Initial       Final       Units
                                    -------       -----       -----
    Surface Potential              0.0000e+00   -4.9125e+02 volts
    Conductor Potential            0.0000e+00    0.0000e+00 volts

 Flux Breakdown:
    Incident Electron Flux        -5.8523e-05   -1.5199e-05 A/m**2
    Electron Secondary Flux        3.7908e-06    3.0361e-06 A/m**2
    Backscattered Electron Flux    2.7606e-06    2.6164e-06 A/m**2

    Incident Ion Flux              4.1548e-07    9.4658e-06 A/m**2
    Ion Secondary Flux             0.0000e+00    1.0897e-07 A/m**2

    Photo Flux                     0.0000e+00    0.0000e+00 A/m**2
    Conduction Flux                0.0000e+00    0.0000e+00 A/m**2
                                   -----------   -----------
    Total Flux                    -5.1556e-05    2.8271e-08 A/m**2

 Init  Sheath Radius= 1.900e+00 meters  AVMACH= 6.700e+00
 Final Sheath Radius= 9.069e+00 meters  ROBJ  = 1.900e+00 meters

 SUCHGR command >>  mate npai
Setting default values for material NPAI

 SUCHGR command >>  charge

 Charged under Space Charge Limited Regime
                                    Initial       Final       Units
                                    -------       -----       -----
    Surface Potential              0.0000e+00   -5.4125e+02 volts
    Conductor Potential            0.0000e+00    0.0000e+00 volts

 Flux Breakdown:
    Incident Electron Flux        -5.8523e-05   -1.5155e-05 A/m**2
    Electron Secondary Flux        4.3803e-06    3.1805e-06 A/m**2
    Backscattered Electron Flux    1.7080e-06    1.5942e-06 A/m**2

    Incident Ion Flux              4.1548e-07    1.0148e-05 A/m**2
    Ion Secondary Flux             0.0000e+00    2.8374e-07 A/m**2

    Photo Flux                     0.0000e+00    0.0000e+00 A/m**2
    Conduction Flux                0.0000e+00    0.0000e+00 A/m**2
                                   -----------   -----------
    Total Flux                    -5.2019e-05    5.1363e-08 A/m**2

 Init  Sheath Radius= 1.900e+00 meters  AVMACH= 6.700e+00
 Final Sheath Radius= 9.390e+00 meters  ROBJ  = 1.900e+00 meters

 SUCHGR command >>  mate aqua
Setting default values for material AQUA

 SUCHGR command >>  charge

 Charged under Space Charge Limited Regime
                                    Initial       Final       Units
                                    -------       -----       -----
```

```
   Surface Potential                 0.0000e+00   -6.0375e+02 volts
   Conductor Potential               0.0000e+00    0.0000e+00 volts

Flux Breakdown:
   Incident Electron Flux           -5.8523e-05   -1.5102e-05 A/m**2
   Electron Secondary Flux           2.2214e-06    1.7910e-06 A/m**2
   Backscattered Electron Flux       1.9551e-06    1.8232e-06 A/m**2

   Incident Ion Flux                 4.1548e-07    1.0997e-05 A/m**2
   Ion Secondary Flux                0.0000e+00    4.0207e-07 A/m**2

   Photo Flux                        0.0000e+00    0.0000e+00 A/m**2
   Conduction Flux                   0.0000e+00    0.0000e+00 A/m**2
                                     -----------   -----------
   Total Flux                       -5.3931e-05   -8.9032e-08 A/m**2

 Init  Sheath Radius= 1.900e+00 meters  AVMACH= 6.700e+00
 Final Sheath Radius= 9.775e+00 meters  ROBJ  = 1.900e+00 meters

 SUCHGR command >>  mate kapt
Setting default values for material KAPT

 SUCHGR command >>  charge

 Charged under Space Charge Limited Regime
                                    Initial       Final       Units
                                    -------       -----       -----
   Surface Potential                0.0000e+00   -6.4125e+02 volts
   Conductor Potential              0.0000e+00    0.0000e+00 volts

 Flux Breakdown:
   Incident Electron Flux          -5.8523e-05   -1.5070e-05 A/m**2
   Electron Secondary Flux          2.8429e-06    1.5059e-06 A/m**2
   Backscattered Electron Flux      1.7080e-06    1.5819e-06 A/m**2

   Incident Ion Flux                4.1548e-07    1.1511e-05 A/m**2
   Ion Secondary Flux               0.0000e+00    4.8213e-07 A/m**2

   Photo Flux                       0.0000e+00    0.0000e+00 A/m**2
   Conduction Flux                  0.0000e+00    0.0000e+00 A/m**2
                                    -----------   -----------
   Total Flux                      -5.3556e-05    1.0892e-08 A/m**2

 Init  Sheath Radius= 1.900e+00 meters  AVMACH= 6.700e+00
 Final Sheath Radius= 1.000e+01 meters  ROBJ  = 1.900e+00 meters

 SUCHGR command >>  mate alum
Setting default values for material ALUM

 SUCHGR command >>  charge

 Charged under Space Charge Limited Regime
                                    Initial       Final       Units
                                    -------       -----       -----
   Surface Potential                0.0000e+00   -5.6625e+02 volts
   Conductor Potential              0.0000e+00    0.0000e+00 volts

 Flux Breakdown:
   Incident Electron Flux          -5.8523e-05   -1.5134e-05 A/m**2
   Electron Secondary Flux          1.8627e-06    1.3977e-06 A/m**2
   Backscattered Electron Flux      3.2424e-06    3.0656e-06 A/m**2

   Incident Ion Flux                4.1548e-07    1.0486e-05 A/m**2
   Ion Secondary Flux               0.0000e+00    1.7658e-07 A/m**2
```

```
   Photo Flux                      0.0000e+00    0.0000e+00 A/m**2
   Conduction Flux                 0.0000e+00    0.0000e+00 A/m**2
                                  -----------   -----------
   Total Flux                     -5.3002e-05   -7.5891e-09 A/m**2

 Init  Sheath Radius= 1.900e+00 meters  AVMACH= 6.700e+00
 Final Sheath Radius= 9.545e+00 meters  ROBJ  = 1.900e+00 meters

 SUCHGR command >> mate tefl
Setting default values for material TEFL

 SUCHGR command >> charge

 Charged under Space Charge Limited Regime
                                  Initial       Final       Units
                                  -------       -----       -----
   Surface Potential              0.0000e+00   -5.2875e+02 volts
   Conductor Potential            0.0000e+00    0.0000e+00 volts

 Flux Breakdown:
   Incident Electron Flux        -5.8523e-05   -1.5166e-05 A/m**2
   Electron Secondary Flux        3.9214e-06    2.7974e-06 A/m**2
   Backscattered Electron Flux    2.1803e-06    2.0504e-06 A/m**2

   Incident Ion Flux              4.1548e-07    9.9798e-06 A/m**2
   Ion Secondary Flux             0.0000e+00    2.6240e-07 A/m**2

   Photo Flux                     0.0000e+00    0.0000e+00 A/m**2
   Conduction Flux                0.0000e+00    0.0000e+00 A/m**2
                                  -----------   -----------
   Total Flux                    -5.2005e-05   -7.6453e-08 A/m**2

 Init  Sheath Radius= 1.900e+00 meters  AVMACH= 6.700e+00
 Final Sheath Radius= 9.312e+00 meters  ROBJ  = 1.900e+00 meters

 SUCHGR command >> mate gold
Setting default values for material GOLD

 SUCHGR command >> charge

 Charged under Space Charge Limited Regime
                                  Initial       Final       Units
                                  -------       -----       -----
   Surface Potential              0.0000e+00   -1.8750e+02 volts
   Conductor Potential            0.0000e+00    0.0000e+00 volts

 Flux Breakdown:
   Incident Electron Flux        -5.8523e-05   -1.5497e-05 A/m**2
   Electron Secondary Flux        3.0267e-06    2.8391e-06 A/m**2
   Backscattered Electron Flux    8.0270e-06    7.8697e-06 A/m**2

   Incident Ion Flux              4.1548e-07    4.7575e-06 A/m**2
   Ion Secondary Flux             0.0000e+00    5.3101e-08 A/m**2

   Photo Flux                     0.0000e+00    0.0000e+00 A/m**2
   Conduction Flux                0.0000e+00    0.0000e+00 A/m**2
                                  -----------   -----------
   Total Flux                    -4.7054e-05    2.2975e-08 A/m**2

 Init  Sheath Radius= 1.900e+00 meters  AVMACH= 6.700e+00
 Final Sheath Radius= 6.429e+00 meters  ROBJ  = 1.900e+00 meters

 SUCHGR command >> mate cpai
```

```
Setting default values for material CPAI

 SUCHGR command >>  charge

 Charged under Space Charge Limited Regime
                                    Initial       Final       Units
                                    -------       -----       -----
    Surface Potential              0.0000e+00   -6.4125e+02 volts
    Conductor Potential            0.0000e+00    0.0000e+00 volts

 Flux Breakdown:
    Incident Electron Flux        -5.8523e-05   -1.5070e-05 A/m**2
    Electron Secondary Flux        2.8429e-06    1.5059e-06 A/m**2
    Backscattered Electron Flux    1.7080e-06    1.5819e-06 A/m**2

    Incident Ion Flux              4.1548e-07    1.1511e-05 A/m**2
    Ion Secondary Flux             0.0000e+00    4.8213e-07 A/m**2

    Photo Flux                     0.0000e+00    0.0000e+00 A/m**2
    Conduction Flux                0.0000e+00    0.0000e+00 A/m**2
                                   -----------   -----------
    Total Flux                    -5.3556e-05    1.0892e-08 A/m**2

 Init  Sheath Radius= 1.900e+00 meters  AVMACH= 6.700e+00
 Final Sheath Radius= 1.000e+01 meters  ROBJ  = 1.900e+00 meters

 SUCHGR command >>  mate silv
Setting default values for material SILV

 SUCHGR command >>  charge

 Charged under Space Charge Limited Regime
                                    Initial       Final       Units
                                    -------       -----       -----
    Surface Potential              0.0000e+00   -2.9438e+02 volts
    Conductor Potential            0.0000e+00    0.0000e+00 volts

 Flux Breakdown:
    Incident Electron Flux        -5.8523e-05   -1.5382e-05 A/m**2
    Electron Secondary Flux        2.8423e-06    2.6023e-06 A/m**2
    Backscattered Electron Flux    6.3595e-06    6.1775e-06 A/m**2

    Incident Ion Flux              4.1548e-07    6.5072e-06 A/m**2
    Ion Secondary Flux             0.0000e+00    1.0787e-07 A/m**2

    Photo Flux                     0.0000e+00    0.0000e+00 A/m**2
    Conduction Flux                0.0000e+00    0.0000e+00 A/m**2
                                   -----------   -----------
    Total Flux                    -4.8906e-05    1.2900e-08 A/m**2

 Init  Sheath Radius= 1.900e+00 meters  AVMACH= 6.700e+00
 Final Sheath Radius= 7.519e+00 meters  ROBJ  = 1.900e+00 meters

 SUCHGR command >>  quit
Want to save a copy of the session?  >>  yes

Exit SUCHGR.
```

The computer **vehicl** was executed with the following standard input and object definition files. Some of the resulting figures are shown in Figure 37.

vehicl Execution Standard Input Polar Orbiting Spacecraft–DMSP

```
nxyz 19  15  27
matplots yes
makeplot 2
plotdir 2 3 5
plotdir -2 -3 -5
end
```

Object Definition File Polar Orbiting Spacecraft–DMSP

```
COMMENT ASSUMING A GRID OF 19,15,27
OFFSET 10 7 13
comment ******  SOLAR CELL ARRAY
comment ******  solar cell panel
CONDUCTOR 8
SLANT
corner -8 0 -2
top solar 0  1 -1
bottom npaint
length 2 6 6
endobj
PATCHW
corner -8 2 -5
face gold 0 1 -1
length 1 1 1
endobj
comment ******  solar cell panel
CONDUCTOR 7
SLANT
corner -6 0 -2
top solar 0  1 -1
bottom npaint
length 2 6 6
endobj
PATCHW
corner -6 3 -4
face gold 0 1 -1
length 1 1 1
endobj
comment ******  solar cell panel
CONDUCTOR 6
SLANT
corner -4 0 -2
top solar 0  1 -1
bottom npaint
length 2 6 6
endobj
PATCHW
corner -4 2 -5
face gold 0 1 -1
length 1 1 1
endobj
comment ******  solar cell panel
CONDUCTOR 5
SLANT
corner -2 0 -2
top solar 0  1 -1
bottom npaint
length 2 6 6
endobj
```

```
PATCHW
corner -2 3 -4
face gold 0 1 -1
length 1 1 1
endobj
comment ******  solar cell panel
CONDUCTOR 4
SLANT
corner 0 0 -2
top solar 0  1 -1
bottom npaint
length 2 6 6
endobj
PATCHW
corner 0 2 -5
face gold 0 1 -1
length 1 1 1
endobj
comment ******  solar cell panel
CONDUCTOR 3
SLANT
corner 2 0 -2
top solar 0  1 -1
bottom npaint
length 2 6 6
endobj
PATCHW
corner 2 3 -4
face gold 0 1 -1
length 1 1 1
endobj
comment ******  solar cell panel
CONDUCTOR 2
SLANT
corner 4 0 -2
top solar 0  1 -1
bottom npaint
length 2 6 6
endobj
PATCHW
corner 4 2 -5
face gold 0 1 -1
length 1 1 1
endobj
comment ******  solar cell panel
CONDUCTOR 1
SLANT
corner 6 0 -2
top solar 0  1 -1
bottom npaint
length 2 6 6
endobj
PATCHW
corner 6 3 -4
face gold 0 1 -1
length 1 1 1
endobj
comment battery boxes twice?
OCTAGON
axis 0 0 -2 0 0 -1
width 6
side 4
comment 10 mil 2nd surface teflon = cpaint
surface *  cpaint
```

```
surface -  cpaint
surface C  cpaint
endobj
comment RSS
OCTAGON
axis 0 0 -4 0 0 0
width 6
side 2
comment 5 mil aluminized 2nd surface teflon is default
surface +   teflon
surface -   teflon
surface C   teflon
endobj
comment ARM motor, oxydized Ti = aquadag ?
PATCHR
corner -1 -1 -4
deltas 2 2 1
surface -z aquadg
endobj
comment RSS truss piece
comment Proper truss is not possible, so extend rss and esm
OCTAGON
axis 0 0 0 0 0 1
width 6
side 2
surface +  teflon
surface -  teflon
surface C  teflon
endobj
comment battery boxes
comment OCTAGON
comment axis 0 0 -2 0 0 -1
comment width 6
comment side 4
comment surface +  cpaint
comment surface -  cpaint
comment surface C  cpaint
comment endobj
comment OCTAGON
comment axis 0 0 -4 0 0 0
comment width 6
comment side 2
comment surface +   teflon
comment surface -   teflon
comment surface C   teflon
comment endobj
comment connector piece
comment OCTAGON
comment axis 0 0 0 0 0 1
comment width 6
comment side 2
comment surface +  cpaint
comment surface -  cpaint
comment surface C  cpaint
comment endobj
comment RSS truss piece
RECTAN
corner -3 -2 1
deltas  6  2 1
surface -x teflon
surface +x teflon
surface -y teflon
surface +y teflon
surface -z teflon
```

```
surface +z teflon
endobj
comment RSS truss piece
WEDGE
corner 0 0 1
face teflon -1 1 0
length 3 3 1
endobj
comment RSS truss piece
WEDGE
corner 0 0 1
face teflon 1 1 0
length 3 3 1
endobj
comment RSS truss lower piece
WEDGE
corner -1 -2 1
face teflon 0 -1 1
length 2 1 1
endobj
comment RSS truss piece lower
TETRAH
corner -1 -2 1
face teflon -1 -1 1
length 1
surface +x teflon
surface +y teflon
surface +z teflon
endobj
comment RSS truss piece lower
TETRAH
corner 1 -2 1
face teflon 1 -1 1
length 1
surface -x teflon
surface +y teflon
surface +z teflon
endobj
comment ************** ESM pieces
RECTAN
corner -3 -2 2
deltas  6  2 7
surface -x kapton
surface +x kapton
comment bottom of ESM is .5mil 2nd surf Al Kapt Dacron cloth ?
comment using npaint just for pictures
surface -y npaint
surface +y kapton
surface -z kapton
surface +z kapton
endobj
WEDGE
corner 0 0 2
face kapton -1 1 0
length 3 3 7
surface +z kapton
endobj
WEDGE
corner 0 0 2
face kapton 1 1 0
length 3 3 7
surface +z kapton
endobj
comment ************* ESM pinwheel louvers
```

```
PATCHW
corner -1 1 3
face aluminum -1 1 0
length 1 1 1
endobj
PATCHW
corner 1 1 3
face aluminum 1 1 0
length 1 1 1
endobj
PATCHR
corner -3 -1 3
deltas 1 1 1
surface -x aluminum
endobj
PATCHR
corner 2 -1 3
deltas 1 1 1
surface +x aluminum
endobj
PATCHW
corner -1 1 5
face aluminum -1 1 0
length 1 1 1
endobj
PATCHW
corner 1 1 5
face aluminum 1 1 0
length 1 1 1
endobj
PATCHR
corner -3 -1 5
deltas 1 1 1
surface -x aluminum
endobj
PATCHR
corner 2 -1 5
deltas 1 1 1
surface +x aluminum
endobj
PATCHW
corner -1 1 7
face aluminum -1 1 0
length 1 1 1
endobj
PATCHW
corner 1 1 7
face aluminum 1 1 0
length 1 1 1
endobj
PATCHR
corner -3 -1 7
deltas 1 1 1
surface -x aluminum
endobj
PATCHR
corner 2 -1 7
deltas 1 1 1
surface +x aluminum
endobj
comment antenna support
RECTAN
corner 1 1 9
deltas 1 2 1
```

```
surface -x kapton
surface +x kapton
surface -y kapton
surface +y kapton
surface -z kapton
surface +z kapton
endobj
comment antena
comment PLATE
comment corner 1 3 9
comment deltas 0 1 1
comment top -x alumin
comment bottom +x alumin
comment endobj
comment more antena
comment SLANT
comment corner 4 4 9
comment top alumin -1 1 0
comment bottom alumin
comment length 3 3 1
comment endobj
comment more antena
comment SLANT
comment corner 3 5 8
comment top alumin -1 1 0
comment bottom alumin
comment length 1 1 3
comment endobj
COMMENT PALLET
PLATE
corner -3 0 9
deltas 6 0 3
top +y teflon
bottom -y teflon
endobj
COMMENT THINGS  ON PALLET
comment sunshade
SLANT
corner 0 1 11
top teflon 0  1 -1
bottom alum
length 2 2 2
endobj
comment wedge to solve triple point
WEDGE
corner 0 0 11
face teflon 0  1 -1
length 2 1 1
surface -x teflon
surface +x teflon
surface -y teflon
surface +y teflon
surface -z teflon
surface +z teflon
endobj
WEDGE
corner -1 0 13
face teflon 0  1 -1
length 1 3 3
surface -x teflon
surface +x teflon
surface -y teflon
surface +y teflon
surface -z teflon
```

```
surface +z teflon
endobj
comment sunshade
WEDGE
corner 2 0 13
face teflon 0  1 -1
length 1 3 3
surface -x teflon
surface +x teflon
surface -y teflon
surface +y teflon
surface -z teflon
surface +z teflon
endobj
WEDGE
corner 0 0 12
face teflon -1 -1 0
length 1 1 1
surface -x teflon
surface +x teflon
surface -y teflon
surface +y teflon
surface -z teflon
surface +z teflon
endobj
comment Slants cannot be placed against any surface Y
comment replaced with wedges
comment SLANT
comment corner 1 -1 12
comment top teflon 1 -1 0
comment bottom alum
comment length 1 1 1
comment endobj
comment SLANT
comment corner 1 -1 12
comment top teflon -1 -1 0
comment bottom alum
comment length 1 1 1
comment endobj
WEDGE
corner 1 -1 12
face teflon 1 -1 0
length 1 1 1
surface -x teflon
surface +x teflon
surface -y teflon
surface +y teflon
surface -z teflon
surface +z teflon
endobj
WEDGE
corner 1 -1 12
face teflon -1 -1 0
length 1 1 1
surface -x teflon
surface +x teflon
surface -y teflon
surface +y teflon
surface -z teflon
surface +z teflon
endobj
WEDGE
corner 2 0 12
face teflon 1 -1 0
```

```
length 1 1 1
surface -x teflon
surface +x teflon
surface -y teflon
surface +y teflon
surface -z teflon
surface +z teflon
endobj
MARKTB 0 -1 12 top
MARKTB 1 -1 12 top
MARKTB -1 -2 12 bottom
MARKTB 2 -2 12 bottom
comment *******  ESA and sunsensor
RECTAN
corner 3 -2 11
deltas 1 2 1
surface -x teflon
surface +x teflon
surface -y gold
surface +y silver
surface -z teflon
surface +z teflon
endobj
MARKTB  3 0 11 top
COMMENT THINGS BELOW PALLET
RECTAN
corner -3 -2 10
deltas 5 2 2
surface -x teflon
surface +x teflon
surface -y teflon
surface +y teflon
surface -z teflon
surface +z teflon
endobj
RECTAN
corner -2 -2 12
deltas 1 1 1
surface -x teflon
surface +x teflon
surface -y teflon
surface +y teflon
surface -z teflon
surface +z teflon
endobj
WEDGE
corner -2 -2 12
face teflon 0 -1 1
length 1 1 1
surface -x teflon
surface +x teflon
surface -y teflon
surface +y teflon
surface -z teflon
surface +z teflon
endobj
RECTAN
corner -2 -3 10
deltas 1 1 2
surface -x teflon
surface +x teflon
surface -y teflon
surface +y teflon
surface -z teflon
```

```
surface +z teflon
endobj
WEDGE
corner -2 -2 10
face teflon 0 -1 -1
length 1 1 1
surface -x teflon
surface +x teflon
surface -y teflon
surface +y teflon
surface -z teflon
surface +z teflon
endobj
WEDGE
corner -2 -2 10
face teflon 0 1 -1
length 1 1 1
surface -x teflon
surface +x teflon
surface -y teflon
surface +y teflon
surface -z teflon
surface +z teflon
endobj
comment new bottom stuff
RECTAN
corner 2 -3 2
deltas  1 1 2
surface -x kapton
surface +x kapton
surface -y kapton
surface +y kapton
surface -z kapton
surface +z kapton
endobj
RECTAN
corner 2 -3 6
deltas  1 1 1
surface -x kapton
surface +x kapton
surface -y kapton
surface +y kapton
surface -z kapton
surface +z kapton
endobj
WEDGE
corner 3 -3 7
face teflon -1 0 1
length 1 1 1
surface -x kapton
surface +x kapton
surface -y kapton
surface +y kapton
surface -z kapton
surface +z kapton
endobj
RECTAN
corner -3 -3 7
deltas  3 1 1
surface -x kapton
surface +x kapton
surface -y kapton
surface +y kapton
surface -z kapton
```

```
surface +z kapton
endobj
WEDGE
corner 0 -3 7
face teflon 1 0 1
length 1 1 1
surface -x kapton
surface +x kapton
surface -y kapton
surface +y kapton
surface -z kapton
surface +z kapton
endobj
RECTAN
cornar 0 -3 5
deltas  1 1 2
surface -x kapton
surface +x kapton
surface -y kapton
surface +y kapton
surface -z kapton
surface +z kapton
endobj
ENDSAT
```

The **orient** standard input defines the mach vector. Here the spacecraft is moving at mach 6.7.

orient Execution Standard Input Polar Orbiting Spacecraft–DMSP

```
vmach  6.7 0.0 0.0
```

The **nterak** execution was completed in nine steps. The standard input files are shown below. The fifth standard input was used for the fifth through ninth continuation.

nterak Execution Standard Input Polar Orbiting Spacecraft–DMSP

```
  DEFAULT
  ISTART NEW
comment
comment  Choose Physical Models to be used.
  igical yes
  sthwake on
  aveprtcl on
  thrmsprd on
comment
comment  Redefine Algorithm parameters
  maxitc 50
  potcon 4
  dvlim 30.
  maxitt 1
  deltat .02
comment Define Computational Grid
  DXMESH 0.25
```

```
  MXADNT 17
  MXADNB 18
  NYADNT 18
  NYADNB 14
  NZADON 11
  NZTAIL 45
comment define the plasma environment
  VMACH 0.0 0.0 6.7
  RATIH 10.0
  DENS 3.55e9
  TEMP 0.2
  DEN2   6.0E5
  TEMP2  8.0E3
  GAUCO  4.0e4
  ENAUT  2.4E4
  DELTA  1.6E4
  POWCO  3.0E11
  PALPHA 1.1
  PCUTL  50.0
  PCUTH  1.6E6
Comment solar arrays not biased in the dark
comment BIAS 2 4.6
comment BIAS 3 9.2
comment BIAS 4 13.7
comment BIAS 5 18.3
comment BIAS 6 22.8
comment BIAS 7 27.4
comment BIAS 8 32.0
comment Iterate on the analytical modules
  what
  PWASON
  CHARGE
  endrun
```

nterak Continuation Run Standard Input Polar Orbiting Spacecraft–DMSP

```
  ISTART cont
comment  Choose Physical Models to be used.
  IGICAL no
comment  Redefine Algorithm parameters
  deltat .02
Comment physics modules
  WHAT
  LOOP 5 PWASON CURREN CHARGE
  endrun
```

nterak Second Continuaton Run Standard Input Polar Orbiting Spacecraft–DMSP

```
comment  Redefine Algorithm parameters
  maxitt 2
  deltat .05
comment physics modules
  what
  LOOP 10 PWASON CURREN CHARGE
  endrun
```

nterak Third Continuation Run Standard Input Polar Orbiting Spacecraft–DMSP

```
comment  Redefine Algorithm parameters
  deltat .05
comment physics modules
  what
  LOOP 10 PWASON CORREN CHARGE
  endrun
```

nterak Fourth Continuation Run Standard Input Polar Orbiting Spacecraft–DMSP

```
comment  Redefine Algorithm parameters
  deltat .1
comment physics modules
  what
  LOOP 10 PWASON CURREN CHARGE
  endrun
```

nterak Fifth Continuation Run Standard Input Polar Orbiting Spacecraft–DMSP

```
comment  Redefine Algorithm parameters
  deltat .2
comment physics modules
  what
  LOOP 10 PWASON CURREN CHARGE
  endrun
```

trmtlk Execution Polar Orbiting Spacecraft–DMSP

The program **trmtlk** was used to examine the potentials reached and the time variation of the surface potentials. A group of surface cells is defined for each of the materials. The final potentials for each of the groups is requested. A history of the potential over time for a selection of cells (including one at ground potential) is requested. The selection was chosen to represent the range of potentials for each material. The single module is used to examine the selected cells in more detail. The time history of potentials on selected surfaces is shown in Figure 38.

```
Welcome to POLAR 1.3 TRMTLK ...

Any AID may be called from any MODULE

     MODULES          AIDS
  ************     ********
     HISTORY          AGAIN
     LATEST           HELP
     SINGLE           LOCATION #
     SPECIAL          OUTLINE
                      SUBSET
                      EXIT
                      SUBSET [GROUP NAME]

Enter any MODULE/AID name or 'HELP' for help -> subset npaint
DEFINITION OF NEW SUBSET NAMED NPAI
```

```
 683 REMAINING IN GROUP

SUBSET command please >> matl npaint
 130 REMAINING IN GROUP

SUBSET command please >> normal -1 1 0
  96 REMAINING IN GROUP

SUBSET command please >> done
GROUP NPAI WITH   96 MEMBERS IS NOW DEFINED
RETURNING TO MODULE  'MAIN'

Enter any MODULE/AID name or 'HELP' for help >> subset npa2
DEFINITION OF NEW SUBSET NAMED NPA2
 683 REMAINING IN GROUP

SUBSET command please >> compl npaint
 587 REMAINING IN GROUP

SUBSET command please >> matl npaint
  34 REMAINING IN GROUP

SUBSET command please >> done
GROUP NPA2 WITH   34 MEMBERS IS NOW DEFINED
RETURNING TO MODULE  'MAIN'

Enter any MODULE/AID name or 'HELP' for help >> subset gold
DEFINITION OF NEW SUBSET NAMED GOLD
 683 REMAINING IN GROUP

SUBSET command please >> matl gold
   9 REMAINING IN GROUP

SUBSET command please >> done
GROUP GOLD WITH    9 MEMBERS IS NOW DEFINED
RETURNING TO MODULE  'MAIN'

Enter any MODULE/AID name or 'HELP' for help >> subset solar
DEFINITION OF NEW SUBSET NAMED SOLA
 683 REMAINING IN GROUP

SUBSET command please >> matl solar
  88 REMAINING IN GROUP

SUBSET command please >> normal 1 -1 0
  88 REMAINING IN GROUP

SUBSET command please >> done
GROUP SOLA WITH   88 MEMBERS IS NOW DEFINED
RETURNING TO MODULE  'MAIN'

Enter any MODULE/AID name or 'HELP' for help >> subset cpaint
DEFINITION OF NEW SUBSET NAMED CPAI
 683 REMAINING IN GROUP

SUBSET command please >> matl cpaint
  36 REMAINING IN GROUP

SUBSET command please >> done
GROUP CPAI WITH   36 MEMBERS IS NOW DEFINED
RETURNING TO MODULE  'MAIN'

Enter any MODULE/AID name or 'HELP' for help >> subset teflon
DEFINITION OF NEW SUBSET NAMED TEFL
```

```
 683 REMAINING IN GROUP

SUBSET command please >> matl teflon
 268 REMAINING IN GROUP

SUBSET command please >> done
GROUP TEFL WITH  268 MEMBERS IS NOW DEFINED
RETURNING TO MODULE  'MAIN'

Enter any MODULE/AID name or 'HELP' for help >> subset aquadg
DEFINITION OF NEW SUBSET NAMED AQUA
 683 REMAINING IN GROUP

SUBSET command please >> matl aquadg
   4 REMAINING IN GROUP

SUBSET command please >> done
GROUP AQUA WITH    4 MEMBERS IS NOW DEFINED
RETURNING TO MODULE  'MAIN'

Enter any MODULE/AID name or 'HELP' for help >> subset kapton
DEFINITION OF NEW SUBSET NAMED KAPT
 683 REMAINING IN GROUP

SUBSET command please >> matl kapton
 123 REMAINING IN GROUP

SUBSET command please >> done
GROUP KAPT WITH  123 MEMBERS IS NOW DEFINED
RETURNING TO MODULE  'MAIN'

Enter any MODULE/AID name or 'HELP' for help >> subset alum
DEFINITION OF NEW SUBSET NAMED ALUM
 683 REMAINING IN GROUP

SUBSET command please >> matl alum
  16 REMAINING IN GROUP

SUBSET command please >> done
GROUP ALUM WITH   16 MEMBERS IS NOW DEFINED
RETURNING TO MODULE  'MAIN'

Enter any MODULE/AID name or 'HELP' for help >> latest

LATEST command or MODE set >> magnitude
MODE RESET

LATEST command or MODE set >> group npaint
POTL IN VOLTS  FOR POLAR CYCLE  57 ... TIME = 1.41E+01 SEC
 647-1.15E+00  659-2.01E+00  649-5.07E+01    8-5.13E+01   10-9.02E+01
 511-9.53E+01  651-9.88E+01  585-1.15E+02  581-1.18E+02  635-1.19E+02
 661-1.44E+02  657-1.55E+02    4-1.68E+02  633-1.71E+02  645-1.77E+02
 105-1.80E+02   99-1.98E+02   60-2.05E+02  503-2.09E+02    2-2.31E+02
   6-2.36E+02   14-2.43E+02   46-2.46E+02  663-2.59E+02  637-3.09E+02
 109-3.12E+02   16-3.25E+02   52-3.43E+02  181-3.53E+02   56-3.64E+02
  54-3.73E+02  173-3.96E+02   22-4.31E+02   40-4.34E+02   26-4.53E+02
 249-4.68E+02  257-4.70E+02  577-4.81E+02   97-4.82E+02   38-4.83E+02
  20-5.01E+02   50-5.03E+02   34-5.05E+02   28-5.16E+02   18-5.27E+02
  48-5.29E+02  325-5.35E+02  185-5.44E+02  499-5.56E+02  404-5.64E+02
  12-5.93E+02  333-5.97E+02  416-6.02E+02   64-6.14E+02  493-6.20E+02
  36-6.24E+02  412-6.30E+02   44-6.31E+02  402-6.35E+02   42-6.38E+02
  24-6.49E+02  261-6.53E+02  491-6.64E+02  631-6.72E+02  323-6.85E+02
 337-6.94E+02  422-7.07E+02  655 7.09E+02   95-7.20E+02  117-7.57E+02
 643-7.61E+02   30-7.70E+02   32-8.01E+02  575-8.15E+02  341-8.18E+02
```

```
 247-8.18E+02  265-8.26E+02  171-8.32E+02  573-8.32E+02  629-8.83E+02
 191-8.99E+02  669-9.32E+02  671-1.00E+03  321-1.04E+03  169-1.05E+03
 245-1.06E+03  667-1.06E+03  400-1.11E+03  489-1.13E+03  673-1.14E+03
 675-1.18E+03  653-1.19E+03  641-1.20E+03  571-1.20E+03  627-1.22E+03
 665-1.29E+03    0 0.00E+00    0 0.00E+00    0 0.00E+00    0 0.00E+00

LATEST command or MODE set >> group npa2
POTL IN VOLTS  FOR POLAR CYCLE  57 ... TIME = 1.41E+01 SEC
 366-1.06E+00  453-1.13E+00  451-1.38E+00  364-1.40E+00  536-1.43E+00
 286-1.44E+00  291-2.04E+01  533-2.57E+01  445-3.29E+01  542-6.84E+01
 282-1.14E+02  449-1.23E+02  442-1.44E+02  544-1.81E+02  437-2.76E+02
 279-3.14E+02  440-3.19E+02  277-3.73E+02  209-4.37E+02  211-4.62E+02
 207-4.65E+02  353-4.71E+02  147-4.82E+02  275-4.84E+02  219-4.85E+02
 351-4.88E+02  356-4.95E+02  205-4.97E+02  133-5.14E+02  137-5.61E+02
 135-5.62E+02  214-5.79E+02  139-6.12E+02  142-7.49E+02    0 0.00E+00

LATEST command or MODE set >> group gold
POTL IN VOLTS  FOR POLAR CYCLE  57 ... TIME = 1.41E+01 SEC
   5-2.32E+02   53-3.07E+02   31-3.57E+02  630-3.60E+02  498-4.30E+02
 658-4.73E+02  617-4.73E+02  324-5.05E+02  180-5.06E+02    0 0.00E+00

LATEST command or MODE set >> group solar
POTL IN VOLTS  FOR POLAR CYCLE  57 ... TIME = 1.41E+01 SEC
 403 1.53E+00  570-8.26E-01  244-1.09E+00   11-1.12E+00   25-1.15E+00
  63-1.16E+00  488-1.21E+00  116-1.25E+00  399-1.26E+00   19-1.26E+00
  17-1.38E+00  320-1.41E+00   37-1.52E+00   29-1.53E+00  640-1.53E+00
 626-1.56E+00  168-1.72E+00  190-1.82E+00    3-2.60E+00  652-3.50E+00
  23-3.50E+00  664-4.10E+00  264-7.25E+00    1-1.28E+01   94-1.35E+01
   9-1.37E+01   47-1.70E+01   35-2.43E+01  340-2.79E+01   98-3.10E+01
  49-3.41E+01  248-6.47E+01  332-9.02E+01   43-1.13E+02  256-1.14E+02
 668-1.22E+02  672-1.25E+02  492-1.30E+02  421-1.36E+02  411-1.37E+02
 574-1.49E+02  670-1.54E+02  104-1.59E+02  644-1.61E+02  172-1.80E+02
  41-1.88E+02  666-2.02E+02  634-2.03E+02   39-2.03E+02  648-2.09E+02
 674-2.31E+02  580-2.35E+02  502-2.37E+02   55-2.58E+02  576-2.66E+02
 415-2.90E+02   21-2.97E+02  322-2.98E+02  660-3.02E+02  656-3.05E+02
  33-3.21E+02  336-3.22E+02  260-3.36E+02   27-3.37E+02  108-3.47E+02
 646-3.57E+02  632-3.67E+02  510-3.80E+02  184-3.84E+02   15-4.04E+02
 401-4.04E+02   96-4.07E+02  246-4.09E+02   13-4.10E+02   45-4.15E+02
 662-4.20E+02  636-4.34E+02  628-4.44E+02  650-4.47E+02  642-4.64E+02
  59-4.93E+02   51-4.95E+02  584-4.96E+02  490-5.09E+02  170-5.11E+02
 572-5.14E+02  654-5.27E+02    7-7.22E+02    0 0.00E+00    0 0.00E+00

LATEST command or MODE set >> group cpaint
POTL IN VOLTS  FOR POLAR CYCLE  57 ... TIME = 1.41E+01 SEC
 589-4.73E+02  586-4.73E+02  519-4.73E+02  517-4.73E+02  515-4.73E+02
 514-4.73E+02  513-4.73E+02  512-4.73E+02  509-4.73E+02  507-4.73E+02
 505-4.73E+02  504-4.73E+02  427-4.73E+02  425-4.73E+02  424-4.73E+02
 423-4.73E+02  419-4.73E+02  417-4.73E+02  196-4.73E+02  194-4.73E+02
 193-4.73E+02  192-4.73E+02  188-4.73E+02  186-4.73E+02  125-4.73E+02
 123-4.73E+02  121-4.73E+02  120-4.73E+02  119-4.73E+02  118-4.73E+02
 115-4.73E+02  113-4.73E+02  111-4.73E+02  110-4.73E+02   68-4.73E+02
  65-4.73E+02    0 0.00E+00    0 0.00E+00    0 0.00E+00    0 0.00E+00

LATEST command or MODE set >> group teflon
POTL IN VOLTS  FOR POLAR CYCLE  57 ... TIME = 1.41E+01 SEC
 616-5.71E-01  305-9.45E-01  555-1.03E+00  461-1.03E+00  563-1.03E+00
 372-1.04E+00  388-1.06E+00  587-1.26E+00  309-1.28E+00   91-1.30E+00
 157-1.35E+00  313-1.35E+00  299-1.38E+00  548-1.48E+00  389-1.49E+00
 314-1.50E+00  568-1.53E+00  582-1.55E+00  567-1.68E+00  267-1.78E+00
 234-1.78E+00  379-1.79E+00  622-1.97E+00  526-3.18E+00  381-3.47E+00
 621-4.57E+00   93-4.66E+00  240-5.47E+00  554-6.05E+00  263-6.19E+00
 386-6.42E+00  460-1.01E+01  473-1.02E+01  471-1.07E+01  383-1.11E+01
 475-1.23E+01   57-1.34E+01  197-1.44E+01  472-2.04E+01  106-2.70E+01
 241-2.95E+01  189-3.49E+01  590-3.59E+01  480-3.68E+01  374-5.36E+01
```

```
 58-5.93E+01  269-5.94E+01  165-6.46E+01   90-6.93E+01   62-7.39E+01
384-8.37E+01   74-9.35E+01  541-9.44E+01   69-9.73E+01  177-1.09E+02
158-1.18E+02   70-1.18E+02   61-1.26E+02   92-1.33E+02  327-1.51E+02
 66-1.61E+02  466-1.63E+02  164-1.68E+02  588-1.75E+02  431-1.75E+02
 67-1.77E+02  235-1.79E+02  107-1.79E+02  524-1.81E+02  569-1.84E+02
343-1.95E+02  516-1.97E+02  408-2.01E+02  161-2.05E+02  231-2.05E+02
149-2.06E+02  127-2.11E+02  251-2.18E+02  112-2.23E+02  198-2.23E+02
187-2.28E+02  482-2.41E+02  203-2.45E+02  566-2.60E+02  182-2.61E+02
595-2.61E+02  160-2.78E+02   71-2.78E+02   73-2.79E+02  525-2.81E+02
274-2.83E+02  382-2.9?E+02  312-2.94E+02  521-2.95E+02  592-3.01E+02
363-3.01E+02  396-3.07E+02  319-3.07E+02  308-3.11E+02  254-3.15E+02
506-3.16E+02  500-3.16E+02  124-3.20E+02  262-3.23E+02  591-3.29E+02
232-3.31E+02  183-3.32E+02  434-3.39E+02  578-3.48E+02  527-3.58E+02
428-3.62E+02  199-3.71E+02  201-3.82E+02  176-3.93E+02  522-3.93E+02
122-4.01E+02  430-4.05E+02   72-4.10E+02  200-4.17E+02  167-4.17E+02
625-4.20E+02  204-4.21E+02  195-4.22E+02  228-4.27E+02  594-4.30E+02
242-4.31E+02  266-4.33E+02  398-4.56E+02  518-4.58E+02  565-4.61E+02
338-4.63E+02  345-4.66E+02  237-4.68E+02  131-4.69E+02  495-4.69E+02
128-4.72E+02  221-4.73E+02  330-4.73E+02  238-4.74E+02  258-4.81E+02
344-4.84E+02  494-4.85E+02  413-5.01E+02  326-5.03E+02  487-5.16E+02
202-5.19E+02  593-5.19E+02  243-5.24E+02  346-5.24E+02  405-5.31E+02
315-5.34E+02  270-5.35E+02  334-5.37E+02  178-5.39E+02  429-5.43E+02
339-5.44E+02  162-5.45E+02  470-5.45E+02  166-5.50E+02  268-5.51E+02
159-5.56E+02  477-5.60E+02  583-5.68E+02  407-5.71E+02  432-5.77E+02
114-5.89E+02  478-5.95E+02  179-5.98E+02  391-5.98E+02  318-6.02E+02
126-6.02E+02  129-6.05E+02  293-6.13E+02  132-6.14E+02  255-6.24E+02
624-6.31E+02  273-6.33E+02  342-6.40E+02  130-6.41E+02  406-6.44E+02
236-6.46E+02  272-6.60E+02  496-6.60E+02  458-6.76E+02  348-6.79E+02
271-6.84E+02  467-6.88E+02  485-6.97E+02  520-6.98E+02  347-6.98E+02
163-7.00E+02  623-7.01E+02  463-7.35E+02  564-7.36E+02  174-7.41E+02
433-7.51E+02  317-7.53E+02  409-7.74E+02  239-7.83E+02  250-7.87E+02
418-8.12E+02  556-8.17E+02  393-8.18E+02  369-8.19E+02  233-8.23E+02
100-8.38E+02  331-8.49E+02  259-8.50E+02  426-8.55E+02  380-8.56E+02
392-8.62E+02  474-8.65E+02  230-8.69E+02  371-8.73E+02  481-8.74E+02
579-8.77E+02  479-8.94E+02  484-9.02E+02  618-9.11E+02  316-9.18E+02
638-9.33E+02  497-9.43E+02  414-9.71E+02  620-1.01E+03  304-1.02E+03
103-1.03E+03  420-1.04E+03  639-1.05E+03  306-1.06E+03  483-1.07E+03
550-1.09E+03  301-1.11E+03  335-1.11E+03  553-1.13E+03  557-1.14E+03
558-1.14E+03  501-1.15E+03  175-1.15E+03  435-1.15E+03  310-1.16E+03
410-1.19E+03  350-1.20E+03  349-1.21E+03  152-1.32E+03  101-1.34E+03
562-1.36E+03  102-1.37E+03  307-1.41E+03  311-1.43E+03  615-1.56E+03
560-1.59E+03  150-1.65E+03  294-1.66E+03  385-1.78E+03  508-1.83E+03
390-1.83E+03  296-1.86E+03  559-1.89E+03  614-1.97E+03  298-2.12E+03
395-2.38E+03  223-2.39E+03  394-2.43E+03  154-2.68E+03  155-2.71E+03
226-2.83E+03  561-2.87E+03  225-3.37E+03    0 0.00E+00    0 0.00E+00

LATEST command or MODE set >> group aquadg
POTL IN VOLTS  FOR POLAR CYCLE  57 ... TIME = 1.41E+01 SEC
 329-4.73E+02  328-4.73E+02  253-4.73E+02  252-4.73E+02    0 0.00E+00

LATEST command or MODE set >> group kapton
POTL IN VOLTS  FOR POLAR CYCLE  57 ... TIME = 1.41E+01 SEC
 545-1.03E+00  543-1.04E+00  373-1.07E+00  613-1.07E+00  537-1.10E+00
 539-1.10E+00  534-1.25E+00   89-1.32E+00  285-1.41E+00  547-1.46E+00
 284-1.46E+00  529-1.55E+00  531-1.57E+00  450-3.23E+00   86-4.29E+00
 599-1.24E+01   80-1.44E+01   88-1.53E+01  441-2.76E+01   84-3.51E+01
 220-4.45E+01  148-5.40E+01  462-7.37E+01  289-1.01E+02  292-1.22E+02
 215-1.34E+02  610-1.66E+02  455-1.77E+02  607-1.77E+02  210-1.83E+02
 145-1.99E+02  549-2.11E+02  606-2.30E+02  156-2.44E+02   76-2.46E+02
 612-2.48E+02  596-2.49E+02  287-2.52E+02   83-2.55E+02  608-2.68E+02
 465-2.75E+02  469-2.77E+02  464-2.83E+02   79-2.95E+02   77-3.03E+02
 281-3.05E+02   81-3.09E+02  206-3.18E+02  375-3.23E+02  376-3.29E+02
 140-3.48E+02  138-3.54E+02  144-3.56E+02  530-3.64E+02  136-3.71E+02
 283-3.79E+02   85-3.81E+02   75-4.06E+02  438-4.12E+02  143-4.30E+02
```

```
216-4.37E+02  278-4.58E+02  459-4.73E+02  280-4.96E+02  532-5.06E+02
535-5.12E+02  290-5.37E+02  276-5.40E+02  448-5.43E+02  370-5.54E+02
134-5.64E+02  609-5.81E+02  303-6.07E+02  604-6.17E+02  528-6.17E+02
377-6.26E+02  288-6.27E+02  552-6.37E+02  546-6.48E+02  360-6.62E+02
457-7.27E+02  300-7.55E+02  523-7.62E+02  436-7.66E+02  358-7.72E+02
213-7.74E+02  600-7.84E+02  597-7.85E+02  146-7.85E+02  368-7.86E+02
218-7.89E+02  454-8.20E+02  598-8.26E+02  603-8.26E+02  540-8.40E+02
551-8.40E+02  468-8.52E+02  302-8.60E+02  538-8.67E+02  439-8.75E+02
602-8.86E+02  229-9.10E+02  355-9.36E+02  378-9.48E+02  141-9.48E+02
456-9.51E+02  362-9.63E+02  447-1.13E+03  444-1.15E+03  367-1.16E+03
227-1.21E+03  151-1.22E+03  334-1.26E+03  352-1.26E+03  359-1.27E+03
357-1.27E+03  361-1.29E+03  365-1.43E+03  297-1.49E+03  295-1.66E+03
153-1.94E+03  222-2.22E+03  224-2.80E+03    0 0.00E+00    0 0.00E+00

LATEST command or MODE set >> group alum
POTL IN VOLTS  FOR POLAR CYCLE  57 ... TIME = 1.41E+01 SEC
 611-4.73E+02  605-4.73E+02  601-4.73E+02  486-4.73E+02  486-4.73E+02
 452-4.73E+02  446-4.73E+02  441-4.73E+02  397-4.73E+02  387-4.73E+02
 217-4.73E+02  212-4.73E+02  208-4.73E+02   87-4.73E+02   82-4.73E+02
  78-4.73E+02    0 0.00E+00    0 0.00E+00    0 0.00E+00    0 0.00E+00

LATEST command or MODE set >> single

SINGLE command or MODE set >> everything
MODE RESET

SINGLE command or MODE set >> 647
-------------------------------------------------------------------
SURFACE NO.  647                    CENTERED AT  10.50   8.50  15.50
MATERIAL IS NPAI                    NORMAL IS     -1    1    0
SHAPE IS RECTANGLE                  SURFACE AREA =  8.8388E-02 M**2

                    POTENTIAL  = -1.1513E+00 VOLTS
                    UNDERLYING CONDUCTOR NUMBER IS  1
                    UNDERLYING CONDUCTOR POTENTIAL = -4.7339E+02 VOLTS
                    DELTA V    =  3.5868E+02 VOLTS
                    INTERNAL FIELD STRESS   =  2.8694E+06 VOLTS/METER
                    EXTERNAL ELECTRIC FIELD =  6.3047E+03 VOLTS/METER
 FLUXES IN AMPS/METER**2
        INCIDENT ELECTRONS              -1.5972E-05
             RESULTING SECONDARIES       3.8630E-06
             RESULTING BACKSCATTER       1.7073E-06
        INCIDENT IONS                    1.1771E-05
             RESULTING SECONDARIES       1.0095E-08
        BULK CONDUCTIVITY                1.6929E-07
        HOPPING CURRENT                  0.0000E+00
        PHOTOCURRENT                     0.0000E+00
                                        ------------
        TOTAL FLUX THROUGH SURFACE       1.3790E-06

SINGLE command or MODE set >> 665
-------------------------------------------------------------------
SURFACE NO.  665                    CENTERED AT   7.50   5.50  17.50
MATERIAL IS NPAI                    NORMAL IS     -1    1    0
SHAPE IS RECTANGLE                  SURFACE AREA =  8.8388E-02 M**2

                    POTENTIAL  = -1.2890E+03 VOLTS
                    UNDERLYING CONDUCTOR NUMBER IS  1
                    UNDERLYING CONDUCTOR POTENTIAL = -4.7339E+02 VOLTS
                    DELTA V    = -8.1557E+02 VOLTS
                    INTERNAL FIELD STRESS   = -6.5245E+06 VOLTS/METER
                    EXTERNAL ELECTRIC FIELD = -1.6220E+04 VOLTS/METER
 FLUXES IN AMPS/METER**2
        INCIDENT ELECTRONS              -1.4566E-05
```

```
          RESULTING SECONDARIES      2.9852E-06
          RESULTING BACKSCATTER      1.5132E-06
     INCIDENT IONS                   6.4632E-06
          RESULTING SECONDARIES      7.6054E-07
     BULK CONDUCTIVITY              -3.8495E-07
     HOPPING CURRENT                 0.0000E+00
     PHOTOCURRENT                    0.0000E+00
                                    ------------
     TOTAL FLUX THROUGH SURFACE     -2.8438E-06

SINGLE command or MODE set >> 403
-------------------------------------------------------------------------
SURFACE NO.  403                    CENTERED AT   9.50   7.50  11.50
MATERIAL IS SOLA                    NORMAL IS     1  -1   0
SHAPE IS RECTANGLE                  SURFACE AREA =  8.8388E-02 M**2

                    POTENTIAL  =  1.5329E+00 VOLTS
                    UNDERLYING CONDUCTOR NUMBER IS  1
                    UNDERLYING CONDUCTOR POTENTIAL = -4.7339E+02 VOLTS
                    DELTA V    =  5.0628E+02 VOLTS
                    INTERNAL FIELD STRESS   =  1.1313E+06 VOLTS/METER
                    EXTERNAL ELECTRIC FIELD =  4.7899E+03 VOLTS/METER
 FLUXES IN AMPS/METER**2
     INCIDENT ELECTRONS             -1.5828E-05
          RESULTING SECONDARIES      1.5728E-06
          RESULTING BACKSCATTER      2.7565E-06
     INCIDENT IONS                   9.9818E-06
          RESULTING SECONDARIES      1.0269E-08
     BULK CONDUCTIVITY               6.6750E-08
     HOPPING CURRENT                 0.0000E+00
     PHOTOCURRENT                    0.0000E+00
                                    ------------
     TOTAL FLUX THROUGH SURFACE      4.9336E-07

SINGLE command or MODE set >> 7
-------------------------------------------------------------------------
SURFACE NO.    7                    CENTERED AT  10.50   8.50   2.50
MATERIAL IS SOLA                    NORMAL IS     1  -1   0
SHAPE IS RECTANGLE                  SURFACE AREA =  8.8388E-02 M**2

                    POTENTIAL  = -7.2236E+02 VOLTS
                    UNDERLYING CONDUCTOR NUMBER IS  1
                    UNDERLYING CONDUCTOR POTENTIAL = -4.7339E+02 VOLTS
                    DELTA V    = -4.9052E+02 VOLTS
                    INTERNAL FIELD STRESS   = -1.0961E+06 VOLTS/METER
                    EXTERNAL ELECTRIC FIELD = -1.0658E+04 VOLTS/METER
 FLUXES IN AMPS/METER**2
     INCIDENT ELECTRONS             -1.5013E-05
          RESULTING SECONDARIES      2.9580E-06
          RESULTING BACKSCATTER      2.5767E-06
     INCIDENT IONS                   7.8588E-06
          RESULTING SECONDARIES      1.9929E-07
     BULK CONDUCTIVITY              -6.4572E-08
     HOPPING CURRENT                 0.0000E+00
     PHOTOCURRENT                    0.0000E+00
                                    ------------
     TOTAL FLUX THROUGH SURFACE     -1.4200E-06

SINGLE command or MODE set >> 616
-------------------------------------------------------------------------
SURFACE NO.  616                    CENTERED AT   7.33  21.67  11.00
MATERIAL IS TEFL                    NORMAL IS     0   0   1
SHAPE IS RIGHT TRIANGLE             SURFACE AREA =  3.1250E-02 M**2
```

```
                    POTENTIAL  = -5.7084E-01 VOLTS
                    UNDERLYING CONDUCTOR NUMBER IS  1
                    UNDERLYING CONDUCTOR POTENTIAL = -4.7339E+02 VOLTS
                    DELTA V    =  4.7282E+02 VOLTS
                    INTERNAL FIELD STRESS   =  1.4892E+06 VOLTS/METER
                    EXTERNAL ELECTRIC FIELD =  5.0770E+04 VOLTS/METER
 FLUXES IN AMPS/METER**2
        INCIDENT ELECTRONS              -1.8100E-05
             RESULTING SECONDARIES       3.6153E-06
             RESULTING BACKSCATTER       2.1799E-06
        INCIDENT IONS                    2.1113E-05
             RESULTING SECONDARIES       0.0000E+00
        BULK CONDUCTIVITY                8.7862E-08
        HOPPING CURRENT                  0.0000E+00
        PHOTOCURRENT                     0.0000E+00
                                        ------------
        TOTAL FLUX THROUGH SURFACE       8.8078E-06

 SINGLE command or MODE set >> 225
 ------------------------------------------------------------------------
 SURFACE NO.  225                   CENTERED AT   6.50  23.00   8.50
 MATERIAL IS TEFL                   NORMAL IS     0   -1    0
 SHAPE IS SQUARE                    SURFACE AREA =  6.2500E-02 M**2

                    POTENTIAL  = -3.3740E+03 VOLTS
                    UNDERLYING CONDUCTOR NUMBER IS  1
                    UNDERLYING CONDUCTOR POTENTIAL = -4.7339E+02 VOLTS
                    DELTA V    = -2.9006E+03 VOLTS
                    INTERNAL FIELD STRESS   = -9.1358E+06 VOLTS/METER
                    EXTERNAL ELECTRIC FIELD = -3.4310E+04 VOLTS/METER
 FLUXES IN AMPS/METER**2
        INCIDENT ELECTRONS              -1.3082E-05
             RESULTING SECONDARIES       2.2823E-06
             RESULTING BACKSCATTER       1.7215E-06
        INCIDENT IONS                    2.5770E-06
             RESULTING SECONDARIES       6.5002E-07
        BULK CONDUCTIVITY               -5.3901E-07
        HOPPING CURRENT                  0.0000E+00
        PHOTOCURRENT                     0.0000E+00
                                        ------------
        TOTAL FLUX THROUGH SURFACE      -9.8510E-06

 SINGLE command or MODE set >> 545
 ------------------------------------------------------------------------
 SURFACE NO.  545                   CENTERED AT   7.50  21.50  12.50
 MATERIAL IS KAPT                   NORMAL IS     1   0   1
 SHAPE IS RECTANGLE                 SURFACE AREA =  8.9388E-02 M**2

                    POTENTIAL  = -1.0330E+00 VOLTS
                    UNDERLYING CONDUCTOR NUMBER IS  1
                    UNDERLYING CONDUCTOR POTENTIAL = -4.7339E+02 VOLTS
                    DELTA V    =  4.7235E+02 VOLTS
                    INTERNAL FIELD STRESS   =  1.4877E+06 VOLTS/METER
                    EXTERNAL ELECTRIC FIELD =  6.8271E+03 VOLTS/METER
 FLUXES IN AMPS/METER**2
        INCIDENT ELECTRONS              -1.6084E-05
             RESULTING SECONDARIES       2.1989E-06
             RESULTING BACKSCATTER       1.7073E-06
        INCIDENT IONS                    1.5555E-05
             RESULTING SECONDARIES       1.1336E-06
        BULK CONDUCTIVITY                8.7776E-08
        HOPPING CURRENT                  0.0000E+00
        PHOTOCURRENT                     0.0000E+00
                                        ------------
```

```
        TOTAL FLUX THROUGH SURFACE      3.3886E-06

SINGLE command or MODE set >> 224
-------------------------------------------------------------------------
SURFACE NO.  224                        CENTERED AT   6.50  22.00   8.50
MATERIAL IS KAPT                        NORMAL IS     0   1   0
SHAPE IS SQUARE                         SURFACE AREA =  6.2500E-02 M**2

                    POTENTIAL  = -2.7976E+03 VOLTS
                    UNDERLYING CONDUCTOR NUMBER IS  1
                    UNDERLYING CONDUCTOR POTENTIAL = -4.7339E+02 VOLTS
                    DELTA V    = -2.3242E+03 VOLTS
                    INTERNAL FIELD STRESS    = -7.3204E+06 VOLTS/METER
                    EXTERNAL ELECTRIC FIELD = -1.9908E+04 VOLTS/METER
 FLUXES IN AMPS/METER**2
        INCIDENT ELECTRONS              -1.3479E-05
             RESULTING SECONDARIES       1.2697E-06
             RESULTING BACKSCATTER       1.3783E-06
        INCIDENT IONS                    3.4794E-06
             RESULTING SECONDARIES       7.5595E-07
        BULK CONDUCTIVITY               -4.3190E-07
        HOPPING CURRENT                  0.0000E+00
        PHOTOCURRENT                     0.0000E+00
                                        ------------
        TOTAL FLUX THROUGH SURFACE      -6.5952E-06

SINGLE command or MODE set >> history

HISTORY command or MODE set >> -1,647,665,403,7

POTL in Volts

  TIME  :     -1       647      665      403        7
--------|-------------------------------------------------------------------
        :     #1       #2       #3       #4       #5       #6       #7
 0.0E+00:-1.03E+00-1.03E+00-1.03E+00-1.03E+00-1.03E+00
 2.0E-02:-5.64E+01-6.04E+01-5.66E+01-6.04E+01-6.04E+01
 4.0E-02:-1.15E+02-1.20E+02-1.15E+02-1.20E+02-7.88E+01
 6.0E-02:-1.73E+02-1.79E+02-1.73E+02-1.79E+02-1.12E+02
 8.0E-02:-2.31E+02-2.38E+02-2.31E+02-2.37E+02-1.45E+02
 1.0E-01:-2.88E+02-2.97E+02-2.87E+02-2.91E+02-1.69E+02
 1.2E-01:-3.26E+02-3.51E+02-3.37E+02-3.33E+02-1.75E+02
 2.2E-01:-4.14E+02-4.11E+02-4.19E+02-3.78E+02-1.68E+02
 3.2E-01:-4.64E+02-4.50E+02-4.77E+02-3.97E+02-1.73E+02
 4.2E-01:-4.74E+02-4.76E+02-4.98E+02-3.97E+02-1.85E+02
 5.2E-01:-4.84E+02-4.77E+02-5.20E+02-3.77E+02-1.57E+02
 6.2E-01:-4.65E+02-4.64E+02-5.16E+02-3.67E+02-1.46E+02
 7.2E-01:-4.59E+02-4.49E+02-5.21E+02-3.25E+02-1.01E+02
 8.2E-01:-4.39E+02-4.41E+02-5.16E+02-3.21E+02-4.49E+01
 9.2E-01:-4.40E+02-4.02E+02-5.29E+02-3.05E+02-6.19E+00
 1.0E+00:-4.24E+02-4.04E+02-5.24E+02-3.07E+02-1.92E+00
 1.1E+00:-4.46E+02-4.07E+02-5.58E+02-2.43E+02-1.65E+00
 1.2E+00:-4.30E+02-4.28E+02-5.57E+02-2.77E+02-1.45E+01
 1.3E+00:-4.59E+02-3.92E+02-5.96E+02-2.39E+02-7.71E+00
 1.4E+00:-4.45E+02-4.28E+02-5.97E+02-2.79E+02-2.71E+01
 1.5E+00:-4.68E+02-3.92E+02-6.29E+02-2.40E+02-3.80E+01
 1.6E+00:-4.57E+02-4.36E+02-6.31E+02-2.63E+02-8.07E+01
 1.7E+00:-4.76E+02-3.92E+02-6.60E+02-2.19E+02-7.06E+01
 1.8E+00:-4.65E+02-4.33E+02-6.60E+02-2.44E+02-8.96E+01
 1.9E+00:-4.89E+02-3.89E+02-6.92E+02-2.01E+02-9.27E+01
 2.0E+00:-4.75E+02-4.38E+02-6.88E+02-2.36E+02-1.22E+02
 2.1E+00:-4.97E+02-3.96E+02-7.19E+02-1.92E+02-1.25E+02
 2.5E+00:-4.79E+02-4.41E+02-7.26E+02-2.26E+02-1.90E+02
 2.9E+00:-5.09E+02-4.09E+02-7.82E+02-1.85E+02-1.89E+02
```

```
3.3E+00:-4.86E+02-4.46E+02-7.83E+02-2.57E+02-2.37E+02
3.7E+00:-5.10E+02-3.94E+02-8.32E+02-2.17E+02-2.46E+02
4.1E+00:-4.87E+02-4.24E+02-8.39E+02-2.86E+02-2.98E+02
4.5E+00:-5.05E+02-3.67E+02-8.80E+02-2.39E+02-3.09E+02
4.9E+00:-4.78E+02-3.79E+02-8.84E+02-3.20E+02-3.57E+02
5.3E+00:-4.95E+02-3.22E+02-9.13E+02-2.65E+02-3.92E+02
5.7E+00:-4.71E+02-3.15E+02-9.19E+02-3.17E+02-4.28E+02
6.1E+00:-4.87E+02-2.70E+02-9.49E+02-2.32E+02-4.71E+02
6.5E+00:-4.69E+02-2.68E+02-9.55E+02-2.67E+02-4.96E+02
6.9E+00:-4.79E+02-2.19E+02-9.87E+02-2.15E+02-5.23E+02
7.3E+00:-4.65E+02-1.81E+02-9.98E+02-2.27E+02-5.62E+02
7.7E+00:-4.73E+02-1.42E+02-1.02E+03-2.06E+02-5.67E+02
8.1E+00:-4.66E+02-1.06E+02-1.04E+03-2.09E+02-5.76E+02
8.5E+00:-4.68E+02-7.07E+01-1.06E+03-1.75E+02-5.69E+02
8.9E+00:-4.62E+02-4.04E+01-1.08E+03-1.64E+02-5.85E+02
9.3E+00:-4.71E+02-1.50E+01-1.10E+03-1.26E+02-6.16E+02
9.7E+00:-4.60E+02-4.83E+00-1.12E+03-1.42E+02-6.30E+02
1.0E+01:-4.77E+02-1.60E+00-1.15E+03-9.92E+01-6.42E+02
1.1E+01:-4.64E+02-1.51E+00-1.16E+03-9.97E+01-6.43E+02
1.1E+01:-4.77E+02-1.37E+00-1.19E+03-6.39E+01-6.26E+02
1.1E+01:-4.64E+02-1.34E+00-1.20E+03-6.09E+01-6.19E+02
1.2E+01:-4.78E+02-1.27E+00-1.23E+03-3.64E+01-5.90E+02
1.2E+01:-4.64E+02-1.24E+00-1.23E+03-3.37E+01-6.01E+02
1.3E+01:-4.74E+02-1.20E+00-1.25E+03-1.52E+01-6.09E+02
1.3E+01:-4.62E+02-1.21E+00-1.24E+03-2.51E+01-6.14E+02
1.3E+01:-4.72E+02-1.16E+00-1.26E+03-1.11E+01-6.50E+02
1.4E+01:-4.61E+02-1.17E+00-1.26E+03-1.51E+01-7.00E+02
1.4E+01:-4.73E+02-1.15E+00-1.29E+03 1.53E+00-7.22E+02
```

1 POTL versus TIME in Seconds

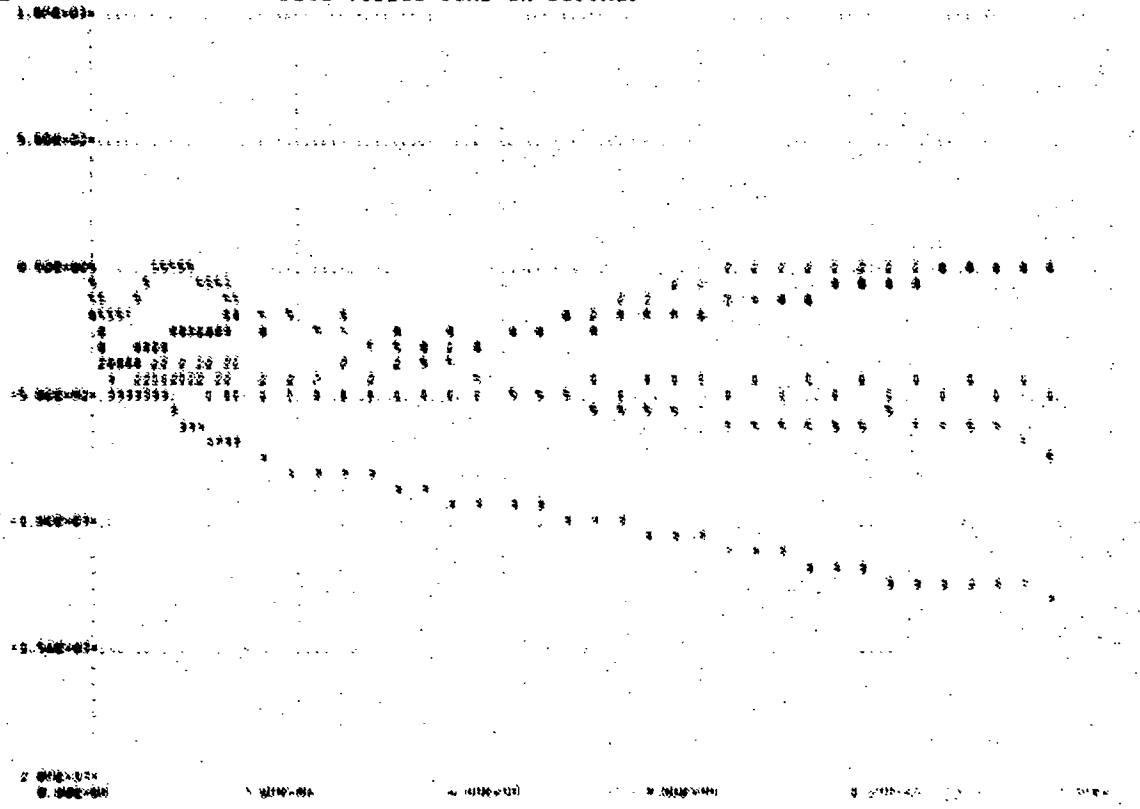

HISTORY command or MODE set >> 616,225,545,224

POTL in Volts

TIME	616	225	545	224			
	#1	#2	#3	#4	#5	#6	#7
0.0E+00	-1.03E+00	-1.03E+00	-1.03E+00	-1.03E+00			
2.0E-02	-5.72E+01	-5.72E+01	-5.70E+01	-5.70E+01			
4.0E-02	-1.15E+02	-1.16E+02	-1.15E+02	-1.15E+02			
6.0E-02	-1.68E+02	-1.74E+02	-1.74E+02	-1.74E+02			
8.0E-02	-2.14E+02	-2.32E+02	-2.32E+02	-2.32E+02			
1.0E-01	-2.52E+02	-2.89E+02	-2.85E+02	-2.88E+02			
1.2E-01	-2.80E+02	-3.40E+02	-3.31E+02	-3.39E+02			
2.2E-01	-2.75E+02	-4.34E+02	-3.75E+02	-4.26E+02			
3.2E-01	-2.47E+02	-5.10E+02	-3.84E+02	-4.90E+02			
4.2E-01	-1.94E+02	-5.61E+02	-3.52E+02	-5.24E+02			
5.2E-01	-1.47E+02	-6.12E+02	-3.19E+02	-5.56E+02			
6.2E-01	-8.31E+01	-6.45E+02	-2.67E+02	-5.69E+02			
7.2E-01	-3.54E+01	-6.84E+02	-2.24E+02	-5.89E+02			
8.2E-01	-5.81E+00	-7.15E+02	-1.78E+02	-6.03E+02			
9.2E-01	-2.19E+00	-7.59E+02	-1.59E+02	-6.34E+02			
1.0E+00	-1.80E+00	-7.90E+02	-1.22E+02	-6.54E+02			
1.1E+00	-1.68E+00	-8.46E+02	-1.18E+02	-7.01E+02			
1.2E+00	-1.48E+00	-8.78E+02	-8.95E+01	-7.22E+02			
1.3E+00	-1.46E+00	-9.39E+02	-8.86E+01	-7.75E+02			
1.4E+00	-1.35E+00	-9.70E+02	-6.03E+01	-7.96E+02			
1.5E+00	-1.33E+00	-1.03E+03	-5.28E+01	-8.44E+02			
1.6E+00	-1.26E+00	-1.06E+03	-2.92E+01	-8.67E+02			
1.7E+00	-1.24E+00	-1.11E+03	-2.04E+01	-9.12E+02			
1.8E+00	-1.18E+00	-1.14E+03	-4.99E+00	-9.34E+02			
1.9E+00	-1.17E+00	-1.20E+03	-2.51E+00	-9.81E+02			
2.0E+00	-1.13E+00	-1.23E+03	-1.99E+00	-9.99E+02			
2.1E+00	-1.12E+00	-1.28E+03	-1.89E+00	-1.04E+03			
2.5E+00	-1.10E+00	-1.36E+03	-1.61E+00	-1.10E+03			
2.9E+00	-1.08E+00	-1.44E+03	-1.49E+00	-1.18E+03			
3.3E+00	-1.07E+00	-1.51E+03	-1.35E+00	-1.24E+03			
3.7E+00	-1.06E+00	-1.59E+03	-1.28E+00	-1.32E+03			
4.1E+00	-1.05E+00	-1.66E+03	-1.21E+00	-1.37E+03			
4.5E+00	-1.04E+00	-1.74E+03	-1.17E+00	-1.45E+03			
4.9E+00	-1.04E+00	-1.81E+03	-1.14E+00	-1.50E+03			
5.3E+00	-1.04E+00	-1.89E+03	-1.12E+00	-1.57E+03			
5.7E+00	-1.04E+00	-1.95E+03	-1.10E+00	-1.62E+03			
6.1E+00	-1.03E+00	-2.03E+03	-1.09E+00	-1.69E+03			
6.5E+00	-1.03E+00	-2.10E+03	-1.08E+00	-1.73E+03			
6.9E+00	-1.03E+00	-2.18E+03	-1.08E+00	-1.80E+03			
7.3E+00	-1.03E+00	-2.25E+03	-1.07E+00	-1.84E+03			
7.7E+00	-1.03E+00	-2.32E+03	-1.06E+00	-1.91E+03			
8.1E+00	-1.03E+00	-2.39E+03	-1.06E+00	-1.96E+03			
8.5E+00	-1.03E+00	-2.45E+03	-1.05E+00	-2.02E+03			
8.9E+00	-1.03E+00	-2.52E+03	-1.05E+00	-2.07E+03			
9.3E+00	-1.03E+00	-2.59E+03	-1.05E+00	-2.13E+03			
9.7E+00	-1.03E+00	-2.65E+03	-1.04E+00	-2.18E+03			
1.0E+01	-1.03E+00	-2.73E+03	-1.04E+00	-2.24E+03			
1.1E+01	-1.03E+00	-2.80E+03	-1.04E+00	-2.30E+03			
1.1E+01	-1.03E+00	-2.86E+03	-1.04E+00	-2.36E+03			
1.1E+01	-1.03E+00	-2.93E+03	-1.04E+00	-2.41E+03			
1.2E+01	-1.03E+00	-2.99E+03	-1.04E+00	-2.47E+03			
1.2E+01	-9.25E-01	-3.05E+03	-1.04E+00	-2.52E+03			
1.3E+01	-8.27E-01	-3.12E+03	-1.04E+00	-2.59E+03			
1.3E+01	-7.59E-01	-3.17E+03	-1.03E+00	-2.63E+03			
1.3E+01	-6.90E-01	-3.24E+03	-1.03E+00	-2.69E+03			
1.4E+01	-6.31E-01	-3.30E+03	-1.03E+00	-2.73E+03			
1.4E+01	-5.71E-01	-3.37E+03	-1.03E+00	-2.80E+03			

```
1                    POTL versus TIME in Seconds
 0.00E+004...11111333.3..3.3.3.3.3.3.3..3.3.3.3.3.3.3.3..3...3.3.3.3.3..3.3.3.3.3 :.
         4  1 3333          .              .              .              .
         4 1133             .              .              .              .
```

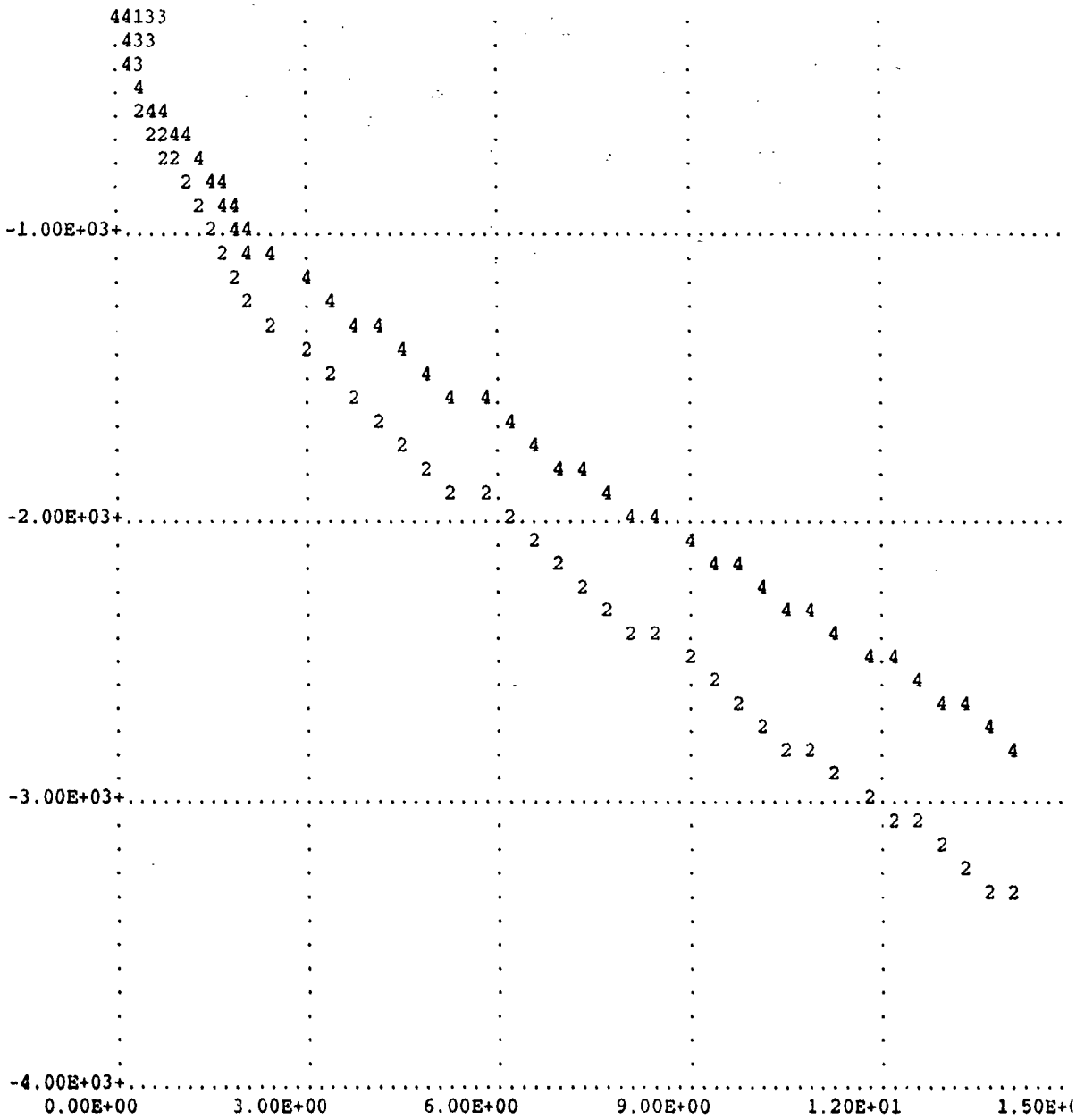


```
HISTORY command or MODE set >> exit
```

shontl Interactive Session Polar Orbiting Spacecraft–DMSP

The program **shontl** was used to create Figures 39. Note that the sheath potential is –0.40393.

```
 [*POLAR 1.3 PLOTTER(SHONTL)*]
IBIAGS(3) defaulted to  1
BIAGS(3) = 0 >> no magnetic limiting in electron presheath
BIAGS(3) > 0 >> FLX = (0.1 + 0.9*Area(DOT)B) * Fnorm
ee nterak/chkprt.f
```

```
NUMDUB=    95 NUMAXG=    100

                                +++COMPUTATION SPACE+++

           THE OBJECT(S) APPEAR TO LIE BETWEEN Z =         1       18


 THE COMP GRID WILL BE SHIFTED BY ONE UNIT IN THE X OR Y DIRECTIONS
 EVERY IDELX OR IDELY UNITS OF Z
           IDELX = 200    IDELY = 200


SO THE COMP GRID NOW HAS THE FOLLOWING FEATURES:
THE X AND Y GRID GROWTH REQUIRED TO FIT THE  OBJECT GRID IN THE DISPLACED
COMP GRID IS:
          NXGRTH =    0 NYGRTH =    0 .
CONSIDERING THE ADD-ONS THE NEW COMP GRID DIMENSIONS ARE:
          NX =    50 NY =    59 NZ =    75

 WELCOME TO THE KEYWORD INPUT PORTION OF SHONTL.  IF YOU NEED
    HELP, TYPE (HELP). AND IF YOU WANT TO LEAVE THIS PROGRAM TYPE (ESC).
SHONTL command >> plots on
plots on
SHONTL command >> levels add -.40393
levels add -.40393
     1 USER SELECTED CONTOUR LEVELS:
                      -4.04E-01
SHONTL command >> levels mark -.40393 s
levels mark -.40393 s
SHONTL command >> pot x
pot x
          ZCLEVS, MIN= -1.34E+03 MAX=  2.00E-03 LEVELS =  10
           CONTOURS ARE:
          -1.4000E+03    -1.2000E+03    -1.0000E+03    -8.0000E+02
          -6.0000E+02    -4.0000E+02    -2.0000E+02    -4.0393E-01
          -2.0000E-01    -2.0000E-02
SHONTL command >> pot y
pot y
          ZCLEVS, MIN= -8.89E+02 MAX=  1.04E-03 LEVELS =   8
           CONTOURS ARE:
          -1.0000E+03    -8.0000E+02    -6.0000E+02    -4.0000E+02
          -2.0000E+02    -4.0393E-01    -2.0000E-01    -2.0000E-02
SHONTL command >> pot z
pot z
          ZCLEVS, MIN= -1.41E+03 MAX=  1.71E-03 LEVELS =  11
           CONTOURS ARE:
          -1.6000E+03    -1.4000E+03    -1.2000E+03    -1.0000E+03
          -8.0000E+02    -6.0000E+02    -4.0000E+02    -2.0000E+02
          -4.0393E-01    -2.0000E-01    -2.0000E-02
SHONTL command >> exit
exit
[*EXIT POLAR PLOTTER, SHONTL*]
```

C.10 A Multibody Problem–EMU Near the Shuttle

Execution of suchgr (fort.3) A Multibody Problem—Shuttle

The computer code **suchgr** was used to determine the electron current collected by the shuttle orbiter.

```
Welcome to SUCHGR 1.3

    Default material is TILE
    Default environment is DMSP

SUCHGR command >> VEND -2625


SUCHGR command >> TABLE IV


Fluxes(A/m**2) as functions of Surface Voltage(eV)

  0.00E+00 -1.29E-04 -1.36E-04  4.26E-06  2.18E-06  8.93E-07  0.00E+00
 -1.25E+02  5.57E-04 -1.56E-05  3.83E-06  2.13E-06  5.56E-04  1.04E-05
 -2.50E+02  1.13E-03 -1.54E-05  3.73E-06  2.10E-06  1.11E-03  2.93E-05
 -3.75E+02  1.71E-03 -1.53E-05  3.66E-06  2.08E-06  1.67E-03  5.38E-05
 -5.00E+02  2.31E-03 -1.52E-05  3.61E-06  2.05E-06  2.22E-03  9.31E-05
 -6.25E+02  2.97E-03 -1.51E-05  3.57E-06  2.04E-06  2.78E-03  2.04E-04
 -7.50E+02  3.68E-03 -1.50E-05  3.53E-06  2.02E-06  3.33E-03  3.57E-04
 -8.75E+02  4.43E-03 -1.49E-05  3.49E-06  2.00E-06  3.89E-03  5.48E-04
 -1.00E+03  5.21E-03 -1.48E-05  3.46E-06  1.98E-06  4.45E-03  7.75E-04
 -1.12E+03  6.02E-03 -1.47E-05  3.43E-06  1.97E-06  5.00E-03  1.03E-03
 -1.25E+03  6.87E-03 -1.46E-05  3.40E-06  1.95E-06  5.56E-03  1.32E-03
 -1.38E+03  7.74E-03 -1.45E-05  3.38E-06  1.94E-06  6.11E-03  1.64E-03
 -1.50E+03  8.64E-03 -1.44E-05  3.35E-06  1.92E-06  6.67E-03  1.98E-03
 -1.62E+03  9.56E-03 -1.43E-05  3.33E-06  1.91E-06  7.22E-03  2.34E-03
 -1.75E+03  1.05E-02 -1.42E-05  3.30E-06  1.89E-06  7.78E-03  2.73E-03
 -1.88E+03  1.15E-02 -1.41E-05  3.28E-06  1.88E-06  8.33E-03  3.14E-03
 -2.00E+03  1.25E-02 -1.40E-05  3.26E-06  1.86E-06  8.89E-03  3.57E-03
 -2.12E+03  1.35E-02 -1.39E-05  3.23E-06  1.85E-06  9.45E-03  4.02E-03
 -2.25E+03  1.45E-02 -1.38E-05  3.21E-06  1.84E-06  1.00E-02  4.49E-03
 -2.38E+03  1.55E-02 -1.38E-05  3.19E-06  1.82E-06  1.06E-02  4.98E-03
 -2.50E+03  1.66E-02 -1.37E-05  3.17E-06  1.81E-06  1.11E-02  5.48E-03
SUCHGR command >> EXIT
```

To determine the ion current to the shuttle orbitor, **vehicl** and **nterak** were used. A rough shuttle model of the appropriate size and shape was created. The standard input and object defintion files are given for the **vehicl** execution.

Standard Input For vehicl Execution A Multibody Problem—Shuttle

```
nxyz 11  13  5
matplots yes
makeplot 2
plotdir 2 3 5
plotdir -2 -3 -5
```

```
end
```

Object Definition File A Multibody Problem—Shuttle

```
comment  This is a crude shuttle model with approximately the correct
comment  surface area.
comment  There is a small patch of teflon to model the EMU
comment  White sputtered tile material
offset  0 0 0
tile
2  0.01  1e-16  7   1.6  0.6  45.4   0.4
200  1.62  0.455  140  2e-5  1e16  15  16
17 18 19 20
rectan
corner   2 2 2
deltas  8   2   2
surface   +x  tile
surface   -x  tile
surface   +y  tile
surface   -y  tile
surface   +z  tile
surface   -z  tile
endobj
rectan
corner  4   4   2
deltas  4   6   2
surface   +x  tile
surface   -x  tile
surface   +z  tile
surface   -z  tile
endobj
wedge
corner  4  4  2
face  tile   -1   1   0
length  2  2  2
surface   +z  tile
surface   -z  tile
endobj
wedge
corner  8  4  2
face  tile   1   1   0
length  2  2  2
surface   +z  tile
surface   -z  tile
endobj
wedge
corner  6  10  2
face  tile   -1   1   0
length  2  2  2
surface   +z  tile
surface   -z  tile
endobj
wedge
corner  6  10  2
face  tile   1   1   0
length  2  2  2
surface   +z  tile
surface   -z  tile
endobj
patchr
corner  6   5   3
deltas 1  1  1
```

```
surface +z teflon
endobj
endsat
```

Execution of nterak A Multibody Problem—Shuttle

The computer code **nterak** was used to evaluate the charging and current collected for several different potentials. The standard input file for the −1 kV case is shown here.

```
  DEFAULT
  ISTART NEW
comment
comment  Choose Physical Models to be used.
  igical yes
  stnwake on
  aveprtcl on
  thrmsprd on
comment
comment  Redefine Algorithm parameters
  maxitc 50
  potcon 4
comment Define Computational Grid
  DXMESH 3.5
  NXADNT 5
  NXADNB 5
  NYADNT 5
  NYADNB 5
  NZADON 5
  NZTAIL 12
comment define the plasma environment
  VMACH 0.0 0.0 8.0
  RATIH 10.0
  DENS  1e10
  TEMP  0.2
  DEN2   6.0E5
  TEMP2  8.0E3
  GAUCO  4.0e4
  ENAUT  2.4E4
  DELTA  1.6E4
  POWCO  3.0E11
  PALPHA 1.1
  PCUTL  50.0
  PCUTH  1.6E6
comment set conductor potential
  CONDV 1  -1000
comment Iterate on the analytical modules
  LOOP 4 PWASON CURREN
  endrun
```

To examine the charging of the EMU, we use the *POLAR* codes. We use **suchgr** to estimate the charging of each of the materials under orbit-limited collection. (The runstream shown here was executed after the environment was defined using **nterak**.)

The suchgr Execution Runstream A Multibody Problem—EMU

```
Welcome to SUCHGR 1.3
```

```
   Default material is BTSP
   Default environment is DMSP

 SUCHGR command >> material teflon
Material is changed to TEFL

 SUCHGR command >> charge

 Charged under Orbit Limited Regime
                                  Initial       Final       Units
                                  -------       -----       -----
    Surface Potential           0.0000E+00  -2.8538E+03 volts
    Conductor Potential         0.0000E+00   0.0000E+00 volts

 Flux Breakdown:
    Incident Electron Flux     -1.7098E-05  -1.3417E-05 A/m**2
    Electron Secondary Flux     3.9940E-06   2.4982E-06 A/m**2
    Backscattered Electron Flux 2.1803E-06   1.7715E-06 A/m**2

    Incident Ion Flux           9.3163E-09   5.8921E-06 A/m**2
    Ion Secondary Flux          4.3398E-11   3.2477E-06 A/m**2

    Photo Flux                  0.0000E+00   0.0000E+00 A/m**2
    Conduction Flux             0.0000E+00   0.0000E+00 A/m**2
                               -----------  -----------
    Total Flux                 -1.0914E-05  -7.8621E-09 A/m**2

 SUCHGR command >> material lexan
Material is changed to LEXA

 SUCHGR command >> charge

 Charged under Orbit Limited Regime
                                  Initial       Final       Units
                                  -------       -----       -----
    Surface Potential           0.0000E+00  -3.2288E+03 volts
    Conductor Potential         0.0000E+00   0.0000E+00 volts

 Flux Breakdown:
    Incident Electron Flux     -1.7098E-05  -1.3156E-05 A/m**2
    Electron Secondary Flux     2.2811E-06   1.2143E-06 A/m**2
    Backscattered Electron Flux 1.7080E-06   1.3400E-06 A/m**2

    Incident Ion Flux           9.3163E-09   6.6651E-06 A/m**2
    Ion Secondary Flux          4.3398E-11   4.0526E-06 A/m**2

    Photo Flux                  0.0000E+00   0.0000E+00 A/m**2
    Conduction Flux             0.0000E+00   0.0000E+00 A/m**2
                               -----------  -----------
    Total Flux                 -1.3099E-05   1.1569E-07 A/m**2

 SUCHGR command >> material alum
Material is changed to ALUM

 SUCHGR command >> charge

 Charged under Orbit Limited Regime
                                  Initial       Final       Units
                                  -------       -----       -----
    Surface Potential           0.0000E+00  -3.3538E+03 volts
    Conductor Potential         0.0000E+00   0.0000E+00 volts

 Flux Breakdown:
```

```
    Incident Electron Flux          -1.7098E-05   -1.3070E-05 A/m**2
    Electron Secondary Flux          1.8093E-06    1.1619E-06 A/m**2
    Backscattered Electron Flux      3.2424E-06    2.5997E-06 A/m**2

    Incident Ion Flux                9.3163E-09    6.9228E-06 A/m**2
    Ion Secondary Flux               2.3273E-11    2.3455E-06 A/m**2

    Photo Flux                       0.0000E+00    0.0000E+00 A/m**2
    Conduction Flux                  0.0000E+00    0.0000E+00 A/m**2
                                    -----------   -----------
    Total Flux                      -1.2037E-05   -4.0196E-08 A/m**2

 SUCHGR command >> material kapton
Material is changed to KAPT

 SUCHGR command >> charge

 Charged under Orbit Limited Regime
                                     Initial       Final       Units
                                     -------       -----       -----
    Surface Potential                0.0000E+00   -3.2288E+03 volts
    Conductor Potential              0.0000E+00    0.0000E+00 volts

 Flux Breakdown:
    Incident Electron Flux          -1.7098E-05   -1.3156E-05 A/m**2
    Electron Secondary Flux          2.2811E-06    1.2143E-06 A/m**2
    Backscattered Electron Flux      1.7080E-06    1.3400E-06 A/m**2

    Incident Ion Flux                9.3163E-09    6.6651E-06 A/m**2
    Ion Secondary Flux               4.3398E-11    4.0526E-06 A/m**2

    Photo Flux                       0.0000E+00    0.0000E+00 A/m**2
    Conduction Flux                  0.0000E+00    0.0000E+00 A/m**2
                                    -----------   -----------
    Total Flux                      -1.3099E-05    1.1569E-07 A/m**2

 SUCHGR command >> material whiten
Material is changed to WHIT

 SUCHGR command >> charge

 Charged under Orbit Limited Regime
                                     Initial       Final       Units
                                     -------       -----       -----
    Surface Potential                0.0000E+00   -3.2288E+03 volts
    Conductor Potential              0.0000E+00    0.0000E+00 volts

 Flux Breakdown:
    Incident Electron Flux          -1.7098E-05   -1.3156E-05 A/m**2
    Electron Secondary Flux          2.6074E-06    1.2395E-06 A/m**2
    Backscattered Electron Flux      1.7080E-06    1.3400E-06 A/m**2

    Incident Ion Flux                9.3163E-09    6.6651E-06 A/m**2
    Ion Secondary Flux               4.3398E-11    4.0526E-06 A/m**2

    Photo Flux                       0.0000E+00    0.0000E+00 A/m**2
    Conduction Flux                  0.0000E+00    0.0000E+00 A/m**2
                                    -----------   -----------
    Total Flux                      -1.2773E-05    1.4088E-07 A/m**2

 SUCHGR command >> exit
Want to save a copy of the session?(YES/NO)  >> yes

Exit SUCHGR.
```

Then we define the EMU object using **vehicl**.

vehicl Standard Input A Multibody Problem—EMU

```
nxyz 17  17   33
matplots yes
makeplot 2
plotdir 2 3 5
plotdir -2 -3 -5
end
```

EMU Object Definition A Multibody Problem—EMU

```
Comment - Object Definition for EVA - Man
comment defined for xmesh of 0.1 m
Comment - Material Definitions
Lexan
3.5       .01       1.E-16 5.  1.8    .2   71.48     .60
290       1.77      .455      140.      .00002        1.E+16 10000.   2000.
17.       18.       19.       20.
ALUMIN
1.        .001      -1.       13.       .97       .3        153.7     .8
220.      1.76      .244      230.      .00004    -1.       10000.    2000.
17.       18.       19.       20.
TEFLON
2.        .01       1.E-16  7.    2.4    .3        45.37      .40
70        1.77      .455      140.      .00002        1.E+16 10000.   2000.
17.       18.       19.       20.
KAPTON
3.5       .01       1.E-16 5.  1.8    .2   71.48     .60
290       1.77      .455      140.      .00002        1.E+16 10000.   2000.
17.       18.       19.       20.
WHITEM
3.5       .01       5.9E-14 5.       2.1       .15       71.5      .60
312.1     1.77      .455      140.      .00002        1.E+13 10000.    2000.
17.       18.       19.       20.
Comment
Comment - Define trunk as two octagons
Octagon
        Axis  -2 -1  0    -2 -1 7
        Width 3
        Side 1
        Surface + Teflon
        Surface - Teflon
        Surface C Teflon
        Endobj
    Octagon
        Axis   1 -1  0     1 -1 7
        Width 3
        Side 1
        Surface + Teflon
        Surface - Teflon
        Surface C Teflon
        Endobj
    Rectan
        Corner -1 -2 0
        Deltas  2  3 8
        Surface +X Teflon
```

```
            Surface -X Teflon
            Surface +Y Teflon
            Surface -Y Teflon
            Surface +Z Teflon
            Surface -Z Teflon
            Endobj
        Octagon
            Axis  -3  -1  6     3  -1  6
            Width 3
            Side 1
            Surface + Teflon
            Surface - Teflon
            Surface C Teflon
            Endobj
        Rectan
            Corner -3 -2 5
            Deltas  6  3 2
            Surface +X Teflon
            Surface -X Teflon
            Surface +Y Teflon
            Surface -Y Teflon
            Surface +Z Teflon
            Surface -Z Teflon
            Endobj
    Comment - Define legs
        Octagon
            Axis -2 -1 -7   -2 -1  0
            Width 3
            Side 1
            Surface + Teflon
            Surface - Teflon
            Surface C Teflon
            Endobj
        Octagon
            Axis +1 -1 -7   +1 -1  0
            Width 3
            Side 1
            Surface + Teflon
            Surface - Teflon
            Surface C Teflon
            Endobj
    Comment - Define feet
        Octagon
            Axis -2  0 -7   -2  0 -6
            Width 3
            Side 1
            Surface + Teflon
            Surface - Teflon
            Surface C Teflon
            Endobj
        Octagon
            Axis +1  0 -7   +1  0 -6
            Width 3
            Side 1
            Surface + Teflon
            Surface - Teflon
            Surface C Teflon
            Endobj
      Rectan
         Corner -2 -2 -7
         Deltas 1 1 1
         Surface +X Aluminum
         Surface -X Aluminum
         Surface +Y Aluminum
```

```
        Surface -Y Aluminum
        Surface +Z Aluminum
        Surface -Z Aluminum
        Endobj
    Rectan
        Corner  1 -2 -7
        Deltas 1 1 1
        Surface +X Aluminum
        Surface -X Aluminum
        Surface +Y Aluminum
        Surface -Y Aluminum
        Surface +Z Aluminum
        Surface -Z Aluminum
        Endobj
Comment - Define Head
    Qsphere
        Center  0  0  10
        Diameter 4
        Side 2
        Material Teflon
        Endobj
    Patchr
        Corner -1 1 9
        Deltas  2 1 2
        Surface +Y Lexan
        Endobj
    Patchw
        Corner -1 1 9
        Face Lexan -1  1 0
        Length   1  1 2
        Endobj
    Patchw
        Corner -1 1 9
        Face Lexan  0  1 -1
        Length   2  1 1
        Endobj
    Patchw
        Corner -1 1 11
        Face Lexan  0  1 1
        Length   2  1 1
        Endobj
    Patchw
        Corner 1 1 9
        Face Lexan 1  1 0
        Length   1  1 2
        Endobj
    Tetrah
        Corner 1 1 9
        Face Lexan 1  1 -1
        Length   1
        Endobj
    Tetrah
        Corner -1 1 9
        Face Lexan -1  1 -1
        Length   1
        Endobj
    Tetrah
        Corner 1 1 11
        Face Lexan 1  1 1
        Length   1
        Endobj
    Tetrah
        Corner -1 1 11
        Face Lexan -1  1 1
```

```
        Length   1
        Endobj
    Patchr
        Corner -1 0 11
        Deltas  2 1 1
        Surface +Z Whiten
        Endobj
    Patchr
        Corner -2 0  9
        Deltas  1 1 2
        Surface -X Whiten
        Endobj
    Patchr
        Corner  1 0  9
        Deltas  1 1 2
        Surface +X Whiten
        Endobj
    Patchw
        Corner  1 0  11
      Face Whiten 1  0 1
      Length 1 1 1
        Endobj
    Patchw
        Corner  -1 0  11
      Face Whiten -1 0 1
      Length 1 1 1
        Endobj
Comment - Define Shoulders
    Qsphere
        Center  -4 -1 6
        Diameter 3
        Side 1
        Material Teflon
        Endobj
    Rectan
        Corner  -4 -2 5
        Deltas   1 3 1
        Surface  +Y Teflon
        Surface  -Y Teflon
        Surface  -X Teflon
        Endobj
    Qsphere
        Center   3 -1 6
        Diameter 3
        Side 1
        Material Teflon
        Endobj
    Rectan
        Corner   3 -2 5
        Deltas   1 3 1
        Surface  +Y Teflon
        Surface  -Y Teflon
        Surface  -Z Teflon
        Endobj
Comment - Upper Arms
    Rectan
        Corner  -5 -1 2
        Deltas   2  1 4
        Surface -X  Teflon
        Surface -Z  Teflon
        Endobj
    Wedge
        Corner  -4 -1 2
        Face Teflon -1 -1 0
```

```
        Length   1  1 4
        Surface -Z  Teflon
        Endobj
    Wedge
        Corner  -4 -1 2
        Face Teflon  1 -1 0
        Length   1  1 4
        Surface -Z  Teflon
        Endobj
    Wedge
        Corner  -4  0 2
        Face Teflon -1  1 0
        Length   1  1 4
        Surface -Z  Teflon
        Endobj
    Wedge
        Corner  -4  0 2
        Face Teflon  1  1 0
        Length   1  1 4
        Surface -Z  Teflon
        Endobj
    Rectan
        Corner   3 -1 2
        Deltas   2  1 4
        Surface +X  Teflon
        Surface -Z  Teflon
        Endobj
    Wedge
        Corner  4 -1 2
        Face Teflon -1 -1 0
        Length   1  1 4
        Surface -Z  Teflon
        Endobj
    Wedge
        Corner  4 -1 2
        Face Teflon  1 -1 0
        Length   1  1 4
        Surface -Z  Teflon
        Endobj
    Wedge
        Corner  4  0 2
        Face Teflon -1  1 0
        Length   1  1 4
        Surface -Z  Teflon
        Endobj
    Wedge
        Corner  4  0 2
        Face Teflon  1  1 0
        Length   1  1 4
        Surface -Z  Teflon
        Endobj
Comment - Forearms
    Rectan
        Corner -5 0 2
        Deltas   2 4 2
        Surface +X Teflon
        Surface -X Teflon
        Surface +Y Kapton
        Surface -Y Teflon
        Surface +Z Teflon
        Surface -Z Teflon
        Endobj
    Rectan
        Corner  3 0 2
```

```
            Deltas   2 4 2
            Surface +X Teflon
            Surface -X Teflon
            Surface +Y Kapton
            Surface -Y Teflon
            Surface +Z Teflon
            Surface -Z Teflon
            Endobj
    Comment - Hands
        Rectan
            Corner -5 4 2
            Deltas   1 1 2
            Surface +X Kapton
            Surface -X Teflon
            Surface +Y Teflon
            Surface -Y Teflon
            Surface +Z Teflon
            Surface -Z Teflon
            Endobj
        Rectan
            Corner  4 4 2
            Deltas   1 1 2
            Surface +X Teflon
            Surface -X Kapton
            Surface +Y Teflon
            Surface -Y Teflon
            Surface +Z Teflon
            Surface -Z Teflon
            Endobj
    Comment - Backpack (PLSS)
        Rectan
            Corner -3  -4  2
            Deltas  6   2  6
            Surface +X Teflon
            Surface -X Teflon
            Surface +Y Teflon
            Surface -Y Teflon
            Surface +Z Teflon
            Surface -Z Teflon
            Endobj
        Rectan
            Corner -2  -6  2
            Deltas  4   1  7
            Surface +X Teflon
            Surface -X Teflon
            Surface +Y Teflon
            Surface -Y Teflon
            Surface +Z Teflon
            Surface -Z Teflon
            Endobj
        Wedge
            Corner  -2  -6  8
            Face  Teflon  -1   0  1
            Length   1   1  1
            Surface  +Y  Teflon
            Surface  -Y  Teflon
            Endobj
        Wedge
            Corner   2  -6  8
            Face  Teflon   1   0  1
            Length   1   1  1
            Surface  +Y  Teflon
            Surface  -Y  Teflon
            Endobj
```

```
    Wedge
        Corner  -2  -3  8
        Face  Teflon    0    1  1
        Length    4    1  1
        Endobj
    Tetrah
        Corner  -2 -3 8
        Face Teflon  -1 1 1
        Length 1
        Endobj
    Tetrah
        Corner   2 -3 8
        Face Teflon   1 1 1
        Length 1
        Endobj
Comment - Brickpack
    Rectan
        Corner -1  1  3
        Deltas  3  1  4
        Surface +X Teflon
        Surface -X Teflon
        Surface +Y Teflon
        Surface -Y Teflon
        Surface +Z Teflon
        Surface -Z Teflon
        Endobj
    Patchr
        Corner  0  1  3
        Deltas  2  1  4
       Surface +Z Aluminum
       Endobj
    Rectan
        Corner -2  1  3
        Deltas  4  1  3
        Surface +X Teflon
        Surface -X Teflon
        Surface +Y Teflon
        Surface -Y Teflon
        Surface -Z Teflon
        Surface -Z Teflon
        Endobj
    Patchr
        Corner  -2  1  5
        Deltas  1  1  1
        Surface +Y Aluminum
        Endobj
Endset
```

Then we execute nterak to examine the charging. This is done in four steps.

nterak Standard Input A Multibody Problem—EMU

```
  DEFAULT
  ISTART NEW
comment
comment  Choose Physical Models to be used.
  igical no
  sthmake off
  orbits
comment
comment  Redefine Algorithm parameters
```

```
  maxits 1
  maxitc 50
  potcon 4
  deltat 0.01
comment Define Computational Grid
  DXMESH .1
  MXADMT 25
  MXADMB 25
  MYADMT 25
  MYADMB 25
  MZADOM 17
  MZTAIL 17
comment define the plasma environment
  VMACH 0.0 0.0 0.001
  RATIH 10.0
  DENS  2.2e7
  TEMP  4.5
  DEN2   6.0E5
  TEMP2  8.0E3
  GAUCO  4.0e4
  EMAUT  2.4E4
  DELTA  1.6E4
  POWCO  3.0E11
  PALPHA 1.1
  PCUTL  50.0
  PCUTH  1.6E6
comment set conductor potential
  CONDV 1  -10
comment Iterate on the analytical modules
  PWASON
  CHARGE
  endrun
```

nterak Standard Input For First Continuation A Multibody Problem—EMU

```
ISTART  cont
WHAT
DELTAT  0.01
LOOP 5 PWASON CHARGE
DELTAT  0.02
LOOP 5 PWASON CHARGE
ENDRUN
```

nterak Standard Input For Second Continuation A Multibody Problem—EMU

```
ISTART  cont
DELTAT  0.05
LOOP 5 PWASON CHARGE
DELTAT  0.10
LOOP 5 PWASON CHARGE
ENDRUN
```

nterak Standard Input For Third Continuation A Multibody Problem—EMU

```
ISTART  cont
DELTAT  0.20
LOOP 5 PWASON CHARGE
DELTAT  0.50
```

```
LOOP 5 PWASON CHARGE
ENDRUN
```

nterak Standard Input For Fourth Continuation A Multibody Problem—EMU

```
ISTART  cont
DELTAT  1
LOOP 5 PWASON CHARGE
DELTAT  2
LOOP 5 PWASON CHARGE
ENDRUN
```

We examine the results using **trmtlk**.

trmtlk Interactive Runstream A Multibody Problem—EMU

```
Welcome to POLAR 1.3 TRMTLK ...

Any AID may be called fr' n any MODULE

    MODULES          AIDS
  **********      ********
    HISTORY          AGAIN
    LATEST           HELP
    SINGLE           LOCATION #
    SPECIAL          OUTLINE
                     SUBSET
                     EXIT
                     SUBSET [GROUP NAME]

Enter any MODULE·AID name or 'HELP' for help >> latest

LATEST command or MODE set >> magnitude
MODE RESET

LATEST command or MODE set >> subset teflon
DEFINITION OF NEW SUBSET NAMED TEFL
 551 REMAINING IN GROUP

SUBSET command please >> matl teflon
 511 REMAINING IN GROUP

SUBSET command please >> done
GROUP TEFL WITH  511 MEMBERS IS NOW DEFINED
RETURNING TO MODULE  'LATE'

LATEST command or MODE set >> subset lexan
DEFINITION OF NEW SUBSET NAMED LEXA
 551 REMAINING IN GROUP

SUBSET command please >> matl lexan
  16 REMAINING IN GROUP

SUBSET command please >> done
GROUP LEXA WITH   16 MEMBERS IS NOW DEFINED
RETURNING TO MODULE  'LATE'

LATEST command or MODE set >> subset whiten
DEFINITION OF NEW SUBSET NAMED WHIT
```

```
 551 REMAINING IN GROUP

SUBSET command please >> matl whiten
   8 REMAINING IN GROUP

SUBSET command please >> done
GROUP WHIT WITH     8 MEMBERS IS NOW DEFINED
RETURNING TO MODULE  'LATE'

LATEST command or MODE set >> subset kapton
DEFINITION OF NEW SUBSET NAMED KAPT
 551 REMAINING IN GROUP

SUBSET command please >> matl kapton
   8 REMAINING IN GROUP

SUBSET command please >> done
GROUP KAPT WITH     8 MEMBERS IS NOW DEFINED
RETURNING TO MODULE  'LATE'

LATEST command or MODE set >> group teflon
POTL IN VOLTS  FOR POLAR CYCLE  42 ... TIME = 3.26E+01 SEC
 161-3.45E+03  160-3.45E+03  159-3.45E+03  158-3.45E+03  538-3.45E+03
 157-3.45E+03  156-3.45E+03  535-3.45E+03  155-3.45E+03  154-3.45E+03
 153-3.45E+03   28-3.45E+03  524-3.45E+03  523-3.45E+03   27-3.45E+03
 150-3.45E+03  149-3.45E+03   70-3.45E+03  512-3.45E+03  511-3.45E+03
 510-3.45E+03  509-3.45E+03  508-3.45E+03  507-3.45E+03   69-3.45E+03
 146-3.45E+03  500-3.45E+03  499-3.45E+03  145-3.45E+03  497-3.45E+03
 144-3.45E+03  495-3.45E+03  494-3.45E+03  493-3.45E+03  492-3.45E+03
 143-3.45E+03  490-3.45E+03  142-3.45E+03  488-3.45E+03  487-3.45E+03
 486-3.45E+03  485-3.45E+03  141-3.45E+03   68-3.45E+03   67-3.45E+03
 138-3.45E+03  480-3.45E+03  479-3.45E+03   66-3.45E+03  136-3.45E+03
 476-3.45E+03  475-3.45E+03  474-3.45E+03  473-3.45E+03  472-3.4 E+03
 471-3.45E+03   65-3.45E+03  467-3.45E+03  134-3.45E+03  465-3.45E+03
 133-3.45E+03   64-3.45E+03  462-3.45E+03   63-3.45E+03  460-3.45E+03
 130-3.45E+03   62-3.45E+03  128-3.45E+03  456-3.45E+03   61-3.45E+03
 126-3.45E+03  453-3.45E+03  125-3.45E+03  124-3.45E+03  450-3.45E+03
 449-3.45E+03  123-3.45E+03  447-3.45E+03  446-3.45E+03   26-3.45E+03
 444-3.45E+03   59-3.45E+03  442-3.45E+03   25-3.45E+03  440-3.45E+03
 439-3.45E+03  438-3.45E+03  437-3.45E+03  436-3.45E+03  435-3.45E+03
 434-3.45E+03  433-3.45E+03  432-3.45E+03  431-3.45E+03  430-3.45E+03
  57-3.45E+03  118-3.45E+03  427-3.45E+03  426-3.45E+03  117-3.45E+03
 424-3.45E+03  423-3.45E+03  422-3.45E+03   24-3.45E+03  420-3.45E+03
 419-3.45E+03   55-3.45E+03   23-3.45E+03  416-3.45E+03  415-3.45E+03
  53-3.45E+03  112-3.45E+03  412-3.45E+03  411-3.45E+03  410-3.45E+03
 409-3.45E+03  408-3.45E+03  407-3.45E+03  406-3.45E+03  405-3.45E+03
 404-3.45E+03  403-3.45E+03  402-3.45E+03  401-3.45E+03  400-3.45E+03
 399-3.45E+03  111-3.45E+03  396-3.45E+03  395-3.45E+03  394-3.45E+03
 110-3.45E+03  392-3.45E+03  391-3.45E+03  109-3.45E+03   52-3.45E+03
 388-3.45E+03  387-3.45E+03   51-3.45E+03   22-3.45E+03  384-3.45E+03
 383-3.45E+03  382-3.45E+03  381-3.45E+03  380-3.45E+03  379-3.45E+03
 378-3.45E+03  377-3.45E+03  376-3.45E+03  375-3.45E+03  374-3.45E+03
 373-3.45E+03  372-3.45E+03  371-3.45E+03  370-3.45E+03  369-3.45E+03
 368-3.45E+03  367-3.45E+03  366 3.45E+03  365-3.45E+03  364-3.45E+03
 363-3.45E+03  362-3.45E+03   21-3.45E+03  360-3.45E+03  359-3.45E+03
 358-3.45E+03  357-3.45E+03  356 3.45E+03  355-3.45E+03  354-3.45E+03
 353-3.45E+03  104-3.45E+03  351-3.45E+03  103-3.45E+03  349-3.45E+03
 348-3.45E+03   20-3.45E+03  346-3.45E+03   19-3.45E+03  344-3.45E+03
  18-3.45E+03  342-3.45E+03  341-3.45E+03   17-3.45E+03  339-3.45E+03
 338-3.45E+03  337-3.45E+03   98-3.45E+03   97-3.45E+03  334-3.45E+03
  96-3.45E+03   32-3.45E+03  331 3.45E+03   95-3.45E+03  329-3.45E+03
 328-3.45E+03   44-3.45E+03  326 3.45E+03   43-3.45E+03  324-3.45E+03
 323-3.45E+03  322-3.45E+03  321-3.45E+03  320 3.45E+03  319-3.45E+03
 318-3.45E+03  317-3.45E+03  316 3.45E+03  315-3.45E+03  314-3.45E+03
```

```
313-3.45E+03  312-3.45E+03  307-3.45E+03  306-3.45E+03  305-3.45E+03
304-3.45E+03  303-3.45E+03  302-3.45E+03  301-3.45E+03  300-3.45E+03
299-3.45E+03  298-3.45E+03  297-3.45E+03  296-3.45E+03  295-3.45E+03
294-3.45E+03  293-3.45E+03  292-3.45E+03  291-3.45E+03  290-3.45E+03
289-3.45E+03  288-3.45E+03  287-3.45E+03   16-3.45E+03   15-3.45E+03
284-3.45E+03  283-3.45E+03  282-3.45E+03  281-3.45E+03   90-3.45E+03
 89-3.45E+03    8-3.45E+03  277-3.45E+03   13-3.45E+03  275-3.45E+03
 38-3.45E+03   37-3.45E+03  272-3.45E+03  271-3.45E+03  270-3.45E+03
269-3.45E+03  268-3.45E+03  267-3.45E+03  266-3.45E+03  265-3.45E+03
264-3.45E+03  263-3.45E+03  262-3.45E+03  261-3.45E+03  260-3.45E+03
255-3.45E+03  254-3.45E+03  253-3.45E+03  252-3.45E+03  251-3.45E+03
250-3.45E+03  249-3.45E+03  248-3.45E+03  247-3.45E+03  246-3.45E+03
245-3.45E+03  244-3.45E+03  243-3.45E+03  242-3.45E+03  241-3.45E+03
240-3.45E+03  239-3.45E+03  238-3.45E+03  237-3.45E+03  236-3.45E+03
235-3.45E+03  234-3.45E+03  233-3.45E+03   84-3.45E+03   83-3.45E+03
230-3.45E+03  229-3.45E+03  228-3.45E+03  227-3.45E+03   82-3.45E+03
 81-3.45E+03   36-3.45E+03  223-3.45E+03   35-3.45E+03  221-3.45E+03
 12-3.45E+03   11-3.45E+03  218-3.45E+03  217-3.45E+03  216-3.45E+03
215-3.45E+03  214-3.45E+03  213-3.45E+03  212-3.45E+03  211-3.45E+03
210-3.45E+03  209-3.45E+03  208-3.45E+03  207-3.45E+03  206-3.45E+03
205-3.45E+03  204-3.45E+03  203-3.45E+03  202-3.45E+03  201-3.45E+03
200-3.45E+03  199-3.45E+03  198-3.45E+03  197-3.45E+03  196-3.45E+03
195-3.45E+03  194-3.45E+03  193-3.45E+03  192-3.45E+03  191-3.45E+03
190-3.45E+03  189-3.45E+03   76-3.45E+03   75-3.45E+03  186-3.45E+03
185-3.45E+03  184-3.45E+03  183-3.45E+03  182-3.45E+03  181-3.45E+03
180-3.45E+03  179-3.45E+03  178-3.45E+03  177-3.45E+03   10-3.45E+03
  7-3.45E+03  174-3.45E+03  173-3.45E+03  172-3.45E+03  171-3.45E+03
170-3.45E+03  169-3.45E+03  168-3.45E+03  167-3.45E+03  166-3.45E+03
165-3.45E+03  164-3.45E+03  163-3.45E+03  162-3.45E+03   50-3.45E+03
 49-3.45E+03   48-3.45E+03   47-3.45E+03  537-3.45E+03  536-3.45E+03
 46-3.45E+03   45-3.45E+03  526-3.45E+03  525-3.45E+03   42-3.45E+03
 41-3.45E+03  514-3.45E+03  513-3.45E+03   40-3.45E+03   39-3.45E+03
498-3.45E+03  496-3.45E+03  491-3.45E+03  489-3.45E+03  484-3.45E+03
483-3.45E+03  482-3.45E+03  481-3.45E+03  478-3.45E+03  477-3.45E+03
 14-3.45E+03  466-3.45E+03  464-3.45E+03  463-3.45E+03    9-3.45E+03
459-3.45E+03  458-3.45E+03  457-3.45E+03  455-3.45E+03  454-3.45E+03
452-3.45E+03  451-3.45E+03  448-3.45E+03  445-3.45E+03  443-3.45E+03
441-3.45E+03  429-3.45E+03  428-3.45E+03  425-3.45E+03  421-3.45E+03
418-3.45E+03  417-3.45E+03  414-3.45E+03  413-3.45E+03  398-3.45E+03
393-3.45E+03  390-3.45E+03  389-3.45E+03  386-3.45E+03  385-3.45E+03
361-3.45E+03  352-3.45E+03  350-3.45E+03  347-3.45E+03  345-3.45E+03
343-3.45E+03  340-3.45E+03  336-3.45E+03  335-3.45E+03  333-3.45E+03
330-3.45E+03  327-3.45E+03  325-3.45E+03  286-3.45E+03  285-3.45E+03
280-3.45E+03  279-3.45E+03  278-3.45E+03  276-3.45E+03  274-3.45E+03
273-3.45E+03  232-3.45E+03  231-3.45E+03  226-3.45E+03  225-3.45E+03
224-3.45E+03  222-3.45E+03  220-3.45E+03  219-3.45E+03  188-3.45E+03
187-3.45E+03  176-3.45E+03  175-3.45E+03  152-3.45E+03  151-3.45E+03
148-3.45E+03  147-3.45E+03  140-3.45E+03  139-3.45E+03  137-3.45E+03
135-3.45E+03  132-3.45E+03  131-3.45E+03  129-3.45E+03  127-3.45E+03
122-3.45E+03  121-3.45E+03  120-3.45E+03  119-3.45E+03  116-3.45E+03
115-3.45E+03  114-3.45E+03  113-3.45E+03  108-3.45E+03  107-3.45E+03
106-3.45E+03  105-3.45E+03  102-3.45E+03  101-3.45E+03  100-3.45E+03
 99-3.45E+03   94-3.45E+03   93-3.45E+03   92-3.45E+03   91-3.45E+03
 88-3.45E+03   87-3.45E+03   86-3.45E+03   85-3.45E+03   80-3.45E+03
 79-3.45E+03   78-3.45E+03   77-3.45E+03   74-3.45E+03   73-3.45E+03
 72-3.45E+03   71-3.45E+03   60-3.45E+03   58-3.45E+03   56-3.45E+03
 54-3.45E+03  548-3.45E+03  547-3.45E+03  540-3.45E+03  539-3.45E+03
528-3.45E+03  527-3.45E+03  516-3.45E+03  515-3.45E+03  502-3.45E+03
501-3.45E+03  469-3.45E+03  461-3.45E+03   34-3.45E+03   33-3.45E+03
 32-3.45E+03   31-3.45E+03    6-3.45E+03    4-3.45E+03    3-3.45E+03
  1 3.45E+03    0 0.00E+00    0 0.00E+00    0 0.00E+00    0 0.00E+00

LATEST command or MODE set -> group lexan
POTL IN VOLTS FOR POLAR CYCLE  42 ... TIME   3.26E+01 SEC
```

```
 520-3.90E+03  545-3.90E+03  544-3.90E+03  519-3.90E+03  534-3.90E+03
 533-3.90E+03  532-3.90E+03  531-3.90E+03  522-3.90E+03  521-3.90E+03
 504-3.90E+03  505-3.90E+03  546-3.90E+03  543-3.90E+03  506-3.90E+03
 503-3.90E+03    0 0.00E+00    0 0.00E+00    0 0.00E+00    0 0.00E+00

LATEST command or MODE set >> group whiten
POTL IN VOLTS  FOR POLAR CYCLE  42 ... TIME = 3.26E+01 SEC
 518-3.89E+03  517-3.89E+03  542-3.89E+03  541-3.89E+03  550-3.89E+03
 549-3.89E+03  530-3.89E+03  529-3.89E+03    0 0.00E+00    0 0.00E+00

LATEST command or MODE set >> group kapton
POTL IN VOLTS  FOR POLAR CYCLE  42 ... TIME = 3.26E+01 SEC
 311-3.90E+03  310-3.90E+03  309-3.90E+03  308-3.90E+03  259-3.90E+03
 258-3.90E+03  257-3.90E+03  256-3.90E+03    0 0.00E+00    0 0.00E+00

LATEST command or MODE set >> history

HISTORY command or MODE set >> 161,520,518,311,-1

POTL in Volts

  TIME  :   161       520       518       311       -1
--------:-------------------------------------------------------------
        :    #1        #2        #3        #4        #5        #6        #7
 0.0E+00:-1.00E+01-1.00E+01-1.00E+01-1.00E+01-1.00E+01
 2.0E-02:-1.32E+03-1.37E+03-1.39E+03-1.37E+03-1.31E+03
 4.0E-02:-2.30E+03-2.42E+03-2.44E+03-2.42E+03-2.30E+03
 6.0E-02:-2.85E+03-3.02E+03-3.04E+03-3.02E+03-2.85E+03
 8.0E-02:-3.14E+03-3.36E+03-3.37E+03-3.36E+03-3.14E+03
 1.0E-01:-3.29E+03-3.55E+03-3.56E+03-3.55E+03-3.30E+03
 1.2E-01:-3.37E+03-3.66E+03-3.66E+03-3.66E+03-3.38E+03
 1.6E-01:-3.43E+03-3.76E+03-3.77E+03-3.76E+03-3.44E+03
 2.0E-01:-3.44E+03-3.82E+03-3.82E+03-3.82E+03-3.47E+03
 2.4E-01:-3.45E+03-3.85E+03-3.84E+03-3.85E+03-3.48E+03
 2.6E-01:-3.45E+03-3.86E+03-3.85E+03-3.86E+03-3.48E+03
 2.8E-01:-3.45E+03-3.86E+03-3.86E+03-3.86E+03-3.48E+03
 3.8E-01:-3.45E+03-3.89E+03-3.88E+03-3.89E+03-3.49E+03
 4.8E-01:-3.45E+03-3.90E+03-3.89E+03-3.90E+03-3.49E+03
 5.3E-01:-3.45E+03-3.90E+03-3.89E+03-3.90E+03-3.50E+03
 5.8E-01:-3.45E+03-3.90E+03-3.90E+03-3.90E+03-3.50E+03
 6.3E-01:-3.45E+03-3.90E+03-3.90E+03-3.90E+03-3.51E+03
 8.3E-01:-3.45E+03-3.90E+03-3.90E+03-3.90E+03-3.51E+03
 1.0E+00:-3.45E+03-3.90E+03-3.90E+03-3.90E+03-3.52E+03
 1.2E+00:-3.45E+03-3.90E+03-3.90E+03-3.90E+03-3.53E+03
 1.4E+00:-3.45E+03-3.90E+03-3.90E+03-3.90E+03-3.54E+03
 1.6E+00:-3.45E+03-3.90E+03-3.90E+03-3.90E+03-3.55E+03
 2.0E+00:-3.45E+03-3.90E+03-3.90E+03-3.90E+03-3.57E+03
 2.4E+00:-3.45E+03-3.90E+03-3.90E+03-3.90E+03-3.58E+03
 2.8E+00:-3.45E+03-3.90E+03-3.90E+03-3.90E+03-3.59E+03
 3.2E+00:-3.45E+03-3.90E+03-3.90E+03-3.90E+03-3.61E+03
 3.6E+00:-3.45E+03-3.90E+03-3.90E+03-3.90E+03-3.62E+03
 4.6E+00:-3.45E+03-3.90E+03-3.90E+03-3.90E+03-3.65E+03
 5.6E+00:-3.45E+03-3.90E+03-3.90E+03-3.90E+03-3.67E+03
 6.6E+00:-3.45E+03-3.90E+03-3.90E+03-3.90E+03-3.69E+03
 7.6E+00:-3.45E+03-3.90E+03-3.90E+03-3.90E+03-3.71E+03
 8.6E+00:-3.45E+03-3.90E+03-3.89E+03-3.90E+03-3.73E+03
 1.1E+01:-3.45E+03-3.90E+03-3.89E+03-3.90E+03-3.75E+03
 1.3E+01:-3.45E+03-3.90E+03-3.89E+03-3.90E+03-3.77E+03
 1.5E+01:-3.45E+03-3.90E+03-3.89E+03-3.90E+03-3.79E+03
 1.7E+01:-3.45E+03-3.90E+03-3.89E+03-3.90E+03-3.80E+03
 1.9E+01:-3.45E+03-3.90E+03-3.89E+03-3.90E+03-3.81E+03
 2.3E+01:-3.45E+03-3.90E+03-3.89E+03-3.90E+03-3.82E+03
 2.7E+01:-3.45E+03-3.90E+03-3.89E+03-3.90E+03-3.83E+03
 2.9E+01:-3.45E+03-3.90E+03-3.89E+03-3.90E+03-3.83E+03
```

```
 3.1E+01:-3.45E+03-3.90E+03-3.89E+03-3.90E+03-3.83E+03
 3.3E+01:-3.45E+03-3.90E+03-3.89E+03-3.90E+03-3.83E+03
1                    POTL versus TIME in Seconds
 0.00E+005................................................................................
          .                   .                   .                   .                   .
          .                   .                   .                   .                   .
          .                   .                   .                   .                   .
          .                   .                   .                   .                   .
          .                   .                   .                   .                   .
          .                   .                   .                   .                   .
          .                   .                   .                   .                   .
          .                   .                   .                   .                   .
          .                   .                   .                   .                   .
          .                   .                   .                   .                   .
          .                   .                   .                   .                   .
-1.00E+03+................................................................................
          .                   .                   .                   .                   .
          .                   .                   .                   .                   .
          .                   .                   .                   .                   .
          5                   .                   .                   .                   .
          3                   .                   .                   .                   .
          .                   .                   .                   .                   .
          .                   .                   .                   .                   .
          .                   .                   .                   .                   .
          .                   .                   .                   .                   .
          .                   .                   .                   .                   .
          .                   .                   .                   .                   .
-2.00E+03+................................................................................
          .                   .                   .                   .                   .
          .                   .                   .                   .                   .
          .                   .                   .                   .                   .
          5                   .                   .                   .                   .
          4                   .                   .                   .                   .
          .                   .                   .                   .                   .
          .                   .                   .                   .                   .
          .                   .                   .                   .                   .
          .                   .                   .                   .                   .
          5                   .                   .                   .                   .
          .                   .                   .                   .                   .
-3.00E+034................................................................................
          .                   .                   .                   .                   .
          5                   .                   .                   .                   .
          1                   .                   .                   .                   .
          5                   .                   .                   .                   .
          51111111 1 1 1 1 1  .1   1   1   1   1  .    1       1   1  .1   1              .
          5555                .                   .                   .                   .
          4  55555            .                   .                   .                   .
          4        5 5 5      .                   .                   .                   .
          4              5 5  .5   5   5          .                   .                   .
          44                  .            5   5  .    5       5   5  .5   5              .
          .4444444 4 4 4 4 4  .4   4   4   4   4  .    4       4   4  .4   4              .
 4.00E+03+................................................................................
    0.00E+00            1.00E+01            2.00E+01            3.00E+01            4.00E+0

HISTORY command or MODE set >> latest

LATEST command or MODE set >> field
MODE RESET

LATEST command or MODE set >> absmag
MODE RESET

LATEST command or MODE set >> group all
FIEL IN VOLTS/METER FOR POLAR CYCLE 42      TIME = 3.26E+01 SEC
```

23-2.17E+05	28-2.17E+05	29-2.04E+05	30-2.04E+05	2-1.92E+05
5-1.92E+05	549-1.76E+05	550-1.76E+05	1-1.75E+05	6-1.75E+05
261-1.74E+05	262-1.74E+05	471-1.74E+05	476-1.74E+05	313-1.72E+05
314-1.72E+05	7-1.71E+05	16-1.71E+05	43-1.59E+05	44-1.59E+05
255-1.54E+05	260-1.54E+05	307-1.52E+05	312-1.52E+05	207-1.50E+05
208-1.50E+05	541-1.49E+05	542-1.49E+05	529-1.46E+05	530-1.46E+05
371-1.46E+05	372-1.46E+05	259-1.45E+05	257-1.45E+05	311-1.43E+05
309-1.43E+05	544-1.42E+05	545-1.42E+05	25-1.39E+05	26-1.39E+05
37-1.36E+05	38-1.36E+05	39-1.36E+05	42-1.36E+05	533-1.35E+05
534-1.35E+05	35-1.29E+05	36-1.29E+05	24-1.27E+05	27-1.27E+05
543-1.27E+05	546-1.27E+05	531-1.26E+05	532-1.26E+05	61-1.21E+05
68-1.21E+05	258-1.20E+05	256-1.20E+05	17-1.19E+05	22-1.19E+05
31-1.18E+05	34-1.18E+05	517-1.17E+05	310-1.17E+05	308-1.17E+05
518-1.16E+05	415-1.13E+05	416-1.13E+05	397-1.12E+05	521-1.12E+05
522-1.11E+05	173-1.10E+05	178-1.10E+05	8-1.08E+05	15-1.08E+05
209-1.08E+05	214-1.08E+05	519-1.02E+05	520-1.01E+05	547-1.01E+05
548-1.01E+05	3-9.89E+04	4-9.89E+04	536-9.86E+04	537-9.86E+04
472-9.70E+04	475-9.70E+04	454-9.67E+04	507-9.67E+04	510-9.67E+04
430-9.66E+04	435-9.66E+04	455-9.65E+04	470-9.48E+04	477-9.46E+04
478-9.46E+04	436-9.40E+04	437-9.39E+04	215-9.35E+04	216-9.35E+04
227-9.26E+04	228-9.26E+04	539-9.26E+04	540-9.26E+04	251-9.17E+04
254-9.17E+04	51-9.07E+04	52-9.07E+04	303-8.93E+04	306-8.92E+04
75-8.77E+04	76-8.77E+04	387-8.72E+04	388-8.72E+04	157-8.60E+04
162-8.60E+04	535-8.40E+04	538-8.39E+04	89-8.26E+04	90-8.26E+04
473-8.24E+04	474-8.24E+04	53-8.19E+04	59-8.19E+04	247-8.05E+04
250-8.05E+04	401-7.98E+04	406-7.98E+04	45-7.80E+04	46-7.80E+04
47-7.75E+04	50-7.75E+04	263-7.67E+04	268-7.67E+04	103-7.64E+04
104-7.64E+04	295-7.61E+04	302-7.61E+04	337-7.57E+04	338-7.56E+04
219-7.56E+04	226-7.56E+04	235-7.55E+04	246-7.55E+04	373-7.52E+04
378-7.52E+04	413-7.52E+04	414-7.52E+04	229-7.49E+04	234-7.49E+04
203-7.48E+04	206-7.48E+04	417-7.42E+04	69-7.42E+04	70-7.42E+04
315-7.41E+04	320-7.41E+04	418-7.39E+04	10-7.30E+04	13-7.30E+04
523-7.24E+04	524-7.24E+04	525-7.22E+04	526-7.22E+04	508-7.17E+04
509-7.17E+04	281-7.10E+04	504-7.10E+04	282-7.10E+04	71-6.99E+04
74-6.99E+04	40-6.98E+04	41-6.98E+04	407-6.97E+04	408-6.97E+04
210-6.94E+04	213-6.94E+04	456-6.93E+04	367-6.90E+04	370-6.89E+04
465-6.88E+04	117-6.88E+04	118-6.88E+04	83-6.83E+04	84-6.83E+04
199-6.73E+04	202-6.73E+04	527-6.72E+04	289-6.72E+04	294-6.72E+04
528-6.71E+04	505-6.71E+04	18-6.67E+04	21-6.67E+04	440-6.67E+04
453-6.67E+04	468-6.66E+04	479-6.63E+04	485-6.62E+04	493-6.59E+04
500-6.54E+04	179-6.47E+04	184-6.47E+04	85-6.46E+04	88-6.46E+04
12-6.45E+04	11-6.45E+04	269-6.45E+04	270-6.45E+04	211-6.43E+04
212-6.43E+04	19-6.42E+04	20-6.42E+04	379-6.38E+04	380-6.38E+04
97-6.30E+04	98-6.30E+04	321-6.24E+04	322-6.24E+04	62-6.08E+04
66-6.08E+04	205-6.06E+04	204-6.06E+04	99-5.98E+04	102-5.98E+04
191-5.94E+04	198-5.94E+04	283-5.92E+04	288-5.92E+04	9-5.90E+04
14-5.90E+04	273-5.86E+04	280-5.86E+04	503-5.82E+04	385-5.82E+04
386-5.82E+04	133-5.80E+04	134-5.80E+04	91-5.75E+04	94-5.75E+04
65-5.74E+04	64-5.74E+04	359-5.72E+04	366-5.72E+04	77-5.71E+04
80-5.71E+04	111-5.65E+04	112-5.65E+04	185-5.63E+04	190-5.63E+04
32-5.62E+04	33-5.62E+04	95-5.62E+04	96-5.62E+04	174-5.59E+04
177-5.59E+04	325-5.58E+04	336-5.58E+04	431-5.47E+04	434-5.47E+04
506-5.43E+04	113-5.42E+04	116-5.42E+04	105-5.36E+04	108-5.36E+04
109-5.33E+04	110-5.33E+04	457-5.32E+04	253-5.24E+04	252-5.23E+04
369-5.19E+04	419-5.16E+04	464-5.15E+04	368-5.12E+04	158-5.11E+04
161-5.11E+04	432-5.10E+04	433-5.10E+04	81-5.07E+04	82-5.07E+04
426-5.01E+04	402-4.96E+04	405-4.96E+04	389-4.93E+04	390-4.92E+04
264-4.88E+04	267-4.88E+04	119-4.77E+04	122-4.77E+04	123-4.76E+04
124-4.76E+04	462-4.76E+04	374-4.73E+04	377-4.73E+04	305-4.71E+04
316-4.68E+04	319-4.68E+04	127-4.63E+04	132-4.63E+04	304-4.63E+04
159-4.62E+04	160-4.62E+04	429-4.61E+04	125-4.58E+04	126-4.58E+04
403-4.57E+04	404-4.57E+04	339-4.57E+04	351-4.57E+04	438-4.56E+04
439-4.56E+04	266-4.53E+04	265-4.53E+04	375-4.36E+04	376-4.36E+04
317-4.33E+04	318-4.33E+04	441-4.17E+04	452-4.17E+04	149-4.07E+04

```
150-4.07E+04  353-4.05E+04  358-4.04E+04  201-3.98E+04  200-3.98E+04
135-3.92E+04  140-3.92E+04  142-3.82E+04  141-3.82E+04   54-3.65E+04
 60-3.65E+04  409-3.50E+04  411-3.50E+04  427-3.49E+04  513-3.36E+04
514-3.36E+04  217-3.35E+04  218-3.35E+04  147-3.33E+04  148-3.33E+04
400-3.32E+04  480-3.19E+04  486-3.19E+04  515-3.14E+04  163-3.14E+04
172-3.14E+04  516-3.11E+04  143-3.05E+04  146-3.05E+04  428-2.96E+04
425-2.86E+04  365-2.84E+04  298-2.79E+04  299-2.78E+04  399-2.78E+04
391-2.75E+04  360-2.74E+04  396-2.74E+04  156-2.73E+04  153-2.73E+04
152-2.71E+04  151-2.71E+04  340-2.70E+04  352-2.69E+04   49-2.68E+04
 48-2.68E+04  381-2.62E+04  383-2.62E+04  197-2.59E+04  192-2.59E+04
 63-2.52E+04   67-2.52E+04  249-2.48E+04  248-2.47E+04  511-2.45E+04
512-2.45E+04  297-2.44E+04  300-2.43E+04   72-2.43E+04   73-2.43E+04
364-2.41E+04  363-2.39E+04   86-2.25E+04   87-2.25E+04  155-2.25E+04
154-2.25E+04  144-2.22E+04  145-2.22E+04  393-2.21E+04  220-2.16E+04
225-2.16E+04  420-2.14E+04  481-2.07E+04  484-2.07E+04  398-2.07E+04
100-2.07E+04  101-2.07E+04  410-2.01E+04  412-2.01E+04  362-2.01E+04
494-1.92E+04  458-1.91E+04  499-1.91E+04  421-1.91E+04  271-1.88E+04
272-1.88E+04  128-1.86E+04  130-1.86E+04  301-1.84E+04  114-1.84E+04
115-1.84E+04  361-1.81E+04  395-1.80E+04   92-1.79E+04   93-1.79E+04
296-1.74E+04  106-1.73E+04  107-1.73E+04  323-1.71E+04  324-1.71E+04
181-1.71E+04  183-1.71E+04  196-1.70E+04  193-1.70E+04  189-1.69E+04
186-1.69E+04  382-1.69E+04  384-1.69E+04  138-1.68E+04  136-1.68E+04
326-1.68E+04  334-1.68E+04  442-1.63E+04  450-1.63E+04  120-1.56E+04
121-1.56E+04   78-1.55E+04   79-1.55E+04  195-1.51E+04  194-1.51E+04
467 1.50E+04  423-1.48E+04  463-1.47E+04  241-1.46E+04  239-1.46E+04
274-1.45E+04  279-1.45E+04  175-1.41E+04  176-1.41E+04  180-1.40E+04
182-1.40E+04  501-1.35E+04  243-1.30E+04  237-1.29E+04  171-1.25E+04
165-1.25E+04  327-1.23E+04  335-1.23E+04  188-1.18E+04  187-1.18E+04
164-1.18E+04  170-1.18E+04  349-1.18E+04  342-1.18E+04  469 1.17E+04
129-1.13E+04  131-1.13E+04  460 1.09E+04  357-1.09E+04  502-1.07E+04
221-1.04E+04  223-1.04E+04  487-1.03E+04  492-1.03E+04  354-1.02E+04
424-1.01E+04  245-1.01E+04  236-1.00E+04  356-9.85E+03  139-9.74E+03
137-9.74E+03  166-9.70E+03  168-9.70E+03   57-9.47E+03   55-9.47E+03
394-8.88E+03  355-8.63E+03  482-8.57E+03  483-8.57E+03  169-8.48E+03
167-8.48E+03  291-8.38E+03  292-8.26E+03  498-8.00E+03  496-7.47E+03
443-7.42E+03  451-7.40E+03   56-7.26E+03   58-7.26E+03  244-6.50E+03
238-6.50E+03  242-6.45E+03  240-6.45E+03  461 5.36E+03  422-5.14E+03
293-4.76E+03  392-4.75E+03  344-4.70E+03  497-4.57E+03  290-4.14E+03
343-3.83E+03  350-3.83E+03  275-3.58E+03  277-3.58E+03  346-3.55E+03
495-3.48E+03  233-3.35E+03  230-3.35E+03  489-3.32E+03  491-3.32E+03
348-3.32E+03  341-3.00E+03  466-2.95E+03  329-2.54E+03  332-2.54E+03
444-2.33E+03  447-2.33E+03  232-2.06E+03  231-2.06E+03  445-1.77E+03
448-1.76E+03  328-1.69E+03  331-1.69E+03  459-1.67E+03  222-1.56E+03
224-1.56E+03  446-9.81E+02  449-9.81E+02  287-7.91E+02  345-7.23E+02
284-6.36E+02  488-4.91E+02  490-4.91E+02  286-3.27E+02  285-3.16E+02
347-3.13E+02  330-1.26E+00  333-1.26E+00  278-5.06E-01  276-5.06E-01
  -1 0.00E+00    0 0.00E+00    0 0.00E+00    0 0.00E+00    0 0.00E+00

LATEST command or MODE set >> stress
MODE RESET

LATEST command or MODE set >> group all
STRE IN VOLTS/METER  FOR POLAR CYCLE  42 ... TIME = 3.26E+01 SEC
 197 3.88E+04  196 3.88E+04  195 3.88E+04  194 3.88E+04  193 3.88E+04
 192 3.88E+04  191 3.88E+04  190 3.88E+04  189 3.88E+04   76 3.88E+04
  75 3.88E+04  186 3.88E+04  185 3.88E+04  538 3.88E+04  184 3.88E+04
 183 3.88E+04  535 3.88E+04  182 3.88E+04  181 3.88E+04  180 3.88E+04
 179 3.88E+04  178 3.88E+04  177 3.88E+04   12 3.88E+04   11 3.88E+04
 174 3.88E+04  173 3.88E+04  524 3.88E+04  523 3.88E+04  172 3.88E+04
 171 3.88E+04  170 3.88E+04  169 3.88E+04  168 3.88E+04  167 3.88E+04
 166 3.88E+04  165 3.88E+04  164 3.88E+04  163 3.88E+04  512 3.88E+04
 511 3.88E+04  510 3.88E+04  509 3.88E+04  508 3.88E+04  507 3.88E+04
 162 3.88E+04  161 3.88E+04  160 3.88E+04  159 3.88E+04  158 3.88E+04
 157 3.88E+04  500 3.88E+04  499 3.88E+04  156 3.88E+04  497 3.88E+04
```

155	3.88E+04	495	3.88E+04	494	3.88E+04	493	3.88E+04	492	3.88E+04
154	3.88E+04	490	3.88E+04	153	3.88E+04	488	3.88E+04	487	3.88E+04
486	3.88E+04	485	3.88E+04	10	3.88E+04	7	3.88E+04	150	3.88E+04
149	3.88E+04	480	3.88E+04	479	3.88E+04	70	3.88E+04	69	3.88E+04
476	3.88E+04	475	3.88E+04	474	3.88E+04	473	3.88E+04	472	3.88E+04
471	3.88E+04	146	3.88E+04	145	3.88E+04	144	3.88E+04	467	3.88E+04
143	3.88E+04	465	3.88E+04	142	3.88E+04	141	3.88E+04	462	3.88E+04
68	3.88E+04	460	3.88E+04	67	3.88E+04	138	3.88E+04	66	3.88E+04
456	3.88E+04	136	3.88E+04	65	3.88E+04	453	3.88E+04	134	3.88E+04
133	3.88E+04	450	3.88E+04	449	3.88E+04	64	3.88E+04	447	3.88E+04
446	3.88E+04	63	3.88E+04	444	3.88E+04	130	3.88E+04	442	3.88E+04
62	3.88E+04	440	3.88E+04	439	3.88E+04	438	3.88E+04	437	3.88E+04
436	3.88E+04	435	3.88E+04	434	3.88E+04	433	3.88E+04	432	3.88E+04
431	3.88E+04	430	3.88E+04	128	3.88E+04	61	3.88E+04	427	3.88E+04
426	3.88E+04	126	3.88E+04	424	3.88E+04	423	3.88E+04	422	3.88E+04
125	3.88E+04	420	3.88E+04	419	3.88E+04	124	3.88E+04	123	3.88E+04
416	3.88E+04	415	3.88E+04	28	3.88E+04	59	3.88E+04	412	3.88E+04
411	3.88E+04	410	3.88E+04	409	3.88E+04	408	3.88E+04	407	3.88E+04
406	3.88E+04	405	3.88E+04	404	3.88E+04	403	3.88E+04	402	3.88E+04
401	3.88E+04	400	3.88E+04	399	3.88E+04	27	3.88E+04	57	3.88E+04
396	3.88E+04	395	3.88E+04	394	3.88E+04	118	3.88E+04	392	3.88E+04
391	3.88E+04	117	3.88E+04	26	3.88E+04	388	3.88E+04	387	3.88E+04
55	3.88E+04	25	3.88E+04	384	3.88E+04	383	3.88E+04	382	3.88E+04
381	3.88E+04	380	3.88E+04	379	3.88E+04	378	3.88E+04	377	3.88E+04
376	3.88E+04	375	3.88E+04	374	3.88E+04	373	3.88E+04	372	3.88E+04
371	3.88E+04	370	3.88E+04	369	3.88E+04	368	3.88E+04	367	3.88E+04
366	3.88E+04	365	3.88E+04	364	3.88E+04	363	3.88E+04	362	3.88E+04
53	3.88E+04	360	3.88E+04	359	3.88E+04	358	3.88E+04	357	3.88E+04
356	3.88E+04	355	3.88E+04	354	3.88E+04	353	3.88E+04	112	3.88E+04
351	3.88E+04	111	3.88E+04	349	3.88E+04	348	3.88E+04	110	3.88E+04
346	3.88E+04	109	3.88E+04	344	3.88E+04	52	3.88E+04	342	3.88E+04
341	3.88E+04	51	3.88E+04	339	3.88E+04	338	3.88E+04	337	3.88E+04
24	3.88E+04	23	3.88E+04	334	3.88E+04	104	3.88E+04	332	3.88E+04
331	3.88E+04	103	3.88E+04	329	3.88E+04	328	3.88E+04	22	3.88E+04
326	3.88E+04	21	3.88E+04	324	3.88E+04	323	3.88E+04	322	3.88E+04
321	3.88E+04	320	3.88E+04	319	3.88E+04	318	3.88E+04	317	3.88E+04
316	3.88E+04	315	3.88E+04	314	3.88E+04	313	3.88E+04	312	3.88E+04
20	3.88E+04	19	3.88E+04	98	3.88E+04	97	3.88E+04	307	3.88E+04
306	3.88E+04	305	3.88E+04	304	3.88E+04	303	3.88E+04	302	3.88E+04
301	3.88E+04	300	3.88E+04	299	3.88E+04	298	3.88E+04	297	3.88E+04
296	3.88E+04	295	3.88E+04	294	3.88E+04	293	3.88E+04	292	3.88E+04
291	3.88E+04	290	3.88E+04	289	3.88E+04	288	3.88E+04	287	3.88E+04
96	3.88E+04	95	3.88E+04	284	3.88E+04	283	3.88E+04	282	3.88E+04
281	3.88E+04	44	3.88E+04	43	3.88E+04	18	3.88E+04	277	3.88E+04
17	3.88E+04	275	3.88E+04	90	3.88E+04	89	3.88E+04	272	3.88E+04
271	3.88E+04	270	3.88E+04	269	3.88E+04	268	3.88E+04	267	3.88E+04
266	3.88E+04	265	3.88E+04	264	3.88E+04	263	3.88E+04	262	3.88E+04
261	3.88E+04	260	3.88E+04	16	3.88E+04	15	3.88E+04	38	3.88E+04
37	3.88E+04	255	3.88E+04	254	3.88E+04	253	3.88E+04	252	3.88E+04
251	3.88E+04	250	3.88E+04	249	3.88E+04	248	3.88E+04	247	3.88E+04
246	3.88E+04	245	3.88E+04	244	3.88E+04	243	3.88E+04	242	3.88E+04
241	3.88E+04	240	3.88E+04	239	3.88E+04	238	3.88E+04	237	3.88E+04
236	3.88E+04	235	3.88E+04	234	3.88E+04	233	3.88E+04	84	3.88E+04
83	3.88E+04	230	3.88E+04	229	3.88E+04	228	3.88E+04	227	3.88E+04
82	3.88E+04	81	3.88E+04	36	3.88E+04	225	3.88E+04	35	3.88E+04
221	3.88E+04	8	3.88E+04	13	3.88E+04	218	3.88E+04	217	3.88E+04
216	3.88E+04	215	3.88E+04	214	3.88E+04	213	3.88E+04	212	3.88E+04
211	3.88E+04	210	3.88E+04	209	3.88E+04	208	3.88E+04	207	3.88E+04
206	3.88E+04	205	3.88E+04	204	3.88E+04	203	3.88E+04	202	3.88E+04
201	3.88E+04	200	3.88E+04	199	3.88E+04	198	3.88E+04	122	3.88E+04
121	3.88E+04	120	3.88E+04	119	3.88E+04	116	3.88E+04	118	3.88E+04
114	3.88E+04	113	3.88E+04	108	3.88E+04	107	3.88E+04	106	3.88E+04
105	3.88E+04	102	3.88E+04	537	3.88E+04	536	3.88E+04	101	3.88E+04
100	3.88E+04	99	3.88E+04	94	3.88E+04	93	3.88E+04	92	3.88E+04

```
 91 3.88E+04   88 3.88E+04  526 3.88E+04  525 3.88E+04   87 3.88E+04
 86 3.88E+04   85 3.88E+04   80 3.88E+04   79 3.88E+04   78 3.88E+04
 77 3.88E+04   74 3.88E+04  514 3.88E+04  513 3.88E+04   73 3.88E+04
 72 3.88E+04   71 3.88E+04   60 3.88E+04   58 3.88E+04   56 3.88E+04
498 3.88E+04  496 3.88E+04  491 3.88E+04  489 3.88E+04  484 3.88E+04
483 3.88E+04  482 3.88E+04  481 3.88E+04  478 3.88E+04  477 3.88E+04
 54 3.88E+04   50 3.88E+04   49 3.88E+04  466 3.88E+04  464 3.88E+04
463 3.88E+04   48 3.88E+04  459 3.88E+04  458 3.88E+04  457 3.88E+04
455 3.88E+04  454 3.88E+04  452 3.88E+04  451 3.88E+04  448 3.88E+04
445 3.88E+04  443 3.88E+04  441 3.88E+04  429 3.88E+04  428 3.88E+04
425 3.88E+04  421 3.88E+04  418 3.88E+04  417 3.88E+04  414 3.88E+04
413 3.88E+04  398 3.88E+04   47 3.88E+04  393 3.88E+04  390 3.88E+04
389 3.88E+04  386 3.88E+04  385 3.88E+04  361 3.88E+04  352 3.88E+04
350 3.88E+04  347 3.88E+04  345 3.88E+04  343 3.88E+04  340 3.88E+04
336 3.88E+04  335 3.88E+04  333 3.88E+04  330 3.88E+04  327 3.88E+04
325 3.88E+04   46 3.88E+04   45 3.88E+04   42 3.88E+04   41 3.88E+04
286 3.88E+04  285 3.88E+04  280 3.88E+04  279 3.88E+04  278 3.88E+04
276 3.88E+04  274 3.88E+04  273 3.88E+04   40 3.88E+04   39 3.88E+04
 14 3.88E+04    9 3.88E+04  232 3.88E+04  231 3.88E+04  226 3.88E+04
225 3.88E+04  224 3.88E+04  222 3.88E+04  220 3.88E+04  219 3.88E+04
188 3.88E+04  187 3.88E+04  176 3.88E+04  175 3.88E+04  152 3.88E+04
151 3.88E+04  148 3.88E+04  147 3.88E+04  140 3.88E+04  139 3.88E+04
137 3.88E+04  135 3.88E+04  132 3.88E+04  131 3.88E+04  129 3.88E+04
127 3.88E+04  515 3.88E+04   32 3.88E+04  461 3.88E+04  548 3.88E+04
547 3.88E+04  528 3.88E+04  527 3.88E+04   31 3.88E+04   34 3.88E+04
502 3.88E+04  501 3.88E+04  540 3.88E+04  539 3.88E+04   33 3.88E+04
469 3.88E+04  516 3.88E+04    4 3.88E+04    3 3.88E+04    6 3.88E+04
  1 3.88E+04  503-6.80E+03  506-6.80E+03  543-6.80E+03  546-6.80E+03
504-6.80E+03  505-6.80E+03  259-6.80E+03  258-6.80E+03  257-6.80E+03
545-6.80E+03  544-6.80E+03  256-6.80E+03  311-6.80E+03  534-6.80E+03
533-6.80E+03  532-6.80E+03  531-6.80E+03  310-6.80E+03  309-6.80E+03
522-6.80E+03  521-6.80E+03  520-6.80E+03  519-6.80E+03  308-6.80E+03
529-6.11E+03  550-6.11E+03  549-6.11E+03  530-6.11E+03  541-6.11E+03
542-6.11E+03  517-6.11E+03  518-6.11E+03    2 2.44E-01  470 2.44E-01
468 2.44E-01  397 2.44E-01   30 2.44E-01   29 2.44E-01    5 2.44E-01
 -1 0.00E+00    0 0.00E+00    0 0.00E+00    0 0.00E+00    0 0.00E+00

LATEST command or MODE set >> exit
```

C.11 Electron Trajectories

NASCAP/GEO codes were used to do the calculations shown in Section 5.6.

Termtalk Execution—Direct Effects of Charging

Termtalk was used to determine the surface cell number of the cell with the detector. The surface normal and position limit commands of subset were used to locate the cell.

```
 CHOOSE ANY MODULE
 HELP IS ALWAYS AVAILABLE   TYPE 'HELP'
>subset
DEFINITION OF NEW SUBSET NAMED $A
 487 REMAINING IN GROUP
 SUBSET INSTRUCTION PLEASE >
>normal 1 0 0
 112 REMAINING IN GROUP
 SUBSET INSTRUCTION PLEASE >
```

```
>ylim -4 to -3
  14 REMAINING IN GROUP
 SUBSET INSTRUCTION PLEASE ?
>zlim 0 to 1
   1 REMAINING IN GROUP
 SUBSET INSTRUCTION PLEASE ?
>which
MEMBERS OF GROUP $A
  402    0    0    0    0    0    0    0    0    0
   1 REMAINING IN GROUP
 SUBSET INSTRUCTION PLEASE ?
>done
REMAINING MEMBER IS  # 402
THIS SUBSET HAS 1 MEMBERS
IT WILL NOT BE CATALOGUED
RETURNING TO MODULE 'MAIN'
 CHOOSE ANY MODULE
 HELP IS ALWAYS AVAILABLE - TYPE 'HELP'
>single
 SINGLE COMMAND OR MODE SET ?
>402
-------------------------------------------------------------------------
  SURFACE CELL NO.  402
                                    CENTERED AT      1.0   -3.5    0.5
                                    MATERIAL IS  KAP1
                        POTENTIAL =-6.510E+02 VOLTS
 SINGLE COMMAND OR MODE SET ?
>exit
```

Nascap Standard Input—Direct Effects of Charging

Nascap was then used to determine the trajectories of electrons normally incident on surface cell 402. The trajectories are shown in Figure 58. The standard input to Nascap follows.

```
rdopt 5
   delta 60.
   longtimestep
   ncyc 20
   ng 2
   nz 33
   zmesh 0.457
   sundir 1 .1 -.2
   sunint 1.
   end
detect
   icell 402
   energy 100
   dnk 10
   theta 0
   phi 0
   nstp 1300
   ns 1
   np 1
   nmx2 1
   finalv 1000
   n 10
   prflux
   plpart
end
```

```
detect
   icell 402
   energy 1000
   dek 10
   theta 0
   phi 0
   nstp 1300
   ne 1
   np 1
   nmu2 1
   finalv 10000
   n 10
   prflux
   plpart
end
end
```

Chapter 5 also shows trajectories for the same spacecraft with all of the surfaces at −651, the surface potential of the surface with the detector. The trajectories were created by Nascap with the following standard input file.

```
rdopt 5
   delta 60.
   longtimestep
   ncyc 20
   ng 2
   nz 33
   xmesh 0.457
   sundir 1 .1 -.2
   sunint 1.
   end
ipa 5
   pcond 1 -651
   end
detect
   icell 402
   energy 100
   dek 10
   theta 0
   phi 0
   nstp 1300
   ne 1
   np 1
   nmu2 1
   finalv 1000
   n 10
   prflux
   plpart
end
detect
   icell 402
   energy 1000
   dek 10
   theta 0
   phi 0
   nstp 1300
   ne 1
   np 1
   nmu2 1
   finalv 10000
   n 10
```

```
    prflux
    plpart
end
end
```

Appendix D
Discharge Equivalent Circuit Response

The equivalent circuit for the discharge test circuit given in Figure 63 of Chapter 6 is shown in Figure 71.

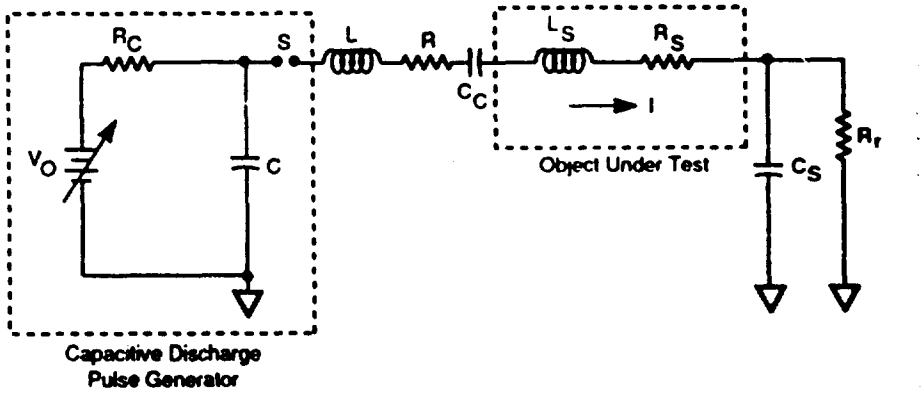

Adjustable Circuit Parameters

V_o	Adjustable charging voltage
R_c	Charging resistor
C	Drive capacitor
L	Added inductance for wave shaping
R	Added resistance for wave shaping
C_c	Capacitive coupling between pulse generator and test object
L_s	Nominal inductance of test object
R_s	Nominal resistance of test object
C_s	Capacitance between test object and pulse generator ground
I	Body current of test object which is charging current for C_s
R_r	Resistance of return line to ground
S	Spark gap

For direct drive, C_c and C are removed from circuit

Figure 71 General capacitive discharge injection model

Note that the entire circuit has been reduced to a charged capacitor being discharged into a series R′, L′, (and C_{eq} for capacitive coupling) which are respectively the sum of the individual elements shown in Figure 63. The basic equation for the current flowing on this circuit as a function of time is:

$$I(t)=\frac{2V_o\eta}{(\eta^2-1)^{1/2}R'}\exp(-\eta\omega_o t)\sinh\omega_o(\eta^2-1)^{1/2} \tag{60}$$

$$\eta=\frac{R}{2}(C/L)^{1/2}=1/2(\tau_2/\tau_1)^{1/2}, \tag{61}$$

$$\omega_o=(L'C)^{-1/2}=1/2(\tau_2/\tau_1)^{-1/2}, \tag{62}$$

$$\tau_1=2L'/R', \tag{63}$$

$$\tau_2=2R'C\ . \tag{64}$$

R′ is the sum of all resistances (except for R_c), L′ the sum of all inductances, and C the charging capacitor in Figure 71.

For capacitive coupling, the circuit becomes a series R, L, C circuit and the appropriate equations for the load current are:

$$I(t)=V_oC_{eq}(\omega_o/\omega)\exp(-t/\tau_1)\ \cosh(\omega t+\omega_1/\omega)-\tau_1^{-1}\sinh(\omega t+\omega_1/\omega), \tag{65}$$

where

$$\frac{R'^2C_{eq}}{4L'}>1\text{(overdamping)}, \tag{66}$$

or

$$I(t)=C_{eq}V_o\exp(-t/\tau_1)(t/\tau_1), \tag{67}$$

where

$$\frac{R'^2C_{eq}}{4L'^2}=1\text{(critical damping)}, \tag{68}$$

or

$$I(t)=V_oC_{eq}(\omega_o/\omega)\exp(-t/\tau_1)\left[\omega\cos(\omega t+\omega_1/\omega)-\tau_1^{-1}\sin(\omega t+\omega_1/\omega)\right], \tag{69}$$

where

$$\frac{R'^2C_{eq}}{4L'^2}<1\text{ (under damped)}\ . \tag{70}$$

In each case

$$\omega_o = \left(L' C_{eq}\right)^{-1/2}, \tag{71}$$

$$\omega = \left|\omega_o^2 - \frac{R'^2}{4L'^2}\right|^{1/2}, \tag{72}$$

$$\tau_1 = \frac{2L'}{R'}, \tag{73}$$

and

$$\omega_1 = 2/\tau_1. \tag{74}$$

The effective capacitance C_{eq} is

$$C_{eq}^{-1} = C^{-1} + C_L^{-1} + C_c^{-1}. \tag{75}$$

The effective resistance R′ is equal to the sum of all the series resistances, while the effective inductance L′ is equal to the sum of all the series inductances.

Glossary

ABORC

Arbitrary Body of Revolution Code.

Absolute charging

The development of a potential of the spacecraft frame relative to the surrounding space plasma.

Anomaly

An unexpected event, usually undesirable. Anomalies range from phantom commands to instrument failure.

Aurora

The precipitation of charged particles in the auroral region that is often connected with geomagnetic substorm activity.

Auroral region

An oval band around each geomagnetic pole, ranging from 75 degrees magnetic latitude at local noon to about 67 degrees magnetic latitude at midnight, in which auroral activity is generally most intense. It widens to both higher and lower latitudes during the expansion phase of a magnetic substorm.

Backscattered electrons

An electron reflected from a material surface with a substantial fraction of its incident energy.

Blow-off discharge

A blow-off discharge is a vacuum discharge characterized by the ejection of current (blow-off of charge) into space surrounding an electrode.

Capacitive direct injection

Capacitive direct injection is a method of inducing a space vehicle response that simulates that response to a blow-off discharge. The method involves injecting current pulses at a given location on the space vehicle through a capacitor formed by a conducting plate near the space vehicle conductive surfaces at the injection location. The capacitive plate coupler allows the current to be distributed over a large area simulating the return of blow-off currents.

Debye length

A distance that indicates the sphere of influence of a charged object in a thermal plasma. It is given by the expression $\lambda_D = \sqrt{\varepsilon_0 \theta / ne}$ where n is the density of the plasma and θ is the temperature.

Differential charging

The change in the potential of one part of the spacecraft with respect to another part of the spacecraft.

DMSP

Defense Meteorological Satellite Program. Some of the DMSP spacecraft have carried particle detectors that are able to measure charging events.

Direct injection excitation

Direct injection excitation is a global current injection method for simulating space vehicle response to blow-off discharges. This method injects current pulses onto the space vehicle over a given area. The injection is performed via a collection of wires that fan out from a common connection at the injection drive point and to make direct contact with the space vehicle over the area to be excited. The contact points that are uniformly distributed over the excitation area are equal to the number of injection wires.

EMU

Extravehicular Mobility Unit—A space suit.

ESD

Electrostatic discharge refers to any breakdown from those produced when people contact metal objects after crossing a wool rug to high voltage breakdowns. Here we are only concerned with discharges due to the surface charging of spacecraft.

EVA

Extravehicular Activity Astronauts in space suits outside the spacecraft.

EUV

Extreme ultraviolet. The portion of the electromagnetic spectrum from approximately 100Å to 1000Å in wavelength.

Faraday cage

An electromagnetically shielded enclosure.

Flash-over discharge

A flash-over discharge is a discharge characterized by a current path that travels along a surface of the material (and sometimes around an edge) to close the path between the electrodes.

Floating potential

The potential of an object in a plasma at which the incident electron current, emitted electron currents, and the ion current to the object exactly balance. So no net current flows to the object.

Geomagnetic coordinates

A system of spherical coordinates for Earth that is inclined about 11 degrees from Earth's rotational axis along the axis of Earth's approximately dipolar magnetic field.

Geosynchronous altitude

The altitude at which a spacecraft orbiting Earth has an orbital period of 23 hours and 56 minutes. This is approximately 6.6 Earth radii from Earth's center.

GEOS

A European Space Agency geostationary satellite.

GOES

Geostationary Operational Environmental Satellite. A series of geosynchronous spacecraft designed to monitor weather and the near-Earth space environment operated by NOAA (National Oceanic and Atmospheric Administration).

IEMCAP

Intrasystem Electromagnetic Compatibility Analysis Program.

K_p index

A world-wide, 3-hour, dimensionless, quasi-logarithmic index ranging from 0 to 9 that provides a measure of the level of disturbance of the geomagnetic field.

Magnetosphere

The region of the upper atmosphere surrounding Earth that extends out for tens of thousands of kilometers and is dominated by Earth's magnetic field.

Matchg

MATerial CHarGing. A zero-dimensional computer code that computes the incident currents and equilibrium surface potentials on a sphere coated with a specified material in a specified environment. It is appropriate for evaluating charging in the laboratory tank environment and at geosynchronous altitudes. It is distributed with the *NASCAP/GEO* computer code.

MIP

Multibody Interactions in Plasma.

MLT

Magnetic local time.

NASCAP/GEO

NASA Charging Analyzer Program for geosynchronous orbit. A set of computer codes that models the charging of spacecraft surfaces in a geosynchronous plasma in three dimensions. The *NASCAP/GEO* codes include **Nascap**, **Termtalk**, **Contours**, **Matchg**, and **PotColor**. The codes allow for a 3-dimensional, finite element representation of a spacecraft within a 16 x 16 x 32 grid. They use orbit-limited current collection algorithms to compute the current incident to surfaces, including secondary electron emission, backscatter, and photoemission. **Nascap** calculates the 3-dimensional electric fields around the object and includes their role in limiting the emission of low energy secondary and photoelectrons.

NEC

Numerical Electromagnetic Code.

Orbit-limited current collection

Collection of current by a biased probe from a surrounding plasma when the plasma density is such that the potential has a range larger than the largest impact parameter and is sufficiently well behaved so that no angular momentum barriers exist.

Paschen breakdown

A self-sustaining arc through a neutral environment between two biased electrodes. Electrons emitted from the cathode traversing the inter-electrode region produce ion-electron pairs at a rate determined by the collision ionization cross-section, neutral density, and the applied electric field. The ions return to the cathode and cause additional electrons to be emitted from the cathode.

Paschen region

The range of pressures at which Paschen discharges occur. At higher pressures, it takes a higher field to accelerate an electron to ionization energy within a mean free path. At low pressures not enough ionizations occur to sustain a chain reaction.

Plasmasphere

A region of cool (low energy), dense plasma surrounding Earth. It may be considered an extension of the ionosphere.

Photoelectrons

Electrons emitted from a surface due to incident, short-wavelength, electromagnetic radiation.

POLAR

Potentials Of Large objects in the Auroral Region. A family of computer codes that models the charging of spacecraft surfaces in an auroral environment in three dimensions. The codes are **vehicl, orient, nterak, shontl,** and **trmtlk**. The codes allow for a 3-dimensional, finite element representation of a spacecraft. It can use either space-charge-limited or orbit-limited current collection algorithms to compute the current incident to surfaces. It includes secondary electron emission, backscatter, and photoemission.

Punch-through discharge

A punch-through discharge is a discharge through the bulk of a dielectric material. The current path is through the bulk of the material, with surfaces on opposite sides of the dielectric acting as electrodes.

SCATHA

The Spacecraft Charging AT High Altitudes program, which included the satellite known as SCATHA or P78-2. The SCATHA program was a joint Air Force/NASA investigation whose objective was to provide the design criteria, materials, techniques, test and analytical methods to ensure control of the absolute and differential charging of spacecraft surfaces. The satellite was spin-stabilized and was in a near-geosynchronous,

near-equatorial Earth orbit. It was launched in January 1979. It carried a variety of instruments to measure surface potentials of different materials, discharge transients, and the environment.

Secondary electrons

Low-energy electrons emitted from a surface from the collision of incident electrons or ions with the surface. The ratio of secondary particles to incident particles can be greater than unity.

SEMCAP

Specification and Electromagnetic Compatibility Program. Calculates the intrasystem electromagnetic coupling within large systems.

Space-charge-limited current collection

Collection of current by a biased probe from a surrounding plasma when the plasma density is such that the space charge of the attracted particles shields the attracting potential and thus limits the range of the potential.

SPICE (and SPICE2 and ISPICE)

Computes the simultaneous solution of unlimited node circuit equations in either the time or frequency domain.

Stopping power

The rate of energy loss for an energetic particle passing through matter.

Substorm

A short term disturbance of Earth's magnetosphere lasting about 1 to 3 hours.

suchgr

SUrface CHarGeR. A zero-dimensional computer code that computes the incident currents and equilibrium surface potentials on a sphere coated with a specified material in a specified environment. It is appropriate for evaluating charging in the auroral region. It is distributed with the *POLAR* package of computer codes.

Wake

The ion depleted region of plasma behind a spacecraft moving at a speed higher than the ion thermal speed.

References

Aarset, B., Cloud, R. W., and Trump, J. G., "Electron Emission from Metals Under High-Energy Hydrogen Ion Bombardment," *Journal of Applied Physics, Vol. 25*, p. 1365, 1954.

Ademec, F. and Calderwood, J. H., "Electrical Conduction in Dielectrics at High Fields," *Journal of Physics, Vol. D-8*, p. 351, 1975.

Ashley, J. C., Tung, C. J., Anderson, V. E., and Ritchie, R. H., "Inelastic Interactions of Electrons with Polystyrene: Calculations of Mean Free Paths, Stopping Powers and CSDA Ranges," *IEEE Transactions on Nuclear Science, Vol. NS-25*, p. 1566, 1978.

Balmain, K. G., "Scaling Laws and Edge Effects for Polymer Surface Discharges," *Spacecraft Charging Technology—1978*, NASA CP-2071, AFGL-TR-79-0082, ADA084626, edited by R. C. Finke and C. P. Pike, p. 646-656, 1979.

Balmain, K. G., Battagin, A., and Dubois, G. R., "Thickness Scaling for Arc Discharges on Electron-beam-charged Dielectrics," *IEEE Transactions on Nuclear Science, Vol. NS-32, No. 6*, p. 4073-4078, 1985.

Balmain, K. G. and Dubois, G. R., "Surface Discharges on Teflon, Mylar, and Kapton," *IEEE Transactions on Nuclear Science, Vol. NS-26, No. 6*, p. 5146-5151, 1979.

Barker, T. G., *Analytic and Observational Approaches to Spacecraft Auroral Charging*, AFGL-TR-87-0021, ADA181456, 1986.

Bogorad, A., Bowman, C., Rayadurg, L., Sterner, T., Loman, J., and Armenti, J., "Amplitude Scaling of Solar Array Discharges," *IEEE Transactions on Nuclear Science, Vol. 37, No. 6*, p. 2112-2119, 1990.

Bowman, C., Bogorad, A., Shih, P., Tasca, D., Shomberg, M., and Armenti, J., "Spacecraft-Level Current-Injection Testing to Investigate Discharge Coupling Models," *IEEE Transactions on Nuclear Science, Vol. NS-36, No. 6*, p. 2033, 1989.

Burke, E. A., Wall, J. A., and Frederickson, A. R., "Radiation-Induced Low Energy Electron Emission from Metals," *IEEE Transactions on Nuclear Science, Vol. NS-17, No. 6*, p. 193-199, 1970.

Burke, G. J. and Poggio, A. J., *Numerical Electromagnetic Code (NEC), Part I and Part II: Program Description*, Lawrence Livermore National Laboratory, UCID-18834, 1981.

Cooke, private communication.

Cooke, D. L., Katz, I., Mandell, M. J., Lilley, J. R., Jr., and Rubin, A. J., "Three-Dimensional Calculation of Shuttle Charging in Polar Orbit," *Spacecraft Environmental*

Interactions Technology 1983, NASA CP-2359, AFGL-TR-85-0018, ADA202020, edited by C. K. Purvis and C. P. Pike, p. 205-227, 1985.

Cooke, D. L., Tautz, M., and Lilley, J. R., Jr., "Polar Code Simulation of DMSP Satellite Auroral Charging," *Proceedings of the Spacecraft Charging Technology Conference - 1989*, edited by R. C. Olsen, Naval Postgraduate School, Monterey, CA, p. 194-203, 1989.

Cousinie, P., Colombie, N., Fert, C., and Simon, R., "Variation du coefficient e'emission electronique secondaire de qualques metaux avec l'energie des ions incidents," *Comptes Rendus, Vol. 249*, p. 387, 1959.

Darlington, E. H. and Cosslett, V. E., "Backscattering of 0.5 - 10 keV Electrons from Solid Targets," *Journal of Physics D, Vol. 5, No. 22*, p. 1969-1981, 1972.

Durgin, D. L., et al., *DEFT Handbook, The Determination of EMP Failure Thresholds*, DNA-4-84-79, 9th Edition, 1983.

Elkman, W. R., Brown, E. M., Wadsworth, D. V. Z., Smith, E. C., and Adams, P. F., "Electrostatics Charging and Radiation Shielding Design Philosophy for a Synchronous Satellite," *Journal of Spacecraft and Rockets, Vol. 20*, p. 417-424, 1983.

EMP Assessment Handbook, AFWL-TR-78-60, BDM, 1980.

EMP Susceptibility Threshold Handbook, D224-10013-1, Boeing Co., 1972.

Everhart, T. E., "Simple Theory Concerning the Reflection of Electrons from Solids," *Journal of Applied Physics, Vol. 31*, p. 1483, 1960.

Fahleson, U., "Plasma-Vehicle Interactions in Space—Some Aspects on Present Knowledge and Future Development," *Photon and Particle Interactions with Surfaces in Space*, edited by R. J. L. Grard, D. Reidel Publishing Co., Dordrecht, Holland, p. 563-569, 1973.

Feldman, C., "Range of 1-10 keV Electrons in Solids," *Physical Review, Vol. 117*, p. 455, 1960.

FLTSATCOM Phase II Experiment Plan, CSC/AFWL SGEMP-P-5091, 1981.

Fontheim, E. G., Stasiewicz, K., Chandler, M. O., Ong, R. S. B., Gombosi, E., and Hoffman, R. A., "Statistical Study of Precipitating Electrons," *Journal of Geophysical Research, Vol. 87, No. A5*, p. 3469-3480, 1982.

Foti, G., Potenza, R., and Triglia, A., "Secondary-Electron Emission from Various Materials Bombarded with Protons at Ep < 2.5 MeV," *Lettere al Nuovo Cimento, Vol. 11*, p. 659, 1974.

Frederickson, A. R., "Radiation Induced Currents and Conductivity in Dielectrics," *IEEE Transactions on Nuclear Science, Vol. NS-24*, p. 2532, 1977.

Frezet, M., Granger, J. P., Levy, L., and Hamelin, J., "Assessment of Charging Behaviour of Meteosat Satellite in Geosynchronous Environment," *IEEE Transactions on Nuclear Science, Vol. 35, No. 6*, p. 1400-1406, 1988.

Frooninckx, T. B. and Sojka, J. J., "Solar Cycle Dependence of Spacecraft Charging in Low Earth Orbit," *Journal of Geophysical Research, Vol. 97, No. A3*, p. 2985-2996, 1992.

Garrett, H. B., Whittlesey, A., and Daughtridge, S., "Environment Induced Anomalies on the TDRS and the Role of Spacecraft Charging," AIAA Paper 90-0178, 1990.

Goldstein, R. D., Brown, E. M., and Maldoon, L. C., "Usage of ITO to Prevent Spacecraft Charging," *IEEE Transactions on Nuclear Science, Vol. NS-29, No. 6*, p. 1621-1628, 1982.

Gore, J. V., "The Design, Construction and Testing of the Communications Technology Satellite Protection Against Spacecraft Charging," *Proceedings of the Spacecraft Charging Technology Conference*, NASA TM X-73537, edited by C. P. Pike and R. R. Lovell, p. 773-788, 1977.

Granger, J. P. and Ferrante, J. G., "Electrostatic-Discharge Coupling in Spacecraft Electronics," *ESA Journal, Vol. 11, No. 14*, p. 19-30, 1987.

Grey, E. W., "Vacuum Surface Flashover: A High-Pressure Phenomenon," *Journal of Applied Physics, Vol. 58, No. 1*, p. 132, 1985.

Gussenhoven, M. S., Hardy, D. A., Rich, F., Burke, W. J., and Yeh, H.-C., "High-Level Spacecraft Charging in the Low-Altitude Polar Auroral Environment," *Journal of Geophysical Research, Vol. 90*, p. 11009-11023, 1985.

Hackenberg, O. and Brauer, W., "Secondary Electron Emission from Solids," *Advances in Electronics and Electron Physics*, edited by L. Marton, Academic Press, New York, p. 413-499, 1959.

Hall, W. M., Leung, P., Katz, I., Jongeward, G. A., Lilley, J. R., Jr., Naneviez, J. E., Thayer, J. S., and Stevens, N. J., "Polar-auroral Charging of the Space Shuttle and EVA Astronaut," *The Aerospace Environment at High Altitudes and its Implications for Spacecraft Charging and Communications*, AGARD-CP-406, p. 34/1-34/9, 1987.

Hardy, D. A., Burke, W. J., Gussenhoven, M. S., Holeman, E., and Yeh, H. C., "Average and Worst-Case Specifications of Precipitating Auroral Electron Environment," *Spacecraft Environmental Interactions Technology 1983*, NASA CP-2359, AFGL-TR-85-0018, ADA202020, edited by C. K. Purvis and C. P. Pike, p. 131-153, 1985.

Hastings, D. E., Weyl, G., and Kauffman, D., "A Threshold Voltage for Arcing in Negatively Biased Solar Arrays," *Proceedings of the Spacecraft Charging Technology Conference - 1989*, edited by R. C. Olsen, Naval Postgraduate School, Monterey, CA, p. 275-292, 1989.

Heiderbrecht, *SEMCAP Program Description, Version 7.4*, TRW, 1975.

Hilbert, R. H., *Comparison of the Trapped-Electron Models AE4 and AE5 with AE2 and AE3*, NSSDC-74-13, NASA, 1979.

Hill, A. G., Buechne, W. W., Clark, J. S., and Fisk, J. B., "The Emission of Secondary Electrons Under High-Energy Positive Ion Bombardment," *Physical Review, Vol. 55*, p. 463, 1939.

Inouye, G. T., "Brushfire Arc Discharge Model," *Spacecraft Charging Technology—1980*, NASA CP-2182, AFGL-TR-81-0270, ADA114426, edited by N. J. Stevens and C. P. Pike, p. 133-162, 1981.

Jongeward, G. A., Katz, I., Mandell, M. J., and Lilley, J. R., Jr., *Charging of a Man in the Wake of the Shuttle*, AFGL-TR-86-0139, ADA182789, 1986.

Katz, I., Mandell, M. J., Jongeward, G. A., and Gussenhoven, M. S., "The Importance of Accurate Secondary Electron Yields in Modeling Spacecraft Charging," *Journal of Geophysical Research, Vol. 91*, p. 13739-13744, 1986.

Katz, I., Parks, D. E., Mandell, M. J., Harvey, J. M., Brownell, J., D. H., and S. S. Wang, M., *A Three Dimensional Dynamic Study of Electrostatic Charging in Materials*, NASA CR-135256, 1977a.

Katz, I., Parks, D. E., Mandell, M. J., Harvey, J. M., Wang, S. S., and Roche, J. C., "NASCAP, A Three-Dimensional Charging Analyzer Program for Complex Spacecraft," *IEEE Transactions on Nuclear Science, Vol. NS-24, No. 6*, p. 2276, 1977b.

Katz, I., Stannard, P. G., Gedeon, L., Roche, J. C., Rubin, A. G., and Tautz, M. F., "NASCAP Simulations of Spacecraft Charging of the SCATHA Satellite," *Spacecraft/Plasma Interactions and Their Influence on Field and Particle Measurements*, ESA SP-198, edited by A. Pedersen, D. Guyenne, and J. Hunt, European Space Agency, Noordwijk, The Netherlands, p. 109-114, 1983.

Keyser, R. C., Leadon, R. E., Weiman, A., and Wilkenfeld, J. M., "Electron Induced Discharge Modeling for SCATHA," *Phenomenology Study and Model Testing*, DNA 4820F-1, 1978.

Koons, H. C. and Gorney, D. J., "Relationship Between Electrostatic Discharges on Spacecraft P78-2 and the Electron Environment," *Journal of Spacecraft and Rockets, Vol. 28, No. 6*, p. 683-688, 1991.

Koons, H. C., Mizera, P. F., Roeder, J. L., and Fennell, J. F., "Severe Spacecraft-Charging Event on SCATHA in September 1982," *Journal of Spacecraft and Rockets, Vol. 25*, p. 239-243, 1988.

Krauss, A. R., "Localized Plasma Sheath Model on Dielectric Discharge of Spacecraft Polymers," *IEEE Trans. Nuc. Sci., Vol. NS-35, No. 6*, 1988.

Laframboise, J. G. and Kamitsuma, M., "The Threshold Temperature Effect in High-Voltage Spacecraft Charging," *Proceedings of the Air Force Geophysics Laboratory Workshop on Natural Charging of Large Space Structures in Near Earth Polar Orbit: 14-15 September 1982*, AFGL-TR-83-0046, ADA134894, edited by R. C. Sagalyn, D. E. Donatelli, and I. Michael, p. 293-308, 1983.

Lai, S. T., Gussenhoven, M. S., and Cohen, H. A., "The Concepts of Critical Temperature and Energy Cutoff of Ambient Electrons in High Voltage Charging of Spacecraft," *Spacecraft/Plasma Interactions and their Influence on Field and Particle Measurements*, ESA SP-198, edited by A. Pedersen, D. Guyenne, and J. Hunt, European Space Agency, Noordwijk, The Netherlands, p. 169-175, 1983.

Leung, M. S., Tueling, M. B., and Mizera, P. F., "Long-Term, Light-Induced Changes in the Dark Conductivity of Kapton," *Journal of Spacecraft and Rockets, Vol. 22, No. 3*, p. 361-366, 1985.

Leung, P., "Characteristics of Electromagnetic Interference Generated by Arc Discharges," *9th Aerospace Testing Seminar*, Los Angeles, CA, p. 40-44, 1986.

Leung, P. L., "Characteristics of Electromagnetic Interference Generated During Discharge of Mylar Samples," *IEEE Transactions on Nuclear Science, Vol. NS-31, No. 6*, p. 1587-1590, 1984.

Leung, P. L. and Plamp, G., "Characteristics of RF Resulting from Dielectric Discharges," *IEEE Transactions on Nuclear Science, Vol. NS-29, No. 6*, p. 1610-1614, 1982.

Levy, L., Reulet, R., Siguier, J. M., and Sarrail, D., "Discharges Triggered on and by Electron Bombarded Dielectrics," *IEEE Transactions on Nuclear Science, Vol. 38, No. 6*, p. 1635-1640, 1991.

Levy, L. and Sarrail, D., "Scaling Laws for Discharges on Floating Supports," *IEEE Transactions on Nuclear Science, Vol. NS-34, No. 6*, p. 1606-1613, 1987.

Lilley, J. R., Jr., Cooke, D. L., Jongeward, G. A., and Katz, I., *POLAR User's Manual*, GL-TR-89-0307, ADA232103, 1989.

Lin, C. S. and Hoffman, R. A., "Characteristics of the Inverted-V Event," *Journal of Geophysical Research, Vol. 84*, p. 1514, 1979a.

Lin, C. S. and Hoffman, R. A., "Fluctuations of Inverted-V Electron Fluxes," *Journal of Geophysical Research, Vol. 84, No. A11*, p. 6471, 1979b.

Ling, D., "Common Approach to Solving SGEMP, DEMP and ESD Survivability," *Proceedings of the Spacecraft Charging Technology Conference*, NASA TM X-73537, edited by C. P. Pike and R. R. Lovell, p. 789-803, 1977.

Lowell, R., Madle, P., and Higgins, D., "Current Injection Techniques for SGEMP Testing of Full Satellite Systems," *IEEE Transactions on Nuclear Science, Vol. NS-27*, p. 1585-1589, 1980.

Mandell, M. J., Katz, I., Schnuelle, G. W., Steen, P. G., and Roche, J. C., "The Decrease in Effective Photocurrents Due to Saddle Points in Electrostatic Potentials Near Differentially Charged Spacecraft," *IEEE Transactions on Nuclear Science, Vol. NS-25, No. 6*, p. 1313-1317, 1978.

Mandell, M. J., Stannard, P. R., and Katz, I., *NASCAP Programmer's Reference Manual*, S-Cubed Division, La Jolla, CA, SSS-R-84-6638, 1984.

McAfee, W. S., "Determination of Energy Spectra of Backscattered Electrons by Use of Everhart's Theory," *Journal of Applied Physics, Vol. 47*, p. 1179, 1976.

Milligan, B., Adamo, R. C., Nanevicz, J. C., Beers, B. L., Delmer, T. N., Pine, V. W., and Hwang, H. C., *Space Discharge Characterization—Test Setup, Quick Look Experiments and Preliminary Model Development*, 1979.

Mullen, E. G. and Gussenhoven, M. S., *High-Level Spacecraft Charging Environments Near Geosynchronous Orbit*, AFGL-TR-82-0063, ADA118791, 1982.

Noise Immunity Comparison of CMOS versus Popular Bipolar Logic Families, AN-707, Motorola,

O'Donnell, E. E. and Beers, B. L., *Characteristics of Electrostatic Discharge on Spacecraft Materials*, SAIC Report, 1982.

Olsen, R. C., "A Threshold Effect for Spacecraft Charging," *Journal of Geophysical Research, Vol. 88*, p. 493-499, 1983.

Purvis, C. K., Garrett, H. B., Whittlesey, A. C., and Stevens, N. J., *Design Guidelines for Assessing and Controlling Spacecraft Charging Effects*, NASA TP 2361, 1984.

Robinson, J. W., "Charge Distributions Near Metal-Dielectric Interfaces Before and After Dielectric Surface Flashover," *Proceedings of the Spacecraft Charging Technology Conference*, AFGL-TR-77-0051, NASA TMX-73537, ADA045459, edited by C. P. Pike and R. R. Lovell, p. 503-516, 1977.

Rosen, A., *Effects of Arcing Due to Spacecraft Charging on Spacecraft Survival*, CR-159593, 1978.

Rostek, P. M., "Avoid Wiring-Inductance Problems," *Electronic Design, Vol. 25*, p. 62, 1974.

Rudie, N. J., et al., *Design Support Guide for Radiation Hardening of Space Electronics Systems*, IRT Corporation, IRT 6409-001, 1981.

Schnuelle, G. W., Stannard, P. R., Katz, I., and Mandell, M. J., "Simulation of Charging Response of SCATHA (P78-2) Satellite," *Spacecraft Charging Technology—1980*, ADA114426, edited by N. J. Stevens and C. P. Pike, p. 580, 1981.

Shimizu, R., "Secondary Electron Yield with Primary Electron Beam of Kilo-Electron-Volts," *Journal of Applied Physics, Vol. 45, No. 5*, p. 2107, 1974.

Siedler, W., Bryars, J., Tumolillo, T., Wondra, J., Keyser, R., Walters, D., Harper, H. T., and Photinos, H. R., "Experimental Evaluation of a Large Grounded Hexagonal Damper and a Ferrite Isolated Data Limit for SGEMP Testing," *IEEE Transactions on Nuclear Science, Vol. NS-28*, 1981a.

Siedler, W., Wondra, J., Walters, D., O'Donnell, H., Tasca, D., and Peden, J., "High Level Test Analysis of the SGEMP Test Analysis and Research Satellite (STARSAT)," *IEEE Transactions on Nuclear Science, Vol. NS-28*, 1981b.

Snyder, D. B., "Discharge Mechanisms in Solar Arrays - Experiment," AIAA Paper 86-0363, 1986.

Stannard, P. R., Katz, I., Gedeon, L., Roche, J. C., Rubin, A. G., and Tautz, M. F., "Validation of the NASCAP Model Using Spaceflight Data," AIAA-82-0269, 1982.

Sternglass, E. J., "Theory of Secondary Electron Emission by High Speed Ions," *Physical Review, Vol. 108, No. 1*, p. 1-12, 1957.

Stettner, R. and Dewald, A. B., "A Surface Discharge Model for Spacecraft Dielectrics," *IEEE Transactions on Nuclear Science, Vol. NS-32, No. 6*, p. 4079-4086, 1985.

Stevens, N. J., Barbay, G. J., Jones, M. R., and Viswanathan, R., "Modeling of Environmentally Induced Transients within Satellites," *Journal of Spacecraft and Rockets, Vol. 24, No. 3*, p. 257-263, 1987.

Stevens, N. J., Berkopec, F. D., Staskus, J. V., Blech, R. A., and Narciso, N. J., "Testing of Typical Spacecraft Materials in a Simulated Substorm Environment," *Proceedings of the Spacecraft Charging Technology Conference*, AFGL-TR-77-0051,

NASA TMX-73537, ADA045459, edited by C. P. Pike and R. R. Lovell, p. 431-457, 1977.

Stevens, N. J., Rosen, A., and Inouye, G. T., *Communication Satellite Experience in the Seventies*, AIAA-87-0473, 1987.

Stevens, N. J., Underwood, C. S., and Jones, M. R., "Interpretation of High Voltage Solar Array Discharge Experiments," *IEEE Transactions on Nuclear Science, Vol. 37, No. 6*, p. 2120-2127, 1990.

Sweton, J. F., *DNA EMP Handbook, Volume 3, Component Response and Test Methods (U)*, DASIAC, DNA 2114H-3, Confidential, 1979.

Treadaway, M. J., Woods, A. J., Flanagan, T. M., Leadon, R. E., Grismore, R., Denson, R., and Weenas, E. P., "Experimental Verification of an ECEMP Spacecraft Discharge Coupling Model," *IEEE Transactions on Nuclear Science, Vol. NS-27, No. 6*, p. 1776-1779, 1980.

Tumolillo, T. A. and Wondra, J. P., "MEEC-3DP: A Computer Code for the Self-Consistent Solution of the Maxwell-Lorentz Equation in Three Dimensions," *IEEE Transactions on Nuclear Science, Vol. NS-24*, p. 4545, 1977.

Wall, J. A., Burke, E. A., and Frederickson, A. R., "Results of Literature Search on Dielectric Properties and Electron Interaction Phenomena Related to Spacecraft Charging," *Proceedings of the Spacecraft Charging Technology Conference*, AFGL-TR-77-0051, ADA045459, edited by C. P. Pike and R. R. Lovell, p. 569-591, 1977.

Whipple, E. C., "Potentials of Surfaces in Space," *Reports on Progress in Physics, Vol. 44*, p. 1197-1250, 1981.

Wilkenfeld, J., "Space Electron-Induced Discharge Coupling into Satellite Electronics," *Proceedings of the Air Force Geophysics Laboratory Workshop on Natural Charging of Large Space Structures in Near Earth Polar Orbit: 14-15 September 1982*, AFGL-TR-83-0046, ADA134894, edited by R. C. Sagalyn, D. E. Donatelli, and I. Michael, p. 215-234, 1983.

Wilkenfeld, J., Judge, R., and Harlacher, B., *Development of Electrical Test Procedures for Qualification of Spacecraft Against EID, Vol. 1*, IRT 8195-018, IRT Corp., 1981.

Wilkinson, D. C., "NOAA's Spacecraft Anomaly Database," AIAA Paper 90-0173, 1990.

Woods, A. J. and Delmer, T. N., *The Arbitrary Body-of-Revolution Code (ABORC) for SGEMP/IEMP*, DNA, 4348T, 1976.

Woods, A. J. and Wenaas, E. P., "Spacecraft Discharge Electromagnetic Interference Coupling Models," *Journal of Spacecraft and Rockets, Vol. 22, No. 3*, p. 265-281, 1985.

Yeh, H.-C. and Gussenhoven, M. S., "The Statistical Electron Environment for Defense Meteorological Satellite Program Eclipse Charging," *Journal of Geophysical Research, Vol. 92, No. A7*, p. 7705-7715, 1987.

Bibliography

General

Finke, R. C. and Pike, C. P., eds., *Spacecraft Charging Technology—1978*, NASA CP-2071, AFGL-TR-79-0082, ADA084626, 1979.

Garrett, H. B. and Pike, C. P., eds., *Space Systems and Their Interactions with Earth's Space Environment*, Progress in Astronautics and Aeronautics, series ed. M. Summerfield, AIAA, New York, 1980.

Grard, R. J. L., eds., *Photon and Particle Interactions with Surfaces in Space*, D. Reidel Publishing Co., Dordrecht, Holland, 1973.

Jursa, A. S., eds., *Handbook of Geophysics and the Space Environment*, AFGL-TR-85-0315, ADA167000, Hanscom AFB, MA, 1985.

Olsen, R. C., eds., *Proceedings of the Spacecraft Charging Technology Conference - 1989*, Naval Postgraduate School, Monterey, CA, 1989.

Pike, C. P. and Lovell, R. R., eds., *Proceedings of the Spacecraft Charging Technology Conference*, AFGL-TR-77-0051, NASA TMX-73537, ADA045459, 1977.

Purvis, C. K. and Pike, C. P., eds., *Spacecraft Environmental Interactions Technology 1983*, NASA CP-2359, AFGL-TR-85-0018, ADA202020, 1985.

Robinson, P. A., Jr., *Spacecraft Environmental Anomalies Handbook*, GL-TR-89-0222, ADA214603, Geophysics Laboratory, Hanscom AFB, MA, 1989.

Rosen, A., eds., *Spacecraft Charging by Magnetospheric Plasma*, Progress in Astronautics and Aeronautics, series ed. M. Summerfield, AIAA, New York, 1975.

Sagalyn, R. C., Donatelli, D. E., and Michael, I., eds., *Proceedings of the Air Force Geophysics Laboratory Workshop on Natural Charging of Large Space Structures in Near Earth Polar Orbit: 14-15 September 1982*, AFGL-TR-83-0046, ADA134894, 1983.

Smith, R. E. and West, G. S., eds., *Space and Planetary Environment Criteria Guidelines for Use in Space Vehicle Development*, NASA TM-82478, 1983.

Space Environment: Prevention of Risks Related to Spacecraft Charging, Cepadues-Editions, Toulouse, France, 1992.

Spacecraft Materials in a Space Environment, SP-178, European Space Agency, 1983.

Spacecraft Materials in Space Environment, SP-232, European Space Agency, 1985.

Spacecraft Materials in Space Environment, ONERA, 1988.

Stevens, N. J., Kirkpatrick, M. E., Chaky, R. C., Howard, J. E., Inouye, G. T., and Beran, E. W., *Environmental Interactions Technology Status*, AFGL-TR-85-0043, ADA210822, Air Force Geophysics Laboratory, Hanscom AFB, MA, 1986.

Stevens, N. J. and Pike, C. P., eds., *Spacecraft Charging Technology—1980*, NASA CP-2182, AFGL-TR-81-0270, ADA114426, 1981.

Spacecraft Charging

Adamo, R. C. and Nanevicz, J. E., "The Causes, Characteristics, and Effects of Spacecraft Charging," *International Aerospace Conference on Lightning and Static Electricity, Vol. 2*, Oxford, England, p. E7/1 - E7/6, 1982.

Aron, P. R. and Staskus, J. V., "Area Scaling Investigations of Charging Phenomena," *Spacecraft Charging Technology—1978*, NASA CP-2071, AFGL-TR-79-0082, ADA084626, edited by R. C. Finke and C. P. Pike, p. 485-506, 1979.

Balebanov, V. M., Gdalevich, G. L., Gubskii, V. F., Dubinin, E. M., Lazarev, V. I., Nikolaeva, N. S., Podgornyi, I. M., Teltsov, M. V., Bnakov, L., and Bochev, A., "Effects of Small-Scale Plasma Disturbance on the IKB-1300 Spacecraft Potential," *34th IAF International Astronautical Congress*, AIAA, Budapest, Hungary, 1983.

Barker, T. G., *Analytic and Observational Approaches to Spacecraft Auroral Charging*, AFGL-TR-87-0021, ADA181456, 1986.

Barker, T. G., *Charging Potentials for Two Sample Sets of Spectra from DMSP Satellites*, AFGL-TR-88-0057, ADA203694, 1988.

Bessarabskii, A. I. and Shustin, E. G., "Nonstationary Potential of a Spacecraft Emitting Electrons into Free Space," *Kosmicheskie Issledovaniia, Vol. 26*, p. 953-956, 1988. In Russian.

Besse, A. L., "Unstable Potential of Geosynchronous Spacecraft," *Journal of Geophysical Research, Vol. 86*, p. 2443-2446, 1981.

Besse, A. L. and Rubin, A. G., "A Simple Analysis of Spacecraft Charging Involving Blocked Photoelectron Currents," *Journal of Geophysical Research, Vol. 85, No. A5*, p. 2324-2328, 1980.

Besse, A. L., Rubin, A. G., and Hardy, D. A., "Charging of DMSP/F6 Spacecraft in Aurora on 10 January 1983," *Spacecraft Environmental Interactions Technology 1983*, NASA CP 2359, AFGL-TR-85-0018, ADA202020, edited by C. K. Purvis and C. P. Pike, p. 125-130, 1985.

Burke, W. J., "Environmental Interactions of Polar Orbiting Satellites," *Proceedings of the Air Force Geophysics Laboratory Workshop on Natural Charging of Large Space Structures in Near Earth Polar Orbit: 14-15 September 1982*, AFGL-TR-83-0046, ADA134894, edited by R. C. Sagalyn, D. E. Donatelli, and I. Michael, p. 163-173, 1983.

Burke, W. J., Hardy, D. A., Rich, F. J., Rubin, A. G., Tautz, M. F., Saflekos, N. A., and Yeh, H. C., "Direct Measurements of Severe Spacecraft Charging in Auroral Ionosphere," *Spacecraft Environmental Interactions Technology 1983*, AFGL-TR-85-0018, ADA202020, p. 109-124, 1985.

Carovillano, R. L., *Spacecraft in the Magnetospheric Environment*, AFGL-TR-86-0134, ADA175490, 1985.

Corso, G. J., "Potential Effects of Cosmic Dust and Rocket Exhaust Particles on Spacecraft Charging," *Acta Astronautica, Vol. 12*, p. 265-267, 1985.

Craubner, S. and Froidevaux, B., "Simulation of the Electrostatic Charge Characteristics in the Case of the Direct Television Satellite TV SAT," *DFVLR-Nachrichten, Vol. 42*, p. 25-31, 1984. In German.

Craubner, S. and Froidevaux, B., "Simulation of the Electrostatic Charging Characteristics of Geostationary Satellites," *Zeitschrift fuer Flugwissenschaften und Weltraumforschung, Vol. 10*, p. 82-91, 1986. In German.

Craven, P. D., "Potential Modulation on the SCATHA Spacecraft," *Journal of Spacecraft and Rockets, Vol. 24, No. 2*, p. 150-157, 1987.

Davies, D. K., "Solar Panel Charging," *Electrostatics*, p. 165-169, 1987.

DeForest, S. E., "Spacecraft Charging at Synchronous Orbit," *Journal of Geophysical Research, Vol. 77*, p. 651-659, 1972.

DeForest, S. E., "Electrostatic Potentials Developed by ATS-5," *Photon and Particle Interactions with Surfaces in Space*, edited by R. J. L. Grard, D. Reidel Publishing Co., Dordrecht, Holland, p. 263-276, 1973.

Fahleson, U., "Plasma-Vehicle Interactions in Space—Some Aspects on Present Knowledge and Future Development," *Photon and Particle Interactions with Surfaces in Space*, edited by R. J. L. Grard, D. Reidel Publishing Co., Dordrecht, Holland, p. 563-569, 1973.

Farthing, W. J., Brown, J. P., and Bryant, W. C., *Differential Spacecraft Charging on the Geostationary Operational Environmental Satellites*, NASA-TM-83908, 1982.

Fennell, J. F., Koons, H. C., Leung, M. S., and Mizera, P. F., "A Review of SCATHA Satellite Results: Charging and Discharging," *Spacecraft/Plasma Interactions and Their Influence on Field and Particle Measurements*, ESA SP-198, edited by A. Pedersen, D. Guyenne, and J. Hunt, European Space Agency, Noordwijk, The Netherlands, p. 3-11, 1983.

Frederickson, A. R., "Electrostatic Charging and Discharging in Space Environment," *Tenth IEEE International Symposium on Discharges and Electrical Insulation in Vacuum*, 1982.

Fredricks, R. W. and Scarf, F. L., "Observations of Spacecraft Charging Effects in Energetic Plasma Regions," *Photon and Particle Interactions with Surfaces in Space*, edited by R. J. L. Grard, D. Reidel Publishing Co., Dordrecht, Holland, p. 277-308, 1973.

Frooninckx, T. B. and Sojka, J. J., "Solar Cycle Dependence of Spacecraft Charging in Low Earth Orbit," *Journal of Geophysical Research, Vol. 97, No. A3*, p. 2985-2996, 1992.

Garrett, H. B., "The Charging of Spacecraft Surfaces," *Reviews of Geophysics, Vol. 19, No. 4*, p. 577-616, 1981.

Garrett, H. B., "Three-dimensional Charging Effects," *Space Environment Technology*, Cepadues-Editions, Toulouse, France, p. 459-495, 1987.

Garrett, H. B. and Gauntt, D. M., "Spacecraft Charging during Eclipse Passage," *Space Systems and Their Interactions with Earth's Space Environment*, edited by H. B. Garrett and C. P. Pike, Progress in Astronautics and Aeronautics, series ed. M. Summerfield, AIAA, New York, p. 227-251, 1980.

Garrett, H. B. and Pike, C. P., "Spacecraft Charging: A Review," *Space Systems and Their Interactions with Earth's Space Environment*, edited by H. B. Garrett and C. P. Pike, Progress in Astronautics and Aeronautics, series ed. M. Summerfield, AIAA, New York, p. 167-226, 1980.

Garrett, H. B. and Rubin, A. G., "Spacecraft Charging at Geosynchronous Orbit-Generalized Solution for Eclipse Passage," *Geophysical Research Letters, Vol. 5*, p. 865-868, 1978.

Garrett, H. B., Rubin, A. G., and Pike, C. P., "Prediction of Spacecraft Potentials at Geosynchronous Orbit," *Solar-Terrestrial Predictions*, NASA TM-81061, edited by R. F. Donnelley, p. 104-118, 1979.

Grard, R., Knott, K., and Pedersen, A., "Interactions Between a Large Body and its Environment in a Low Polar Orbit," *Proceedings of the Air Force Geophysics Laboratory Workshop on Natural Charging of Large Space Structures in Near Earth Polar Orbit: 14-15 September 1982*, AFGL-TR-83-0046, ADA134894, edited by R. C. Sagalyn, D. E. Donatelli, and I. Michael, p. 175-184, 1983.

Grard, R. J. L., Knott, K., and Pedersen, M. R., "Spacecraft Charging Effects," *Space Science Review, Vol. 34, No. 3*, p. 289-304, 1983.

Gussenhoven, M. S., Hardy, D. A., Rich, F., Burke, W. J., and Yeh, H.-C., "High-Level Spacecraft Charging in the Low-Altitude Polar Auroral Environment," *Journal of Geophysical Research, Vol. 90*, p. 11009-11023, 1985.

Hall, D. F., "Spacecraft Charging/Contamination Experiment on SCATHA," *Proceedings of the Spacecraft Charging Technology Conference*, AFGL-TR-77-0051, NASA TMX-73537, ADA045459, edited by C. P. Pike and R. R. Lovell, p. 699, 1977.

Hall, W. M., Leung, P., Katz, I., Jongeward, G. A., Lilley, J. R., Jr., Nanevicz, J. E., Thayer, J. S., and Stevens, N. J., "Polar-auroral Charging of the Space Shuttle and EVA Astronaut," *The Aerospace Environment at High Altitudes and its Implications for Spacecraft Charging and Communications*, AGARD-CP-406, p. 34/1-34/9, 1987.

Hardy, D. A., Gussenhoven, M. S., and H.-C. Yeh, "Spacecraft Hazards in the Low Altitude Polar-Space Environment," AIAA Paper 86-0517, 1986.

Hill, J. R. and Whipple, J., E. C., "Charging of Large Structures in Space with Application to the Solar Sail Spacecraft," *Journal of Spacecraft and Rockets, Vol. 22*, p. 245-253, 1985.

Inouye, G. T., "Spacecraft Potentials in a Substorm Environment," *Spacecraft Charging by Magnetospheric Plasmas*, edited by A. Rosen, Progress in Astronautics and Aeronautics, series ed. M. Summerfield, AIAA, New York, p. 103-120, 1976.

Johnstone, A. D. and Wrenn, G. L., "Observations of Differential Charging with METEOSAT," *Proceedings of the Air Force Geophysics Laboratory Workshop on Natural Charging of Large Space Structures in Near Earth Polar Orbit: 14-15 September*

1982, AFGL-TR-83-0046, ADA134894, edited by R. C. Sagalyn, D. E. Donatelli, and I. Michael, p. 185-195, 1983.

Jongeward, G. A., Katz, I., Mandell, M. J., and Lilley, J. R., Jr., *Charging of a Man in the Wake of the Shuttle*, AFGL-TR-86-0139, ADA182789, 1986.

Katz, I., Cooke, D. L., Parks, D. E., and Mandell, M. J., "Polar Orbit Electrostatic Charging of Objects in the Shuttle Wake," *Spacecraft Environment Interactions Technology—1983*, p. 229, 1985.

Katz, I. and Mandell, M. J., "Differential Charging of High-Voltage Spacecraft: the Equilibrium Potential of Insulated Surfaces," *Journal of Geophysical Research, Vol. 87*, p. 4,533-4,541, 1982.

Katz, I., Mandell, M. J., Jongeward, G. A., Lilley, J. R., Jr., Hall, W. N., and Gussenhoven, M. S., "Analysis of DMSP Charging and the Implications for Polar Shuttle Missions," *Houston Shuttle and Environment Interactions Workshop*, 1985.

Katz, I., Mandell, M. J., Jongeward, G. A., Lilley, J. R., Jr., Hall, W. N., and Rubin, A. G., "Astronaut Charging in the Wake of a Polar Orbiting Shuttle," *AIAA Shuttle Environment and Operations II Conference*, Houston, TX, 1985.

Katz, I. and Parks, D. E., "Space Shuttle Orbiter Charging," *Journal of Spacecraft and Rockets, Vol. 20, No. 1*, p. 22-25, 1983.

Katz, I., Parks, D. E., Mandell, M. J., Harvey, J. M., Brownell, J., D. H., and S. S. Wang, M., *A Three Dimensional Dynamic Study of Electrostatic Charging in Materials*, NASA CR-135256, 1977.

Katz, I., Wilson, A., Parke, L. W., Rothwell, P. L., and Rubin, A. G., "Static and Dynamic Behavior of Spherical Probe and Satellite Plasma Sheaths," *IEEE Transactions on Nuclear Science, Vol. NS-23, No. 6*, p. 1814, 1976.

Knott, K., "The Equilibrium Potential of a Magnetospheric Satellite in an Eclipse Situation," *Planetary and Space Science, Vol. 20*, p. 1137-1146, 1972.

Knott, K., Pedersen, A., Decreau, P. M. E., Korth, A., and Wrenn, G. L., "The Potential of an Electrostatically Clean Geostationary Satellite and its Use is Plasma Diagnostics," *Planetary and Space Science, Vol. 32*, p. 227-237, 1984.

Koons, H. C. and Gorney, D. J., "Relationship Between Electrostatic Discharges on Spacecraft P78-2 and the Electron Environment," *Journal of Spacecraft and Rockets, Vol. 28, No. 6*, p. 683-688, 1991.

Koons, H. C., Mizera, P. F., Roeder, J. L., and Fennell, J. F., "Severe Spacecraft-Charging Event on SCATHA in September 1982," *Journal of Spacecraft and Rockets, Vol. 25*, p. 239-243, 1988.

Laframboise, J. F., Kamitsuma, M., and Godard, R., "Multiple Floating Potentials, 'Threshold-Temperature' Effects and 'Barrier' Effects in High-Voltage Charging of Exposed Surfaces on Spacecraft," *Spacecraft Materials in a Space Environments*, ESA SP-178, Toulouse, France, p. 269-275, 1982.

Laframboise, J. G. and Kamitsuma, M., "The Threshold Temperature Effect in High-Voltage Spacecraft Charging," *Proceedings of the Air Force Geophysics Laboratory Workshop on Natural Charging of Large Space Structures in Near Earth Polar Orbit*

14-15 September 1982, AFGL-TR-83-0046, ADA134894, edited by R. C. Sagalyn, D. E. Donatelli, and I. Michael, p. 293-308, 1983.

Laframboise, J. G. and Luo, J., "High-Voltage Polar-Orbit and Beam-Induced Charging of a Dielectric Spacecraft: A Wake-Induced Barrier Effect Mechanism," *Journal of Geophysical Research, Vol. 94*, p. 9033-9048, 1989.

Laframboise, J. G. and Parker, L. W., *Progress toward Predicting High-Voltage Charging of Spacecraft in Low Polar Orbit*, AFGL-TR-86-0261, ADA176939, 1986.

Laframboise, J. G. and Parker, L. W., "Spacecraft Charging in the Auroral Plasma: Progress Toward Understanding the Physical Effects Involved," *The Aerospace Environment at High Altitudes and its Implications for Spacecraft Charging and Communications*, p. 13/1-13/16, 1987.

Laframboise, J. G. and Prokopenko, S. M. L., "Predictions of High-Voltage Differential Charging on Geostationary Spacecraft," *Proceedings of the 1978 Symposium on the Effect of the Ionosphere on Space and Terrestrial Systems*, 1978 0-277-182, edited by J. M. Goodman, U. S. Government Printing Office, Washington DC, p. 293-301, 1978.

Lai, S. T., "Triple-Root Jump in Spacecraft Charging—Theory and Observation," *Spacecraft Materials in Space Environment*, ONERA, Toulouse, France, p. 251-258, 1988.

Lai, S. T., Gussenhoven, M. S., and Cohen, H. A., "The Concepts of Critical Temperature and Energy Cutoff of Ambient Electrons in High Voltage Charging of Spacecraft," *Spacecraft/Plasma Interactions and their Influence on Field and Particle Measurements*, ESA SP-198, edited by A. Pedersen, D. Guyenne, and J. Hunt, European Space Agency, Noordwijk, The Netherlands, p. 169-175, 1983.

Lam, H.-L. and Hruska, J., "Magnetic Signatures for Satellite Anomalies," *Journal of Spacecraft and Rockets, Vol. 28, No. 1*, p. 93-99, 1991.

Leadon, R. and Treadaway, M., *Literature Review of Spacecraft Charging*, AFGL-TR-83-0294, ADA140543, 1983.

Leung, M. S. and Kan, H. K. A., "Laboratory Study of the Charging of Spacecraft Materials," *Journal of Spacecraft and Rockets, Vol. 18, No. 6*, p. 510-514, 1981.

Levy, L., "Discharge Phenomena," *Space Environment Technology*, Cepadues-Editions, Toulouse-France, p. 523-543, 1987. In French.

Levy, L., Sarrail, D., Phillipon, J. P., Cetani, J. P., and Fourquet, J. M., "On the Possibility of a Several-Kilovolt Differential Charge in the Day Sector of a Geosynchronous Orbit," *The Aerospace Environment at High Altitudes and its Implications for Spacecraft Charging and Communications*, p. 17/1-17/12, 1987.

Li, W.-W. and Whipple, E. C., "A Study of SCATHA Eclipse Charging," *Journal of Geophysical Research, Vol. 93*, p. 10041-10046, 1988.

Mandell, M. J., Katz, I., and Cooke, D. L., "Potentials on Large Spacecraft in LEO," *IEEE Transactions on Nuclear Science, Vol. NS-29, No. 6*, p. 1584-1588, 1982.

Marque, J. P., Grando, J., Delannoy, A., and Labaune, G., "Spacecraft Charging and Electromagnetic Effects on Geostationary Satellites," *Annales des Telecommunications, Vol. 43*, p. 615-624, 1988. In French.

Massaro, M. J. and Ling, D., "Spacecraft Charging Results for the DSCS-III Satellite," *Spacecraft Charging Technology—1978*, NASA CP-2071, AFGL-TR-79-0082, ADA084626, edited by R. C. Finke and C. P. Pike, p. 158-178, 1979.

McPherson, D. A. and Schober, W., "Spacecraft Charging at High Altitudes: The SCATHA Satellite Program," *Spacecraft Charging by Magnetospheric Plasmas*, edited by A. Rosen, Progress in Astronautics and Aeronautics, series ed. M. Summerfield, AIAA, New York, p. 15-30, 1976.

Mileev, V. N., Novikov, L. S., and Ozhiganov, S. L., "Features of the Electrification of Geostationary Satellites in the Multicomponent Cosmic Plasma," *Magnetospheric Physics*, Izdatel'stvo Nauka, Moscow, p. 121-132, 1985. In Russian.

Mizera, P. F., "Natural and Artificial Charging-Results from the Satellite Surface Potential Monitor Flown on P78-2," AIAA Paper 80-0334, 1980.

Mizera, P. F., "Charging Results from the Satellite Surface Potential Monitor," *Journal of Spacecraft and Rockets, Vol. 18, No. 6*, p. 506-509, 1981. AIAA Paper 80-0334.

Mizera, P. F., "A Summary of Spacecraft Charging Results," *Journal of Spacecraft and Rockets, Vol. 20, No. 5*, p. 438, 1982.

Mizera, P. F., Koons, H. C., Schnauss, E. R., Croley, D. R., Jr., Kan, H. K. A., Leung, M. S., Stevens, N. J., Berkopec, F., Staskus, J., Lehn, W. L., and Nanewics, J. E., "First Results of Material Charging in the Space Environment," *Applied Physics Letters, Vol. 37, No. 3*, 1980.

Mizera, P. F., Schnauss, E. R., Vandre, R., and Mullen, E. G., "Description and Charging Results from the SSPM," *Spacecraft Charging Technology—1978*, NASA CP-2071, AFGL-TR-79-0082, ADA084626, edited by R. C. Finke and C. P. Pike, p. 91-100, 1979.

Mullen, E. G., Gussenhoven, M. S., and Hardy, D. A., "SCATHA Survey of High-level Spacecraft Charging in Sunlight," *Journal of Geophysical Research, Vol. 91*, p. 1474-1490, 1986.

Nanevicz, J. E. and Adamo, R. C., "Status of Critical Issues in the Area of Spacecraft Charging," *10th International Aerospace and Ground Conference on Lightning and Static Electricity and 17th Congres International Aeronautique*, Paris, France, p. 475-484, 1985.

Nanevicz, J. E., Thayer, J. S., and Hewitt, K. L., "Effects of Ambient Electron Plasma On Spacecraft Charging and Discharging," *Spacecraft Materials in Space Environment*, ONERA, Toulouse, France, p. 607-616, 1988.

Nishimoto, H., Fujii, H., and Abe, T., "Observation of Surface Charging on Engineering Test Satellite V of Japan," Reno, NV, 1989.

Olsen, R. C., "A Threshold Effect for Spacecraft Charging," *Journal of Geophysical Research, Vol. 88*, p. 493-499, 1983.

Olsen, R. C., "Record Charging Events from Applied Technology Satellite 6," *Journal of Spacecraft and Rockets, Vol. 24, No. 4*, p. 362-366, 1987.

Olsen, R. C., McIlwain, C. E., and Whipple, E. C., Jr., "Observations of Differential Charging Effects on ATS-6," *Journal of Geophysical Research, Vol. 86*, p. 6809-6819, 1981.

Olsen, R. C. and Purvis, C. K., "Observations of Charging Dynamics," *Journal of Geophysical Research, Vol. 88*, p. 5657-5667, 1983.

Olsen, R. C. and Whipple, E. C., "An Unusual Charging Event on ISEE 1," *Journal of Geophysical Research, Vol. 93, No. A6*, p. 5568-5578, 1988.

Parker, L. W., "Differential Charging and Sheath Asymmetry of Nonconducting Spacecraft Due to Plasma Flow," *Journal of Geophysical Research, Vol. 83*, p. 4873-4876, 1978.

Parker, L. W., "Differential Charging of Nonconducting Spacecraft," *Proceedings of the 1978 Symposium on the Effect of the Ionosphere on Space and Terrestrial Systems*, 1978 0-277-182, edited by J. M. Goodman, U. S. Government Printing Office, Washington DC, 1978.

Parker, L. W., *Potential Barriers and Asymmetric Sheaths due to Differential Charging of Nonconducting Spacecraft*, AFGL-TR-78-0045, ADA053618, 1978.

Parks, D. E. and Katz, I., "Charging of a Large Object in Low Polar Earth Orbit," *Spacecraft Charging Technology—1980*, NASA CP-2182, AFGL-TR-81-0270, ADA114426, edited by N. J. Stevens and C. P. Pike, p. 979-989, 1981.

Parks, D. E. and Katz, I., "Mechanisms That Limit Potentials on Ionospheric Satellites," *Journal of Geophysical Research, Vol. 88*, p. 9155, 1983.

Prokopenko, S. M. L. and Laframboise, J. G., "Prediction of Large Negative Shaded-Side Spacecraft Potentials," *Proceedings of the Spacecraft Charging Technology Conference*, AFGL-TR-77-0051, NASA TMX-73537, ADA045459, edited by C. P. Pike and R. R. Lovell, p. 369-387, 1977.

Prokopenko, S. M. L. and Laframboise, J. G., "High-Voltage Differential Charging of Geostationary Spacecraft," *Journal of Geophysical Research, Vol. 85, No. A8*, p. 4125-4131, 1980.

Purvis, C. K., "Configuration Effects on Satellite Charging Response," AIAA Paper 80-0040, 1980.

Purvis, C. K., "The Role of Potential Barrier Formation in Spacecraft Charging," *Spacecraft/Plasma Interactions and Their Influence on Field and Particle Measurements*, ESA SP-198, edited by A. Pedersen, D. Guyenne, and J. Hunt, European Space Agency, Noordwijk, The Netherlands, p. 115-124, 1983.

Purvis, C. K., Staskus, J. V., Roche, J. C., and Berkopec, F. D., "Charging Rates of Metal-Dielectric Structures," *Spacecraft Charging Technology—1978*, NASA CP-2071, AFGL-TR-79-0082, ADA112052, edited by R. C. Finke and C. P. Pike, p. 507-523, 1979.

Purvis, C. K., Stevens, N. J., and Olgebay, J. C., "Charging Characteristics of Materials: Comparison of Experimental Results with Simple Analytical Models,"

Proceedings of the Spacecraft Charging Technology Conference, AFGL-TR-77-0051, NASA TMX-73537, ADA045459, edited by C. P. Pike and R. R. Lovell, p. 459-486, 1977.

Raitt, W. J., "Space Shuttle Charging Results," *Proceedings of the Air Force Geophysics Laboratory Workshop on Natural Charging of Large Space Structures in Near Earth Polar Orbit: 14-15 September 1982*, AFGL-TR-83-0046, ADA134894, edited by R. C. Sagalyn, D. E. Donatelli, and I. Michael, p. 107-118, 1983.

Reagan, J. B., Meyerott, R. E., Gaines, E. E., Nightingale, R. W., Filbert, P. C., and Imhof, W. L., "Space Charging Currents and Their Effects on Spacecraft Systems," *IEEE Transactions on Electrical Insulation, Vol. EI-18*, p. 354-365, 1983.

Reasoner, D. L., Lennartsson, W., and Chappell, C. R., "Relationship Between ATS-6 Spacecraft Charging Occurrences and Warm Plasma Encounters," *Spacecraft Charging by Magnetospheric Plasmas*, edited by A. Rosen, Progress in Astronautics and Aeronautics, series ed. M. Summerfield, AIAA, New York, p. 89-101, 1976.

Reddy, J. and Serene, B. E., "Effects of Electron Irradiation on Large Insulating Surfaces Used for European Communications Satellites," *Spacecraft Charging Technology—1978*, NASA CP-2071, AFGL-TR-79-0082, ADA084626, edited by R. C. Finke and C. P. Pike, p. 570-586, 1979.

Roberts, B., "Vehicle Charging and Potential (VCAP)," *Solar Terrestrial Observatory Space Station Workshop*, p. 24-25, 1986.

Rose, M. F., "Electrical Insulations and Dielectrics in the Space Environment," *IEEE Transactions on Electrical Insulation, Vol. EI-22, No. 5*, p. 555-571, 1987.

Rosen, A., *RGA Analysis: Findings Regarding Correlation of Satellite Anomalies with Magnetospheric Substorms and Laboratory Test Results*, 09670-7020-RO-00, TRW Defense and Space Systems, 1972.

Rubin, A. G. and Besse, A., "Charging of a Manned Maneuvering Unit in the Shuttle Wake," AIAA Paper 83-2612, 1983.

Rubin, A. G. and Besse, A. L., "Shuttle Orbiter Charging in Polar Earth Orbit," *Proceedings of the Air Force Geophysics Laboratory Workshop on Natural Charging of Large Space Structures in Near Earth Polar Orbit: 14-15 September 1982*, AFGL-TR-83-0046, ADA134894, edited by R. C. Sagalyn, D. E. Donatelli, and I. Michael, p. 253-263, 1983.

Rubin, A. G. and Garrett, H. B., "ATS-5 and ATS-6 Potentials During Eclipse," *Spacecraft Charging Technology—1978*, NASA CP-2071, AFGL-TR-79-0082, ADA084626, edited by R. C. Finke and C. P. Pike, p. 38-43, 1979.

Samir, U. and Willmore, A. P., "The Equilibrium Potential of a Spacecraft in the Ionosphere," *Planetary and Space Science, Vol. 14*, p. 1131-1137, 1966.

Satellite Contamination, AFML-TR-78-15, 1978.

Semenov, V. A., "Laboratory Modeling of the High-voltage Electrostatic Charging of Bodies in Space," *Kosmicheskaia Nauka i Tekhnika, No. 3*, p. 57-61, 1988. In Russian.

Spearman, K. R., "DSP Experience with Spacecraft Charging," *Spacecraft Anomalies Conference*, p. 110, 1984.

Stannard, P. R., Katz, I., and Parks, D. E., "Bootstrap Charging of Surfaces Composed of Multiple Materials," *IEEE Transactions on Nuclear Science, Vol. NS-28, No. 6*, p. 4563-4567, 1981.

Stannard, P. R., Schnuelle, G. W., Katz, I., and Mandell, M. J., "Representation and Material Charging Response of GEO Plasma Environments," *Spacecraft Charging Technology—1980*, NASA CP-2182, AFGL-TR-81-0270, ADA114426, edited by N. J. Stevens and C. P. Pike, p. 560-579, 1981.

Stevens, J. R. and Vampola, A. L., *Description of the Space Test Program P78-2 Spacecraft and Payloads*, The Aerospace Corporation, SAMSO TR-78-24, 1978.

Stevens, N. J., "Review of Interactions of Large Space Structures with the Environment," *Space Systems and Their Interactions with Earth's Space Environment*, edited by H. B. Garrett and C. P. Pike, Progress in Astronautics and Aeronautics, series ed. M. Summerfield, AIAA, New York, p. 437-454, 1980.

Stevens, N. J., "Analytical Modeling of Satellites in Geosynchronous Environment," *Spacecraft Charging Technology—1980*, NASA CP-2182, AFGL-TR-81-0270, ADA114426, edited by N. J. Stevens and C. P. Pike, p. 717-729, 1981.

Stevens, N. J., "Influence of Charging Environments on Spacecraft Materials and System Performance," *Space Environmental Effects on Materials Workshop*, p. 535-542, 1989.

Stevens, N. J., "Spacecraft Charging," *Space Environmental Effects on Materials Workshop*, 2, p. 577-584, 1989.

Stevens, N. J., Lovell, R. R., and Gore, V., "Spacecraft-Charging Investigation for the CTS Project," *Spacecraft Charging by Magnetospheric Plasmas*, edited by A. Rosen, Progress in Astronautics and Aeronautics, series ed. M. Summerfield, AIAA, New York, p. 264-275, 1976.

Treadaway, J. J., "The Effects of High-Energy Electrons on the Charging of Spacecraft Dielectrics," *IEEE Transactions of Nuclear Science, Vol. NS-26, No. 6*, p. 5102-5106, 1979.

Vakulin, I. I., Grafodatskii, O. S., Gusel'nikov, V. I., Degtiarev, V. I., and Zherebtsov, G. A., "The Main Geophysical Characteristics of the Electrification of the Gorizont Series of Geostationary Satellites," *Kosmicheskie Issledovaniia, Vol. 27*, p. 102-112, 1989. In Russian.

Whipple, E. C., "Potentials of Surfaces in Space," *Reports on Progress in Physics, Vol. 44*, p. 1197-1250, 1981.

Whipple, E. C., Jr., "An Overview of Charging of Large Space Structures in Polar Orbit," *Proceedings of the Air Force Geophysics Laboratory Workshop on Natural Charging of Large Space Structures in Near Earth Polar Orbit: 14-15 September 1982*, AFGL-TR-83-0046, ADA134894, edited by R. C. Sagalyn, D. E. Donatelli, and I. Michael, p. 11-28, 1983.

Whipple, E. C., Krinsky, I. S., Torbert, R. B., and Olsen, R. C., "Anomalously High Potentials Observed on ISEE," *Spacecraft/Plasma Interactions and Their Influence on*

Field and Particle Measurements, ESA SP-198, edited by A. Pedersen, D. Guyenne, and J. Hunt, European Space Agency, Noordwijk, The Netherlands, p. 35-40, 1983.

Whipple, E. C., Jr. and Olsen, R. C., "High Spacecraft Potentials on ISEE-1 in Sunlight," *The Aerospace Environment at High Altitudes and its Implications for Spacecraft Charging and Communications*, AGARD-CP-406, p. 8/1-8/10, 1987.

Wrenn, G. L., "Spacecraft Charging Effects," *Solar Terrestrial Predictions Workshop*, Sydney, Australia, 1989.

Wrenn, G. L. and Johnstone, A. D., "Spacecraft Charging: METEOSAT Experience," *The Aerospace Environment at High Altitudes and its Implications for Spacecraft Charging and Communications*, AGARD-CP-406, p. 15/1-15/14, 1987.

Design

Adamo, R. C., Nanevicz, J. E., and Hanum, J., "Spacecraft Charging Protection for Future Space Systems," *Proceedings of the International Aerospace Conference on Lightning and Static Electricity*, St. Catherine's College, Oxford, p. E6-1 – E6-7, 1982.

Bower, S. P., "Spacecraft Charging Characteristics and Protection," *IEEE Transactions on Nuclear Science, Vol. NS-24, No. 6*, p. 2266-2269, 1977.

Broihanne, L., "Spacecraft Protection Against Electrostatic Discharge—Application to the ARABSAT Spacecraft," *The Aerospace Environment at High Altitudes and its Implications for Spacecraft Charging and Communications*, AGARD-CP-406, p. 22/1-22/11, 1987.

Dodi, D., "Design Rules and System Testing Methods," *Space Environment: Prevention of Risks Related to Spacecraft Charging*, Toulouse, France, p. 471-487, 1992.

Elkman, W. R., Brown, E. M., Wadsworth, D. V. Z., Smith, E. C., and Adams, P. F., "Electrostatics Charging and Radiation Shielding Design Philosophy for a Synchronous Satellite," *Journal of Spacecraft and Rockets, Vol. 20*, p. 417-424, 1983.

Fellas, C. N., "Spacecraft Charging: How to Make a Large Communications Satellite Immune to Arcing," *Spacecraft Materials in Space Environment*, ESA SP-232, p. 305-309, 1985.

Kamen, R. E., Holman, A. B., Stevens, N. J., and Berkopec, F. D., "Design Guidelines for the Control of Spacecraft Charging," *Spacecraft Charging Technology—1978*, NASA CP-2071, AFGL-TR-79-0082, ADA084626, edited by R. C. Finke and C. P. Pike, p. 817-818, 1979.

Lechte, H. G., "Electrostatic Immunity of Geostationary Satellites," *The Aerospace Environment at High Altitudes and its Implications for Spacecraft Charging and Communications*, AGARD-CP-406, p. 24/1-24/8, 1987.

Lechte, H. G., "A Way Towards Electrostatic Immunity in the Geostationary Orbit," *Journal of Electrostatics, Vol. 20*, p. 31-42, 1987.

Levadou, F., "Proprietes Electriques Des Materiaux," *Space Environment: Prevention of Risks Related to Spacecraft Charging*, Cepadues-Editions, Toulouse, France, p. 261-278, 1992. In French.

Lewis, R. O., Jr., "Viking and STP P78-2 Electrostatic Charging Designs and Testing," *Proceedings of the Spacecraft Charging Technology Conference*, AFGL-TR-77-0051, NASA TMX-73537, ADA045459, edited by C. P. Pike and R. R. Lovell, p. 753-772, 1977.

MIL-STD-1541, *Electromagnetic Compatibility Requirements for Space Systems*, MIL-STD-1541A (USAF), 1987.

Newell, D. M., "Radiation Effects and Spacecraft Charging Protective Design of the Intelsat-V Communications Satellite," Orlando, FL, 1982.

Purvis, C. K., Garrett, H. B., Whittlesey, A. C., and Stevens, N. J., *Design Guidelines for Assessing and Controlling Spacecraft Charging Effects*, NASA TP 2361, 1984.

Stevens, N. J., *Design Practices for Controlling Spacecraft Charging Interactions*, NASA TM 82781, 1982.

Vampola, A. L., Mizera, P. F., Koons, H. C., Fennell, J. F., and Hall, D. F., *The Aerospace Spacecraft Charging Document*, SD-TR-85-26,AD-A157 664, 1985.

Whittlesey, A. C., "Voyager Electrostatic Discharge Protection Program," *IEEE International Symposium on Electromagnetic Compatibility*, p. 377-383, 1978.

Geosynchronous Environment

Al'pert, Y. L., *The Near-Earth and Interplanetary Plasma, Vol. 1 & 2*, Cambridge University Press, Cambridge, 1983.

Baker, D. N., Belian, R. D., Higbie, P. R., Klebesadel, R. W., and Blake, J. B., "Hostile Energetic Particle Radiation Environments in Earth's Outer Magnetosphere," *The Aerospace Environment at High Altitudes and its Implications for Spacecraft Charging and Communications*, AGARD-CP-406, p. 4/1-4/16, 1987.

Barfield, J. N. and Burch, J. L., "Initial Dynamics Explorer 1 Hot Plasma Results," *1982-4 MIT Symposia on the Physics of Plasmas*, Cambridge, MA, 1984.

Cummings, W. C., Barfield, J. N., and Coleman, P. J., "Magnetospheric Substorms Observed at the Synchronous Orbit," *Journal of Geophysical Research, Vol. 73*, p. 6687-6698, 1968.

Daly, E. J., "The Evaluation of Space Radiation Environments for ESA Projects," *ESA Journal, Vol. 12, No. 2*, p. 229-247, 1988.

DeForest, S. E., "The Plasma Environment at Geosynchronous Orbit," *Proceedings of the Spacecraft Charging Technology Conference*, AFGL-TR-77- 0051, NASA TMX-73537, ADA045459, edited by C. P. Pike and R. R. Lovell, p. 37-52, 1977.

Deutsch, M.-J. C., "Worst Case Earth Charging Environment," *Journal of Spacecraft and Rockets, Vol. 19, No. 5*, p. 473-477, 1982.

Gabriel, S. B. and Garrett, H. B., "An Overview of Charging Environments," *Space Environmental Effects on Materials Workshop*, p. 495-509, 1989.

Garrett, H. B., Schwank, D. C., and DeForest, S. E., "A Statistical Analysis of the Low-Energy Geosynchronous Plasma Enviroment-I. Electrons," *Planetary and Space Science, Vol. 29*, p. 1021-1044, 1981.

Garrett, H. B., Schwank, D. C., and DeForest, S. E., "A Statistical Analysis of the Low-Energy Geosynchronous Plasma Enviroment-II. Ions," *Planetary and Space Science, Vol. 29*, p. 1045, 1981.

Garrett, H. B., Schwank, D. C., Higbie, P. R., and Baker, D. N., "Comparison Between the 30- and 80-keV Electron Channels on ATS 6 and 1976-059A During Conjunction and Application to Spacecraft Charging Predictions," *Journal of Geophysical Research, Vol. 85, No. A3*, p. 1155-1162, 1980.

Garrett, H. B. and Spitale, G. C., "Magnetospheric Plasma Modeling (0-100 keV)," *Journal of Spacecraft and Rockets, Vol. 22, No. 3*, p. 231-244, 1985.

Gussenhoven, M. S. and Mullen, E. G., "A "Worst Case" Spacecraft Charging Environment as Observed by SCATHA on 24 April 1979," AIAA Paper 82-0271, 1982.

Gussenhoven, M. S. and Mullen, E. G., "Geosynchronous Environment for Severe Spacecraft Charging," *Journal of Spacecraft and Rockets, Vol. 20*, p. 26-34, 1983.

McIlwain, C. E. and Whipple, E. C., "The Dynamic Behavior of Plasmas Observed Near Geosynchronous Orbit," *IEEE Transactions on Plasma Science, Vol. PS-14*, p. 874-890, 1986.

Mullen, E. G. and Gussenhoven, M. G., *SCATHA Environmental Atlas*, AFGL-TR-83-0002, ADA131456, 1983.

Mullen, E. G. and Gussenhoven, M. S., *High-Level Spacecraft Charging Environments Near Geosynchronous Orbit*, AFGL-TR-82-0063, ADA118791, 1982.

Mullen, E. G., Hardy, D. A., Garrett, H. B., and Whipple, E. C., "P78-2 SCATHA Environmental Data Atlas," *Spacecraft Charging Technology—1980*, NASA CP-2182, AFGL-TR-81-0270, ADA114426, edited by N. J. Stevens and C. P. Pike, p. 802-813, 1981.

Sharp, R. D., "Preliminary Results of a Low-Energy Particle Survey at Synchronous Altitude," *Journal of Geophysical Research, Vol. 75*, p. 6092-6101, 1970.

Young, D. T., "Near-Equatorial Magnetospheric Particles From ~1 eV to ~1 MeV," *Reviews of Geophysics, Vol. 21*, p. 402-418, 1983.

Polar Environment

Barfield, J., Burch, J., Gurgiolo, C., Lin, C., Winningham, D., and Saflekos, N., "Polar Plasmas as Observed by Dynamics Explorer 1 and 2," *Spacecraft Environmental Interactions Technology 1983*, NASA CP-2359, AFGL-TR-85-0018, ADA202020, edited by C. K. Purvis and C. P. Pike, p. 155-176, 1985.

Barker, T. G., *Analytic and Observational Approaches to Spacecraft Auroral Charging*, AFGL-TR-87-0021, ADA181456, 1986.

Fontheim, E. G., Stasiewicz, K., Chandler, M. O., Ong, R. S. B., Gombosi, E., and Hoffman, R. A., "Statistical Study of Precipitating Electrons," *Journal of Geophysical Research, Vol. 87, No. A5*, p. 3469-3480, 1982.

Garrett, H., "Auroral-Polar Cap Environment and its Impact on Spacecraft Plasma Interactions," *Spacecraft Environmental Interactions Technology 1983*, p. 177-193, 1985.

Gorney, D. J., Evans, D. S., Gussenhoven, M. S., and Mizera, P. F., "A Multiple-Satellite Observation of the High-Latitude Auroral Activity on January 11, 1983," *Journal of Geophysical Research, Vol. 91, No. A1*, p. 339-346, 1986.

Hardy, D. A., Burke, W. J., Gussenhoven, M. S., Holeman, E., and Yeh, H. C., "Average and Worst-Case Specifications of Precipitating Auroral Electron Environment," *Spacecraft Environmental Interactions Technology 1983*, NASA CP-2359, AFGL-TR-85-0018, ADA202020, edited by C. K. Purvis and C. P. Pike, p. 131-153, 1985.

Hoffman, R. A. and Lin, C. S., "Study of Inverted-V Auroral Precipitation Events," *Physics of Auroral Arc Formation*, edited by S. I. Akasofu and J. R. Kan, American Geophysical Union, Washington DC, p. 80-90, 1981.

Krukonis, A. P. and Whalen, J. A., "Occurrence and Lifetimes of Discrete Auroras Near Midnight," *Journal of Geophysical Research, Vol. 85*, p. 119, 1980.

Lin, C. S., Barfield, J. N., Burch, J. L., and Winningham, J. D., "Near-Conjugate Observations of Inverted-V Electron Precipitation Using DE-1 and DE-2," *Journal of Geophysical Resarch, Vol. 90*, p. 1669-1682, 1985.

Lin, C. S. and Hoffman, R. A., "Characteristics of the Inverted-V Event," *Journal of Geophysical Research, Vol. 84*, p. 1514, 1979a.

Lin, C. S. and Hoffman, R. A., "Fluctuations of Inverted-V Electron Fluxes," *Journal of Geophysical Research, Vol. 84, No. A11*, p. 6471, 1979b.

Lin, C. S. and Hoffman, R. A., "Narrow Bursts of Intense Electron Precipitation Fluxes within Inverted-V Events," *Geophysical Research Letters, Vol. 9*, p. 211, 1982.

Lin, C. S. and Hoffman, R. A., "Observations of Inverted-V Electron precipitation," *Space Sciences Review, Vol. 33*, p. 415, 1982.

Lin, C. S., Mauk, B., Gurgiolo, C., DeForest, S., and McIlwain, C. E., "Temperature Characteristics of Electron Beams and Ambient Particles," *Journal of Geophysical Research, Vol. 84, No. A6*, p. 265, 1979.

Sauer, H. H., *An Atlas of Polar Cap Energetic Particle Observations*, NOAA/ERL/SEL-3,-4, U.S. Dept. of Commerce, 1984.

Sharber, J. R. and Winningham, J. D., "Dynamics Explorer-2 Measurements During an Isolated Auroral Substorm," *Third Finish-American Auroral Workshop*, Sodankyla, Finland, 1986.

Yeh, H.-C. and Gussenhoven, M. S., "The Statistical Electron Environment for Defense Meteorological Satellite Program Eclipse Charging," *Journal of Geophysical Research, Vol. 92, No. A7*, p. 7705-7715, 1987.

Material Properties

Aarset, B., Cloud, R. W., and Trump, J. G., "Electron Emission from Metals Under High-Energy Hydrogen Ion Bombardment," *Journal of Applied Physics, Vol. 25*, p. 1365, 1954.

Antolak, A. J. and Williamson, W., Jr., "Electron Backscattering from Bulk Materials," *Journal of Applied Physics, Vol. 58, No. 1*, p. 526-534, 1985.

Belanger, V. J. and Eagles, A. E., "Secondary Emission Conductivity of High Purity Silica Fabric," *Proceedings of the Spacecraft Charging Technology Conference*, AFGL-TR-77-0051, NASA TMX-73537, ADA045459, edited by C. P. Pike and R. R. Lovell, p. 655-686, 1977.

Borovsky, J. E. and Suszcynsky, D. M., "Experimental Investigation of the z^2 Scaling Law of Fast-Ion-Produced Secondary-Electron Emission," *Physical Review A, Vol. 43, No. 3*, p. 1416-1432, 1991.

Borovsky, J. E. and Suszcynsky, D. M., "Reduction of Secondary-Electron Yields by Collective Electric Fields within Metals," *Physical Review A, Vol. 43, No. 3*, p. 1433-1440, 1991.

Bowman, C., Bogorad, A., Brucker, G., Seehra, S., and Lloyd, T., "ITO-Coated RF Transparent Materials for Antenna Sunscreen: Space Environment Effects," *IEEE Transactions on Nuclear Science, Vol. 37, No. 6*, p. 2134-2127, 1990.

Bronshteyn, I. M. and Protsenko, A. N., "Inelastic Electron Scattering and the Secondary Electron Emission of Insulators," *Radio Engineering and Electronic Physics, Vol. 15, No. 4*, p. 677, 1970.

Budd, P. A., Javidi, B., and Robinson, J. W., "Secondary Electron Emission from a Charged Dielectric," *IEEE Transactions on Electical Insulation, Vol. EI-20, No. 3*, p. 485-491, 1985.

Burke, E. A., "Secondary Emission from Polymers," *IEEE Transactions on Nuclear Science, Vol. NS-27, No. 6*, p. 1760-1764, 1980.

Burke, E. A., Wall, J. A., and Frederickson, A. R., "Radiation-Induced Low Energy Electron Emission from Metals," *IEEE Transactions on Nuclear Science, Vol. NS-17, No. 6*, p. 193-199, 1970.

Chase, R. W., *Secondary Electron Emission Yield from Aluminum Alloy Surfaces*, Case Western Reserve University, 1979.

Chung, M. S. and Everhart, T. E., "Simple Calculations of Energy Distribution of Low-Energy Secondary Electrons Emitted from Metals Under Electron Bombardment," *Journal of Applied Physics, Vol. 45, No. 2*, p. 707-709, 1974.

Clouvas, A., Rothard, H., Burkhard, M., Kroneberger, K., Biedermann, C., Kemmler, J., Groeneveld, K. O., Kirsch, R., Misaelides, P., and Katsanos, A., "Secondary Electron Emission from Thin Foils under Fast-Ion Bombardment," *Physical Review B, Vol. 39, No. 10*, p. 6316-6319, 1989.

Cotts, D. B. and Reyes, Z., *New Polymeric Materials Expected to Have Superior Properties for Space-Based Uses*, RADC, Bedford, MA, RADC-TR-85-129, ADA160285, 1985.

Cotts, D. B. and Reyes, Z., *Electrically Conductive Organic Polymers for Advanced Applications*, Noyes Data Corporation, Park Ridge, NJ, 212, 1986.

Cousinie, P., Colombie, N., Fert, C., and Simon, R., "Variation du coefficient e'emission electronique secondaire de qualques metaux avec l'energie des ions incidents," *Comptes Rendus, Vol. 249*, p. 387, 1959.

Darlington, E. H. and Cosslett, V. E., "Backscattering of 0.5 - 10 keV Electrons from Solid Targets," *Journal of Physics D, Vol. 5, No. 22*, p. 1969-1981, 1972.

De, B. R., "Conductorlike Behavior of Photoemitting Dielectric Surface," *Journal of Geophysical Research, Vol. 84, No. A6*, p. 2655-2656, 1979.

Dekker, A. J., *Secondary Electron Emission, Vol. 6*, Solid State Physics, Advances in Research and Applications, series ed. F. Seitz and D. Turnbull, Academic Press, New York, 251-311, 1958.

Eagles, A. E., Amore, L. J., Belanger, V. J., and Schmidt, R. E., *Spacecraft Static Charge Control Materials, Part I*, AFML-TR-77-105, General Electric Space Division, 1977.

Eagles, A. E., Amore, L. J., Belanger, V. J., and Schmidt, R. E., *Spacecraft Static Charge Control Materials, Part II*, AFML-TR-77-105, General Electric Space Division, 1978.

Eagles, A. E., Schmidt, R. E., Amore, L. J., and Belanger, V. J., *Transparent Antistatic Satellite Materials, Part I*, AFML-TR-77-174, General Electric Space Division, 1977.

Eagles, A. E., Schmidt, R. E., Amore, L. J., and Belanger, V. J., *Transparent Antistatic Satellite Materials, Part II*, AFML-TR-77-174, General Electric Space Division, 1978.

Ehrenberg, W. and Gibbons, D. J., *Electron Bombardment Induced Conductivity*, Academic Press, New York, NY, 1981.

Everhart, T. E., "Simple Theory Concerning the Reflection of Electrons from Solids," *Journal of Applied Physics, Vol. 31*, p. 1483, 1960.

Feldman, C., "Range of 1-10 keV Electrons in Solids," *Physical Review, Vol. 117*, p. 455, 1960.

Feuerbacher, B. and Fitton, B., "Experimental Investigation of Photoemission from Satellite Surface Materials," *Journal of Applied Physics, Vol. 43, No. 4*, p. 1562-1572, 1972.

Foti, G., Potenza, R., and Triglia, A., "Secondary-Electron Emission from Various Materials Bombarded with Protons at Ep < 2.5 MeV," *Lettere al Nuovo Cimento, Vol. 11*, p. 659, 1974.

Frederickson, A. R., "Dielectrics for Long Term Space Exposure and Spacecraft Charging: A Briefing," *Space Environmental Effects on Materials Workshop, Part 2*, p. 473-494, 1989.

Frederickson, A. R., Wall, J. A., Cotts, D. B., and Bouquet, F. L., *Spacecraft Dielectric Material Properties and Spacecraft Charging, Vol. 107*, Progress in Astronautics and Aeronautics, series ed. M. Summerfield, AIAA, New York, 1986.

Gibbons, D. J., "Secondary Electron Emission," *Physical Electronics*, edited by A. H. Beck, Handbook of Vacuum Physics, Pergamon Press, Oxford, p. 301-395, 1966.

Guillaumon, J. C., "New Space Paints," *Spacecraft Materials in Space Environment*, Noordwijk, The Netherlands, p. 239-243, 1985.

Hackenberg, O. and Brauer, W., "Secondary Electron Emission from Solids," *Advances in Electronics and Electron Physics*, edited by L. Marton, Academic Press, New York, p. 413-499, 1959.

Henrich, V. E., "Fast, Accurate Secondary-Electron Yield Measurements at Low Primary Energies," *Review of Scientific Instruments, Vol. 44, No. 4*, p. 456-462, 1973.

Hill, A. G., Buechne, W. W., Clark, J. S., and Fisk, J. B., "The Emission of Secondary Electrons Under High-Energy Positive Ion Bombardment," *Physical Review, Vol. 55*, p. 463, 1939.

Javidi, B., *Secondary Electron Emission from a Charged Dielectric in the Presence of Normal and Oblique Electric Fields*, NASA-CR-168558, 1982.

Kanaya, K. and Kawakatsu, H., "Secondary Electron Emission Due to Primary and Backscattered Electrons," *Journal of Physics D, Vol. 5*, p. 1727-1742, 1972.

Kanter, H., "Energy Dissipation and Secondary Electron Emission in Solids," *Physical Review, Vol. 121*, p. 677, 1961.

Katz, I., Parks, D. E., Mandell, M. J., Harvey, J. M., Brownell, J., D. H., and S. S. Wang, M., *A Three Dimensional Dynamic Study of Electrostatic Charging in Materials*, NASA CR-135256, 1977.

Krainsky, I., Lundin, W., Gordon, W. L., and Hoffman, R. W., "Secondary Electron Emission Yields," *Spacecraft Charging Technology—1980*, NASA CP-2182, AFGL-TR-81-0270, ADA114426, edited by N. J. Stevens and C. P. Pike, p. 179-197, 1981.

Laframboise, J. G., "Calculation of Secondary-Electron Escape Currents from Inclined Spacecraft Surfaces in a Magnetic Field," *Spacecraft Environmental Interactions Technology 1983*, NASA CP-2359, AFGL-TR-85-0018, ADA202020, edited by C. K. Purvis and C. P. Pike, p. 277-286, 1985.

Lebreton, J.-P., "Spacecraft Paint Layer Electrical Characteristics Measurements by the Langmuir Probe Technique," *Spacecraft Materials in Space Environment*, ONERA, Toulouse, France, p. 589-598, 1988.

Lehn, W. L., "SCATHA Conductive Spacecraft Materials Development," *Journal of Spacecraft and Rockets, Vol. 20, No. 2*, p. 182-185, 1983.

Leung, M. S., Tueling, M. B., and Mizera, P. F., "Long-Term, Light-Induced Changes in the Dark Conductivity of Kapton," *Journal of Spacecraft and Rockets, Vol. 22, No. 3*, p. 361-366, 1985.

Levadou, F., "Proprietes Electriques Des Materiaux," *Space Environment: Prevention of Risks Related to Spacecraft Charging*, Cepadues-Editions, Toulouse, France, p. 261-278, 1992. In French.

Levadou, F., Bosma, S. J., and Paillous, A., "Materials Characterization Study of Conductive Flexible Second Surface Mirrors," *Spacecraft Charging Technology - 1980*, NASA CP 2182, AFGL-TR-81-0270, ADA114426, edited by N. J. Stevens and C. P. Pike, p. 237-260, 1981.

Levadou, F., "Discharge Prevention of Geosynchronous Orbit-Conductive Thermal Control Materials and Grounding Systems," *Space Environment Technology*, Cepadues-Editions, Toulouse, France, p. 695-715, 1987. In French.

Levy, L., Paillous, A., and Catani, J. P., "Experimental Study of Thermal Control Material Charging and Discharging," *Spacecraft Materials in a Space Environment*, ESA SP-178, p. 243-251, 1983.

Levy, L., Paillous, A., and Sarrail, D., *Satellite Charging Control Materials*, ONERA, Centre D'Etudes et de Recherches de Toulouse, AFWAL-TR-81-4033, 1981.

Levy, L., Sarrail, D., and Siguier, J. M., "Conductivity and Secondary Emission Properties of Dielectrics as Required by NASCAP," *Spacecraft Materials in Space Environment*, Noordwijk, The Netherlands, p. 113-123, 1985.

Lucas, A. A., "Fundamental Processes in Particle and Photon Interactions with Surfaces in Space," *Photon and Particle Interactions with Surfaces in Space*, edited by R. J. L. Grard, D. Reidel Publishing Co., Dordrecht, Holland, p. 3-21, 1973.

Makhov, A. F., "An Empirical Relation for the Secondary Electron Emission of Solids," *Soviet Physics-Solid State, Vol. 17, No. 8*, 1976.

Mandell, M. J., Katz, I., Schnuelle, G. W., and Roche, J. C., "Photoelectron Charge Density and Transport Near Differentially Charged Spacecraft," *IEEE Transactions on Nuclear Science, Vol. NS-26, No. 6*, p. 5107, 1979.

Marco, J., Paillous, A., and Levadou, F., "Combined Radiation Effects on Optical Reflectance of Thermal Control Coatings," *Spacecraft Materials in Space Environment*, ONERA, Toulouse, France, p. 121-132, 1988.

McAfee, W. S., "Determination of Energy Spectra of Backscattered Electrons by Use of Everhart's Theory," *Journal of Applied Physics, Vol. 47*, p. 1179, 1976.

Norman, K. and Freeman, R. M., "Energy Distribution of Photoelectrons Emitted from a Surface on the OGO-5 Satellite and Measurements of Satellite Potential," *Photon and Particle Interactions with Surfaces in Space*, edited by R. J. L. Grard, D. Reidel Publishing Co., Dordrecht, Holland, p. 231-244, 1973.

Passenheim, B. C., Van Lint, V. A. J., Riddell, J. D., and Kitterer, R., "Electrical Conductivity and Discharge in Spacecraft Thermal Control Dielectrics," *IEEE Transactions on Nuclear Science, Vol. NS-29, No. 6*, p. 1594-1600, 1982.

Rafla-Yuan, H. and Cordaro, J. F., "Optical Reflectance of Aluminum-Doped Zinc Oxide Powders," *Journal of Applied Physics, Vol. 69, No. 2*, p. 959-964, 1991.

Reulet, R., "Moyens D'Irradiation," *Space Environment: Prevention of Risks Related to Spacecraft Charging*, Cepadues-Editions, Toulouse, France, p. 335-365, 1992. In French.

Riddell, J. D., Chervenak, J. G., and Van Lint, V. A. J., "Ionization-induced Breakdown and Conductivity of Satellite Dielectrics," *IEEE Transactions on Nuclear Science, Vol. NS-29, No. 6*, p. 1754-1759, 1982.

Riddell, J. R. and Passenheim, B. C., *Electrical Conductivity of Spacecraft Thermal Control Dielectrics*, AFWL, Albuquerque, NM, 1982.

Rittenhouse, J. B. and Singletar, J. B., *Space Material Handbook*, NASA SP-3051, 1969.

Robinson, J. W. and Budd, P. A., "Oblique-Incidence Secondary Emission from Charged Dielectrics," *Spacecraft Charging Technology - 1980*, NASA CP 2182, AFGL-TR-81-0270, ADA114426, edited by N. J. Stevens and C. P. Pike, p. 198-210, 1981.

Rose, A., eds., *Concepts in Photoconductivity and Allied Problems*, John Wiley, 1963.

Samson, J. A. R. and Cairns, R. B., "Photoelectric Yield of Aluminum from 300 to 1300 Angstroms," *Review of Scientific Instruments, Vol. 36, No. 1*, p. 19-21, 1965.

Satellite Spacecraft Charging Control Materials, AFWAL-TR-80-4029, 1980.

Schmidt, R. E., *Charging Control Satellite Materials, Part 1*, AFWAL-TR-80-4017, 1980.

Schmidt, R. E., *Charging Control Satellite Materials, Part 2, Materials Demonstration*, AFWAL-TR-80-4017, 1981.

Schmitz, W., "Development of Solar Generator Substrates: Simple Anticharging (AC) and Conductive Thermal Control (TC) Materials (GEO), and Some LEO Aspects," *Spacecraft Materials in Space Environment*, ESA, p. 133-141, 1986.

Schwarz, S. A., "Application of a Semi-Empirical Sputtering Model to Secondary Electron Emission," *Journal of Applied Physics, Vol. 68, No. 5*, p. 2382-2391, 1990.

Shimizu, R., "Secondary Electron Yield with Primary Electron Beam of Kilo-Electron-Volts," *Journal of Applied Physics, Vol. 45, No. 5*, p. 2107, 1974.

Simpson, J. C. and Cordaro, J. F., "Photocapacitance and Photoconductance of Bi-Doped ZnO," *Journal of Applied Physics, Vol. 69, No. 7*, p. 4011-4016, 1991.

Sternglass, E. J., "Secondary Electron Emission and Atomic Shell Structure," *Physical Review, Vol. 80, No. 5*, p. 925-926, 1950.

Sternglass, E. J., "Backscattering of Kilovolt Electrons from Solids," *Physical Review, Vol. 95, No. 2*, p. 345-358, 1954.

Sternglass, E. J., "Theory of Secondary Electron Emission by High Speed Ions," *Physical Review, Vol. 108, No. 1*, p. 1-12, 1957.

Stevens, N. J., "Influence of Charging Environments on Spacecraft Materials and System Performance," *Space Environmental Effects on Materials Workshop*, p. 535-542, 1989.

Sun, Y.-N., "Electron Yield Behaviour from Kapton," *Spacecraft Materials in Space Environment*, Toulouse, France, p. 617-619, 1988.

Svensson, B., Holmen, G., and Buren, A., "Angular Dependence of the Ion-Induced Secondary-Electron Yield from Solids," *Physical Review B, Vol. 24, No. 7*, p. 3749-3755, 1981.

Verdin, D. and Duck, M. J., "Conductive Coatings to Minimise the Electrostatic Charging of Kapton," *Spacecraft Materials in Space Environment*, Noordwijk, The Netherlands, p. 125-131, 1985.

Wall, J. A., Burke, E. A., and Frederickson, A. R., "Results of Literature Search on Dielectric Properties and Electron Interaction Phenomena Related to Spacecraft Charging," *Proceedings of the Spacecraft Charging Technology Conference*, AFGL-TR-77-0051, ADA045459, edited by C. P. Pike and R. R. Lovell, p. 569-591, 1977.

Weissler, G. L., "Photoionization in Gases and Photoelectric Emission from Solids," *Handbuch der Physik, Vol. XXI*, p. 360-363, 1973.

Williamson, W., Jr., Antolak, A. J., and Meredith, R. J., "An Energy-Dependent Electron Backscattering Coefficient," *Journal of Applied Physics, Vol. 61, No. 9*, p. 4612-4618, 1987.

Williamson, W. S., Dulgeroff, C. R., Hymann, J., and Viswanathan, R., "Kapton Charging Characteristics: Effects of Material Thickness and Electron-Energy Distribution," *Spacecraft Environmental Interactions Technology 1983*, NASA CP-2359, AFGL-TR-85-0018, ADA202020, edited by C. K. Purvis and C. P. Pike, p. 547-558, 1985.

Willis, R. F. and Skinner, D. K., "Secondary Electron Emission Yield Behavior of Polymers," *Solid State Communications, Vol. 13, No. 6*, p. 685-688, 1973.

Wrenn, G. L. and Heikkila, W. J., "Photoelectrons Emitted from ISIS Spacecraft," *Photon and Particle Interactions with Surfaces in Space*, edited by R. J. L. Grard, D. Reidel Publishing Co., Dordrecht, Holland, p. 221-230, 1973.

Yang, K., Gordon, W. L., and Hoffman, R. W., "Electron Yields from Spacecraft Materials," *Spacecraft Environmental Interactions Technology 1983*, NASA CP-2359, AFGL-TR-85-0018, ADA202020, edited by C. K. Purvis and C. P. Pike, p. 537-545, 1985.

Young, D. T., "Energy Distributions and Yields of Secondary Ions and Electrons Emitted by GIOTTO During Halley Encounter," *Spacecraft/Plasma Interactions and Their Influence on Field and Particle Measurements*, ESA SP-198, edited by A. Pedersen, D. Guyenne, and J. Hunt, European Space Agency, Noordwijk, The Netherlands, p. 143-150, 1983.

Zimcik, D. G., Wertheimer, M. R., Balmain, K. B., and Tennyson, R. C., "Plasma-Deposited Protective Coatings for Spacecraft Applications," *Journal of Spacecraft and Rockets, Vol. 28, No. 6*, p. 652-657, 1991.

Effect of Material Properties on Spacecraft Charging

Besse, A. L. and Rubin, A. G., "A Simple Analysis of Spacecraft Charging Involving Blocked Photoelectron Currents," *Journal of Geophysical Research, Vol. 85, No. A5*, p. 2324-2328, 1980.

Cauffman, D. P., "The Effects of Photoelectron Emission on a Multiple-Probe Spacecraft Near the Plasmapause," *Photon and Particle Interactions with Surfaces in*

Space, edited by R. J. L. Grard, D. Reidel Publishing Co., Dordrecht, Holland, p. 153-161, 1973.

Garrett, H. B. and DeForest, S. E., "Time-Varying Photoelectron Flux Effects on Spacecraft Potentials at Geosynchronous Orbit," *Journal of Geophysical Research, Vol. 84*, p. 2083-2088, 1979.

Grard, R. J. L., "Properties of the Satellite Photoelectron Sheath Derived from Photoemission Laboratory Measurements," *Journal of Geophysical Research, Vol. 78*, p. 2885-2906, 1973.

Grard, R. J. L. and Tunaley, J. K. E., "Photoelectron Sheath Near a Planar Probe in Interplanetary Space," *Journal of Geophysical Research, Vol. 76*, p. 2498-2505, 1971.

Katz, I. and Mandell, M. J., "Secondary Electron Generation, Emission and Transport: Effects on Spacecraft Charging and NASCAP Models," *Journal of Electrostatics, Vol. 20*, p. 109-121, 1987.

Katz, I., Mandell, M. J., Jongeward, G. A., and Gussenhoven, M. S., "The Importance of Accurate Secondary Electron Yields in Modeling Spacecraft Charging," *Journal of Geophysical Research, Vol. 91*, p. 13739-13744, 1986.

Laframboise, J. G., Prokopenko, S. M. L., Kamitsuma, M., and Godard, R., "Results from a Two-Dimensional Spacecraft-Charging Simulation and Comparison with a Surface Photocurrent Model," *Spacecraft Charging Technology—1980*, NASA CP-2182, AFGL-TR-81-0270, ADA114426, edited by N. J. Stevens and C. P. Pike, p. 709-716, 1981.

Leung, M. S., Tueling, M. B., and Schnauss, E. R., "Effects of Secondary Electron Emission on Charging," *Spacecraft Charging Technology—1980*, NASA CP-2182, AFGL-TR-81-0270, ADA114426, edited by N. J. Stevens and C. P. Pike, p. 163-178, 1981.

Mandell, M. J., Katz, I., Schnuelle, G. W., Steen, P. G., and Roche, J. C., "The Decrease in Effective Photocurrents Due to Saddle Points in Electrostatic Potentials Near Differentially Charged Spacecraft," *IEEE Transactions on Nuclear Science, Vol. NS-25, No. 6*, p. 1313-1317, 1978.

Moskalenko, A. M., "Electric Field and Plasma Structure Near a Small Body in the Presence of Photoelectron Emission" *Geomagnetizm i Aeronomiia, Vol. 23*, p. 750-754, 1983. In Russian.

Purvis, C. K., "Effects of Secondary Yield Parameter Variation on Predicted Equilibrium Potentials of an Object in a Charging Environment," 1979.

Purvis, C. K., Stevens, N. J., and Olgebay, J. C., "Charging Characteristics of Materials: Comparison of Experimental Results with Simple Analytical Models," *Proceedings of the Spacecraft Charging Technology Conference*, AFGL-TR-77-0051, NASA TMX-73537, ADA045459, edited by C. P. Pike and R. R. Lovell, p. 459-486, 1977.

Sanders, N. L. and Inouye, G. T., "Secondary Emission Effects on Spacecraft Charging: Energy Distribution Considerations," *Spacecraft Charging Technology—1978*,

NASA CP-2071, AFGL-TR-79-0082, ADA084626, edited by R. C. Finke and C. P. Pike, p. 747-755, 1979.

Whipple, E. C., Jr., "Observation of Photoelectrons and Secondary Electrons Reflected from a Potential Barrier in the Vicinity of ATS-6," *Journal of Geophysical Research, Vol. 81*, p. 715-719, 1976.

Modeling of Spacecraft Charging

Cooke, D., Parker, L. W., and McCoy, J. E., "Three-Dimensional Space Charge Model for Large High-Voltage Satellites," *Spacecraft Charging Technology—1980*, NASA CP-2182, AFGL-TR-81-0270, ADA114426, edited by N. J. Stevens and C. P. Pike, p. 957-978, 1981.

Cooke, D. L., Katz, I., Mandell, M. J., Lilley, J. R., Jr., and Rubin, A. J., "Three-Dimensional Calculation of Shuttle Charging in Polar Orbit," *Spacecraft Environmental Interactions Technology 1983*, NASA CP-2359, AFGL-TR-85-0018, ADA202020, edited by C. K. Purvis and C. P. Pike, p. 205-227, 1985.

Cooke, D. L., Tautz, M., and Lilley, J. R., Jr., "Polar Code Simulation of DMSP Satellite Auroral Charging," *Proceedings of the Spacecraft Charging Technology Conference - 1989*, edited by R. C. Olsen, Naval Postgraduate School, Monterey, CA, p. 194-203, 1989.

Daly, E. J. and Burke, W. R., *Simulations of the Electrostatic Charging of ESA Communications Satellites*, ESA-STM-239, European Space Agency, ESTEC, Noordwijk, The Netherlands, 1987.

Frezet, M., "Charging Calculations for the HIPPARCOS Satellite," *Space Environment Technology*, Cepadues-Editions, Toulouse, France, p. 631-650, 1987. In French.

Frezet, M., Granger, J. P., Daly, E. J., and Hamelin, J., "Assessment of Electrostatic Charging of Satellites in the Geostationary Environment," *ESA Journal, Vol. 13, No. 2*, p. 89-116, 1989.

Frezet, M., Granger, J. P., Levy, L., and Hamelin, J., "Assessment of Charging Behaviour of Meteosat Satellite in Geosynchronous Environment," *IEEE Transactions on Nuclear Science, Vol. 35, No. 6*, p. 1400-1406, 1988.

Hoge, D. G., "METEOSAT Spacecraft Charging Investigation," *Spacecraft Charging Technology—1980*, NASA CP-2182, AFGL-TR-81-0270, ADA144226, edited by N. J. Stevens and C. P. Pike, p. 814-834, 1981.

Jongeward, G. A., Mandell, M. J., Lilley, J. R., Jr., and Katz, I., *POLAR 2.0 Validation and Preflight SPEAR I Calculations*, AGFL-TR-88-0056, ADA201094, 1988.

Katz, I., Cassidy, J. J., Mandell, M. J., Schnuelle, G. W., Steen, P. G., and Roche, J. C., "The Capabilities of the NASA Charging Analyzer Program," *Spacecraft Charging Technology—1978*, NASA CP-2071, AFGL-TR-79-0082, ADA084626, edited by R. C. Finke and C. P. Pike, p. 101-122, 1979.

Katz, I., Cooke, D. L., Mandell, M. J., Parks, D. E., Lilley, J. R., Jr., Alexander, J. H., and Rubin, A. G., "POLAR Code Development," *Proceedings of the Air Force Geophysics Laboratory Workshop on Natural Charging of Large Space Structures in Near Earth Polar Orbit: 14-15 September 1982*, AFGL-TR-83-0046, ADA134894, edited by R. C. Sagalyn, D. E. Donatelli, and I. Michael, p. 321-332, 1983.

Katz, I., Cooke, D. L., Parks, D. E., Mandell, M. J., and Rubin, A. G., "A Three-Dimensional Wake Model for Low Earth Orbit," *Journal of Spacecraft and Rockets, Vol. 21*, p. 125, 1984.

Katz, I., Parks, D. E., Mandell, M. J., Harvey, J. M., Wang, S. S., and Roche, J. C., "NASCAP, A Three-Dimensional Charging Analyzer Program for Complex Spacecraft," *IEEE Transactions on Nuclear Science, Vol. NS-24, No. 6*, p. 2276, 1977.

Katz, I., Stannard, P. G., Gedeon, L., Roche, J. C., Rubin, A. G., and Tautz, M. F., "NASCAP Simulations of Spacecraft Charging of the SCATHA Satellite," *Spacecraft/Plasma Interactions and Their Influence on Field and Particle Measurements*, ESA SP-198, edited by A. Pedersen, D. Guyenne, and J. Hunt, European Space Agency, Noordwijk, The Netherlands, p. 109-114, 1983.

Laframboise, J. G., Godard, R., and Prokopenko, S. M. L., "Numerical Calculations of High-Altitude Differential Charging: Preliminary Results," *Spacecraft Charging Technology—1978*, NASA CP-2071, AFGL-TR-79-0082, ADA084626, edited by R. C. Finke and C. P. Pike, p. 188-196, 1979.

Lilley, J. R., Jr., Cooke, D. L., Jongeward, G. A., and Katz, I., *POLAR User's Manual*, GL-TR-89-0307, ADA232103, 1989.

Lilley, J. R., Jr., Waisman, S. G., Peterka, D., Daou, D., and Mandell, M. J., *Spacecraft/Environment Interactions CAE Tool User's Manual*, S-Cubed Division, La Jolla, CA, 1988.

Mandell, M. J., Katz, I., and Parks, D. E., "NASCAP Simulation of Laboratory Spacecraft Charging Tests Using Multiple Electron Guns," *IEEE Transactions on Nuclear Science, Vol. NS-28, No. 6*, p. 4568-4570, 1981.

Mandell, M. J., Stannard, P. R., and Katz, I., *NASCAP Programmer's Reference Manual*, S-Cubed Division, La Jolla, CA, SSS-R-84-6638, 1984.

Massaro, M. J., Green, T., and Ling, D., "A Charging Model for Three-Axis Stabilized Spacecraft," *Proceedings of the Spacecraft Charging Technology Conference*, AFGL-TR-77-0051, NASA TMX-73537, ADA045459, p. 237-269, 1977.

Murphy, G. and Katz, I., "The POLAR Code Wake Model: Comparison with In Situ Observations," *Journal of Geophysical Research, Vol. 94*, p. 9065-9075, 1989.

Rubin, A. G., Katz, I., Mandell, M., Schnuelle, G., Steen, P., Parks, D., Cassidy, J., and Roche, J., "A Three-dimensional Spacecraft-Charging Computer Code," *Space Systems and Their Interactions with Earth's Space Environment*, edited by H. B. Garrett and C. P. Pike, Progress in Astronautics and Aeronautics, series ed. M. Summerfield, AIAA, New York, p. 318-336, 1980.

Schnuelle, G. W., Parks, D. E., Katz, I., Mandell, M. J., Steen, P. G., Cassidy, J. J., and Rubin, A. G., "Charging Analysis of the SCATHA Satellite," *Spacecraft Charging*

Technology—1978, NASA CP-2071, AFGL-TR-79-0082, ADA084626, edited by R. C. Finke and C. P. Pike, 1979.

Stevens, N. J., "Modeling of Environmentally-Induced Effects Within Satellites, Part I NASCAP Modeling of Satellites," *Space Environment Technology*, Cepadues-Editions, Toulouse, France, p. 497, 1987.

Stevens, N. J., Barbay, G. J., Jones, M. R., and Viswanathan, R., "Modeling of Environmentally Induced Transients within Satellites," *Journal of Spacecraft and Rockets, Vol. 24, No. 3*, p. 257-263, 1987.

Stevens, N. J. and Purvis, C. K., *NASCAP Modeling Computations on Large Optics Spacecraft in Geosynchronous Substorm Environment*, NASA TM-81395, 1980.

Discharges

Adamo, R. C. and Matarrese, J. R., "Transient Pulse Monitor Data from the P78-2 (SCATHA) Spacecraft," *Journal of Spacecraft and Rockets*, p. 432-437, 1983. AIAA Paper 82-0265.

Adamo, R. C. and Nanevicz, J. E., "Spacecraft-Charging Studies of Voltage Breakdown Processes on Spacecraft Thermal Control Mirrors," *Spacecraft Charging by Magnetospheric Plasmas*, edited by A. Rosen, Progress in Astronautics and Aeronautics, series ed. M. Summerfield, AIAA, New York, p. 225-235, 1976.

Balmain, K. G., "Scaling Laws and Edge Effects for Polymer Surface Discharges," *Spacecraft Charging Technology—1978*, NASA CP-2071, AFGL-TR-79-0082, ADA084626, edited by R. C. Finke and C. P. Pike, p. 646-656, 1979.

Balmain, K. G., "Surface Discharge Arc Propagation and Damage on Spacecraft Dielectrics," *Spacecraft Materials in Space Environment*, edited by J. Dauphin and D. Guyenne, European Space Agency, p. 209-215, 1979.

Balmain, K. G., "Surface Discharge Effects-Induced Electric Arcs from Spacecraft Dielectric Sheets," *Space Systems and Their Interactions with Earth's Space Environment*, edited by H. B. Garrett and C. P. Pike, Progress in Astronautics and Aeronautics, series ed. M. Summerfield, AIAA, New York, p. 276-298, 1980.

Balmain, K. G., *Charge Accumulation and Arc Discharges on Spacecraft Materials and Components*, AD-A166216, AFOSR-86-0057TR, 1985.

Balmain, K. G., "Arc Propagation, Emission and Damage on Spacecraft Dielectrics," *The Aerospace Environment at High Altitudes and its Implications for Spacecraft Charging and Communications*, AGARD-CP-406, p. 16/1-16/7, 1987.

Balmain, K. G., Battagin, A., and Dubois, G. R., "Thickness Scaling for Arc Discharges on Electron-beam-charged Dielectrics," *IEEE Transactions on Nuclear Science, Vol. NS-32, No. 6*, p. 4073-4078, 1985.

Balmain, K. G., Cuchanski, M., and Kremer, P. C., "Surface Micro-Discharges on Spacecraft Dielectrics," *Proceedings of the Spacecraft Charging Technology Conference*, AFGL-TR-77-0051, NASA TMX-73537, ADA045459, edited by C. P. Pike and R. R. Lovell, p. 519-526, 1977.

Balmain, K. G. and Dubois, G. R., "Surface Discharges on Teflon, Mylar, and Kapton," *IEEE Transactions on Nuclear Science, Vol. NS-26, No. 6*, p. 5146-5151, 1979.

Balmain, K. G. and Gossland, M., "Spacecraft Fiberglass Strut Charging/Discharging and EMI," *IEEE Transactions on Nuclear Science, Vol. NS-32, No. 6*, p. 4438-4440, 1985.

Balmain, K. G., Gossland, M., Reeves, R. D., and Kuller, W. G., "Phenomenology of Surface Arcs on Spacecraft Dielectric Materials," *Spacecraft Materials in a Space Environment*, SP-178, ESA, p. 263-268, 1983.

Balmain, K. G. and Hirt, W., "Dielectric Surface Discharges: Dependence on Incident Electron Flux," *IEEE Transactions on Nuclear Science, Vol. NS-27, No. 6*, p. 1770-1775, 1980.

Balmain, K. G. and Hirt, W., "Dielectric Surface Discharges-Effects of Combined Low-Energy and High-Energy Incident Electrons," *IEEE Transactions on Electrical Insulation, Vol. EI-18*, p. 498-503, 1983.

Balmain, K. G., Orszag, M., and Kremer, P., "Surface Discharges on Spacecraft Dielectric in a Scanning Electron Microscope," *Spacecraft Charging by Magnetospheric Plasmas*, edited by A. Rosen, Progress in Astronautics and Aeronautics, series ed. M. Summerfield, AIAA, New York, p. 213-223, 1976.

Bartnikas, R., "1987 Whitehead Memorial Lecture: A Commentary on Partial Discharge Measurement and Detection," *IEEE Transactions on Electrical Insulation, Vol. 1-22, No. 5*, p. 629-653, 1987.

Beers, B. L., Pine, V. W., Hwang, H. C., Bloomberg, H. W., Lin, D. L., Schmidt, M. J., and Strickland, D. J., *First Principles Numerical Model of Avalanche-Induced Arc Discharges in Electron-Irradiated Dielectrics*, NASA CR-159560, 1979.

Beers, B. L., Pine, V. W., and Ives, S. T., *Continued Development of a Detailed Model of Arc Discharge Dynamics*, NASA CR-167977, 1982.

Berolo, O., "Damage and Deterioration of Teflon Second-Surface Mirrors by Space Simulated Electron Irradiation," *Spacecraft Materials in a Space Environment*, ESA SP-178, Toulouse, France, p. 231-240, 1982.

Bogorad, A., Bowman, C., Lloyd, T., Loman, J., and Armenti, J., "Electrostatic Discharge Induced Thermo-Optical Degradation of Optical Solar Reflectors (OSRs)," *IEEE Transactions on Nuclear Science, Vol. 38, No. 6*, p. 1608-1613, 1991.

Bogorad, A., Bowman, C., Loman, J., Bouknight, R., Armenti, J., and Lloyd, T., "Relation Between Electrostatic Discharge Rate and Outgassing Rate," *IEEE Transactions on Nuclear Science, Vol. 36, No. 6*, p. 2021-2026, 1989.

Capart, J. J. and Dumesnil, J. J., "The Electrostatic-Discharge Phenomena on Marecs-A," *ESA Bulletin, Vol. 34*, p. 22-27, 1983.

Catani, J.-P., "Introduction to the Problem of Environmentally-Induced Discharges by the Environment," *Space Environment Technology*, Cepadues-Editions, Toulouse-France, p. 413-428, 1987. In French.

Christou, C., "Even Satellites Aren't Safe From Electrostatic Discharge," *Microwaves & RF, Vol. 23*, p. 97-101, 1984.

Coakley, P., Kitterrer, B., and Treadaway, M., "Charging and Discharging Characteristics of Dielectric Material Exposed to Low-and Mid-Energy Electrons," *IEEE Transactions on Nuclear Science, Vol. NS-29, No. 6*, p. 1639-1643, 1982.

Coakley, P., Treadway, M., Wild, N., and Kitterer, B., "Discharge Characteristics of Dielectric Materials Examined in Mono-, Dual-, and Spectral Energy Electron Charging Environments," *Spacecraft Environmental Interactions Technology 1983*, NASA CP-2359, AFGL-TR-85-0018, ADA202020, edited by C. K. Purvis and C. P. Pike, p. 511-524, 1985.

Daughtridge, S., "Environment-Induced Anomalies on the TDRS and the Role of Spacecraft Charging," *Journal of Spacecraft and Rockets, Vol. 28, No. 3*, p. 324-329, 1991.

Davies, D. K., "Radiation Charging and Breakdown of Insulators," *The Aerospace Environment at High Altitudes and its Implications for Spacecraft Charging and Communications*, AGARD-CP-406, p. 19/1 - 19/7, 1987.

Dollery, A. A. and Verdin, D., "Electrostatic Discharging Behaviour of Kapton and Other Dielectric Materials in a Simulated Space Environment," *Environmental Effects on Materials for Space Applications*, AGARD, 1983.

Edmonds, L., *Approximations Useful for the Prediction of Electrostatic Discharges for Simple Electrode Geometries*, JPL 86-36, 1986.

Frederickson, A. R., "Electric Discharge Pulses in Irradiated Solid Dielectrics in Space," *IEEE Transactions on Electrical Insulation, Vol. EI-18*, p. 337-349, 1983.

Frederickson, A. R., "Discharge Pulse Phenomenology," *Spacecraft Environmental Interactions Technology 1983*, NASA CP-2359, AFGL-TR-85-0018, ADA202020, edited by C. K. Purvis and C. P. Pike, p. 483-509, 1985.

Frederickson, A. R., "Partial Discharge Phenomena in Space Applications," *Spacecraft Materials in Space Environment*, ONERA, Toulouse, France, p. 221-231, 1988.

Fujii, H., Shibuya, Y., Abe, T., Kasai, R., and Nishoto, H., "Electrostatic Charging and Arc Discharges on Satellite Dielectrics Simulated by Electron Beam," *Journal of Spacecraft and Rockets, Vol. 25*, p. 156-161, 1988.

Gal'perin, I. I., Gladyshev, V. A., Kozlov, A. I., and Molchanov, O. A., "Results on the Reduction of the Level of Discharge Phenomena in the Near-Satellite Plasma on the Aureole-3 Satellite," *Vol. 26*, p. 279-288, 1988. In Russian.

Garreau, M., "Electrostatic Discharges in Geostationary Orbit: The Case of Telecom 1," *Space Environment Technology*, Cepadues-Editions, Toulouse, France, p. 717-733, 1987. In French.

Garrett, H. B., Whittlesey, A., and Daughtridge, S., "Environment Induced Anomalies on the TDRS and the Role of Spacecraft Charging," AIAA Paper 90-0178, 1990.

Grossland, M. and Balmain, K. G., "Barriers to Flashover Discharge Arcs on Teflon." *IEEE Transactions on Nuclear Science, Vol. NS-29, No. 6*, p. 1618-1620, 1982.

Grossland, M. and Balmain, K. G., "Incident Ion Effects on Polymer Surface Discharges," *IEEE Transactions on Nuclear Science, Vol. NS-30, No. 6*, p. 4302-4306, 1983.

Haffner, J. W., "An Analysis of GPS Electrostatic Discharge Rates," *27th Aerospace Sciences Meeting*, Reno, NV, 1989.

Hoffmaster, D. K. and Sellen, J. M., Jr., "Spacecraft Material Response to Geosynchronous Substorm Conditions," *Spacecraft Charging by Magnetospheric Plasmas*, edited by A. Rosen, Progress in Astronautics and Aeronautics, series ed. M. Summerfield, AIAA, New York, p. 185-211, 1976.

Inouye, G. T., "Brushfire Arc Discharge Model," *Spacecraft Charging Technology—1980*, NASA CP-2182, AFGL-TR-81-0270, ADA114426, edited by N. J. Stevens and C. P. Pike, p. 133-162, 1981.

Inouye, G. T., Sanders, N. L., Komatsu, G. K., Valles, J. R., and Sellen, J. M., Jr., "Thermal Blanket Metallic Film Groundstrap and Second Surface Mirror Vulnerability to Arc Discharges," *Spacecraft Charging Technology—1978*, NASA CP-2071, AFGL-TR-79-0082, ADA084626, edited by R. C. Finke and C. P. Pike, p. 667-682, 1979.

Inouye, G. T. and Sellen, J. M., Jr., "A Proposed Mechanism for the Initiation and Propagation of Dielectric Surface Discharges," *Proceedings of the 1978 Symposium on the Effect of the Ionosphere on Space and Terrestrial Systems*, 1978 0-277-182, edited by J. M. Goodman, U. S. Government Printing Office, Washington DC, 1978.

Johnstone, A. D., Wrenn, G. L., Huber, A., and Hoge, D., "First Results from Meteosat-2 Discharge Experiments," *ESA Bulletin, Vol. 29*, p. 84-89, 1982.

Katz, I., Mandell, M. J., Parks, D. E., and Schnuelle, G. W., "A Theory of Dielectric Surface Discharges," *IEEE Transactions on Nuclear Science, Vol. NS-27, No. 6*, p. 1786-1791, 1980.

Koons, H. C., "Characteristics of Electrical Discharges on the P78-2 Satellite (SCATHA)," AIAA Paper 80-0333, 1980.

Koons, H. C., "Aspect Dependence and Frequency Spectrum of Electrical Discharges on the P78-2 (SCATHA) Satellite," *Spacecraft Charging Technology—1980*, NASA CP-2182, AFGL-TR-81-0270, ADA114426, edited by N. J. Stevens and C. P. Pike, p. 478-492, 1981.

Koons, H. C., "Summary of Environmentally Induced Electrical Discharges on the P78-2 (SCATHA) Satellite," *Journal of Spacecraft and Rockets, Vol. 20*, p. 425-431, 1983.

Larigaldie, S., Lecourtdeberu, H., Surget, J., Brunet, A., Faurer, F., Marque, J. P., and Veyrat, D., *Study of Surface Discharges*, ONERA-RF-11/7236-PY, ETN-87-99387, 1979.

Leadon, R. and Wilkenfeld, J., "Model for Breakdown Process in Dielectric Discharges," *Spacecraft Charging Technology—1978*, NASA CP-2071, AFGL-TR-79-0082, ADA084626, edited by R. C. Finke and C. P. Pike, p. 704-710, 1979.

Levy, L., "A New Understanding of Breakdowns in the Day Sections of Geosynchronous Orbit," *Proceedings of the International Aerospace Conference on Lightning and Static Electricity*, Paris, France, p. 467-474, 1985.

Levy, L., "Discharge Phenomena," *Space Environment Technology*, Cepadues-Editions, Toulouse-France, p. 523-543, 1987. In French.

Levy, L., Paillous, A., and Catani, J. P., "Experimental Study of Thermal Control Material Charging and Discharging," *Spacecraft Materials in a Space Environment*, ESA SP-178, p. 243-251, 1983.

Levy, L. and Sarail, D., "Phenomenology of Discharges in Space: Application to a Solar Generator," *Photovoltaic Generators in Space*, p. 109-114, 1985.

Levy, L. and Sarrail, D., "Scaling Laws for Discharges on Floating Supports," *IEEE Transactions on Nuclear Science, Vol. NS-34, No. 6*, p. 1606-1613, 1987.

Marque, J. P., "Statistical Behavior of Dielectric Discharges on Satellites - A New Experimental Approach," *International Aerospace and Ground Conference on Lightning and Static Electricity*, ONERA TP 1986-2, 1986.

Marque, J. P., "Surface Discharge on E-irradiated Materials," *Workshop on Electrostatic Charges and Discharges and Cosmic Ray Interaction in Satellites*, ONERA, TP 1986-194, 1986.

Marque, J. P., "Dielectric Discharges and Electromagnetic Disturbances on Geostationary Satellites," *4th Colloque sur la Compatibilite Electromagnetique*, ONERA, TP 1987-82, 1987. In French.

Marque, J. P., "Electrostatic Discharges and Geostationary Satellites," *L'Aeronautique et l'Astronautique, Vol. 122*, p. 41-55, 1987. In French.

Marque, J. P., "Phenomenology of E-irradiated Polymer Breakdown," *Vacuum, Vol. 39, No. 5*, p. 443-452, 1989.

Meulenberg, A., Jr., "Evidence for a New Discharge Mechanism for Dielectrics in a Plasma," *Spacecraft Charging by Magnetospheric Plasmas*, edited by A. Rosen, Progress in Astronautics and Aeronautics, series ed. M. Summerfield, AIAA, New York, p. 237-246, 1976.

Nanevicz, J. E. and Adamo, R. C., "Occurrence of Arcing and Its Effects on Space Systems," *Space Systems and Their Interactions with Earth's Space Environment*, edited by H. B. Garrett and C. P. Pike, Progress in Astronautics and Aeronautics, series ed. M. Summerfield, AIAA, New York, p. 252-275, 1980.

Payan, D., "Charge Electrostatique Par Electrons De Haute Energie," *Space Environment: Prevention of Risks Related to Spacecraft Charging*, Cepadues-Editions, Toulouse, France, p. 279-310, 1992. In French.

Purvis, C. K., "Arc Discharges of Electron-Irradiated Polymers: Results from the Spacecraft Charging Investigation," *Conference on Electrical Insulation and Dielectric Phenomena*, p. 277-283, 1979.

Robinson, J. W., "Charge Distributions Near Metal-Dielectric Interfaces Before and After Dielectric Surface Flashover," *Proceedings of the Spacecraft Charging Technology Conference*, AFGL-TR-77-0051, NASA TMX-73537, ADA045459, edited by C. P. Pike and R. R. Lovell, p. 503-516, 1977.

Rosen, A., *Effects of Arcing Due to Spacecraft Charging on Spacecraft Survival*, CR-159593, 1978.

Shaw, R. R., Nanevicz, J. E., and Adamo, R. C., "Observations of Electrical Discharges Caused by Differential Satellite Charging," *Spacecraft Charging by*

Magnetospheric Plasmas, edited by A. Rosen, Progress in Astronautics and Aeronautics, series ed. M. Summerfield, AIAA, New York, p. 61-76, 1976.

Snyder, D. B., "Discharge Mechanisms in Solar Arrays - Experiment," AIAA Paper 86-0363, 1986.

Stettner, R. and Dewald, A. B., "A Surface Discharge Model for Spacecraft Dielectrics," *IEEE Transactions on Nuclear Science, Vol. NS-32, No. 6*, p. 4079-4086, 1985.

Stettner, R. and Duerksen, G., "The Discharge of Spacecraft Dielectrics and the Theory of Lichtenberg Figure Formation," *IEEE Transactions on Nuclear Science, Vol. NS-31, No. 6*, p. 1375-1380, 1984.

Stevens, N. J., "Environmentally Induced Discharges on Satellites," *2nd ESTEC Spacecraft Electromagnetic Compatibility Seminar*, p. 161-172, 1983.

Stevens, N. J., Mills, H. E., and Orange, L., "Voltage Gradients in Solar Array Cavities as a Possible Site in Spacecraft-Charging-Induced Discharges," *IEEE Transactions on Nuclear Science, Vol. NS-28, No. 6*, p. 4558-4562, 1981.

Wadham, P. N., "The Effects of Electrostatic Discharge Phenomena on Telesat's Domestic Communication Satellites," *The Aerospace Environment at High Altitudes and its Implications for Spacecraft Charging and Communications*, AGARD-CP-406, p. 25/1-25/10, 1987.

Wilkinson, D. C., "NOAA's Spacecraft Anomaly Database," AIAA Paper 90-0173, 1990.

Yadlowsky, E. J. and Hazelton, R. C., "Studies of Microdamage in Dielectric Discharges," *Journal of Spacecraft and Rockets, Vol. 22*, p. 282-286, 1985.

Yadlowsky, E. J., Hazelton, R. C., and Churchill, R. J., "Puncture Discharge in Surface Dielectrics as Contaminant Sources in Spacecraft Environments," *International Spacecraft Contamination Conference*, NASA CP-2039, edited by J. M. Jemiola, Air Force Materials Lab, p. 945-969, 1978.

Yang, Z., Zhou, Y., and Ge, R., "Charging and Discharging of Dielectric Films Irradiated by High-/ Medium-/ Low-energy Electrons," *IAF 36th International Astronautical Congress*, Stockholm, Sweden, 1985.

Coupling of Discharges with Spacecraft Electronics

Alliot, J. C., "Electromagnetic Interaction Between an Electric Discharge and Cabling Inside a Satellite," *Space Environment Technology*, Cepadues-Editions, Toulouse, France, p. 561-587, 1987. In French.

Bowman, C., Bogorad, A., Shih, P., Tasca, D., Shomberg, M., and Armenti, J., "Spacecraft-Level Current-Injection Testing to Investigate Discharge Coupling Models," *IEEE Transactions on Nuclear Science, Vol. NS-36, No. 6*, p. 2033, 1989.

Brett, L., Estienne, J. P., Ferrante, J. G., Frezet, M., Grange, J. P., Noel, P., Labaune, G., Levy, L., and Catani, J. P., *Electrostatic Discharge Effects on Satellite Electronic Devices.*, ESA-CR(P)-2229, 1985.

Catani, J.-P., "Electromagnetic Discharges: Effects on the Circuit," *Space Environment Technology*, Cepadues-Editions, Toulouse-France, p. 589-611, 1987. In French.

Granger, J. P. and Ferrante, J. G., "Electrostatic-Discharge Coupling in Spacecraft Electronics," *ESA Journal, Vol. 11, No. 14*, p. 19-30, 1987.

Keyser, R. C. and Wilkenfeld, J. M., "Internal Responses of a Complex Satellite Model to Two Electron-Induced Discharge Simulation Techniques," *IEEE Transactions on Nuclear Science, Vol. NS-26, No. 6*, p. 5121-5126, 1979.

Leung, P., "Characteristics of Electromagnetic Interference Generated by Arc Discharges," *9th Aerospace Testing Seminar*, Los Angeles, CA, p. 40-44, 1986.

Nanevicz, J. E. and Adamo, R. C., "Laboratory Studies of Spacecraft Response to Transient Discharge Pulses," *Spacecraft Environmental Interactions Technology 1983*, NASA CP-2359, AFGL-TR-85-0018, ADA202020, edited by C. K. Purvis and C. P. Pike, p. 453-463, 1985.

Stevens, N. J., "Modeling of Environmentally-Induced Transients Within Satellites, Part 2 Discharge Coupling," *Space Environment Technology*, Cepadues-Editions, Toulouse, France, p. 511, 1987.

Treadaway, M. J., Woods, A. J., Flanagan, T. M., Leadon, R. E., Grismore, R., Denson, R., and Weenas, E. P., "Experimental Verification of an ECEMP Spacecraft Discharge Coupling Model," *IEEE Transactions on Nuclear Science, Vol. NS-27, No. 6*, p. 1776-1779, 1980.

Wilkenfeld, J., "Space Electron-Induced Discharge Coupling into Satellite Electronics," *Proceedings of the Air Force Geophysics Laboratory Workshop on Natural Charging of Large Space Structures in Near Earth Polar Orbit: 14-15 September 1982*, AFGL-TR-83-0046, ADA134894, edited by R. C. Sagalyn, D. E. Donatelli, and I. Michael, p. 215-234, 1983.

Woods, A. J., Treadaway, M. J., Grismore, R., Leadon, R. E., Flanagan, T. M., and Wenaas, E. P., "Model of Coupling of Discharges into Spacecraft Structures," *Spacecraft Charging Technology—1980*, NASA CP-2182, AFGL-TR-81-0270, ADA114426, edited by N. J. Stevens and C. P. Pike, p. 745-754, 1981.

Woods, A. J. and Wenaas, E. P., "Spacecraft Discharge Electromagnetic Interference Coupling Models," *Journal of Spacecraft and Rockets, Vol. 22, No. 3*, p. 265-281, 1985.

Testing

Bogorad, A., Bowman, C., Rayadurg, L., Sterner, T., Loman, J., and Armenti, J., "Amplitude Scaling of Solar Array Discharges," *IEEE Transactions on Nuclear Science, Vol. 37, No. 6*, p. 2112-2119, 1990.

Bowman, C., Bogorad, A., Shih, P., Tasca, D., Shomberg, M., and Armenti, J., "Spacecraft-Level Current-Injection Testing to Investigate Discharge Coupling Models," *IEEE Transactions on Nuclear Science, Vol. NS-36, No. 6*, p. 2033, 1989.

Catani, J.-P., "Satellite Qualification Tests for Electrostatic Discharges," *Proceedings of the International Symposium on Environmental Testing for Space Programmes—Test Facilities & Methods*, ESA SP-304, Noordwijk, The Netherlands, p. 507-510, 1990.

Coakley, P., *ECEMP Test Specification for Electronic Hardware*, JAYCOR, San Diego, CA, 1986.

Hall, W. N., "Space System Electrostatic Discharge Testing," *10th Aerospace Testing Seminar*, Los Angeles, CA, p. 77-82, 1987.

Levadou, F., "Proprietes Electriques Des Materiaux," *Space Environment: Prevention of Risks Related to Spacecraft Charging*, Cepadues-Editions, Toulouse, France, p. 261-278, 1992. In French.

Levy, L., Paillous, A., and Sarrail, D., *Satellite Charging Control Materials*, ONERA, Centre D'Etudes et de Recherches de Toulouse, AFWAL-TR-81-4033, 1981.

Pourtau, J. C., "Methodes D'Analyses Et D'Essais Aux Decharges Electrostatiques Des Equipements Electroniques D'Un Satellite Regles De Conception," *Space Environment: Prevention of Risks Related to Spacecraft Charging*, Cepadues-Editions, Toulouse, France, p. 441-467, 1992. In French.

Reddy, J., "Electron Irradiation Tests on European Meteorological Satellite," *Spacecraft Charging Technology—1980*, NASA CP-2182, AFGL-TR-81-0270, ADA114426, edited by N. J. Stevens and C. P. Pike, p. 835-855, 1981.

Staskus, J. V. and Roche, J. C., *Testing of a Spacecraft Model in a Combined Environment Simulator*, NASA TM-82723, 1981.

Stevens, N. J., Berkopec, F. D., Staskus, J. V., Blech, R. A., and Narciso, N. J., "Testing of Typical Spacecraft Materials in a Simulated Substorm Environment," *Proceedings of the Spacecraft Charging Technology Conference*, AFGL-TR-77-0051, NASA TMX-73537, ADA045459, edited by C. P. Pike and R. R. Lovell, p. 431-457, 1977.

Whittlesey, A. and Inouye, G., "Voyager Spacecraft Electrostatic Discharge Testing," *Journal of Environmental Science, Vol. 23, No. 2*, p. 29-33, 1980.

Whittlesey, A. and Leung, P., "Simulation of External and Internal Electrostatic Discharges at the Spacecraft System Test Level," *8th Aerospace Testing Seminar*, Los Angeles, CA, 1984.

Wilkenfeld, J., Judge, R., and Harlacher, B., *Development of Electrical Test Procedures for Qualification of Spacecraft Against EID, Vol. 1*, IRT 8195-018, IRT Corp., 1981.

Wilkenfeld, J. M., Harlacher, B. L., and Mathews, D., *Development of Electrical Test Procedures for Qualification of Spacecraft Against EID, Vol. 2*, IRT-8195-022-1, NASA CR-165590, IRT Corp., 1982.

Passive Charge Control

Degraffenreid, K. J. and Evans, R. C., "A Plan for Controlling Electrostatic Discharges on Geosynchronous Spacecraft," *25th IEEE International Symposium on Electromagnetic Compatibility*, Arlington, VA, p. 362-365, 1983.

Eagles, A. E., Amore, L. J., Belanger, V. J., and Schmidt, R. E., *Spacecraft Static Charge Control Materials, Part I*, AFML-TR-77-105, General Electric Space Division, 1977.

Eagles, A. E., Amore, L. J., Belanger, V. J., and Schmidt, R. E., *Spacecraft Static Charge Control Materials, Part II*, AFML-TR-77-105, General Electric Space Division, 1978.

Eagles, A. E. and Belanger, V. J., *Conductive Coatings for Satellites*, AFML-TR-75-233, General Electric Space Division, Valley Forge, PA, 1976.

Eagles, A. E., Schmidt, R. E., Amore, L. J., and Belanger, V. J., *Transparent Antistatic Satellite Materials, Part I*, AFML-TR-77-174, General Electric Space Division, 1977.

Eagles, A. E., Schmidt, R. E., Amore, L. J., and Belanger, V. J., *Transparent Antistatic Satellite Materials, Part II*, AFML-TR-77-174, General Electric Space Division, 1978.

Fujii, H., Nakanishi, K., Abe, T., Ohmura, T., and Nishimoto, H., "Suppression of Surface Potential Formation on Spacecraft," *16th International Symposium on Space Technology and Science*, 2, Sapporo, Japan, p. 1613-1619, 1988.

Gilligan, J. E., Yamauchi, T., Wolf, R. E., and Ray, C., *Electrically Conductive Paints for Satellites*, IIT Research Institute, IL, 1976.

Goldstein, R. D., Brown, E. M., and Maldoon, L. C., "Usage of ITO to Prevent Spacecraft Charging," *IEEE Transactions on Nuclear Science, Vol. NS-29, No. 6*, p. 1621-1628, 1982.

Lechte, H. G., "Stopping Differential Charging of Solar Arrays," *Fifth European Symposium on Photovoltaic Generators in Space*, p. 189-193, 1987.

Lehn, W. L., "SCATHA Conductive Spacecraft Materials Development," *Journal of Spacecraft and Rockets, Vol 20, No. 2*, p. 182-185, 1983.

Levadou, F., "Discharge Prevention of Geosynchronous Orbit-Conductive Thermal Control Materials and Grounding Systems," *Space Environment Technology*, Cepadues-Editions, Toulouse, France, p. 6[illegible]5-715, 1987. In French.

Lu, Y. and Li, H., "Preparation and Evaluation of Conductive Thin Films for Controlling Charging State on Spacecraft Surface," *40th IAF International Astronautical Congress, IAF Paper 89-322*, Malaga, Spain, 1989.

Rubin, A. G., Rothwell, P. L., and Yates, G. K., "Reduction of Spacecraft Charging Using Highly Emissive Materials," *Proceedings of the 1978 Symposium on the Effect of the Ionosphere on Space and Terrestrial Systems*, 1978 0-277-182, edited by J. M. Goodman, U. S. Government Printing Office, Washington DC, p. 313-316, 1978.

Rubin, A. G., Rothwell, P. L., and Yates, G. K., *Reduction of Spacecraft Charging Using Highly Emissive Surface Materials*, AFGL-TR-79-0086, AD A068291, 1979.

Satellite Spacecraft Charging Control Materials, AFWAL-TR-80-4029, 1980.

Schmidt, R. E., *Charging Control Satellite Materials. Part 1*, AFWAL-TR-80-4017, 1980.

Schmidt, R. E., *Charging Control Satellite Materials. Part 2. Materials Demonstration*, AFWAL-TR-80-4017, 1981.

Schmitz, W., "Development of Solar Generator Substrates: Simple Anticharging (AC) and Conductive Thermal Control (TC) Materials (GEO), and Some LEO Aspects," *Spacecraft Materials in Space Environment*, ESA, p. 133-141, 1986.

Sellappan, R. G., "Electro-static Surface Control of a Large Radiometer Spacecraft," *Guidance and Control Conference*, Gatlinburg, Tennessee, p. 618-621, 1983.

Verdin, D. and Duck, M. J., "Surface Modifications to Minimise the Electrostatic Charging of Kapton in the Space Environment," *The Aerospace Environment at High Altitudes and Its Implications for Spacecraft Charging and Communications*, AGARD-CP-406, p. 26/1-26/12, 1987.

Active Charge Control

Bartlett, R. O., DeForest, S. E., and Goldstein, P., "Spacecraft Charging Control Demonstration at Geosynchronous Altitude," AIAA Paper 75-359, 1975.

Bartlett, R. O. and Purvis, C. K., "Summary of the Two-Year NASA Program for Active Control of ATS-5/6 Environmental Charging," *Spacecraft Charging Technology—1978*, NASA CP-2071, AFGL-TR-79-0082, ADA084626, edited by R. C. Finke and C. P. Pike, p. 44-58, 1979.

Beattie, J. R. and Goldstein, R., "Active Spacecraft Potential Control System Selection for the Jupiter Orbiter with Probe Mission," *Proceedings of the Spacecraft Charging Technology Conference*, AFGL-TR-77-0051, NASA TMX-73537, ADA045459, edited by C. P. Pike and R. R. Lovell, p. 143-166, 1977.

Beattie, J. R., Williamson, W. S., Matossoan, J. N., Vourgourakis, E. J., and Burch, J. L., "High-current Plasma Contactor Neutralizer System," *3rd International Conference on Tethers in Space–Towards Flight*, CP892, AIAA, San Francisco, CA, 1989.

Cohen, H. A., Chesley, A. L., Aggson, T., Gussenhoven, M. S., Olsen, R. C., and Whipple, E., "A Comparison of Three Techniques of Discharging Satellites," *Spacecraft Charging Technology—1980*, NASA CP-2182, AFGL-TR-81-0270, ADA114426, edited by N. J. Stevens and C. P. Pike, p. 888-893, 1981.

Cohen, H. A. and Lai, S., "Discharging the P78-2 Satellite Using Ions and Electrons," AIAA Paper 82-0266, 1982.

Davis, V. A., Katz, I., Mandell, M. J., and Parks, D. E., "Hollow Cathodes as Electron Emitting Plasma Contactors: Theory and Computer Modeling," *Journal of Spacecraft and Rockets, Vol. 25*, p. 175, 1988.

DeForest, S. E. and Goldstein, R., *A Study of Electrostatic Charging of ATS-5 During Ion Thruster Operation*, NASA CR-145910, 1973.

Deininger, W. D., Aston, G., and Pless, L. C., "Hollow Cathode Plasma Source for Active Spacecraft Charge Control," *Review of Scientific Instruments, Vol. 58*, p. 1053-1062, 1987.

Goldstein, R., "Active Control of Potential of the Geosynchronous Satellites ATS-5 and ATS-6," *Proceedings of the Spacecraft Charging Technology Conference*, AFGL-TR-77-0051, NASA TMX-73537, ADA045459, edited by C. P. Pike and R. R. Lovell, p. 121-129, 1977.

Goldstein, R. and DeForest, S. E., "Active Control of Spacecraft Potentials at Geosynchronous Orbit," *Spacecraft Charging by Magnetospheric Plasmas*, edited by A. Rosen, Progress in Astronautics and Aeronautics, series ed. M. Summerfield, AIAA, New York, p. 169-181, 1976.

Gonfalone, A., Pedersen, A., Fahleson, U. V., Falthammar, C.-G., Mozer, F. S., and Torbert, R. B., "Spacecraft Potential Control on ISEE-1," *Spacecraft Charging Technology—1978*, NASA CP-2071, AFGL-TR-79-0082, ADA084626, edited by R. C. Finke and C. P. Pike, p. 256-267, 1979.

Grard, R. J. L., "Spacecraft Potential Control and Plasma Diagnostic Using Electron Field Emission Probes," *Space Science Instruments, Vol. 1*, p. 363-376, 1975.

Groh, K. H., Bescherer, K., Nikolaizig, N. K., and Loeb, H. W., "Interaction between the RIT 10 Exhaust and Negatively Charged Surfaces," *Journal of Spacecraft and Rockets, Vol. 19, No. 2*, p. 125-128, 1982. AIAA Paper 81-0726.

Gussenhoven, M. S., Mullen, E. G., and Hardy, D. A., "Artificial Charging of Spacecraft Due to Electron Beam Emission," *IEEE Transactions on Nuclear Science, Vol. NS-34, No. 6*, p. 1614-1619, 1987.

Hastings, D. E., "The Use of Electrostatic Noise to Control High-voltage Differential Charging of Spacecraft," *Journal of Geophysical Research, Vol. 91*, p. 5719-5724, 1986.

James, H. G., "Discharge of RF-Induced Spacecraft DC Potential by Positive Ions," *Planetary and Space Science, Vol. 35*, p. 105-118, 1987.

Kawashima, N., "Experimental Studies of the Neutralization of a Charged Vehicle in Space and in the Laboratory in Japan," *Artificial Particle Beams in Space Plasma Studies*, edited by B. Grandal, Plenum Press, New York, p. 597-626, 1982.

Komatsu, G. K. and Sellen, J. M., Jr., "A Plasma Bridge Neutralizer for the Neutralization of Differentially Charged Surfaces," *Effect of the Ionosphere on Space and Terrestrial Systems*, edited by J. Goodman, U.S. Government Printing Office, p. 317-321, 1978.

Lai, S. T., McNeil, W. J., and Aggson, T. L., "Spacecraft Charging During Ion Beam Emissions in Sunlight," AIAA Paper 90-0636, 1990.

Lebreton, J. P., "Active Control of the Potential of ISEE-1 by an Electron Gun," *Spacecraft/Plasma Interactions and Their Influence on Field and Particle Measurements*, ESA SP-198, edited by A. Pedersen, D. Guyenne, and J. Hunt, European Space Agency, Noordwijk, The Netherlands, p. 191-197, 1983.

Lin, C. S. and Koga, J., "Spacecraft Charging Potential during Electron-beam Injections into Space Plasma," *IEEE Transactions on Plasma Science, Vol. 17*, p. 205, 1989.

Linson, L. M., "Charge Neutralization as Studied Experimentally and Theoretically," *Artificial Particle Beams in Space Plasma Studies*, edited by B. Grandal, Plenum Press, New York, p. 573-595, 1982.

Olsen, R. C., "Modification of Spacecraft Potentials by Plasma Emission," *Journal of Spacecraft and Rockets, Vol. 18*, p. 462-469, 1981.

Olsen, R. C., "Modification of Spacecraft Potentials by Thermal Electron Emission on ATS-5," *Journal of Spacecraft and Rockets, Vol. 18*, p. 527-532, 1981.

Olsen, R. C., "Experiments in Charge Control at Geosynchronous Orbit - ATS-5 and ATS-6," *Journal of Spacecraft and Rockets, Vol. 22*, p. 254-264, 1985.

Olsen, R. C., Whipple, E. C., and Purvis, C. K., "Active Modification of the ATS-5 and ATS-6 Spacecraft Potentials," *Proceedings of the 1978 Symposium on the Effect of the Ionosphere on Space and Terrestrial Systems*, 1978 0-277-182, edited by J. M. Goodman, U. S. Government Printing Office, Washington DC, p. 328-336, 1978.

Pederson, A., Chapell, C. R., Knott, K., and Olsen, R. C., "Methods for Keeping a Conductive Spacecraft Near the Plasma Potential," *Spacecraft/Plasma Interactions and Their Influence on Field and Particle Measurements*, ESA SP-198, edited by A. Pedersen, D. Guyenne, and J. Hunt, European Space Agency, Noordwijk, The Netherlands, p. 185-190, 1983.

Purvis, C. K. and Bartlett, R. O., "Active Control of Spacecraft Charging," *Space Systems and Their Interactions with Earth's Space Environment*, edited by H. B. Garrett and C. P. Pike, Progress in Astronautics and Aeronautics, series ed. M. Summerfield, AIAA, New York, p. 299-317, 1980.

Purvis, C. K., Bartlett, R. O., and DeForest, S. E., "Active Control of Spacecraft Charging on ATS-5 and ATS-6," *Proceedings of the Spacecraft Charging Technology Conference*, AFGL-TR-77-0051, NASA TMX-73537, ADA045459, edited by C. P. Pike and R. R. Lovell, p. 107-120, 1977.

Riedler, W., Goldstein, R., Hamelin, M., Machlum, B. N., Troim, J., Olsen, R. C., Pedersen, A., Grard, R. J. L., Schmidt, R., and Rudenauer, F., "Active Spacecraft Potential Control: An Ion Emitter Experiment Cluster Mission," *The Cluster Mission: Scientific and Technical Aspects of the Instruments*, ESA, p. 95-102, 1989.

Robson, R. R. and Williamson, W. W., *Flight Model Discharge System Report*, AFGL-TR-88-0150, 1988.

Sasaki, S., Kawashima, N., Kuriki, K., Yanagisawa, M., Obayshi, T., Roberts, W. T., Reasoner, D. L., Williamson, P. R., Banks, P. M., Taylor, W. L., Akai, K., and Burch, J. L., "Neutralization of Beam-emitting Spacecraft by Plasma Injection," *Journal of Spacecraft and Rockets, Vol. 24*, p. 227-231, 1987.

Schmidt, R., Arends, H., Nikolaizig, N., and Riedler, W., "Ion Emission to Actively Control the Floating Potential of a Spacecraft," *Advances in Space Research, Vol. 8, No. 1*, p. 187-192, 1988.

Shuman, B. M. and Cohen, H. A., "Automatic Charge Control System for Satellites," *Spacecraft Environmental Interactions Technology 1983*, NASA CP-2359, AFGL-TR-85-0018, ADA202020, edited by C. K. Purvis and C. P. Pike, p. 477-481, 1985.

Shuman, B. M., Cohen, H. A., Hyman, J., Robson, R. R., and Williamson, W. S., *A Charge Control System for Spacecraft Protection*, AFGL-TR-88-0246, ADA199904, 1988.

Trinke, H., "Aerospace Vehicles Charging by Thruster Plumes," *FAA Eighth International Aerospace and Ground Conference on Lightning and Static Electricity*, p. 6, 1983.

Wikolaizig, N. K., Bescherer, K. W., Groh, K. H., and Loeb, H. W., "The Possibility of Controlling Spacecraft Charging by Means of the Electric Propulsion System RIT 10," *Spacecraft Electromagnetic Compatibility Seminar*, p. 173-178, 1983.

Monitoring

Sturman, J. C., "Development and Design of Three Monitoring Instruments for Spacecraft Charging," NASA TP-1800, 1981.

Index